Methods in Molecular Biology 1904

Springer Protocols

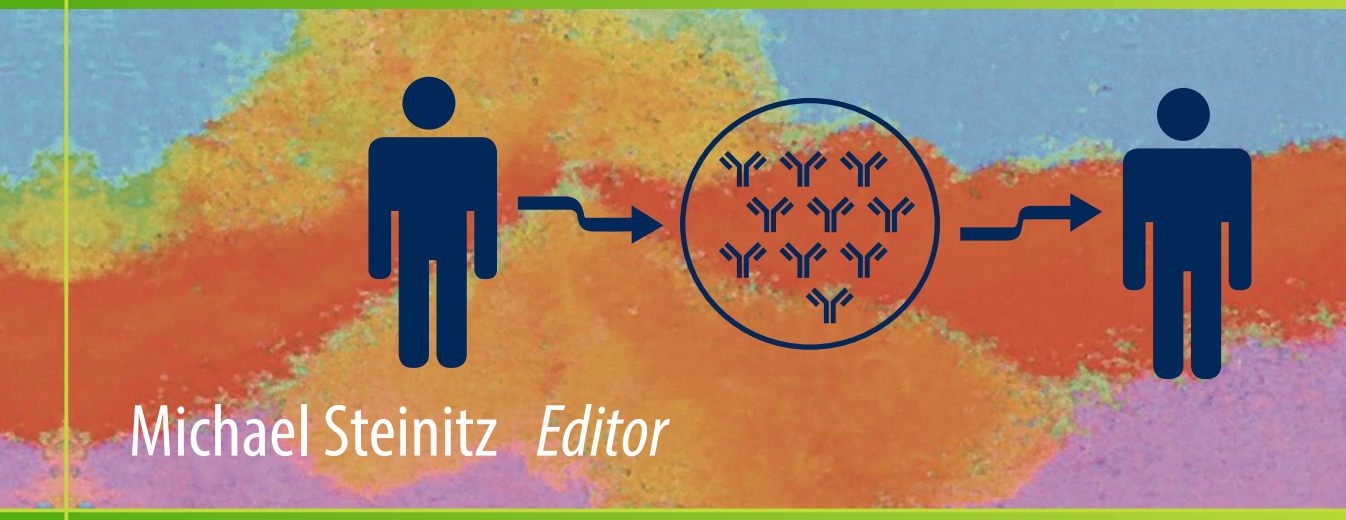

Michael Steinitz *Editor*

Human Monoclonal Antibodies

Methods and Protocols

Second Edition

Humana Press

METHODS IN MOLECULAR BIOLOGY

Series Editor
John M. Walker
School of Life and Medical Sciences
University of Hertfordshire
Hatfield, Hertfordshire, AL10 9AB, UK

For further volumes:
http://www.springer.com/series/7651

Human Monoclonal Antibodies

Methods and Protocols

Second Edition

Edited by

Michael Steinitz

Department of Pathology, The Hebrew University, Hadassah Medical School, Jerusalem, Israel

Humana Press

Editor
Michael Steinitz
Department of Pathology
The Hebrew University
Hadassah Medical School
Jerusalem, Israel

ISSN 1064-3745 ISSN 1940-6029 (electronic)
Methods in Molecular Biology
ISBN 978-1-4939-8957-7 ISBN 978-1-4939-8958-4 (eBook)
https://doi.org/10.1007/978-1-4939-8958-4

Library of Congress Control Number: 2018964050

This Humana Press imprint is published by the registered company Springer Science+Business Media, LLC, part of Springer Nature.
The registered company address is: 233 Spring Street, New York, NY 10013, U.S.A.

Dedication

This book is dedicated to George Klein, 1925–2016, a giant creative and stimulating scientist of infinite knowledge, friend, and mentor. His legacy is a never-fading light house to hundreds of former students, co-workers, colleagues, and friends.

Preface

A second edition of Springer Protocols book *Human Monoclonal Antibodies* is a natural outcome of the rapid developments in the area and the remarkable interest attracted by our 2014 first edition of the book.

It is amazing what a rapid and dramatic development has occurred in the field of human monoclonal antibodies since the first time these were produced in the laboratory. It was the pioneering study initiated by Professor George Klein in Stockholm in 1977 [1] that showed the feasibility of making such antibodies from immortalized peripheral blood antigen-committed human B lymphocytes.

The extensive basic immune research which has taken place during the last years rapidly converged into the clinic. The Fast and dramatic development of novel immune treatments in the clinic using human monoclonal antibodies urged the improvements of traditional and also completely new techniques involved in the production of the antibodies. The introduction of monoclonal antibodies directed against lymphocyte cell-surface costimulatory/immune checkpoint receptors that mediate the immune response has been revolutionary. These antibodies enable overcome immune unresponsiveness (i.e., tolerance) of T cells. Antibodies against costimulatory lymphocyte receptors which now are used in the clinic proved very beneficial for tumor patients at least in relation to some types of cancer.

Continuous progress in molecular techniques enables genuine management of antibody molecules. Such reagents introduced into cytotoxic T cells promise new horizons for the treatment of cancer patients.

The present Springer Protocols book reflects some of the recent developments in the area. It includes several completely new chapters related to topics that were not discussed in the first edition. In addition, some chapters from the first edition are updated with necessary revisions. Similar to the first edition, besides the detailed specific technical protocols, there are a few review manuscripts too.

Jerusalem, Israel *Michael Steinitz*

Reference

1. Steinitz M, Klein G, Koskimies S, Mäkelä O (1977) EBV virus induced B lymphocyte cell lines producing specific antibody. Nature 269:420–422

Contents

Contributors

Azimah Ahmad • *Institute for Research in Molecular Medicine, Universiti Sains Malaysia, Penang, Malaysia*

Michihiko Aoyama • *Division of Biological Chemistry and Biologicals, National Institute of Health Sciences, Kawasaki, Kanagawa, Japan*

Nicolas Aubrey • *UMR Université-INRA ISP 1282, BioMAP, Université de Tours, Tours, France*

Ivan Babic • *Department of Translational Neurosciences and Neurotherapeutics, John Wayne Cancer Institute, Santa Monica, CA, USA*

Ina Becker • *Department of Radiation Oncology, Universitätsklinikum Erlangen, Friedrich-Alexander-Universität Erlangen-Nürnberg, Erlangen, Germany*

Itai Benhar • *School of Molecular Cell Biology and Biotechnology, The George S. Wise Faculty of Life Sciences, Tel-Aviv University, Ramat Aviv, Israel*

Madhuri Bhandaru • *Department of Dermatology and Skin Science, University of British Columbia, Vancouver, BC, Canada*

Joyeeta Bhattacharyya • *Department of Cardiac Research, Cumballa Hill Hospital and Heart Institute, Mumbai, India*

Philippe Billiald • *School of Pharmacy, Paris-Sud University, Châtenay-Malabry, France*

Racheli Birnboim-Perach • *School of Molecular Cell Biology and Biotechnology, The George S. Wise Faculty of Life Sciences, Tel-Aviv University, Ramat Aviv, Israel*

Patricia Blundell • *Liverpool School of Tropical Medicine, Liverpool, UK*

Angela Chiew Wen Ch'ng • *Institute for Research in Molecular Medicine, Universiti Sains Malaysia, Penang, Malaysia*

Marco Dal Ferro • *Department of Life Sciences, University of Trieste, Trieste, Italy*

Anna-Jasmina Donaubauer • *Department of Radiation Oncology, Universitätsklinikum Erlangen, Friedrich-Alexander-Universität Erlangen-Nürnberg, Erlangen, Germany*

Stav Dror • *School of Molecular Cell Biology and Biotechnology, The George S. Wise Faculty of Life Sciences, Tel-Aviv University, Ramat Aviv, Israel*

Haley L. Dugan • *Committee on Immunology, University of Chicago, Chicago, IL, USA*

Mahboobeh Fereidan-Esfahani • *Department of Neurology, Mayo Clinic, Rochester, MN, USA*

Fortunato Ferrara • *Specifica Inc., Santa Fe, NM, USA*

Rainer Fietkau • *Department of Radiation Oncology, Universitätsklinikum Erlangen, Friedrich-Alexander-Universität Erlangen-Nürnberg, Erlangen, Germany*

Benjamin Frey • *Department of Radiation Oncology, Universitätsklinikum Erlangen, Friedrich-Alexander-Universität Erlangen-Nürnberg, Erlangen, Germany*

Viola Fühner • *Abteilung Biotechnologie, Institut für Biochemie, Biotechnologie und Bioinformatik, Technische Universität Braunschweig, Braunschweig, Germany*

Udo S. Gaipl • *Department of Radiation Oncology, Universitätsklinikum Erlangen, Friedrich-Alexander-Universität Erlangen-Nürnberg, Erlangen, Germany*

Mark C. Glassy • *Department of Translational Neurosciences and Neurotherapeutics, John Wayne Cancer Institute, Santa Monica, CA, USA; Translational Neuro-Oncology Laboratory, UCSD Moores Cancer Center, La Jolla, CA, USA; Nascent Biotech, Inc., San Diego, CA, USA*

África González-Fernández • *Immunology, Centro de Investigaciones Biomédicas (CINBIO), Centro de Investigación Singular de Galicia, Instituto de Investigación Sanitaria Galicia Sur, Universidad de Vigo, Vigo, Spain*
Yehudit Grinberg • *School of Molecular Cell Biology and Biotechnology, The George S. Wise Faculty of Life Sciences, Tel-Aviv University, Ramat Aviv, Israel*
Jenna J. Guthmiller • *Department of Medicine, Section of Rheumatology, The Knapp Center for Lupus and Immunology, University of Chicago, Chicago, IL, USA*
Hiroshi Hamana • *Department of Immunology, Graduate School of Medicine and Pharmaceutical Sciences, University of Toyama, Toyama, Japan*
Koji Hashimoto • *Department of Life Sciences, Graduate School of Arts and Sciences, The University of Tokyo, Tokyo, Japan*
Kunihiro Hattori • *Research Division, Chugai Pharmaceutical, Kamakura, Kanagawa, Japan*
Philip Alexander Heine • *Abteilung Biotechnologie, Institut für Biochemie, Biotechnologie und Bioinformatik, Technische Universität Braunschweig, Braunschweig, Germany*
Charles L. Howe • *Department of Neurology, Mayo Clinic, Rochester, MN, USA*
Michael Hust • *Abteilung Biotechnologie, Institut für Biochemie, Biotechnologie und Bioinformatik, Technische Universität Braunschweig, Braunschweig, Germany*
Tomoyuki Igawa • *Chugai Pharmabody Research Pte. Ltd., Singapore, Singapore*
Akiko Ishii-Watabe • *Division of Biological Chemistry and Biologicals, National Institute of Health Sciences, Kawasaki, Kanagawa, Japan*
Santosh Kesari • *Department of Translational Neurosciences and Neurotherapeutics, John Wayne Cancer Institute, Santa Monica, CA, USA*
Jeremy D. King • *Department of Molecular Medicine, Beckman Research Institute at City of Hope, Duarte, CA, USA*
Hiroyuki Kishi • *Department of Immunology, Graduate School of Medicine and Pharmaceutical Sciences, University of Toyama, Toyama, Japan*
Eiji Kobayashi • *Department of Immunology, Graduate School of Medicine and Pharmaceutical Sciences, University of Toyama, Toyama, Japan*
Zoltán Konthur • *Department of Biomolecular Systems, Max Planck Institute of Colloids and Interfaces, Potsdam, Germany*
Taichi Kuramochi • *Chugai Pharmabody Research Pte. Ltd., Singapore, Singapore*
Kohei Kurosawa • *Department of Life Sciences, Graduate School of Arts and Sciences, The University of Tokyo, Tokyo, Japan*
Linda Yu-Ling Lan • *Committee on Immunology, University of Chicago, Chicago, IL, USA*
Theam Soon Lim • *Institute for Research in Molecular Medicine, Universiti Sains Malaysia, Penang, Malaysia; Analytical Biochemistry Research Centre, Universiti Sains Malaysia, Penang, Malaysia*
Dana Litvak-Greenfeld • *School of Molecular Cell Biology and Biotechnology, The George S. Wise Faculty of Life Sciences, Tel-Aviv University, Ramat Aviv, Israel*
Immacolata Luisi • *Department of Life Sciences, University of Trieste, Trieste, Italy*
Susana Magadán Mompó • *Immunology, Centro de Investigaciones Biomédicas (CINBIO), Centro de Investigación Singular de Galicia, Instituto de Investigación Sanitaria Galicia Sur, Universidad de Vigo, Vigo, Spain*
Francesca Marano • *Department of Life Sciences, University of Trieste, Trieste, Italy*
Ilaria Marrocco • *Department of Biological Regulation, Weizmann Institute of Science, Rehovot, Israel*

Doris Meier • *Abteilung Biotechnologie, Institut für Biochemie, Biotechnologie und Bioinformatik, Technische Universität Braunschweig, Braunschweig, Germany*
Keichiro Mihara • *Department of Hematology and Oncology, Research Institute for Radiation Biology and Medicine, Hiroshima University, Hiroshima, Japan*
Massimo Morbidelli • *ETH Zurich, Institute for Chemical and Bioengineering, Zurich, Switzerland*
Gustavo Marçal Schmidt Garcia Moreira • *Abteilung Biotechnologie, Institut für Biochemie, Biotechnologie und Bioinformatik, Technische Universität Braunschweig, Braunschweig, Germany*
Thomas Müller-Späth • *ETH Zurich, Institute for Chemical and Bioengineering, Zurich, Switzerland*
Atsushi Muraguchi • *Department of Immunology, Graduate School of Medicine and Pharmaceutical Sciences, University of Toyama, Toyama, Japan*
Limor Nahary • *School of Molecular Cell Biology and Biotechnology, The George S. Wise Faculty of Life Sciences, Tel-Aviv University, Ramat Aviv, Israel*
Tarek Nayfeh • *Department of Neurology, Mayo Clinic, Rochester, MN, USA*
Karlynn E. Neu • *Department of Medicine, Section of Rheumatology, The Knapp Center for Lupus and Immunology, University of Chicago, Chicago, IL, USA; Committee on Immunology, University of Chicago, Chicago, IL, USA*
Kunihiro Ohta • *Department of Life Sciences, Graduate School of Arts and Sciences, The University of Tokyo, Tokyo, Japan*
Tatsuhiko Ozawa • *Department of Immunology, Graduate School of Medicine and Pharmaceutical Sciences, University of Toyama, Toyama, Japan*
Richard Pleass • *Liverpool School of Tropical Medicine, Liverpool, UK*
Serena Rizzo • *Department of Life Sciences, University of Trieste, Trieste, Italy*
Emanuela Rizzo • *Department of Life Sciences, University of Trieste, Trieste, Italy*
Moses Rodriguez • *Department of Neurology, Mayo Clinic, Rochester, MN, USA*
Donatella Romaniello • *Department of Biological Regulation, Weizmann Institute of Science, Rehovot, Israel*
Kristian Daniel Ralph Roth • *Abteilung Biotechnologie, Institut für Biochemie, Biotechnologie und Bioinformatik, Technische Universität Braunschweig, Braunschweig, Germany*
Anand Rotte • *Department of Clinical Pharmacology, Genentech Research and Early Development, South San Francisco, CA, USA; Department of Clinical and Regulatory Affairs, Nevro Corp., Redwood City, CA, USA*
Paul F. Rühle • *Department of Radiation Oncology, Universitätsklinikum Erlangen, Friedrich-Alexander-Universität Erlangen-Nürnberg, Erlangen, Germany*
Giulio Russo • *Abteilung Biotechnologie, Institut für Biochemie, Biotechnologie und Bioinformatik, Technische Universität Braunschweig, Braunschweig, Germany*
Daniele Sblattero • *Department of Life Sciences, University of Trieste, Trieste, Italy*
Hidetaka Seo • *Department of Life Sciences, Graduate School of Arts and Sciences, The University of Tokyo, Tokyo, Japan*
Maria Felicia Soluri • *Department of Health Sciences and IRCAD, University of Piemonte Orientale (UPO), Novara, Italy*
Minoru Tada • *Division of Biological Chemistry and Biologicals, National Institute of Health Sciences, Kawasaki, Kanagawa, Japan*
Olga Tarasiuk • *Department of Health Sciences and IRCAD, University of Eastern Piedmont, Novara, Italy*

Hiroyuki Tsunoda • *Research Division, Chugai Pharmaceutical, Kamakura, Kanagawa, Japan*
Nicole Ulmer • *ETH Zurich, Institute for Chemical and Bioengineering, Zurich, Switzerland*
Lilach Vaks • *School of Molecular Cell Biology and Biotechnology, The George S. Wise Faculty of Life Sciences, Tel-Aviv University, Ramat Aviv, Israel*
Sebastian Vogg • *ETH Zurich, Institute for Chemical and Bioengineering, Zurich, Switzerland*
Herman Waldmann • *Sir William Dunn School of Pathology, Oxford University, Oxford, UK*
Arthur Warrington • *Department of Neurology, Mayo Clinic, Rochester, MN, USA*
John C. Williams • *Department of Molecular Medicine, Beckman Research Institute at City of Hope, Duarte, CA, USA*
Patrick C. Wilson • *Department of Medicine, Section of Rheumatology, The Knapp Center for Lupus and Immunology, University of Chicago, Chicago, IL, USA; Committee on Immunology, University of Chicago, Chicago, IL, USA*
Yosef Yarden • *Department of Biological Regulation, Weizmann Institute of Science, Rehovot, Israel*
Tetsumi Yoshida • *Department of Hematology and Oncology, Research Institute for Radiation Biology and Medicine, Hiroshima University, Hiroshima, Japan*
Kilian Johannes Carl Zilkens • *YUMAB GmbH, Braunschweig, Germany*

Chapter 1

Human Monoclonal Antibodies: The Benefits of Humanization

Herman Waldmann

Abstract

The major reasons for developing human monoclonal antibodies were to be able to efficiently manipulate their effector functions while avoiding immunogenicity seen with rodent antibodies. Those effector functions involve interactions with the complement system and naturally occurring Fc receptors on diverse blood white cells. Antibody immunogenicity results from the degree to which the host immune system can recognize and react to these therapeutic agents. Thus far, there is still no generally applicable technology guaranteed to render therapeutic antibodies antigenically silent. This is not to say that the task is impossible, but rather that we need to train the immune system to help us. This can be achieved if we take advantage of natural mechanisms by which an individual can be rendered tolerant of "foreign" antigens, and as a corollary minimize the potential immunogenicity of any contaminating protein aggregates, or "aggregates" arising from antibodies complexing with their antigen. I here summarize our efforts to engineer antibodies to harness optimal effector functions, while also minimizing their immunogenicity. Potential avenues to achieve the latte are predicted from classical work showing that monomeric "foreign" immunoglobulins are good tolerogens, while aggregates of immunoglobulins ate intrinsically immunogenic. Consequently, I argue that one solution to the immunogenicity problem lies in ensuring a temporal quantitative advantage of tolerogenic non-cell-bound monomer over the cell-binding immunogenic form.

Key words Therapeutic antibodies, Complement system, Fc receptors, Immunogenicity, Adjuvanticity, High dose tolerance, Humanized and human antibodies

1 Introduction

Although monoclonal antibodies were first described in 1975 [1], their potential as therapeutic agents was not properly appreciated until technology evolved to replace, to different degrees, the original rodent forms with human equivalents [2–8]. The reasons for this are complex, but relate to a combination of perceptions related to patentability, immunogenicity, effector function, and wish to avoid undesirable side effects. Undoubtedly, the terms *human* or *humanized* (Fig. 1) carried some emotive advantage over *rodent*, *murine*, or *rat* in giving comfort that agents close to the human form were

Michael Steinitz (ed.), *Human Monoclonal Antibodies: Methods and Protocols*, Methods in Molecular Biology, vol. 1904, https://doi.org/10.1007/978-1-4939-8958-4_1,

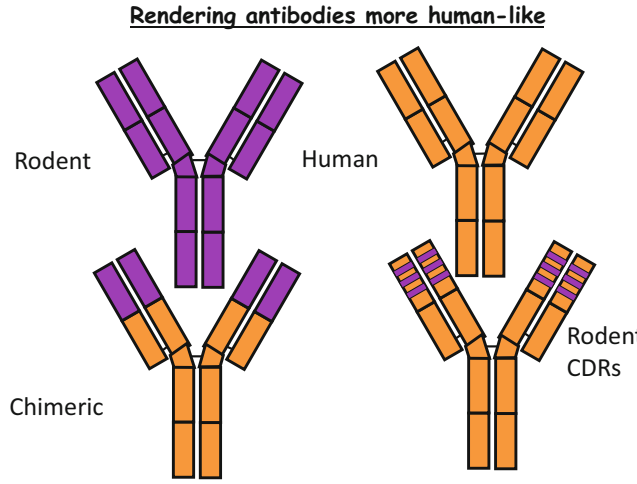

Fig. 1 The construction of chimeric and humanized antibodies. The bulk of the humanized Ab (so-called frameworks-in orange) is tolerated as if "self." The complementarity determining regions (CDRs) which bind antigen will however be regarded by the immune system as foreign

somehow preferable, even before all the evidence was in [9]. That emotive argument has even been extended to comparisons between *fully human* as opposed to more *humanized* antibodies, as if there were some important and significant functional difference. Undoubtedly though, the commercially driven demand for human antibodies has, to its credit, catalyzed technologies related to antibody engineering and manufacture which have aided commercialization in a very productive way. The basic human constructs and expression vectors generated for the purpose have also served as templates to enable generation of antibody variants designed to deliver improved therapeutic performance [10].

In this short chapter I will discuss our past work assessing the ability of human immunoglobulin subclasses to harness natural effector mechanisms, and the extent to which engineering therapeutic antibodies to human forms has provided solution to the "immunogenicity" problem.

2 Antibody Effector Functions

Early work with rodent "therapeutic" monoclonal antibodies taught us that choice of antibody class and subclass were important in harnessing therapeutic effector mechanisms in vitro and in vivo [11–13]. In the first steps toward derivation of engineered "human" antibodies reagents chimeric for human Fc (constant) regions with rodent variable regions (Fig. 1) proved invaluable in driving decisions as to which human Fc region was best suited to

achieve a desired therapeutic effect [14]. In one of the first of such in vitro studies [15, 16] a series of chimeric antibodies were constructed all having identical variable regions binding to a defined hapten (4-hydroxy-3-nitrophenacetyl). Whereas IgM, IgG1, and IgG3 constant regions bound C1q efficiently, and could mediate lysis with human complement, IgE, IgG2, and IgG4 were very weak in that regard. In cell mediated lysis studies IgG1 and IgG3 were efficient, while IgM, IgG2, IgG4, IgA, and IgE were very weak. This hierarchy of IgG subclasses in mediating effector functions was also demonstrated with the humanized antibody CAMPATH-1H [5] (Fig. 1). In the case of a humanized anti-CD3 antibody we wished to find an immunoglobulin Fc region that would not allow mitogenicity and cytokine release [17], as these had been associated with significant toxicity due to a cytokine storm in patients treated with the original rodent forms of anti-CD3 antibodies. We observed that all of the IgG subclasses, IgE and IgA were mitogenic in vitro, whereas a mutated IgG1 constant region mutated to lose the glycosylation site (Asn297) by changing to alanine, was non-mitogenic. The aglycosyl IgG1 form was less able to generate cytokine release in hCD3 transgenic mice [17, 18], unlike the parental IgG1 form. However, the mutant form, although non-lytic, has proven immunosuppressive both in vitro and in vivo [17–20]. Although the native hIgG1 form of humanized anti-CD3 antibody failed to activate human complement lysis in vitro, an engineered monovalent form was able to do so [21].

In. summary then, these studies taught us that selected human IgG isotypes, both natural and engineered, could be adopted for desired effector activity in therapeutic application. In more recent times, especially in the arena of checkpoint blockade, selection of human immunoglobulin isotypes in relation to binding particular Fc receptors, may be of great importance [22].

3 Immunogenicity

It has long been known that “foreign” polyclonal antibodies are potentially immunogenic in humans and in experimental animals. Seminal studies from Chiller and Weigle, and Dresser indicated that even though human immunoglobulins were foreign to mice, when given as monomers, they were tolerogenic rather than immunogenic [10]. However, given as heat induced aggregates, they were obligate immunogens. At high doses the monomers could tolerize both T-helper cells and B-cells, but at low doses would only tolerize the T-helper cells [10]. As therapeutic antibodies tended to target antigens within the body, it was likely that, when bound to cell surface antigens, they would be generating “immunogenic” aggregates within the treated hosts. Whereas polyclonal antibodies might

bind to multiple epitopes within the antigen, monoclonal antibodies would be restricted to just one or very few such targets.

In 1986, we examined a series of rat antibodies that were directed toward mouse leucocyte antigens, and found that virtually all proved immunogenic, except antibodies to the CD4 molecule [23].

In contrast, monomeric rat monoclonal immunoglobulins that did not bind to leucocytes, proved non-immunogenic, but were actually tolerogenic, in markedly reducing the antibody response to cell-binding antibodies given at a later time. It also emerged that the anti-CD4 antibodies were indeed directing the immune system to regard them as tolerogens, as well as other proteins that might be given under the umbrella of the anti-CD4 therapy. This observation formed the basis for many subsequent studies on therapeutic reprogramming of the immune system through recruitment of host tolerance mechanisms [24]. These findings suggested that antibodies binding to leucocytes simulated the Chiller-Weigle aggregates in generating sufficient adjuvanticity to evoke immune responses, but also left some questions about what target cell type or antigen was needed for that purpose. To this day, there has been very little attention to this question. For example, what if the target antigen was a monomer in solution, or a trimer (such as TNF)? Would therapeutic antibodies to these be immunogenic? As mentioned earlier, tolerogenicity can be quite dose dependent, and therapeutic doses of antibodies may not always achieve the level required to tolerize both T- and B-cells.

As humans are largely tolerant of the constant regions of their own antibodies (self-tolerance), it was assumed that human antibodies, or engineering of antibodies to a human form, would bypass the immunogenicity problem. The concept was supported by evidence that the closer a monoclonal immunoglobulin was engineered toward host-type, then the less immunogenic it proved [3]. In a study comparing a humanized anti-CD52 antibody with a previous administration of the rodent form, the humanized version appeared far less immunogenic after a single course [25].

However, the humanization approach depended on retention of the original murine CDRs within the new human framework, and so eventual immunogenicity was still a potential issue. The notion of fully human antibodies implied that humans would be tolerant to the CDRs and framework-overlapping regions of antibodies derived from a human repertoire. This cannot be the case [9]. We know from past work that anti-idiotype responses can be generated to one's own antibodies [26]; and we also know that in the evolution of an antibody response, VJ and VDJ recombinations as well as somatic hypermutation can change the CDRs away from their germ line configuration. Consequently, there is still no evidence-based argument that would make the general case for fully human antibodies being less immunogenic than humanized

antibodies. In a published study of the humanized CD52 antibody (CAMPATH-1H or alemtuzumab) the majority of patients treated with a second course of antibody made strong anti-idiotypic responses to the humanized therapeutic [27]. This teaches us that the CDRs can remain a focus of the host immune response to humanized (and probably also human) monoclonal antibodies.

4 Overcoming the Immunogenicity Problem

The current portfolio of antibody therapeutics comprises members for whom immunogenicity has yet to be identified as a problem, and others where immunogenicity is well documented. In some scenarios the use of a synergistic immunosuppressive drug may not only benefit the target disease, but also mask the extent of antibody immunogenicity [28]. Where immunogenicity has arisen, options may be available to switch to a different agent serving the same purpose, or even to a different antibody target, as in anti-TNF therapy. Where immunogenicity has not occurred, we may not always be able to establish why. In other words, is lack of immunogenicity a feature of the target antigen, the dose, or some unique feature of the therapeutic agent?

Nevertheless, when all the information from clinical studies is made available, there will surely be examples of human antibodies where immunogenicity will have been shown to limit clinical utility. What can be done to more effectively control immunogenicity? There are a number of directions that might be considered.

First, and not insignificant, is the issue of natural aggregates resulting from the biopharmaceutical processing. Somehow these can create immunogenicity in their own right, irrespective of the therapeutic antibody binding to its target. A discussion of such natural aggregates is beyond the scope of this article, but the reader is directed to a few recent reviews dealing with this complex problem. Some of the solutions may involve approaches discussed below, but others may require attention to the bioprocessing and formulation of given products [29–33].

When it comes to immunogenicity of the desired drug product, then one needs to recognize that in order for T-cells to recognize the "foreign" determinants it is essential that the antibody is processed into peptides that can bind to MHC Class II [34–37] while B-cells may have special requirements for recognition of conformational epitopes [36, 37]. By scanning the primary sequence of antibody heavy and light chains for potential antigenic epitopes, it has been claimed that one can purge the therapeutic of T-cell epitopes, and reduce the number of B-cell epitopes [36, 37]. The success of this depends upon such drugs being manufactured and assessed in clinical trials, as there really is no in-vitro system that can replace the in-vivo assessment. Until that is achieved in a head to

head comparison with a conventional antibody, we cannot be certain that this will eliminate the problem.

Another route to eliminate immunogenicity is to find a route to tolerize the patient to the therapeutic antibody, so that any immune response to T-cell or B-cell would be rendered impossible [38]. This may sound counterintuitive, but we know from Chiller and Weigle that this ought to be possible. In principle a tolerogenic form of the therapeutic antibody might be generated if one could produce a limited number of mutations in the key CDRs concerned with antigen binding. A few mutations that could drastically reduce binding might provide a tolerogenic version which would be given ahead of the non-mutated therapeutic form of the antibody. The feasibility of this approach has been demonstrated in mice transgenic for the human CD52 antigen [39]. A human IgG1 antibody to CD52 was used to ablate mouse T-lymphocytes. This ablation was associated with immunogenicity of the foreign antibody. In contrast, mice that had previously received single or double mutant forms of the antibody which were markedly reduced in their binding (Fig. 2), could not be immunized to either the tolerogen nor to

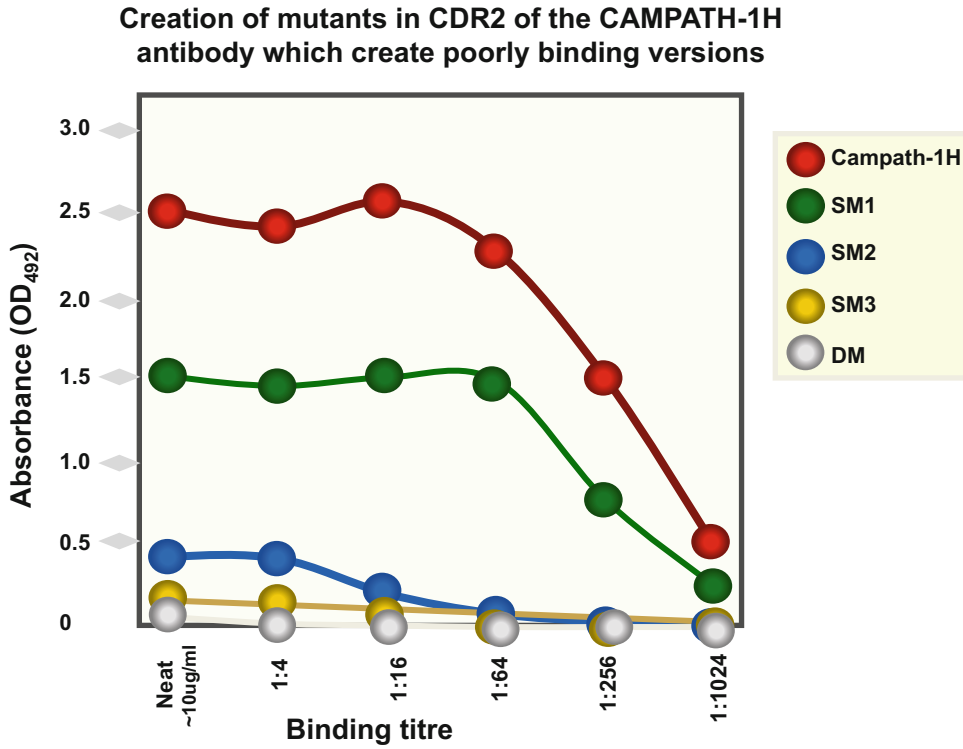

Fig. 2 Mutants can be created in the CDR regions which render the antibody far less able to bind to cells. In this case mutants were created in CDR2 of the heavy chain of the CAMPATH-1H anti-CD52 antibody. *SM* single mutations, *DM* double mutants. Binding to antigen is substantially reduced by three (blue, yellow, and gray symbols) of the four mutant antibodies compared to the original therapeutic (red) (Adapted from Gilliland et al. [39])

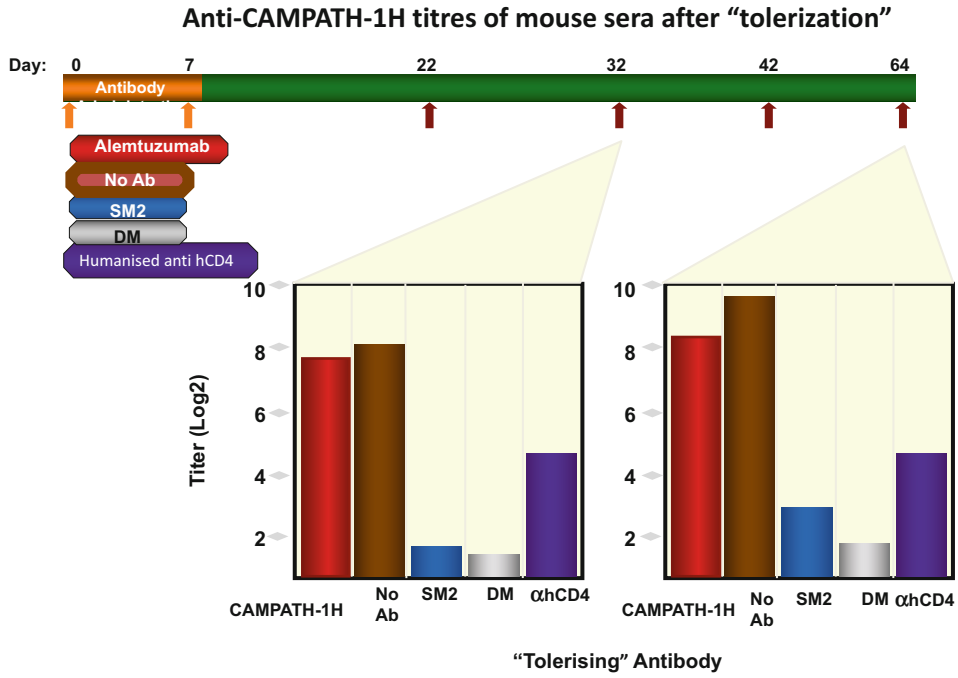

Fig. 3 Poorly-binding mutants tolerize CD52-transgenic mice to subsequent CAMPATH-1H treatment. CD52 transgenic mice were pretreated with two injections of 1 mg of a poorly binding mutant in CDR2 of the heavy chain of CAMPATH-1H, or a control anti-human CD4 antibody from 22 days onwards mice were given multiple challenges with the wild-type therapeutic antibody. "Tolerogen" pretreated mice made negligible antibody responses to the therapeutic (Adapted from Gilliland et al. [39])

challenge with the therapeutic form (Fig. 3). This provides a clear demonstration that high dose tolerance to the mutant prevented a response to the therapeutic version.

This two stage tolerizing protocol was applied in a small scale clinical study in patients given the IgG1 CD52 antibody, alemtuzumab, as a treatment for multiple sclerosis. A mutant "tolerogen" given before treatment substantially diminished the antibody response to a primary course of the therapeutic, as well as a second course given one year later [27].

Although impressive the disadvantage of this tolerizing approach is the need to manufacture and utilize two antibody forms. Thus far, no pharmaceutical company has made use of this strategy.

Is it possible that one could produce a version of the therapeutic antibody which can serve both as a tolerogen, yet still be able to exert its functional effect on cells? Such a one-step strategy has been achieved by engineering a covalently attached antigen mimotope into the antibody-binding site [40]. As the blocker mimotope renders the major proportion of antibody molecules "non-binding" at the time of infusion, it allows tolerogenesis before the bulk

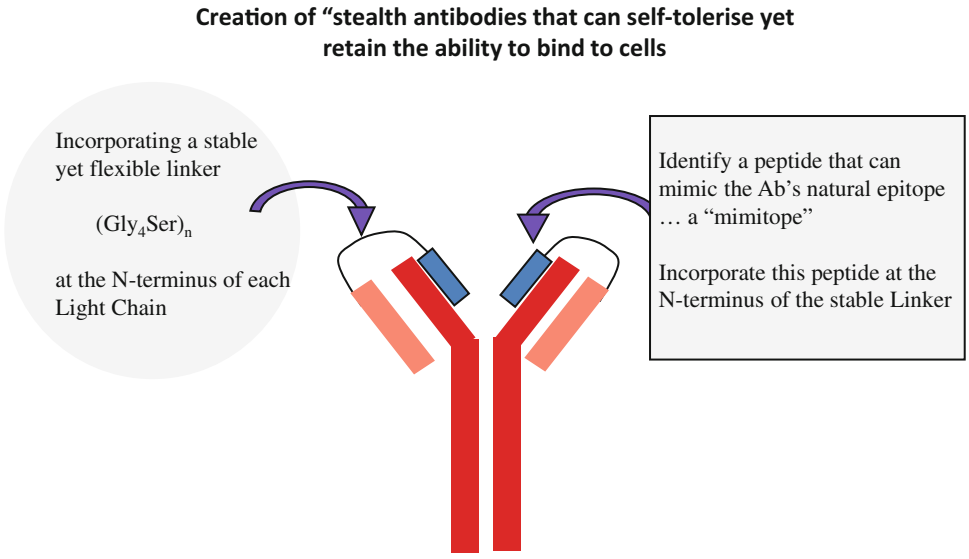

Fig. 4 Creation of "stealth antibodies that can self-tolerize yet retain the ability to bind to cells. (From issued patent US 7465,790B2-Therapeutic Antibodies). A peptide mimotope of the CD52 epitope is covalently bound into the CAMPATH-1H-binding site. This severely impairs binding, allows tolerogenesis but still retains, in the antibody, a capacity for cell-lysis

cell-binding consequences become effective. This sort of "stealth" antibody (Fig. 4), although tolerogenic in the mouse model, has not yet been subject to a clinical test. By reducing the pace of the lytic effect of the drug, it has also been possible to diminish some of the "cytokine" release-dependent side-effects of CD52 antibody therapy. There are obvious variations of this approach that could include concomitant administration of reversible "chemical" blockers of the antigen-binding site given together with the therapeutic, creating an initial "blocked" tolerogen whose cell binding eventually returns once the blocker is cleared.

It should be noted that the experimental models shown above both used human antibodies given to mice. Tolerization was achieved despite the extensive degree of "foreigness." However, even if humans prove tolerizable to rodent antibodies, it is obvious that one should apply "tolerization" approaches using antibodies whose constant regions are human, so making the task of tolerization easier. Moreover, as human constant regions are likely to be subject to various engineering strategies to optimize function, then one should regard the human rather than rodent frameworks as the template for such improvements.

5 Prospects and Conclusions

Thus far human antibodies seem to have satisfied the requirements of the biopharmaceutical industry even with antibodies where immunogenicity has been established. The need to do more to prevent this has become an issue of investment against likely demand, and at this stage of the therapeutic antibody experience, the need for active tolerization to the therapeutic has, sadly, not become a priority. I would venture that for some antibodies immunogenicity will never be a problem, but for others it may substantially enhance the longevity of the antibody as a drug. Given this, we should continue to evolve methodologies that can guarantee elimination of immunogenicity.

References

1. Kohler G, Milstein C (1975) Continuous cultures of fused cells secreting antibody of predefined specificity. Nature 256 (5517):495–497
2. Steinitz M et al (1977) EB virus-induced B lymphocyte cell lines producing specific antibody. Nature 269(5627):420–422
3. Bruggemann M et al (1989) The immunogenicity of chimeric antibodies. J Exp Med 170 (6):2153–2157
4. Jones PT et al (1986) Replacing the complementarity-determining regions in a human antibody with those from a mouse. Nature 321(6069):522–525
5. Riechmann L et al (1988) Reshaping human antibodies for therapy. Nature 332 (6162):323–327
6. Lonberg N (2005) Human antibodies from transgenic animals. Nat Biotechnol 23 (9):1117–1125
7. Winter G et al (1994) Making antibodies by phage display technology. Annu Rev Immunol 12:433–455
8. Bruggemann M et al (1989) A repertoire of monoclonal antibodies with human heavy chains from transgenic mice. Proc Natl Acad Sci U S A 86(17):6709–6713
9. Clark M (2000) Antibody humanization: a case of the 'Emperor's new clothes'? Immunol Today 21(8):397–402
10. Chiller JM, Habicht GS, Weigle WO (1970) Cellular sites of immunologic unresponsiveness. Proc Natl Acad Sci U S A 65(3):551–556
11. Cobbold SP et al (1984) Therapy with monoclonal antibodies by elimination of T-cell subsets in vivo. Nature 312(5994):548–551
12. Neuberger MS, Williams GT, Fox RO (1984) Recombinant antibodies possessing novel effector functions. Nature 312 (5995):604–608
13. Bruggemann M et al (1989) A matched set of rat/mouse chimeric antibodies. Identification and biological properties of rat H chain constant regions mu, gamma 1, gamma 2a, gamma 2b, gamma 2c, epsilon, and alpha. J Immunol 142(9):3145–3150
14. Morrison SL et al (1984) Chimeric human antibody molecules: mouse antigen-binding domains with human constant region domains. Proc Natl Acad Sci U S A 81(21):6851–6855
15. Bruggemann M et al (1987) Comparison of the effector functions of human immunoglobulins using a matched set of chimeric antibodies. J Exp Med 166(5):1351–1361
16. Bindon CI et al (1988) Human monoclonal IgG isotypes differ in complement activating function at the level of C4 as well as C1q. J Exp Med 168(1):127–142
17. Bolt S et al (1993) The generation of a humanized, non-mitogenic CD3 monoclonal antibody which retains in vitro immunosuppressive properties. Eur J Immunol 23(2):403–411
18. Kuhn C et al (2011) Human CD3 transgenic mice: preclinical testing of antibodies promoting immune tolerance. Sci Transl Med 3 (68):68ra10
19. Friend PJ et al (1999) Phase I study of an engineered aglycosylated humanized CD3 antibody in renal transplant rejection. Transplantation 68(11):1632–1637

20. Keymeulen B et al (2005) Insulin needs after CD3-antibody therapy in new-onset type 1 diabetes. N Engl J Med 352(25):2598–2608
21. Routledge EG et al (1991) A humanized monovalent CD3 antibody which can activate homologous complement. Eur J Immunol 21 (11):2717–2725
22. Beers SA, Glennie MJ, White AL (2016) Influence of immunoglobulin isotype on therapeutic antibody function. Blood 127 (9):1097–1101
23. Benjamin RJ et al (1986) Tolerance to rat monoclonal antibodies. Implications for serotherapy. J Exp Med 163(6):1539–1552
24. Waldmann H, Adams E, Cobbold S (2008) Reprogramming the immune system: co-receptor blockade as a paradigm for harnessing tolerance mechanisms. Immunol Rev 223:361–370
25. Rebello PR et al (1999) Anti-globulin responses to rat and humanized CAMPATH-1 monoclonal antibody used to treat transplant rejection. Transplantation 68(9):1417–1420
26. Eichmann K (1973) Idiotype expression and the inheritance of mouse antibody clones. J Exp Med 137(3):603–621
27. Somerfield J et al (2010) A novel strategy to reduce the immunogenicity of biological therapies. J Immunol 185(1):763–768
28. Feldmann M, Maini RN (2001) Anti-TNF alpha therapy of rheumatoid arthritis: what have we learned? Annu Rev Immunol 19:163–196
29. Jefferis R (2011) Aggregation, immune complexes and immunogenicity. MAbs 3 (6):503–504
30. Joubert MK et al (2012) Highly aggregated antibody therapeutics can enhance the in vitro innate and late-stage T-cell immune responses. J Biol Chem 287(30):25266–25279
31. Moussa EM et al (2016) Immunogenicity of therapeutic protein aggregates. J Pharm Sci 105(2):417–430
32. Sauerborn M et al (2010) Immunological mechanism underlying the immune response to recombinant human protein therapeutics. Trends Pharmacol Sci 31(2):53–59
33. St Clair JB et al (2017) Immunogenicity of Isogenic IgG in Aggregates and Immune Complexes. PLoS One 12(1):e0170556
34. De Groot AS, Scott DW (2007) Immunogenicity of protein therapeutics. Trends Immunol 28(11):482–490
35. Harding FA et al (2010) The immunogenicity of humanized and fully human antibodies: residual immunogenicity resides in the CDR regions. MAbs 2(3):256–265
36. Griswold KE, Bailey-Kellogg C (2016) Design and engineering of deimmunized biotherapeutics. Curr Opin Struct Biol 39:79–88
37. Nagata S, Pastan I (2009) Removal of B cell epitopes as a practical approach for reducing the immunogenicity of foreign protein-based therapeutics. Adv Drug Deliv Rev 61 (11):977–985
38. Isaacs JD, Waldmann H (1994) Helplessness as a strategy for avoiding antiglobulin responses to therapeutic monoclonal antibodies. Ther Immunol 1(6):303–312
39. Gilliland LK et al (1999) Elimination of the immunogenicity of therapeutic antibodies. J Immunol 162(6):3663–3671
40. Waldmann HF, Gillilkand MK, Graca L (2008) Therapeutic antibodies. Patent US 7,465,790 B2

Chapter 2

Cancer Immunotherapy: The Dawn of Antibody Cocktails

Ilaria Marrocco, Donatella Romaniello, and Yosef Yarden

Abstract

Since the approval of the first monoclonal antibody (mAb), rituximab, for hematological malignancies, almost 30 additional mAbs have been approved in oncology. Despite remarkable advances, relatively weak responses and resistance to antibody monotherapy remain major open issue. Overcoming resistance might require combinations of drugs blocking both the major target and the emerging secondary target. We review clinically approved combinations of antibodies and either cytotoxic regimens (chemotherapy and irradiation) or kinase inhibitors. Thereafter, we focus on the most promising and currently very active arena that combines mAbs inhibiting immune checkpoints or growth factor receptors. Clinically approved and experimental oligoclonal mixtures of mAbs targeting different antigens (hetero-combinations) or different epitopes of the same antigen (homo-combinations) are described. Effective oligoclonal mixtures of antibodies that mimic the polyclonal immune response will likely become a mainstay of cancer therapy.

Key words Antibody mixtures, Cancer, Chemotherapy, Immune checkpoints, Immunotherapy

1 The Power of Drug Combinations: A Systems Biology Perspective

It is worthwhile considering the evolution of biological systems and networks as a prelude for discussing pharmacological attempts to block pathological versions of biological networks. Viewed from an evolutionary perspective, the two genome duplications that created all metazoans generated families of four genes and laid the cornerstone for the modular structure of biological networks, a key feature of robustness [1]. Robustness was further boosted by means of training to overcome internal (mutational) and external (environmental) perturbations. However, due to low frequency, perturbations were introduced one at a time [2]. Hence, when challenged by two or more simultaneous perturbations, networks often expose remarkable fragilities [3]. This fundamental attribute of network training translates to high efficacy of pharmacological strategies utilizing drug combinations (poly-pharmacology). For example, kinome-wide profiling and *Drosophila* genetics showed that concurrent inhibition of three pathways, Ret and Raf, Src and ribosomal S6-kinase, was required for optimal survival of a Ret-driven

Michael Steinitz (ed.), *Human Monoclonal Antibodies: Methods and Protocols*, Methods in Molecular Biology, vol. 1904,
https://doi.org/10.1007/978-1-4939-8958-4_2,

fly model of multiple endocrine neoplasia [4]. Accordingly, combining targeted therapies (TTs), such as protein kinase inhibitors (PKIs) and monoclonal antibodies (mAbs), is considered a major future arena of medical oncology [5, 6]. It is notable that the ability of biological networks to resist common perturbations is greatly enhanced by their capacity to rewire information and metabolic circuitries [7]. This non-mutational mechanism of adaptation to a changing environment underlays many mechanisms that confer resistance to TTs [8, 9]. A similarly important mode of resistance entails genetic aberrations: either emergence of pre-existing mutant-expressing clones (tumor heterogeneity) [10] or de novo amplification/mutagenesis of drug targets [11]. Herein we review the short history of TT, with a focus on mAbs, their various modes of action and mechanisms underlying emergence of resistance to antibodies. Following brief descriptions of the main therapeutic antibodies, we review several efficacious combinations of antibodies with chemotherapy (CT), radiotherapy (RT), and PKIs. Lastly, we focus on the emerging, highly successful trend of combining several different antibodies to the same antigen (homo-combinations) and other mixtures of antibodies, including immune checkpoint inhibitors, recognizing distinct protein targets (hetero-combinations).

2 An Introduction to Cancer Therapy, Including Molecular Targeted Therapy

Cancer treatment depends on several factors: type of tumor, stage of the disease (local or metastatic), patient's age, and health status. Surgery, radiation therapy, and chemotherapy represent the primary modalities of cancer treatment [12]. The dawn of the third millennium witnessed the birth of molecular targeted therapy, which includes the use of antibodies specific to either cell surface molecules or soluble antigens. Surgery is the oldest treatment and, if cancer has not spread, this approach can completely cure a patient. For example, the excision of primary melanomas is sufficient to cure this type of cancer in 90% of cases. In some other cases, surgery can be employed to reduce the bulk of tumor prior to treatment of the residual cancer. Surgery is not only an important treatment modality but it can also be used for prevention, such as prophylactic mastectomy in women with BRCA mutations. Resection of primary solid tumors, when these are confined to the anatomic side of origin, is the first application of surgery in cancer.

Radiation therapy (RT) is used as an initial treatment, alone or in combination with other treatments, in 30–50% of all cancer patients [13]. In many patients this translates to high-energy external-beam photon therapy. Ionizing radiation affects normal cell division, causes DNA damage, and finally induces cell death. Electrons can be used to treat superficial tumors (for instance, skin and breast cancer) since they can penetrate up to 6-cm of tissue. In the

case of deeper tumors photons are used because they spare the skin and deposit dose along the path until the beam leaves the body. Radiation can be used alone, when the tumor is localized and surgery is not an option, or it can be associated with either chemotherapy or TT in case of locally advanced or aggressive cancers. RT causes side effects in normal tissues because ionizing radiation is unable to discriminate between cancer and healthy tissues. The tissues most affected by RT are those that depend on rapid self-renewal, such as skin and mucosal surfaces (e.g., organs of the gastrointestinal tract). In addition, a decrease in lymphocyte count is observed following irradiation [13].

Chemotherapy (CT) is the most widely used approach in cancer treatment. In principle, CT may cure even advanced cancers. However, the major issues are raised by drug toxicity toward normal tissues and emergence of resistance. CT is used as a primary treatment in patients with advanced cancers that cannot receive other types of treatment, or it is used as neoadjuvant treatment aimed at reducing tumor mass before proceeding with local therapy (i.e., surgery or RT). Chemotherapy can also be combined with RT or with TT. The main classes of chemotherapeutic drugs include alkylating agents, platinum compounds, antimetabolites like 5-fluorouracil, topoisomerase inhibitors, such as irinotecan, and anti-microtubule agents, like paclitaxel. Similar to RT, organs with rapid self-renewal are damaged by CT. Toxicity to the bone marrow with consequent leukopenia and increased risk of infections is a common side effect of most of the chemotherapeutic drugs.

Treatment of cancer has profoundly changed since the introduction of TT and the birth of precision medicine, namely pharmacological interventions able to specifically block mutation-bearing drivers of cancer or signaling pathways essential for survival of tumor cells [14]. Targeted therapies include small-molecule drugs and mAbs, which will be the focus of this review. The first small molecule to be approved for cancer treatment was the BCR-ABL protein kinase inhibitor (PKI) called imatinib, which was approved in 2001 for the treatment of chronic myeloid leukemia (CML) [15]. Since then many other small molecules have been approved. For example, PKIs specific to the epidermal growth factor receptor (EGFR), such as erlotinib, afatinib, and osimertinib, are commonly used to treat lung cancer tumors harboring mutant forms of EGFR [16]. Similarly, mAbs to the vascular endothelial growth factor (VEGF), EGFR, and its closely related protein, called HER2 or ERBB2, entered clinical applications around the turn of the millennium [17]. Accordingly, their first biosimilars are becoming available worldwide. Notably, these and additional antibodies are often combined with CT or RT. In this review we argue that mixtures of mAbs (oligoclonal antibodies) might be the welcome swallows of a spring of synergistic anti-cancer antibodies.

3 A Primer to Therapeutic Antibodies

The immune system plays a general defensive role against infectious agents, such as bacteria and viruses, which present a threat to human health. This system consists of two arms: the innate immune response, which engages soluble proteins, cytokines and physical barriers, recognizes many invaders without any specificity, whereas the adaptive immune response shows high target specificity and can be divided into humoral (antibody-mediated) and cellular (cell-mediated) responses [18]. The first use of antibodies as therapeutic tools dates back to the late nineteenth and the early twentieth centuries when infectious diseases were treated with serum from patients who had recovered from that specific disease.

Antibodies, also called immunoglobulins (Ig), are proteins consisting of four polypeptide chains, two heavy chains, and two light chains, which interact with each other through disulphide bonds and globally form a typical "Y" shape [19]. The light and heavy chains of a mAb contain variable (V_H and V_L) and constant (C_H and C_L) regions. The constant region determines the mechanism responsible for the destruction of the antigen (e.g., recruitment of macrophages, natural killer cells, or neutrophils). Based on the structure of the constant regions and thus on the immune function, immunoglobulins are divided into five classes: IgM, IgG, IgA, IgD, and IgE. The most common isotype of immunoglobulins used as therapeutic antibodies is IgG. The variable regions of both heavy and light chains present hypervariable amino acid sequences, called CDRs (complementarity determining regions), which are responsible for the interaction and specificity toward different antigens. One IgG molecule contains three pairs of different CDRs: CDR1, CDR2, and CDR3, with CDR3 showing the highest variability. The first mAbs were isolated from hybridoma cells by Cesar Milstein and Georges Kohler in 1975 [20]. The first therapeutic antibody, muromonab (OKT-3), was a murine antibody directed against the CD3 receptor expressed on the surface of T cells. Muromonab was approved in 1986 for organ acute rejection [21]. Notably, this antibody was not very effective in preventing organ rejection, mainly because it induced a strong human anti-mouse antibody (HAMA) response in treated patients [22]. For this reason and due to the introduction of alternative treatments, OKT-3 was discontinued in 2010. In general, the use of murine antibodies in the clinic is limited because of the differences between the rodent and human immune system and the HAMA-mediated allergic response [23].

Even though the hybridoma technology instigated an enormous step forward, similar to muromonab, the initial mAbs were murine and immunogenic when injected into humans, which limited their clinical use. This problem was initially overcome by the

replacement of the murine *C* (constant) chains with the human constant sequences (i.e., chimerization) [24]. Notably, the first murine/human chimeric mAb, abciximab [25], was approved in 1994 for hemostasis. Typically, 65% of the sequence of chimeric antibodies is derived from human sequences, which reduces HAMA responses. Rituximab and cetuximab are examples of chimeric antibodies approved in 1997 and in 2004, respectively, for the treatment of non-Hodgkin lymphoma (rituximab) and colorectal cancer (cetuximab; see below). Another attempt to overcome the rodent origin of murine antibodies has been the introduction of humanized antibodies, in which the mouse hypervariable regions are grafted onto the human IgG backbone (humanization). In this case the human sequence represents about 95% of the entire molecule. Daclizumab (Zenapax), the first humanized mAb, was approved in 1997 for kidney transplant rejection [26]. Later, the introduction of transgenic mice and phage display platforms allowed the production of fully human antibodies [27]. Adalimumab was the first fully human mAb to be approved, for the treatment of rheumatoid arthritis. Similarly, the fully human anti-EGFR antibody panitumumab was first approved in 2006 for the treatment of metastatic colorectal cancer [28]. The use of mAbs in cancer therapy has been particularly productive [29]. These molecules display high specificity and thus can be used to target with high selectivity specific antigens, which are mainly expressed by tumors (targeted therapy). As a result, the number of clinically approved therapeutic antibodies has steadily increased in the last decade (*see* Table 1), and many more are in clinical trials for cancer and other diseases. The targeted antigens of cancer-specific mAbs include surface glycoproteins playing roles in growth or differentiation, such as CD20, which has been successfully targeted by rituximab [30]. Other antigens that can be targeted in cancer are growth factor receptors. The humanized anti-HER2 antibody, trastuzumab, was the first antibody to be successfully used in the treatment of solid tumors [31]. In addition, antibodies can bind and neutralize soluble antigens. Bevacizumab, a humanized antibody that effectively binds with the vascular endothelial growth factor (VEGF), has been approved for several types of cancer.

4 Mechanisms of Action of Therapeutic Antibodies

In general, the mechanisms enabling therapeutic antibodies to inhibit growth of, or kill, cancer cells can be divided into two categories: immune-mediated mechanisms (e.g., ADCC, antibody-dependent cellular cytotoxicity and CDC, complement-dependent cytotoxicity) and mechanisms that interfere with pathways of tumorigenesis (e.g., triggering apoptosis, inhibiting cell proliferation or blocking angiogenesis). In order to trigger

Table 1
Monoclonal antibodies currently approved for use in oncology

Antibody	Brand name (company)	Target	Type	Year of first FDA/EMA approval	Therapeutic indication
Rituximab	Rituxan/MabThera (Genentech)	CD20	Chimeric IgG1k	1997/1998	NHL, CLL
Trastuzumab	Herceptin (Genentech)	HER2	Humanized IgG1k	1998/2000	HER2-overexpressing breast cancer, HER2-overexpressing metastatic gastric or GEJ adenocarcinoma
Ibritumomab tiuxetan	Zevalin (Spectrum Pharms)	CD20	Murine IgG1k (ARC)	2002/2004	NHL
Cetuximab	Erbitux (ImClone)	EGFR	Chimeric IgG1	2004/2004	HNSCC, CRC
Bevacizumab	Avastin (Genentech)	VEGF-A	Humanized IgG1	2004/2005	Metastatic CRC, NSCLC, metastatic breast cancer, glioblastoma multiforme; metastatic RCC
Panitumumab	Vectibix (Amgen)	EGFR	Human IgG2	2006/2007	Metastatic CRC
Ofatumumab	Arzerra (Glaxo Grp Ltd)	CD20	Human IgG1	2009/2010	CLL
Denosumab	Xgeva (Amgen)	RANK Ligand	Human IgG2	2010/2011	Giant cell tumors of the bone, prevention of SREs in patients with MM and bone metastases from solid tumors
Ipilimumab	Yervoy (Bristol Myers Squibb)	CTLA-4	Human IgG1	2011/2011	Melanoma, RCC
Brentuximab vedotin	Adcetris (Seattle Genetics)	CD30	Chimeric IgG1 (ADC)	2011/2012	HL, systemic ALCL

Pertuzumab	Perjeta (Genentech)	HER2	Humanized IgG1	2012/2013	HER2+ metastatic breast cancer
Ado-Trastuzumab emtansine	Kadcyla (Genentech)	HER2	Humanized IgG1 (ADC)	2013/2013	HER2+ metastatic breast cancer
Obinutuzumab	Gazyva/Gazyvaro (Genentech)	CD20	Humanized IgG1	2013/2014	CLL
Ramucirumab	Cyramza (Eli Lilly)	VEGFR2	Human IgG1	2014/2014	Gastric cancer, NSCLC, CRC
Pembrolizumab	Keytruda (Merck Sharp Dohme)	PD-1	Humanized IgG4	2014/2015	Melanoma, NSCLC, HNSCC, HL, large B-cell lymphoma, urothelial carcinoma, gastric cancer, cervical cancer
Blinatumomab	Blincyto (Amgen)	CD19/CD3	BiTE	2014/2015	Precursor cell lymphoblastic leukemia-lymphoma
Nivolumab	Opdivo (Bristol Myers Squibb)	PD-1	Human IgG4	2014/2015	Urothelial carcinoma, NSCLC, RCC, HL, melanoma, CRC, HNSCC, hepatocellular carcinoma
Dinutuximab	Unituxin (United Therapeutics)	GD2	Human IgG1/κ	2015/W	Neuroblastoma
Necitumumab	Portrazza (Eli Lilly)	EGFR	Human IgG1	2015/2016	NSCLC
Elotuzumab	Empliciti (Bristol Myers Squibb)	SLAMF7	Humanized IgG1	2015/2016	MM
Daratumumab	Darzalex (Janssen Biotech)	CD38	Human IgG1/κ	2015/2016	MM
Olaratumab	Lartruvo (Eli Lilly)	PDGFR-α	Human IgG1	2016/2016	Soft tissue sarcoma
Atezolizumab	Tecentriq (Genentech-Roche)	PD-L1	Humanized IgG1	2016/2017	

(continued)

Table 1
(continued)

Antibody	Brand name (company)	Target	Type	Year of first FDA/EMA approval	Therapeutic indication
					Metastatic NSCLC, urothelial carcinoma
Durvalumab	Imfinzi (Astrazeneca UK)	PD-L1	Human IgG1/κ	2017/NA	Metastatic urothelial carcinoma, NSCLC
Avelumab	Bavencio (EMD Serono INC.)	PD-L1	Human IgG1/κ	2017/2017	Metastatic Merkel cell carcinoma, urothelial carcinoma
Inotuzumab ozogamicin	Besponsa (Wyeth Pharmaceuticals Inc.)	CD22	Humanized IgG4/k (ADC)	2017/2017	B-cell precursor ALL
Gemtuzumab ozogamicin	Mylotarg (Wyeth Pharmaceuticals Inc.)	CD33	Humanized IgG4 (ADC)	2017/2018	CD33-positive AML
Bevacizumab-awwb	Mvasi (Amgen/Allergen)	VEGF-A	Biosimilar to Bevacizumab	2017/2018	CRC, NSCLC, glioblastoma,RCC, cervical cancer
Trastuzumab-dkst	Ogivri (Mylan GMBH)	HER2	Biosimilar to Trastuzumab	2017/NA	HER2-overexpressing breast or metastatic gastric or GEJ adenocarcinoma

Listed are all clinically used mAbs, their immunoglobulin types, year of first approval by the Food and Drug Administration (FDA; United States) or by the European Medicines Agency (EMA), as well as the respective major therapeutic indications. Note that gemtuzumab ozogamicin was first approved in 2000, but in 2010 it was withdrawn. ADC, antibody-drug conjugate; ALCL, anaplastic large cell lymphoma; ALL, acute lymphoblastic leukemia; AML, acute myeloid leukemia; ARC, antibody-radionuclide conjugate; BiTE, bispecific T-cell engager; CLL, chronic lymphocytic leukemia; CRC, colorectal cancer; GEJ, gastroesophageal junction; HL, Hodgkin lymphoma; HNSCC, head and neck squamous cell cancer; MM, multiple myeloma; NA, not approved; NHL, non-Hodgkin lymphoma; NSCLC, non-small cell lung cancer; RCC, renal cell carcinoma; SREs, skeletal-related events; W, withdrawn

ADCC, the antibody has to bind a specific antigen expressed on the surface of a cancer cell. This event leads to the recruitment of immune effector cells, such as natural killer (NK) cells, macrophages, or neutrophils. Subsequently, the F_C region of the antibody interacts with an F_C receptor on an effector cell, which enables lysis of the target tumor cells [32]. For example, one mechanism of action of the anti-CD20 antibody, rituximab, harnesses ADCC. Two lines of evidence exemplify ADCC involvement: Firstly, rituximab was not effective when tested in $F_{C\gamma}R^{-/-}$ mice, which do not express the stimulatory Fc-gamma receptor type III, and conversely, it exhibited enhanced activity when tested in mice lacking the inhibitory $F_{C\gamma}R$ type IIb [33]. Secondly, polymorphisms in the FcRIIIa gene affect the response rates of NHL patients to rituximab: in humans, a polymorphism in FcRIIIa places either a valine (V) or a phenylalanine (F) at position 158. Several studies have shown that patients with receptor homozygous for V in position 158 (158V/V) respond better to rituximab as compared with patients displaying the 158V/F or the 158F/F receptor [34]. This has been attributed to higher in vitro affinity of 158V/V FcRIIIa toward IgG1 compared to the other isoforms, 158V/F or 148F/F [35]. Similarly, polymorphisms in Fc receptors have been associated with the efficacy of cetuximab in colorectal cancer [36]. Interestingly, cetuximab is an IgG1 antibody, which induces ADCC, while another anti-EGFR antibody, panitumumab, which is an IgG2 molecule, is unable to trigger immune responses because IgG2 molecules do not recognize $F_{C\gamma}$ receptors on immune effector cells [37]. CDC starts when the antibody-antigen complex interacts with C1q, thereby forms the membrane attack complex (MAC). This results in the activation of the complement cascade, which is regulated by several zymogens (C1–C9) and inhibitory proteins, such as CD35, CD46, CD55, and CD59 [38]. As a final result, the target cell undergoes lysis. Several studies in mice suggest that CDC is one of the mechanisms of action of rituximab: mice lacking C1q display reduced sensitivity to rituximab and complement inhibitory proteins are able to inhibit cell death induced by rituximab [39, 40]. In addition, whereas blocking the inhibitory proteins enhances rituximab-induced CDC.

The non-immune modes of actions of anti-cancer mAbs may be exemplified by bevacizumab, an anti-VEGF antibody, which binds and inactivates the soluble growth factor with no known involvement of immune mechanisms [41]. Other antibodies may bind a receptor on the target cell surface, and this often leads to blocking ligand binding or receptor dimerization. Alternatively, by virtue of their bivalence, mAbs may induce internalization and degradation of oncogenic/survival receptors. As a result, mAbs may modulate signaling pathways controlling important cellular processes such as apoptosis, proliferation, and angiogenesis. Apoptosis is a programmed cell death process involving activation of several

proteases, known as caspases, and occurring via two pathways: the intrinsic pathway, activated by intracellular signals, such as stress, which leads to release of cytochrome C from the mitochondria, and the extrinsic pathway, activated by the binding of extracellular cytokines to death receptors localized at the cell surface, and formation of a complex that activates the caspase cascade. Binding of rituximab to CD20, a modulator of calcium channels [42], may induce apoptosis via accelerating calcium fluxes. Similarly, the anti-HER2 antibody trastuzumab may induce apoptosis by inhibiting the AKT and the mitogen-activated protein kinase (MAPK) pathways, as well as by enhancing the TRAIL- (tumor necrosis factor-related apoptosis-inducing ligand) mediated apoptosis pathway [43]. Alternatively, the anti-EGFR antibody, cetuximab, induces an increase in the expression levels of the apoptotic protein BAX and a decrease in the levels of the anti-apoptosis protein BCL-2 [44]. Another common mechanism used by antibodies to inhibit cell proliferation is the modulation of key proteins of the cell cycle [45]. Trastuzumab induces upregulation of the cyclin-dependent kinase inhibitor (CDKI) p27kip1, which arrests cancer cells in the G1 phase of the cell cycle [45]. Another important mechanism of action of therapeutic antibodies is the inhibition of angiogenesis. It has been reported that trastuzumab inhibits angiogenesis in different cancer models [46]. Antibodies targeting growth factor receptors, such as cetuximab or trastuzumab, may also exert their antitumor activity by blocking the mitogenic signaling pathways downstream of the respective receptors. Cetuximab prevents binding of ligands to EGFR and inhibits receptor dimerization [47, 48]. It has been shown that anti-HER2 mAbs induce internalization and degradation of HER2 through the activation of the Cbl ubiquitin ligase [49]. In addition, a specific subset of anti-HER2 mAbs inhibits formation of heterodimers containing HER2 [50]. It was later reported that certain anti-HER2 mAbs, such as pertuzumab, bind to subdomain II of HER2 and inhibit formation of heterodimers containing other EGFR family members, thereby inhibit the ability of HER2 to enhance downstream signaling [51].

5 Resistance to Therapeutic Antibodies

Since mAbs were introduced in oncology wards, they have significantly improved the treatment of cancer. For example, rituximab in combination with chemotherapy (CHOP; cyclophosphamide, doxorubicin, vincristine and prednisone) has significantly improved the overall survival of patients with non-Hodgkin lymphoma (NHL) within the first five years after approval of the mAb [52]. This anti-CD20 antibody has also modified the treatment of patients with follicular lymphoma (FL), even though it has not changed the final patient outcome. Every other patient with

relapsed/refractory FL shows no response to rituximab, and in about 60% of cases that show initial positive response, patients stop responding to a second treatment [53]. Similarly, the introduction of trastuzumab has clearly improved the outcome in breast cancer patients, but the median response to this treatment is still modest [54]. In general, the failure of mAb therapy might be due to several resistance mechanisms. The resistance can be intrinsic or acquired: in intrinsic mechanisms the antibody is not effective, even if the antigen is present on tumor cells. By contrast, in acquired resistance, tumor cells display initial sensitivity to the treatment, but after a variable period of time they stop responding. The underlying mechanisms of resistance include heterogeneity of HER2 downregulation in the tumor, signaling pathway promiscuity [55], as well as immune escape due to impairment of ADCC or CDC [6]. Loss or modifications of the antigens can be responsible for resistance to mAb treatment. Loss of CD20 expression on the cell surface is one of the mechanisms responsible for resistance to rituximab [56]. Likewise, expression of the truncated p95-HER2 isoform is related to diminished sensitivity to trastuzumab in breast cancer patients [57]. In addition to loss of the target antigen, or its masking by other molecules, such as MUC4 [58], one common resistance mechanism to mAbs is the presence of mutations in downstream signaling molecules or compensatory activation of other receptors. Patients with advanced colorectal cancer do not respond to anti-EGFR therapy (cetuximab or panitumumab) if KRAS mutations are present in the tumors [59]. Likewise, evidence from cellular and animal models indicate that treatment of EGFR-mutated lung cancer cells with an anti-EGFR antibody causes upregulation of other members of the EGFR family of receptors, primarily HER2 and HER3, with consequent hyper-activation of ERK-MAPK, but co-treatment with anti-EGFR, anti-HER2 and anti-HER3 antibodies completely abrogated activation of the compensatory pathway [60]. Similarly, upregulation of the receptors for the insulin-like growth factor 1 (IGF1R) and the hepatocyte growth factor (MET) has been related to resistance to trastuzumab in models of breast cancer [61, 62]. In a number of patients, mutations in PIK3CA or low expression of PTEN, which lead to activation of the PI3K-to-AKT pathway, are associated with poor prognosis after trastuzumab treatment [63].

6 Examples of mAbs Employed to Treat Cancer

Cancer treatment has dramatically changed since 2000, primarily due to the clinical approval of recombinant mAbs and kinase inhibitors. Remarkably, the new agents significantly enrich the armamentarium of clinical oncology rather than replace the relatively nonspecific cytotoxic treatments, such as radiotherapy and

chemotherapy. It is also notable that in comparison to small-molecule drugs, like PKIs, mAbs display very narrow target selectivity, hence toxicity due to off-target interactions is less common in immunotherapy.

6.1 mAbs for Hematological Tumors

Hematological malignancies comprise several different types of blood cancers, which are divided into four groups: leukemia, Hodgkin lymphoma, non-Hodgkin lymphoma (NHL), and myeloma. Rituximab, the first antibody to be approved for hematological tumors, is still the most widely used mAb for treatment of B cell-NHL and for chronic lymphocytic leukemia (CLL). Rituximab is a chimeric IgG1 antibody that binds to CD20, a B-lymphocyte transmembrane antigen, which is expressed on the surface of both non-neoplastic B cells (pre-, immature, mature, and activated) and malignant B cells [64]. Given that CD20 is not expressed on the surface of hematopoietic stem cells, normal B cells can regenerate after stopping treatment with rituximab. The mechanisms of action of rituximab include ADCC, CDC, and induction of apoptosis. The antibody was first approved 1997 for NHL and subsequently, in 2009, for the treatment of CLL patients. Later, rituximab became a standard component of the treatment of follicular lymphoma, diffuse large B-cell lymphoma, CLL, and mantle cell lymphoma. Importantly, several clinical trials have shown that rituximab is able to extend the time to disease progression and also the overall survival rates [65]. Following 20 years of post-marketing surveillance, the major side effects to rituximab in B-cell malignancies are quite well known, with the most common being infusion-related reactions (IRRs), the cytokine release syndrome, bronchospasm, and hypotension. In the majority of cases, IRRs occur after the first injection of rituximab, but later their incidence decreases. Other common adverse events to rituximab include cardiovascular events, infections, and hematological side effects, like neutropenia. Despite the clear efficacy of rituximab in patients with B-cell malignancies, some patients do not respond to the first-line therapy and some other patients become resistant following an initial response. Resistance to rituximab involves loss of CD20 expression [66] and impairment of either CDC (because of complement protein depletion), ADCC (polymorphism of the FcRIIIa on immune effector cells may alter the sensitivity of the tumor cells to ADCC), or apoptosis (upregulation of antiapoptotic proteins) [67]. The enormous success of anti-CD20 treatment in B-cell malignancies led to the development of additional antibodies against this antigen. Ofatumumab is a fully human anti-CD20 antibody, which was approved in 2009 for CLL. Similarly, obinutuzumab, a humanized glycoengineered anti-CD20 antibody, was approved in 2013 for the treatment of CLL and later also for FL. This antibody, as a result of posttranslational glycoengineering modification, lacks a fucose residue in the IgG oligosaccharides of the Fc region, resulting in

enhanced binding affinity to the FcRIII on the surface of immune effector cells [68]. Antibodies directed against other antigens (e.g., anti-CD19, inebilizumab, and anti-CD22, epratuzumab) have been investigated, but they did not show promising results in clinical trials. Furthermore, two mAbs were recently approved for clinical use, namely the humanized anti-SLAMF7 mAb called elotuzumab and daratumumab, an anti-CD38 mAb.

6.2 mAbs for Solid Tumors

The approval of trastuzumab, an anti-HER2 antibody, in 1998, for the treatment of patients with HER2-positive metastatic breast cancer instigated the era of solid tumor treatment. The receptor tyrosine kinase (RTK) called HER2 is overexpressed in 15–20% of invasive breast cancers, and high HER2 expression levels are correlated with poor prognosis [69]. While anti-HER2 mAbs were able to inhibit growth of HER2-overexpressing mammary cancer cells, both in vitro and in vivo, the parent of trastuzumab, the murine antibody MuMAb4D5, showed no inhibitory activity toward normal cells or toward tumor cells devoid of HER2. Thus, because HER2 is mainly overexpressed in tumor cells, there is only low risk of toxicity associated with anti-HER2 treatments. The parent anti-HER2 murine antibody was humanized in order to obtain a recombinant antibody comprising almost 95% of human sequence. Trastuzumab is directed against the extracellular subdomain IV of the receptor [70]. Trastuzumab decreased receptor signaling, while increasing HER2 internalization and subsequent degradation [49]. In addition, trastuzumab induces apoptosis and inhibits angiogenesis. Because response rates to trastuzumab administered alone (monotherapy) are relatively low, usually this mAb is administered together with chemotherapeutic drugs, such as paclitaxel or docetaxel, with consequent improvement in response rates, overall survival, and disease progression [71]. Despite initial responses to therapy based on this mAb, within 12–18 months many patients become resistant to the drug. The proposed resistance mechanisms include expression of a truncated isoform of HER2, overexpression of other RTKs, and loss of PTEN, a lipid phosphatase [72]. Another approved anti-HER2 humanized recombinant antibody is pertuzumab. Pertuzumab binds to the extracellular dimerization domain II of HER2, which is distinct from the epitope recognized by trastuzumab [73].

Other important mAbs used for treatment of solid tumors include the anti-EGFR antibodies cetuximab, panitumumab, and necitumumab. The EGFR signaling pathway is involved in processes crucial for tumor growth and progression, cell proliferation, angiogenesis, and inhibition of apoptosis [74]. Cetuximab was first approved in 2004 for the treatment of metastatic colorectal cancer, either alone, after failure of chemotherapy, or in combination with chemotherapy as first-line treatment. Because it was later observed that this mAb confers no benefit when used to treat colorectal

tumors harboring KRAS mutations [75], the antibody is not indicated for the treatment of tumors with RAS mutations. In 2011 cetuximab was also approved for head and neck cancer, in combination with radiotherapy or with chemotherapy, or as a single agent after failure of chemotherapy [76]. Cetuximab is a chimeric mAb which binds with extracellular domain III of EGFR and blocks the binding of the ligand, thereby inhibits activation of the receptor and all downstream signaling pathways. In addition, the antibody induces ADCC and promotes receptor internalization and degradation [77]. The anti-EGFR human mAb called panitumumab was approved in 2006 for the treatment of KRAS wild type metastatic colorectal cancer. Another human anti-EGFR antibody, necitumumab, was approved in 2015 for clinical application in combination with two chemotherapeutic drugs (gemcitabine and cisplatin), because it offers a survival advantage for patients with advanced squamous NSCLC [78].

Given the essential roles played by VEGF-A and VEGFR-2 in tumor angiogenesis, the blockade of this pathway represents a suitable strategy to inhibit cancer progression [79]. Bevacizumab, a recombinant humanized anti-VEGF-A monoclonal antibody, was first approved in 2004 for the treatment of metastatic colorectal cancer, in combination with chemotherapy. The binding of bevacizumab to VEGF-A prevents its interaction with the receptors and their activation, which leads to regression of immature tumor vasculature and inhibition of angiogenesis. In 2006, bevacizumab was also approved for the treatment of metastatic HER2-negative breast cancer, in combination with chemotherapy, based on preliminary analysis of the E2100 clinical trial. However, approval for this breast cancer treatment was revoked in 2011, following completion of additional trials [80]. Currently, bevacizumab is approved for the treatment of colorectal cancer, non-small cell lung cancer, glioblastoma, renal cell carcinoma, cervical cancer, ovarian cancer, fallopian tube cancer, and peritoneal cancer.

7 Immune Checkpoint Inhibitors

The immune response to a specific antigen requires interactions among antigen-presenting cells, T cells, and target cells. The activation of T cell requires a first signal, which involves the interaction of the antigen, bound to the MHC (major histocompatibility complex), with the T-cell receptor, and a second signal, the binding of the T-cell activator CD28 to a member of the B7 co-stimulatory molecules (CD80 or CD86). These events lead to autocrine production of interleukin-2 (IL-2) and subsequent T-cell activation. Tumors can escape the immune response by means of several mechanisms [81], for example by activating immunoregulatory mechanisms, also known as immune checkpoints. Targeting the

immune checkpoints with antibodies represents an effective way to enhance the anti-tumor immune response.

Cytotoxic T lymphocyte-associated protein 4 (CTLA-4) potently regulates T-cell responses [82]: after engagement of the T-cell receptor (TCR) and a co-stimulatory signal mediated by CD28, CTLA-4 outcompetes CD28 for binding to CD80 and CD86, two co-stimulatory proteins. This interaction arrests both proliferation and activation of T cells [83]. Hence, blocking CTLA-4 translates to enhanced T-cell activation. Two mAbs against CTLA-4 were developed: ipilimumab and tremelimumab. The success of a large phase III clinical trial, which compared ipilimumab with standard dacarbazine chemotherapy [84], which showed that the antibody improved overall survival of patients with metastatic melanoma, led to the approval of this mAb, in 2011, for the treatment of unresectable or metastatic melanoma. Unfortunately, given the mechanism of action of this antibody, namely T-cell proliferation and activation, the toxicity to this drug is common and it mainly involves inflammatory side effects, mostly confined to skin and to the gastrointestinal tract. However, in some cases it can affect also liver and endocrine glands [85].

Another key immune checkpoint of T cells is the programmed death 1 (PD-1) molecule, which is expressed not only on T cells, but also on natural killer (NK) cells and B cells. When PD-1 binds to its ligand, PD-L1, which is broadly expressed by tumor cells and also by many somatic cells upon exposure to proinflammatory cytokines, it causes inhibition of T-cell proliferation, cytokine production, and cytotoxicity, as well as elevated apoptosis [86]. Hence, blocking PD-1 is another approach that has been used in order to enhance the immune response against cancer cells. In vivo studies confirmed that the blockade of PD-1 with antibodies led to enhancement of anti-tumor immunity [87]. Subsequently, several clinical trials in patients with advanced melanoma [88], NSCLC [89], renal cell carcinoma [90], bladder cancer [91], and Hodgkin's lymphoma [92], led to the approval of nivolumab, an anti-PD1 mAb, in all the aforementioned indications. Currently, five antibodies that target the PD-1/PD-L1 axis have been approved: nivolumab and pembrolizumab, which target PD-1, and three anti-PD-L1 antibodies, atezolizumab, avelumab, and durvalumab [93].

8 Combinations of Antibodies and Cytotoxic Treatments (*See* Fig. 1)

It is important noting that the labels of many clinically approved mAbs indicate combinations with cytotoxic regimens, namely chemotherapy or, in a fewer cases, radiotherapy. For example randomized clinical trials comparing CHOP (cyclophosphamide, doxorubicin, vincristine, and prednisone) regimen alone or in combination with rituximab (R-CHOP) in NHL showed that

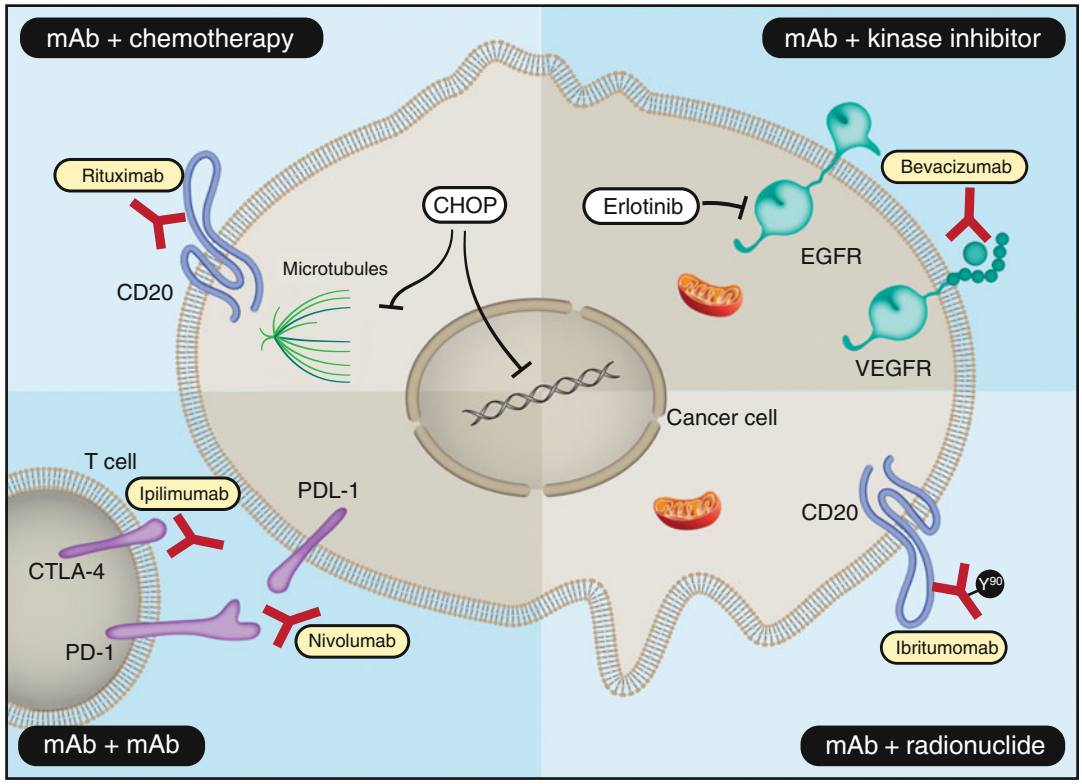

Fig. 1 Clinically approved combinations of antibodies and other pharmacological approaches. Four different examples of pharmacological strategies are presented. The upper left corner presents a combination of a monoclonal anti-CD20 antibody (rituximab) and chemotherapy (CHOP; cyclophosphamide, doxorubicin, vincristine and prednisone), which is approved for non-Hodgkin lymphoma. The upper right corner presents a combination of a monoclonal anti-VEGF antibody (bevacizumab) and an EGFR-specific kinase inhibitor (erlotinib). This combination has been approved as first-line treatment of patients with unresectable metastatic (or recurrent) NSCLC presenting EGFR mutations. The lower left corner presents a combination of two monoclonal antibodies recognizing T-cell antigens: CTLA-4 (ipilimumab) and PD-1 (nivolumab). This combination has been approved for patients with unresectable or metastatic melanoma, as well as some types of kidney and colon tumors. The lower right corner presents treatment with an anti-CD20 antibody (ibritumomab), which is conjugated to a radioactive isotope, Yttrium-90 (Y-90). This construct is approved for patients with relapsed or refractory low-grade CD20-positive B-cell non-Hodgkin lymphoma

co-treatment with the mAb and chemotherapy significantly increased the overall survival, as well as progression-free survival of treated patients [94]. Likewise, a phase III combination trial comparing chemotherapy alone (two regimens: anthracycline plus either cyclophosphamide or paclitaxel) and in combination with trastuzumab showed that patients receiving paclitaxel and trastuzumab displayed a median time to progression of 6.9 months, as compared to 3.0 months in the group treated only with paclitaxel, while patients treated with anthracycline, cyclophosphamide, and trastuzumab showed a median time to progression of 7.8 months,

compared to 6.1 months in the chemotherapy regimen [95]. More lately, trastuzumab has also been approved for adjuvant treatment of HER2-overexpressing breast cancer, both node positive and node negative, in combination with chemotherapy (e.g., doxorubicin, cyclophosphamide, and paclitaxel/docetaxel). Similarly, the anti-EGFR antibody cetuximab was approved in metastatic colorectal cancer in combination with different chemotherapeutic regimens. This antibody was also approved with radiotherapy in head and neck cancer since it has been shown that the combination reduces mortality without increasing the toxic effects of radiotherapy treatments [96].

mAbs can be used to deliver radiation or cytotoxic drugs directly to the tumor site. In the radioimmunotherapy approach radionuclides, typically β-emitters, are conjugated to an antibody. Ibritumomab tiuxetan (an anti-CD20 antibody labeled with the radionuclide ^{90}Y) and tositumumab (an anti-CD20 antibody labeled with ^{131}I) were approved in 2002 and 2003, respectively, for the treatment of NHL. Two antibody-drug conjugates (ADC) have been approved for clinical use: brentuximab vedotin (BV, in 2011) and ado-trastuzumab emtansine (TE, in 2013). BV consists of an anti-CD30 antibody conjugated to mono-methyl auristatin E. BV was approved for relapsed Hodgkin lymphoma based on a phase II trial which showed overall response rate of 75%, with complete remission in 34% of patients [97], and for systemic anaplastic large-cell lymphoma (ALCL) on the basis of another phase II trial, in which brentuximab vedotin induced objective responses in the majority of patients and complete responses in more than half of patients with recurrent systemic ALCL [98]. Ado-trastuzumab emtansine was prepared by conjugating maytansinoid DM1 to trastuzumab. Its approval in 2013 was based on a phase III study which showed that this ADC prolonged overall survival compared to lapatinib plus capecitabine in patients with HER2-positive metastatic breast cancer previously treated with trastuzumab and a taxane [99].

9 Combinations of mAbs and Protein Kinase Inhibitors (PKIs; *See* Fig. 1)

Imatinib, a BCR-ABL tyrosine kinase inhibitor, was the first PKI to be approved, in 2001, for the treatment of chronic myeloid leukemia (CML). The introduction of this PKI into the clinic has turned CML, a fatal cancer, into a manageable disease. Since then several other PKIs have been successfully used to treat cancer, including several generations of EGFR-specific PKIs (e.g., erlotinib, gefitinib, afatinib, and osimertinib), which are used to treat NSCLC [100]. Currently, the major issue with EGFR PKIs and similar drugs is the inevitable emergence of resistance after a variable period of time [5]. The most common mechanism of resistance to

PKI therapy is the appearance of point mutations within the kinase domain, resulting in decreased affinity of the inhibitor to the ATP-binding site. For example, resistance to first generation EGFR-PKIs, erlotinib and gefitinib, is mainly due to a secondary point mutation in the kinase domain of the receptor, namely the T790M mutation [101]. Another mechanism of resistance entails gene amplification, or other modes that upregulate expression levels of compensatory RTKs. Amplification of MET has been found in 20% of cases of resistance to first generation EGFR-PKIs in patients with NSCLC [102]. In addition, emergence of resistance to PKIs can be due to alterations in intracellular signaling pathways. Thus, resistance to erlotinib in EGFR-mutated lung cancer has been shown to be related to PTEN loss and consequent activation of AKT [103]. Considering all possible mechanisms leading to PKI resistance, several attempts to combine PKIs and mAbs have been conducted. Combining cetuximab and erlotinib or gefitinib caused inhibition of tumor growth and induction of apoptosis in head and neck and lung cancer cell lines [104]. Likewise, specific combinations of EGFR-specific mAbs and EGFR-PKIs showed a synergistic effect in terms of reducing cell proliferation and inhibiting the RAS signaling in triple-negative breast cancer cell lines [105]. The combination of three monoclonal antibodies (anti-EGFR, anti-HER2, anti-HER3) with osimertinib, a third generation EGFR-PKI, was highly effective in reducing tumor growth in NSCLC xenografts [60, 106]. Interestingly, when applied in vitro and in animals, the PKI induced apoptosis whereas the triple combination of mAbs induced senescence of EGFR-driven tumor cells. Several clinical trials examined combinations of PKIs and mAbs. A combination of an anti-MET antibody, onartuzumab, and erlotinib was tested in a phase III clinical study in NSCLC patients presenting MET amplification. However, this study showed that adding onartuzumab to erlotinib did not improve clinical outcome [107]. Another study, the JO25567 trial, analyzed a combination of erlotinib and bevacizumab in EGFR-driven lung cancer patients [108]. This study showed a clear improvement in progression-free survival. Another phase II trial confirmed the efficacy of combining erlotinib with bevacizumab in NSCLC patients with activating EGFR mutations [109], which led to clinical approval in 2016, in Europe. Lastly, a dual-specificity PKI, lapatinib, which blocks both EGFR and HER2, showed synergistic effects when mixed with trastuzumab and applied on HER2-overexspressing breast cancer cell lines [110]. Two explanations for the synergistic in vitro effect could be downregulation of survivin and enhanced tumor cell apoptosis. However, although several clinical studies showed that the combination of lapatinib and trastuzumab has better efficacy in comparison to the respective single agent treatments in metastatic HER2-positive breast cancer, the combinations also induced relatively high toxicity [111].

10 Applications of Oligoclonal Combinations of Antibodies

10.1 Homo-Combinations of Antibodies Targeting RTKs

Along with their ability to harness immune mechanisms, antibodies to receptors critical for cell growth and survival often induce extensive, although slow, degradation of their target receptors [38]. Ligand-induced rapid endocytosis and degradation of the cognate RTKs is considered a major physiological mechanism that terminates growth signals in normal cells, but cancer cells often employ tricks that delay receptor endocytosis [112, 113]. An anti-EGFR antibody able to inhibit tumor growth was shown to induce down-regulation of the receptor [114]. Studies that examined different mAbs specific to HER2 showed that administration of certain mixtures of antibodies resulted in synergistic anti-tumor effects [115]. Using two other sets of anti-HER2 antibodies, synergy was associated with enhanced ADCC and more extensive receptor degradation [116, 117]. Yet another study demonstrated that synergy in terms of HER2 degradation and tumor inhibition required engagement of two nonoverlapping epitopes of HER2 [118]. Because combinations of antibodies to the homologous receptor, EGFR, reduced surface receptor levels by inhibiting recycling back to the plasma membrane [77, 119], it is plausible that formation of large aggregates of RTKs, by means of two or more non-competitive mAbs, is followed by rapid receptor endocytosis and degradation, with minimal recycling.

Pertuzumab and trastuzumab are both approved for the treatment of HER2-positive breast cancer. These anti-HER2 antibodies target different epitopes of the extracellular part of the receptor (*see* Fig. 2). Binding of trastuzumab to the juxtamembrane domain of HER2 inhibits cleavage of HER2 by an extracellular protease and inhibits intracellular mitogenic pathways [120]. Pertuzumab binds with domain II, thereby blocks a pocket necessary for the dimerization of HER2 with other HER/ERBB family members [51]. In light of the nonoverlapping binding sites, combining the two antibodies is a valid approach to inhibiting HER2 signaling. Early studies along this line demonstrated that admixing these two anti-HER2 antibodies strongly inhibited cancer cell growth in vitro [121] and in HER2-positive breast xenografts [122]. The underlying mechanisms may entail enhanced HER2 degradation, augmented ADCC, or the complementary functions of trastuzumab and pertuzumab. In line with the preclinical studies, the Cleopatra phase III clinical trial, which tested pertuzumab plus trastuzumab plus docetaxel in patients with HER2-positive metastatic breast cancer reported statistically significant and clinically meaningful survival benefit with this combination [123, 124]. NeoSphere compared four groups as neoadjuvant treatment in HER2-positive breast cancer: docetaxel plus trastuzumab, docetaxel plus pertuzumab, docetaxel plus trastuzumab plus pertuzumab, and

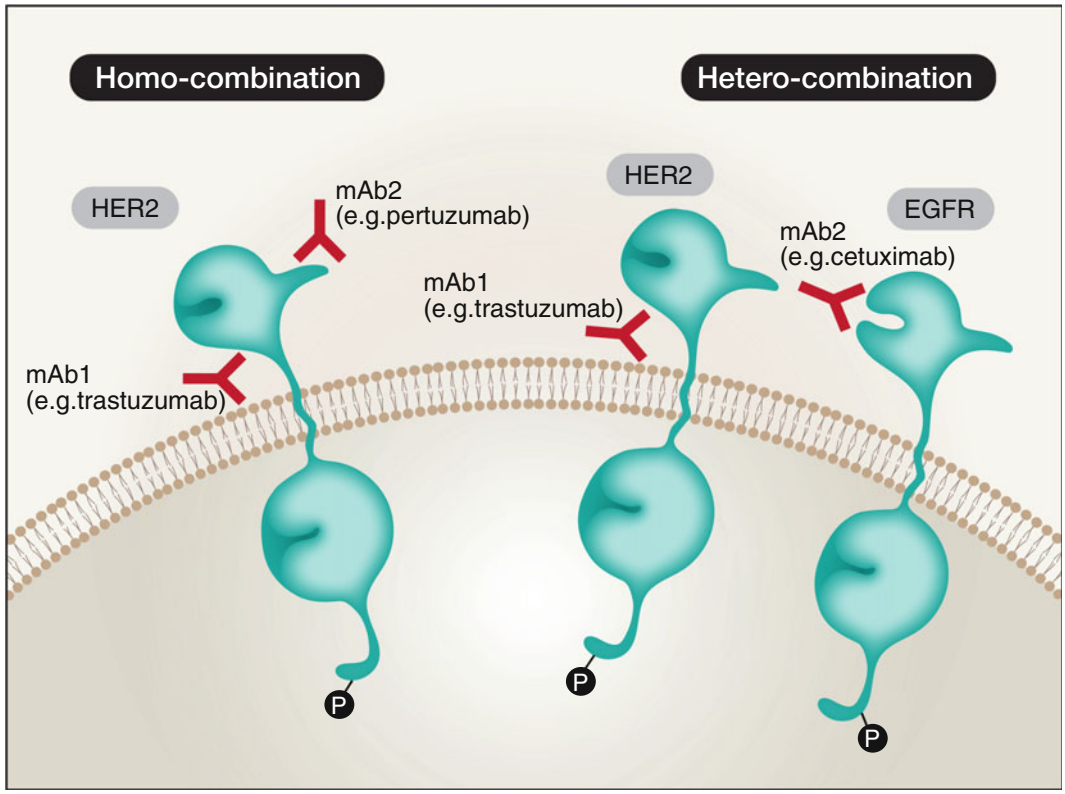

Fig. 2 Classes of oligoclonal antibody mixtures. The homo-combination class combines monoclonal antibodies targeting two or more nonoverlapping antigenic determinants (epitopes) of an antigen. For example, trastuzumab and pertuzumab engage domain IV and domain II, respectively, of the HER2 protein. The mixture of these antibodies, in combination with docetaxel, has been approved for HER2-positive metastatic breast cancer. The hetero-combination class combines monoclonal antibodies targeting two or more antigens. Examples include a mixture of antibodies specific to CTLA-4 and PD-1 (ipilimumab and nivolumab, respectively; not shown), which has been approved for advanced melanoma, CRC and renal cancer, and an experimental combination of antibodies simultaneously targeting the homologous receptors EGFR and HER2. Encircled P letters mark tyrosine auto-phosphorylation sites of EGFR and HER2

pertuzumab plus trastuzumab. The pathological complete response rate in the docetaxel/trastuzumab/pertuzumab group was 46% compared to 29% in the docetaxel/trastuzumab group. In addition, no substantial differences in terms of toxicity were found [125]. In another trial, APHINITY, the adjuvant treatment with pertuzumab, trastuzumab, and chemotherapy, was tested in node-positive or high-risk node-negative HER2-positive breast cancer. In the cohort of patients with node-positive disease, the 3-year rate of invasive disease-free survival was 92% in the pertuzumab/trastuzumab/chemotherapy group as compared with 90.2% in trastuzumab/chemotherapy group [126]. Accordingly, the combination of trastuzumab, pertuzumab, and chemotherapy was approved in

2017 as adjuvant treatment for patients with HER-positive breast cancer at high risk of recurrence.

In similarity to the case of HER2, experimental data relevant to mAb-induced degradation of EGFR have been reported. However, no combination of anti-EGFR mAbs has so far been approved. Early studies that employed a radiolabeled cetuximab confirmed endocytosis of the antibody [127]. In addition, combining two mAbs to EGFR strongly accelerated receptor degradation, provided that the antibodies engaged nonoverlapping epitopes [119]. Sym004 is a mixture of two anti-EGFR monoclonal antibodies, futuximab and modotuximab, that engage nonoverlapping epitopes within the extracellular domain III of the receptor, while inhibiting cancer cell growth by blocking activation of EGFR and by causing internalization and degradation of the receptor [128]. When evaluated in a phase I trial in patients with colorectal cancer (CRC) who acquired resistance to an anti-EGFR antibody, Sym004 induced tumor shrinkage in 17 out of 39 patients and partial response was observed in five additional patients [129]. In the Sym005-05 phase II trial chemo-refractory patients with metastatic CRC and acquired resistance to approved anti-EGFR antibodies were treated with different dose regimens of Sym004. Although Sym004 did not improve overall survival or progression-free survival in unselected patients, profiling of circulating DNA identified a subgroup of patients with no mutations in RAS, BRAF, and EGFR (extracellular), who derived clinical benefit from the treatment with Sym004 [130]. In analogy to EGFR, targeting the hepatocyte growth factor receptor, c-MET, offers a hub amenable for inhibition of several malignancies [131]. In gastric and in NSCLC tumors, amplification of the *MET* gene has been associated with poor prognosis [132, 133], but so far no antibodies targeting MET have been approved. The anti-MET antibody onartuzumab binds to the extracellular domain of MET, and inhibits HGF binding, but a phase III study reported no improvement in clinical outcomes in patients with MET-positive NSCLC treated with onartuzumab plus erlotinib compared to an erlotinib group [107]. An alternative strategy, which combines two antibodies targeting different epitopes within the extracellular domain of MET, is not only able to disrupt the interaction with HGF but also induce receptor internalization, along with CDC and ADCC [134]. This mixture of two anti-MET antibodies is currently being tested in a phase I clinical trial (ClinicalTrials.gov; identifier: NCT02648724). Table 2 lists all phase II and III clinical trials currently addressing combinations of antibodies in various oncology indications.

Table 2
Antibody-based drug combinations currently examined by specific clinical trials

Drug combination	Antibody target	Major tumor types	ClinicalTrial.gov identifier (NTC0)
Atezolizumab + ado-trastuzumab emtansine	PD-L1 + HER2	Breast cancer	2924883
Atezolizumab + anetumab ravtansine	PD-L1 + mesothelin (ADC)	NSCLC	3455556
Atezolizumab + daratumumab	PD-L1 + CD38	NSCLC	3023423
Atezolizumab + mosunetuzumab	PD-L1 + CD20/CD3 (BsAb)	NHL, CLL	2500407
Atezolizumab + MTIG7192A	PD-L1 + TIGIT	NSCLC	3563716
Atezolizumab + obinutuzumab + CT	PD-L1 + CD20	FL	2596971
Atezolizumab + obinutuzumab + ibrutinib	PD-L1 + CD20	CLL	2846623
Atezolizumab + obinutuzumab + lenalidomide	PD-L1 + CD20	FL	2631577
Atezolizumab + obinutuzumab + polatuzumab vedotin, atezolizumab + rituximab + polatuzumab vedotin	PD-L1 + CD20 + CD79b (ADC), PD-L1 + CD20 + CD79b (ADC)	FL, DLBCL	2729896
Atezolizumab + pertuzumab + trastuzumab	PDL-1 + HER2 + HER2	Breast cancer	3417544
Atezolizumab + RO6958688	PD-L1 + CEA/CD3 (BsAb)	NSCLC	3337698
Atezolizumab + trastuzumab + pertuzumab + CT	PD-L1 + HER2 + HER2	Breast cancer	3125928
Avelumab + PF-04518600, PF-04518600 + utomilumab, avelumab + utomilumab	PD-L1 + OX40, OX40 + CD137, PD-L1 + CD137	AML	3390296
Avelumab + utomilumab + rituximab	PD-L1 + CD137 + CD20	DLBCL (Ib/III)	2951156 (Ib/III)

Avelumab + utomilumab, avelumab + PD 0360324, avelumab + PF-05082566 + PF-04518600	PD-L1 + CD137, PD-L1 + CSF1, PD-L1 + OX40	Advanced malignancies	2554812
Avelumab + utomilumab, avelumab + PF-04518600, avelumab + utomilumab + PF-04518600	PD-L1 + CD137, PD-L1 + OX40, PD-L1 + CD137 + OX40	Advanced malignancies	3217747
Bevacizumab + atezolizumab	VEGF-A + PD-L1	Ovarian, cervical cancer, RCC (III), HCC (III),	More than five trials
Bevacizumab + atezolizumab + CT	VEGF-A + PD-L1	CRC (III), NSCLC (III)	More than three trials
Bevacizumab + atezolizumab + endocrine therapy	VEGF-A + PD-L1	Breast cancer	3280563
Bevacizumab + atezolizumab + Entinostat	VEGF-A + PD-L1	RCC	3024437
Bevacizumab + atezolizumab + ipatasertib/ cobimetinib	VEGF-A + PD-L1	Breast, ovarian cancer	3395899, 3363867
Bevacizumab + atezolizumab, atezolizumab + ladiratuzumab vedotin	VEGF-A + PD-L1, PD-L1 + LIV-1 (ADC)	Breast cancer	3424005
Bevacizumab + avelumab + Ad-CEA vaccine + CT	VEGF-A + PD-L1	CRC	3050814
Bevacizumab + brentuximab vedotin	VEGF-A + CD30 (ADC)	Germ cell tumor	2988843
Bevacizumab + carotuximab	VEGF-A + endoglin	GTD	2664961
Bevacizumab + cetuximab + CT	VEGF-A + EGFR	CRC (III)	0265850 (III)
Bevacizumab + pembrolizumab	VEGF-A + PD-1	RCC	2348008
BGB-A333 + BGB-A317	PD-L1 + PD-1	Advanced solid tumors	3379259
BI-1206 + CD20 Ab	CD32b + CD20	B-cell malignancy	2933320
Cetuximab + avelumab	EGFR + PD-L1	HNSCC	3494322
Cetuximab + Hu5F9-G4	EGFR + CD47	CRC	2953782

(continued)

Table 2
(continued)

Drug combination	Antibody target	Major tumor types	ClinicalTrial.gov identifier (NTC0)
Cetuximab + pembrolizumab	EGFR + PD-1	HNSCC	3082534
Cetuximab + pembrolizumab, pembrolizumab + trastuzumab, pembrolizumab + ado-trastuzumab emtansine	EGFR + PD-1, PD-1 + HER2, PD-1 + HER2	Advanced cancer	2318901
Durvalumab + daratumumab	PD-L1 + CD38	MM	2807454
Durvalumab + rituximab	PDL-1 + CD20	Lymphoma, CLL	2733042
Durvalumab + cetuximab + RT	PD-L1 + EGFR	HNSCC	3051906
Iodine I 131 tositumomab + rituximab + CT	CD20 + CD20	NHL	0770224
Ipilimumab + cemiplimab + CT	CTLA-4 + PD-1	NSCLC (III)	3409614 (III), 3430063
Ipilimumab + nivolumab	CTLA-4 + PD-1	TCC, melanoma (III), NSCLC (III/IV), CRC, breast, ovarian, pancreatic, gastric, prostate, bladder, thyroid, uterine cancer, RCC (IV), CNS malignancies, HNSCC, SCLC, esophageal adenocarcinoma (III), hematological malignancies, HCC, glioblastoma	More than 60 trials
Ipilimumab + nivolumab + CT	CTLA-4 + PD-1	Soft tissue sarcoma, NSCLC (III), TCC (III)	3138161, 3215706 (III), 3036098 (III)
Ipilimumab + nivolumab + dentritic cell based p53 vaccine	CTLA-4 + PD-1	SCLC	3406715
Ipilimumab + nivolumab + epacadostat, nivolumab + lirilumab + epacadostat	CTLA-4 + PD-1, PD-1 + KIR	Advanced or metastatic malignancies	3347123

Ipilimumab + nivolumab + glembatumumab vedotin	CTLA-4 + PD-1 + GPNMB	Solid tumors	3326258
Ipilimumab + nivolumab + INCAGN01876, INCAGN01876 + ipilimumab, INCAGN01876 + nivolumab	CTLA-4 + PD-1 + GITR, GITR + CTLA-4, GITR + PD-1	Advanced or metastatic malignancies	3126110
Ipilimumab + nivolumab + lirilumab, nivolumab + lirilumab	CTLA-4 + PD-1 + KIR, PD-1 + KIR	Advanced solid tumors	1714739
Ipilimumab + nivolumab + panitumab	CTLA-4 + PD-1 + EGFR	CRC	3442569
Ipilimumab + nivolumab + prednisolone	CTLA-4 + PD-1	Melanoma	3563729
Ipilimumab + nivolumab + RT	CTLA-4 + PD-1	SCLC, NSCLC, pancreatic cancer	3043599, 2696993, 2866383
Ipilimumab + nivolumab + trametinib/ nintedanib/binimetinib	CTLA-4 + PD-1	CRC, NSCLC	3377361, 3377023, 3271047
Ipilimumab + nivolumab + trastuzumab, nivolumab + trastuzumab + CT	CTLA-4 + PD-1 + HER2, PD-1 + HER2	Esophagogastric adenocarcinoma	3409848
Ipilimumab + nivolumab, nivolumab + BMS-986016, nivolumab + daratumumab	CTLA-4 + PD-1, PD-1 + LAG-3, PD-1 + CD38	CRC	2060188
Ipilimumab + nivolumab, nivolumab + lirilumab, nivolumab + daratumumab	CTLA-4 + PD-1, PD-1 + KIR, PD-1 + CD38	Hematologic malignancies	1592370
Ipilimumab + nivolumab, nivolumab + relatlimab	CTLA-4 + PD-1, PD-1 + LAG3	NSCLC (III), RCC	2750514, 2996110
Ipilimumab + pembrolizumab	CTLA-4 + PD-1	Melanoma	2743819
Isatuximab + Cemiplimab	CD38 + PD-1	MM	3194867
JNJ-63723283 + daratumumab	PD-1 + CD38	Advanced solid tumors	3547037

(continued)

Table 2
(continued)

Drug combination	Antibody target	Major tumor types	ClinicalTrial.gov identifier (NTC0)
LAG525 + PDR001	LAG3 + PD-1	Advanced solid and hematologic malignancies	2460224, 3365791
LAG525 + spartalizumab	LAG3 + PD-1	Breast cancer	3499899
MBG453 + PDR001	TIM3 + PD-1	Advanced malignancies	2608268
MGD007 + MGA012	gpA33/CD3 (DART) + PD-1	CRC	3531632
NIS793 + PDR001	TGFβ + PD-1	Advanced malignancies	2947165
Nivolumab + andecaliximab	PD1 + MMP9	Gastric or GEJ adenocarcinoma	2864381
Nivolumab + APX005M	PD-1 + CD40	Melanoma, NSCLC	3123783
Nivolumab + APX005M + Cabiralizumab	PD-1 + CD40 + CSF1R	Melanoma, NSCLC, RCC	3502330
Nivolumab + bevacizumab	PD-1 + VEGF-A	Ovarian, fallopian tube or peritoneal cancer	2873962
Nivolumab + BMS-986012	PD-1 + fucosyl-GM1	SCLC	2247349
Nivolumab + BMS-986179	PD-1 + CD73	Advanced solid tumors	2754141
Nivolumab + BMS-986218	PD-1 + CTLA-4	Advanced solid tumors	3110107
Nivolumab + BMS-986253	PD-1 + IL-8	Advanced cancers	3400332
Nivolumab + brentuximab vedotin	PD-1 + CD30 (ADC)	HL, NHL	2572167, 2581631
Nivolumab + elotuzumab	PD-1 + SLAMF7	MM	2612779, 3227432
Nivolumab + nimotuzumab	PD-1 + EGFR	NSCLC	2947386
Nivolumab + oregovomab	PD-1 + CA125	Ovarian cancer	3100006

Nivolumab + relatlimab	PD-1 + LAG-3	Advanced solid tumors, melanoma (II/III)	1968109, 3470922 (II/III)
Nivolumab + rituximab + CT	PD-1 + CD20	DLBCL	3259529
Nivolumab + rituximab + lenalidomide	PD-1 + CD20	DLBCL, CNS lymphoma	3558750
Nivolumab + urelumab	PD-1 + CD137	Advanced/metastatic solid tumors, NHL, bladder TCC	2253992
Nivolumab + varlilumab	PD-1 + CD27	Advanced solid tumors, B-cell lymphoma	2335918, 3038672
Nivolumab + BMS-986249	PD-1 + CTLA-4	Advanced solid tumors	3369223
Nivolumab and/or ipilimumab + BMS-986178	PD-1 and/or CTLA-4 + OX40	Advanced solid tumors	2737475
Nivolumab or pembrolizumab + glembatumumab vedotin, glembatumumab vedotin + varlilumab	PD-1 + GPNMB (ADC), GPNMB (ADC) + CD27	Melanoma	2302339
Obinutuzumab + polatuzumab vedotin	CD20 + CD79b (ADC)	NHL	1691898
Obinutuzumab + polatuzumab vedotin + lenalidomide, rituximab + polatuzumab vedotin + lenalidomide	CD20 + CD79b (ADC), CD20 + CD79b (ADC)	FL, DLBCL	2600897
Obinutuzumab + polatuzumab vedotin + venetoclax, rituximab + polatuzumab vedotin + venetoclax	CD20 + CD79b (ADC), CD20 + CD79b (ADC)	FL, DLBCL	2611323
Pembrolizumab + anetumab ravtansine	PD-1 + mesothelin (ADC)	Mesothelioma	3126630
Pembrolizumab + APX005M	PD-1 + CD40	Melanoma	2706353
Pembrolizumab + B-701	PD-1 + FGFR3	TCC	3123055
Pembrolizumab + bavituximab	PD-1 + phosphatidylserine	HCC	3519997
Pembrolizumab + mogamulizumab	PD-1 + CCR4	Lymphomas	3309878

(continued)

Table 2
(continued)

Drug combination	Antibody target	Major tumor types	ClinicalTrial.gov identifier (NTC0)
Rituximab + BI-1206	CD20 + CD32b	NHL	3571568
Rituximab + Hu5F9-G4	CD20 + CD47	NHL	2953509
Rituximab + ibritumomab tiuxetan	CD20 + CD20 (ARC)	NHL	732498
Rituximab + ibritumomab tiuxetan + bortezomib	CD20 + CD20 (ARC)	FL, NHL	372905
SAR439459 + REGN2810	TGFβ + PD-1	Advanced solid tumors	3192345
Trastuzumab + avelumab + CT, trastuzumab + avelumab + utomilumab + CT, trastuzumab + avelumab + utomilumab	HER2 + PD-L1, HER2 + PD-L1 + CD137, HER2 + PD-L1 + CD137	Breast cancer	3414658
Trastuzumab + pembrolizumab + CT	HER2 + PD-1	Gastric cancer	2901301
Trastuzumab + pertuzumab	HER2 + HER2	Breast cancer (III)	2625441 (III)
Trastuzumab + pertuzumab + CT	HER2 + HER2	Breast cancer (III)	1796197, 2402712 (III)
Tremelimumab + durvalumab	CTLA-4 + PD-L1	Bladder, ovarian, prostate, urinary tract cancer, germ cell tumors, TCC (III), HNSCC (III), CRC, NSCLC (III), SCLC, glioma, RCC, advanced solid malignancies (III)	More than 25 trials
Tremelimumab + durvalumab + CT	CTLA-4 + PD-L1	HNSCC, CRC, SCLC (III)	3019003, 3202758, 3043872 (III)
Tremelimumab + durvalumab + hormone therapy	CTLA-4 + PD-L1	Breast cancer	3430466
Tremelimumab + durvalumab + IMCgp100	CTLA-4 + PD-L1	Melanoma	2535078

Tremelimumab + durvalumab + olaparib	CTLA-4 + PD-L1	Ovarian, fallopian tube, or primary peritoneal cancer	2953457
Tremelimumab + durvalumab + proton therapy	CTLA-4 + PD-L1	HNSCC	3450967
Tremelimumab + durvalumab + RT	CTLA-4 + PD-L1	Pancreatic, biliary tract cancer, HNSCC, HCC, CRC	More than three trials

Listed are all current phase II and III studies employing two or more antibodies in oncology (phase I studies were excluded). The information was extracted in July 2018 from the following internet site: www.clinicaltrials.gov. Note that only major clinical indications are indicated. Lists of clinical trial identifiers have been abbreviated. ACC, adenoid cystic carcinoma, ADC, antibody-drug conjugate; Ad-CEA, carcinoembryonic antigen; AML, acute myeloid leukemia; BiTE, bispecific T-cell engager; BTC, biliary tract cancer; CLL, chronic lymphocytic leukemia; CNS, central nervous system; CRC, colorectal cancer; CT, chemotherapy; DART, dual-affinity re-targeting antibody; DLBCL, diffuse large B-cell lymphoma; ESCC, esophageal squamous cell carcinoma; FL, follicular lymphoma; GEJ, gastroesophageal junction; GTD, gestational trophoblastic disease; HCC, hepatocellular carcinoma; HL, Hodgkin lymphoma; HNSCC, head and neck squamous cell carcinoma; mBCC, metastatic basal cell carcinoma; MCL, mantle cell lymphoma; MM, multiple myeloma; NHL, non-Hodgkin lymphoma; NSCLC, non-small cell lung cancer; RCC, renal cell carcinoma; RMC, renal medullary carcinoma; RT, radiotherapy; SCLC, small cell lung cancer; TCC, transitional cell carcinoma.

10.2 Hetero-Combinations of Antibodies Targeting RTKs (See Fig. 2)

Resistance to targeted therapies (PKIs or mAbs) commonly involves secondary mutations or activation of compensatory pathways. For example, inhibition of AKT in a wide spectrum of tumor types induces a conserved set of RTKs, including HER3 and the insulin receptor [135]. Likewise, resistance to anti-EGFR antibodies in models of NSCLC and head and neck cancer was associated with upregulation of specific members of the EGFR family [136]. Accordingly, concurrently targeting EGFR, HER2, and HER3 with pan-HER (a mixture of six antibodies targeting these three receptors) in lung and head and neck cancer led to extensive shrinkage of tumor models [137]. In a similar way, treatment of NSCLC models driven by mutant forms of EGFR caused upregulation of HER2 and HER3, which resulted in strong activation of the MAPK pathway [60]. Moreover, a combination of three antibodies, including the approved anti-EGFR cetuximab and anti-HER2 trastuzumab, plus an anti-HER3 antibody, was able to overcome resistance to EGFR-specific PKIs [106]. Another hetero-combination of anti-RTK antibodies made use of a mixture of cetuximab and the anti-HER3 antibody U3-1287, which blocked activation of the MAPK and AKT pathways in cetuximab-resistant NSCLC cell lines [138]. This combination was also effective in blocking HER2 activation. Because mutations and amplification of the *HER3* gene were associated with malignancy, this kinase-defective orthologue of EGFR is emerging as a suitable target for antibodies [139]. For example, patritumab, a human anti-HER3 mAb, has shown anticancer activity in preclinical models. When combined with trastuzumab and paclitaxel in patients with HER2-overexpressing metastatic breast cancer, the antibody was found to be tolerable and efficacious [140]. In conclusion, several hetero-combinations of antibodies, which are in various stages of development, might emerge as pharmacological agents able to overcome emergence of resistance to targeted therapies in diverse indications of oncology.

10.3 Hetero-Combinations of Immune Checkpoint Inhibitors

Experimental combinations of various immune checkpoint inhibitors currently dominate the field of oncology clinical trials (*see* Table 2). This new era of immunotherapy reflects complementary features of different immune checkpoints, which offer additive or synergistic therapeutic effects. Specifically, blocking either CTLA-4 or PD-1 engages subsets of exhausted-like CD8 T cells, but blocking CTLA-4 also induces expansion of an ICOS+ Th1-like CD4 effector population [141]. Both CTLA-4 and PD-1 regulate immune checkpoints that act at different stages during T-cell activation: while CTLA-4 is involved in the early stages of T-cell activation, PD-1 modulates late stages in the tumor microenvironment. In addition, while the main site of action of CTLA-4 is confined to the draining lymph node, PD-1 physically binds with PD-L1 molecules residing on the surface of tumor cells, meaning that anti-PD-1 antibodies act upon both tumor cells and immune cells in the

immediate tumor microenvironment [93]. Clinical tests combining an anti-CTLA-4 mAb (ipilimumab) and an anti-PD-1 mAb (nivolumab) were initially performed in melanoma [142, 143] and later applied to NSCLC [144]. Phase I studies, which combined ipilimumab and nivolumab in patients with advanced melanoma, showed high response rates, as compared with studies that tested each mAb as monotherapy [142]. A subsequent phase III study that recruited metastatic melanoma patients reported a median progression-free survival of 11.5 months in the ipilimumab plus nivolumab group [143]. This was clearly superior to the other arms: 2.9 months in the ipilimumab group and 6.9 in the nivolumab group. Along with increased efficacy, adverse events should be considered when combining functionally different immune checkpoint inhibitors: 55% of patients treated with the combination of antibodies had adverse events of grade 3 or 4, compared with 16.3% in the nivolumab group and 27.3% in the ipilimumab arm [145]. Moreover, approximately 40% of patients with advanced melanoma who entered clinical trials with ipilimumab plus nivolumab had to stop treatment because of the adverse events [146]. Interestingly, retrospective analyses uncovered similar efficacy outcomes between patients who discontinued treatment because of adverse events and those who did not discontinue because of side effects. In other words, many patients may continue to derive benefit from the mAb combination even after discontinuation of treatment. Although no biomarker able to predict response to the mAb combination is available so far, it seems that low tumor expression of PD-L1 may associate with improved survival with the combination therapy, as compared to treatment with nivolumab alone. Following a promising phase I trial in lung cancer, a phase III trial was performed, which enrolled patients with stage IV or recurrent NSCLC that was not previously treated with chemotherapy [144]. Patients received nivolumab plus ipilimumab, nivolumab plus chemotherapy, or chemotherapy alone. The 1-year progression-free survival rate was 42.6% with nivolumab plus ipilimumab versus 13.2% with chemotherapy, and the objective response rate was 45.3% with nivolumab plus ipilimumab versus 26.9% with chemotherapy. These observations revealed benefit of nivolumab plus ipilimumab in NSCLC. In conclusion, the relatively efficacious combination of CTLA-4 and PD-1 blockers in two clinical indications highlights the enormous potential offered by the many other immune checkpoint inhibitors.

11 Bispecific Antibodies

The need to simultaneously block multiple protein targets, in order to better kill tumor cells, led to the development of bispecific antibodies (BsAbs). BsAbs can recognize two different epitopes on the same or on different antigens [147]. Based on their

functions, they can be divided into BsAbs that act directly on their targets, while modulating their activities, and BsAbs that are used to deliver a therapeutic payload. BsAbs can also be classified on the basis of their structures: IgG-like molecules, containing an Fc region, and non-IgG-like molecules that do not contain an Fc region. As expected, IgG-like BsAbs can induce Fc-mediated effector functions, such as CDC and ADCC. The other group of BsAbs usually comprises relatively small molecules. Hence, they are endowed with an enhanced ability to penetrate into tissues, and since they lack the Fc region, they less potently activate nonspecific immune responses. Nevertheless, because of their small size, they have a short half-life. Two bispecific antibodies have been approved so far: catumaxomab and blinatumomab, for EpCAM (epithelial cell adhesion molecule) positive ovarian and gastric cancer (catumaxomab) and for relapsed or refractory Philadelphia-chromosome negative or positive B-cell acute lymphoblastic leukemia (ALL; blinatumomab). Catumaxomab is an IgG2a molecule that combines specificities to both CD3 of T cells and EpCAM of cancer cells. Notably, the Fc portion of catumaxomab recruits to tumor cells several types of antigen-presenting cells, like macrophages. Blinatumumab is a single-chain bispecific mAb which belongs to the class of antibody fragments called BiTE (bispecific T-cell engager). One of its arms binds with CD19, a common B-cell marker, and the other binds with CD3, the co-stimulatory T-cell receptor. Hence, this BsAb redirects unstimulated primary T cells against CD19 positive lymphoma cells, leading to tumor lysis and release of cytokines and chemokines, with consequent activation and proliferation of T cells [148].

12 Conclusions

For many decades, the armamentarium of medical oncologists comprised surgery, radiation, and chemotherapy. Since 1998 this has gradually changed: targeted therapies able to specifically recognize protein molecules involved in malignant transformation already outnumber the arsenal of chemotherapeutic drugs. Thus, approximately 30 antibodies, 35 kinase inhibitors, and several additional drugs, such as steroid hormone blockers, offer relatively safe and effective boosters or replacements of cytotoxic regimens. Emergence of resistance due to compensatory pathways, pre-existing, or newly acquired mutations currently limits the application of molecular targeted drugs. This adaptation to pharmacological pressure is an intrinsic feature of biological networks and in many instances it reflects the genetic and clonal heterogeneity of tumors. Once an adaptation mechanism is molecularly resolved, the next logical step would be combining a drug blocking the primary target and another drug targeting the secondary target.

Empirically, this principle translates to admixing two or more drugs, each employing a different mechanism of action. In analogy, highly effective cocktails of protease inhibitors and nucleoside/nucleotide reverse transcriptase inhibitors practically keep the HIV epidemic at bay, but single-agent therapies are ineffective. Similarly, advanced stage colorectal cancer is commonly treated using combinations of 3–4 chemotherapeutic drugs, such as folinic acid, fluorouracil, oxiplatin, and irinotecan. In this monograph we reviewed animal and clinical data documenting the already identified combinations of targeted therapies, with an emphasis on monoclonal antibodies. Treatments with chemotherapy and a mAbs (e.g., CHOP and rituximab), or radiotherapy and an antibody (e.g., concurrent treatment of head/neck cancer with radiation and cetuximab) are among the past breakthrough of oncology. Although combinations of certain kinase inhibitors and antibodies may evolve into a major pharmacological endeavor, as we describe herein, the most promising drug mixtures will likely comprise oligoclonal antibodies, namely 2–3 antibodies engaging nonoverlapping epitopes of the same protein antigen (homo-combinations) and two or more antibodies, each blocking another antigen (hetero-combinations). A combination of trastuzumab and pertuzumab represents the first clinically approved homo-combination (for breast cancer). Similarly, a combination of two antibodies collectively blocking PD-1 (nivolumab) and CTLA-4 (ipilimumab) represents the first clinically available hetero-combination, which is approved for advanced melanoma, as well as for additional types of cancer (e.g., microsatellite instability high or mismatch repair-deficient metastatic CRC and for intermediate or poor-risk advanced renal cell carcinoma). Predictably, more mAb pairs or higher order oligoclonal antibodies will soon become a mainstay of oncology.

Acknowledgments

Our laboratory has been supported by the European Research Council, the Israel Science Foundation, the Israel Cancer Research Fund, and the Dr. Miriam and Sheldon G. Adelson Medical Research Foundation. I.M. and D.R. received the Sergio Lombroso Fellowship for postdoctoral cancer research. Y.Y. is the incumbent of the Harold and Zelda Goldenberg Professorial Chair. Our studies were performed in the Marvin Tanner Laboratory for Research on Cancer.

References

1. Kitano H (2007) The theory of biological robustness and its implication in cancer. Ernst Schering Res Found Workshop 61:69–88
2. Amit I, Wides R, Yarden Y (2007) Evolvable signaling networks of receptor tyrosine kinases: relevance of robustness to malignancy and to cancer therapy. Mol Syst Biol 3:151
3. Hase T, Tanaka H, Suzuki Y, Nakagawa S, Kitano H (2009) Structure of protein interaction networks and their implications on drug design. PLoS Comput Biol 5:e1000550
4. Dar AC, Das TK, Shokat KM, Cagan RL (2012) Chemical genetic discovery of targets and anti-targets for cancer polypharmacology. Nature 486:80–84
5. Mancini M, Yarden Y (2015) Mutational and network level mechanisms underlying resistance to anti-cancer kinase inhibitors. Semin Cell Dev Biol 50:164–176
6. Carvalho S, Levi-Schaffer F, Sela M, Yarden Y (2016) Immunotherapy of cancer: from monoclonal to oligoclonal cocktails of anti-cancer antibodies: IUPHAR Review 18. Br J Pharmacol 173:1407–1424
7. Kholodenko BN, Hancock JF, Kolch W (2010) Signalling ballet in space and time. Nat Rev Mol Cell Biol 11:414–426
8. Camidge DR, Pao W, Sequist LV (2014) Acquired resistance to TKIs in solid tumours: learning from lung cancer. Nat Rev Clin Oncol 11:473–481
9. Garraway LA, Janne PA (2012) Circumventing cancer drug resistance in the era of personalized medicine. Cancer Discov 2:214–226
10. Piotrowska Z, Niederst MJ, Karlovich CA, Wakelee HA, Neal JW, Mino-Kenudson M, Fulton L, Hata AN, Lockerman EL, Kalsy A, Digumarthy S, Muzikansky A, Raponi M, Garcia AR, Mulvey HE, Parks MK, DiCecca RH, Dias-Santagata D, Iafrate AJ, Shaw AT, Allen AR, Engelman JA, Sequist LV (2015) Heterogeneity underlies the emergence of EGFRT790 wild-type clones following treatment of T790M-positive cancers with a third-generation EGFR inhibitor. Cancer Discov 5:713–722
11. Hata AN et al (2016) Tumor cells can follow distinct evolutionary paths to become resistant to epidermal growth factor receptor inhibition. Nat Med 22:262–269
12. DeVita JVT, Lawrence TS, Rosenberg SA, D'ePinho RA, Weinberg RAA (2015) DeVita, Hellman, and Rosenberg's cancer: principles and practice of oncology. Wolthers Kluwer, Alphen aan den Rijn
13. Munoz-Garzon V, Rovirosa A, Ramos A (2013) Global radiation oncology waybill. Rep Pract Oncol Radiother 18:321–328
14. Hanahan D, Weinberg RA (2011) Hallmarks of cancer: the next generation. Cell 144:646–674
15. Hunter T (2007) Treatment for chronic myelogenous leukemia: the long road to imatinib. J Clin Invest 117:2036–2043
16. Troiani T, Napolitano S, Della Corte CM, Martini G, Martinelli E, Morgillo F, Ciardiello F (2016) Therapeutic value of EGFR inhibition in CRC and NSCLC: 15 years of clinical evidence. ESMO Open 1:e000088
17. Yarden Y, Pines G (2012) The ERBB network: at last, cancer therapy meets systems biology. Nat Rev Cancer 12:553–563
18. Treviño SR, Permenter AR, England MJ, Parthasarathy N, Gibbs PH, Waag DM, Chanh TC, Trevin SR (2006) Monoclonal antibodies passively protect BALB/c mice against Burkholderia mallei aerosol challenge. Infect Immun 74:1956–1961
19. Stanfield RL, Wilson IA (2009) Antibody molecular structure. In: An Z (ed) Therapeutic monoclonal antibodies: from bench to clinic. John Wiley & Sons, Inc., Hoboken, NJ
20. Köhler G, Milstein C (1975) Continuous cultures of fused cells secreting antibody of predefined specificity. Nature 256:495–497
21. Thistlethwaite JRJ, Haag BW, Gaber AO, Stuart JK, Aronson AJ, Mayes JT, Lloyd DM, FP S (1987) The use of OKT3 to treat steroid-resistant renal allograft rejection in patients receiving cyclosporine. Transplant Proc 19:1901–1904
22. Kurosawa N, Yoshioka M, Fujimoto R, Yamagishi F, Isobe M (2012) Rapid production of antigen-specific monoclonal antibodies from a variety of animals. BMC Biol 10:80
23. Reff ME, Hariharan K, Braslawsky G (2002) Future of monoclonal antibodies in the treatment of hematologic malignancies. Cancer Control 9:152–166
24. Morrison SL, Johnson MJ, Herzenberg LA, Oi VT (1984) Chimeric human antibody molecules: mouse antigen-binding domains with human constant region domains. Proc Natl Acad Sci U S A 81:6851–6855

25. Faulds D, Sorkin EM (1994) Abciximab (c7E3 Fab). A review of its pharmacology and therapeutic potential in ischaemic heart disease. Drugs 48:583–598
26. Vincenti F, Kirkman R, Light S, Bumgardner G, Pescovitz M, Halloran P, Neylan J, Wilkinson A, Ekberg H, Gaston R et al (1998) Interleukin-2-receptor blockade with daclizumab to prevent acute rejection in renal transplantation. N Engl J Med 338:161–165
27. Ahmad ZA, Yeap SK, Ali AM, Ho WY, Alitheen NBM, Hamid M (2012) ScFv antibody: principles and clinical application. *Clin Dev Immunol* 2012:1–15
28. Giusti RM, Shastri KA, Cohen MH, Keegan P, Pazdur R (2007) FDA drug approval summary: panitumumab (Vectibix). Oncologist 12:577–583
29. Fauvel B, Yasri A (2014) Antibodies directed against receptor tyrosine kinases: current and future strategies to fight cancer. MAbs 6:10–11
30. Maloney DG, Grillo-Lopez AJ, White CA, Bodkin D, Schilder RJ, Neidhart JA, Janakiraman N, Foon KA, Liles TM, Dallaire BK, Wey K, Royston I, Davis T, Levy R (1997) IDEC-C2B8 (Rituximab) anti-CD20 monoclonal antibody therapy in patients with relapsed low-grade non-Hodgkin's lymphoma. Blood 90:2188–2195
31. Shak S (1999) Overview of the trastuzumab (Herceptin) anti-HER2 monoclonal antibody clinical program in HER2-overexpressing metastatic breast cancer. Herceptin Multinational Investigator Study Group. Semin Oncol 26:71–77
32. Zafir-Lavie I, Michaeli Y, Reiter Y (2007) Novel antibodies as anticancer agents. Oncogene 26:3714–3733
33. Clynes RA, Towers TL, Presta LG, Ravetch JV (2000) Inhibitory Fc receptors modulate in vivo cytoxicity against tumor targets. Nat Med 6:443–446
34. Kim DH, Jung HD, Kim JG, Lee J-J, Yang D-H, Park YH, Do YR, Shin HJ, Kim MK, Hyun MS, Sohn SK (2006) FCGR3A gene polymorphisms may correlate with response to frontline R-CHOP therapy for diffuse large B-cell lymphoma. Blood 108:2720–2725
35. Koene HR, Kleijer M, Algra J, Roos D, von dem Borne AE, de Haas M (1997) Fc gammaRIIIa-158V/F polymorphism influences the binding of IgG by natural killer cell Fc gammaRIIIa, independently of the Fc gammaRIIIa-48L/R/H phenotype. Blood 90:1109–1114
36. Zhang W, Gordon M, Schultheis AM, Yang DY, Nagashima F, Azuma M, Chang HM, Borucka E, Lurje G, Sherrod AE, Iqbal S, Groshen S, Lenz HJ (2007) FCGR2A and FCGR3A polymorphisms associated with clinical outcome of epidermal growth factor receptor expressing metastatic colorectal cancer patients treated with single-agent cetuximab. J Clin Oncol 25:3712–3718
37. Holubec L, Polivka JJ, Safanda M, Karas M, Liska V (2016) The role of cetuximab in the induction of anticancer immune response in colorectal cancer treatment. Anti Cancer Res 36:4421–4426
38. Ben-Kasus T, Schechter B, Sela M, Yarden Y (2007) Cancer therapeutic antibodies come of age: targeting minimal residual disease. Mol Oncol 1:42–54
39. Di Gaetano N, Cittera E, Nota R, Vecchi A, Grieco V, Scanziani E, Botto M, Introna M, Golay J (2003) Complement activation determines the therapeutic activity of rituximab in vivo. J Immunol 171:1581–1587
40. Di Gaetano N, Cittera E, Nota R, Vecchi A, Grieco V, Scanziani E, Botto M, Introna M, Golay J (2006) The role of complement in the therapeutic activity of rituximab in a murine B lymphoma model homing in lymph nodes. Haematologica 91:176–183
41. Ferrara N, Hillan KJ, Gerber HP, Novotny W (2004) Discovery and development of bevacizumab, an anti-VEGF antibody for treating cancer. Nat Rev Drug Discov 3:391–400
42. Bubien JK, Zhou LJ, Bell PD, Frizzell RA, Tedder TF (1993) Transfection of the CD20 cell surface molecule into ectopic cell types generates a Ca2+ conductance found constitutively in B lymphocytes. J Cell Biol 121:1121–1132
43. Cuello M, Ettenberg SA, Clark AS, Keane MM, Posner RH, Nau MM, Dennis PA, Lipkowitz S (2001) Down-regulation of the erbB-2 receptor by trastuzumab (herceptin) enhances tumor necrosis factor-related apoptosis-inducing ligand-mediated apoptosis in breast and ovarian cancer cell lines that overexpress erbB-2. Cancer Res 61:4892–4900
44. Huang SM, Bock JM, Harari PM (1999) Epidermal growth factor receptor blockade with C225 modulates proliferation, apoptosis, and radiosensitivity in squamous cell carcinomas of the head and neck. Cancer Res 59:1935–1940
45. Marches R, Uhr JW (2004) Enhancement of the p27Kip1-mediated antiproliferative effect of trastuzumab (Herceptin) on HER2-overexpressing tumor cells. Int J Cancer 112:492–501

46. Lange T, Nentwich MF, Lüth M, Yekebas E, Schumacher U (2011) Trastuzumab has anti-metastatic and anti-angiogenic activity in a spontaneous metastasis xenograft model of esophageal adenocarcinoma. Cancer Lett 308:54–61
47. Li S, Schmitz KR, Jeffrey PD, Wiltzius JJ, Kussie P, Ferguson KM (2005) Structural basis for inhibition of the epidermal growth factor receptor by cetuximab. Cancer Cell 7:301–311
48. Sunada H, Magun BE, Mendelsohn J, MacLeod CL (1986) Monoclonal antibody against epidermal growth factor receptor is internalized without stimulating receptor phosphorylation. Proc Natl Acad Sci U S A 83:3825–3829
49. Klapper LN, Waterman H, Sela M, Yarden Y (2000) Tumor-inhibitory antibodies to HER-2/ErbB-2 may act by recruiting c-Cbl and enhancing ubiquitination of HER-2. Cancer Res 60:3384–3388
50. Klapper LN, Vaisman N, Hurwitz E, Pinkas-Kramarski R, Yarden Y, Sela M (1997) A subclass of tumor-inhibitory monoclonal antibodies to ErbB-2/HER2 blocks crosstalk with growth factor receptors. Oncogene 14:2099–2109
51. Agus DB, Akita RW, Fox WD, Lewis GD, Higgins B, Pisacane PI, Lofgren JA, Tindell C, Evans DP, Maiese K, Scher HI, Sliwkowski MX (2002) Targeting ligand-activated ErbB2 signaling inhibits breast and prostate tumor growth. Cancer Cell 2:127–137
52. Coiffier B, Lepage E, Briere J, Herbrecht R, Tilly H, Bouabdallah R, Morel P, Van Den Neste E, Salles G, Gaulard P, Reyes F, Lederlin P, Gisselbrecht C (2002) CHOP chemotherapy plus rituximab compared with CHOP alone in elderly patients with diffuse large-B-cell lymphoma. N Engl J Med 346:235–242
53. Davis TA, Grillo-López AJ, White CA, McLaughlin P, Czuczman MS, Link BK, Maloney DG, Weaver RL, Rosenberg J, Levy R (2000) Rituximab anti-CD20 monoclonal antibody therapy in non-Hodgkin's lymphoma: safety and efficacy of re-treatment. J Clin Oncol 18:3135–3143
54. Gajria D, Chandarlapaty S (2011) HER2-amplifiedbreast cancer: mechanisms of trastuzumab resistance and novel targeted therapies. Expert Rev Anticancer Ther 11:263–275
55. Esteva FJ, Yu D, Hung M-C, Hortobagyi GN (2010) Molecular predictors of response to trastuzumab and lapatinib in breast cancer. Nat Rev Clin Oncol 7:98–107
56. Pavanello F, Zucca E, Ghielmini M (2017) Rituximab: 13 open questions after 20 years of clinical use. Cancer Treat Rev 53:38–46
57. Scaltriti M, Rojo F, Ocana A, Anido J, Guzman M, Cortes J, Di Cosimo S, Matias-Guiu X, Ramon y Cajal S, Arribas J, Baselga J (2007) Expression of p95HER2, a truncated form of the HER2 receptor, and response to anti-HER2 therapies in breast cancer. J Natl Cancer Inst 99:628–638
58. Nagy P, Friedlander E, Tanner M, Kapanen AI, Carraway KL, Isola J, Jovin TM (2005) Decreased accessibility and lack of activation of ErbB2 in JIMT-1, a herceptin-resistant, MUC4-expressing breast cancer cell line. Cancer Res 65:473–482
59. Lievre A, Bachet JB, Le Corre D, Boige V, Landi B, Emile JF, Cote JF, Tomasic G, Penna C, Ducreux M, Rougier P, Penault-Llorca F, Laurent-Puig P (2006) KRAS mutation status is predictive of response to cetuximab therapy in colorectal cancer. Cancer Res 66:3992–3995
60. Mancini M, Gaborit N, Lindzen M, Salame TM, Dall'Ora M, Sevilla-Sharon M, Abdul-Hai A, Downward J, Yarden Y (2015) Combining three antibodies nullifies feedback-mediated resistance to erlotinib in lung cancer. Sci Signal 8:ra53
61. Lu Y, Zi X, Zhao Y, Mascarenhas D, Pollak M (2001) Insulin-like growth factor-I receptor signaling and resistance to trastuzumab (Herceptin). J Natl Cancer Inst 93:1852–1857
62. Shattuck DL, Miller JK, Carraway KL III, Sweeney C (2008) Met receptor contributes to trastuzumab resistance of Her2-overexpressing breast cancer cells. Cancer Res 68:1471–1477
63. Berns K, Horlings HM, Hennessy BT, Madiredjo M, Hijmans EM, Beelen K, Linn SC, Gonzalez-Angulo AM, Stemke-Hale K, Hauptmann M, Beijersbergen RL, Mills GB, van de Vijver MJ, Bernards R (2007) A functional genetic approach identifies the PI3K pathway as a major determinant of trastuzumab resistance in breast cancer. Cancer Cell 12:395–402
64. Marshall MJE, Stopforth RJ, Cragg MS (2017) Therapeutic antibodies: what have we learnt from targeting CD20 and where are we going? Front Immunol 8:1245
65. Salles G, Barrett M, Foa R, Maurer J, O'Brien S, Valente N, Wenger M, Maloney DG (2017) Rituximab in B-cell hematologic malignancies: a review of 20 years of clinical experience. Adv Ther 34:2232–2273

66. Hiraga J, Tomita A, Sugimoto T, Shimada K, Ito M, Nakamura S, Kiyoi H, Kinoshita T, Naoe T (2009) Down-regulation of CD20 expression in B-cell lymphoma cells after treatment with rituximab-containing combination chemotherapies: its prevalence and clinical significance. Blood 113:4885–4893
67. Czuczman MS, Olejniczak S, Gowda A, Kotowski A, Binder A, Kaur H, Knight J, Starostik P, Deans J, FJ H-I (2008) Acquirement of rituximab resistance in lymphoma cell lines is associated with both global CD20 gene and protein down-regulation regulated at the pretranscriptional and posttranscriptional levels. Clin Cancer Res 14:1561–1570
68. Goede V, Klein C, Stilgenbauer S (2015) Obinutuzumab (GA101) for the treatment of chronic lymphocytic leukemia and other B-cell non-Hodgkin's lymphomas: a glycoengineered type II CD20 antibody. Oncol Res Treat 38:185–192
69. Slamon DJ, Godolphin W, Jones LA, Holt JA, Wong SG, Keith DE, Levin WJ, Stuart SG, Udove J, Ullrich A et al (1989) Studies of the HER-2/neu proto-oncogene in human breast and ovarian cancer. Science 244:707–712
70. Carter PJ (2006) Potent antibody therapeutics by design. Nat Rev Immunol 6:343–357
71. Dean-Colomb W, Esteva FJ (2008) Her2-positive breast cancer: herceptin and beyond. Eur J Cancer (Oxford) 1990(44):2806–2812
72. Vu T, Claret FX (2012) Trastuzumab: updated mechanisms of action and resistance in breast cancer. Front Oncol 18:62–81
73. Franklin MC, Carey KD, Vajdos FF, Leahy DJ, de Vos AM, Sliwkowski MX (2004) Insights into ErbB signaling from the structure of the ErbB2-pertuzumab complex. Cancer Cell 5:317–328
74. Schneider MR, Yarden Y (2016) The EGFR-HER2 module: a stem cell approach to understanding a prime target and driver of solid tumors. Oncogene 35:2949–2960
75. Bronte G, Silvestris N, Castiglia M, Galvano A, Passiglia F, Sortino G, Cicero G, Rolfo C, Peeters M, Bazan V, Fanale D, Giordano A, Russo A (2015) New findings on primary and acquired resistance to anti-EGFR therapy in metastatic colorectal cancer: do all roads lead to RAS? Oncotarget 6:24780–24796
76. Vermorken JB, Mesia R, Rivera F, Remenar E, Kawecki A, Rottey S, Erfan J, Zabolotnyy D, Kienzer HR, Cupissol D, Peyrade F, Benasso M, Vynnychenko I, De Raucourt D, Bokemeyer C, Schueler A, Amellal N, Hitt R (2008) Platinum-based chemotherapy plus cetuximab in head and neck cancer. N Engl J Med 359:1116–1127
77. Spangler JB, Neil JR, Abramovitch S, Yarden Y, White FM, Lauffenburger DA, Wittrup KD (2010) Combination antibody treatment down-regulates epidermal growth factor receptor by inhibiting endosomal recycling. Proc Natl Acad Sci U S A 107:13252–13257
78. Park K, Cho EK, Bello M, Ahn M-J, Thongprasert S, Song E-K, Soldatenkova V, Depenbrock H, Puri T, Orlando M (2017) Efficacy and safety of first-line necitumumab plus gemcitabine and cisplatin versus gemcitabine and cisplatin in East Asian patients with stage IV squamous non-small cell lung cancer: a subgroup analysis of the phase 3, open-label, randomized SQUIRE study. Cancer Res Treat 49:937–946
79. Ferrara N, Kerbel RS (2005) Angiogenesis as a therapeutic target. Nature 438:967–974
80. Seddon AN, Cuellar S, Haaf CM (2014) The life, death, and attempted rebirth of bevacizumab in breast cancer. J Oncol Pharm Pract 20:433–444
81. Dunn GP, Old LJ, Schreiber RD (2004) The three Es of cancer immunoediting. Annu Rev Immunol 22:329–360
82. Leach DR, Krummel MF, Allison JP (1996) Enhancement of antitumor immunity by CTLA-4 blockade. Science (New York, NY) 271:1734–1736
83. Chambers CA, Kuhns MS, Egen JG, Allison JP (2001) CTLA-4-mediated inhibition in regulation of T cell responses: mechanisms and manipulation in tumor immunotherapy. Annu Rev Immunol 19:565–594
84. Robert C, Thomas L, Bondarenko I, O'Day S, Weber J, Garbe C, Lebbe C, Baurain J-F, Testori A, Grob J-J, Davidson N, Richards J, Maio M, Hauschild A, Miller WH Jr, Gascon P, Lotem M, Harmankaya K, Ibrahim R, Francis S, Chen T-T, Humphrey R, Hoos A, Wolchok JD (2011) Ipilimumab plus dacarbazine for previously untreated metastatic melanoma. N Engl J Med 364:2517–2526
85. Postow MA, Sidlow R, Hellmann MD (2018) Immune-related adverse events associated with immune checkpoint blockade. N Engl J Med 378:158–168
86. Dong H, Strome SE, Salomao DR, Tamura H, Hirano F, Flies DB, Roche PC, Lu J, Zhu G, Tamada K, Lennon VA, Celis E, Chen L (2002) Tumor-associated B7-H1 promotes T-cell apoptosis: a potential mechanism of immune evasion. Nat Med 8:793–800

87. Iwai Y, Ishida M, Tanaka Y, Okazaki T, Honjo T, Minato N (2002) Involvement of PD-L1 on tumor cells in the escape from host immune system and tumor immunotherapy by PD-L1 blockade. Proc Natl Acad Sci U S A 99:12293–12297
88. Topalian SL, Sznol M, McDermott DF, Kluger HM, Carvajal RD, Sharfman WH, Brahmer JR, Lawrence DP, Atkins MB, Powderly JD, Leming PD, Lipson EJ, Puzanov I, Smith DC, Taube JM, Wigginton JM, Kollia GD, Gupta A, Pardoll DM, Sosman JA, Hodi FS (2014) Survival, durable tumor remission, and long-term safety in patients with advanced melanoma receiving nivolumab. J Clin Oncol 32:1020–1030
89. Brahmer J et al (2015) Nivolumab versus docetaxel in advanced squamous-cell non-small-cell lung cancer. N Engl J Med 373:123–135
90. Motzer RJ et al (2015) Nivolumab versus Everolimus in advanced renal-cell carcinoma. N Engl J Med 373:1803–1813
91. Sharma P, Retz M, Siefker-Radtke A, Baron A, Necchi A, Bedke J, Plimack ER, Vaena D, Grimm M-O, Bracarda S, Arranz JA, Pal S, Ohyama C, Saci A, Qu X, Lambert A, Krishnan S, Azrilevich A, Galsky MD (2017) Nivolumab in metastatic urothelial carcinoma after platinum therapy (CheckMate 275): a multicentre, single-arm, phase 2 trial. Lancet Oncol 18:312–322
92. Ansell SM, Lesokhin AM, Borrello I, Halwani A, Scott EC, Gutierrez M, Schuster SJ, Millenson MM, Cattry D, Freeman GJ, Rodig SJ, Chapuy B, Ligon AH, Zhu L, Grosso JF, Kim SY, Timmerman JM, Shipp MA, Armand P (2015) PD-1 blockade with nivolumab in relapsed or refractory Hodgkin's lymphoma. N Engl J Med 372:311–319
93. Ribas A, Wolchok JD (2018) Cancer immunotherapy using checkpoint blockade. Science (New York, NY) 359:1350–1355
94. Kahl B (2008) Chemotherapy combinations with monoclonal antibodies in non-Hodgkin's lymphoma. Semin Hematol 45:90–94
95. Slamon DJ, Leyland-Jones B, Shak S, Fuchs H, Paton V, Bajamonde A, Fleming T, Eiermann W, Wolter J, Pegram M, Baselga J, Norton L (2001) Use of chemotherapy plus a monoclonal antibody against HER2 for metastatic breast cancer that overexpresses HER2. N Engl J Med 344:783–792
96. Bonner JA, Harari PM, Giralt J, Azarnia N, Shin DM, Cohen RB, Jones CU, Sur R, Raben D, Jassem J, Ove R, Kies MS, Baselga J, Youssoufian H, Amellal N, Rowinsky EK, Ang KK (2006) Radiotherapy plus cetuximab for squamous-cell carcinoma of the head and neck. N Engl J Med 354:567–578
97. Younes A, Gopal AK, Smith SE, Ansell SM, Rosenblatt JD, Savage KJ, Ramchandren R, Bartlett NL, Cheson BD, de Vos S, Forero-Torres A, Moskowitz CH, Connors JM, Engert A, Larsen EK, Kennedy DA, Sievers EL, Chen R (2012) Results of a pivotal phase II study of brentuximab vedotin for patients with relapsed or refractory Hodgkin's lymphoma. J Clin Oncol 30:2183–2189
98. Pro B, Advani R, Brice P, Bartlett NL, Rosenblatt JD, Illidge T, Matous J, Ramchandren R, Fanale M, Connors JM, Yang Y, Sievers EL, Kennedy DA, Shustov A (2012) Brentuximab vedotin (SGN-35) in patients with relapsed or refractory systemic anaplastic large-cell lymphoma: results of a phase II study. J Clin Oncol 30:2190–2196
99. Verma S, Miles D, Gianni L, Krop IE, Welslau M, Baselga J, Pegram M, Oh DY, Dieras V, Guardino E, Fang L, Lu MW, Olsen S, Blackwell K (2012) Trastuzumab emtansine for HER2-positive advanced breast cancer. N Engl J Med 367:1783–1791
100. Zhong W-Z, Zhou Q, Wu Y-L (2017) The resistance mechanisms and treatment strategies for EGFR-mutant advanced non-small-cell lung cancer. Oncotarget 8:71358–71370
101. Kobayashi S, Boggon TJ, Dayaram T, Janne PA, Kocher O, Meyerson M, Johnson BE, Eck MJ, Tenen DG, Halmos B (2005) EGFR mutation and resistance of non-small-cell lung cancer to gefitinib. N Engl J Med 352:786–792
102. Bean J, Brennan C, Shih JY, Riely G, Viale A, Wang L, Chitale D, Motoi N, Szoke J, Broderick S, Balak M, Chang WC, Yu CJ, Gazdar A, Pass H, Rusch V, Gerald W, Huang SF, Yang PC, Miller V, Ladanyi M, Yang CH, Pao W (2007) MET amplification occurs with or without T790M mutations in EGFR mutant lung tumors with acquired resistance to gefitinib or erlotinib. Proc Natl Acad Sci U S A 104:20932–20937
103. Sos ML, Koker M, Weir BA, Heynck S, Rabinovsky R, Zander T, Seeger JM, Weiss J, Fischer F, Frommolt P, Michel K, Peifer M, Mermel C, Girard L, Peyton M, Gazdar AF, Minna JD, Garraway LA, Kashkar H, Pao W, Meyerson M, Thomas RK (2009) PTEN loss contributes to erlotinib resistance in EGFR-mutant lung cancer by activation of Akt and EGFR. Cancer Res 69:3256–3261
104. Huang S, Armstrong EA, Benavente S, Chinnaiyan P, Harari PM (2004) Dual-agent molecular targeting of the epidermal growth factor receptor (EGFR): combining anti-

EGFR antibody with tyrosine kinase inhibitor. Cancer Res 64:5355–5362

105. El Guerrab A, Bamdad M, Kwiatkowski F, Bignon Y-J, Penault-Llorca F, Aubel C (2016) Anti-EGFR monoclonal antibodies and EGFR tyrosine kinase inhibitors as combination therapy for triple-negative breast cancer. Oncotarget 7:73618–73637
106. Mancini M, Gal H, Gaborit N, Mazzeo L, Romaniello D, Salame TM, Lindzen M, Mahlknecht G, Enuka Y, Burton DG, Roth L, Noronha A, Marrocco I, Adreka D, Altstadter RE, Bousquet E, Downward J, Maraver A, Krizhanovsky V, Yarden Y (2017) An oligoclonal antibody durably overcomes resistance of lung cancer to third-generation EGFR inhibitors. EMBO Mol Med 10:294–308
107. Spigel DR, Edelman MJ, O'Byrne K, Paz-Ares L, Mocci S, Phan S, Shames DS, Smith D, Yu W, Paton VE, Mok T (2017) Results from the phase III randomized trial of onartuzumab plus erlotinib versus erlotinib in previously treated stage IIIB or IV non-small-cell lung cancer: METLung. J Clin Oncol 35:412–420
108. Herbst RS, O'Neill VJ, Fehrenbacher L, Belani CP, Bonomi PD, Hart L, Melnyk O, Ramies D, Lin M, Sandler A (2007) Phase II study of efficacy and safety of bevacizumab in combination with chemotherapy or erlotinib compared with chemotherapy alone for treatment of recurrent or refractory non small-cell lung cancer. J Clin Oncol 25:4743–4750
109. Rosell R et al (2017) Erlotinib and bevacizumab in patients with advanced non-small-cell lung cancer and activating EGFR mutations (BELIEF): an international, multicentre, single-arm, phase 2 trial. Lancet Respir Med 5:435–444
110. Xia W, Mullin RJ, Keith BR, Liu LH, Ma H, Rusnak DW, Owens G, Alligood KJ, Spector NL (2002) Anti-tumor activity of GW572016: a dual tyrosine kinase inhibitor blocks EGF activation of EGFR/erbB2 and downstream Erk1/2 and AKT pathways. Oncogene 21:6255–6263
111. Ahn ER, Vogel CL (2012) Dual HER2-targeted approaches in HER2-positive breast cancer. Breast Cancer Res Treat 131:371–383
112. Mosesson Y, Mills GB, Yarden Y (2008) Derailed endocytosis: an emerging feature of cancer. Nat Rev Cancer 8:835–850
113. Abella JV, Park M (2009) Breakdown of endocytosis in the oncogenic activation of receptor tyrosine kinases. Am J Physiol Endocrinol Metab 296:E973–E984
114. Fan Z, Masui H, Altas I, Mendelsohn J (1993) Blockade of epidermal growth factor receptor function by bivalent and monovalent fragments of 225 anti-epidermal growth factor receptor monoclonal antibodies. Cancer Res 53:4322–4328
115. Drebin JA, Link VC, Greene MI (1988) Monoclonal antibodies reactive with distinct domains of the neu oncogene-encoded p185 molecule exert synergistic anti-tumor effects in vivo. Oncogene 2:273–277
116. Spiridon CI, Ghetie MA, Uhr J, Marches R, Li JL, Shen GL, Vitetta ES (2002) Targeting multiple Her-2 epitopes with monoclonal antibodies results in improved antigrowth activity of a human breast cancer cell line in vitro and in vivo. Clin Cancer Res 8:1720–1730
117. Kasprzyk PG, Song SU, Di Fiore PP, King CR (1992) Therapy of an animal model of human gastric cancer using a combination of anti-erbB-2 monoclonal antibodies. Cancer Res 52:2771–2776
118. Ben-Kasus T, Schechter B, Lavi S, Yarden Y, Sela M (2009) Persistent elimination of ErbB-2/HER2-overexpressing tumors using combinations of monoclonal antibodies: relevance of receptor endocytosis. Proc Natl Acad Sci U S A 106:3294–3299
119. Friedman LM, Rinon A, Schechter B, Lyass L, Lavi S, Bacus SS, Sela M, Yarden Y (2005) Synergistic down-regulation of receptor tyrosine kinases by combinations of mAbs: implications for cancer immunotherapy. Proc Natl Acad Sci U S A 102:1915–1920
120. Junttila TT, Akita RW, Parsons K, Fields C, Lewis Phillips GD, Friedman LS, Sampath D, Sliwkowski MX (2009) Ligand-independent HER2/HER3/PI3K complex is disrupted by trastuzumab and is effectively inhibited by the PI3K inhibitor GDC-0941. Cancer Cell 15:429–440
121. Nahta R, Hung MC, Esteva FJ (2004) The HER-2-targeting antibodies trastuzumab and pertuzumab synergistically inhibit the survival of breast cancer cells. Cancer Res 64:2343–2346
122. Scheuer W, Friess T, Burtscher H, Bossenmaier B, Endl J, Hasmann M (2009) Strongly enhanced antitumor activity of trastuzumab and pertuzumab combination treatment on HER2-positive human xenograft tumor models. Cancer Res 69:9330–9336
123. Swain SM, Baselga J, Kim SB, Ro J, Semiglazov V, Campone M, Ciruelos E, Ferrero JM, Schneeweiss A, Heeson S, Clark E, Ross G, Benyunes MC, Cortes J, Group CS (2015) Pertuzumab, trastuzumab, and

docetaxel in HER2-positive metastatic breast cancer. N Engl J Med 372:724–734

124. Swain SM, Kim S-B, Cortes J, Ro J, Semiglazov V, Campone M, Ciruelos E, Ferrero J-M, Schneeweiss A, Knott A, Clark E, Ross G, Benyunes MC, Baselga J (2013) Pertuzumab, trastuzumab, and docetaxel for HER2-positive metastatic breast cancer (CLEOPATRA study): overall survival results from a randomised, double-blind, placebo-controlled, phase 3 study. Lancet Oncol 14:461–471
125. Gianni L, Eiermann W, Semiglazov V, Lluch A, Tjulandin S, Zambetti M, Moliterni A, Vazquez F, Byakhov MJ, Lichinitser M, Climent MA, Ciruelos E, Ojeda B, Mansutti M, Bozhok A, Magazzu D, Heinzmann D, Steinseifer J, Valagussa P, Baselga J (2014) Neoadjuvant and adjuvant trastuzumab in patients with HER2-positive locally advanced breast cancer (NOAH): follow-up of a randomised controlled superiority trial with a parallel HER2-negative cohort. Lancet Oncol 15:640–647
126. von Minckwitz G et al (2017) Adjuvant pertuzumab and trastuzumab in early HER2-positive breast cancer. N Engl J Med 377:122–131
127. Jaramillo ML, Leon Z, Grothe S, Paul-Roc B, Abulrob A, O'Connor McCourt M (2006) Effect of the anti-receptor ligand-blocking 225 monoclonal antibody on EGF receptor endocytosis and sorting. Exp Cell Res 312:2778–2790
128. Pedersen MW, Jacobsen HJ, Koefoed K, Hey A, Pyke C, Haurum JS, Kragh M (2010) Sym004: a novel synergistic anti-epidermal growth factor receptor antibody mixture with superior anticancer efficacy. Cancer Res 70:588–597
129. Dienstmann R, Patnaik A, Garcia-Carbonero-R, Cervantes A, Benavent M, Rosello S, Tops BB, van der Post RS, Argiles G, Skartved NJ, Hansen UH, Hald R, Pedersen MW, Kragh M, Horak ID, Braun S, Van Cutsem E, Tolcher AW, Tabernero J (2015) Safety and activity of the first-in-class Sym004 anti-EGFR antibody mixture in patients with refractory colorectal cancer. Cancer Discov 5:598–609
130. Montagut C et al (2018) Efficacy of Sym004 in patients with metastatic colorectal cancer with acquired resistance to anti-EGFR therapy and molecularly selected by circulating tumor DNA analyses: a phase 2 randomized clinical trial. JAMA Oncol 4:e175245
131. Vigna E, Comoglio PM (2014) Targeting the oncogenic Met receptor by antibodies and gene therapy. Oncogene 34:1883–1889
132. Kawakami H, Okamoto I, Arao T, Okamoto W, Matsumoto K, Taniguchi H, Kuwata K, Yamaguchi H, Nishio K, Nakagawa K, Yamada Y (2013) MET amplification as a potential therapeutic target in gastric cancer. Oncotarget 4:9–17
133. Dimou A, Non L, Chae YK, Tester WJ, Syrigos KN (2014) MET gene copy number predicts worse overall survival in patients with non-small cell lung cancer (NSCLC); a systematic review and meta-analysis. PLoS One 9:e107677
134. Grandal MM, Havrylov S, Poulsen TT, Koefoed K, Dahlman A, Galler GR, Conrotto P, Collins S, Eriksen KW, Kaufman D, Woude GFV, Jacobsen HJ, Horak ID, Kragh M, Lantto J, Bouquin T, Park M, Pedersen MW (2017) Simultaneous targeting of two distinct epitopes on MET effectively inhibits MET- and HGF-driven tumor growth by multiple mechanisms. Mol Cancer Ther 16:2780–2791
135. Chandarlapaty S, Sawai A, Scaltriti M, Rodrik-Outmezguine V, Grbovic-Huezo O, Serra V, Majumder PK, Baselga J, Rosen N (2011) AKT inhibition relieves feedback suppression of receptor tyrosine kinase expression and activity. Cancer Cell 19:58–71
136. Wheeler DL, Huang S, Kruser TJ, Nechrebecki MM, Armstrong EA, Benavente S, Gondi V, Hsu KT, Harari PM (2008) Mechanisms of acquired resistance to cetuximab: role of HER (ErbB) family members. Oncogene 27:3944–3956
137. Iida M, Bahrar H, Brand TM, Pearson HE, Coan JP, Orbuch RA, Flanigan BG, Swick AD, Prabakaran PJ, Lantto J, Horak ID, Kragh M, Salgia R, Kimple RJ, DL W (2016) Targeting the HER family with pan-HER effectively overcomes resistance to cetuximab. Mol Cancer Ther 15:2175–2186
138. Iida M, Brand TM, Starr MM, Huppert EJ, Luthar N, Bahrar H, Coan JP, Pearson HE, Salgia R, Wheeler DL (2014) Overcoming acquired resistance to cetuximab by dual targeting HER family receptors with antibody-based therapy. Mol Cancer 13:242
139. Gaborit N, Lindzen M, Yarden Y (2016) Emerging anti-cancer antibodies and combination therapies targeting HER3/ERBB3. Hum Vaccin Immunother 12:576–592
140. Mukai H, Saeki T, Aogi K, Naito Y, Matsubara N, Shigekawa T, Ueda S, Takashima S, Hara F, Yamashita T, Ohwada S, Sasaki Y (2016) Patritumab plus trastuzumab and paclitaxel in human epidermal growth factor receptor 2-overexpressing metastatic breast cancer. Cancer Sci 107:1465–1470

141. Wei SC, Levine JH, Cogdill AP, Zhao Y, Anang N-AAS, Andrews MC, Sharma P, Wang J, Wargo JA, Pe'er D, Allison JP (2017) Distinct cellular mechanisms underlie anti-CTLA-4 and anti-PD-1 checkpoint blockade. Cell 170:1120–1133.e17

142. Wolchok JD, Kluger H, Callahan MK, Postow MA, Rizvi NA, Lesokhin AM, Segal NH, Ariyan CE, Gordon RA, Reed K, Burke MM, Caldwell A, Kronenberg SA, Agunwamba BU, Zhang X, Lowy I, Inzunza HD, Feely W, Horak CE, Hong Q, Korman AJ, Wigginton JM, Gupta A, Sznol M (2013) Nivolumab plus ipilimumab in advanced melanoma. N Engl J Med 369:122–133

143. Postow MA, Chesney J, Pavlick AC, Robert C, Grossmann K, McDermott D, Linette GP, Meyer N, Giguere JK, Agarwala SS, Shaheen M, Ernstoff MS, Minor D, Salama AK, Taylor M, Ott PA, Rollin LM, Horak C, Gagnier P, Wolchok JD, Hodi FS (2015) Nivolumab and ipilimumab versus ipilimumab in untreated melanoma. N Engl J Med 372:2006–2017

144. Hellmann MD, Ciuleanu T-E, Pluzanski A, Lee JS, Otterson GA, Audigier-Valette C, Minenza E, Linardou H, Burgers S, Salman P, Borghaei H, Ramalingam SS, Brahmer J, Reck M, O'Byrne KJ, Geese WJ, Green G, Chang H, Szustakowski J, Bhagavatheeswaran P, Healey D, Fu Y, Nathan F, Paz-Ares L (2018) Nivolumab plus ipilimumab in lung cancer with a high tumor mutational burden. N Engl J Med 378:2093–2104

145. Larkin J et al (2015) Combined nivolumab and ipilimumab or monotherapy in untreated melanoma. N Engl J Med 373:23–34

146. Schadendorf D, Wolchok JD, Hodi FS, Chiarion-Sileni V, Gonzalez R, Rutkowski P, Grob J-J, Cowey CL, Lao CD, Chesney J, Robert C, Grossmann K, McDermott D, Walker D, Bhore R, Larkin J, MA P (2017) efficacy and safety outcomes in patients with advanced melanoma who discontinued treatment with nivolumab and ipilimumab because of adverse events: a pooled analysis of randomized phase II and III trials. J Clin Oncol 35:3807–3814

147. Krishnamurthy A, Jimeno A (2018) Bispecific antibodies for cancer therapy: a review. Pharmacol Ther 185:122–134

148. Wu J, Fu J, Zhang M, Liu D (2015) Blinatumomab: a bispecific T cell engager (BiTE) antibody against CD19/CD3 for refractory acute lymphoid leukemia. J Hematol Oncol 8:104

Chapter 3

IgM Natural Autoantibodies in Physiology and the Treatment of Disease

Mahboobeh Fereidan-Esfahani, Tarek Nayfeh, Arthur Warrington, Charles L. Howe, and Moses Rodriguez

Abstract

Antibodies are vital components of the adaptive immune system for the recognition and response to foreign antigens. However, some antibodies recognize self-antigens in healthy individuals. These autoreactive antibodies may modulate innate immune functions. IgM natural autoantibodies (IgM-NAAs) are a class of primarily polyreactive immunoglobulins encoded by germline V-gene segments which exhibit low affinity but broad specificity to both foreign and self-antigens. Historically, these autoantibodies were closely associated with autoimmune disease. Nevertheless, not all human autoantibodies are pathogenic and compelling evidence indicates that IgM-NAAs may exert a spectrum of effects from injurious to protective depending upon cellular and molecular context. In this chapter, we review the current state of knowledge regarding the potential physiological and therapeutic roles of IgM-NAAs in different disease conditions such as atherosclerosis, cancer, and autoimmune disease. We also describe the discovery of two reparative IgM-NAAs by our laboratory and delineate their proposed mechanisms of action in central nervous system (CNS) disease.

Key words IgM, Natural, Autoantibody, Physiology, Atherosclerosis, Cancer, Central nervous system, Multiple sclerosis, Remyelination, Oligodendrocyte, B-1a

1 Introduction

B cells produce immunoglobulins (Igs) as one of the essential components of the adaptive immune response. Immunoglobulins are classified by five isotypes, namely IgG, IgM, IgA, IgE, and IgD, that mediate a variety of functions involving identification and neutralization of pathogens through interactions with isotype-specific Fc receptors and downstream activation of the complement system [1, 2].

An autoantibody is defined as an Ig directed against self-antigens [3]. The first report of the presence of autoantibodies in humans was published in the early 1900s [4]. Paul Eherlich described the concept of natural autoantibodies (NAAs). He was awarded the Nobel Prize in Physiology or Medicine in 1908 in part

Michael Steinitz (ed.), *Human Monoclonal Antibodies: Methods and Protocols*, Methods in Molecular Biology, vol. 1904, https://doi.org/10.1007/978-1-4939-8958-4_3,

based on his hypothesis that healthy individuals produced antibodies to all potential non-self-antigens even before immune exposure [5]. Since then, several efforts have been made to characterize the nature of these antibodies. The term "natural" derives from the fact that the antibodies arise spontaneously without specific immunization and exist independently of exposure to foreign antigens. Studies show that such antibodies exist even in mice raised under germ-free conditions [6]. Moreover, these Igs fulfill the definition of "autoantibody," since they are self-reactive but not self-specific.

NAAs are primarily polyreactive and are encoded by germline V-gene segments, with low affinity but broad specificity to both foreign and self-antigens [7]. Historically, autoreactive autoantibodies were thought to be primarily associated with autoimmune disease. However, compelling evidence indicates that not all human autoantibodies are pathogenic. Based on the context in which NAAs encounter antigenic targets, these Igs have the specific ability to exert either physiological or pathological effector functions. Although NAAs may belong to all Ig isotypes, self-reactive IgM antibodies are common in healthy individuals and are already present in the cord blood of human newborns [8, 9]. These low-affinity natural IgM autoantibodies usually lack N-region additions and are germline-encoded or exhibit minimal somatic hypermutation [10]. In contrast, pathogenic NAAs found in adults are predominantly high-affinity, somatically mutated IgGs that may result from failure of counter selection processes against specific autoantigens (Table 1).

2 IgM-NAA Properties

The IgM isotype is one of the most abundant Ig classes in the body. The molecular weight of monomeric IgM is 190 kDa, but the predominant form of circulating IgM is a closed ring (pentameric) composed of five 7S subunits and a J chain forming a macromolecule of about 970 kDa. In healthy individuals, circulating polyclonal IgM is generally present at a concentration of 1–2 mg/ml of blood, with a half-life of about 5 days [11]. The following receptors have been recognized as binding sites for IgM:

(a) *Complement receptors (CR)* are expressed widely by many different cell types. For example, B cells express cell surface complement receptor type 1 (CR1/CD35) and complement receptor type 2 (CR2/CD21) which can bind to IgM-antigen complexes that have aggregated activated complement molecules [12].

(b) *Fcα/μ Receptors (Fcα/μR)* are type I transmembrane proteins that bind both IgA and IgM isotypes [13]. These receptors are constitutively expressed on marginal zone B lymphocytes,

Table 1
Characteristics of natural autoantibodies versus pathogenic autoantibodies

Features	Natural autoantibodies	Pathogenic autoantibodies
Serum titer	Low	High
Isotype	IgM > IgG > IgA	IgG > IgM > IgA
Antigen specificity	Low	High
Sequence	Germline or near germline with few somatic mutations, no affinity maturation	Somatically mutated, affinity maturated

follicular dendritic cells and binding of IgM to these cells may suppress germinal center formation, affinity maturation, and memory B-cell generation in response to T-cell-independent antigen challenge [14].

(c) *Polymeric Ig receptors(poly-IgR)* are expressed on epithelial cells and bind polymeric IgA and IgM via the J-chain. These receptors mediate transport of polymeric J-chain-containing Ig at mucosal sites [15, 16].

(d) *FAIM3/TOSO receptors* were initially identified as "Fas apoptosis inhibitory molecule 3" (FAIM3) [17]. However, these receptors were recently rediscovered as an IgM-specific Fc receptor or *FcμR*. *FcμR* is the only identified receptor that binds exclusively to the Fc portion of pentameric IgM with high affinity [17]. This receptor is present on a variety of cell types such as macrophages, dendritic cells, and T cells, with highest expression observed in B cells [18, 19]. Binding of IgM, especially pentameric IgM, to this receptor enhances B and T-cell cooperation and increases antibody-dependent cell-mediated cytotoxicity and complement activation [20, 21]. Signaling pathways engaged by FcμR are still poorly understood but warrant further study.

(e) *Sialic acid-binding immunoglobulin-like lectins* such as Siglec-G and CD22 are expressed on B-cell membranes and bind sialic acid residues on IgM, resulting in inhibition of downstream B-cell receptor (BCR) signaling [22, 23]. CD22, an inhibitory co-receptor on B cells, also plays a role as a receptor for the glycoconjugates on soluble IgM via its sialoprotein-binding domain. The absence of either Siglec-G or CD22 alone does not lead to autoimmune disease development, but the lack of both receptors results in spontaneous lupus-like disease in mice [23]. In the absence of these receptors, B cells become hyperactive due to increased BCR signaling, leading to development of autoimmune disease [24, 25].

3 Role of B-1a Cells as the Source of IgM-NAA

Determining and subsequently examining the source of NAA has been the subject of intense research since the late 1960s. The B-lineage compartment includes two main B-cell subsets: B-1 cells that constitutively produce NAAs which are most often of the IgM isotype; and B-2 cells that are recruited into T-cell-dependent germinal centers upon protein antigen exposure (Fig. 1) [26, 27]. Many studies discuss differences between these cell populations, regarding ontogeny, anatomical localization, antibody repertoire, antigen stimulus, and role in the immune response [21, 28]. B-2 cells are produced in the bone marrow from hematopoietic stem cells (HSCs) and migrate to secondary lymphoid

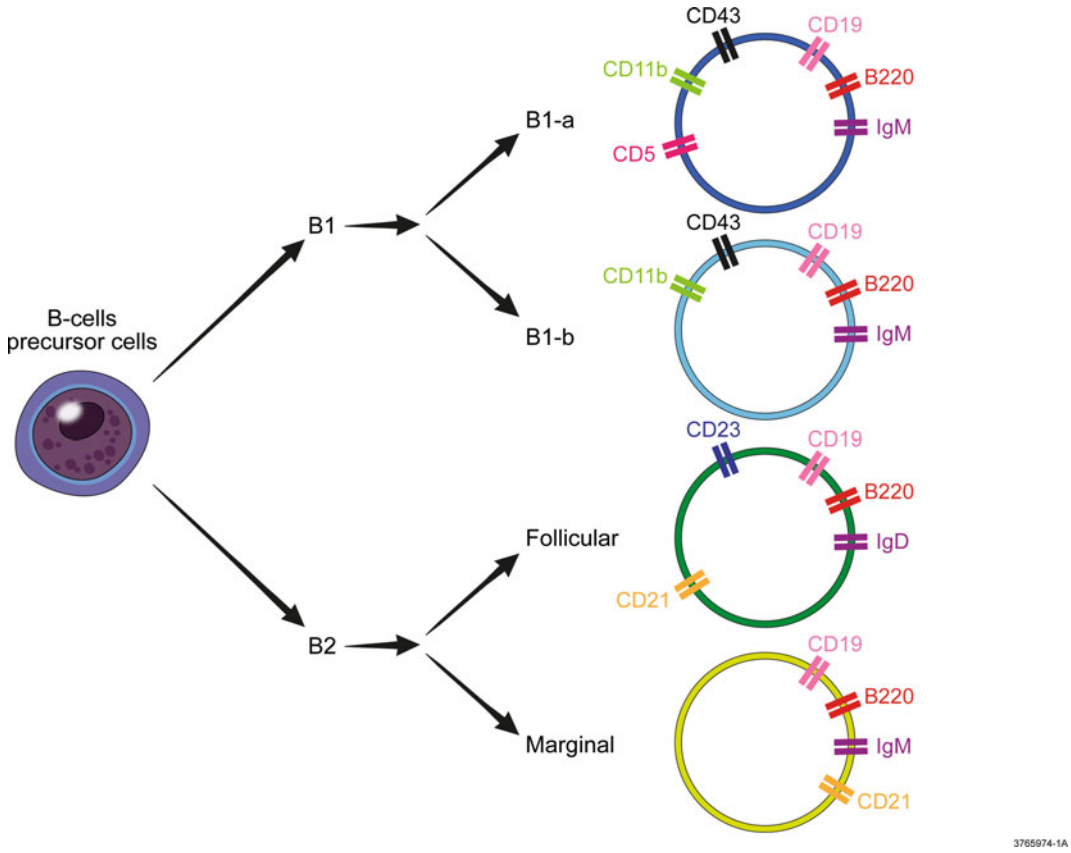

Fig. 1 B-cells CD markers in mice: The B-lineage compartment includes B-1 and B2 cells. B-1 constitutively produce natural autoantibodies which are mainly IgM, but can be IgG and IgA isotypes; B-1a cells that express CD5 have long been considered the major source of natural IgM. Marginal zone B cells are responsible for response to encapsulated organisms and their non-protein antigens; and follicular B cells are recruited into T-cell-dependent germinal centers upon protein antigen exposure. Marginal zone B cells and B1 cells have shared IgM specificities, but it is unclear to what extent splenic marginal zone B cells contribute to natural IgM production

organs as immature B cells where they differentiate into follicular and marginal zone B cells [29]. The majority of B-1 cells reside in peritoneal and pleural cavities and constitute only a small fraction of B cells in the spleen [30]. B-1 cells originate and develop primarily during the fetal stage from distinct B-2 cell precursors [31, 32]. In mice, B-1 cells are distinguished from B-2 cells by surface expression of CD5 (pan-T cell marker), CD11b, high IgM, low IgD, and the absence of CD23 [33, 34]. In addition, CD5 expression also subdivides B-1 cells into two different subsets: B-1a cells, which are $CD5^+$, and B-1b cells, which are $CD5^-$ (Fig. 2) [33, 35]. However, identification of the human counterpart for these cell types has been controversial. A study by Ghosen et al. [36] reported $CD20^+CD27^+CD43^+$ memory B cells as the human B-1 cell equivalent. They also showed that HSCs sorted from adult mice bone marrow and transferred to lethally irradiated recipients evidently give rise to B-2 and B-1b cells but do not detectably reconstitute B-1a cells [36]. These data suggest that B-1a cells are a separate B-cell lineage that is distinct from B-2 cells and B-1b cells in humans.

B-1a cells specialize in the recognition of diverse antigens. Consequently, they provide distinct immune effector functions, such as a T-cell-independent rapid response to antigens and production of majority of NAAs in serum [37, 38]. Furthermore, it has been postulated that these cells also act as antigen presenting cells (APCs) [39, 40]. B-1a cells also have unique capacity for self-renewal, which leads to constant production of IgM-NAAs throughout life [41].

4 The Physiologic Role of IgM-NAAs

IgM-NAAs have been shown to play several roles in the immune system, including immediate protection from infection, regulation of B-cell responses [42], control of B-cell development [43], selection of the B-cell repertoire [43, 44], suppression of allergic responses [45, 46], and protection against cancer [47, 48].

(a) *Providing the first line of defense against pathogen*: The adaptive arm of the immune system generates specific and long-term immunity to pathogens, such as long-lasting anti-viral antibodies following vaccination. Notably, IgM-NAAs serve as a parallel, immediate, innate response to invading microbes through neutralization of pathogens, activation of the classical complement pathway, opsonization of pathogens, enhancement of phagocytosis, and transport of antigens to lymphoid tissue [49–55] (Fig. 2).

(b) *Shaping the subsequent immune response to antigen*: The unique pentameric structure and polyreactivity of IgM provide

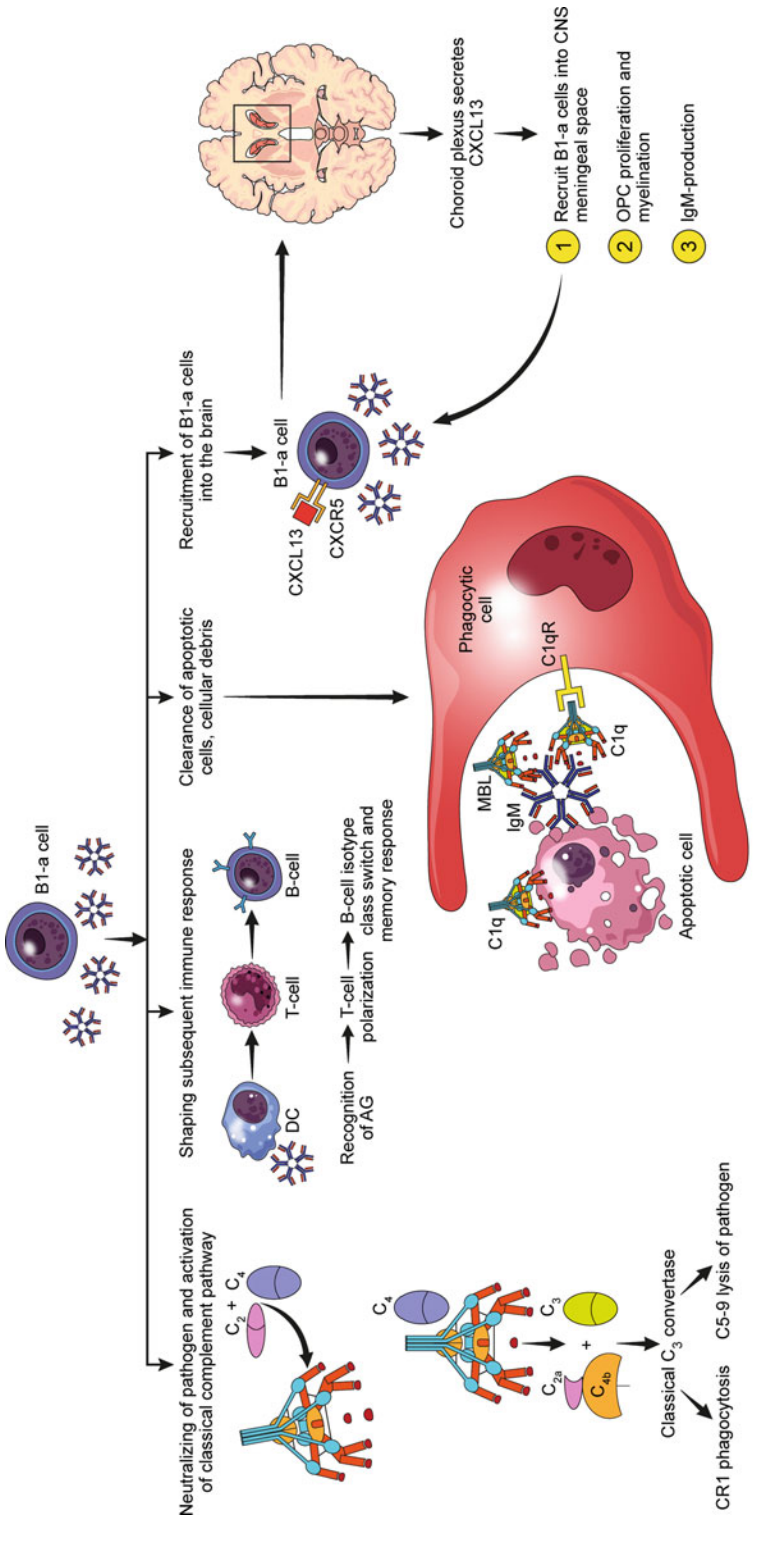

Fig. 2 Physiological role of IgM-natural autoantibodies in the body: Natural IgM autoantibodies can act as the first line of defense against invading microbes through neutralizing the pathogen and activating the complement pathways. Natural IgM can also shape the subsequent immune response to a pathogen by influencing the T-cell polarization and B-cell class-switch. They recognize the apoptotic cell membranes, cellular debris and decorate them with complement system and mannose-binding lectin (MBL) to promote the clearance by phagocytes such as dendritic cells (DC) and macrophages. Also, natural IgM secreted from B-1a cells in the central nervous system lead to oligodendrocyte proginator cell proliferation and myelination

the ability to interact directly with the pathogens. IgM-NAAs can simultaneously bind to different conserved structures, such as nucleic acids, phospholipids, and carbohydrates, on the same pathogen and promote recognition and presentation by APCs, ultimately leading to activation of acquired immunity and memory responses [56, 57] (Fig. 2).

(c) *Clearance of apoptotic cells, misfolded proteins, and altered cells.* Safe removal of dying cells is a fundamental process required throughout the life of an organism. Decoration of dying cell surface membranes with soluble innate immune molecules such as complement C1Q and mannose-binding lectin promotes recognition by cells that initiate a process of phagocytosis termed "efferocytosis" [58]. The IgM-dependent deposition of C1Q has a major role in determining the efficiency clearance of apoptotic cells by macrophages. In the healthy individual, apoptotic cells do not present a threat to the host because efferocytosis ensures rapid and efficient clearance of cell corpses by macrophages and dendritic cells. Defects in efferocytosis, as postulated by Walport et al. [59] in the "waste disposal" hypothesis, may be linked to autoimmune disease. A defect in clearance of apoptotic cells may progress to secondary necrosis which leads to release of pathogenic factors such as heat shock proteins, high-mobility group box 1 protein, and other components of dying cells. These factors along with novel autoantigens released by necrotic cells may activate pathogenic B and T cells and cause inflammatory responses and development of autoimmune disease in a susceptible individual [11] (Fig. 2).

(d) *Recruiting B-1a cells into the developing brain*: cells in peritoneal and pleural cavity express CXCL13. Binding of this chemokine to its receptor (CXCR5) is a crucial step for the promotion of IgM-NAAs production [60]. CXCL13 secretes from choroid plexus and recruits B-1a cells into meningeal space which subsequently lead to oligodendrocyte progenitor cell (OPC) proliferation, myelination, and IgM-NAAs production in brain [61] (Fig. 2).

5 IgM-NAA and Atherosclerosis

Several animal studies have shown an atheroprotective effect of IgM-NAAs. This fact was first brought to light by the observation that injection of mice with apoptotic cells or phosphatidylserine-containing liposomes (PSL) attenuated development of atherosclerotic plaques [62]. Similarly, immunization of low-density lipoprotein receptor (LDLr) knock-out mice with streptococcus pneumonia vaccine induces anti-phosphatidylcholine IgM

antibodies that correlate with a reduction in atherosclerotic lesions [63]. The IgM-NAA (T15/EO6) was isolated from the plasma of mice vaccinated with heat-killed phosphatidylcholine-containing pneumococcal extracts and this antibody exerts a protective effect by interfering in the interaction between oxidized LDL (OxLDL) and macrophages, thereby preventing the formation of foam cells [64, 65] and limiting the pro-inflammatory effects of OxLDL. Likewise, T15/EO6 IgM may enhance clearance of oxidized phospholipid-bearing apoptotic cells that accumulate in atherosclerotic plaques [66, 67]. The cardiovascular protective qualities of the anti-OxLDL autoantibody produced in response to 23-valent pneumococcal vaccine in humans emphasize the concept that molecular mimicry may exist between phosphatidylcholine of streptococcus pneumonia and that of OxLDL [65] [68]. It is also notable that presence of anti-phosphatidylcholine IgM in patients with systemic lupus erythematosis (SLE) correlates with lower risk of myocardial ischemia [69]. Finally, another mechanism by which anti-OxLDL antibodies may exert anti-atherosclerotic effect is through binding of oxidation-specific epitopes (OSEs) found on apoptotic cells, OxLDL, and circulating microparticles [70]. Microparticles are membrane-derived small vesicles originating from Malondialdehyde epitopes. Such epitopes are elevated in the atherosclerotic lesions of patients with myocardial ischemia.

6 IgM-NAA and Cancer

Some studies elucidated the anti-proliferative action of IgM-NAAs. Several tumor-specific antibodies were isolated from plasma of patients with various types of cancer [71]. These antibodies were screened for binding to a broad spectrum of epithelial carcinomas. The antibodies called PAM-1, LM-1, PM-2, SAM-3, SAM-4, SAM-6, PM-1, and CM-1 bound a broad array of cancer specimens, whereas binding of antibodies SC-1, CM-2, and SAM-2 was more tumor-specific; SC-1 to adenocarcinoma of the stomach, CM-2 to adenocarcinoma of the colon, and SAM-2 to squamous cell carcinoma of the esophagus. Similarly, antibodies NORM-1 and NORM-2, found on tumor-specific receptors and isolated from the sera of normal individuals, reacted with several tumor tissues. All of the aforementioned antibodies were isolated from B1 cells and had an inhibitory effect on tumor growth through binding to specific surface epitopes (mostly carbohydrates) and inducing apoptosis; PAM-1 binds to a variant of the cysteine-rich fibroblast growth factor receptor 1 (CFR-1), hinders cell growth, and induces apoptosis [72]. SAM-6 identifies a cell surface receptor and binds to OxLDL [73] leading to uptake of the antibody/OxLDL complex with subsequent formation of lipid depots and release of cytochrome c from mitochondria. The final result is

activation of caspases causing apoptosis. SC-1 targets a glycosylation variant of the decay accelerating factor (DAF/CD55) [74]. Binding causes internalization of the SC-1/CD55 complex and ultimately activates caspase-6 leading to the apoptotic lysis of the cell. Apoptotic activity of SC-1 was also demonstated in animal models and clinically in stomach cancer patients [74, 75]. LM-1, PM-1, PM-2, CM-1, and CM-2 showed promising potential in the treatment of lymphoproliferative diseases [76, 77]. Their antiproliferative mechanism involves cross-linkage of Fas receptors, downstream activation of caspase-3, and reduction in mitochondrial transmembrane potential, culminating in growth arrest and cell death. These natural antibodies may also induce apoptosis through binding to Fc receptors present on the surface of hematopoietic cells [78, 79].

Anti-tumor IgMs also exert their cytotoxicity through their ability to activate complement [80]. IgM-NAA found in serum of healthy individuals are the underlying cause of the plasma exchange efficacy in the treatment of neuroblastoma. Anti-neuroblastoma IgMs can destroy cancerous cells by complement activation, complement independent recruitment of granulocytes and inducing the apoptosis process [81–83]. The complement-dependent cytolytic activity of IgMs could be implicated in the future therapy of metastatic melanoma by way of harnessing the prevalence of anti-αGal antibody (antibody to cell surface α1,3 galactose) in human serum [84].

7 IgM-NAA, Autoimmunity, Inflammation, and Infection

Significant modulation of immune responses by IgM-NAAs has been illustrated in several studies. Several IgM-enriched Ig preparations, pooled from plasma of healthy donors, demonstrated therapeutic efficacy in a variety of diseases. Pentaglobin (12% IgM) showed a beneficial effect on infections in post-bone marrow transplantation, in the course of autoimmune diseases and patients with sepsis and septic shock [85–91]. Pentaglobin most likely benefits from the presence of a common VH4–34 encoded natural IgM which has a high capacity for binding to lipopolysaccharides (LPS), the trigger of infection-induced cardiovascular collapse [92]. Another pilot IgM-enriched preparation (IVIgM) (90% IgM) illustrated efficacy in treating a wide range of autoimmune diseases including complement-dependent inflammatory conditions, experimental models of uveitis, myasthenia gravis, and multiple sclerosis (MS). IVIgM conveys these effects through several modes of action including induction of apoptosis of mononuclear cells, suppression of T cells, and the complement cascade and presence of anti-idiotypic IgM antibodies that neutralize

pathogenic IgG autoantibodies [76, 90, 93–95]. Anti-idiotypic IgM antibodies produced in the serum of patients in remission of anti-neutrophil cytoplasmic antigen-positive vasculitis correlation with the clearance of pathogenic IgG autoantibodies [96, 97]. This indicates that IVIgM may be considered in the management of systemic vasculitis.

The presence of anti-dsDNA IgM in SLE patients protected against glomerulonephritis [98]. Administering anti-dsDNA IgM in the lupus model of mice prevented the development of nephritis. This is in part due to IgM competitively binding to circulating antigens forming fewer IgG immune complexes. Furthermore, anti-dsDNA IgM immune complexes are more actively phagocytosed resulting in less deposition in the glomeruli. Investigators also postulated that anti-dsDNA IgM decreases the production of pathogenic IgG autoantibodies by downregulating autoreactive B cells. Similarly, Rheumatoid Factor (IgM-RF) exerts its glomeruloprotective qualities through interfering in the binding of C3b of the complement to glomeruli receptors, preventing the deposition of immune complexes and causing glomerulonephritis [99]. These observations imply a potential role for IgM preparations for use in the management of all immune complex forming diseases. Moreover, administering small amounts of IgM-NAAs prevented the development of insulitis and diabetes in the non-obese diabetic (NOD) mouse model of human insulin-dependent diabetes predicting a promising role for IgM rich products in treatment of diabetes [100].

IgM-NAAs show an inhibitory effect on the complement cascade by reacting with activated components of the complement system including C3b and C4b and inhibiting the binding of C1q, thus controlling the classical pathway of the complement cascade while sparing the alternative pathway. This comprises an advantage for IVIgM to be used in the management of conditions where there is excessive activation of the classical complement pathway, such as prevention of hyper-acute rejection or treatment of acute vascular rejection in xenotransplantation, while at the same time preserving the capacity to defend against infections [101].

Studies on the mouse model of ischemia-induced acute kidney injury (AKI) showed a protective role of bone marrow dendritic cells (BMDCs) pretreated with natural IgM. This protection stems from the ability of IgM to modulate the innate immune response through inhibiting effector T cells, downregulating CD40 and NF-κB switching activated BMDC to a regulatory phenotype, and by inhibiting chemotaxis preventing activated inflammatory cells from infiltrating the ischemic kidney tissue. This supports future cellular therapies in which IgM-pretreated DCs are used to prevent ischemic acute renal failure (ARF) such as in patients undergoing cardiac surgery or delayed graft function after kidney transplantation [102–104].

8 IgM-NAA in Central Nervous System Disease

The pathogenic nature of antibodies directed against self-antigens in neurological diseases such as myasthenia gravis or Lambert-Eaton syndrome has led to a general perception that all autoantibodies are "bad." However, recent diagnostic and therapeutic findings regarding NAAs in several central nervous system (CNS) disorders suggest that a more nuanced understanding of these antibodies is required.

Alzheimer's disease (AD) is the most common neurodegenerative cause of dementia in older adults. From a mechanistic perspective, it seems probable that the earliest molecular events underlying AD pathogenesis occur decades prior to cognitive manifestations. Hence, identification of biomarkers predictive for AD might facilitate therapeutic interventions that prevent AD [105]. Extracellular deposition of the amyloid beta (Aβ) peptide is one of the essential pathologic hallmarks in AD and Aβ42 predominates amyloid plaques in the AD. As the disease progresses, the total number and size of amyloid plaques increase through brain tissue [106]. Induction of antibodies against Aβ in animal models of AD led to reduced plaque pathology and improved behavioral outcome [107]. Three strategies have been employed to generate antibodies against Aβ in AD models [108]: (a) *Direct immunization with full-length Aβ42* to stimulate APCs, T cell, and B-cell responses. This technique eventually drives B cells to produce anti-Aβ antibodies and experiments using such immunization led to the new field of Aβ immunotherapy. (b) *Injection of small synthetic fragments of Aβ conjugated to an unrelated carrier protein*: This approach uses a carrier peptide to stimulate T helper cells, providing cytokines that are necessary for vigorous B-cell responses. (c) *Passive administration of anti-Aβ antibodies*: This approach does not require host immune responses and is, therefore, a potential alternative in the elderly and other individuals who do not respond adequately to Aβ immunization. All these approaches have focused on the role of high-affinity IgGs directed against aspects of Aβ deposition. Pharmaceutical industry has ignored, to this point, the potential benefit of IgM-NAAs in AD despite evidence that human monoclonal IgM also reverses cognitive deficits in AD models [109].

NAAs against Aβ peptides are present in the serum and cerebrospinal fluid (CSF) of both healthy controls and AD patients. Marcello et al. [110] reported that the level of anti-Aβ IgM was significantly decreased in AD patients compared to sex and age-matched healthy individuals, suggesting that IgM-NAAs directed against Aβ might be a plasma biomarker for AD risk and highlights the possibility that such NAAs might be protective. IgM-NAAs directed against Aβ isolated from patients with Waldenstrom macroglobulinemia enzymatically cleave Aβ peptides in

plaques [111]. However, anti-Aβ IgM-NAAs have not been tested in clinical trials in AD and there is a paucity of data regarding the diagnostic and therapeutic role of IgM-NAAs in AD. These concepts warrant greater investigation.

MS is a progressive CNS demyelinating disease and the most common cause of non-traumatic disability in young people. It impacts more than two million individuals worldwide and currently there is no effective treatment to significantly prevent progression or reverse the disease course. Disease-modifying therapies that prevent inflammatory cell migration across the blood-brain barrier (BBB) and therapies that enhance production of anti-inflammatory cytokines and inhibition of pro-inflammatory factors are currently the best strategies for slowing MS. However, the failure of current immunomodulatory therapies to halt disease progression and the inexorable loss of function that occurs in MS patients suggests that our understanding of MS etiology and pathogenesis is incomplete. New biotechnologies that stimulate myelin repair and nerve regeneration are vital to preventing and reversing long-term disability in MS patients. One such biotechnology, first discovered and developed by our laboratory at Mayo Clinic, utilizes naturally occurring IgM autoantibodies to promote CNS repair. The discovery of IgM-NAAs that promote CNS remyelination (rHIgM22) and neurite outgrowth (rHIgM12) provides a fundamentally new strategy for treating not only MS, but a multitude of CNS disorders that involve injury and/or loss of oligodendrocytes (OLs), axons, and neurons. In the following sections, we describe the current information regarding these IgM-NAAs.

9 Discovery of Oligodendrocyte-Binding IgM-NAAs as Remyelination-Promoting Antibodies

A narrative of discovery: For a long time it has been generally accepted that the humoral immune response plays a purely pathogenic role in CNS demyelinating disease. On this basis, we expected that passive transfer of antisera and antibodies generated against myelin components into animals with active demyelination would exacerbate disease. To test this, we immunized mice chronically infected with Theiler's murine encephalomyelitis virus (TMEV) with spinal cord homogenate (SCH). Surprisingly, instead of worsening of disease all immunized animals exhibited substantial remyelination in the spinal cord compared to controls immunized with liver homogenate [112]. Similar findings were also observed in the experimental autoimmune encephalomyelitis (EAE) model in guinea pigs upon immunization with myelin after disease induction [113]. The concept that autoreactive naturally occurring Abs directly enhance myelination was further established by showing

that suppression of B-cell responses and consequent lack of Igs from birth resulted in an increased number and severity of demyelinated lesions in TMEV-infected mice [114]. These innovative experiments were the first to demonstrate that autoreactive antibodies could play a beneficial role in promoting CNS remyelination.

Therapeutic efficacy of mouse IgM-NAAs in disease models: Despite compelling evidence that Igs were involved, SCH immunization may also lead to remyelination and repair via mechanisms that involve direct stimulatory effects on oligodendrocyte proliferation, via depletion of inflammatory cells, or by stimulating axonal regeneration [115–117]. Therefore, we began to systematically study the specificities and mechanisms of action for antibodies raised against SCH. Using SCH as the antigen, mice were immunized and standard techniques were used to generate antibody-producing hybridomas. Several hybridomas were screened for reparative efficacy in the TMEV model, yielding the first remyelination-promoting IgM-NAA referred to as SCH94.03 [118]. This poly-reactive mouse IgM induced nearly complete remyelination in approximately 30% of the lesions in TMEV-infected mice [119]. Conversely, control IgMs induced remyelination in less than 5% of lesions. Over a 5 year period in the 1990s we identified a group of OL-specific murine IgM-NAAs (O1, O4, A2B5, and HNK-1) that induced robust remyelination in demyelinated mice [120] (Table 2).The effective mouse IgMs all bound to myelin and OLs, but each had clearly different antigenic targets, leading us to propose that CNS repair was not driven by binding to a single epitope.

Discovery of human IgM-NAAs: Following the identification of robust remyelination induced by murine IgM-NAAs, we sought to identify equivalent IgM-NAAs with remyelinating potential in humans. We recruited patients with Waldenstrom's macroglobulinemia, multiple myeloma, lymphoma, or monoclonal gammopathies, diseases that involve production of tremendous amounts of monoclonal Ig. We screened the Mayo Clinic serum bank collection of 140,000 patient samples for donors without a history of neurological or immunological disorders and the presence of a monoclonal Ig spike of at least 20 mg/ml. From this, we identified 102 serum-derived human IgMs (sHIgMs) and IgGs (sHIgGs) and subsequently applied the conserved character of murine IgM-NAAs to identify the first reparative human IgM-NAAs [121].

Screening the human remyelination-promoting IgM-NAAs. Early in this work we postulated that OL binding is a primary feature of the remyelination-promoting effect of IgM-NAAs. Therefore, we screened binding of sHIgMs and sHIgGs to the surface of OLs in mixed primary glial cultures and to white matter tracts in unfixed rat cerebellar slices. Six out of 52 sHIgMs and zero of 50 sHIgGs exhibited binding affinity for cultured rodent OLs

Table 2
Properties of mouse and human remyelination-promoting IgM natural autoantibodies

Antibody	Possible targets	CNS cell signals
O1	GalC, MGDG and psychosine	Ca^{2+}
O4	POA and sulfatide	Ca^{2+}, P-MAPK, caspase-3, P-SFKs
A2B5	Ganglioside GQ1c and other antigens found in GMx, GDx, GTx and PGs	Ca^{2+}
HNK-1	Sulfated glucuronic acid-containing glycolipids expressed on neural cell adhesion molecules (e.g. N-CAM, L1, J1), MAG and ependymins	Ca^{2+}
SCH 79.08	MBP and cytoskeletal proteins (e.g., Vimentin)	Ca^{2+}
SCH 94.03	Surface and cytoplasmic antigens, cytoskeletal proteins (e.g., Vimentin, Spectrin, Tubulin, Actin and Kinesin)	Ca^{2+}
SCH 94.32	Surface and cytoplasmic antigens, cytoskeletal proteins (e.g., Vimentin, Spectrin, Tubulin and Actin)	Ca^{2+}
rHIgM22	Sulfated antigens (e.g., GlcC-S, LacC-3-S, seminolipid, SB1a and SB2)	Ca^{2+}P-MAPK, caspase-3, P-SFKs
sHIgM46	Myelin	Ca^{2+}, caspase-3

GalC galactocerebroside, *MGDG* monogalactosyl-diglyceride, POA proligodendroblast antigen, *PGs* polysialogangliosides, *GTx* trisialogangliosides, *GDx* disialogangliosides, *GMx* monosialogangliosides, *MAG* myelin-associated glycoprotein, *MBP* myelin basic protein, *REM* remyelination protein, *GlcC-S* glucosylcerebroside-sulfate, *LacC-3-S* lactosylceramide-3-sulfate, *SB1a* bis-sulphogangliotetraosylceramide, *SB2* bis-sulphogangliotriaosylceramide

[122]. We also cultured OLs derived from the neural tissue of epilepsy patients undergoing temporal lobectomy and identified sHIgMs that readily bound to human OLs [121].

Therapeutic efficacy of human IgM-NAA in animal models. We assessed the efficacy of six OL-binding sHIgMs to induce remyelination in the TMEV model. sHIgM22 and sHIgM46 IgMs both derived from Waldenstrom's macroglobulinemia patients promoted robust remyelination in demyelinated mice. Using molecular cloning techniques, we generated a recombinant form of sHIgM22 (rHIgM22) to make enough reagent for research and clinical testing. After isolating a stable F3B6 hybridoma production clone, we created research and Good Manufacturing Practice-certified cell lines for the production of rHIgM22 [123]. rHIgM22 maintained key characteristics of the serum-derived form, OL binding, as well as robust induction of CNS remyelination in demyelinated mice [124]. We further showed that human IgM-NAAs enhance remyelination via activation of OL lineage cells rather than by altering the immune system [125]. rHIgM22-induced remyelination was confirmed in some

models of demyelination; chronic infection with TMEV, focal lesion induced by lysolecithin, and widespread demyelination after systemic cuprizone toxicity [122, 126]. Notably, we did not observe an IgM-induced improvement in the EAE model, or exacerbation of disease, supporting the premise that these CNS-binding IgM-NAAs do not directly modulate inflammation, but instead act by modulating OL lineage proliferation and maturation [127]. A recent study by Cui et al. [128] demonstrated that rHIgM22 accelerates remyelination of the corpus callosum in the brains of cuprizone-treated mice. They also investigated the effect of rHIgM22 on hippocampal myelination and on hippocampal-dependent learning and memory in the cuprizone model. rHIgM22 not only enhances hippocampal remyelination, but also reduces memory deficits induced by cuprizone treatment.

Penetration of human IgM-NAAs into the CNS compartment. The BBB makes the CNS compartment one of the most challenging sites for therapeutic targeting due to restrictions on drug penetration. Large molecules such as circulating antibodies, especially IgMs, are tightly restricted at the BBB. However, BBB permeability changes during inflammatory conditions and may allow greater CNS access. Animal studies have shown only 0.01–0.4% of peripheral doses of antibodies cross the BBB, regardless of the disease model [129]. A similar low level of CNS delivery is reported in nearly all Abs based trials for AD. Increasing the level of the drug with the CSF can be achieved by intrathecal delivery or micropumps. However, there is still debate how delivery of a drug to the CSF reflects concentration in the brain parenchyma.

Targeting of rHIgM22 to brain lesions was performed in mice receiving radio-tagged rHIgM22 and assayed using T2-weighted MRI scanning. We found that over 48 h the IgM crosses the BBB, enters the CNS, and accumulates at brain lesions [130]. In dosing studies we found than even a single 500 ng dose of rHIgM22 can induce significant remyelination in TMEV-infected mice five weeks after IgM treatment [131].

Mechanism of action of remyelination-promoting IgM-NAAs: To date, the precise mechanism of action of IgM-mediated remyelination is elusive. Spanning four decades of data generated in the Rodriguez laboratory, two main hypotheses have been proposed:

(a) The direct hypothesis states that IgM-NAAs recognize myelinating cells and promote the synthesis of new myelin. Supporting evidence comes from the observations that remyelination-promoting IgM-NAAs bind OLs in culture, isolated myelin and myelin tracks in cerebellar slice cultures [118, 120–122, 131, 132]. All tested human and mouse remyelination-promoting IgM-NAAs induce Ca^{+2} influx in cells of the OL-lineage, which suggests activation of intracellular signaling pathways for remyelination [133]. Moreover,

rHIgM22 mediates the inhibition of OL differentiation and apoptotic signaling in enriched OPC cultures in vitro through a Src family kinase (Lyn) which causes a fourfold decrease in the expression of the mature OL markers myelin basic protein (MBP) and myelin oligodendrocyte glycoprotein (MOG), and a more than tenfold reduction in the activation of caspase-3 and caspase-9 respectively [134]. Following binding of rHIgM22 to OLs, activating Lyn, ERK1, and ERK2 in OPCs lead to inhibition of OPC differentiation and reduced apoptotic signaling [134]. rHIgM22 also alters gene expression upon calcium influx through CNQX-sensitive AMPA channels in OLs.

The high affinity of remyelination promoting IgMs to myelin also suggests direct binding to the target underlies the mechanism of action. Because many IgM-NAAs are considered polyreactive due to their near germline variable regions their binding affinity has been assumed to be low. However, when the dissociation constants (K_d) for binding to myelin for several remyelination-promoting IgMs were derived the values were found to be unexpectedly high. The mouse IgMs O4 and O1 that bind to sulfatide and galactosylceramide, respectively, bind myelin at 2.2×10^{-9} mol/l and (2.4×10^{-9} mol/l [135]; Fig. 3).

(b) The indirect hypothesis proposes IgM-NAAs activate either immune cells or cell types other than cells of the OL lineage within the CNS, which, in turn, stimulate OPCs or OLs (i.e., by secreting remyelination-promoting factors). The idea of the indirect hypothesis comes from the observation that remyelination-promoting IgM-NAAs stimulate Ca^{+2} signaling in glial fibrillary acidic protein (GFAP) $^{+}$ astrocytes [136]. Interestingly, the astrocytic response to IgM-NAAs is immediate and precedes the OLs response. Although the mechanisms of Ca^{+2} influxes into astrocytes and OPCs are different, the identification of PDGFα receptor as a part of OPC-signaling for rHIgM22-mediated actions suggests the involvement of the astroglial growth factor PDGF in rHIgM22-mediated actions in OPCs [134]. The critical point is that we were able to detect IgM-mediated OPC proliferation only in cultures containing substantial amounts of astrocytes, microglia, and OPCs (mixed glial cultures), but not in highly enriched OPC populations [137]. The growth factor PDGF and potentially other secreted microglial and astrocytic factors or direct cellular contact between OPCs and other glial cells are considered essential steps for the proliferative response. It seems probable that all three cell types (OPCs, microglia, and astrocytes) are required for the IgM-NAAs-mediated proliferation of OPCs in vitro. It has

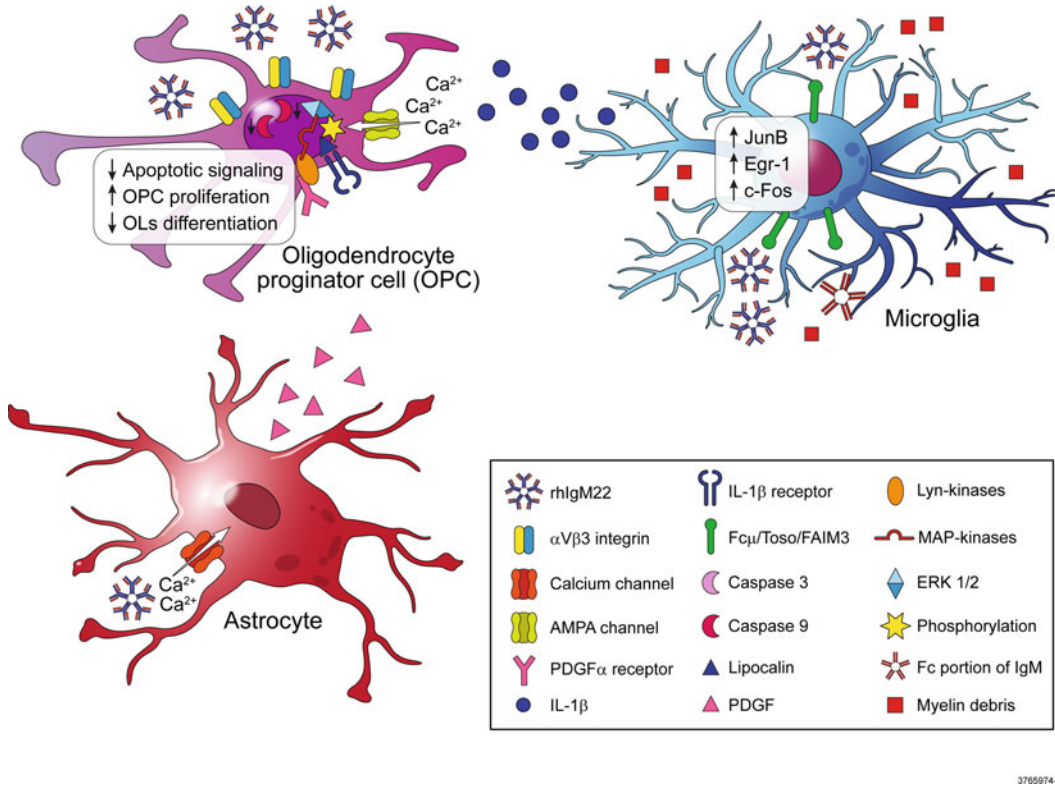

Fig. 3 Direct and indirect mechanisms of remyelination by rHIgM22 natural autoantibodies. *Direct mechanism*: Remyelination-promoting natural IgM binds to oligodendrocytes (OLs) and induces calcium influx in cells of OL-linage. rHIgM22 alters gene expression upon slow calcium influx through CNQX-sensitive AMPA channels in OLs. rHIgM22 mediates the inhibition of OL differentiation and apoptotic signaling through a Src family kinase (Lyn) and reduction in the activation of caspase-3 and caspase-9. Following binding of rHIgM22 to OLs, activating Lyn, ERK1, and ERK2 in oligodendrocyte progenitor cells (OPCs) lead to inhibition of OPC differentiation and reduced apoptotic signaling *Indirect mechanism*: rHIgM22 also stimulates calcium signaling in astrocytes. The astrocytic response to rHIgM22 is fast and precedes the OLs response. PDGFα receptor was identified as part of OPC-signaling for rHIgM22-mediated actions suggests the involvement of the astroglial-derived growth factor PDGF in rHIgM22-mediated signaling in OPCs. Activated microglia may also contribute in remyelination process of rHIgM22. The Fc portion of human IgM shifts microglia to an activated phenotype, reduces glial proliferation, upregulates several immediate early genes including JunB, Egr-1, and c-Fos, and stimulates microglial production and release of IL-1β. Microglia-derived IL-1β consequently prompts transcriptional upregulation of immediate early genes in mixed glial cultures, and induces the upregulation of late response genes such as lipocalin in purified OLs. Microglia and macrophages also enhance phagocytosis of myelin, thus allowing the normal remyelination process to take place

been shown that mice overexpressing PDGF have higher levels of proliferating OPCs and less OPC apoptosis in the chemical-demyelinated lesion [138]. However, it is well established that the PDGF is not sufficient by itself to stimulate OPC survival or proliferation in vitro [139–141]. We believe that additional factors are required to activate the PDGF response in vivo. Further investigations in O1 or O4 knocked

out mice are necessary to postulate whether IgM-NAAs binding to glial cells but not OPCs are enough to induce repair in the lesions.

We showed that IgM-NAAs might also lead to remyelination through activating of microglia cells. The support for this notion stems from the earlier work that showed the Fc portion of human IgM shifts microglia to an activated phenotype, reduces glial proliferation, upregulates several immediate early genes including JunB, Egr-1, and c-Fos, and stimulates microglial production and release of IL-1β. Microglia-derived IL-1β consequently prompts transcriptional upregulation of immediate early genes such as c-Jun, Egr-1, and c-Fos in mixed glial cultures, and induces the upregulation of late response genes such as lipocalin in purified OLs. Treatment with an IL-1β receptor antagonist abolished the effects of Fcμ on glial proliferation and prevented the upregulation of lipocalin in response to Fcμ, but did not prevent Fcμ-mediated upregulation of IL-1β, indicating that IL-1β mediates at least some of the downstream effects of Fcμ in mixed glial cultures. We believe that Fcμ-mediated IL-1β-induced upregulation of immediate early and late response genes in OLs may promote CNS repair [142]. Moreover, recent evidence shows that rHIgM22 labels the myelin debris and makes rHIgM22/myelin complex. This complex undergoes complement opsonization and provides a recognizable ligand on microglia receptors. Binding of complement opsonized rHIgM22/myelin to the microglia receptors leads to phagocytic uptake and prompts the clearance of extracellular myelin, consequently increasing OPC proliferation [143] (Fig. 3).

Therapeutic efficacy of IgM-NAAs in clinical trials: rHIgM22 has completed Phase 1a/b clinical trials (NCT01803867 and NCT02398461) in 85 MS patients without any safety concerns or therapeutic intervention due to major adverse effects at any administered dose (0.025–2.0 mg/kg). A major concern of the FDA that an autoreactive monoclonal (mAb) IgM would exacerbate pre-existing autoimmune disease was not supported by the results of the trial. mAb was detected in the CSF of all patients assayed from day 2 to 29 after a single dose, confirming the ability of rHIgM22 to cross the BBB in humans.

10 Discovery of Neuron-Binding IgM-NAAs and Their Therapeutic Efficacy in Neuronal Protection

Characterization of rHIgM12-NAA: In our quest to find IgM-NAAs that bind to OLs and promote remyelination in live slices of the cerebellum, we discovered other IgMs that bind to the

surface of neurons and support neurite outgrowth. A recombinant form of the serum-derived IgM12 was generated in CHO cells with biological properties identical to sHIgM12 [144]. rHIgM12 does not induce Ca^{+2} influx in glial cells in vitro, in contrast to all IgMs that promote remyelination [136]. However, rHIgM12 binds to neurons and promotes significant neurite outgrowth in a variety of primary neurons including cerebellar neurons, retinal ganglion neurons, and cortical neurons [144]. Xu et al. [145] showed that rHIgM12 promotes neuronal attachment and guides neurite outgrowth from hippocampal neurons using microcontact printing.

Therapeutic efficacy in animal models: Following administration, a single 10 mg/kg dose of rHIgM12 in TMEV-infected mice significantly increased NAA concentration within the brain stem and improved neurological function [146, 147]. We assessed the effect of rHIgM12 in two different models of amyotrophic lateral sclerosis (ALS); SOD1-G86R mice with the mutation in SOD1 gene represents a model for rapidly progressive ALS, and SOD1-G93A with multiple copies of a mutant human SOD1 allele that represents a slower progressive form of the disease. Administration of a single intraperitoneal dose of rHIgM12 protected axons and significantly improved survival of both strains [148]. Mice with rapidly progressive ALS also had significantly more $NeuN^{+}$ in neurons of the anterior horn of thoracic and lumbar spinal cord, demonstrating attenuated neurodegeneration [149].

Identifying the molecular target of rHIgM12: Recognizing the antigens of neuron-binding IgM-NAA could provide a rationale to utilize these agents in the treatment of neurodegenerative diseases.

Neural cell-adhesion molecule (NCAM) is a glycoprotein expressed on the surface of many cell types including neurons, glia, skeletal cells, and natural killer cells [150]. NCAM has been implicated in the mechanism of neurodegeneration likely through its effect on synaptic transmission and neurite outgrowth [151]. Because neurite outgrowth is the main effect observed in tissue culture when neurons are grown in a substrate containing rHIgM12, NCAM became a likely target of the antibody. NCAM is usually associated chemically with PSA (poly-sialylated adhesion molecule) thus forming PSA-NCAM. The developing brain expresses PSA thus being a crucial carbohydrate in different stages of neuronal development such as axonal extension and OPC migration [152]. The addition of PSA to NCAM interferes with NCAM interactions within the surrounding environment [152]. PSA-NCAM is expressed profoundly during neural developmental stages and during the process of axonal sprouting, guidance, and targeting, whereas in adults it is limited to regions that show self-renewal or plasticity such as the olfactory bulb, suprachiasmatic nucleus, hippocampus, hypothalamus, and specific spinal cord

nuclei. Interestingly, PSA-NCAM is re-expressed on demyelinated axons and is found in demyelinated MS plaques [153].

We identified PSA as the antigen for rHIgM12 using NCAM knock-out strain and enzymatic digestion of PSA via endoneuraminidase, an enzyme that cleaves explicitly α 2- to 8-linked PSA polymers present on NCAM and other proteins. Western blotting using rHIgM12 did not detect any antigen from endoneuraminidase digested brain tissues. Several other methods including immunoprecipitation, mass spectroscopy, immunocytochemistry, and immunohistochemistry all confirmed that rHIgM12 binds to tissue is solely in the presence of PSA attached to NCAM [154].

Earlier studies indicated that sHIgM12 binds to the surface of neurons and overrides the inhibitory effects of myelin on neurite outgrowth [144, 155]. rHIgM12 also is required to alter neuronal lipid-raft microdomains in order to drive axon extension [156]. Gangliosides can serve as receptors for ligand and antibody-mediated neuronal signaling. rHIgM12 binds with high affinity to gangliosides GD1a and GT1b. Moreover, myelin-associated glycoprotein (MAG) also recognizes these gangliosides within the neuronal plasma membrane [157, 158]. MAG facilitates the interactions between OLs and axons to preserve long-term axonal stability and restrict further neurite extensions [159].

Studies [148, 160] show that the addition of fused MAG-Fc complex to rat cerebrocortical cultures diminishes α-tubulin tyrosination and increases levels of de-tyrosinated tubulin and acetylated α-tubulin. This supports the hypothesis that MAG raises microtubule stability. Nonetheless, if rHIgM12 is added to cortical neurons in cultures then a significant rise in α-tubulin tyrosination is observed [148]. Adding rHIgM12 to neurons in culture in the presence of MAG results in the increase of tubulin tyrosination and decrease in tubulin acetylation over a few hours [148]. Our data suggest that there is competition between rHIgM12 and MAG for binding to the surface of neurons in vitro. Therefore rHIgM12 overcomes MAG-mediated tubulin stability and promotes a more dynamic state of the cytoskeleton driving neurite outgrowth. These findings provide evidence that gangliosides have a role in balancing neural stimulatory and inhibitory signals supplied by rHIgM12 and MAG. Based on the CNS cell type affected, subcellular rHIgM12 recognition of PSA-NCAM and gangliosides provides essential insights into rHIgM12-induced signaling for neurite outgrowth.

11 New Investigations Highlight the Biological Background of IgM-NAA in the Developing Brain

A recent study by Tanabe et al. [61] elegantly described the crucial role of IgM-NAA in promoting oligodendrogenesis during brain development. They used flow-cytometry to quantify the ratio of

lymphocyte phenotypes in developing brain from embryonic day E16, E18, postnatal day P1, P5, P10 and week 8. They found high levels of $CD19^+CD45R^+$ B cells compared to $CD4^+$ or $CD8^+$ cells in developing brain peaking at 5% on P1. B cells were mostly localized in choroid plexus, lateral ventricle, and meningeal space of cerebellum and spinal cord. During the neonatal stage of development, immature B cells in the blood "transitional B cells" [161] infiltrate the brain and differentiate into mature B-1a cells which comprise the most abundant B-cell subtype in the neonatal brain. Data also showed that by adding B-1a cells to neurospheres in culture, a significant increase in the number of cells of OL lineage is observed. Cultures from dissociated neurospheres are heterogeneous, containing cells such as astrocytes and neurons. Therefore, in order to exclude the possibility that B-1a cells promote oligodendrogenesis through other cell types such as astrocyte or neurons, researchers isolated PDGF-receptor-α-positive ($PDGFR\alpha^+$) OPCs, and cocultured them with B-1a cells. The proportion of proliferating OPCs and MBP^+ OLs was significantly higher in the presence of B-1a cells. These results suggest that B-1a cells directly affect oligodendrogenesis by promoting OPC proliferation. Moreover, it has been shown in vivo that depletion of B-1a cells using blocking antibodies against B-cell-activating factor reduces the number of OLs in the developing brain. Investigators proposed that B-1a cells promote proliferation of OPCs via IgM-Fcα/μR signaling. To confirm the hypothesis, they performed immunohistochemistry in the P5 mouse brain and found that $PDGFR\alpha^+$ OPCs expressed Fcα/μR, while MBP^+ mature OLs did not. To assess whether Fcα/μR contributed to the in vivo proliferation of OPCs, neutralizing anti-Fcα/μR antibodies were injected into the lateral ventricle in P1 mice, which were then analyzed at P7. Anti-Fcα/μR treatment diminished the number of cells with OL-lineage. Furthermore, recombinant IgM-NAA directed against a lectin injected into the ventricles colocalized with Fcα/μR in $PDGFR\alpha^+$ OPCs and resulted in increased proportion of $Ki67^+PDGFR\alpha^+Olig2^+$ cells, which subsequently promoted the proliferation of OPCs in the corpus callosum at P7. These results suggest that IgM–Fcα/μR signaling mediates oligodendrogenesis by regulating the proliferation of OPCs in the developing brain.

To determine whether IgM-NAA from B-1a cells promotes the proliferation of OPCs through Fcα/μR, they cocultured OPCs with B-1a cells in vitro in the presence of neutralizing anti-Fcα/μR antibody or IgG. They postulated that the number of $PDGFR\alpha^+$ OPCs increased significantly when cocultured with B-1a cells. However, this effect was eliminated by anti-Fcα/μR treatment. These results indicate that IgM-NAAs secreted from B-1a cells induce the proliferation of OPCs in vitro via Fcα/μR signaling pathway.

It is important to mention that Fcα/μR is not the only Ig receptor that is implicated in OPCs differentiation. Nakahara et al. [162] over 10 years ago provided evidence that the common γ chain of the Ig Fc receptor is involved in the activation of Fyn tyrosine kinase—a critical signaling pathway for OPCs differentiation. FcRγ cross-linking by IgG on OPCs promotes the activation of Fyn signaling and induces rapid morphological differentiation via upregulation of MBP expression levels. In 2006, we hypothesized binding of Fc portion of IgM to Fcμ mediates IL-1β-induced upregulation of some rapid and late response genes in OLs which may lead to the CNS repair [142]. In 2008, TOSO/FAIM3, rediscovered as Fcμ receptor, was found to be expressed in high levels on OPCs which shed more light on the anti-apoptotic feature of remyelination-promoting IgM-NAAs [17, 163]. These data support the underlying biological process of rHIgM22. However, the effect of IgM-NAA on neurons has been overlooked. We believe that B-1a cells secret the cocktail of polyclonal natural autoantibodies which may exert various functions in the brain according to their binding sites. Further investigations are required to show if B-1a cells lead to neurite extension by signaling via neurons.

12 Conclusion Remarks

In summary, human self-reactive natural IgM antibodies are common in health and disease and can play fundamental roles in tissue homeostasis and the maintenance of immune equilibrium. Accumulating evidence suggests that natural IgM may have protective properties in cardiovascular disease and autoimmunity. IgM-NAAs could be a promising candidate for cancer therapy and AD.

A combinatorial therapeutic approach using a human remyelination-promoting antibody (rHIgM22) and neuroprotective antibody (rHIgM12) may be a promising option for CNS repair in diseases such as MS where myelin is the primary target, and neuronal injury determines long-term deficits. The recent investigations on the role of B-1a cells in oligodendrogenesis in the neonates along with our theories about remyelination inducing effect of IgM-NAAs in the CNS create a new challenge for researchers seeking to apply this science in other diseases such as cerebral palsy in pediatric patients. We believe that our knowledge about IgM-NAA in CNS is still in its infancy. Future efforts should focus on the mechanisms of PSA-NCAM signaling via rHIgM12 and on identifying the role of different IgM receptors in CNS remyelination.

Acknowledgment

M.F.S. is supported by grant from the National MS Society (NMSS).

References

1. Walport MJ (2001) Complement. First of two parts. N Engl J Med 344(14):1058–1066
2. Toapanta FR, Ross TM (2006) Complement-mediated activation of the adaptive immune responses: role of C3d in linking the innate and adaptive immunity. Immunol Res 36 (1–3):197–210
3. Aggarwal A (2014) Role of autoantibody testing. Best Pract Res Clin Rheumatol 28 (6):907–920
4. Zaichik A, Churilov LP, Utekhin VJ (2008) Autoimmune regulation of genetically determined cell functions in health and disease. Pathophysiology 15(3):191–207
5. Piro A, Tagarelli A, Tagarelli G et al (2008) Paul Ehrlich: the Nobel Prize in physiology or medicine 1908. Int Rev Immunol 27 (1–2):1–17
6. Haury M, Sundblad A, Grandien A et al (1997) The repertoire of serum IgM in normal mice is largely independent of external antigenic contact. Eur J Immunol 27 (6):1557–1563
7. Boes M (2000) Role of natural and immune IgM antibodies in immune responses. Mol Immunol 37(18):1141–1149
8. Meffre E, Salmon JE (2007) Autoantibody selection and production in early human life. J Clin Invest 117(3):598–601
9. Merbl Y, Zucker-Toledano M, Quintana FJ, Cohen IR (2007) Newborn humans manifest autoantibodies to defined self molecules detected by antigen microarray informatics. J Clin Invest 117(3):712–718
10. Elkon K, Casali P (2008) Nature and functions of autoantibodies. Nat Clin Pract Rheumatol 4(9):491–498
11. Kaveri SV, Silverman GJ, Bayry J (2012) Natural IgM in immune equilibrium and harnessing their therapeutic potential. J Immunol 188(3):939–945
12. Carroll MC (1998) The role of complement and complement receptors in induction and regulation of immunity. Annu Rev Immunol 16:545–568
13. Sakamoto N, Shibuya K, Shimizu Y et al (2001) A novel Fc receptor for IgA and IgM is expressed on both hematopoietic and non-hematopoietic tissues. Eur J Immunol 31(5):1310–1316
14. Shibuya A, Sakamoto N, Shimizu Y et al (2000) Fc alpha/mu receptor mediates endocytosis of IgM-coated microbes. Nat Immunol 1(5):441–446
15. Kaetzel CS (2005) The polymeric immunoglobulin receptor: bridging innate and adaptive immune responses at mucosal surfaces. Immunol Rev 206:83–99
16. Johansen FE, Pekna M, Norderhaug IN et al (1999) Absence of epithelial immunoglobulin A transport, with increased mucosal leakiness, in polymeric immunoglobulin receptor/secretory component-deficient mice. J Exp Med 190(7):915–922
17. Kubagawa H, Carroll MC, Jacob CO et al (2015) Nomenclature of Toso, Fas apoptosis inhibitory molecule 3, and IgM FcR. J Immunol 194(9):4055–4057
18. Kubagawa H, Kubagawa Y, Jones D et al (2014) The old but new IgM Fc receptor (FcmuR). Curr Top Microbiol Immunol 382:3–28
19. Kubagawa H, Oka S, Kubagawa Y et al (2009) Identity of the elusive IgM Fc receptor (FcmuR) in humans. J Exp Med 206 (12):2779–2793
20. Shima H, Takatsu H, Fukuda S et al (2010) Identification of TOSO/FAIM3 as an Fc receptor for IgM. Int Immunol 22 (3):149–156
21. Berland R, Wortis HH (2002) Origins and functions of B-1 cells with notes on the role of CD5. Annu Rev Immunol 20:253–300
22. Peaker CJ, Neuberger MS (1993) Association of CD22 with the B cell antigen receptor. Eur J Immunol 23(6):1358–1363
23. Muller J, Nitschke L (2014) The role of CD22 and Siglec-G in B-cell tolerance and autoimmune disease. Nat Rev Rheumatol 10 (7):422–428
24. O'Keefe TL, Williams GT, Davies SL et al (1996) Hyperresponsive B cells in CD22-deficient mice. Science 274(5288):798–801
25. Jellusova J, Nitschke L (2011) Regulation of B cell functions by the sialic acid-binding

receptors siglec-G and CD22. Front Immunol 2:96
26. Hardy RR, Hayakawa K (2001) B cell development pathways. Annu Rev Immunol 19:595–621
27. LeBien TW, Tedder TF (2008) B lymphocytes: how they develop and function. Blood 112(5):1570–1580
28. Herzenberg LA, Herzenberg LA (1989) Toward a layered immune system. Cell 59 (6):953–954
29. Chung JB, Silverman M, Monroe JG (2003) Transitional B cells: step by step towards immune competence. Trends Immunol 24 (6):343–349
30. Deenen GJ, Kroese FG (1993) Kinetics of peritoneal B-1a cells (CD5 B cells) in young adult mice. Eur J Immunol 23(1):12–16
31. Kantor AB, Stall AM, Adams S et al (1992) Adoptive transfer of murine B-cell lineages. Ann N Y Acad Sci 651:168–169
32. Kantor AB, Stall AM, Adams S et al (1992) Differential development of progenitor activity for three B-cell lineages. Proc Natl Acad Sci U S A 89(8):3320–3324
33. Tung JW, Mrazek MD, Yang Y et al (2006) Phenotypically distinct B cell development pathways map to the three B cell lineages in the mouse. Proc Natl Acad Sci U S A 103 (16):6293–6298
34. Herzenberg LA, Stall AM, Lalor PA et al (1986) The Ly-1 B cell lineage. Immunol Rev 93:81–102
35. Hayakawa K, Hardy RR, Parks DR et al (1983) The "Ly-1 B" cell subpopulation in normal immunodefective, and autoimmune mice. J Exp Med 157(1):202–218
36. Ghosn EE, Yamamoto R, Hamanaka S et al (2012) Distinct B-cell lineage commitment distinguishes adult bone marrow hematopoietic stem cells. Proc Natl Acad Sci U S A 109 (14):5394–5398
37. Martin F, Oliver AM, Kearney JF (2001) Marginal zone and B1 B cells unite in the early response against T-independent blood-borne particulate antigens. Immunity 14 (5):617–629
38. Choi YS, Baumgarth N (2008) Dual role for B-1a cells in immunity to influenza virus infection. J Exp Med 205(13):3053–3064
39. Griffin DO, Holodick NE, Rothstein TL (2011) Human B1 cells in umbilical cord and adult peripheral blood express the novel phenotype CD20+ CD27+ CD43+ CD70. J Exp Med 208(1):67–80
40. Wong SC, Chew WK, Tan JE et al (2002) Peritoneal CD5+ B-1 cells have signaling properties similar to tolerant B cells. J Biol Chem 277(34):30707–30715
41. Hayakawa K, Hardy RR, Stall AM et al (1986) Immunoglobulin-bearing B cells reconstitute and maintain the murine Ly-1 B cell lineage. Eur J Immunol 16(10):1313–1316
42. Boes M, Esau C, Fischer MB et al (1998) Enhanced B-1 cell development, but impaired IgG antibody responses in mice deficient in secreted IgM. J Immunol 160 (10):4776–4787
43. Nguyen TT, Elsner RA, Baumgarth N (2015) Natural IgM prevents autoimmunity by enforcing B cell central tolerance induction. J Immunol 194(4):1489–1502
44. Freitas AA, Viale AC, Sundblad A et al (1991) Normal serum immunoglobulins participate in the selection of peripheral B-cell repertoires. Proc Natl Acad Sci U S A 88 (13):5640–5644
45. Kearney JF, Patel P, Stefanov EK et al (2015) Natural antibody repertoires: development and functional role in inhibiting allergic airway disease. Annu Rev Immunol 33:475–504
46. Patel PS, Kearney JF (2015) Neonatal exposure to pneumococcal phosphorylcholine modulates the development of house dust mite allergy during adult life. J Immunol 194(12):5838–5850
47. Vollmers HP, Brandlein S (2009) Natural antibodies and cancer. New Biotechnol 25 (5):294–298
48. Madi A, Bransburg-Zabary S, Maayan-Metzger A, Dar G, Ben-Jacob E, Cohen IR (2015) Tumor-associated and disease-associated autoantibody repertoires in healthy colostrum and maternal and newborn cord sera. J Immunol 194(11):5272–5281
49. Heyman B (2000) Regulation of antibody responses via antibodies, complement, and Fc receptors. Annu Rev Immunol 18:709–737
50. Heyman B, Pilstrom L, Shulman MJ (1988) Complement activation is required for IgM-mediated enhancement of the antibody response. J Exp Med 167(6):1999–2004
51. Ochsenbein AF, Fehr T, Lutz C et al (1999) Control of early viral and bacterial distribution and disease by natural antibodies. Science 286(5447):2156–2159
52. Zhou ZH, Zhang Y, Hu YF et al (2007) The broad antibacterial activity of the natural antibody repertoire is due to polyreactive antibodies. Cell Host Microbe 1(1):51–61

53. Stager S, Alexander J, Kirby AC, Botto M, Rooijen NV, Smith DF et al (2003) Natural antibodies and complement are endogenous adjuvants for vaccine-induced CD8+ T-cell responses. Nat Med 9(10):1287–1292
54. Kohler H, Bayry J, Nicoletti A et al (2003) Natural autoantibodies as tools to predict the outcome of immune response? Scand J Immunol 58(3):285–289
55. Jayasekera JP, Moseman EA, Carroll MC (2007) Natural antibody and complement mediate neutralization of influenza virus in the absence of prior immunity. J Virol 81 (7):3487–3494
56. Rapaka RR, Ricks DM, Alcorn JF et al (2010) Conserved natural IgM antibodies mediate innate and adaptive immunity against the opportunistic fungus Pneumocystis murina. J Exp Med 207(13):2907–2919
57. Fernandez Gonzalez S, Jayasekera JP, Carroll MC (2008) Complement and natural antibody are required in the long-term memory response to influenza virus. Vaccine 26(Suppl 8):I86–I93
58. Henson PM (2017) Cell removal: efferocytosis. Annu Rev Cell Dev Biol 33:127–144
59. Manderson AP, Botto M, Walport MJ (2004) The role of complement in the development of systemic lupus erythematosus. Annu Rev Immunol 22:431–456
60. Ansel KM, Harris RB, Cyster JG (2002) CXCL13 is required for B1 cell homing, natural antibody production, and body cavity immunity. Immunity 16(1):67–76
61. Tanabe S, Yamashita T (2018) B-1a lymphocytes promote oligodendrogenesis during brain development. Nat Neurosci 21 (4):506–516
62. Hosseini H, Li Y, Kanellakis P et al (2015) Phosphatidylserine liposomes mimic apoptotic cells to attenuate atherosclerosis by expanding polyreactive IgM producing B1a lymphocytes. Cardiovasc Res 106 (3):443–452
63. Binder CJ, Horkko S, Dewan A et al (2003) Pneumococcal vaccination decreases atherosclerotic lesion formation: molecular mimicry between Streptococcus pneumoniae and oxidized LDL. Nat Med 9(6):736–743
64. Hörkkö S, Bird DA, Miller E et al (1999) Monoclonal autoantibodies specific for oxidized phospholipids or oxidized phospholipid–protein adducts inhibit macrophage uptake of oxidized low-density lipoproteins. J Clin Invest 103(1):117–128
65. Binder CJ, Hörkkö S, Dewan A et al (2003) Pneumococcal vaccination decreases atherosclerotic lesion formation: molecular mimicry between Streptococcus pneumoniae and oxidized LDL. Nat Med 9:736
66. Thorp E, Cui D, Schrijvers DM et al (2008) Mertk receptor mutation reduces efferocytosis efficiency and promotes apoptotic cell accumulation and plaque necrosis in atherosclerotic lesions of Apoe−/− mice. Arterioscler Thromb Vasc Biol 28(8):1421–1428
67. Chang MK, Bergmark C, Laurila A et al (1999) Monoclonal antibodies against oxidized low-density lipoprotein bind to apoptotic cells and inhibit their phagocytosis by elicited macrophages: evidence that oxidation-specific epitopes mediate macrophage recognition. Proc Natl Acad Sci U S A 96(11):6353–6358
68. Suthers B, Hansbro P, Thambar S et al (2012) Pneumococcal vaccination may induce antioxidized low-density lipoprotein antibodies that have potentially protective effects against cardiovascular disease. Vaccine 30 (27):3983–3985
69. Grönwall C, Vas J, Silverman G (2012) Protective roles of natural IgM antibodies. Front Immunol 3:66
70. Tsiantoulas D, Perkmann T, Afonyushkin T et al (2015) Circulating microparticles carry oxidation-specific epitopes and are recognized by natural IgM antibodies. J Lipid Res 56 (2):440–448
71. Brändlein S, Pohle T, Ruoff N et al (2003) Natural IgM antibodies and immunosurveillance mechanisms against epithelial cancer cells in humans. Cancer Res 63 (22):7995–8005
72. Brandlein S, Pohle T, Vollmers C et al (2004) CFR-1 receptor as target for tumor-specific apoptosis induced by the natural human monoclonal antibody PAM-1. Oncol Rep 11 (4):777–784
73. Brandlein S, Rauschert N, Rasche L et al (2007) The human IgM antibody SAM-6 induces tumor-specific apoptosis with oxidized low-density lipoprotein. Mol Cancer Ther 6(1):326–333
74. Hensel F, Hermann R, Schubert C et al (1999) Characterization of glycosylphosphatidylinositol-linked molecule CD55/decay-accelerating factor as the receptor for antibody SC-1-induced apoptosis. Cancer Res 59(20):5299–5306
75. Hermann R, Hensel F, Muller EC et al (2001) Deactivation of regulatory proteins hnRNP A1 and A2 during SC-1 induced apoptosis. Hum Antibodies 10(2):83–90

76. Varambally S, Bar-Dayan Y, Bayry J et al (2004) Natural human polyreactive IgM induce apoptosis of lymphoid cell lines and human peripheral blood mononuclear cells. Int Immunol 16(3):517–524
77. Brandlein S, Lorenz J, Ruoff N et al (2002) Human monoclonal IgM antibodies with apoptotic activity isolated from cancer patients. Hum Antibodies 11(4):107–119
78. Daeron M (1997) Fc receptor biology. Annu Rev Immunol 15:203–234
79. Ravetch JV, Clynes RA (1998) Divergent roles for Fc receptors and complement in vivo. Annu Rev Immunol 16:421–432
80. Schwartz-Albiez R (2012) Naturally occurring antibodies directed against carbohydrate tumor antigens. In: Lutz HU (ed) Naturally occurring antibodies (NAbs). Springer, New York, NY, pp 27–43
81. Erttmann R (2008) Treatment of neuroblastoma with human natural antibodies. Autoimmun Rev 7(6):496–500
82. Ollert MW, David K, Schmitt C, Hauenschild A et al (1996) Normal human serum contains a natural IgM antibody cytotoxic for human neuroblastoma cells. Proc Natl Acad Sci U S A 93(9):4498–4503
83. David K, Heiligtag S, Ollert MW et al (2001) Initial characterization of the apoptosis-inducing receptor for natural human anti-neuroblastoma IgM. Med Pediatr Oncol 36 (1):251–257
84. Larkin JMG, Norsworthy PJ, A'Hern RP et al (2006) Anti-αGal-dependent complement-mediated cytotoxicity in metastatic melanoma. Melanoma Res 16(2):157–163
85. Poynton CH, Jackson S, Fegan C et al (1992) Use of IgM enriched intravenous immunoglobulin (pentaglobin) in bone marrow transplantation. Bone Marrow Transplant 9 (6):451–457
86. Kreymann KG, de Heer G, Nierhaus A et al (2007) Use of polyclonal immunoglobulins as adjunctive therapy for sepsis or septic shock. Crit Care Med 35(12):2677–2685
87. Norrby-Teglund A, Haque KN, Hammarstrom L (2006) Intravenous polyclonal IgM-enriched immunoglobulin therapy in sepsis: a review of clinical efficacy in relation to microbiological aetiology and severity of sepsis. J Intern Med 260(6):509–516
88. Haque KN, Zaidi MH, Bahakim H (1988) IgM-enriched intravenous immunoglobulin therapy in neonatal sepsis. Am J Dis Child (1960) 142(12):1293–1296
89. Stehr SN, Knels L, Weissflog C et al (2008) Effects of IGM-enriched solution on polymorphonuclear neutrophil function, bacterial clearance, and lung histology in endotoxemia. Shock (Augusta, GA) 29 (2):167–172
90. Rieben R, Roos A, Muizert YT et al (1999) Immunoglobulin M-enriched human intravenous immunoglobulin prevents complement activation in vitro and in vivo in a rat model of acute inflammation. Blood 93(3):942–951
91. Maddur MS, Vani J, Lacroix-Desmazes S et al (2010) Autoimmunity as a predisposition for infectious diseases. PLoS Pathog 6(11): e1001077
92. Marcia MB, Neelima MB, Nelson NHT (1995) Anti-endotoxin human monoclonal antibody A6H4C5 (HA-1A) utilizes the VH4.21 gene. Clin Infect Dis 21:S186–S1S9
93. Hurez V, Kazatchkine MD, Vassilev T et al (1997) Pooled normal human polyspecific IgM contains neutralizing anti-idiotypes to IgG autoantibodies of autoimmune patients and protects from experimental autoimmune disease. Blood 90(10):4004–4013
94. Vassilev T, Yamamoto M, Aissaoui A et al (1999) Normal human immunoglobulin suppresses experimental myasthenia gravis in SCID mice. Eur J Immunol 29 (8):2436–2442
95. Vassilev T, Mihaylova N, Voynova E et al (2006) IgM-enriched human intravenous immunoglobulin suppresses T lymphocyte functions in vitro and delays the activation of T lymphocytes in hu-SCID mice. Clin Exp Immunol 145(1):108–115
96. Jayne DR, Esnault VL, Lockwood CM (1993) ANCA anti-idiotype antibodies and the treatment of systemic vasculitis with intravenous immunoglobulin. J Autoimmun 6 (2):207–219
97. Rossi F, Jayne DR, Lockwood CM et al (1991) Anti-idiotypes against anti-neutrophil cytoplasmic antigen autoantibodies in normal human polyspecific IgG for therapeutic use and in the remission sera of patients with systemic vasculitis. Clin Exp Immunol 83 (2):298–303
98. Yehuda S, Elias T (2005) Protective autoantibodies: role in homeostasis, clinical importance, and therapeutic potential. Arthritis Rheum 52(9):2599–2606
99. Bolton WK, Schrock JH, Davis JS IV (1982) Rheumatoid factor inhibition of in vitro binding of IgG complexes in the human glomerulus. Arthritis Rheum 25(3):297–303
100. Andersson A, Forsgren S, Soderstrom A et al (1991) Monoclonal, natural antibodies prevent development of diabetes in the

non-obese diabetic (NOD) mouse. J Autoimmun 4(5):733–742

101. Walpen AJ, Laumonier T, Aebi C et al (2004) Immunoglobulin M-enriched intravenous immunoglobulin inhibits classical pathway complement activation, but not bactericidal activity of human serum. Xenotransplantation 11(2):141–148
102. Lobo PI, Schlegel KH, Bajwa A et al (2015) Natural IgM switches the function of lipopolysaccharide-activated murine bone marrow-derived dendritic cells to a regulatory dendritic cell that suppresses innate inflammation. J Immunol 195(11):5215–5226
103. Lobo PI, Bajwa A, Schlegel KH et al (2012) Natural IgM anti-leukocyte autoantibodies attenuate excess inflammation mediated by innate and adaptive immune mechanisms involving Th-17. J Immunol 188 (4):1675–1685
104. Ehrenstein MR, Notley CA (2010) The importance of natural IgM: scavenger, protector and regulator. Nat Rev Immunol 10 (11):778–786
105. Bibl M, Esselmann H, Otto M et al (2004) Cerebrospinal fluid amyloid beta peptide patterns in Alzheimer's disease patients and non-demented controls depend on sample pretreatment: indication of carrier-mediated epitope masking of amyloid beta peptides. Electrophoresis 25(17):2912–2918
106. Giacobini E, Becker RE (2007) One hundred years after the discovery of Alzheimer's disease. A turning point for therapy? J Alzheimers Dis 12(1):37–52
107. Bard F, Cannon C, Barbour R et al (2000) Peripherally administered antibodies against amyloid beta-peptide enter the central nervous system and reduce pathology in a mouse model of Alzheimer disease. Nat Med 6(8):916–919
108. Lambracht-Washington D, Rosenberg RN (2013) Advances in the development of vaccines for Alzheimer's disease. Discov Med 15 (84):319–326
109. Banks WA, Farr SA, Morley JE et al (2007) Anti-amyloid beta protein antibody passage across the blood-brain barrier in the SAMP8 mouse model of Alzheimer's disease: an age-related selective uptake with reversal of learning impairment. Exp Neurol 206 (2):248–256
110. Marcello A, Wirths O, Schneider-Axmann T, Degerman-Gunnarsson M, Lannfelt L, Bayer TA (2011) Reduced levels of IgM autoantibodies against N-truncated pyroglutamate Abeta in plasma of patients with Alzheimer's disease. Neurobiol Aging 32(8):1379–1387
111. Taguchi H, Planque S, Nishiyama Y et al (2008) Autoantibody-catalyzed hydrolysis of amyloid beta peptide. J Biol Chem 283 (8):4714–4722
112. Lang W, Rodriguez M, Lennon VA et al (1984) Demyelination and remyelination in murine viral encephalomyelitis. Ann N Y Acad Sci 436:98–102
113. Traugott U, Stone SH, Raine CS (1982) Chronic relapsing experimental autoimmune encephalomyelitis. treatment with combinations of myelin components promotes clinical and structural recovery. J Neurol Sci 56 (1):65–73
114. Rodriguez M, Kenny JJ, Thiemann RL et al (1990) Theiler's virus-induced demyelination in mice immunosuppressed with anti-IgM and in mice expressing the xid gene. Microb Pathog 8(1):23–35
115. Rodriguez M, Lennon VA (1990) Immunoglobulins promote remyelination in the central nervous system. Ann Neurol 27(1):12–17
116. Rodriguez M (1991) Immunoglobulins stimulate central nervous system remyelination: electron microscopic and morphometric analysis of proliferating cells. Lab Investig 64 (3):358–370
117. Rodriguez M, Lennon VA, Benveniste EN et al (1987) Remyelination by oligodendrocytes stimulated by antiserum to spinal cord. J Neuropathol Exp Neurol 46(1):84–95
118. Miller DJ, Sanborn KS, Katzmann JA et al (1994) Monoclonal autoantibodies promote central nervous system repair in an animal model of multiple sclerosis. J Neurosci 14 (10):6230–6238
119. Miller DJ, Bright JJ, Sriram S et al (1997) Successful treatment of established relapsing experimental autoimmune encephalomyelitis in mice with a monoclonal natural autoantibody. J Neuroimmunol 75(1–2):204–209
120. Asakura K, Miller DJ, Pease LR et al (1998) Targeting of IgMkappa antibodies to oligodendrocytes promotes CNS remyelination. J Neurosci 18(19):7700–7708
121. Warrington AE, Asakura K, Bieber AJ et al (2000) Human monoclonal antibodies reactive to oligodendrocytes promote remyelination in a model of multiple sclerosis. Proc Natl Acad Sci U S A 97(12):6820–6825
122. Bieber AJ, Warrington A, Asakura K et al (2002) Human antibodies accelerate the rate of remyelination following lysolecithin-induced demyelination in mice. Glia 37 (3):241–249

123. Mitsunaga Y, Ciric B, Van Keulen V et al (2002) Direct evidence that a human antibody derived from patient serum can promote myelin repair in a mouse model of chronic-progressive demyelinating disease. FASEB J 16(10):1325–1327
124. Wootla B, Denic A, Watzlawik JO et al (2016) Antibody-mediated oligodendrocyte remyelination promotes axon health in progressive demyelinating disease. Mol Neurobiol 53 (8):5217–5228
125. Ciric B, Van Keulen V, Paz Soldan M, Rodriguez M, Pease LR (2004) Antibody-mediated remyelination operates through mechanism independent of immunomodulation. J Neuroimmunol 146(1–2):153–161
126. Mullin AP, Cui C, Wang Y et al (2017) rHIgM22 enhances remyelination in the brain of the cuprizone mouse model of demyelination. Neurobiol Dis 105:142–155
127. Wright BR, Warrington AE, Edberg DD et al (2009) Cellular mechanisms of central nervous system repair by natural autoreactive monoclonal antibodies. Arch Neurol 66 (12):1456–1459
128. Cui C, Wang J, Mullin AP et al (2018) The antibody rHIgM22 facilitates hippocampal remyelination and ameliorates memory deficits in the cuprizone mouse model of demyelination. Brain Res 1694:73–86
129. Banks WA, Terrell B, Farr SA et al (2002) Passage of amyloid beta protein antibody across the blood-brain barrier in a mouse model of Alzheimer's disease. Peptides 23 (12):2223–2226
130. Pirko I, Ciric B, Gamez J et al (2004) A human antibody that promotes remyelination enters the CNS and decreases lesion load as detected by T2-weighted spinal cord MRI in a virus-induced murine model of MS. FASEB J 18(13):1577–1579
131. Warrington AE, Bieber AJ, Ciric B et al (2007) A recombinant human IgM promotes myelin repair after a single, very low dose. J Neurosci Res 85(5):967–976
132. Asakura K, Miller DJ, Murray K et al (1996) Monoclonal autoantibody SCH94.03, which promotes central nervous system remyelination, recognizes an antigen on the surface of oligodendrocytes. J Neurosci Res 43 (3):273–281
133. Howe CL, Bieber AJ, Warrington AE et al (2004) Antiapoptotic signaling by a remyelination-promoting human antimyelin antibody. Neurobiol Dis 15(1):120–131
134. Watzlawik J, Holicky E, Edberg DD et al (2010) Human remyelination promoting antibody inhibits apoptotic signaling and differentiation through Lyn kinase in primary rat oligodendrocytes. Glia 58(15):1782–1793
135. Wittenberg NJ, Im H, Xu X et al (2012) High-affinity binding of remyelinating natural autoantibodies to myelin-mimicking lipid bilayers revealed by nanohole surface plasmon resonance. Anal Chem 84(14):6031–6039
136. Paz Soldan MM, Warrington AE, Bieber AJ et al (2003) Remyelination-promoting antibodies activate distinct Ca2+ influx pathways in astrocytes and oligodendrocytes: relationship to the mechanism of myelin repair. Mol Cell Neurosci 22(1):14–24
137. Watzlawik JO, Warrington AE, Rodriguez M (2013) PDGF is required for remyelination-promoting IgM stimulation of oligodendrocyte progenitor cell proliferation. PLoS One 8 (2):e55149
138. Vana AC, Flint NC, Harwood NE et al (2007) Platelet-derived growth factor promotes repair of chronically demyelinated white matter. J Neuropathol Exp Neurol 66 (11):975–988
139. Colognato H, Baron W, Avellana-Adalid V et al (2002) CNS integrins switch growth factor signalling to promote target-dependent survival. Nat Cell Biol 4(11):833–841
140. Frost EE, Buttery PC, Milner R et al (1999) Integrins mediate a neuronal survival signal for oligodendrocytes. Curr Biol 9 (21):1251–1254
141. Baron W, Shattil SJ, Ffrench-Constant C (2002) The oligodendrocyte precursor mitogen PDGF stimulates proliferation by activation of alpha(v)beta3 integrins. EMBO J 21 (8):1957–1966
142. Howe CL, Mayoral S, Rodriguez M (2006) Activated microglia stimulate transcriptional changes in primary oligodendrocytes via IL-1beta. Neurobiol Dis 23(3):731–739
143. Zorina Y, Stricker J, Caggiano AO et al (2018) Human IgM antibody rHIgM22 promotes phagocytic clearance of myelin debris by microglia. Sci Rep 8(1):9392
144. Xu X, Warrington AE, Wright BR et al (2011) A human IgM signals axon outgrowth: coupling lipid raft to microtubules. J Neurochem 119(1):100–112
145. Xu X, Wittenberg NJ, Jordan LR et al (2013) A patterned recombinant human IgM guides neurite outgrowth of CNS neurons. Sci Rep 3:2267
146. Denic A, Bieber A, Warrington A et al (2009) Brainstem 1H nuclear magnetic resonance (NMR) spectroscopy: marker of

demyelination and repair in spinal cord. Ann Neurol 66(4):559–564

147. Wootla B, Denic A, Watzlawik JO et al (2015) A single dose of a neuron-binding human monoclonal antibody improves brainstem NAA concentrations, a biomarker for density of spinal cord axons, in a model of progressive multiple sclerosis. J Neuroinflammation 12:83
148. Xu X, Denic A, Jordan LR et al (2015) A natural human IgM that binds to gangliosides is therapeutic in murine models of amyotrophic lateral sclerosis. Dis Model Mech 8 (8):831–842
149. Ripps ME, Huntley GW, Hof PR et al (1995) Transgenic mice expressing an altered murine superoxide dismutase gene provide an animal model of amyotrophic lateral sclerosis. Proc Natl Acad Sci U S A 92(3):689–693
150. Pollerberg EG, Sadoul R, Goridis C et al (1985) Selective expression of the 180-kD component of the neural cell adhesion molecule N-CAM during development. J Cell Biol 101(5 Pt 1):1921–1929
151. Kleene R, Mzoughi M, Joshi G et al (2010) NCAM-induced neurite outgrowth depends on binding of calmodulin to NCAM and on nuclear import of NCAM and fak fragments. J Neurosci 30(32):10784–10798
152. Giza J, Biederer T (2010) Polysialic acid: a veteran sugar with a new site of action in the brain. Proc Natl Acad Sci U S A 107 (23):10335–10336
153. Czepiel M, Leicher L, Becker K et al (2014) Overexpression of polysialylated neural cell adhesion molecule improves the migration capacity of induced pluripotent stem cell-derived oligodendrocyte precursors. Stem Cells Transl Med 3(9):1100–1109
154. Watzlawik JO, Kahoud RJ, Ng S et al (2015) Polysialic acid as an antigen for monoclonal antibody HIgM12 to treat multiple sclerosis and other neurodegenerative disorders. J Neurochem 134(5):865–878
155. Warrington AE, Bieber AJ, Van Keulen V et al (2004) Neuron-binding human monoclonal antibodies support central nervous system neurite extension. J Neuropathol Exp Neurol 63(5):461–473
156. Xu X, Denic A, Warrington AE et al (2013) Therapeutics to promote CNS repair: a natural human neuron-binding IgM regulates membrane-raft dynamics and improves motility in a mouse model of multiple sclerosis. J Clin Immunol 33(Suppl 1):S50–S56
157. Lopez PH, Schnaar RL (2009) Gangliosides in cell recognition and membrane protein regulation. Curr Opin Struct Biol 19 (5):549–557
158. Vyas AA, Patel HV, Fromholt SE et al (2002) Gangliosides are functional nerve cell ligands for myelin-associated glycoprotein (MAG), an inhibitor of nerve regeneration. Proc Natl Acad Sci U S A 99(12):8412–8417
159. Sheikh KA, Sun J, Liu Y et al (1999) Mice lacking complex gangliosides develop Wallerian degeneration and myelination defects. Proc Natl Acad Sci U S A 96(13):7532–7537
160. Nguyen T, Mehta NR, Conant K et al (2009) Axonal protective effects of the myelin-associated glycoprotein. J Neurosci 29 (3):630–637
161. Montecino-Rodriguez E, Dorshkind K (2012) B-1 B cell development in the fetus and adult. Immunity 36(1):13–21
162. Nakahara J, Tan-Takeuchi K, Seiwa C et al (2003) Signaling via immunoglobulin Fc receptors induces oligodendrocyte precursor cell differentiation. Dev Cell 4(6):841–852
163. Nielsen JA, Maric D, Lau P et al (2006) Identification of a novel oligodendrocyte cell adhesion protein using gene expression profiling. J Neurosci 26(39):9881–9891

Chapter 4

Monoclonal Antibodies for the Treatment of Melanoma: Present and Future Strategies

Madhuri Bhandaru and Anand Rotte

Abstract

Metastatic melanoma is a dreadful type of skin cancer arising due to uncontrolled proliferation of melanocytes. It has very poor prognosis, low 5-year survival rates and until recently there were only handful of treatment options for metastatic melanoma patients. The drugs that were approved for the treatment had low response rates and were associated with severe adverse events. With the introduction of monoclonal antibodies against inhibitory immune checkpoints the treatment landscape for metastatic melanoma has changed dramatically. Ipilimumab, the first monoclonal antibody to be approved for the treatment of metastatic melanoma, showed significant improvements in durable response rates in patients and paved the way for next class of monoclonal antibodies. Nivolumab and pembrolizumab, the anti-PD-1 antibodies that were approved 3-years after the approval of ipilimumab, had decent response rates, low relapse rates and showed manageable safety profile. Antibodies against ligands for PD-1 receptors were then developed to overcome the adverse effects of anti-PD-1 antibodies and combination of monoclonal antibodies (ipilimumab plus nivolumab) was tested to increase the response rates. Additional target receptors that regulate T cell activity were identified on T cells and monoclonal antibodies against potential targets such as TIGIT, TIM-3, and LAG-3 were developed. This chapter discusses the details of monoclonal antibodies used for the treatment of melanoma along with the ones that could be introduced in the near future with emphasis on mechanisms by which antibodies stimulate anti-tumor immune response and the specifics of target molecules of the antibodies.

Key words Co-stimulation, Checkpoints, T cells, CTLA-4, PD-1, TIGIT, TIM-3, LAG-3, ADCC

1 Introduction

Melanoma is the most deadly type of skin cancer caused due to uncontrolled proliferation of the melanin-producing cells, known as melanocytes located at the basal layer (Stratum basale) of skin epidermis [1]. Though it accounts for less than 5% of all skin cancer types, it is the most aggressive type of skin cancer and nearly 80% of the skin cancer-related deaths are due to melanoma. Studies from USA reported it as the fifth most frequent cancer in men and seventh most frequent cancer in women [2, 3]. Melanoma is more prevalent in Caucasian population. According to the data

Michael Steinitz (ed.), *Human Monoclonal Antibodies: Methods and Protocols*, Methods in Molecular Biology, vol. 1904, https://doi.org/10.1007/978-1-4939-8958-4_4,

published by International Agency for Research on Cancer (IARC), American Hawaii Islands have the highest incidence of melanoma followed by Queensland, Australia [4–6]. Within United States, melanoma is reported to be more prevalent in California, Florida, New York, Pennsylvania, and Texas [4]. Exposure to UV radiation and familial history are considered the most common causative factors. When detected in early stage, melanoma can be treated by surgical resection and primary melanoma has a very good posttreatment prognosis rate. However, if the tumors metastasize, melanoma has poor prognosis and less than 15% of the metastatic melanoma patients survive for 5-years [2, 3, 7, 8]. Until recently, there were only a handful of treatment options available for patients with metastatic melanoma. Dacarbazine and high-dose IL-2 were the only FDA-approved drugs available for metastatic melanoma patients for several decades [9, 10]. In the past decade, there have been considerable advances in the treatment of melanoma. The approvals of vemurafenib (specific inhibitors of BrafV600E; BRAF harboring a point mutation resulting from a substitution of valine at amino-acid 600 with glutamine) and ipilimumab (monoclonal antibody against cytotoxic T-lymphocyte-associated antigen 4; anti-CTLA-4) in 2011 are considered major milestones in treatment of melanoma; the drugs increased the survival rates of patients and laid foundation for further research in targeted therapy and immunotherapy of melanoma respectively. Especially, the success of ipilimumab in stabilizing the disease and increasing the overall survival has particularly interested clinicians in monoclonal antibodies that can stimulate immune response and paved the way for the next class of monoclonal antibodies targeting programmed cell death protein 1 (PD-1) receptors on immune effector cells such as T cells and NK cells [11]. Two anti-PD-1 antibodies, pembrolizumab and nivolumab, were approved for the treatment of unresectable metastatic melanoma in 2014, just 3 years after the approval of Ipilimumab (Fig. 1; Table 1). In the following months, their use was approved for other major cancer types such as non-small cell lung cancer (NSCLC), renal cell carcinoma (RCC), classic Hodgkin's lymphoma, and head and neck squamous cell carcinoma (HNSCC) [12–14]. Anti-PD-1 antibody, pembrolizumab, also got a broad approval for the treatment of any solid tumor with microsatellite instability-high (MSI-H) or mismatch repair deficient (dMMR) abnormalities [15–17]. To overcome the immune-related adverse events commonly seen with anti-PD-1 therapy, researchers developed monoclonal antibodies against PD-L1, the ligand for PD-1 receptors commonly found on tumor surface. Three anti-PD-L1 monoclonal antibodies including atezolizumab, avelumab, and durvalumab have been approved for various cancer subtypes such as bladder cancer and NSCLC, and are in advanced stages of clinical testing for melanoma. Following the favorable outcomes from anti-CTLA-4, anti-PD-1, and anti-PD-

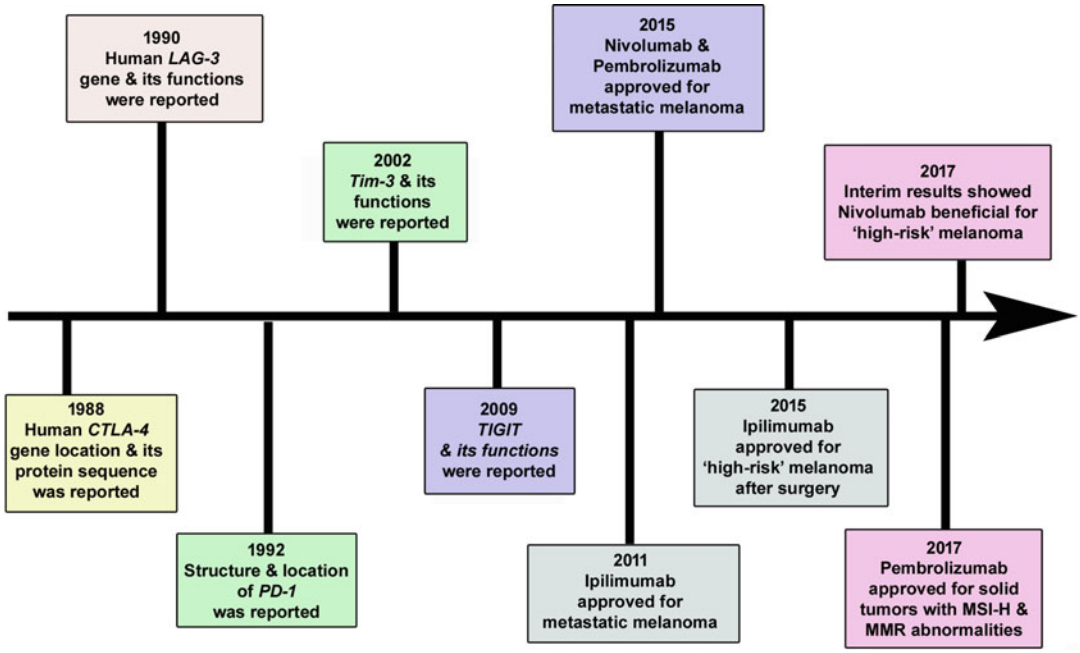

Fig. 1 Milestones in immunotherapy of melanoma

Table 1
List of immune-based drugs approved for the treatment of melanoma

Drug	Marketed by	Category	Indication
Aldesleukin (proleukin)	Prometheus	Cytokine	Metastatic melanoma
Interferon-a2b (intron-A)	Merck	Cytokine	Surgically resected "high-risk" melanoma
Pegylated interferon-a2b (sylatron)	Merck	Cytokine	Surgically resected "high-risk" melanoma
Ipilimumab (Yervoy)	Bristol-Myers Squibb	Monoclonal antibody	Metastatic melanoma and surgically resected "high-risk" melanoma
Nivolumab (Opdivo)	Bristol-Myers Squibb	Monoclonal antibody	Metastatic melanoma
Pembrolizumab (Keytruda)	Merck	Monoclonal antibody	Metastatic melanoma
Talimogene laherparepvec (Imlygic)	Amgen	Oncolytic virus	Local melanoma lesions

L1 antibodies, researchers identified the additional target receptors on immune cells (T cells and NK cells) such as T-cell immunoglobulin and ITIM domain (TIGIT), T-cell immunoglobulin-3 (TIM-3), and lymphocyte activation gene 3 (LAG-3) and

developed monoclonal antibodies against the receptors; the antibodies are in clinical testing and are in advanced stages of approval. This chapter highlights the potential of monoclonal antibodies in stimulating anti-tumor immune response and discusses key details that regulate their mechanism of action. Antibodies can activate immune response by two mechanisms: one by activating the immune effector cell-mediated antibody-dependent cellular cytotoxicity (ADCC) and other by activating T cells. The key events in the initiation of immune response such as ADCC and activation of T cells are discussed in the following sections to help in understanding mechanism of action of monoclonal antibodies.

2 ADCC and Effector Functions

ADCC is a non-phagocytic, complement as well as MHC restriction independent mechanism through which innate immune cells such as macrophages, DCs, neutrophils, and NK cells kill the antibody-bound target cells (Table 2). The target-bound antibody achieves the specificity of ADCC and it can be induced in vitro by comparatively lower concentrations of antibody than that is required to activate complement-mediated lysis [18]. The initial step in the activation of ADCC is the binding of Ig-antibodies (exogenous or endogenous) to the receptors or antigens present on the target cell. The Fc- region of the antibody then binds to the Fc-γ receptors on the surface of cytotoxic leukocytes and connects the target cell to effector cells. ADCC effector cells express two types of Fc-γ receptors (Fc-γRs); stimulatory Fc-γRs, which have immunoreceptor tyrosine-based activating motif (ITAM) in their protein structure and inhibitory Fc-γRs, which have immunoreceptor tyrosine-based inhibitory motif (ITIM) in their protein structure [18]. In humans, Fc-γRI (CD64), Fc-γ RIIa, Fc-γ RIIc (CD32), and Fc-γ RIIIa (CD16) are the activating Fc-γ receptors and Fc-γRIIb is the inhibitory Fc-γ receptor (Table 2). Binding of antibodies to activating Fc-γ receptors results in the release of cytotoxic mediators such as perforin, granzyme, tumor necrosis factor-α (TNF-α), and reactive oxygen species (ROS) on to the target cell surface and induces target cell lysis. The expression of Fc-γRs on the effector cell surface and the binding affinity of the IgG isotype to Fc-γR regulate the induction of ADCC by antibody [19–22]. NK cells are the most commonly studied cells for ADCC and macrophages are the only cells in humans that express all the three types of activating Fc-γRs [18, 23, 24]. Similarly, antibodies with IgG1 backbone have highest affinity to all the three stimulatory Fc-γRs and can induce significant ADCC whereas IgG2-based antibodies do not induce ADCC and are preferred when ADCC is undesirable in the therapy (Table 3).

Table 2
Fcγ expression on effector cells (summarized from [19, 21, 22, 108])

	Activating receptors with IC ITAM motif				No IC motif	Inhibitory receptor with ITIM motiff
Cell type	Fcγ RI	Fcγ RIIA	Fcγ RIIC	Fcγ RIIIA	Fcγ RIIIB	Fcγ RIIB
Monocytes	+	+	−	+	−	+
Macrophages	+	+	−	+	−	+
DCs	Inducible in immature DCs	+	−	−	−	+
Neutrophils	Inducible	+	−	−	+	+
NK cells	−	−	+	Expressed in 10% of individuals	−	−
B-cells	−	−	−	−	−	+

Table 3
Fcγ binding affinity of IgG (summarized from [20])

Antibody isotype	Affinity (K_A) for Fcγ RI	K_A for Fcγ RIIA	K_A for Fcγ RIIB/C	K_A for Fcγ RIIIA	K_A for Fcγ RIIIB
IgG1	+++	++	+	++	+
IgG2	n.m.	+	+	+	n.m.
IgG3	+++	+	+	++	++
IgG4	+++	+	+	+	n.m.

+++, 100–700 × 10^5 M^{-1}; ++, 10–100 × 10^5 M^{-1}; +, 0.1–10 × 10^5 M^{-1}; not measured

3 Activation of T Cells

Adaptive immune system is evolved to initiate antigen-specific responses and the critical step during initiation of meticulous responses is activation of T cells that can recognize and act against specific antigen-expressing cells. Antigen-presenting cells (APCs) such as dendritic cells (DCs) play an important role in the process by capturing antigens, processing the antigens, migrating to lymph nodes, and presenting the processed antigens on major histocompatibility complex I/II (MHC I/II) molecules to antigen-specific T cells [25]. Activation of T cells involves presentation of antigens on MHC I/II molecules to T cell receptor (TCR) on T cells along with a second set of activating signal, which most commonly is from the interaction between CD28 receptors on T cells and B7-ligands (CD80/CD86) on DCs. "Two-signal stimulation" of T cells is

Table 4
Co-stimulatory and inhibitory receptors on T cells and their respective ligands

Receptor	Ligand/s
Co-stimulatory receptors	
CD28	B7–1 (CD80) and B7–2 (CD86)
OX40	OX40L
ICOS	B7RP-1
CD40	CD40L
CD27	CD70
4-1BB	4-1BBL
DNAM1	CD155 and CD112
GITR	GITRL
RANK-L	TRANCE (RANK)
CD30	CD30L
LFA-1	ICAM-1
ICAM3	DC-SIGN
CD2	CD58
Inhibitory/checkpoint receptors	
CTLA-4	B7-1 (CD80) and B7-2 (CD86)
PD-1	PD-L1 and PD-L2
TIGIT	CD155 and CD112
BTLA-4	HVEM
TIM-3	Galectin-9, CEACAM and phosphatidyl serine
LAG-3	MHC II molecules and LSECtin
NKG2A	HLA-E
CD96	CD155
CEACAM1	CEACAM1
KIR	HLA class I
KLRG1	E-, N-, and R-cadherins
CD160	HVEM

commonly known as co-stimulation and in addition to CD28, several other receptors also function as co-stimulatory receptors; the receptors and their respective ligands are listed in Table 4. Co-stimulation is an essential requirement for priming of T cells and in the absence of co-stimulation, antigen presentation to T cells

results in anergy and apoptosis instead of activation. Co-stimulation thus mainly helps in preventing the initiation of T cell response against possibly harmless antigen [26]. Uncontrolled T cell activation and initiation of T cell response against harmless self-antigens is also prevented by specialized receptors on T cells called "checkpoint receptors," which act by binding to their respective ligands on DCs (APCs). Under resting conditions, the expression of checkpoint receptors is usually not detectable but can be induced upon TCR activation [27]. Cytotoxic T-lymphocyte-associated protein-4 (CTLA-4) and programmed cell death protein-1 (PD-1), discussed in the following sections, are the main checkpoints that regulate T cell activation in lymph nodes. The fate of the T cell that is presented with antigen by DCs depends on: degree of TCR activation, number of co-stimulatory receptors, presence of co-stimulatory ligands on DCs as well as on the number of checkpoint receptors [14]. Activated T cells then leave the lymph nodes, enter circulation, and migrate to the target site. Interestingly, T cells can interact again with a new APC or other immune cells at the target site resulting in a second set of activation or inhibition. The second interaction is not a compulsory event but the colocalization of immune cells in narrow tissue spaces introduces the possibility of interactions between immune cells such as T cell:DC, T cell:T cell, T cell:NK cell, and so on. The second interaction in the tissues could possibly decide the outcome of immune response and whether an activated T cell should proceed with effector functions or should be shut down and prevented from causing damage to the tissues. Some immunologists proposed a two-step activation theory of T cells to explain the significance of second interaction; they proposed that the first step of activation takes place in the lymph nodes and the second step of activation takes place in the peripheral tissues. According to the "two-step" activation model, T cells are primed and activated in the first step but are not fully committed to the effector phenotype. Only after the second interaction, referred to as second "touch" in the tissues, complete differentiation and commitment to effector functions takes place [28]. Though there is not enough data to support the two-step activation model, the possibility of interactions between immune cells and their outcomes needs to be considered during immune response. While co-stimulatory receptors on T cells would further activate the T cells and amplify the immune response during "second touch," inhibitory checkpoint receptors would inhibit the T cells and dampen the response (Fig. 2). Checkpoint receptors such as CTLA-4, PD-1, TIGIT, TIM-3, and LAG-3 are found to be the main regulators of T cell activity in the tumor microenvironment and their potential as targets for immunotherapy has been demonstrated in clinical testing (Table 5). They are therefore the focus of this chapter and are discussed in detail in the following sections.

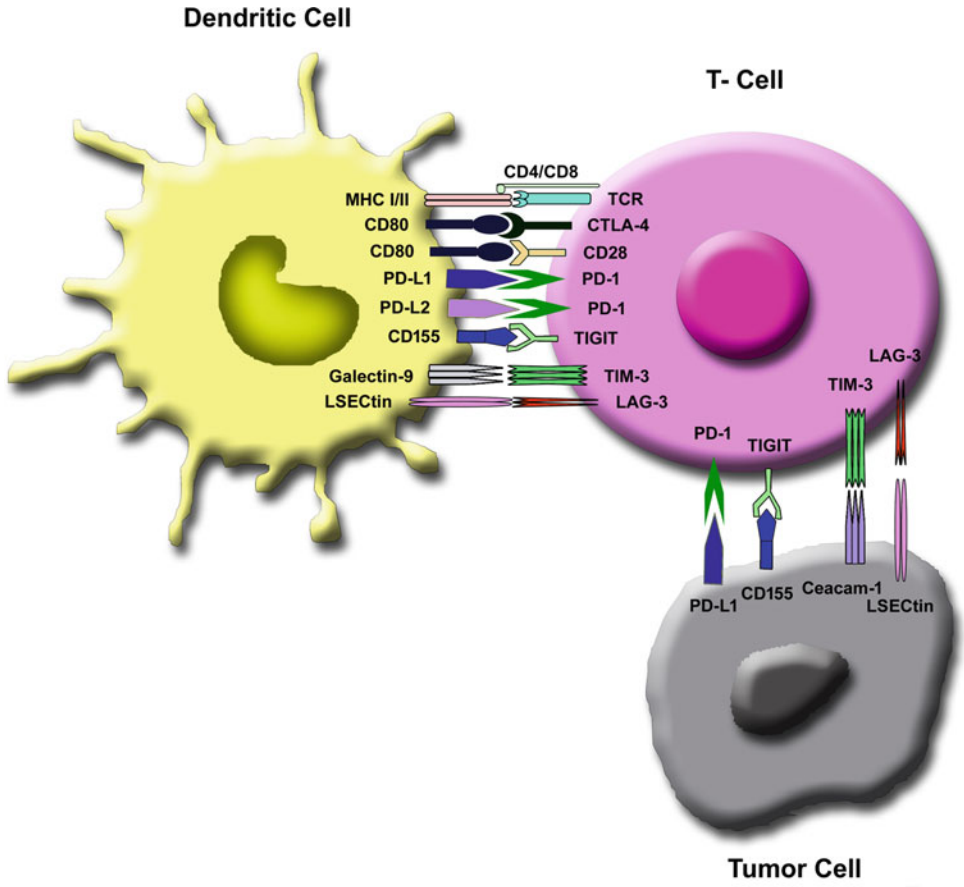

Fig. 2 Regulation of T cell activation. The outcome of T-cell priming in lymph node depends on the degree of TCR activation and on the levels of co-stimulatory/checkpoint receptor expression on T cells

4 Checkpoints Targeted for Melanoma Treatment

4.1 Cytotoxic T-Lymphocyte Associated Protein 4 (CTLA-4)

4.1.1 Structure and Expression

CTLA-4 is also known as cluster of differentiation 152 (CD152). It was discovered in 1987 by Brunet et al., through screening of mouse cytolytic T-cell-derived cDNA libraries and was described as a 223-amino acid protein belonging to immunoglobulin (Ig) super family (Table 5). The protein was mainly found to be expressed in activated lymphocytes and was co-induced with T-cell-mediated cytotoxicity [29]. Located on chromosome 2q33, human *CTLA-4* gene encodes a type 1 transmembrane glycoprotein belonging to Ig super family that is composed of four domains including a single peptide, an extracellular ligand-binding domain, a transmembrane domain, and a short cytoplasmic tail [30, 31]. CTLA-4 expression is minimal in resting T cells; it is induced at both mRNA and protein level in response to TCR activation, requires entry into cell cycle and peak expression is

Table 5
Commonly targeted checkpoints for the treatment of cancer

Receptor (synonyms)	Ligands	Cells expressing receptor	Cells expressing ligands
CTLA-4 (CD152)	CD80 and CD86	Effector T cells and TRegs	APCs
PD-1 (PDCD1 and CD279)	PD-L1 and PD-L2	Effector T cells, TRegs, NK cells, and macrophages	APCs, hematopoietic and nonhematopoietic cells and tumor cells
TIGIT (WUCAM)	PVR/CD155 and CD112	Effector T cells, memory T cells, TRegs, NK cells, and NKT cells	APCs, fibroblasts, endothelial cells, and tumor cells
TIM-3 (HAVCR2)	Ceacam-1, Galectin-9, HMGB-1, and phosphatidyl serine	Effector T cells, TRegs, DCs, NK cells, and monocytes	APCs and tumor cells
LAG-3 (CD223)	MHC II class LSECtin and galectin-3	Effector T cells, TRegs, and NK cells	APCs Liver cells and tumor cells

seen at 24–48 h post TCR stimulation [32, 33]. As listed in Table 5, CTLA-4 is generally expressed on activated T cells, however unlike other effector cells, regulatory T cells or TRegs constitutively express CTLA-4 owing to their high expression of forkhead transcription factor FoxP3, a known regulator of CTLA-4 expression [34].

4.1.2 Role in Immune Response

CTLA-4 binds to B7 ligands (B7-1 and B7-2) on APCs. Due to high degree of shape complementarity found in the binding interface of CTLA-4 and B7 ligands, the two are packed in a periodic arrangement in the crystal lattice where bivalent CTLA-4 homodimers bridge the bivalent B7-1 homodimers, forming stable signaling complexes at the T-cell surface [35]. During T-cell activation, CTLA-4 binds to B7 ligands with higher affinity and at a much lower surface density compared to CD28 and suppresses the activation by competing with CD28 for binding with B7 ligands expressed on APCs. Blockade of CD28-B7 ligand interaction prevents the T cell from receiving the second activation signal and induces anergy in T cells (Fig. 3) [27]. CTLA-4 sequesters B7-ligands, followed by trans-endocytosis and degradation of endocytosed ligands resulting in significant depletion of the B7 ligands from the surface of APCs and induction of a tolerogenic

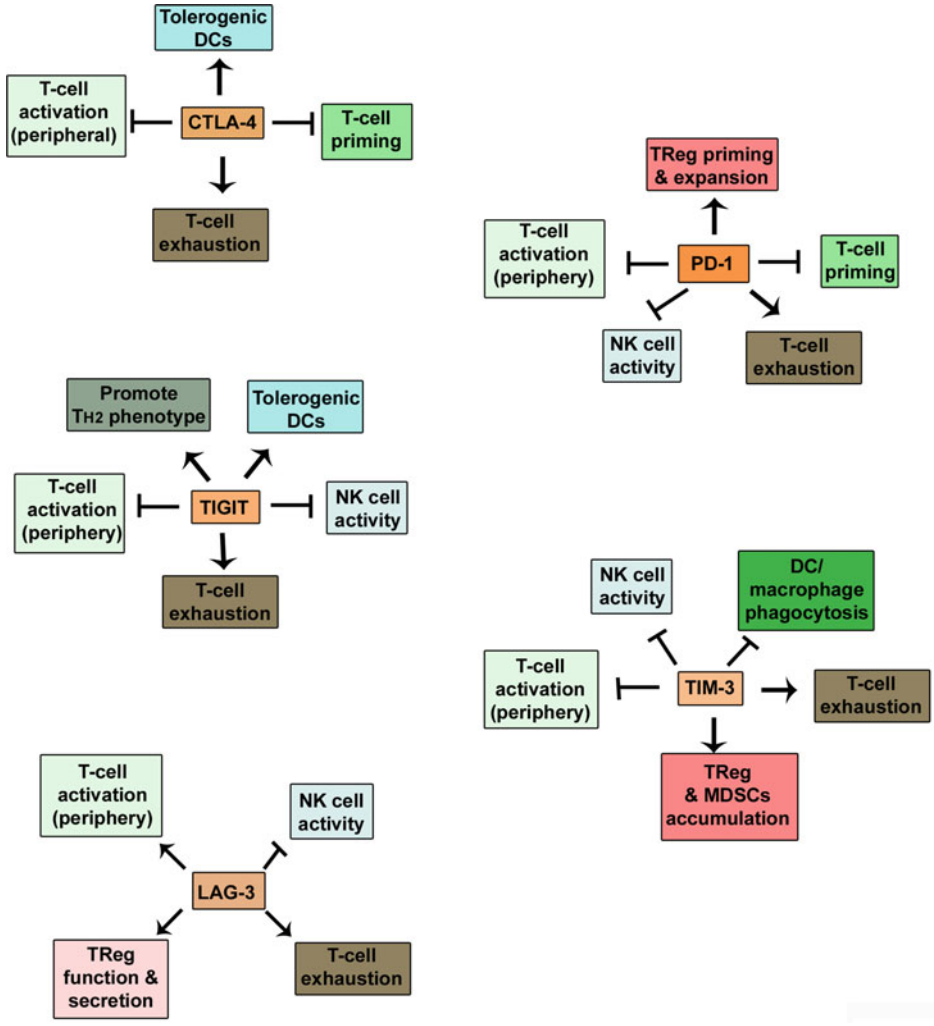

Fig. 3 Effects of checkpoint inhibition on immune response. The distinct role of checkpoint receptors CTLA-4, PD-1, TIGIT, TIM-3, and LAG-3 in regulation of T-cell responses are shown in the figure

phenotype in APCs [36]. The significance of CTLA-4 in regulation of immune response can be understood from the severe autoimmune phenotype of *Ctla-4* knock-out mice; *Ctla-4*$^{-/-}$ mice were reported to develop rapidly progressive and fatal autoimmune disease characterized by massive lymphoproliferation, multiorgan tissue destruction, and death by 3–4 weeks of age [37, 38].

4.1.3 Signal Transduction

CTLA-4 mainly acts by competitively inhibiting the co-stimulatory binding of CD28 of T cells with the B7 ligands on APCs. However, studies into the intracellular events that follow CTLA-4 engagement also illustrated activation of cell-intrinsic signaling cascades and cross-talks with pathways regulating cell survival and proliferation [39, 40]. CTLA-4 was shown to inhibit TCR-mediated ERK

activation, T-cell proliferation, and cytokine production independent of B7 binding [41]. The cytoplasmic domain of CTLA-4 was shown to regulate the vesicular trafficking and transendocytosis of B7 ligands and interact with a number of signaling molecules that could inhibit downstream signaling of TCR and CD28 [39]. CTLA-4 was also reported to inhibit IL-2 production and induce cell cycle arrest through cross-talks with phosphatidylinositol 3-kinase (PI3K) and NFκB pathways. Additionally, CTLA-4 was shown to upregulate anti-apoptotic factor Bcl-xL, inhibit nuclear accumulation of transcription factors such as AP1, NFAT, and NFκB, and inhibit cell cycle regulating proteins such as CDK4, CDK6, and cyclin D3 [42–44].

4.1.4 Target for Cancer Immunotherapy

The potential of CTLA-4 as a target for cancer immunotherapy was demonstrated through in vivo administration of anti-CTLA-4 antibodies, which resulted in rejection of tumors including the pre-established tumors. More importantly, the study showed that mice treated with anti-CTLA-4 antibodies developed immune memory against tumors and resisted secondary exposure to tumor cells [45]. Three antibodies, ipilimumab (MDX-010; Yervoy™, Bristol-Myers Squibb), tremelimumab (CP-642206; formerly known as ticilimumab), and CP-642570 (parental antibody of tremelimumab) entered clinical trials. CP-642570 administration reportedly caused treatment-related thrombocytopenia and was discontinued from development [11]. Both ipilimumab and tremelimumab are fully human monoclonal antibodies but differ in their IgG backbone and their ability to initiate effector response. While ipilimumab is IgG1 monoclonal antibody with full effector functions (Table 6), tremelimumab is a IgG2 monoclonal antibody with no effector functions. Ipilimumab is approved for unresectable metastatic melanoma as well as adjuvant to surgery for "high-risk" melanoma. Tremelimumab is not yet approved for the treatment of cancer, but is in advanced stages of clinical development [11, 46].

4.2 Programmed Cell Death Protein 1 (PD-1)

4.2.1 Structure and Expression

PD-1, also known as PDCD1 and CD279, is a cell surface receptor expressed commonly on T cells. It was first described by Honjo and his coworkers from studies on pathways of programmed cell death [47]. Human *PD-1* gene is located on chromosome 2q37.3; it encodes a type I transmembrane protein belonging to Ig super family (Table 5). PD-1 is composed of 288 amino acids with an extracellular N-terminal IgV-like domain, a transmembrane domain, and a cytoplasmic tail [48]. The extracellular domain of PD-1 is partly similar to CTLA-4 with 21–33% sequence homology, but it lacks the extracellular cysteine residue required for covalent dimerization and exists as a monomer on the cell surface as well as in solution, unlike CTLA-4, which is a dimer. Its cytoplasmic domain consists of two tyrosine residues including

Table 6
Details of origin, IgG subtype, Fcg binding, binding affinity to receptor, ADCC for monoclonal antibodies approved for the treatment of cancer

Drug	Origin	IgG sub-type	Molecular weight (kDa)	Kd for target molecule	Affinity to activating FcγR	ADCC	Reference
Ipilimumab	Human	IgG1	148	5.24 nM	High	High	[46]
Nivolumamb	Human	IgG4	146	3.06 nM	Low	Low	[62, 63, 109]
Pembrolizumab	Humanized	IgG4	149	29 pM	Low-none	None	[62, 110]
Atezolizumab	Humanized	IgG1	145	0.433 nM	None (FcγR-binding region deleted)	None	[62]
Avelumab	Human	IgG1	147	0.667 nM	High	High	[64]
Durvalumab	Human	IgG1	146	0.0467 nM	None (FcγR-binding region deleted)	None	[64]

immunoreceptor tyrosine-based inhibitory motif (ITIM) and immunoreceptor tyrosine-based switch motif (ITSM). Studies on PD-1 cytoplasmic domain found that the amino acid sequence surrounding ITSM domain was conserved between human and mouse protein and that the tyrosine residue located within ITSM was essential for the inhibitory function of PD-1 [12]. PD-1 expression is not detected on naïve T cells, whereas B cells have basal levels of PD-1 expression. Activation of TCR/BCR leads to induction in PD-1 expression and/or recruitment of PD-1 to the surface. In addition to activated T cells and B cells, PD-1 expression is also seen on TRegs, natural killer T cells (NKT), natural killer (NK) cells, activated monocytes and on myeloid DCs (Table 5). Two ligands, PD-L1 (B7-H1) and PD-L2 (B7-DC), have been identified to bind to PD-1 receptors. PD-L1 is the widely expressed ligand for PD-1; it is expressed on T cells, B cells, macrophages, DCs as well as non-hematopoietic cell types such as vascular endothelial cells, fibroblastic reticular cells, epithelia, pancreatic islet cells, astrocytes, and neurons. PD-L1 expression is also seen in cells at sites of immune privilege including trophoblasts in the placenta and retinal pigment epithelial cells and neurons in the eye. The second ligand for PD-1, PD-L2 is not as widely expressed as PD-L1 and is mainly seen on activated macrophages and DCs [49–51]. However, PD-L2 reportedly has higher binding affinity to PD-L1 and has ~three-fold lower K_d value compared to PD-L1 [52].

4.2.2 Role in Immune Response

PD-1 receptors inhibit the characteristic features of immune responses such as cell proliferation, cytokine secretion, and cytotoxic ability [40]. In addition, PD-1 signaling was also found to enhance FoxP3 expression and regulate the differentiation of induced TReg (iTReg) cells in murine models [53]. Like CTLA-4, PD-1 receptors are critical regulators of immune response as seen by spontaneous autoimmune phenotype of *PD-1* knock-out mice. However, the phenotype of PD-1 deficient mice is relatively mild compared to CTLA-4 and was reported to be dependent on the genetic background of the mouse. Lupus-like syndrome, characterized by glomerulonephritis and arthritis with delayed onset, was seen in *Pdcd*$^{-/-}$ mice from C57Bl/6 background whereas autoimmune dilated cardiomyopathy was reported in *Pdcd*$^{-/-}$ mice from BALB/c background [54, 55]. The main purpose of PD-1:PD-L pathway is to control the extent of immune cell activation and prevent the damage to healthy neighboring tissues. PD-L1 expression is induced on the surface of the normal tissues in response to IFN-γ as a protective mechanism from T-cell-mediated damage. Tumor cells utilize this normal physiological mechanism and develop resistance to anti-tumor immune response by expressing PD-L1 [34]. Additionally, under conditions such as chronic infections and tumors, the presence of increased levels of inflammatory cytokines and antigens results in T-cell exhaustion and dysfunction characterized by increased expression of PD-1 [56].

4.2.3 Signal Transduction

Upon recruitment to immune synapse and ligation, PD-1 sends inhibitory signals leading to inhibition of glucose consumption, cytokine production, proliferation, and survival of T cells. Stimulation of PD-1 receptors results in phosphorylation on the tyrosine residue located within the ITSM motifs of the cytoplasmic tail, leading to recruitment of phosphatases SHP1 and SHP2, which then dephosphorylate downstream effectors such as Syk, PI3K, ZAP70, and CD3ζ in T- and B cells. Inhibition of PI3K pathway prevents the activation of the cell survival factor Bcl-xL and the expression of transcription factors such as GATA-3, T-bet, and Eomes that regulate the effector functions of T cells [50]. In contrast to CTLA-4, which blocks phosphorylation of Akt, via activation of protein phosphatase 2 (PP2A), PD-1 recruits SHP2 and blocks the proximal activation of PI3K and thereby prevents activation of Akt [57]. The extent of PD-1-mediated inhibition thus depends on TCR signal strength and can be abrogated in the presence of T cell co-stimulation via CD28 or IL-2 [12]. Strikingly, IL-2 was shown to rescue T cells from PD-1-mediated effects by direct activation of Akt via STAT5 and circumvent the PD-1 interference [58]. Apart from IL-2, other cytokines such as IL-7 and IL-15 that induce activation of STAT5, were also found to abate the inhibitory effects of PD-1 ligation [59].

4.2.4 Target for Cancer Immunotherapy

The importance of targeting PD-1:PD-L pathway for treatment of cancer can be seen from the reports showing the expression of PD-1 by TILs and exhausted T cells, and PD-L1 in several cancer types including bladder, lung, colon, breast, kidney, ovary, cervix, melanoma, glioblastoma, multiple myeloma, and T-cell lymphoma. Targeting PD-1/PD-L1 to enhance anti-tumor immune response proved to be the most successful strategy to date; three antibodies including pembrolizumab (MK-3475; formerly known as lambrolizumab; anti-PD-1; Merck), nivolumab (BMS96558; anti-PD-1; Bristol-Myers Squibb), Atezolizumab (anti-PD-L1; Genentech/Roche), Avelumab (anti-PD-L1; Pfizer), and Durvalumab (anti-PD-L1, AstraZeneca) are approved by US FDA for the treatment of different types of cancer [60]. Pembrolizumab and nivolumab were approved for the treatment of metastatic melanoma in 2014. They both have IgG4 backbone, with low FcγR binding and were not found to induce ADCC in in vitro studies. Pembrolizumab is a humanized antibody with comparatively higher PD-1 affinity, whereas nivolumab is a fully human antibody with slightly lower affinity (Table 6). Anti-PD-L1 antibodies, atezolizumab, avelumab, and durvalumab are yet to be approved for the treatment of melanoma. Atezolizumab is a humanized antibody and Avelumab and Durvalumab are fully human antibodies; while all the three antibodies have IgG1 isotype, only Avelumab has FcγR-binding ability and therefore has intact ADCC functions. FcγR-binding region of Atezolizumab and Durvalumab is engineered to prevent the binding of the antibody to Fcγ receptors and subsequent induction of ADCC [61–64].

5 Novel Targets in Clinical Testing

5.1 T-Cell Immunoglobulin and ITIM Domain (TIGIT)

5.1.1 Structure and Expression

TIGIT is a recently discovered inhibitory receptor belonging to the CD28 family and Ig superfamily. The expression of TIGIT on TRegs, activated and memory T cells was identified by scientists from Genentech in 2008 through a genomic search for T-cell-specific genes with protein domain structures representative of potential inhibitory receptors [65]. Later in the same year Boles et al. reported TIGIT as a novel immunoreceptor, Washington University Cell Adhesion Molecule (WUCAM) on human follicular B helper T cells (TFH) that bound to Polio Virus Receptor (PVR; also known as CD155 and nectin-like protein 5), expressed on follicular DCs under both static and flow conditions [66]. *TIGIT* gene is located on chromosome 3q13.31; the encoded 244-amino acid protein consists of single extracellular immunoglobulin domain, a type 1 transmembrane region and a single intracellular ITIM domain [65]. TIGIT is mainly expressed on resting $CD4^{+}CD25^{hi}$ TReg cells, memory T cells, activated T cells, NKT cells, and NK cells, but it is not detected on naïve $CD4^{+}$ T cells.

TIGIT expression is induced at mRNA levels upon activation of naïve $CD4^+$ T cells, memory T cells and TRegs [65–67]. TIGIT expression has been reported to be a characteristic marker for exhausted $CD8^+$ T cells and TRegs in the tumor microenvironment and also in viral infections [68–70].

5.1.2 Role in Immune Response

TIGIT mainly acts by competing with the co-stimulatory receptors CD226 (also known as DNAM1) and CD96 expressed on T cells for PVR and PVRL2 ligands (also known as CD112 and nectin 2) (Table 5). TIGIT binds to PVR ligands with greater affinity and outcompetes CD226 and the pathway resembles the CD28, CTLA-4, and B7 ligand axis. TIGIT-PVR interaction inhibits the activation, proliferation, and differentiation of T cells. In addition to inhibition of proliferation, TIGIT engagement also activates the survival pathways and ensures the survival of inhibited T cells for long time. On the other hand, interaction of PVR on DCs with TIGIT skews the cytokine secretion profile of DCs with decreased IL-12 production and increased IL-10 production, thereby inducing a tolerogenic phenotype in DCs. Activation of TIGIT on NK cells results in decreased IFN-γ production, cytotoxic granule polarization, and NK cell cytotoxicity [71]. Finally, TIGIT engagement on TRegs results in shifting of the cytokine balance and promotes a Th2 phenotype while suppressing Th1 or Th17-phenotype [69]. However, the overall role of TIGIT in regulation of immune response appears to be comparatively less critical as seen by milder phenotype of $Tigit^{-/-}$ mouse [65].

5.1.3 Signal Transduction

The intracellular signaling events that follow after TIGIT engagement are not well characterized in T cells. Based on the presence of ITIM domain in the protein structure of TIGIT, it was initially thought to recruit protein tyrosine phosphatases SHP-1 and SHP-2 and inhibit cell proliferation [66]. However, the initial in vitro studies using cultured cells expressing full-length TIGIT did not find evidence of phosphorylation, an indicator of signaling cascade after TIGIT-PVR interaction. Studies also showed that TIGIT did not significantly influence T-cell antigen receptor signaling in primary human $CD45RO^+$ T cells and blocking TIGIT using anti-TIGIT antibody or siRNA reportedly did not have any substantial effect on CD3-induced T-cell proliferation and cytokine production [65]. Intracellular TIGIT signaling has been mostly demonstrated in NK cells where its intracellular ITIM domain was shown to regulate PI3K and MAPK signaling cascades [72, 73]. Using TIGIT-deficient mice and TIGIT-transgenic mice, Li et al. showed that TIGIT-PVR interaction causes TIGIT phosphorylation, followed by association of β-arrestin 2 with TIGIT and recruitment of SHIP1 (SH2-containing inositol phosphatase 1). SHIP1 was shown to impair the TNF receptor-associated factor 6 (TRAF6) autoubiquitination and NF-κB

activation leading to decreased IFN-γ production in NK cells [74]. Further, *Fusobacterium nucleatum*, a bacterium present in colon adenocarcinoma, was shown to interact directly with TIGIT via protein Fap2 and inhibit NK cell cytotoxicity, indicating PVR-independent functions of TIGIT in NK cells [75]. Later studies by Joller et al., using agonistic anti-TIGIT antibody, showed cell-intrinsic effects of TIGIT and downregulation of components of TCR complex upon TIGIT engagement [76]. Interestingly, binding of PVR with TIGIT was found to have cell-intrinsic effects on DCs and result in increased IL-10 production as well as decreased IL-12 production from DCs [65].

5.1.4 Target for Cancer Immunotherapy

Upregulation of TIGIT ligands, PVR and PVRL2, on tumor cell surface was identified even before the discovery of TIGIT. Expression of PVR and PVRL2 was detected on tumors from epithelial origin such as non-small cell lung cancer, colon cancer, and metastatic neuroblastoma as well as hematopoietic origin such as myeloid leukemia [77–79]. Genentech is leading in the development of anti-TIGIT antibodies for the treatment of cancer and its molecule MTIG7192A/RG6058 is currently in clinical trials. Targeting TIGIT has gained importance in the recent months and more companies including Bristol Myers Squibb and Compugen are investing in the clinical development of anti-TIGIT antibodies [14].

5.2 T-Cell Immunoglobulin-3 (TIM-3)

5.2.1 Structure and Expression

TIM-3, also known as Hepatitis A Virus Cellular Receptor 2 (HAVCR2), was identified by Kuchroo and associates in 2002, as a cell surface receptor expressed on differentiated $CD4^+$ Th1 cells. Human *TIM-3* gene is located on the chromosome 5q33.3 and its mouse counterpart is located on chromosome 11. Murine TIM-3 protein was reported as a type I membrane protein of 281 amino acids, with an extracellular domain consisting of immunoglobulin variable-region-like domain followed by a mucin-like domain and cytoplasmic region containing a tyrosine phosphorylation motif. Human TIM-3 protein is made of 301 amino acids and the sequence has 63% similarity to that of mouse Tim-3 and the cytoplasmic region shares 77% identity including the tyrosine phosphorylation motif [80]. Apart from Th1 cells, TIM-3 is also expressed on activated $CD8^+$ T cells, TRegs, and other innate immune cells such as DCs, NK cells, as well as monocytes [71, 81]. Three years after the identification of TIM-3, galectin-9, a C-type lectin, expressed on APCs was identified as the ligand for TIM-3 [82]. Later other ligands including Ceacam-1, HMGB-1, and phosphatidyl serine were identified to interact with TIM-3 [71]. Unlike the ligands for other checkpoints such as TIGIT, the ligands for TIM-3 have a broad expression profile and are expressed on a variety of cell types including cancer cells [81]. Recently, CEACAM-1, identified as a novel TIM-3 ligand, was shown to be

co-expressed with TIM-3 on $CD4^+$ as well as $CD8^+$ T cells with tolerant or dysfunctional phenotype. CEACAM-1 was shown to be required for proper TIM-3 function and more interestingly, CEACAM-1:TIM-3 binding was found to occur in both cis and trans manner. The cis interaction was shown to promote the stability of mature TIM-3 glycoprotein on the cell surface and together with trans interaction drive the immunosuppressive function of TIM-3 [71, 83].

5.2.2 Role in Immune Response

TIM-3 was initially thought to suppress immune responses mainly by limiting the activity of Th1 cells and inducing Th1 cell-apoptosis but its role in suppression of $CD8^+$ T-cell activity has been gaining interest recently [71, 81, 84]. TIM-3 has also been implicated in accumulation of immunosuppressor cell types such as TRegs and MDSCs, promotion of T-cell exhaustion, and the maintenance of peripheral tolerance by DCs and macrophages [85, 86]. Blockade of TIM-3 pathway by treatment of the mice with TIM-3-Ig fusion protein was shown to enhance the clinical and pathological severity of experimental autoimmune encephalomyelitis (EAE) [80]. Role of TIM-3 in development of tolerance was further shown through studies in *Tim-3*$^{-/-}$ mice, which were found to be refractory to induction of antigen-specific tolerance [87, 88].

5.2.3 Signal Transduction

The evidence for the occurrence of intracellular signaling following TIM-3 activation was provided by the study by Zhu et al., which showed a Galectin-9-induced intracellular calcium flux in $TIM\text{-}3^+$ Th1 cells [82]. However, TIM-3 does not have a conventional signaling motif in its cytoplasmic tail and depends on the conserved tyrosine residues in the cytoplasmic region for phosphorylation-mediated initiation of signaling cascade [71]. Src kinases and ITK (interleukin-2-inducible T-cell kinase) were shown to phosphorylate the cytoplasmic tyrosine residues of TIM-3 at Y256 and Y263 positions, and regulate the binding of BAT-3 (HLA-B-associated transcript 3), the subunits of PI3K, as well as the tyrosine kinases Fyn and Lck to the C-terminal tail of TIM-3. BAT-3 plays an important role in the control of TIM-3 signaling; under basal conditions when TIM-3 is not activated by its ligand, BAT3 is bound to TIM-3 where it blocks SH2 domain-binding sites in the TIM-3 tails and also promotes the TCR signaling by recruiting catalytically active form of Lck [89]. Upon activation of TIM-3 via binding to Galectin-9 or Ceacam-1, Y256 and Y263 are phosphorylated leading to the release of BAT-3 from the TIM-3 tail, thereby allowing the binding of SH2 domains to Src kinases and subsequent inhibition of TCR signaling [71]. Fyn, a kinase implicated in the induction of T-cell anergy and known to activate phosphoprotein associated with glycosphingolipid microdomains (PAG) that suppress Lck function by recruiting Csk, also binds to the BAT-3-binding region of Tim-3 cytoplasmic tail. It is believed

that a possible switch between TIM-3:BAT-3 and TIM-3-Fyn could change the TIM-3 function from allowing TCR signaling to inhibiting TCR signaling [71, 90].

5.2.4 Target for Cancer Immunotherapy

The potential for TIM-3-based cancer immunotherapy was illustrated by studies in tumor samples from patients with advanced melanoma, non-small cell lung cancer (NSCLC), and follicular B cell non-Hodgkin lymphoma, which found TIM-3 expression on exhausted T cells that correlated positively with cancer severity and prognosis [71]. Anti-TIM-3 antibodies are not yet approved for the treatment of cancer and are currently in clinical trials. Commercial development of anti-TIM-3 antibodies is being pursued by Novartis, Tesaro, and Roche [14].

5.3 Lymphocyte Activation Gene 3 (LAG-3)

LAG-3 (also known as CD223) was discovered nearly three decades ago as a CD4-related molecule that is undetectable in resting peripheral blood lymphocytes and found on activated T cells as well as NK cells [91]. Interestingly, *Lag-3*$^{-/-}$ mice were initially thought to have no T-cell-related defects but subsequent studies identified LAG-3-mediated negative regulation of T-cell expansion [92, 93]. In addition to activated CD4$^+$ T cells, CD8$^+$ T cells, and NK cells, LAG-3 expression is also seen on both natural and induced TRegs [71]. *LAG-3* gene is located on chromosome 12p13.32 adjacent to the *CD4* gene and the protein shares 20% similarity in amino-acid sequence to that of CD4 [71, 94]. LAG-3 protein is composed of 498-amino acids with four extracellular IgSF domains, including a V-SET domain, which consists of an extra loop in the middle of the domain and an unusual intrachain disulfide bridge and three C2-SET domains [91]. The cytoplasmic tail of LAG-3 has three regions: a serine phosphorylation site-containing region, a KIEELE motif-containing region, and a glutamic acid-proline repeat-containing region [95]. Owing to its structural resemblance to CD4 co-receptor, LAG-3 binds to MHC class II molecules with a higher affinity than CD4 [71]. The presence of additional ligands for LAG-3 was speculated from the fact that LAG-3 regulated the functions of CD8$^+$ T cells and NK cells, which do not interact with MHC class II molecules. LSECtin, a member of DC-SIGN family of molecules, expressed in liver as well as several tumor subtypes has been suggested as a LAG-3 ligand in CD8$^+$ T cells and NK cells [96].

5.3.1 Structure and Expression

5.3.2 Role in Immune Response

Like other negative regulators of immune response, LAG-3 inhibits the effector cell responses and promotes suppressive activity of TRegs. The receptor is thought to mainly function in coordination with other checkpoints such as PD-1 and promote the development of tolerance [71]. Especially, LAG-3 is believed to play an important role in T-cell dysfunction and exhaustion; its expression

correlated with severity of infection in LCMV models and it was shown to co-express along with PD-1 on virus-specific exhausted $CD8^+$ T cells [97, 98]. Further, LAG-3 also plays a key role in suppressor functions and the IL-10 secretion capacity of TRegs (56). However, the inhibitory effects of LAG-3 are considered to be comparatively mild, as the *LAG-3*-deficient mice do not develop autoimmune disorders directly. Only when *LAG-3* deficiency and administration of anti-LAG-3 antibodies are tested in mice with a permissive genetic background such as NOD mice, its negative effects are demonstrated as acceleration of type I diabetes development in the mice [99]. Similarly, increased susceptibility to Hg-induced autoimmunity is seen in *LAG-3*-deficient mice from B6.SJL background [100].

5.3.3 Signal Transduction

The negative effects of LAG-3 on effector T cells are known to be due to its association with CD3 and the subsequent LAG-3:CD3 ligation-mediated inhibition of T-cell proliferation, cytokine production, and calcium flux [101]. Interestingly, LAG-3 has differential effects on T-cell subtypes; while it inhibits the activity of effector T cells, LAG-3 promotes the suppressive activity of TRegs. The mechanisms involved in these varying effects and the signaling events that occur after LAG-3 activation are not completely understood. The KIEELE motif in the cytoplasmic region was shown to be critical for the inhibition of $CD4^+$ effector T cells [95]. However, the intracellular proteins bound to KIEELE motif, the kinases, and phosphatases that are activated or deactivated and if the motif is needed for promoting TReg cell activity needs to be clarified.

5.3.4 Target for Cancer Immunotherapy

Increased expression of LAG-3 along with other checkpoints such as PD-1 is a characteristic feature of T-cell exhaustion and studies in tumor samples from lung, ovarian, and colorectal cancer patients showed a positive correlation between LAG-3 expression on tumor infiltrating lymphocytes and tumor progression [102–104]. Roche, Novartis, Tesaro, and BMS have shown interest in targeting LAG-3 for treatment of cancer and are separately developing monoclonal antibodies against LAG-3 receptors [14].

6 Summary and Perspective

Immunotherapy has transformed the treatment of melanoma in the past decade with significant increase in durable response rates. While other strategies to stimulate anti-tumor immune response like cancer vaccines and chimeric antigen receptor engineered T cells (CAR T-cells) are also promising, the monoclonal antibodies against inhibitory checkpoints are the most successful class of

immunotherapeutics and are approved for melanoma treatment both as monotherapy and in combination [11–13]. By discussing the details of immune activation, this chapter aims to support the development of future antibodies. As described in the previous sections, checkpoints play a critical role in the initial T-cell activation in lymph nodes, in the second activation in tissues, and also in T-cell exhaustion. Though there is some overlap in inhibitory functions, each checkpoint also has distinct functions (Fig. 3). For example, as seen from studies in knock-out mice and in vitro experiments, T-cell activation in lymph nodes and tolerance to self-antigens is mainly regulated by CTLA-4 and PD-1 [37, 38, 54, 55]. Other checkpoints such as TIGIT, TIM-3, and LAG-3 have less critical role in T-cell priming and tolerance to self-antigens [65, 88, 92]. Blockade of CTLA-4 and PD-1 could thus have severe adverse reactions whereas blockade of TIGIT, TIM-3, and LAG-3 could have relatively mild adverse effects. Similarly, CTLA-4 and TIGIT are involved in induction of tolerogenic phenotype in the APCs and PD-1 is involved in stimulation of TReg differentiation from naïve $CD4^+$ T cells [14]. Thus blockade of CTLA-4, TIGIT, and PD-1 could affect the levels of TRegs in the patients. Further, all the checkpoint receptors are found to regulate the activity of NK cells except CTLA-4 and while all the checkpoint receptors are known to induce T-cell exhaustion, PD-1 appears to be critically important for the effect [14].

Ability of the antibodies to induce ADCC can also be different based on the IgG subtype; antibodies with IgG1 backbone have the highest potential of inducing ADCC followed by antibodies with IgG4 backbone [19]. Ipilimumab (anti-CTLA-4), atezolizumab (anti-PD-L1), durvalumab (anti-PD-L1), and avelumab (anti-PD-L1) have IgG1 backbone and are expected to induce ADCC [105]. The Fc domains of atezolizumab and durvalumab are engineered to eliminate ADCC but ipilimumab and avelumab are known to have intact ADCC effects [106]. Anti-PD-1 antibodies, pembrolizumab and nivolumab, have IgG4 backbone and in vitro studies showed that both antibodies have minimal ability to induce ADCC [61, 107]. Factors such as cells expressing the target molecules and the need for ADCC are considered during the development of antibodies. When the target molecule is abundantly expressed on the cells that need to be killed, for example tumor cells (PD-L1) or TRegs (CTLA-4), induction of ADCC could add to the stimulation of T-cell activity. However when the target molecule is mainly expressed on the cells that need to be activated, as seen with PD-1 receptors on T cells, induction of ADCC is not desired as it could antagonize the stimulatory effects. In summary, monoclonal antibodies that can activate anti-tumor immune response have been immensely successful in the treatment of cancer. The effects of the antibodies depend on their molecular targets, the cell types expressing the respective targets, binding affinity of the

antibodies to FcγRs, and their ability to induce ADCC. The design of the antibodies should be based on factors such as immune cell types that need to be targeted and the need for ADCC.

References

1. Miller AJ, Mihm MC Jr (2006) Melanoma. N Engl J Med 355(1):51–65. https://doi.org/10.1056/NEJMra052166
2. Siegel R, Naishadham D, Jemal A (2013) Cancer statistics, 2013. CA Cancer J Clin 63 (1):11–30. https://doi.org/10.3322/caac.21166
3. Siegel RL, Miller KD, Jemal A (2016) Cancer statistics, 2016. CA Cancer J Clin 66 (1):7–30. https://doi.org/10.3322/caac.21332
4. Rotte A, Bhandaru M (2016) Melanoma – introduction, history and epidemiology (Immunotherapy of melanoma). Springer, Cham
5. Ferlay J, Soerjomataram I, Dikshit R, Eser S, Mathers C, Rebelo M et al (2015) Cancer incidence and mortality worldwide: sources, methods and major patterns in GLOBOCAN 2012. Int J Cancer 136(5):E359–E386. https://doi.org/10.1002/ijc.29210
6. Forman D, Bray F, Brewster DH, Gombe Mbalawa C, Kohler B, Piñeros M et al (eds) (2014) Cancer incidence in five continents Vol. X (Vol. X, IARC Scientific Publication no. 164). IARC Publications, Lyon
7. Balch CM, Gershenwald JE, Soong SJ, Thompson JF, Atkins MB, Byrd DR et al (2009) Final version of 2009 AJCC melanoma staging and classification. J Clin Oncol 27(36):6199–6206. https://doi.org/10.1200/JCO.2009.23.4799
8. Gershenwald JE, Scolyer RA, Hess KR, Sondak VK, Long GV, Ross MI et al (2017) Melanoma staging: evidence-based changes in the American Joint Committee on Cancer eighth edition cancer staging manual. CA Cancer J Clin 67(6):472–492. https://doi.org/10.3322/caac.21409
9. Rotte A, Bhandaru M, Zhou Y, McElwee KJ (2015) Immunotherapy of melanoma: present options and future promises. Cancer Metastasis Rev 34(1):115–128. https://doi.org/10.1007/s10555-014-9542-0
10. Rotte A, Bhandaru M (2016) Melanoma – treatment (immunotherapy of melanoma). Springer, Cham
11. Rotte A, Bhandaru M (2016) Ipilimumab (immunotherapy of melanoma). Springer, Cham
12. Rotte A, Bhandaru M (2016) Nivolumab (immunotherapy of melanoma). Springer, Cham
13. Rotte A, Bhandaru M (2016) Pembrolizumab (immunotherapy of melanoma). Springer, Cham
14. Rotte A, Jin JY, Lemaire V (2018) Mechanistic overview of immune checkpoints to support the rational design of their combinations in cancer immunotherapy. Ann Oncol 29 (1):71–83. https://doi.org/10.1093/annonc/mdx686
15. Le DT, Durham JN, Smith KN, Wang H, Bartlett BR, Aulakh LK et al (2017) Mismatch-repair deficiency predicts response of solid tumors to PD-1 blockade. Science. https://doi.org/10.1126/science.aan6733
16. FDA (2017) FDA approves first cancer treatment for any solid tumor with a specific genetic feature. https://www.fda.gov/newsevents/newsroom/pressannouncements/ucm560167.htm
17. FDA (2017) FDA grants nivolumab accelerated approval for MSI-H or dMMR colorectal cancer. https://www.fda.gov/Drugs/InformationOnDrugs/ApprovedDrugs/ucm569366.htm
18. Teillaud J-L (2001) Antibody-dependent cellular cytotoxicity (ADCC). In: eLS. John Wiley & Sons, Ltd
19. Furness AJ, Vargas FA, Peggs KS, Quezada SA (2014) Impact of tumour microenvironment and Fc receptors on the activity of immunomodulatory antibodies. Trends Immunol 35(7):290–298. https://doi.org/10.1016/j.it.2014.05.002
20. Bruhns P, Iannascoli B, England P, Mancardi DA, Fernandez N, Jorieux S et al (2009) Specificity and affinity of human Fcgamma receptors and their polymorphic variants for human IgG subclasses. Blood 113 (16):3716–3725. https://doi.org/10.1182/blood-2008-09-179754
21. DiLillo DJ, Ravetch JV (2015) Fc-receptor interactions regulate both cytotoxic and immunomodulatory therapeutic antibody effector functions. Cancer Immunol Res 3 (7):704–713. https://doi.org/10.1158/2326-6066.CIR-15-0120

22. Nimmerjahn F, Gordan S, Lux A (2015) FcgammaR dependent mechanisms of cytotoxic, agonistic, and neutralizing antibody activities. Trends Immunol 36(6):325–336. https://doi.org/10.1016/j.it.2015.04.005
23. Wang W, Erbe AK, Hank JA, Morris ZS, Sondel PM (2015) NK cell-mediated antibody-dependent cellular cytotoxicity in cancer immunotherapy. Front Immunol 6:368. https://doi.org/10.3389/fimmu.2015.00368
24. Seidel UJ, Schlegel P, Lang P (2013) Natural killer cell mediated antibody-dependent cellular cytotoxicity in tumor immunotherapy with therapeutic antibodies. Front Immunol 4:76. https://doi.org/10.3389/fimmu.2013.00076
25. Rotte A, Bhandaru M (2016) Dendritic cells (immunotherapy of melanoma). Springer, Cham
26. Smith-Garvin JE, Koretzky GA, Jordan MS (2009) T cell activation. Annu Rev Immunol 27:591–619. https://doi.org/10.1146/annurev.immunol.021908.132706
27. Fife BT, Bluestone JA (2008) Control of peripheral T-cell tolerance and autoimmunity via the CTLA-4 and PD-1 pathways. Immunol Rev 224:166–182. https://doi.org/10.1111/j.1600-065X.2008.00662.x
28. Ley K (2014) The second touch hypothesis: T cell activation, homing and polarization. F1000Res 3:37. https://doi.org/10.12688/f1000research.3-37.v2
29. Brunet JF, Denizot F, Luciani MF, Roux-Dosseto M, Suzan M, Mattei MG et al (1987) A new member of the immunoglobulin superfamily—CTLA-4. Nature 328 (6127):267–270. https://doi.org/10.1038/328267a0
30. Dariavach P, Mattei MG, Golstein P, Lefranc MP (1988) Human Ig superfamily CTLA-4 gene: chromosomal localization and identity of protein sequence between murine and human CTLA-4 cytoplasmic domains. Eur J Immunol 18(12):1901–1905. https://doi.org/10.1002/eji.1830181206
31. Metzler WJ, Bajorath J, Fenderson W, Shaw SY, Constantine KL, Naemura J et al (1997) Solution structure of human CTLA-4 and delineation of a CD80/CD86 binding site conserved in CD28. Nat Struct Biol 4 (7):527–531
32. Perkins D, Wang Z, Donovan C, He H, Mark D, Guan G et al (1996) Regulation of CTLA-4 expression during T cell activation. J Immunol 156(11):4154–4159
33. Alegre ML, Noel PJ, Eisfelder BJ, Chuang E, Clark MR, Reiner SL et al (1996) Regulation of surface and intracellular expression of CTLA4 on mouse T cells. J Immunol 157 (11):4762–4770
34. Pardoll DM (2012) The blockade of immune checkpoints in cancer immunotherapy. Nat Rev Cancer 12(4):252–264. https://doi.org/10.1038/nrc3239
35. Stamper CC, Zhang Y, Tobin JF, Erbe DV, Ikemizu S, Davis SJ et al (2001) Crystal structure of the B7-1/CTLA-4 complex that inhibits human immune responses. Nature 410 (6828):608–611. https://doi.org/10.1038/35069118
36. Wing K, Onishi Y, Prieto-Martin P, Yamaguchi T, Miyara M, Fehervari Z et al (2008) CTLA-4 control over Foxp3+ regulatory T cell function. Science 322 (5899):271–275. https://doi.org/10.1126/science.1160062
37. Tivol EA, Borriello F, Schweitzer AN, Lynch WP, Bluestone JA, Sharpe AH (1995) Loss of CTLA-4 leads to massive lymphoproliferation and fatal multiorgan tissue destruction, revealing a critical negative regulatory role of CTLA-4. Immunity 3(5):541–547
38. Chambers CA, Sullivan TJ, Allison JP (1997) Lymphoproliferation in CTLA-4-deficient mice is mediated by costimulation-dependent activation of CD4+ T cells. Immunity 7 (6):885–895
39. Intlekofer AM, Thompson CB (2013) At the bench: preclinical rationale for CTLA-4 and PD-1 blockade as cancer immunotherapy. J Leukoc Biol 94(1):25–39. https://doi.org/10.1189/jlb.1212621
40. Carreno BM, Bennett F, Chau TA, Ling V, Luxenberg D, Jussif J et al (2000) CTLA-4 (CD152) can inhibit T cell activation by two different mechanisms depending on its level of cell surface expression. J Immunol 165 (3):1352–1356
41. Chikuma S, Abbas AK, Bluestone JA (2005) B7-independent inhibition of T cells by CTLA-4. J Immunol 175(1):177–181
42. Schneider H, Valk E, Leung R, Rudd CE (2008) CTLA-4 activation of phosphatidylinositol 3-kinase (PI 3-K) and protein kinase B (PKB/AKT) sustains T-cell anergy without cell death. PLoS One 3(12):e3842. https://doi.org/10.1371/journal.pone.0003842
43. Fraser JH, Rincon M, McCoy KD, Le Gros G (1999) CTLA4 ligation attenuates AP-1, NFAT and NF-kappaB activity in activated T cells. Eur J Immunol 29(3):838–844

44. Olsson C, Riesbeck K, Dohlsten M, Michaelsson E (1999) CTLA-4 ligation suppresses CD28-induced NF-kappaB and AP-1 activity in mouse T cell blasts. J Biol Chem 274 (20):14400–14405
45. Leach DR, Krummel MF, Allison JP (1996) Enhancement of antitumor immunity by CTLA-4 blockade. Science 271 (5256):1734–1736
46. CHMP (2011) Assessment report for Yervoy (Ipilimumab): procedure no.: EMEA/H/C/002213 (2011). In: C.f.M.P.f.H.U. (CHMP) (Ed.). EMA, London
47. Ishida Y, Agata Y, Shibahara K, Honjo T (1992) Induced expression of PD-1, a novel member of the immunoglobulin gene superfamily, upon programmed cell death. EMBO J 11(11):3887–3895
48. Shinohara T, Taniwaki M, Ishida Y, Kawaichi M, Honjo T (1994) Structure and chromosomal localization of the human PD-1 gene (PDCD1). Genomics 23(3):704–706. https://doi.org/10.1006/geno.1994.1562
49. Keir ME, Butte MJ, Freeman GJ, Sharpe AH (2008) PD-1 and its ligands in tolerance and immunity. Annu Rev Immunol 26:677–704. https://doi.org/10.1146/annurev.immunol.26.021607.090331
50. Francisco LM, Sage PT, Sharpe AH (2010) The PD-1 pathway in tolerance and autoimmunity. Immunol Rev 236(1):219–242. https://doi.org/10.1111/j.1600-065X.2010.00923.x
51. Latchman Y, Wood CR, Chernova T, Chaudhary D, Borde M, Chernova I et al (2001) PD-L2 is a second ligand for PD-1 and inhibits T cell activation. Nat Immunol 2(3):261–268. https://doi.org/10.1038/85330
52. Cheng X, Veverka V, Radhakrishnan A, Waters LC, Muskett FW, Morgan SH et al (2013) Structure and interactions of the human programmed cell death 1 receptor. J Biol Chem 288(17):11771–11785. https://doi.org/10.1074/jbc.M112.448126
53. Francisco LM, Salinas VH, Brown KE, Vanguri VK, Freeman GJ, Kuchroo VK et al (2009) PD-L1 regulates the development, maintenance, and function of induced regulatory T cells. J Exp Med 206 (13):3015–3029. https://doi.org/10.1084/jem.20090847
54. Nishimura H, Nose M, Hiai H, Minato N, Honjo T (1999) Development of lupus-like autoimmune diseases by disruption of the PD-1 gene encoding an ITIM motif-carrying immunoreceptor. Immunity 11(2):141–151
55. Nishimura H, Okazaki T, Tanaka Y, Nakatani K, Hara M, Matsumori A et al (2001) Autoimmune dilated cardiomyopathy in PD-1 receptor-deficient mice. Science 291 (5502):319–322. https://doi.org/10.1126/science.291.5502.319
56. Pauken KE, Wherry EJ (2015) Overcoming T cell exhaustion in infection and cancer. Trends Immunol 36(4):265–276. https://doi.org/10.1016/j.it.2015.02.008
57. Parry RV, Chemnitz JM, Frauwirth KA, Lanfranco AR, Braunstein I, Kobayashi SV et al (2005) CTLA-4 and PD-1 receptors inhibit T-cell activation by distinct mechanisms. Mol Cell Biol 25(21):9543–9553. https://doi.org/10.1128/MCB.25.21.9543-9553.2005
58. Malek TR, Castro I (2010) Interleukin-2-receptor signaling: at the interface between tolerance and immunity. Immunity 33 (2):153–165. https://doi.org/10.1016/j.immuni.2010.08.004
59. Bennett F, Luxenberg D, Ling V, Wang IM, Marquette K, Lowe D et al (2003) Program death-1 engagement upon TCR activation has distinct effects on costimulation and cytokine-driven proliferation: attenuation of ICOS, IL-4, and IL-21, but not CD28, IL-7, and IL-15 responses. J Immunol 170(2):711–718
60. Bhandaru M, Rotte A (2017) Blockade of programmed cell death protein-1 pathway for the treatment of melanoma [short communication]. J Dermatol Res Ther 1(3):1–11. https://doi.org/10.14302/issn.2471-2175.jdrt-17-1760
61. Wang C, Thudium KB, Han M, Wang XT, Huang H, Feingersh D et al (2014) In vitro characterization of the anti-PD-1 antibody nivolumab, BMS-936558, and in vivo toxicology in non-human primates. Cancer Immunol Res 2(9):846–856. https://doi.org/10.1158/2326-6066.CIR-14-0040
62. Mahoney KM, Rennert PD, Freeman GJ (2015) Combination cancer immunotherapy and new immunomodulatory targets. Nat Rev Drug Discov 14(8):561–584. https://doi.org/10.1038/nrd4591
63. Tan S, Zhang H, Chai Y, Song H, Tong Z, Wang Q et al (2017) An unexpected N-terminal loop in PD-1 dominates binding by nivolumab. Nat Commun 8:14369. https://doi.org/10.1038/ncomms14369
64. Tan S, Liu K, Chai Y, Zhang CW, Gao S, Gao GF et al (2018) Distinct PD-L1 binding characteristics of therapeutic monoclonal antibody durvalumab. Protein Cell 9(1):135–139. https://doi.org/10.1007/s13238-017-0412-8

65. Yu X, Harden K, Gonzalez LC, Francesco M, Chiang E, Irving B et al (2009) The surface protein TIGIT suppresses T cell activation by promoting the generation of mature immunoregulatory dendritic cells. Nat Immunol 10 (1):48–57. https://doi.org/10.1038/ni.1674
66. Boles KS, Vermi W, Facchetti F, Fuchs A, Wilson TJ, Diacovo TG et al (2009) A novel molecular interaction for the adhesion of follicular CD4 T cells to follicular DC. Eur J Immunol 39(3):695–703. https://doi.org/10.1002/eji.200839116
67. Stanietsky N, Simic H, Arapovic J, Toporik A, Levy O, Novik A et al (2009) The interaction of TIGIT with PVR and PVRL2 inhibits human NK cell cytotoxicity. Proc Natl Acad Sci U S A 106(42):17858–17863. https://doi.org/10.1073/pnas.0903474106
68. Johnston RJ, Comps-Agrar L, Hackney J, Yu X, Huseni M, Yang Y et al (2014) The immunoreceptor TIGIT regulates antitumor and antiviral CD8(+) T cell effector function. Cancer Cell 26(6):923–937. https://doi.org/10.1016/j.ccell.2014.10.018
69. Kurtulus S, Sakuishi K, Ngiow SF, Joller N, Tan DJ, Teng MW et al (2015) TIGIT predominantly regulates the immune response via regulatory T cells. J Clin Invest 125 (11):4053–4062. https://doi.org/10.1172/JCI81187
70. Chew GM, Fujita T, Webb GM, Burwitz BJ, Wu HL, Reed JS et al (2016) TIGIT marks exhausted T cells, correlates with disease progression, and serves as a target for immune restoration in HIV and SIV infection. PLoS Pathog 12(1):e1005349. https://doi.org/10.1371/journal.ppat.1005349
71. Anderson AC, Joller N, Kuchroo VK (2016) Lag-3, Tim-3, and TIGIT: co-inhibitory receptors with specialized functions in immune regulation. Immunity 44 (5):989–1004. https://doi.org/10.1016/j.immuni.2016.05.001
72. Manieri NA, Chiang EY, Grogan JL (2017) TIGIT: a key inhibitor of the cancer immunity cycle. Trends Immunol 38(1):20–28. https://doi.org/10.1016/j.it.2016.10.002
73. Liu S, Zhang H, Li M, Hu D, Li C, Ge B et al (2013) Recruitment of Grb2 and SHIP1 by the ITT-like motif of TIGIT suppresses granule polarization and cytotoxicity of NK cells. Cell Death Differ 20(3):456–464. https://doi.org/10.1038/cdd.2012.141
74. Li M, Xia P, Du Y, Liu S, Huang G, Chen J et al (2014) T-cell immunoglobulin and ITIM domain (TIGIT) receptor/poliovirus receptor (PVR) ligand engagement suppresses interferon-gamma production of natural killer cells via beta-arrestin 2-mediated negative signaling. J Biol Chem 289(25):17647–17657. https://doi.org/10.1074/jbc.M114.572420
75. Gur C, Ibrahim Y, Isaacson B, Yamin R, Abed J, Gamliel M et al (2015) Binding of the Fap2 protein of Fusobacterium nucleatum to human inhibitory receptor TIGIT protects tumors from immune cell attack. Immunity 42(2):344–355. https://doi.org/10.1016/j.immuni.2015.01.010
76. Joller N, Hafler JP, Brynedal B, Kassam N, Spoerl S, Levin SD et al (2011) Cutting edge: TIGIT has T cell-intrinsic inhibitory functions. J Immunol 186(3):1338–1342. https://doi.org/10.4049/jimmunol.1003081
77. Sakisaka T, Takai Y (2004) Biology and pathology of nectins and nectin-like molecules. Curr Opin Cell Biol 16(5):513–521. https://doi.org/10.1016/j.ceb.2004.07.007
78. Fuchs A, Colonna M (2006) The role of NK cell recognition of nectin and nectin-like proteins in tumor immunosurveillance. Semin Cancer Biol 16(5):359–366. https://doi.org/10.1016/j.semcancer.2006.07.002
79. Masson D, Jarry A, Baury B, Blanchardie P, Laboisse C, Lustenberger P et al (2001) Overexpression of the CD155 gene in human colorectal carcinoma. Gut 49(2):236–240
80. Monney L, Sabatos CA, Gaglia JL, Ryu A, Waldner H, Chernova T et al (2002) Th1-specific cell surface protein Tim-3 regulates macrophage activation and severity of an autoimmune disease. Nature 415 (6871):536–541. https://doi.org/10.1038/415536a
81. Gorman JV, Colgan JD (2014) Regulation of T cell responses by the receptor molecule Tim-3. Immunol Res 59(1–3):56–65. https://doi.org/10.1007/s12026-014-8524-1
82. Zhu C, Anderson AC, Schubart A, Xiong H, Imitola J, Khoury SJ et al (2005) The Tim-3 ligand galectin-9 negatively regulates T helper type 1 immunity. Nat Immunol 6 (12):1245–1252. https://doi.org/10.1038/ni1271
83. Huang YH, Zhu C, Kondo Y, Anderson AC, Gandhi A, Russell A et al (2015) CEACAM1 regulates TIM-3-mediated tolerance and exhaustion. Nature 517(7534):386–390. https://doi.org/10.1038/nature13848
84. Anderson AC (2014) Tim-3: an emerging target in the cancer immunotherapy

landscape. Cancer Immunol Res 2 (5):393–398. https://doi.org/10.1158/2326-6066.CIR-14-0039

85. Sehrawat S, Suryawanshi A, Hirashima M, Rouse BT (2009) Role of Tim-3/galectin-9 inhibitory interaction in viral-induced immunopathology: shifting the balance toward regulators. J Immunol 182(5):3191–3201. https://doi.org/10.4049/jimmunol.0803673
86. Dardalhon V, Anderson AC, Karman J, Apetoh L, Chandwaskar R, Lee DH et al (2010) Tim-3/galectin-9 pathway: regulation of Th1 immunity through promotion of CD11b+Ly-6G+ myeloid cells. J Immunol 185(3):1383–1392. https://doi.org/10.4049/jimmunol.0903275
87. Sabatos CA, Chakravarti S, Cha E, Schubart A, Sanchez-Fueyo A, Zheng XX et al (2003) Interaction of Tim-3 and Tim-3 ligand regulates T helper type 1 responses and induction of peripheral tolerance. Nat Immunol 4(11):1102–1110. https://doi.org/10.1038/ni988
88. Sanchez-Fueyo A, Tian J, Picarella D, Domenig C, Zheng XX, Sabatos CA et al (2003) Tim-3 inhibits T helper type 1-mediated auto- and alloimmune responses and promotes immunological tolerance. Nat Immunol 4(11):1093–1101. https://doi.org/10.1038/ni987
89. Rangachari M, Zhu C, Sakuishi K, Xiao S, Karman J, Chen A et al (2012) Bat3 promotes T cell responses and autoimmunity by repressing Tim-3-mediated cell death and exhaustion. Nat Med 18(9):1394–1400. https://doi.org/10.1038/nm.2871
90. Salmond RJ, Filby A, Qureshi I, Caserta S, Zamoyska R (2009) T-cell receptor proximal signaling via the Src-family kinases, Lck and Fyn, influences T-cell activation, differentiation, and tolerance. Immunol Rev 228 (1):9–22. https://doi.org/10.1111/j.1600-065X.2008.00745.x
91. Triebel F, Jitsukawa S, Baixeras E, Roman-Roman S, Genevee C, Viegas-Pequignot E et al (1990) LAG-3, a novel lymphocyte activation gene closely related to CD4. J Exp Med 171(5):1393–1405
92. Miyazaki T, Dierich A, Benoist C, Mathis D (1996) LAG-3 is not responsible for selecting T helper cells in CD4-deficient mice. Int Immunol 8(5):725–729
93. Workman CJ, Cauley LS, Kim IJ, Blackman MA, Woodland DL, Vignali DA (2004) Lymphocyte activation gene-3 (CD223) regulates the size of the expanding T cell population following antigen activation in vivo. J Immunol 172(9):5450–5455
94. He Y, Rivard CJ, Rozeboom L, Yu H, Ellison K, Kowalewski A et al (2016) Lymphocyte-activation gene-3, an important immune checkpoint in cancer. Cancer Sci 107 (9):1193–1197. https://doi.org/10.1111/cas.12986
95. Workman CJ, Dugger KJ, Vignali DA (2002) Cutting edge: molecular analysis of the negative regulatory function of lymphocyte activation gene-3. J Immunol 169(10):5392–5395
96. Xu F, Liu J, Liu D, Liu B, Wang M, Hu Z et al (2014) LSECtin expressed on melanoma cells promotes tumor progression by inhibiting antitumor T-cell responses. Cancer Res 74 (13):3418–3428. https://doi.org/10.1158/0008-5472.CAN-13-2690
97. Richter K, Agnellini P, Oxenius A (2010) On the role of the inhibitory receptor LAG-3 in acute and chronic LCMV infection. Int Immunol 22(1):13–23. https://doi.org/10.1093/intimm/dxp107
98. Wherry EJ, Kurachi M (2015) Molecular and cellular insights into T cell exhaustion. Nat Rev Immunol 15(8):486–499. https://doi.org/10.1038/nri3862
99. Bettini M, Szymczak-Workman AL, Forbes K, Castellaw AH, Selby M, Pan X et al (2011) Cutting edge: accelerated autoimmune diabetes in the absence of LAG-3. J Immunol 187 (7):3493–3498. https://doi.org/10.4049/jimmunol.1100714
100. Jha V, Workman CJ, McGaha TL, Li L, Vas J, Vignali DA et al (2014) Lymphocyte activation gene-3 (LAG-3) negatively regulates environmentally-induced autoimmunity. PLoS One 9(8):e104484. https://doi.org/10.1371/journal.pone.0104484
101. Hannier S, Tournier M, Bismuth G, Triebel F (1998) CD3/TCR complex-associated lymphocyte activation gene-3 molecules inhibit CD3/TCR signaling. J Immunol 161 (8):4058–4065
102. Thommen DS, Schreiner J, Muller P, Herzig P, Roller A, Belousov A et al (2015) Progression of lung cancer is associated with increased dysfunction of T cells defined by coexpression of multiple inhibitory receptors. Cancer Immunol Res 3(12):1344–1355. https://doi.org/10.1158/2326-6066.CIR-15-0097
103. Matsuzaki J, Gnjatic S, Mhawech-Fauceglia P, Beck A, Miller A, Tsuji T et al (2010) Tumor-infiltrating NY-ESO-1-specific CD8+ T cells are negatively regulated by LAG-3 and PD-1 in human ovarian cancer. Proc Natl Acad Sci

U S A 107(17):7875–7880. https://doi.org/10.1073/pnas.1003345107

104. Chen J, Chen Z (2014) The effect of immune microenvironment on the progression and prognosis of colorectal cancer. Med Oncol 31(8):82. https://doi.org/10.1007/s12032-014-0082-9
105. Lee HT, Lee JY, Lim H, Lee SH, Moon YJ, Pyo HJ et al (2017) Molecular mechanism of PD-1/PD-L1 blockade via anti-PD-L1 antibodies atezolizumab and durvalumab. Sci Rep 7(1):5532. https://doi.org/10.1038/s41598-017-06002-8
106. Madorsky Rowdo FP, Baron A, Urrutia M, Mordoh J (2015) Immunotherapy in cancer: a combat between tumors and the immune system; you win some, you lose some. Front Immunol 6:127. https://doi.org/10.3389/fimmu.2015.00127
107. Scapin G, Yang X, Prosise WW, McCoy M, Reichert P, Johnston JM et al (2015) Structure of full-length human anti-PD1 therapeutic IgG4 antibody pembrolizumab. Nat Struct Mol Biol 22(12):953–958. https://doi.org/10.1038/nsmb.3129
108. Nimmerjahn F, Ravetch JV (2005) Divergent immunoglobulin G subclass activity through selective Fc receptor binding. Science 310(5753):1510–1512. https://doi.org/10.1126/science.1118948
109. Brahmer J, Reckamp KL, Baas P, Crino L, Eberhardt WE, Poddubskaya E et al (2015) Nivolumab versus docetaxel in advanced squamous-cell non-small-cell lung cancer. N Engl J Med 373(2):123–135. https://doi.org/10.1056/NEJMoa1504627
110. Hamid O, Carvajal RD (2013) Anti-programmed death-1 and anti-programmed death-ligand 1 antibodies in cancer therapy. Expert Opin Biol Ther 13(6):847–861. https://doi.org/10.1517/14712598.2013.770836

Chapter 5

An Efficient Method to Generate Monoclonal Antibodies from Human B Cells

Jenna J. Guthmiller, Haley L. Dugan, Karlynn E. Neu, Linda Yu-Ling Lan, and Patrick C. Wilson

Abstract

In the age of personalized medicine, an efficient method to generate monoclonal antibodies (mAbs) is essential for biomedical and immunotherapeutic research. Numerous aspects of basic B-cell biology can be studied at the monoclonal level, including B-cell development, antibody responses to infection or vaccination, and autoimmune responses. Single-cell B-cell receptor cloning allows for the rapid generation of antigen-specific mAbs in a matter of several weeks. In this chapter, we provide an efficient method to generate mAbs from peripheral blood plasmablasts and memory B cells induced by infection and vaccination. Additionally, we provide a protocol on how to optimize single-cell B-cell sorting for both single-cell B-cell receptor cloning and single-cell RNA-sequencing, for the application of studying B-cell specificity and function (spec-seq). This protocol can be easily adapted for other B-cell populations, B cells in tissues, and B cells from other organisms.

Key words Monoclonal antibody, B-cell receptor, Plasmablast, Memory B-cell, Cloning, Single-cell RNA-sequencing, Spec-seq, Humoral immunity, Vaccination, Infection

1 Introduction

Monoclonal antibodies (mAb) are monovalent proteins expressed by B cells that can precisely target a 3-dimensional epitope, making them an attractive therapeutic. With over 70 FDA-approved mAb--based drugs, mAbs have revolutionized modern medicine by providing precision medicine against many diseases. MAbs can target specific immunological pathways to turn on the immune system to eliminate cancer [1, 2], limit overactive immune responses during autoimmunity and transplantation [3–5], and alleviate cardiovascular disease [6]. Additionally, mAbs have prophylactic and therapeutic potential for preventing and limiting infection with highly pathogenic and variable pathogens such as *Bacillus anthracis*, human immunodeficiency viruses, and influenza viruses [7–12]. MAbs can be generated to study the human B-cell

Michael Steinitz (ed.), *Human Monoclonal Antibodies: Methods and Protocols*, Methods in Molecular Biology, vol. 1904, https://doi.org/10.1007/978-1-4939-8958-4_5,

repertoire, antibody-secreting cells induced after infection and vaccination, memory B-cell (MBC) responses, and pathogenic B-cell responses during autoimmune disease [7, 13–20]. Therefore, an efficient method to generate antigen-specific mAbs is essential to streamline immunotherapeutic and basic B-cell immunology research.

MAbs are generated from the pairing of a heavy chain (HC) and light chain from a B-cell. MAbs were first generated by making hybridomas, in which a single B-cell is fused with an immortalized immunoglobulin-deficient myeloma cell [21]. More efficient technologies to generate mAbs, including single-cell B-cell receptor (BCR) cloning and phage-display libraries, have largely replaced hybridoma practices and have become the default method for generating human mAbs. Single-cell BCR cloning allows for the rapid production of dozens, and potentially hundreds, of antigen-specific mAbs in a matter of several weeks, as mAbs are cloned from infection or vaccination-induced plasmablasts and antigen-baited MBCs [7, 16, 18, 22, 23] or plasma cells isolated from healthy and inflamed tissues [20, 24]. Additionally, mAbs generated using single-cell BCR cloning are generated with the biologically induced pairing of the HC and light chain from a single B-cell. In contrast to single-cell BCR cloning, phage-display libraries scan thousands of mAbs for antigen-specificity and only result in a few antigen-specific "hits" that are often of low affinity [25, 26]. Additionally, phage-display libraries largely generate mAbs from random pairings of heavy and light chain genes isolated from naïve B cells and MBCs and do not recapitulate B-cell responses during ongoing immune responses induced by infection, vaccination, and autoimmunity. Therefore, single-cell BCR cloning provides an efficient, robust, and quick approach to study the specificity of B cells in many different disease states.

Single-cell BCR cloning involves the amplification of the HC and light chain of the BCR from a single B-cell. This protocol is optimized for the amplification of both the kappa chain (KC) or lambda chain (LC) genes of the antibody's light chain [27, 28]. We have also included a protocol on how to efficiently amplify HC and light chain sequences from cells that express low levels of HC and light chain transcripts, such as naïve B cells and MBCs. Additionally, the cloning process has been simplified by utilizing Gibson Assembly, in which each end of the HC or KC/LC amplicon is tagged to match and allow for proper ligation with the respective expression vectors [29, 30]. Gibson assembly eliminates the need for digestion of cloning PCR products and the accidental digestion of HC and KC/LC genes with unknown restriction enzyme sites.

This chapter also includes a protocol for simultaneous mAb production and transcriptional profiling from the same cell (spec-seq; Neu et al. in press). The spec-seq protocol was constructed from merging multiple independently powerful pre-existing tools

[27, 29, 31], but their influence has been enhanced through this merger. The single-cell RNA-sequencing aspect was adapted from the smart-seq2 protocol, which relies on an oligodT primer for amplification of all cellular mRNA [31]. An aliquot of full-length cDNA is removed and utilized for PCR-based BCR cloning and downstream receptor functional characterization [27, 29]. This process generates the biologically induced mAb for specificity and functional characterization, the full-length BCR sequence to explore repertoire biases, B-cell phylogeny, or somatic hypermutation frequencies as well as the entire gene expression profile of the original B-cell. Notably, spec-seq allows for retrospective single-cell RNA sequencing of B cells with defined specificity instead of blind interrogation of the transcriptome of a B-cell without defined specificity, saving valuable resources for antigen-specific B cells.

Although initially developed for B cells, spec-seq can be easily modified for other adaptive immune cell populations, where identifying the unique somatically rearranged receptor expressed by the cell is critical to understanding the cellular identity and function. Fortunately, even if primers for receptor PCR amplification are not available, tools have recently been developed that assemble the full-length adaptive receptor sequence from within human and murine single-cell RNA-sequencing data [32–35]. These algorithms provide critical repertoire information that could be combined with downstream sequence-guided receptor synthesis to facilitate receptor functional characterization.

While spec-seq provides an opportunity to generate both a mAb and transcriptome from a single B-cell, spec-seq is still labor intensive and expensive. Single-cell technologies are rapidly evolving, with tools to assemble the BCR of a single B-cell from single-cell RNA-sequencing data recently being described [32, 35]. Using the 10× Genomics platform or similar platforms, protocols are being adapted to assemble immune receptors and single-cell RNA--sequencing data from single cells using bulk-sorted cells or whole tissue [36–38]. Single-cell RNA-sequencing and mAb generation from bulk-sorted cells will significantly reduce labor and turnaround time on both RNA-sequencing and mAb generation.

Overall, this chapter paves the way for the production of mAbs from many different B-cell populations and for transcriptome profiling in the context of the antigen receptor of single human B cells. Spec-seq allows for the characterization of antigen-specific cells across time or distinct tissues niches, as well as the identification of clonally-related cells. This advance has obvious benefits for personalized medicine (ex. cancer, autoimmunity, and transplant immunology), where the identification of clonal expansions is key for diagnosis, and where understanding pathologic or tumor infiltrating cellular identity is essential for selecting appropriate treatment options. Additionally, spec-seq provides an opportunity for basic B-cell research in the context of B-cell development,

repertoire analysis, B cells induced by infection and vaccination, and pathogenic B-cell responses during autoimmunity.

2 Materials

2.1 Equipment

- BD FACSAria™ Fusion flow cytometer (BD Biosciences, 656700) or equivalent.
- BioRad S1000™ Thermal Cycler with 96-well Fast Reaction Module (BioRad) or equivalent.
- Forma™ Series II 3110 Water-Jacketed CO_2 Incubators (ThermoFisher, 3110) or equivalent.
- Eppendorf™ 5810R Centrifuge and Rotor (Eppendorf, 05-413-112) or equivalent.
- NanoDrop™ 2000 Spectrophotometer (ThermoFisher).

2.2 Reagents

General Reagents

- Hard-shell low-profile thin-wall 96-well skirted PCR plates (Bio-Rad).
- Microseal "F" foil seals (Bio-Rad).
- 0.2 ml Flat PCR Tube 8-Cap Strips (Bio-Rad) + Strip Cap Tool (Bio-Rad).
- Nuclease-Free Water (Ambion).
- 200 μl filtered multichannel pipette tips.
- 20 μl filtered multichannel pipette tips.
- 1000 μl filtered pipette tips.
- 200 μl filtered pipette tips.
- 20 μl filtered pipette tips.
- 10 μl filtered pipette tips.
- Microcentrifuge tubes—1.7 ml (Dot Scientific).
- DNA-OFF and RNAse-OFF (Clontech).

2.3 Reagents for Subheading 2.1

2.3.1 B-Cell Isolation from Peripheral Blood

- RosetteSep Human B Cell Enrichment Cocktail (STEMCELL).
- Lymphoprep separation media (STEMCELL).
- 1× PBS, sterile-filtered (Sigma-Aldrich).
- Bovine Serum Albumin (Sigma-Aldrich).
- Falcon 70 μM cell strainer (ThermoFisher).

2.3.2 Cell-Staining

- Staining Buffer (1× PBS sterile-filtered, 0.02% BSA).
- Anti-human CD3 FITC, clone 7D6 (Invitrogen).
- Anti-human CD19 Pacific Blue, clone H1B19 (Biolegend).
- Anti-human CD27 PE, clone O323 (Biolegend).

- Anti-human CD38 AF647, clone HIT2 (Biolegend).
- Fluorophore-conjugated antigen for antigen-specific MBC baiting (*see* **Note 1**).
- Anti-human IgM PE, clone UHB (Southern Biotech).
- Anti-human CD27 BV605, clone O323 (Biolegend).
- Anti-human CD38 PE-Cy7, clone HIT2 (Biolegend).
- NHS-PEG-4 biotin kit (ThermoFisher).
- SA-AF647 (ThermoFisher, S21374).

2.3.3 Preparing 96-Well Plates for Single B-Cell Sorting

- 96-well PCR plates compatible with PCR thermocycler and cell sorting instrument (*see* **Note 2**).
- Reagents for Catch Buffer A, B, or C (*see* Subheading 3.1.3 Methods for description of each):

Catch Buffer A

- Nuclease-free water.
- Tris base (ThermoFisher).
- RNasin (Promega).

Catch Buffer B

- TCL Buffer (Qiagen).
- β-mercaptoethanol (Pierce).

Catch Buffer C

- Nuclease-free water.
- 0.1% Triton X-100 (Sigma-Aldrich) in sterile nuclease-free water.
- dNTPs (10 μM each) (Roche).
- 5′-biotinylated Oligo-dT (Integrated DNA Technologies, Table 1).
- RNAse inhibitor (Clontech).

2.3.4 Cell Sorting

- Falcon FACS tubes—regular and 35 μm nylon mesh filter cap (5 ml) (ThermoFisher).
- Complete RPMI media (500 ml RPMI, (Invitrogen), 1% penicillin-streptomycin (Gibco), 1% HEPES (Invitrogen), 1% L-Glutamine (Gibco), 10% heat-inactivated FBS (Gibco).
- Reagents for sorting catch buffer A, B, or C (*see* Subheadings 3.1.2 and 3.1.3 reagents).

Table 1
Primers

Primer	Sequence	PCR
OligoDt	AAGCAGTGGTATCAACGCAGAGTACT(30)VN	Catch Buffer C
TSO	AAGCAGTGGTATCAACGCAGAGTACATrGrG+G	Spec-seq cDNA synthesis
ISPCR	AAGCAGTGGTATCAACGCAGAGT	Spec-seq Preamplification
5′ L-VH 1	ACAGGTGCCCACTCCCAGGTGCAG	1st PCR
5′ L-VH 3	AAGGTGTCCAGTGTGARGTGCAG	1st PCR
5′ L-VH 4/6	CCCAGATGGGTCCTGTCCCAGGTGCAG	1st PCR
5′ L-VH 5	CAAGGAGTCTGTTCCGAGGTGCAG	1st PCR
3′ HuIgG-const-anti	TCTTGTCCACCTTGGTGTTGCT	1st PCR
3′ Cm CH1 (IgM)	GGGAATTCTCACAGGAGACGA	1st PCR
3′ IgA1-RT	CCTGGCTGGGTGGGAAGTTT	1st PCR
5′ L Vk 1/2	ATGAGGSTCCCYGCTCAGCTGCTGG	1st PCR
5′ L Vk 3	CTCTTCCTCCTGCTACTCTGGCTCCCAG	1st PCR
5′ L Vk 4	ATTTCTCTGTTGCTCTGGATCTCTG	1st PCR
3′ Ck 543–566	GTTTCTCGTAGTCTGCTTTGCTCA	1st PCR
5′ L Vl 1	GGTCCTGGGCCCAGTCTGTGCTG	1st PCR
5′ L Vl 2	GGTCCTGGGCCCAGTCTGCCCTG	1st PCR
5′ L Vl 3	GCTCTGTGACCTCCTATGAGCTG	1st PCR
5′ L Vl 4/5/9	GGTCTCTCTCSCAGCYTGTGCTG	1st PCR
5′ L Vl 6	GTTCTTGGGCCAATTTTATGCTG	1st PCR
5′ L Vl 7	GGTCCAATTCYCAGGCTGTGGTG	1st PCR
5′ L Vl 8	GAGTGGATTCTCAGACTGTGGTG	1st PCR
3′ Cl	CACCAGTGTGGCCTTGTTGGCTTG	1st PCR
5′ VH3a-sense	SARGTGCAGCTCGTGGAG	2nd PCR
5′ VH3b-sense	GAGGTGCAGCTGTTGGAG	2nd PCR
5′ VH1/5/7-sense	CTGCAACCGGTGTACATTCCGAGGTGCAGCTGG TGCAG	2nd PCR
5′ VH4-sense	CTGCAACCGGTGTACATTCCCAGGTGCAGC TGCAGGAG	2nd PCR
3′ Cgamma (IgG)	AGTAGTCCTTGACCAGGCAGCCCAG	2nd PCR
3′ MuD (IgM)	GGAATTCTCACAGGAGACGA	2nd PCR

(continued)

Table 1
(continued)

Primer	Sequence	PCR
3′ IgA1	CAGAGGCTCAGCGGGAAGACC	2nd PCR
5′ Pan Vk	ATGACCCAGWCTCCABYCWCCCTG	2nd PCR
3′ Ck 494–516	GTGCTGTCCTTGCTGTCCTGCT	2nd PCR
5′ AgeI Vl 1	CTGCTACCGGTTCCTGGGCCCAGTCTGTGC TGACKCAG	2nd PCR
5′ AgeI Vl 2	CTGCTACCGGTTCCTGGGCCCAGTCTGCCC TGACTCAG	2nd PCR
5′ AgeI Vl 3	CTGCTACCGGTTCTGTGACCTCCTATGAGC TGACWCAG	2nd PCR
5′ AgeI Vl 4/5/9	CTGCTACCGGTTCTCTCTCSCAGCYTGTGC TGACTCA	2nd PCR
5′ AgeI Vl 6	CTGCTACCGGTTCTTGGGCCAATTTTATGC TGACTCAG	2nd PCR
5′ AgeI Vl 7/8	CTGCTACCGGTTCCAATTCYCAGRCTGTGG TGACYCAG	2nd PCR
3′ XhoI Cl	CTCCTCACTCGAGGGYGGGAACAGAGTG	2nd PCR
5′ VH1/5/7	ATCCTTTTTCTAGTAGCAACTGCAACCGGTG TACATTCCGAGGTGCAGCTGGTGCAG	Cloning PCR
5′ VH3	ATCCTTTTTCTAGTAGCAACTGCAACCGGTG TACATTCTGAGGTGCAGCTGGTGGAG	Cloning PCR
5′ VH3–23	ATCCTTTTTCTAGTAGCAACTGCAACCGGTG TACATTCTGAGGTGCAGCTGTTGGAG	Cloning PCR
5′ VH4	ATCCTTTTTCTAGTAGCAACTGCAACCGGTG TACATTCCCAGGTGCAGCTGCAGGAG	Cloning PCR
5′ VH4–34	ATCCTTTTTCTAGTAGCAACTGCAACCGGTG TACATTCCCAGGTGCAGCTACAGCAGTG	Cloning PCR
5′ VH3–9/30/33	ATCCTTTTTCTAGTAGCAACTGCAACCGGTG TACATTCTGAAGTGCAGCTGGTGGAG	Cloning PCR
5′ VH6–1	ATCCTTTTTCTAGTAGCAACTGCAACCGGTG TACATTCCCAGGTACAGCTGCAGCAG	Cloning PCR
5′ Vk1	ATCCTTTTTCTAGTAGCAACTGCAACCGGTG TACATTCTGACATCCAGATGACCCAGTC	Cloning PCR
5′ Vk1–9/1–13	ATCCTTTTTCTAGTAGCAACTGCAACCGGTG TACATTCAGACATCCAGTTGACCCAGTCT	Cloning PCR
5′ Vk1D–43/1–8	ATCCTTTTTCTAGTAGCAACTGCAACCGGTG TACATTGTGCCATCCGGATGACCCAGTC	Cloning PCR

(continued)

Table 1
(continued)

Primer	Sequence	PCR
5′ Vk2	ATCCTTTTTCTAGTAGCAACTGCAACCGGTG TACATGGGGATATTGTGATGACCCAGAC	Cloning PCR
5′ Vk2–28/2–30	ATCCTTTTTCTAGTAGCAACTGCAACCGGTG TACATGGGGATATTGTGATGACTCAGTC	Cloning PCR
5′ Vk3–11/3D-11	ATCCTTTTTCTAGTAGCAACTGCAACCGGTG TACATTCAGAAATTGTGTTGACACAGTC	Cloning PCR
5′ Vk3–15/3D-15	ATCCTTTTTCTAGTAGCAACTGCAACCGGTG TACATTCAGAAATAGTGATGACGCAGTC	Cloning PCR
5′ Vk3–20/3D-20	ATCCTTTTTCTAGTAGCAACTGCAACCGGTG TACATTCAGAAATTGTGTTGACGCAGTCT	Cloning PCR
5′ Vk4–1	ATCCTTTTTCTAGTAGCAACTGCAACCGGTG TACATTCGGACATCGTGATGACCCAGTC	Cloning PCR
5′ Vl1	ATCCTTTTTCTAGTAGCAACTGCAACCGGTTCC TGGGCCCAGTCTGTGCTGACKCAG	Cloning PCR
5′ Vl2	ATCCTTTTTCTAGTAGCAACTGCAACCGGTTCC TGGGCCCAGTCTGCCCTGACTCAG	Cloning PCR
5′ Vl3	ATCCTTTTTCTAGTAGCAACTGCAACCGGTTC TGTGACCTCCTATGAGCTGACWCAG	Cloning PCR
5′ Vl4/5	ATCCTTTTTCTAGTAGCAACTGCAACCGGTTC TCTCTCSCAGCYTGTGCTGACTCA	Cloning PCR
5′ Vl6	ATCCTTTTTCTAGTAGCAACTGCAACCGGTTC TTGGGCCAATTTTATGCTGACTCAG	Cloning PCR
5′ Vl7/8	ATCCTTTTTCTAGTAGCAACTGCAACCGG TTCCAATTCYCAGRCTGTGGTGACYCAG	Cloning PCR
3′ JH1/2	GGAAGACCGATGGGCCCTTGGTCGACGCC TGAGGAGACGGTGACCAG	Cloning PCR
3′ JH4/5	GGAAGACCGATGGGCCCTTGGTCGACGC TGAGGAGACGGTGACCAG	Cloning PCR
3′ JH3	GGAAGACCGATGGGCCCTTGGTCGACGC TGAAGAGACGGTGACCATTG	Cloning PCR
3′ JH6	GGAAGACCGATGGGCCCTTGGTCGACGC TGAGGAGACGGTGACCGTG	Cloning PCR
3′ Jk1/2/4	AAGACAGATGGTGCAGCCACCGTACGTTTGA TYTCCACCTTGGTC	Cloning PCR
3′ Jk3	AAGACAGATGGTGCAGCCACCGTACGTTTGATA TCCACTTTGGTC	Cloning PCR
3′ Jk5	AAGACAGATGGTGCAGCCACCGTACGTTTAATC TCCAGTCGTGTC	Cloning PCR

(continued)

Table 1
(continued)

Primer	Sequence	PCR
3′ Cl	TGTTGGCTTGAAGCTCCTCACTCGAGGG YGGGAACAGAGTG	Cloning PCR
Abvec-sense	GCTTCGTTAGAACGCGGCTAC	Miniprep sequencing

2.4 Reagents for Subheading 3.2

2.4.1 cDNA Synthesis for Catch Buffer A

- Maxima cDNA Synthesis Kit (ThermoFisher).
- IGEPAL CA-603 (Sigma-Aldrich).

2.4.2 cDNA Synthesis for Catch Buffer B

- Agencort RNAClean XP Kit, SPRI Beads (Beckman Coulter).
- Magnetic Stand (ThermoFisher).
- 200 Proof Ethanol (Decon Laboratories).
- SuperScript IV Synthesis System (ThermoFisher includes SuperScript IV Reverse Transcriptase, DTT, Oligod$(T)_{20}$, dNTPs, RNAseOUT, and 5× SuperScript RT Buffer).

2.4.3 cDNA Synthesis for Catch Buffer C

- PrimeScript Reverse Transcriptase (Clontech), includes 200 U/μl. PrimeScript Reverse Transcriptase and 5× PrimeScript Buffer.
- RNAse inhibitor (Clontech).
- 5 M Betaine (Sigma-Aldrich).
- 1 M $MgCl_2$ (Life Technologies).
- 5′ biotinylated TSO Primer (Integrated DNA Technologies, Table 1).
- KAPA HiFi HotStart ReadyMix (KAPA Biosystems).
- 5′ biotinylated IS PCR Primers (Integrated DNA Technologies, Table 1).
- Elution Buffer Solution (Qiagen).
- AMPure XP Beads (Beckman Coulter).

2.5 Reagents for Subheading 3.3

- DreamTaq Green PCR 2× MasterMix (ThermoFisher).
- NEBuffer 3 (NE Biolabs, B7003S).
- CIP (NE Biolabs).
- ExoI (NE Biolabs).
- All 1st, 2nd, and cloning PCR primers (Integrated DNA Technologies, Table 1).

2.6 Reagents for Subheading 3.4

- QIAquick gel extraction kit (Qiagen).
- FastDigest AgeI (NE Biolabs).
- FastDigest SalI (NE Biolabs).
- FastDigest BsiWI (NE Biolabs).
- FastDigest XhoI (NE Biolabs).
- 10× CutSmart Buffer (included with restriction enzymes).
- FastAP (ThermoFisher).
- GeneJet Gel Extraction Kit (ThermoFisher).
- 5-alpha competent *E. coli* (NE Biolabs).
- SOC Media (ThermoFisher).
- LB agar (Fisher, B9724) + 100 μg/ml Ampicillin (Roche).
- QIAprep 96 Plus Kit (Qiagen), includes 96-well flat-bottom block.
- Genepure Plasmid Maxi Kit (Roche).
- LB broth (ThermoFisher) + 100 μg/ml Ampicillin.
- Glycerol (ThermoFisher).
- AbVec Primer (Integrated DNA Technologies, Table 1).

2.7 Reagents for Subheading 3.5

- 150 mm × 25 mm tissue culture plates (Falcon).
- Adherent 293T human embryonic kidney cells (ATCC).

2.7.1 Transfection of 293 Cells with HC and KC/LC Maxipreps

- Complete Advanced Dulbecco's Modified Eagle's Medium (DMEM): 500 ml. Advanced DMEM (Gibco) supplemented with 10% heat-inactivated ultralow IgG fetal calf serum (Gibco), 1% 200 mM L-Glutamine (Gibco), and 1% Antibiotic/Antimycotic (Gibco).
- Dulbecco's Modified Eagle's Medium (DMEM, Gibco).
- Polyethyleneimine (PEI) solution: 25,000 MW PEI (Polysciences) dissolved to a concentration of 1 mg/ml in sterile Milli-Q water (*see* **Note 3**).
- Protein-Free Hybridoma Medium (PFHM-II, Gibco).

2.7.2 Recombinant Antibody Purification

- Pierce Protein A Agarose Beads (ThermoFisher).
- 1× PBS, sterile-filtered (Sigma-Aldrich).
- NaCl (ThermoFisher).
- Glycine (Sigma-Aldrich).
- HCl (Sigma-Aldrich, 320331).
- Tris base (ThermoFisher).
- Amicon Ultra-4 30 kDa Centrifugal Filter Units (Millipore Sigma).
- Sodium azide (ThermoFisher).

3 Methods

3.1 Preparing Cells and Plates for Cell Sorting

This protocol is optimized for the isolation of human B cells from fresh peripheral blood. For optimal results, it is suggested that blood be processed immediately after collection to ensure maximum plasmablast and MBC viability (*see* **Note 4**). However, the procedures do work with reduced efficiency on frozen blood and tissue samples. The section outlined below describes the detailed sorting protocol for single-cell plasmablasts and antigen-baited MBCs from peripheral blood. It is important that the correct sorting catch buffer (A, B, or C) be used for compatibility with downstream applications.

3.1.1 B-Cell Isolation from Peripheral Blood

This section describes the protocol for isolating B cells from human peripheral blood for subsequent sorting.

1. Combine a maximum of 50 ml blood collected in acid citrate dextrose (ACD) tubes into a conical tube (*see* **Notes 5** and **6**).
2. Enrich for B cells by adding 125 μl RosetteSep to 50 ml blood (or 2.5 μl per 1 ml blood sample obtained). Mix well by slow pipetting or inverting. Incubate at room temperature for 20 min.
3. Aliquot 25 ml blood into separate 50 ml tubes and dilute 1:1 with filter-sterilized PBS 0.2% BSA.
4. Prepare 50 ml tubes with 12.5 ml Lymphoprep separation media. Carefully overlay 25 ml (no more than 30 ml) of diluted blood onto the Lymphoprep separation media by slowly pipetting along the side of the tube. Centrifuge at room temperature at 800 × *g* for 20 min, break off.
5. Collect the B-cell-enriched mononuclear cell layer, which has a velvety texture and lies above the Lymphoprep separation media layer and below the serum layer. Transfer to a new conical tube and wash in PBS 0.2% BSA at 4 °C for 5 min at 500 × *g*, break on. Discard the supernatant.
6. Combine autologous cell pellets from the same patients if desired, and wash again in PBS 0.2% BSA at 4 °C for 5 min at 500 × *g*, break on. Discard the supernatant.
7. Resuspend cells in the desired counting volume and filter cells through a 70 μM cell strainer into a new conical tube.
8. Count the cells. Partition the desired number of cells if ELISPOT is to be performed. Refer to the following protocols for instructions on performing ELISPOTs [29, 39].
9. Wash once more in PBS 0.2% BSA at 4 °C for 5 min at 500 × *g*, break on.
10. Discard the supernatant. Cells are ready for the appropriate staining protocol.

Table 2
Cell staining protocol A

Antibody-Fluorophore	For 1 ml staining volume
α-CD3 FITC	20 μl (1:50)
α-CD19 Pacific Blue	10 μl (1:100)
α-CD27 PE	10 μl (1:100)
α-CD38 AF647	5 μl (1:200)

3.1.2 Cell Staining

Cell Staining Protocol A

Cell Staining Protocol A is optimized for the single-cell sorting of plasmablasts only, and not for antigen-baited MBC sorting (*see* Subheading "Cell Staining Protocol B" below).

1. Resuspend the remaining sample at a staining concentration of ~1×10^7 cells per 1 ml PBS 0.2% BSA.
2. Remove ~0.5×10^6 cells (50 μl) from the cell suspension and separate into a new FACS tube for compensation. Fill to 500 μl with PBS 0.2% BSA and partition 100 μl into each of five FACS tubes (1×10^5 cells per fluorophore used + unstained control). Replace the volume taken from the original sample with PBS 0.2% BSA.
3. Create the sample staining master mix on ice, in the dark (Table 2).
4. Add the antibody-fluorophores (Table 2) to samples on ice, in the dark. Incubate for 30 min.
5. Concurrent with the sample incubation, stain cells for compensation with the corresponding antibody-fluorophore for 30 min. This protocol does not include details on how to perform proper compensation (*see* **Note 7**).
6. Wash samples and compensation tubes in PBS 0.2% BSA at 4 °C for 5 min at 500 × *g*.
7. Resuspend the sample in PBS 0.2% BSA at a concentration of ~1×10^7 cells/ml and filter through a 35 μm nylon mesh filter cap FACS tube. Keep on ice and avoid light until sort.

Cell-Staining Protocol B

As antigen-specific MBCs are rare in the total MBC pool, we typically utilize antigen-baited MBC sorting to generate mAbs. However, it is notable that particular subsets of recently induced memory B cells do have increased frequencies of antigen-specific cells [23, 40]. Cell-staining Protocol B is adapted for baiting influenza hemagglutinin (HA)-specific MBCs from B-cell-enriched samples. The protocol below includes details for biotinylation of the HA probe for conjugation to a streptavidin (SA)-linked fluorophore, as well as the staining instructions specific for our B-cell

panel. This protocol is specific for bait-sorting with recombinant HA protein (*see* **Note 8**), and will need to be optimized for the use of other antigens.

1. Dilute recombinant HA protein to a working concentration of 1 mg/ml in 100 μl.
2. Biotinylate 100 μl (100 μg) of HA protein using the NHS-PEG-4 biotin kit, according to the manufacturer's instructions.
3. Complex biotinylated HA with SA-AF647.
   (a) Suspend 10 μg (10 μl) of biotinylated HA in 85 μl PBS.
      - Add 1 μl of SA-AF647 per 95 μl of diluted HA every 20 min, five times, at 4 °C or on ice. The final concentration of HA-SA complex is 100 μg/ml.

   (b) Simultaneously, suspend 10 μg (10 μl) of non-biotinylated HA in 85 μl PBS. Add SA-AF647 to the non-biotinylated HA identically to the biotinylated HA, as described above. This step will generate a mock HA-SA complex to be used to set the HA-gate on the sorter.

   (c) The biotinylated HA-SA complex and the mock HA-SA complex are stable for 3 months at 4 °C protected from light.
4. Suspend cells for staining at 1×10^7 cells/ml. Remove 170 μl for a negative control stain and compensations. Aliquot 10 μl into seven tubes for compensations (all fluorophores and an unstained control) and add 90 μl of PBS 2% BSA to each tube. Remaining 100 μl of cells is a negative control and will receive all fluorophores and the mock HA-SA complex.
5. Add the appropriate HA-SA complex and antibody-fluorophores (Table 3). Incubate on ice for 30 min in the

Table 3
Cell staining protocol B

Antibody-Fluorophore	For 1 ml staining volume
α-CD3 FITC	20 μl (1:50)
α-CD19 Pacific Blue	10 μl (1:100)
α-CD27 BV605	10 μl (1:100)
α–CD38 PE-Cy7	2 μl (1:500)
α-IgM PE	1.24 μl (1:800)
HA biotin-AF647	5 μl (1:200)
HA-AF647 (negative control)	5 μl (1:200)

dark. For the mock HA-SA staining, scale down the staining protocol for staining in 100 μl.

6. Prepare FACS tubes for compensation and incubate with the corresponding antibody-fluorophore for 30 min, concurrent with sample staining. Use anti-CD38-AF647 rather than HA-SA complex for AF647 compensation, as there will be very few HA^+ cells to accurately set the compensation values.
7. Wash samples and compensation tubes twice with PBS 0.2% BSA at 4 °C for 5 min at 500 × *g*.
8. Resuspend cells at a concentration of ~1 × 10^7 cells/ml in PBS 0.2% BSA filter through a 35 μm nylon mesh filter cap FACS tube. Keep on ice and avoid light until sort.

3.1.3 Catch Buffer and Plate Preparation

This section describes the protocol for preparing 96-well sorting plates with catch buffer compatible with downstream RNA isolation and mAb cloning, or mAb cloning in parallel with RNA-sequencing (spec-seq). Due to the sensitivity of the single-cell BCR cloning and RNA-sequencing protocol, it is critical that proper RNA work precautions be taken when preparing all catch buffers. There are three possible catch buffers that may be used: A, B, or C. Please see below for a description of each catch buffer in order to choose one that is compatible with your research interests.

1. Catch Buffer A is compatible for the mAb cloning protocol from cells with high expression of HC and KC/LC genes, such as plasmablasts, but not for cells with few transcripts for HC and KC/LC genes, such as MBCs and naïve B cells. It is not compatible with our single-cell RNA-sequencing (spec-seq) protocol.
2. Catch Buffer B is compatible with our mAb cloning protocol, but not spec-seq. This protocol is recommended when Catch Buffer A is insufficient for successful amplification of HC and KC/LC genes. The RNA bead purification step compatible with this catch buffer improves the amplification of lowly expressed HC and KC/LC transcripts, such as for naïve B cells, MBCs, intestinal IgA plasma cells, and murine B cells [24, 29].
3. Catch Buffer C is necessary for our spec-seq protocol. Catch Buffer C is compatible with producing mAbs from plasmablasts, MBCs, and other B-cell populations [23].
   (a) Prepare the master mix for Catch Buffer A, B, or C (Tables 4, 5, and 6, depending on which downstream processing protocol is to be used). It is advised that the master mix and plates be prepared fresh in a sterile RNA hood, ensuring proper cleanliness using DNA-OFF and

Table 4
Master mix for catch buffer A

Reagent	Volume for 1 half plate (×50 wells)
Nuclease-free water	579 µl
1 M Tris-HCl pH 8.0	6 µl
RNase inhibitor	15 µl

Table 5
Master mix for catch buffer B

Reagent	Volume for 1 half plate (×50 wells)
TCL buffer	247.5 µl
1% β-mercaptoethanol (vol/vol)	2.5 µl

Table 6
Master mix for catch buffer C

Reagent	Volume for 1 half plate (×50 wells)
Nuclease-free water	45 µl
0.1% Triton-X	95 µl
dNTPs (10 µM each)	50 µl
Oligo-dT (100 µM)	5 µl
RNAse inhibitor	5 µl

RNAse OFF to clean the work space and all tools and reagents used.

(b) Pipette the master mix into a sterile basin, ensuring not to create bubbles.

(c) Use a multichannel with filter tips to pipette 10 µl per well (Catch Buffer A), 5 µl per well (Catch Buffer B), or 4 µl (Catch Buffer C) into each half plate, rows A1-H6.

(d) Stack the plates and seal the top plate with a foil microseal. Place plates on dry ice until beginning the sort.

3.1.4 Cell Sorting

1. For the bulk B-cell population sort, prepare three FACS tubes per subject with 500 µl complete RPMI prior to the sort. Keep on ice. For antigen-specific MBC baiting, cells can be directly single-cell sorted from the B-cell-enriched sample.

2. Bulk sort naïve B-cell ($CD19^+CD3^-CD27^{lo}CD38^{int}$), MBC ($CD19^+CD3^-CD27^+CD38^{int}$), and plasmablast ($CD19^+CD3^-CD27^{hi}CD38^{hi}$) populations into each of the three FACS tubes containing 500 µl complete RPMI. We have optimized this protocol for sorting these populations 7 days post-influenza vaccination (*see* Fig. 1 for complete gating strategies). Bulk sorting of antigen-baited MBCs is not required.
3. Perform a purity check on bulk sorted populations by recording ~100 events per sample.
4. From the bulk-sorted plasmablast tube, single-cell sort plasmablasts into half plates (wells A1-G6). Leave row H empty for subsequent steps as a negative control for contamination.
5. For antigen-baited MBCs, single-cell sort antigen-baited MBCs directly from the B-cell-enriched sample (*see* Fig. 1b for HA baiting gating strategy) into half plates (wells A1-G6). Leave row H empty for subsequent steps as a negative control for contamination.
6. Immediately seal each sorted plate using microseal foil plate seals. When handling plates during the sort, it is recommended that RNAse-OFF wipes be used to clean gloves as well as the work area. Place sealed plates back on dry ice.
7. Store the sorted plates at −80 °C until further processing. Plates may be stored up to several years if necessary. If desired, any remaining bulk sorted cells may be pelleted and lysed in a lysis buffer compatible with commercial RNA isolation kits and stored at −80 °C (*see* **Note 9**). Additionally, bulk-sorted cells can be frozen down in media.

3.2 RNA Isolation and cDNA Synthesis

3.2.1 cDNA Synthesis for Cells Sorted into Catch Buffer A

1. Thaw the sorted 96-well plate on ice.
2. While the plate is thawing, prepare reverse transcription (RT) mix (Table 7).
3. Aliquot 6 µl of RT mix to each well with a sample. The final volume is 16 µl.
4. Mix by pipetting and spin plate down at 700 × *g* for 10 s at room temperature.
5. Run the RT program on the thermocycler (Table 7).
6. After running the RT program, plates can be stored at −20 °C or −80 °C for 6 months or longer.

3.2.2 RNA Isolation and cDNA Synthesis for Cells Sorted into Catch Buffer B

For B cells with low BCR mRNA copies, such as naïve B cells and MBCs, cellular debris can interfere with cDNA synthesis and downstream PCR efficiency. Therefore, purification of cellular RNA is critical to increase BCR amplification efficiency. We recommend using Solid Phase Reversible Immobilization (SPRI) beads that bind RNA and washing steps to eliminate cellular debris.

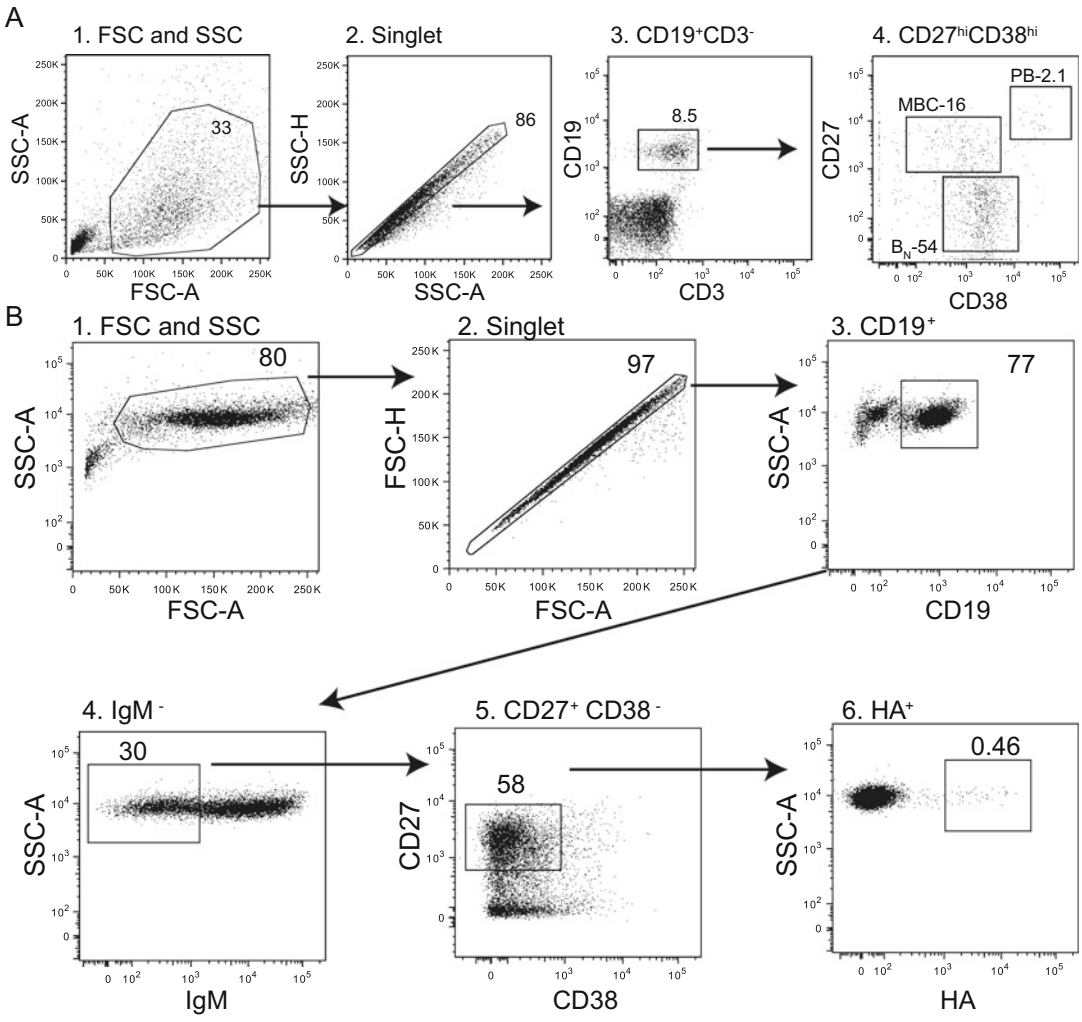

Fig. 1 Plasmablast and memory B cells gating strategies. (**a**) Gating strategy for bulk plasmablasts (PB; $CD19^+CD3^-CD27^{hi}CD38^{hi}$), naïve B cells ($B_N$; $CD19^+CD3^-CD27^-CD38^{int}$) and memory B cells (MBC; $CD19^+CD3^-CD27^+CD38^{int}$). $CD19^+$ B cells were isolated from human peripheral blood 7 days post influenza virus vaccination. If desired, an additional $IgM^-IgD^-IgG^+$ or $IgM^-IgD^-IgA^+$ gate may be set to improve PCR efficiency for amplifying IgG or IgA transcripts, respectively. (**b**) Gating strategy for HA-baited memory B cells ($CD19^+IgM^-CD27^+CD38^-HA^+$). $CD19^+$ B cells were enriched from human peripheral blood 28 days post influenza virus vaccination

1. Thaw the sorted 96-well plate on ice. Warm SPRI beads to room temperature prior to use.
2. Spin the plate down at 700 × *g* for 10 s at room temperature. Add 10 μl of nuclease-free water to each well.
3. Vortex SPRI beads well and add 33 μl to each sample. Mix by pipetting.

Table 7
Reverse transcription master mix for cells sorted into catch buffer A with lid heated to 90 °C

Reagent	Volume per well	Program
5× Buffer mix	3 µl	25 °C—10 min
5% IGEPAL	1.5 µl	50 °C—30 min
Maxima Enzyme Mix	1.5 µl	85 °C—5 min
Catch Buffer + Cell	10 µl	4 °C—hold
Total volume per well	16 µl	

4. Let the samples sit for 10 min at room temperature. Cover the plate to prevent contamination (*see* **Note 10**).
5. Prepare fresh 80% ethanol for the washing step. Make enough for 200 µl/wash × 2 washes × the number of samples.
6. Place the plate on a magnetic stand, covered, at room temperature for 5 min. The plate will remain on the magnetic stand through **step 9**.
7. Wash the plate with 200 µl 80% ethanol, incubate for 30 s, and discard ethanol.
8. Repeat **step 7** one more time.
9. Remove the residue 80% EtOH by pipetting.
10. Let the plate air dry for 3 min, covered. Once dry, remove from magnetic stand.
11. Add 12 µl of RNA annealing mix to each sample to elute RNA from beads (Table 8). Pipette to mix five times.
12. Incubate the plate off the magnetic stand for 5 min, covered.
13. Place the plate on the magnetic stand and leave for 2 min or until the solution appears clear and beads have accumulated in a corner of the well.
14. Transfer the supernatant (~10 µl) to a new 96-well plate without disturbing the beads.
15. Spin the plate down at 300 × *g* for 30 s at room temperature.
16. Run the RNA anneal PCR program (Table 8).
17. Place the plate on ice for 1 min.
18. Add 10 µl of reverse transcription mix, spin the plate down at 300 × *g* for 30 s at room temperature, and run the reverse transcription PCR program (Table 9).
19. cDNA can be used immediately for downstream BCR PCR and cloning or stored at −20 °C or −80 °C for 6 months or longer.

Table 8
RNA annealing for cells sorted into catch buffer B with lid heated to 70 °C

Reagent	Volume per well	Program
10 mM dNTPs	1.25 µl	65 °C—5 min
Oligod$(T)_{20}$	1 µl	4 °C—hold
Nuclease-free water	7.75 µl	
Total volume per well	10 µl	

Table 9
cDNA synthesis for cells sorted into catch buffer B with lid heated to 85 °C

Reagent	Volume per well	Program
5× SuperScript IV RT Buffer	4 µl	50 °C—60 min
100 mM DTT	1 µl	80 °C—10 min
RNAseOut	0.5 µl	4 °C—hold
SuperScript IV Reverse Transcriptase	0.25 µl	
Nuclease-free water	4.25 µl	
Total volume per well	20 µl	

3.2.3 RNA Isolation and cDNA Synthesis for Spec-seq, Based on Cells Sorted Using Catch Buffer C

1. Thaw the sorted 96-well plate on ice.
2. While the plate is thawing, prepare spec-seq reverse transcription mix (Table 10, *see* **Note 11**).
3. Once the plate has thawed, incubate at 72 °C with a heated lid (80 °C) for 3 min. This step is essential for oligodt primer annealing to RNA in each well.
4. Place plate immediately back on ice.
5. In the RNA hood, add 5.7 µl of spec-seq reverse transcription mix from **step 2** to each well, for a final volume of 10 µl/well. Pipette up and down five times to mix. Avoid forming bubbles. Use either foil plate covers or caps to cover the plate.
6. Spin down the plate at 700 × *g* for 10 s at room temperature.
7. Run the primescriptRT reaction on a thermocycler (Table 11). Lid should be heated to 80 °C.
8. After the PCR reaction, spin down the plate at 700 × *g* for 10 s at room temperature.
9. Prepare the PCR preamplification mix (Table 12).

Table 10
cDNA synthesis for spec-seq

Reagent	Volume per well
PrimeScript (200 U/μl) RT	0.5 μl
RNAse inhibitor	0.25 μl
PrimeScript buffer (5×)	2 μl
Betaine (5 M)	2 μl
$MgCl_2$ (1 M)	0.06 μl
TSO (100 μM)	0.1 μl
Nuclease-free water	0.79 μl
Total volume per well	5.7 μl

Table 11
Primescript reverse transcription PCR program with lid heated to 80 °C

Cycles	Temperature	Time
1×	42 °C	90 min
10×	50 °C 42 °C	2 min 2 min
1×	70 °C	15 min
1×	4 °C	Hold

Table 12
PCR preamplification mix

Reagent	Volume per well
First-strand reaction—from cDNA synthesis	10 μl
KAPA HiFi HotStart Ready Mix	12.5 μl
IS PCR Primers (100 μM)	0.0625 μl
Nuclease-free water	2.44 μl
Total volume per well	25 μl

10. Add 15 μl of the PCR preamplification mix to each well, for a final volume of 25 μl/well. Vortex the plate to mix and spin down at 700 × *g* for 10 s at room temperature.
11. Run the PCR preamplification program on a thermocycler (Table 13). Lid should be heated to 100 °C. The PCR product can be stably stored at −20 °C or −80 °C for 6 months or longer.

Table 13
PCR preamplification program with lid heated to 102 °C

Cycles	Temperature	Time
1×	98 °C	3 min
20×	98 °C 67 °C 72 °C	20 s 15 s 6 min
1×	72 °C	5 min
1×	4 °C	Hold

12. To optimize downstream RNAseq, cDNA must next be purified from preamplification PCR step, utilizing AMPure XP beads.
13. Allow the beads to warm to room temperature for 15 min. Vortex well.
14. Prepare fresh 80% ethanol for the washing step. Make enough for 200 μl/wash × 2 washes × the number of samples.
15. Centrifuge the plate at 280 × *g* for 1 min at room temperature.
16. Add 25 μl of beads to each sample. Pipette to mix ten times. Incubate for 8 min, covered (*see* **Note 10**).
17. Put plate on magnetic stand for 5 min, covered. Plate should be left on magnetic stand through **step 21**.
18. Remove and dispose of the supernatant, ~45 μl.
19. Add 200 μl of 80% ethanol. Wait 30 s and remove ethanol.
20. Repeat **step 19**.
21. After removing all ethanol, allow the plate to air dry for 5 min. The plate should remain covered to prevent contamination.
22. Remove the plate from the magnetic stand and add 23 μl of elution buffer solution. Pipette ten times, making sure to resuspend all beads from the sides of the wells. Incubate for 2–3 min.
23. Place the plate back on magnetic stand for 2 min.
24. Transfer 20 μl of the supernatant to a new 96-well plate. Avoid disturbing beads or transferring beads.
25. To determine cDNA quality for downstream RNA sequencing, remove 3 μl and use a Bioanalyzer (Agilent Genomics) and high-sensitivity DNA chip to perform quality control.
26. cDNA can be stored at −20 °C or −80 °C for 6 months or longer.

Table 14
First PCR master mix for one half-plate

PCR reaction for 50 reactions	HC	KC	LC
2× Master Mix Dream Taq Green	500 µl	500 µl	500 µl
5′ Primers (60 µM)	8 µl × 4	8 µl × 3	8 µl × 7
3′ Primers (60 µM)	8 µl × 3	8 µl × 1	8 µl × 1
Nuclease-free water	400 µl	400 µl	400 µl
Total volume per well	20 µl		

3.3 Amplification of Heavy and Light Chain Genes

3.3.1 First PCR

1. Prepare the first PCR mix (Table 14; *see* **Note 12**) to amplify HC, KC, and LC genes. Three separate mixes should be prepared for each chain. Refer to Table 1 for primers.
2. Add 18 µl of the first PCR mix to each well. First PCR mixes should be added to one of three corresponding plates (HC, KC, or LC).
3. Remove 2 µl of cDNA generated in Subheadings 3.2.1 and 3.2.2 or 1 µl of cDNA generated in **step 23** in Subheading 3.2, and add to each 96-well plate with first PCR mix. The final volume is 20 µl or 19 µl, respectively.
4. Mix by pipetting. Spin down the plate at 700 × *g* for 10 s at room temperature.
5. Run the first PCR program on a thermocycler (Table 15).
6. The plate can be stored at −20 °C or −80 °C for 6 months or longer.

3.3.2 Second PCR

1. Prepare the second PCR mix (Table 16) with nested primers to further amplify HC, KC, and LC genes. Three separate mixes should be prepared for each chain. Refer to Table 1 for primers.
2. Add 18 µl of the second PCR mix to each well. Second PCR mixes should be added to one of three corresponding plates (HC, KC, or LC).
3. Remove 2 µl of template from the first PCR plate and add to the new plate with the corresponding second PCR mix (e.g., first PCR HC template to second PCR HC mix). Final volume is 20 µl.
4. Mix by pipetting and spin the plate down at 700 × *g* for 10 s at room temperature.
5. Run the second PCR program on thermocycler (Table 17).
6. Run 2 µl of second PCR products from all wells on a 1.2% agarose gel (*see* **Note 13**).

Table 15
First PCR program with lid heated to 105 °C

Cycles	Temperature	Time
1×	94 °C	5 min
15×	94 °C 51 °C 72 °C	30 s 30 s 55 s
30×	94 °C 56 °C 72 °C	30 s 30 s 55 s
1×	72 °C	8 min
1×	4 °C	Hold

Table 16
Second PCR master mix for one half-plate

PCR reaction for 50 reactions	HC	KC	LC
2× Master Mix Dream Taq Green	500 µl	500 µl	500 µl
5′ Primers (60 µM)	8 µl × 2	8 µl × 1	8 µl × 6
3′ Primers (60 µM)	8 µl × 3	8 µl × 1	8 µl × 1
Nuclease-free water	400 µl	400 µl	400 µl
Total volume per well	20 µl		

Table 17
First PCR Program with lid heated to 105 °C

Cycles	Temperature	Time
1×	94 °C	4 min
50×	94 °C 57 °C 72 °C	30 s 30 s 45 s
1×	72 °C	10 min
1×	4 °C	Hold

7. The gel should reveal HC and LC/KC bands for wells for which cells were sorted into (*see* **Note 14**, Fig. 2). Expected PCR products should be approximately 400 bp. No bands should be in wells H1–12, as no cells were sorted into these wells. Record which wells had amplicons of both a HC and KC/LC.

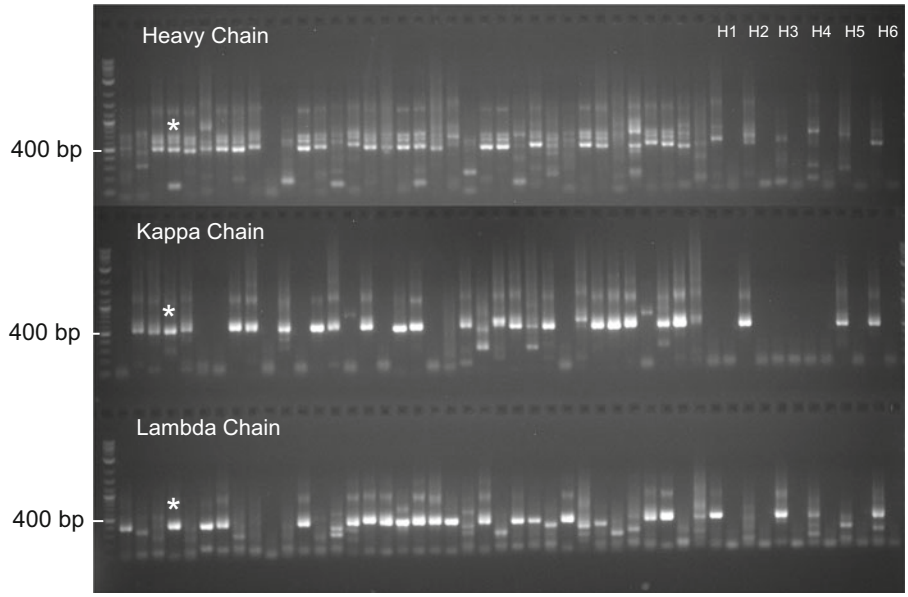

Fig. 2 Second PCR HC, KC, and LC amplicons from memory B cells. Representative images of HC, KC, and LC amplicons after first and second PCR from the same subject and sorted plate. Each well contains a cDNA from a single B-cell except for the far left lane that contains a DNA ladder and wells H1–6, which are contamination controls. The same samples were used for each image. Asterisk (*) refers to one B-cell expressing both a KC and LC. Numerous cells in the image express both a KC and LC

Table 18
PCR Cleanup Mix and Program with lid heated to 105 °C

Reagent	Volume per well	Program
Nuclease-free water	0.7 μl	37 °C—30 min
NEBuffer	0.7 μl	80 °C—20 min
CIP (10 U/μl)	0.1 μl	4 °C—hold
ExoI	0.5 μl	
PCR product	5 μl	
Total volume per well	7 μl	

8. Prepare to send samples with successful amplification of both the HC and KC/LC genes for sequencing by performing PCR cleanup (Table 18).
9. Send PCR cleanup for sequencing.

3.3.3 Cloning PCR

Before setting up the cloning PCR, determine the V and J genes used by both the HC and KC/LC of each antibody by using the NCBI's IgBLAST or the IMGT database. Use the correct V gene

and J gene primers (listed in Table 1). The V gene primer serves as the 5′ primer and the J gene primer as the 3′ primer. For example, if an antibody utilizes VH1-18 and JH4-02 use the VH1/5/7 primer and the JH4/5 primer. Use the 3′ Cl primer for all antibodies that use a LC. Separate cloning PCR reactions are required for the HC and LC.

1. Prepare the cloning PCR master mix (Table 19) with appropriate primers.
2. Add 23.5 μl of the appropriate master mix to the corresponding well in a 96-well plate. Also include a no-template control well for each V/J primer combination to confirm there is no contamination.
3. Add 1.5 μl of template from the first PCR reaction to the corresponding well with master mix and appropriate primers.
4. Mix by pipetting and spin the plate down at 700 × *g* for 10 s at room temperature.
5. Run the cloning PCR program (Table 20).

Table 19
Cloning PCR Master Mix for single reaction with lid heated to 105 °C

Reagent	Volume per well
2× Master Mix DreamTaq Green	12.5 μl
VH, VK, or VL primer (10 μM)	1 μl
JH or JK primer (10 μM)	1 μl
Nuclease-free water	9 μl
Template from first PCR reaction	1.5 μl
Total volume per well	25 μl

Table 20
Cloning PCR Program with lid heated to 105 °C

Cycles	Temperature	Time
1×	94 °C	4 min
40×	94 °C 58 °C 72 °C	30 s 30 s 45 s
1×	72 °C	8 min
1×	4 °C	Hold

Table 21
Digestion of 1 μg of vector

HC		KC		LC	
Reagent	**Volume**	**Reagent**	**Volume**	**Reagent**	**Volume**
10× FastDigest buffer	2 μl	10× FastDigest buffer	2 μl	10× FastDigest buffer	2 μl
SalI	1 μl	BsiWI	1 μl	XhoI	1 μl
AgeI	1 μl	AgeI	1 μl	AgeI	1 μl
Nuclease-free water	14 μl	Nuclease-free water	14 μl	Nuclease-free water	14 μl

6. After running PCR, run 2 μl of reactions on 1.5% agarose gel to confirm amplification.
7. Quantify the PCR product on a nanodrop. The concentration should be 5–12 ng/μl.

3.4 Plasmid DNA Preparation, Transformation, and Mini- and Maxiprep Generation

3.4.1 Vector Digestion and Ligation

1. Set up digestion reactions in 8-well strip tubes. Add 1 μg of either the HC, KC, or LC vector to the appropriate well. Vector sequences can be found on NCBI GenBank: accession numbers FJ475055, FJ475056, and FJ517647, for HC, KC, and LC, respectively. The heavy chain is in a human IgG1 backbone. The circular vectors are available upon request.
2. Make master mix for digestion of HC, KC, and LC circular vectors (Table 21).
3. Incubate at 37 °C for 60 min.
4. Add 2.5 μl of FastAP and incubate at 37 °C for another 10 min.
5. Run on a 1.2% agarose gel at 100 V for 5 min and then 75 V for 75 min.
6. Cut out bands of digested vectors (~6000 bp) and purify digests by following the manufacturer's protocol in the GeneJET Gel Extraction Kit.
7. Elute in 25 μl H_2O.
8. Quantify vector concentration on a nanodrop. The concentration should be 25–40 ng/μl.
9. Prepare for the ligation step. A 4:1 ratio of vector to insert should be used; 40 ng of vector and 10 ng of insert.
10. Assemble the ligation mix following the order in Table 22 in a 96-well plate. Add NE Builder HiFi DNA Assembly master mix last, as this contains the ligase. This will prevent reassembly of the linearized vector without the insert.
11. Mix by pipetting and spin down the plate at 700 × *g* for 10 s at room temperature.

Table 22
Plasmid DNA ligation

Step	Reagent	Volume/quantity
1	Nuclease-free water	To a final volume of 10 µl
2	Insert—HC, KC, or LC	10 ng, ~1 µl
3	Linearized HC, KC, or LC vector	40 ng, ~1–2 µl
4	NE Builder HiFi DNA Assembly Master Mix	4 µl

12. Incubate the plate at 50 °C for 1 h.
13. The assembled vectors with inserts can be stored at −20 °C until transformations are performed.

3.4.2 Transformations and Miniprep and Maxiprep Generation

1. Thaw DH5α *E. coli* cells on ice. Aliquot 45 µl into prechilled 1.7 ml microcentrifuge tubes.
2. Add 10 µl of assembled vector to cells and mix gently. Incubate on ice for 30 min.
3. Heat shock DH5α cells at 42 °C for 40 s.
4. Immediately place cells back on ice for 5 min. Add 150 µl of room-temperature SOC media.
5. Shake cells horizontally at 200 rpm at 37 °C for 40–60 min.
6. Plate 150 µl onto LB Agar + Ampicillin plates and incubate overnight at 37 °C.
7. Pick 4 colonies per plate and grow in a 96-well plate format, containing 1.7 ml of LB broth supplemented with Ampicillin per well. Incubate cultures at 37 °C for 20–24 h with vigorous shaking.
8. Make glycerol stocks by combining 700 µl of bacterial culture from each well to 300 µl of 1:1 mixture of LB broth and glycerol. Store in 1.5 ml tube at −80 °C. Stocks are stable for several years.
9. With the remaining culture, follow instructions for preparing minipreps with the QIAprep 96 Plus Kit.
10. Send 5 µl of miniprep for sequencing using the AbVec primer (Table 1).
11. Align the four miniprep sequences to generate a consensus sequence. Determine the maxiprep that best fits the consensus sequence and the sequence from the second PCR (*see* **Note 15**).

12. Prepare 14 ml round-bottom tubes with 5 ml of LB broth + ampicillin and inoculate desired minipreps by scraping a small amount of bacteria from the glycerol stock. Incubate culture at 37 °C and 225 rpm for 4–5 h.
13. Transfer the cultures to 500 ml flasks containing 250 ml LB Broth + ampicillin. Incubate at 37 °C and 225 rpm overnight.
14. Isolate plasmid DNA using Genepure Plasmid Maxi Kit.
15. Quantify maxipreps on a nanodrop and store at −20 °C. Maxipreps are stable for years and after many freeze-thaw cycles.

3.5 Recombinant Monoclonal Antibody Production and Purification

Upon successful maxiprep generation, recombinant mAbs can be produced and purified within a timeframe of just 6 days. This section describes the straightforward process for producing recombinant mAbs in 293 cells and the final purification protocol for the use of mAbs in desired downstream applications.

3.5.1 Transfection of 293 Cells for Antibody Production

This section describes the protocol for producing recombinant mAbs in 293 cells.

1. Culture human embryonic kidney 293 cells in 150 mm plates under standard conditions (37 °C, 5% CO_2) in 25 ml Complete Advanced DMEM. Cells should be grown to 80% confluency prior to transfection and transfection is optimal when cells are in exponential growth phase (*see* **Note 16**).
2. Combine 9 μg each of corresponding heavy and light chain plasmid DNA in 2.4 ml of DMEM. Add 100 μl of 1 mg/ml PEI solution for a total of 2.5 ml and mix well by vortexing. Incubate at room temperature for 15 min prior to transfecting.
3. During incubation of PEI and plasmid DNA, remove all but 18 ml of culture medium from each cell culture dish used for transfection. Carefully add transfection mixture (plasmid + PEI) to each culture dish. Swirl plates to evenly distribute transfection mixture. The transfections should be left to incubate for 12–18 h under standard conditions.
4. Aspirate transfection media from each plate and re-supplement cells with 25 ml of PFHM-II. Culture for 4 days under standard conditions. During this time, assembled heavy and light chain pairs will be secreted from transfected cells into the supernatant.
5. After 4 days, harvest supernatants in 50 ml tubes and proceed to the purification protocol in Subheading 3.5.2 (*see* **Note 17**).

3.5.2 Recombinant Antibody Purification

The protocol below outlines the process for the final purification of recombinant mAbs, which can then be used in a variety of downstream applications.

1. Centrifuge 25 ml of the collected supernatants from Subheading 3.5.1, **step 5** at 1800 × *g* for 10 min at 4 °C to pellet cell debris that may interfere with purification. Save the supernatant and discard pellet.
2. Transfer 500 μl of Protein A Agarose beads per sample to a 50 ml tube and wash in 1× PBS at 1800 × *g* for 10 min at 4 °C, break OFF (important: *see* **Note 18**).
3. Transfer 25 ml of each transfection supernatant to a 50 ml conical tube containing 500 μl of washed Protein A Agarose beads. Fill tubes to 50 ml with 1× PBS (*see* **Note 19**).
4. Incubate the supernatants with beads horizontally on a tabletop rocker at room temperature for 4 h on a low setting to avoid damage to beads. If you do not wish to proceed immediately with the purification, supernatants and beads may be incubated for 2 h at room temperature and subsequently transferred to a rocker at 4 °C overnight prior to purification.
5. After 4 h rocking at room temperature or the next day after overnight incubation at 4 °C, centrifuge the supernatants with beads at 1800 × *g* for 10 min at 4 °C, break off.
6. Aspirate the supernatants, taking care not to disturb or aspirate beads. Fill tubes to 50 ml with 1 M sterile-filtered NaCl solution. Spin 1800 × *g* for 10 min at 4 °C, break off.
7. Aspirate the supernatants and fill tubes to 50 ml with sterile-filtered 1× PBS. Spin 1800 × *g* for 10 min at 4 °C, break off.
8. Repeat **step 7**.
9. Aspirate the supernatants and add 3 ml of 0.1 M sterile-filtered glycine-HCl solution (pH 2.7). Incubate on a tabletop orbital shaker on medium speed at room temperature for 10 min (*see* **Note 20**). During this step, mAbs will be eluted from beads and the supernatants be saved hereafter.
10. Centrifuge the beads with glycine–HCl at 1800 × *g* for 10 min at 4 °C, break off. Prepare 15 ml tubes with 100–200 μl of Tris–HCl solution (pH 8.8) to neutralize eluted mAbs (*see* **Note 21**).
11. Transfer the supernatants to 15 ml tubes containing 1 M Tris–HCl and neutralize to pH 7–7.4. If there are beads in the vial, centrifuge at 1800 × *g* for 10 min at 4 °C, break off. This step is recommended, as the presence of beads will interfere during the protein concentration step. Proceed with the bead regeneration protocol (*see* Subheading 3.5.3).
12. Transfer the supernatant from **step 10** (3–4 ml) to the top of an Amicon protein concentrator (4 ml capacity, 30 kDa molecular weight cutoff). Centrifuge for 10–12 min 1800 × *g* at 4 °C, break on (*see* **Note 22**). Discard the flow through.

13. Buffer exchange the mAb preparation to remove residual glycine and Tris–HCl by washing the column three times with 1× PBS. Centrifuge for 10–12 min 1800 × *g* at 4 °C, break on.
14. Transfer the concentrated mAb sample from the concentrator (0.250–1 ml) to a clean microcentrifuge tube. If desired, preserve the antibody with 0.05% (wt/vol) NaN_3 (*see* **Notes 23** and **24**). MAb concentration is typically between 250 μg/ml and 2 mg/ml, with some purifications yielding up to 10 mg/ml protein. The 260/280 ratio should be between 0.45 and 0.55, but may be outside this range if NaN_3 has been added.

3.5.3 Protein A Agarose Bead Regeneration

Beads can be regenerated and used in subsequent purifications up to ten times as suggested by the manufacturer.

1. To regenerate beads, incubate for 1 h at room temperature on a tabletop rocker on low speed with 50 ml of 0.1 M glycine–HCl (pH 2.7).
2. Centrifuge 1800 × *g* for 10 min at 4 °C, break off.
3. Aspirate glycine–HCl and wash three times with 1× PBS, 1800 × *g* for 10 min at 4 °C, break off.
4. Store in conical vials at 4 °C in 1× PBS containing 0.05% NaN3 (wt/vol) for up to 6 months (*see* **Note 25**).

3.6 Analysis

In this protocol, we have described a highly detailed method for the rapid cloning of human mAbs from single-human B cells. We have optimized this protocol in our laboratory for the isolation of mAbs highly specific for influenza immunogen [7, 16, 18]. We are able to recover a substantial percentage of plasmablasts (Fig. 1a) and HA-specific memory B cells after vaccination (Fig. 1b). The specificity of these mAbs can be validated against relevant vaccinating antigens using ELISA (Fig. 3). In our laboratory, we have also used these antibodies to study the human immune response to influenza using hemagglutination inhibition assays, virus microneutralization assays, and in vivo prophylactic protection studies in mice. Single-cell BCR cloning can also be used to generate mAbs from naïve B cells, developing B cells, and autoreactive B cells [13–15, 17, 19, 20]. Thus, this protocol yields a substantial amount of mAbs generated from single human B cells that can be tested in a variety of downstream applications, depending on the specific research question. This is a powerful tool for studying the human humoral immune response to infection and vaccination, as serology limits the quality of data that can be obtained regarding antibody specificity and epitope binding.

Spec-seq allows for simultaneous analysis of both a single B-cell's specificity and transcriptional profile (Neu et al. in press).

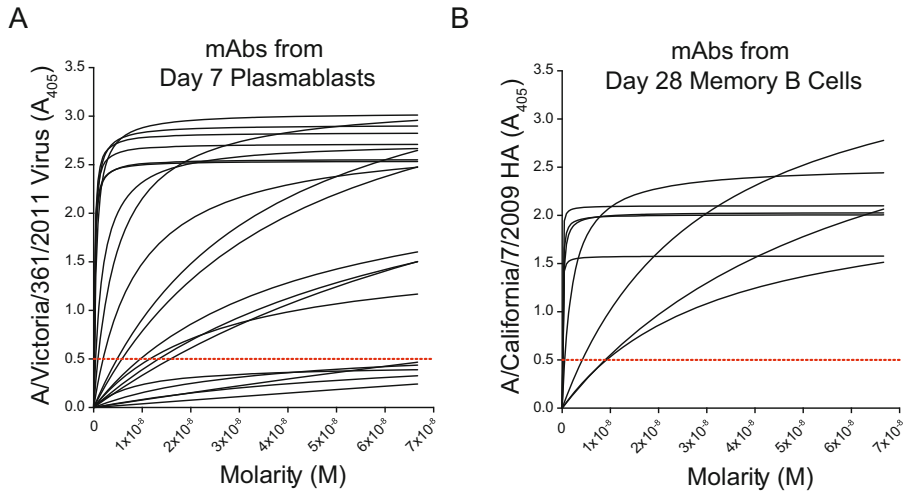

Fig. 3 Characterization of mAb binding and affinity by enzyme-linked ELISA. (**a**) Recombinant mAbs were purified from representative subjects and tested for antigen binding using ELISA. (**a**) mAbs from plasmablasts day 7 post vaccination were tested against A/Victoria/361/2011 whole virus. (**b**) MAbs generated from HA-baited memory B cells 28 days post vaccination were tested against recombinant A/California/7/2009 HA. Distinct binding kinetics can be observed for individual mAbs, indicated by the curves generated from the serial dilutions tested (Molarity, M). An A_{405} value greater than or equal to 0.50 at a starting concentration of 1×10^{-8} M is considered positive for test antigen. Each line depicted represents an individual mAb

While this protocol was developed for analysis of plasmablasts and MBCs induced by influenza virus infection and vaccination, this protocol can easily be adapted for other B-cell subsets or for B cells from other organisms. The protocol outlined within this chapter only provides detailed instructions on single-cell B-cell isolation, cDNA generation and purification, BCR cloning, and mAb generation. We recommend the smart-seq2 protocol for downstream transcriptional profiling [31].

4 Notes

1. The antigen-specific sorting of immune cell populations was first described for antigen-specific T cells [41] and methods have since been developed and utilized for sorting antigen-specific MBCs [42]. Our laboratory has optimized an antigen-specific HA-baiting strategy to isolate influenza-specific MBCs after influenza infection or vaccination. This protocol relies on the biotin-conjugation of recombinant hemagglutinin protein, which can then be conjugated to a SA-linked fluorophore compatible with our described B-cell staining protocol. Subheading 3.1.1 of this protocol includes a detailed protocol for antigen-baiting with recombinant HA protein.

2. We recommend Bio-Rad low-profile full skirted hardshell 96-well plates (*HSP9601*) for sorting, as they are more stable compared to un-skirted or semi-skirted plates and sit evenly on the plate sorting apparatus. They are compatible with most cell sorting machines and thermocyclers (*see* Bio-Rad website for more details).
3. PEI powder should be dissolved in preheated water at 80 °C on a magnetic stir plate. Upon addition of PEI, the solution must be immediately transferred to a magnetic stir plate with no heat and solution must cool to room temperature. Upon cooling, the mixture will turn cloudy and it may take several hours for PEI to go into solution. When PEI has dissolved, the solution will be colorless and acidic and should be neutralized to pH 7 with concentrated NaOH. If cloudiness persists after cooling to room temperature, neutralizing the solution to pH 7 may assist with dissolving. In this case, the solution should sit for at least one hour prior to aliquoting to allow for stabilization of pH. Once pH has stabilized, the solution can be filtered, aliquoted, and stored at −80 °C until future use. Once in use, the solution should be kept at 4 °C and re-freezing should be avoided as it may alter the structure of the PEI polymer.
4. In our hands, the percentage of plasmablasts in human blood substantially declines after 48 h post-blood draw or after freezing.
5. The blood processing and B-cell isolation protocol may be modified depending on the volume of blood sample obtained. For best results, it is suggested that the ratio of blood:diluent: separation media be kept 1:1:1.
6. Prior to adding RosetteSep, 1 ml of blood may be aliquoted into microcentrifuge tubes and centrifuged at 2700 × *g* for 5 min at room temperature for the collection of plasma.
7. The antibody-fluorophore dilutions described herein are optimized for the specific reagents/vendors and cells listed. Antibodies should be titrated to optimize staining protocols.
8. HA binds to sialic acids on host cells. For HA-baiting of MBCs, we utilize a receptor-binding site mutant HA (kindly provided by Dr. Florian Krammer and the NIH) to prevent non-specific binding.
9. If 10,000 cells or more are recovered after the MBC and plasmablast sort, cells may be lysed for RNA isolation and subsequent repertoire sequencing. We recommend lysing in Qiagen Buffer RLT + β-mercaptoethanol (0.1%, vol/vol) for downstream use with Qiagen RNeasy isolation kits.

10. To cover the plate sitting on or off the magnetic stand, we use the plastic lid from a 200 μl pipette tip box that has been wiped down with RNAseOff and DNAOff.
11. We prepare all plates and all steps before cDNA synthesis in a designated RNA hood. We also use extreme precautions to reduce DNAse/RNAse and DNA contaminations and thoroughly wipe all tip boxes, pipettes, etc. with RNAseOff and DNAOff.
12. The first PCR reaction requires different volumes of cDNA, based on the method of cDNA generation.
13. There is no need to add loading dye, as the DreamTaq Green master mix already contains a loading dye.
14. Occasionally, a single B-cell will express both a KC and LC. Proceed with sequencing of both KC and LC for a single B-cell. If both the KC and LC return with a sequence, proceed with cloning, generating an assembled vector, transformation, and miniprep/maxiprep generation. Often, only the HC/KC or HC/LC will result in a productive antibody at the transfection step. Therefore, both antibody pairs should be transfected, purified, quantified, and tested by ELISA.
15. In rare instances, none of the miniprep sequences will match the miniprep consensus sequence or the second PCR sequence. If this is the case, pick four new colonies and repeat the miniprep process.
16. 293 cells should be kept below 30 passages for recovering optimal yields of protein, and transfection is optimal when cells are split 24 h prior to transfection.
17. For pre-screening antibody specificity prior to proceeding with purification, transfections may be appropriately scaled down for antibody production in 24-well culture plates. Supernatants from the mini-transfections can be screened by ELISA using a desired antigen, and large-scale (150 mm plate) transfection and purification may then be performed for antibodies of chosen specificity.
18. Protein A Agarose Beads consist of purified Protein A covalently immobilized to beaded agarose and are ideal for the purification of IgG mAbs. All steps involving centrifugation of beads should ensure that the break is OFF, as high break speeds disturb the bead pellet and can damage the beads, reducing mAb protein yields.
19. All steps involving bead purification should ensure that tubes are filled to capacity with the appropriate buffer solution. When tubes are dry, beads will adhere to plastic and this will prevent proper elution of mAbs during the glycine-HCl elution step.

20. The time that mAbs are in glycine solution should be minimized as much as possible, as prolonged time at low pH will cause damage to mAbs.
21. Volume of 1 M Tris–HCl (pH 8.8) may vary depending on exact volume and pH of glycine used to elute mAbs from beads. The pH of neutralized mAbs should be tested using litmus paper to ensure proper neutralization, and volume of Tris–HCl should be optimized accordingly.
22. Amicon protein concentrators should be equilibrated with 1× PBS prior to adding samples. Add 4 ml 1× PBS to each concentrator, spin 10–12 min 1800 × *g* at 4 °C, break on. Discard flow through.
23. Biological assays using live cells (i.e., viral infection neutralization assays) are sensitive to NaN_3, so mAb storage method may depend on downstream application.
24. MAbs may be used up to one year post-purification at 4 °C. After one year, the antibodies will begin to denature and results using mAbs will not be accurate. Do not freeze mAbs.
25. It is recommended that beads not be pooled, to minimize the possibility of contaminating future protein preparations with residual mAbs. It is critical that the re-generation protocol be completed thoroughly to reduce the possibility of contamination.

Acknowledgments

The authors would like to thank Anna-Karin Palm, Nai-Ying Zheng, and Min Huang for critical feedback on the manuscript. This work was funded in parts from the National Institute of Allergy and Infectious Disease (NIAID), National Institutes of Health grant numbers U19AI082724, U19AI109946, U19AI057266, and the NIAID Centers of Excellence for Influenza Research and Surveillance (CEIRS), HHSN272201400005C.

References

1. Topalian SL, Hodi FS, Brahmer JR, Gettinger SN, Smith DC, McDermott DF, Powderly JD, Carvajal RD, Sosman JA, Atkins MB, Leming PD, Spigel DR, Antonia SJ, Horn L, Drake CG, Pardoll DM, Chen L, Sharfman WH, Anders RA, Taube JM, McMiller TL, Xu H, Korman AJ, Jure-Kunkel M, Agrawal S, McDonald D, Kollia GD, Gupta A, Wigginton JM, Sznol M (2012) Safety, activity, and immune correlates of anti-PD-1 antibody in cancer. N Engl J Med 366(26):2443–2454. https://doi.org/10.1056/NEJMoa1200690
2. Romond EH, Perez EA, Bryant J, Suman VJ, Geyer CE Jr, Davidson NE, Tan-Chiu E, Martino S, Paik S, Kaufman PA, Swain SM, Pisansky TM, Fehrenbacher L, Kutteh LA, Vogel VG, Visscher DW, Yothers G, Jenkins RB, Brown AM, Dakhil SR, Mamounas EP, Lingle WL, Klein PM, Ingle JN, Wolmark N (2005) Trastuzumab plus adjuvant chemotherapy for operable HER2-positive breast cancer.

N Engl J Med 353(16):1673–1684. https://doi.org/10.1056/NEJMoa052122

3. Ahmed AR, Spigelman Z, Cavacini LA, Posner MR (2006) Treatment of pemphigus vulgaris with rituximab and intravenous immune globulin. N Engl J Med 355(17):1772–1779. https://doi.org/10.1056/NEJMoa062930
4. Weinblatt ME, Keystone EC, Furst DE, Moreland LW, Weisman MH, Birbara CA, Teoh LA, Fischkoff SA, Chartash EK (2003) Adalimumab, a fully human anti-tumor necrosis factor alpha monoclonal antibody, for the treatment of rheumatoid arthritis in patients taking concomitant methotrexate: the ARMADA trial. Arthritis Rheum 48(1):35–45. https://doi.org/10.1002/art.10697
5. Vincenti F, Kirkman R, Light S, Bumgardner G, Pescovitz M, Halloran P, Neylan J, Wilkinson A, Ekberg H, Gaston R, Backman L, Burdick J (1998) Interleukin-2-receptor blockade with daclizumab to prevent acute rejection in renal transplantation. Daclizumab Triple Therapy Study Group. N Engl J Med 338(3):161–165. https://doi.org/10.1056/NEJM199801153380304
6. Robinson JG, Farnier M, Krempf M, Bergeron J, Luc G, Averna M, Stroes ES, Langslet G, Raal FJ, El Shahawy M, Koren MJ, Lepor NE, Lorenzato C, Pordy R, Chaudhari U, Kastelein JJ, Investigators OLT (2015) Efficacy and safety of alirocumab in reducing lipids and cardiovascular events. N Engl J Med 372(16):1489–1499. https://doi.org/10.1056/NEJMoa1501031
7. Chen YQ, Wohlbold TJ, Zheng NY, Huang M, Huang Y, Neu KE, Lee J, Wan H, Rojas KT, Kirkpatrick E, Henry C, Palm AE, Stamper CT, Lan LY, Topham DJ, Treanor J, Wrammert J, Ahmed R, Eichelberger MC, Georgiou G, Krammer F, Wilson PC (2018) Influenza infection in humans induces broadly cross-reactive and protective neuraminidase-reactive antibodies. Cell 173(2):417–429 e410. https://doi.org/10.1016/j.cell.2018.03.030
8. Walker LM, Phogat SK, Chan-Hui PY, Wagner D, Phung P, Goss JL, Wrin T, Simek MD, Fling S, Mitcham JL, Lehrman JK, Priddy FH, Olsen OA, Frey SM, Hammond PW, Protocol GPI, Kaminsky S, Zamb T, Moyle M, Koff WC, Poignard P, Burton DR (2009) Broad and potent neutralizing antibodies from an African donor reveal a new HIV-1 vaccine target. Science 326(5950):285–289. https://doi.org/10.1126/science.1178746
9. Wu X, Yang ZY, Li Y, Hogerkorp CM, Schief WR, Seaman MS, Zhou T, Schmidt SD, Wu L, Xu L, Longo NS, McKee K, O'Dell S, Louder MK, Wycuff DL, Feng Y, Nason M, Doria-Rose N, Connors M, Kwong PD, Roederer M, Wyatt RT, Nabel GJ, Mascola JR (2010) Rational design of envelope identifies broadly neutralizing human monoclonal antibodies to HIV-1. Science 329 (5993):856–861. https://doi.org/10.1126/science.1187659
10. Shriver Z, Trevejo JM, Sasisekharan R (2015) Antibody-based strategies to prevent and treat influenza. Front Immunol 6:315. https://doi.org/10.3389/fimmu.2015.00315
11. (1998) Palivizumab, a humanized respiratory syncytial virus monoclonal antibody, reduces hospitalization from respiratory syncytial virus infection in high-risk infants. The IMpact-RSV Study Group. Pediatrics 102(3 Pt 1):531–537
12. Migone TS, Subramanian GM, Zhong J, Healey LM, Corey A, Devalaraja M, Lo L, Ullrich S, Zimmerman J, Chen A, Lewis M, Meister G, Gillum K, Sanford D, Mott J, Bolmer SD (2009) Raxibacumab for the treatment of inhalational anthrax. N Engl J Med 361 (2):135–144. https://doi.org/10.1056/NEJMoa0810603
13. Wardemann H, Yurasov S, Schaefer A, Young JW, Meffre E, Nussenzweig MC (2003) Predominant autoantibody production by early human B cell precursors. Science 301 (5638):1374–1377. https://doi.org/10.1126/science.1086907
14. Koelsch K, Zheng NY, Zhang Q, Duty A, Helms C, Mathias MD, Jared M, Smith K, Capra JD, Wilson PC (2007) Mature B cells class switched to IgD are autoreactive in healthy individuals. J Clin Invest 117 (6):1558–1565. https://doi.org/10.1172/JCI27628
15. Duty JA, Szodoray P, Zheng NY, Koelsch KA, Zhang Q, Swiatkowski M, Mathias M, Garman L, Helms C, Nakken B, Smith K, Farris AD, Wilson PC (2009) Functional anergy in a subpopulation of naive B cells from healthy humans that express autoreactive immunoglobulin receptors. J Exp Med 206 (1):139–151. https://doi.org/10.1084/jem.20080611
16. Henry Dunand CJ, Leon PE, Huang M, Choi A, Chromikova V, Ho IY, Tan GS, Cruz J, Hirsh A, Zheng NY, Mullarkey CE, Ennis FA, Terajima M, Treanor JJ, Topham DJ, Subbarao K, Palese P, Krammer F, Wilson PC (2016) Both neutralizing and non-neutralizing human H7N9 influenza vaccine-induced monoclonal antibodies confer protection. Cell Host Microbe 19

(6):800–813. https://doi.org/10.1016/j.chom.2016.05.014

17. Tiller T, Tsuiji M, Yurasov S, Velinzon K, Nussenzweig MC, Wardemann H (2007) Autoreactivity in human IgG+ memory B cells. Immunity 26(2):205–213. https://doi.org/10.1016/j.immuni.2007.01.009
18. Andrews SF, Huang Y, Kaur K, Popova LI, Ho IY, Pauli NT, Henry Dunand CJ, Taylor WM, Lim S, Huang M, Qu X, Lee JH, Salgado-Ferrer M, Krammer F, Palese P, Wrammert J, Ahmed R, Wilson PC (2015) Immune history profoundly affects broadly protective B cell responses to influenza. Sci Transl Med 7 (316):316ra192. https://doi.org/10.1126/scitranslmed.aad0522
19. Andrews SF, Zhang Q, Lim S, Li L, Lee JH, Zheng NY, Huang M, Taylor WM, Farris AD, Ni D, Meng W, Luning Prak ET, Wilson PC (2013) Global analysis of B cell selection using an immunoglobulin light chain-mediated model of autoreactivity. J Exp Med 210 (1):125–142. https://doi.org/10.1084/jem.20120525
20. Di Niro R, Mesin L, Zheng NY, Stamnaes J, Morrissey M, Lee JH, Huang M, Iversen R, du Pre MF, Qiao SW, Lundin KE, Wilson PC, Sollid LM (2012) High abundance of plasma cells secreting transglutaminase 2-specific IgA autoantibodies with limited somatic hypermutation in celiac disease intestinal lesions. Nat Med 18(3):441–445. https://doi.org/10.1038/nm.2656
21. Kohler G, Milstein C (1975) Continuous cultures of fused cells secreting antibody of predefined specificity. Nature 256 (5517):495–497
22. Wrammert J, Koutsonanos D, Li GM, Edupuganti S, Sui J, Morrissey M, McCausland M, Skountzou I, Hornig M, Lipkin WI, Mehta A, Razavi B, Del Rio C, Zheng NY, Lee JH, Huang M, Ali Z, Kaur K, Andrews S, Amara RR, Wang Y, Das SR, O'Donnell CD, Yewdell JW, Subbarao K, Marasco WA, Mulligan MJ, Compans R, Ahmed R, Wilson PC (2011) Broadly cross-reactive antibodies dominate the human B cell response against 2009 pandemic H1N1 influenza virus infection. J Exp Med 208(1):181–193. https://doi.org/10.1084/jem.20101352
23. Lau D, Lan LY, Andrews SF, Henry C, Rojas KT, Neu KE, Huang M, Huang Y, DeKosky B, Palm AE, Ippolito GC, Georgiou G, Wilson PC (2017) Low CD21 expression defines a population of recent germinal center graduates primed for plasma cell differentiation. Sci Immunol 2(7). https://doi.org/10.1126/sciimmunol.aai8153
24. Bunker JJ, Erickson SA, Flynn TM, Henry C, Koval JC, Meisel M, Jabri B, Antonopoulos DA, Wilson PC, Bendelac A (2017) Natural polyreactive IgA antibodies coat the intestinal microbiota. Science 358(6361). https://doi.org/10.1126/science.aan6619
25. Walker LM, Bowley DR, Burton DR (2009) Efficient recovery of high-affinity antibodies from a single-chain Fab yeast display library. J Mol Biol 389(2):365–375. https://doi.org/10.1016/j.jmb.2009.04.019
26. Hammers CM, Stanley JR (2014) Antibody phage display: technique and applications. J Invest Dermatol 134(2):1–5. https://doi.org/10.1038/jid.2013.521
27. Smith K, Garman L, Wrammert J, Zheng NY, Capra JD, Ahmed R, Wilson PC (2009) Rapid generation of fully human monoclonal antibodies specific to a vaccinating antigen. Nat Protoc 4(3):372–384. https://doi.org/10.1038/nprot.2009.3
28. Wrammert J, Smith K, Miller J, Langley WA, Kokko K, Larsen C, Zheng NY, Mays I, Garman L, Helms C, James J, Air GM, Capra JD, Ahmed R, Wilson PC (2008) Rapid cloning of high-affinity human monoclonal antibodies against influenza virus. Nature 453 (7195):667–671. https://doi.org/10.1038/nature06890
29. Ho IY, Bunker JJ, Erickson SA, Neu KE, Huang M, Cortese M, Pulendran B, Wilson PC (2016) Refined protocol for generating monoclonal antibodies from single human and murine B cells. J Immunol Methods 438:67–70. https://doi.org/10.1016/j.jim.2016.09.001
30. Gibson DG, Young L, Chuang RY, Venter JC, Hutchison CA 3rd, Smith HO (2009) Enzymatic assembly of DNA molecules up to several hundred kilobases. Nat Methods 6 (5):343–345. https://doi.org/10.1038/nmeth.1318
31. Picelli S, Faridani OR, Bjorklund AK, Winberg G, Sagasser S, Sandberg R (2014) Full-length RNA-seq from single cells using Smart-seq2. Nat Protoc 9(1):171–181. https://doi.org/10.1038/nprot.2014.006
32. Canzar S, Neu KE, Tang Q, Wilson PC, Khan AA (2017) BASIC: BCR assembly from single cells. Bioinformatics 33(3):425–427. https://doi.org/10.1093/bioinformatics/btw631
33. Eltahla AA, Rizzetto S, Pirozyan MR, Betz-Stablein BD, Venturi V, Kedzierska K, Lloyd AR, Bull RA, Luciani F (2016) Linking the T cell receptor to the single cell transcriptome in antigen-specific human T cells. Immunol Cell Biol 94(6):604–611. https://doi.org/10.1038/icb.2016.16

34. Stubbington MJT, Lonnberg T, Proserpio V, Clare S, Speak AO, Dougan G, Teichmann SA (2016) T cell fate and clonality inference from single-cell transcriptomes. Nat Methods 13 (4):329–332. https://doi.org/10.1038/nmeth.3800
35. Upadhyay AA, Kauffman RC, Wolabaugh AN, Cho A, Patel NB, Reiss SM, Havenar-Daughton C, Dawoud RA, Tharp GK, Sanz I, Pulendran B, Crotty S, Lee FE, Wrammert J, Bosinger SE (2018) BALDR: a computational pipeline for paired heavy and light chain immunoglobulin reconstruction in single-cell RNA--seq data. Genome Med 10(1):20. https://doi.org/10.1186/s13073-018-0528-3
36. Zheng GX, Terry JM, Belgrader P, Ryvkin P, Bent ZW, Wilson R, Ziraldo SB, Wheeler TD, McDermott GP, Zhu J, Gregory MT, Shuga J, Montesclaros L, Underwood JG, Masquelier DA, Nishimura SY, Schnall-Levin M, Wyatt PW, Hindson CM, Bharadwaj R, Wong A, Ness KD, Beppu LW, Deeg HJ, McFarland C, Loeb KR, Valente WJ, Ericson NG, Stevens EA, Radich JP, Mikkelsen TS, Hindson BJ, Bielas JH (2017) Massively parallel digital transcriptional profiling of single cells. Nat Commun 8:14049. https://doi.org/10.1038/ncomms14049
37. Patil VS, Madrigal A, Schmiedel BJ, Clarke J, O'Rourke P, de Silva AD, Harris E, Peters B, Seumois G, Weiskopf D, Sette A, Vijayanand P (2018) Precursors of human CD4(+) cytotoxic T lymphocytes identified by single-cell transcriptome analysis. Sci Immunol 3(19). https://doi.org/10.1126/sciimmunol.aan8664
38. Zemmour D, Zilionis R, Kiner E, Klein AM, Mathis D, Benoist C (2018) Single-cell gene expression reveals a landscape of regulatory T cell phenotypes shaped by the TCR. Nat Immunol 19(3):291–301. https://doi.org/10.1038/s41590-018-0051-0
39. Andrews SF, Kaur K, Pauli NT, Huang M, Huang Y, Wilson PC (2015) High preexisting serological antibody levels correlate with diversification of the influenza vaccine response. J Virol 89(6):3308–3317. https://doi.org/10.1128/JVI.02871-14
40. Ellebedy AH, Jackson KJ, Kissick HT, Nakaya HI, Davis CW, Roskin KM, McElroy AK, Oshansky CM, Elbein R, Thomas S, Lyon GM, Spiropoulou CF, Mehta AK, Thomas PG, Boyd SD, Ahmed R (2016) Defining antigen-specific plasmablast and memory B cell subsets in human blood after viral infection or vaccination. Nat Immunol 17 (10):1226–1234. https://doi.org/10.1038/ni.3533
41. Altman JD, Moss PA, Goulder PJ, Barouch DH, McHeyzer-Williams MG, Bell JI, McMichael AJ, Davis MM (1996) Phenotypic analysis of antigen-specific T lymphocytes. Science 274(5284):94–96
42. Nair N, Buti L, Faenzi E, Buricchi F, Nuti S, Sammicheli C, Tavarini S, Popp MW, Ploegh H, Berti F, Pizza M, Castellino F, Finco O, Rappuoli R, Del Giudice G, Galli G, Bardelli M (2013) Optimized fluorescent labeling to identify memory B cells specific for Neisseria meningitidis serogroup B vaccine antigens ex vivo. Immun Inflamm Dis 1(1):3–13. https://doi.org/10.1002/iid3.3

Chapter 6

Isolation of Antigen-Specific, Antibody-Secreting Cells Using a Chip-Based Immunospot Array

Hiroyuki Kishi, Tatsuhiko Ozawa, Hiroshi Hamana, Eiji Kobayashi, and Atsushi Muraguchi

Abstract

Antigen-specific monoclonal antibodies are useful tools to detect very small amounts of antigenic materials and are applicable for antibody therapeutics. To produce mouse monoclonal antibodies, a hybridoma between B lymphocytes and myeloma cells is used to produce antigen-specific monoclonal antibodies. However, a good hybridoma system is not available to obtain human monoclonal antibodies. To produce antigen-specific human monoclonal antibodies, transformation of B lymphocytes with Epstein-Barr viruses or a phage-display system is used. Here, we describe the screening of antigen-specific, antibody-secreting cells using microwell array chips to obtain antigen-specific human monoclonal antibodies. The system can be applied to screen antigen-specific, antibody-secreting cells from any animal species.

Key words Antigen-specific antibody, Antibody-secreting cell, Microwell-array chip, Immunospot array assay on a chip

1 Introduction

The production of antibody-secreting cell lines from B lymphocytes is the basal technique to obtain antigen-specific antibodies. In the murine system, the production of a hybridoma between B lymphocytes and myeloma cells is used to obtain antibody-secreting cell lines [1]. In other animal species, including humans, efficient and stable hybridoma-producing systems are not available. In humans, the production of Epstein-Barr virus-transformed B-cell lines is often used to produce cell lines that produce human monoclonal antibodies [2, 3]. In addition, phage libraries that express antibody fragments on their surface are used to screen antigen-specific human antibodies [4, 5]. Time-consuming and laborious steps in both methods include preparing libraries of cells or phages that produce antibodies. It takes a month to several months to obtain libraries, and it is not easy for any laboratories to prepare good libraries (containing antibody-producing cells or phages with large

Michael Steinitz (ed.), *Human Monoclonal Antibodies: Methods and Protocols*, Methods in Molecular Biology, vol. 1904, https://doi.org/10.1007/978-1-4939-8958-4_6,

varieties of antigen specificities), making it difficult to produce personal libraries from individual volunteers or patients who produce self-antigen-reactive autoantibodies in blood.

Recently, we developed microwell array chips that have 45,000–230,000 microwells and whose size and shape are fit specifically to capture single cells in each microwell [6–9]. First, live human B lymphocytes were arrayed on the chip, and antigen-specific, antibody-producing B lymphocytes were detected by stimulating them with antigen and analyzing the alteration of the intracellular Ca^{2+} concentration in antigen-stimulated B lymphocytes or by detecting the binding of fluorescence-labeled antigen to B-cell antigen receptors on B lymphocytes on the chip. The precision to detect antigen-specific B lymphocytes, however, was not very high for these two protocols due to the background noises in the assay. Thus, we have developed the third protocol to detect lymphocytes that secrete antigen-specific antibodies on the chip [10]. Regarding the corresponding microwell array chips, Love et al. developed a microengraving method that uses microwell array chips with microwells of 50 nm diameter and depth [11]. To analyze single cells, they need to adjust the cell concentration by limiting the dilution. Thus, it is difficult to trap single cells in most wells. Deutsch et al. [12], as well as Biran and Walt [13], reported the microwell arrays that could accommodate single cells in each well, whereas their microwells were not suitable to detect antibody secretion from the accommodated cells and retrieve the detected target cells. In this context, our microwell array chips are unique for their capacities to capture single cells in each microwell, detecting antibody secretion from single cells and enabling the retrieval of objective cells.

2 Materials

2.1 Preparation of Antibody-Secreting Cells

1. Heparin: Stored at 4 °C.
2. Syringe.
3. Needle: 21G.
4. Ficoll-Conray solution: Lymphocyte Separation Medium (PromoCell).
5. Phosphate-buffered saline (PBS): 8.0 g NaCl, 0.2 g KCl, 1.44 g Na_2HPO_4, and 0.24 g KH_2PO_4 into 1-L ultrapure water prepared by purifying deionized and distilled water attaining a sensitivity of 18 MΩ cm at 25 °C. Sterilize by autoclaving at 121 °C for 20 min.
6. Hemocytometer.
7. Türk's solution.
8. CD138 MicroBeads (Miltenyi Biotec) (*see* **Note 1**).

9. AutoMACS pro (Miltenyi Biotec).
10. AutoMACS column (Miltenyi Biotec).
11. AutoMACS Running buffer (Miltenyi Biotec).
12. Cellbanker (TaKaRa).
13. R-848 (Enzo Life Sciences) dissolved in dimethyl sulfoxide at 5 mg/mL and stored at −20 °C.
14. Human interleukin-2 (hIL2) (PeproTech) dissolve in purified deionized and distilled water at 10^6 U/mL and stored at −20 °C.
15. Human interleukin-4 (hIL4) (PeproTech): Dissolved in purified deionized and distilled water at 10 μg/mL and stored at −20 °C.
16. Human interleukin-17 (hIL17) (PeproTech) dissolved in purified deionized and distilled water at 100 μg/mL and stored at −20 °C.
17. Human interleukin-21 (hIL21) (PeproTech) dissolved in purified, deionized, and distilled water at 100 μg/mL and stored at −20 °C.
18. Human B-cell activating factor (hBAFF) (PeproTech) dissolved in purified deionized and distilled water at 100 μg/mL and stored at −20 °C.
19. Anti-CD40 antibody (R&D systems): dissolve in purified, deionized, and distilled water at 5 mg/mL and store at −20 °C.
20. CpG2006 (5′-TCGTCGTTTTGTCGTTTTGTCGT-3′): dissolve in purified, deionized, and distilled water at 2.5 mg/mL and store at −20 °C.
21. Cell culture medium: RPMI1640 (Invitrogen, Tokyo, Japan) supplemented with 10% fetal calf serum, 100 U/mL penicillin, and 100 μg/mL streptomycin, and 50 μM 2-mercaptoethanol (*see* **Note 2**).
22. In vitro stimulation medium: Cell culture medium with 5 μg/mL of R-848, 1000 IU/mL of hIL2, 10 ng/mL of hIL4, 2 ng/mL of hIL17, 100 ng/mL of hIL21, 100 ng/mL of hBAFF, 2.5 μg/mL of anti-CD40 antibody, and 2.5 μg/mL of CpG2006 [14].

2.2 Preparation of Antigen-Coated Microwell Array Chips

1. Kimwipe™ paper (Kimberly-Clark Worldwide, Inc.).
2. Lipidure: 5% Lipidure BL-103 (NOF, Tokyo, Japan). Dilute the Lipidure to 0.01% (500-fold) in PBS before use. Store at room temperature until use.
3. Vacuum pump.

2.3 Immunospot Array Assay on a Chip (ISAAC)

1. Microwell array chip containing 62,500 microwells (15 μm in diameter) provided by BliNK BIOMEDECAL (Lyon, France). The ISAAC method is covered by patents that have been exclusively licensed to BliNK BIOMEDECAL (*see* **Note 3**).
2. PBS.
3. Antigen (*see* **Note 4**).
4. Lipidure BL-103 (Provided as 5 wt % solution from NOF Corporation, Tokyo, Japan) (*see* **Note 5**).
5. PBS-L: PBS containing 0.01% Lipidure BL-103.
6. Cy3-conjugated anti-IgG stored according to the manufacturer's instruction (*see* **Note 6**).
7. Cell Trace Oregon green 488 (Invitrogen): Dissolve in dimethyl sulfoxide at 1 mg/mL and store at −20 °C. Dilute to 0.5 μg/mL just prior to use with PBS-L.
8. CO_2 incubator: 5% CO_2 in air, 37 °C.
9. Incubation box (*see* **Note 7**).
10. Fluorescence microscope with a halogen lamp and optical filters to observe FITC (for observing Oregon Green) and Cy3.
11. Digital camera for a microscope, which can observe Oregon Green and Cy3.

2.4 Retrieval of Antigen-Specific Antibody-Secreting Cells

1. Fluorescence microscope.
2. Micromanipulator (TransferMan NK2; Eppendorf).
3. Microinjector (CellTram vario; Eppendorf).
4. Capillary (16 μm in diameter (Primetech)).
5. Paraffin oil.
6. Dynabeads mRNA DIRECT Kit (Invitrogen).
7. Dynabead Oligo$(dT)_{25}$ and Lysis/Binding Buffer kit component from Dynabeads mRNA DIRECT Kit.
8. Cell lysis buffer (30 μg of Dynabead Oligo$(dT)_{25}$, 3 μL of Lysis/Binding Buffer, and 0.25 pmol of each specific primer of human Gamma RT, Kappa RT, and Lambda RT).
9. Oligonucleotide primer sequences are shown in Table 1 (*see* also ref. 15).

2.5 Amplifying Antibody cDNAs from Single Cells

1. ThermalCycler (Applied Biosystems 2720 Thermal Cycler).
2. DynaMag-96 Side Magnet (Thermo Fisher).
3. Elution Buffer, kit component from Dynabeads mRNA DIRECT Kit (Invitrogen).
4. SuperScriptIII (Invitrogen).
5. RNase inhibitor, Murine (New England Biolabs).

Table 1
Oligonucleotide primer used for single-cell 5′-RACE

Oligonucleotide name	Sequence 5′–3′	Used for
human Gamma RT	ACGGTCACCACGCTGCTGAGGGA	RT primer
human Gamma 1st	ACGCTGCTGAGGGAGTAGAGTCCTGAG	1st PCR primer
human Gamma Nest	AGCCGGGAAGGTGTGCACGCCGCTG	Nested PCR primer
human Kappa RT	GAGTTACCCGATTGGAGGGCGTTAT	RT primer
human Kappa 1st	CCACCTTCCACTGTACTTTGGCCTC	1st PCR primer
human Kappa Nest	ACAACAGAGGCAGTTCCAGATTTCAACTGC	Nested PCR primer
human Lambda RT	ACTGTCTTCTCCACGGTGCTCC	RT primer
human Lambda 1st	CTTCTCCACGGTGCTCCCTTCAT	1st PCR primer
human Lambda Nest	AGTGTGGCCTTGTTGGCTTG	Nested PCR primer
dC-adaptor primer	AGCAGTAGCAGCAGTTCGATAACTTCGA ATTCTGCAGTCGACGGTACCGCGGGCCCGG GATCCCCCCCCCCCCCDN[a]	1st PCR primer
Adaptor primer	AGCAGTAGCAGCAGTTCGATAA	Nested PCR primer

[a]Mixture of A, T, G, and C

6. Terminal Deoxynucleotidyl Transferase (Roche).
7. 10 mM dGTP (TaKaRa).
8. PrimeSTAR DNA polymerase with GC Buffer (TaKaRa).
9. Oligonucleotide primer sequences are shown in Table 1 (*see* also ref. 15).
10. 1 M $MgCl_2$.
11. 1 M potassium buffer [1 M K_2HPO_4, 1 M KH_2PO_4, (pH 7.0)].
12. 2.5 mM each dNTP (TaKaRa).
13. 0.1 M DTT.
14. RT solution (10 μL/sample): 4.4 μL of DEPC-H_2O, 2.0 μL of 5× First-Strand Buffer, 2.0 μL of 2.5 mM each dNTP, 1.0 μL of 0.1 M DTT, 0.4 μL of RNase Inhibitor (Murine, 40,000 units/mL), and 0.2 μL of SuperScriptIII.
15. Tailing solution (5 μL/sample): 3.5 μL of H_2O, 0.5 μL of 1 M potassium buffer, 0.5 μL of 10 mM dGTP, 0.4 μL of 0.1 M $MgCl_2$, 0.1 μL of Terminal Deoxynucleotidyl Transferase (400 U/μL).
16. First PCR reaction mix: 0.3 U of PrimeSTAR DNA polymerase, 1× PrimeSTAR GC buffer, 0.2 mM of each dNTP,

0.2 pmol of dC-adaptor primer, human Gamma 1st, Kappa 1st, Lambda 1st.

17. Nested PCR reaction mix: 0.3 U of PrimeSTAR DNA polymerase, 1× PrimeSTAR GC buffer, 0.2 mM of each dNTP, 0.2 pmol of adaptor primer and human Gamma Nest, Kappa Nest, or Lambda Nest.

2.6 Preparation of Antibody Expression Vector

1. QIAquick PCR Purification Kit (QIAGEN).
2. Gibson Assembly Master Mix (New England Biolabs).
3. LB/Amp/plate, LB medium with 1% agarose and 100 μg/mL ampicillin.

2.7 Production of Monoclonal Antibodies

1. Expi293 Expression System (Thermo Fisher Scientific) and incubator for Expi293 cell culture.
2. Protein G column (GE healthcare life sciences).

3 Methods

3.1 Preparation of Peripheral Blood Mononuclear Cells

Human experiments should be performed with the approval of the Ethical Committee at the appropriate organization, and informed consent should be obtained from the subjects.

1. Collect 10–20 mL (50 mL if possible) of peripheral blood from a subject into a syringe (*see* **Note 8**).
2. Divide 5 mL of blood into 15 mL conical tubes, and dilute it with 5 mL of PBS.
3. Insert a sterile Pasteur pipette into blood (Fig. 1 and *see* **Note 9**).
4. Add 3 mL of Lymphocyte Separation Medium to the tube through the Pasteur pipette. The blood is layered on top of the Lymphocyte Separation Medium.
5. Centrifuge the tube at 740 × *g* (2000 rpm) for 30 min at room temperature (*see* **Note 10**).
6. The ring of mononuclear cells is layered in the interphase over the Lymphocyte Separation Medium. Harvest the mononuclear cells using a Pasteur pipette (*see* **Note 11**), and transfer them to another 15 mL conical tube.
7. Dilute the cells with PBS to 10 mL, and centrifuge at 740 × *g* for 10 min at room temperature.
8. Discard the supernatant with decantation, resuspend the cells with approximately 10 mL of PBS, and centrifuge the cells at 420 × *g* (1500 rpm) for 5 min at room temperature.
9. Repeat **step 8**.

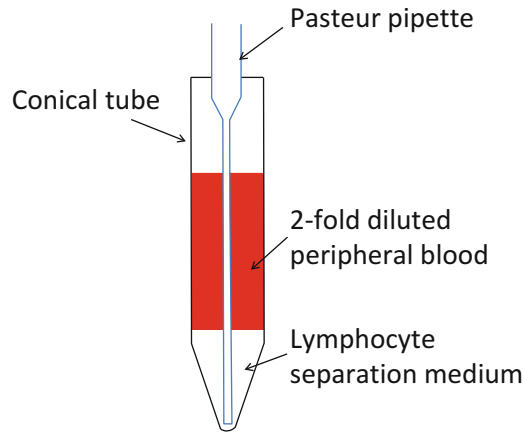

Fig. 1 Layering peripheral blood over the Lymphocyte separation medium. A sterile Pasteur pipette is inserted into the twofold diluted peripheral blood. Lymphocyte separation medium is then poured into the blood from the top of the Pasteur pipette

10. Discard the supernatant with decantation, and resuspend the cells in 10 mL of PBS.
11. Count the cell number using Türk's solution (*see* **Note 12**).
12. Centrifuge the cells at 420 × *g* for 5 min at room temperature.
13–15 (**Optional**).
13. Remove the supernatant as completely as possible.
14. Add Cellbanker to the cells at density of 0.2–1 × 10^7 cells/mL.
15. Freeze and store the cells at −80 °C until use.

3.2 Stimulation of PBMCs to Prepare Antibody-Secreting Cells (Optional)

PBMCs are stimulated with toll-like receptor agonists R-848 and CpG and cytokines to induce antibody secretion in B lymphocytes.

1. Thaw the frozen PBMCs in a water bath at 37 °C.
2. Add five- to tenfold of the culture medium to the cells.
3. Centrifuge the cells at 420 × *g* for 5 min at room temperature.
4. Discard the supernatant, and resuspend the cells in in vitro stimulation medium to a cell density of 1 × 10^6 cells/mL.
5. Incubate the cells at 37 °C for 6–8 days in a humidified CO_2 incubator.

3.3 Separation of CD138⁺ Antibody-Secreting Cells

Antibody-secreting cells are enriched by separating $CD138^+$ cells.

1. Harvest the cells, and count the cell number using Türk's solution (*see* **Note 12**).
2. Centrifuge the cells at 420 × *g* for 5 min at room temperature.
3. Remove the supernatant completely, and add 80 μL of auto-MACS running buffer per 10^7 cells.

4. Add 20 μL of CD138-microbeads to the cells per 10^7 cells.
5. Incubate the cells at 4 °C for 15 min.
6. Add 10 mL of autoMACS running buffer to the cells, and centrifuge them at 420 × *g* for 5 min at room temperature.
7. Remove the supernatant as completely as possible, and add 500 μL of autoMACS running buffer.
8. Separate $CD138^+$ cells using AutoMACS Pro according to the manufacturer's instructions.
9. Count the cell number (*see* **Note 13**).
10. Spin down the cells at 420 × *g* for 5 min at room temperature.
11. Discard the supernatant and resuspend the cells in cell culture medium to the cell density of 5×10^6 cells/mL.
12. Keep the cells at room temperature until use.

3.4 Preparation of Antigen-Coated Microwell Array Chips

Antigen is coated on the chip overnight, and then, the chip is used for ISAAC.

1. Add 100 μL of antigen (*see* **Notes 4** and **14**) in PBS onto the well area on a microwell array chip.
2. Put the chip in a humidified incubation box (Fig. 2).
3. Incubate the chip overnight at 4 °C or room temperature (*see* **Note 15**).
4. Wash the chip by aspirating the antigen solution with a Kimwipe paper (or a filter paper) and then add 100 μL of PBS-L.
5. Repeat **step 4**.
6. Remove the air in microwells using a vacuum pump.
7. Incubate the chip for 15 min at room temperature (Blocking).

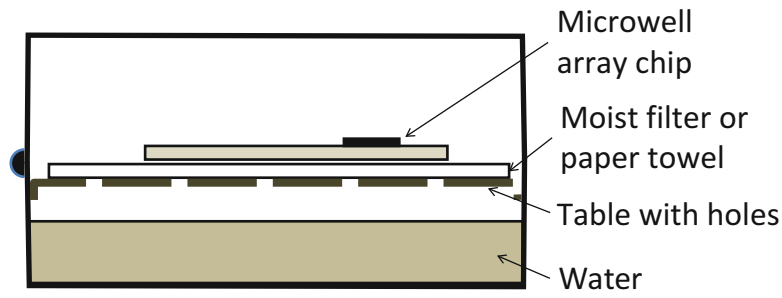

Fig. 2 Humidified incubation box for the incubation of the microwell array chip. To avoid drying out of the solution on the chip during the incubation, the microwell array chip was incubated in the humidified box. We conventionally used an empty box for micropipette tips. It has a table with holes. Water is on the bottom, and a wet paper towel or filter paper was placed on the table. The chip was placed on the filter paper for the incubation

8. Wash the chip as in **step 4** using the cell culture medium instead of PBS-L (*see* **Note 16**).
9. Use the chip for ISAAC.

3.5 Immunospot Array Assay on a Chip (ISAAC) (See Note 17)

When the chip is incubated, put the chip in a humidified black box to avoid drying the chip.

1. Remove the medium by aspirating it with a Kimwipe paper (or a filter paper), and then, add 50 μL of cells (2.5×10^5 cells) (*see* **Note 18**).
2. Incubate the cells at room temperature for 10 min until the cells settle down into the wells.
3. Mix the cell suspension with a pipette to make cells outside the wells float, and incubate the chip for 5 min at room temperature (*see* **Note 19**).
4. Repeat **step 3** once.
5. Mix the cell suspension with a pipette to make cells outside the wells float, and remove the cell suspension by aspirating it with a Kimwipe paper (or a filter paper). Add 100 μL of cell culture medium.
6. Repeat **step 5** twice.
7. Incubate the cells in microwells on the chip at 37 °C for three hours in a humidified CO_2 incubator.
8. Remove the medium by aspiration with a Kimwipe paper (or a filter paper), and then, add 100 μL of PBS.
9. Repeat **step 8** twice.
10. Remove PBS by aspiration with a Kimwipe paper (or a filter paper), add 100 μL of Cy3-conjugated anti-IgG (1 μg/mL in PBS-L), and then incubate the chip at room temperature for 30 min.
11. Remove the antibody solution with a Kimwipe paper (or a filter paper), and then add 100 μL of PBS.
12. Repeat **step 11** twice.
13. Remove PBS by aspiration with a Kimwipe paper (or a filter paper), add 100 μL of Cell Trace Oregon green 488 (0.5 μg/mL in PBS-L), and then, incubate at room temperature for 5 min (*see* **Note 20**).
14. Wash the chip as in **step 11** three times.

3.6 Retrieval of Antigen-Specific Antibody-Secreting Cells

1. Observe antibody secretion with Cy3 signals (*see* **Note 21**) and the cells with Oregon green signals under a fluorescence microscope (*see* Figs. 3 and 4) (*see* **Note 22**). The Cy3 circular signal is observed around the well containing the target cell-secreting antigen-specific IgG.

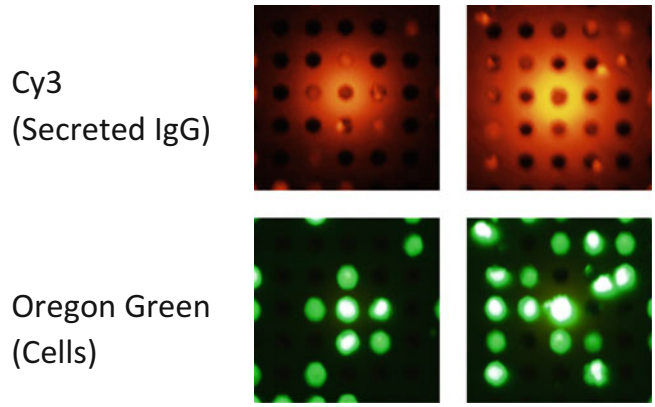

Fig. 3 ISAAC signals. Top, Cy3 signals showing secreted IgG. Bottom, Oregon green signals showing cells in microwells

2. Bring the capillary and micromanipulator to the "retrieval position" as in Fig. 4b. Adjust the tip of the capillary to the target-cell position under a microscope using a CellTransferman NK2 (Fig. 4c). Aspirate cells with a microaspirator (CellTram Vario) (Fig. 4c).
3. Lift the capillary to the "ejection position" (Fig. 4d), and eject cells from the capillary by forming a tiny drop (~0.2 μL) of buffer (Fig. 4e).
4. Transfer a drop containing the cell to cell lysis buffer by adding the drop to the buffer (Fig. 4f, *see* **Note 22**).

3.7 Amplifying Antibody cDNAs from Single Cells

1. Set the tube containing a cell and Dynabeads on DynaMag-96 Side Magnet for 30 s.
2. Remove the Cell lysis buffer, and add 10 μL of the Elution Buffer.
3. Mix gently by vortexing.
4. Set the tube on a DynaMag-96 Side Magnet for 30 s, and remove the Elution Buffer.
5. Add 10 μL of the RT solution, and mix gently by vortexing.
6. Incubate the tube for 40 min at 50 °C using a ThermalCycler.
7. Set the tube on a DynaMag-96 Side Magnet for 30 s, and remove the RT solution.
8. Add 5 μL of the Tailing solution and mix gently by vortexing.
9. Incubate the tube for 40 min at 37 °C using a ThermalCycler.
10. Set the tube on a DynaMag-96 Side Magnet for 30 s, and remove the Tailing solution.
11. Add 25 μL of the first PCR reaction mix, and mix gently by vortexing.

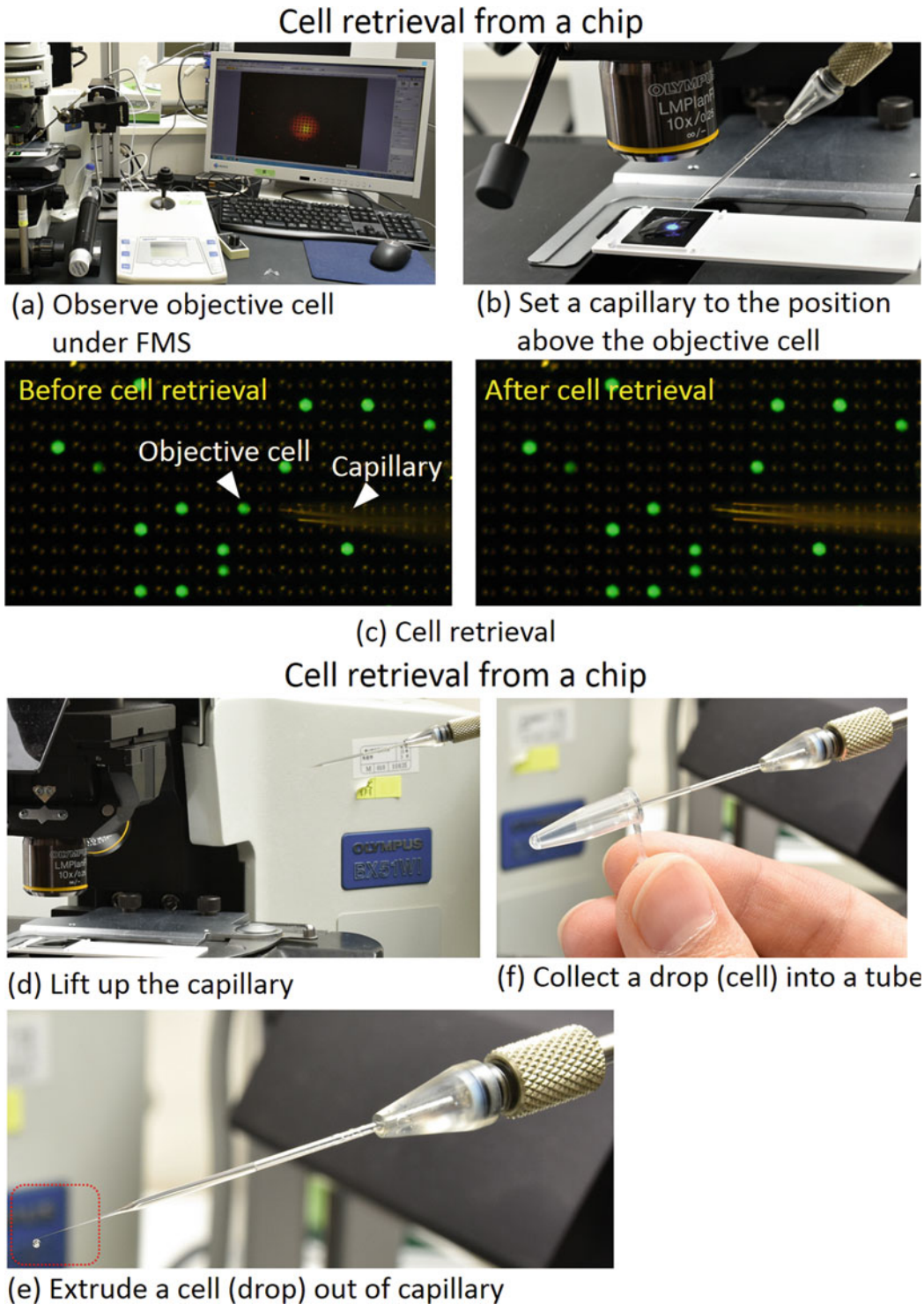

Fig. 4 Cell retrieval with micromanipulator. (**a**) Antigen-specific, antibody-secreting cells were observed under the fluorescence microscope (FMS). (**b**) The capillary is set to the position above the objective cell for cell retrieval. (**c**) Cell retrieval. Left, the capillary is approaching the objective cell. Right, the objective cell has been retrieved, and the well became empty. (**d**) The capillary is raised. (**e**) The retrieved cell is extruded out of the capillary. (**f**) A drop containing an extruded cell is collected into a PCR tube

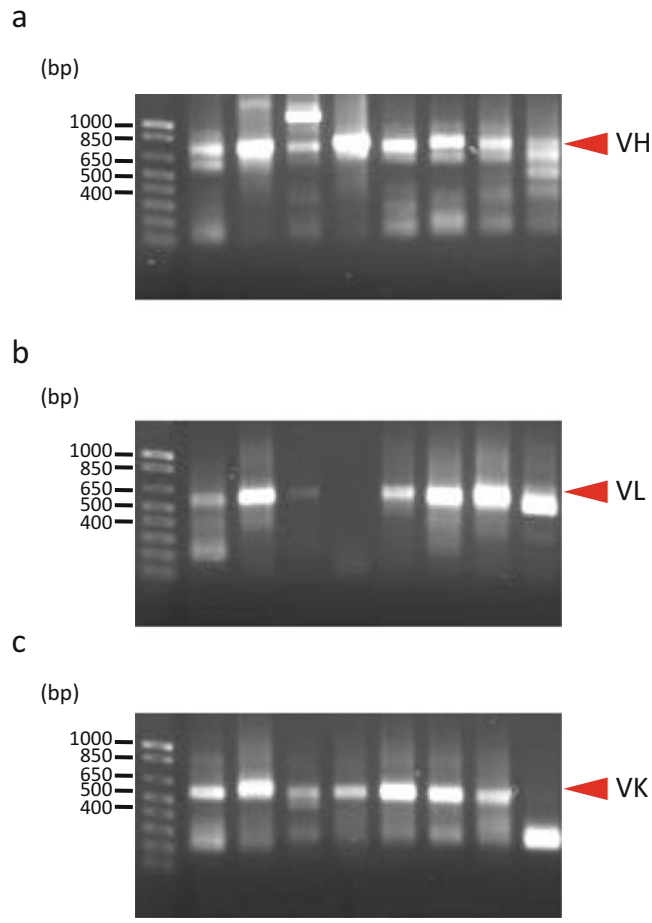

Fig. 5 Amplification of the variable regions Gamma (**a**), Kappa (**b**), and Lambda (**c**) using a single-cell 5′-RACE procedure. The PCR products were analyzed by agarose gel electrophoresis. The sizes are shown at the left. The positions of the gamma, kappa and lambda fragment are indicated with arrow heads on the right

12. Set the tube on a ThermalCycler, and perform PCR reaction as follows: 5 min at 95 °C followed by 30 cycles of 15 s at 95 °C, 5 s at 60 °C, and 1 min at 72 °C.
13. Add 75 μL of water to the resultant PCR products.
14. Transfer 2 μL of the diluted PCR products into a new PCR tube containing 23 μL of the Nested PCR reaction mix.
15. Perform PCR as follows: 5 min at 95 °C followed by 35 cycles of 15 s at 95 °C, 5 s at 60 °C, and 1 min at 72 °C.
16. Analyze the PCR products by agarose gel electrophoresis (Fig. 5) (*see* **Note 23**).

3.8 Preparation of Antibody Expression Vector

1. Purify the PCR products using the QIAquick PCR Purification Kit according to the manufacturer's instructions (*see* **Note 24**).
2. Mix the purified PCR product, vector, and Gibson Assembly Master Mix, and then, incubate the mixture for homologous recombination according to the manufacturer's instructions (*see* **Note 25**).
3. Perform heat shock for the transformation of competent cells, and then, plate them on the LB/Amp/plate for colony formation according to standard protocols.
4. Inoculate the colony with LB/Amp medium, and then isolate the plasmid DNA according to standard protocols.
5. Sequence the plasmid DNA according to standard protocols (*see* **Note 26**).
6. Analyze the immunoglobulin gene repertoire with the ImMunoGeneTics (IMGT)/V-Quest tool (http://www.imgt.org/) [16].

3.9 Production of Monoclonal Antibodies

1. Isolate a large amount of plasmid DNA according to standard protocols (*see* **Note 27**).
2. Co-transfect both the heavy and light chain plasmid DNA to Expi293 cells, and culture the cells according to the manufacturer's instructions.
3. One week after the culture, centrifuge the cell suspension at 13,000 × *g* for 5 min at room temperature.
4. Harvest the supernatant.
5. Purify the antibodies using the protein G column according to the manufacturer's instructions.

4 Notes

1. For isolating human CD138 positive plasma cells.
2. 2-Mercaptoethanol is optional.
3. It is necessary to contact BliNK BIOMEDECAL. The home page of BliNK BIOMEDICAL is http://www.blinkbiomedical.com.
4. The antigen should be dissolved in PBS in the absence of a stabilizer such as bovine serum albumin. It is recommended to check whether good and specific signals are obtained in enzyme-linked immunosorbent assay (ELISA) using the same antigen and positive control anti-serum.
5. Blocking reagent. Any other blocking reagents can be used if the blocking reagents produce a good signal/noise ratio in ELISA. We use Lipidure because it shows a blocking effect very rapidly and efficiently.

6. To detect antigen-specific, IgG-secreting cells, use anti-IgG (Fc-specific). When anti-IgG (whole molecule) is used, the reagent contains anti-immunoglobulin light chain antibodies and it reacts with other antibody classes, including IgM, IgA, and IgE.
7. For the chip incubation, it was put in a humidified incubation box as shown in Fig. 2. You can use an empty tip box for the micropipette.
8. The number of antigen-specific, antibody-secreting cells that circulate in peripheral blood peaks 7 days after the vaccination and then rapidly decreases within several days [17].
9. The Glass Pasteur pipettes are sterilized at 180 °C for 2 h in a dry incubator.
10. The brake should be off.
11. First, remove the upper layer that contains plasma and most of the platelets, and then harvest the mononuclear cells.
12. Mix the cells well with a Pasteur pipette. Harvest 10 μL of the cell suspension, and mix with 90 μL of Türk's solution. Mix the cell suspension well, transfer an aliquot of cell suspension to a hemocytometer, and count the cell number.
13. The volume of CD138-positive cells is approximately 2 mL after separation by AutoMACS Pro.
14. The optimum concentration should be determined for each antigen. Usually, 1–10 μg/mL of antigen is sufficient.
15. When the antigen is labile, coat the chip with antigen at 4 °C. When the antigen is stable, coat the chip with the antigen at room temperature.
16. Be careful not to dry the chip. After aspiration of the buffer, add the medium as quickly as possible.
17. The ISAAC is covered by patents that have been exclusively licensed to BliNK BIOMEDICAL (Lyon, France).
18. The cell number is three to four times the number of microwells, i.e., $1.9–2.5 \times 10^5$ cells for the 62,500-well chip.
19. The cells inside the wells tend to stay in the wells during the mixing of the cell suspension. Mix the cells mildly but strongly enough to float cells outside of the wells.
20. Oregon Green fluorescence is strong and can be detected with the optical filter for Cy3. Strong Oregon Green fluorescence interfered with the observation of the Cy3 signals. Adjust the concentration of Oregon Green and incubation time to label the cells for the optimal strength of the fluorescence signals.
21. Antibodies secreted from a cell in a microwell diffuse in all directions. The secreted antibody bound on the chip is

observed as a circular signal of Cy3. It looks like a doughnut and is easily distinguished from noise signals.

22. Be careful not to puncture the fingers or eyes with the glass capillary. Wear glasses to protect eyes.
23. PCR products for Kappa and Lambda chains will be observed at approximately 700 base pairs; for Gamma chain, 550 base pairs (Fig. 5).
24. Purification of PCR products may be performed by another method.
25. Homologous recombination may be performed by another method.
26. Sequence primer: CMV (5′-ATTGACGCAAATGGGCGGTA-3′), human Gamma Nest, Kappa Nest, and Lambda Nest.
27. More than 10 μg of DNA is necessary for DNA transfection into Expi293 cells.

Acknowledgment

This work was supported by grants from the Toyama Medical Bio-Cluster Project and Hokuriku Innovation Cluster for Health Science of the Ministry of Education, Culture, Sports, Science and Technology, Japan. This work was also supported by JSPS KAKENHI Grant Number JP16H06499 (H.K.), the Platform Project for Supporting in Drug Discovery and Life Science Research (Platform for Drug Discovery, Informatics, and Structural Life Science) from the Ministry of Education, Culture, Sports, Science (MEXT) and the Japan Agency for Medical Research and Development (AMED) (A.M.), and the Platform Project for Supporting Drug Discovery and Life Science Research (Basis for Supporting Innovative Drug Discovery and Life Science Research (BINDS)) from AMED under Grant Number JP18am0101077 (T.O.).

References

1. Kohler G, Milstein C (1975) Continuous cultures of fused cells secreting antibody of predefined specificity. Nature 256:495–497
2. Kozbor D, Roder JC (1981) Requirements for the establishment of high-titered human monoclonal antibodies against tetanus toxoid using the Epstein-Barr virus technique. J Immunol 127:1275–1280
3. Traggiai E, Becker S, Subbarao K, Kolesnikova L, Uematsu Y, Gismondo MR et al (2004) An efficient method to make human monoclonal antibodies from memory B cells: potent neutralization of SARS coronavirus. Nat Med 10:871–875
4. McCafferty J, Griffiths AD, Winter G, Chiswell DJ (1990) Phage antibodies: filamentous phage displaying antibody variable domains. Nature 348:552–554
5. Winter G, Griffiths AD, Hawkins RE, Hoogenboom HR (1994) Making antibodies by phage display technology. Annu Rev Immunol 12:433–455
6. Ozawa T, Kinoshita K, Kadowaki S, Tajiri K, Kondo S, Honda R et al (2009) MAC-CCD

system: a novel lymphocyte microwell-array chip system equipped with CCD scanner to generate human monoclonal antibodies against influenza virus. Lab Chip 9:158–163

7. Tajiri K, Kishi H, Tokimitsu Y, Kondo S, Ozawa T, Kinoshita K et al (2007) Cell-microarray analysis of antigen-specific B-cells: single cell analysis of antigen receptor expression and specificity. Cytometry A 71:961–967
8. Tokimitsu Y, Kishi H, Kondo S, Honda R, Tajiri K, Motoki K et al (2007) Single lymphocyte analysis with a microwell array chip. Cytometry A 71:1003–1010
9. Yamamura S, Kishi H, Tokimitsu Y, Kondo S, Honda R, Rao SR et al (2005) Single-cell microarray for analyzing cellular response. Anal Chem 77:8050–8056
10. Jin A, Ozawa T, Tajiri K, Obata T, Kondo S, Kinoshita K et al (2009) A rapid and efficient single-cell manipulation method for screening antigen-specific antibody-secreting cells from human peripheral blood. Nat Med 15:1088–1092
11. Love JC, Ronan JL, Grotenbreg GM, van der Veen AG, Ploegh HL (2006) A microengraving method for rapid selection of single cells producing antigen-specific antibodies. Nat Biotechnol 24:703–707
12. Deutsch M, Deutsch A, Shirihai O, Hurevich I, Afrimzon E, Shafran Y et al (2006) A novel miniature cell retainer for correlative high-content analysis of individual untethered non-adherent cells. Lab Chip 6:995–1000
13. Biran I, Walt DR (2002) Optical imaging fiber-based single live cell arrays: a high-density cell assay platform. Anal Chem 74:3046–3054
14. Zaimoku Y, Takamatsu H, Hosomichi K, Ozawa T, Nakagawa N, Imi T et al (2017) Identification of an HLA class I allele closely involved in the autoantigen presentation in acquired aplastic anemia. Blood 129:2908–2916
15. Kurosawa N, Yoshioka M, Fujimoto R, Yamagishi F, Isobe M (2012) Rapid production of antigen-specific monoclonal antibodies from a variety of animals. BMC Biol 10:80
16. Giudicelli V, Chaume D, Lefranc MP (2004) IMGT/V-QUEST, an integrated software program for immunoglobulin and T cell receptor V-J and V-D-J rearrangement analysis. Nucleic Acids Res 32:W435–W440
17. Bernasconi NL, Traggiai E, Lanzavecchia A (2002) Maintenance of serological memory by polyclonal activation of human memory B cells. Science 298:2199–2202

Chapter 7

Purification of Human Monoclonal Antibodies and Their Fragments

Nicole Ulmer, Sebastian Vogg, Thomas Müller-Späth, and Massimo Morbidelli

Abstract

This chapter summarizes the most common chromatographic mAb and mAb fragment purification methods, starting by elucidating the relevant properties of the compounds and introducing the various chromatography modes that are available and useful for this application. A focus is put on the capture step affinity and ion-exchange chromatography. Aspects of scalability play an important role in judging the suitability of the methods. The chapter introduces also analytical chromatographic methods that can be utilized for quantification and purity control of the product. In the case of mAbs, for most purposes the purity obtained using an affinity capture step is sufficient. Polishing steps are required if material of particularly high purity needs to be generated. For mAb fragments, affinity chromatography is not yet fully established, and the capture step potentially may not provide material of high purity. Therefore, the available polishing techniques are touched upon briefly. In the case of mAb isoform and bispecific antibody purification, countercurrent chromatography techniques have proven to be very useful and a part of this chapter has been dedicated to them, paying tribute to the rising interest in these antibody formats in research and industry.

Key words Purification, Downstream processing, Preparative chromatography, Affinity chromatography, Cation-exchange chromatography, Size-exclusion chromatography, Hydrophobic interaction chromatography, Protein A, Bind-elute chromatography, Flow-through chromatography

1 Introduction

As the expression of monoclonal antibodies (mAbs) using recombinant cell technology has been developed and refined since the 1970s [1] so have been the technologies to purify them. Early antibody purification strategies comprised non-chromatographic steps such as flocculation and precipitation, which are in part re-discovered today [2]. Nevertheless, due to the availability of very robust and powerful chromatographic stationary phases providing excellent impurity clearance, manufacturing costs for

Nicole Ulmer, Sebastian Vogg, and Thomas Müller-Späth contributed equally to this work.

Michael Steinitz (ed.), *Human Monoclonal Antibodies: Methods and Protocols*, Methods in Molecular Biology, vol. 1904, https://doi.org/10.1007/978-1-4939-8958-4_7,

mAbs have dropped to 20–100 $/g [3]. By today, many biopharmaceutical companies producing mAbs have developed fully industrialized generic platform downstream processes comprising of two to three chromatographic steps [3–9] (*see* **Note 1**). As first step, affinity chromatography is used almost exclusively. In many cases, cation-exchange chromatography (CEX) is used in bind-elute mode as second step (first polishing). Anion-exchange chromatography (AEX) in flow-through mode is frequently used as third chromatography step (second polishing). Very roughly speaking, in the aforementioned three-step purification process, the purpose of the capture step is the concentration of mAb as well as removal of a large part of the host cell proteins while the main purpose of the ion-exchange (IEX) steps is the removal of aggregates (CEX), host cell DNA, and leached affinity ligand (AEX).

1.1 Properties of mAbs and mAb Fragments

1.1.1 Isoelectric Point

Most mAbs and mAb fragments possess a high isoelectric point (pI) in the range of pH 8–9 [10]. To account for the presence of charge isoforms (*see* Subheading 1.1.3), often a pI range is reported in the literature when a specific mAb is discussed. The high pI allows for purification by cation-exchange chromatography at neutral or slightly acidic pH since most impurities have a pI in the neutral or acidic range (for instance, the pI of DNA is at pH 2–3) and will remain in the liquid phase while the mAb is retained on the negative surface.

1.1.2 Aggregates and Fragments

High (HMW) and low molecular weight (LMW) species constitute the key product-related impurities as they typically exhibit a high degree of immunogenicity [11]. The susceptibility of monoclonal antibodies to irreversible aggregation is dependent on their protein sequence, their conformation, and the environmental conditions [12]. Irreversible aggregates comprise mainly mAb dimers and form already during cell culture. For modern antibodies, typically 1–3% mAb aggregates are observed in cell culture supernatants. Another major source of aggregates is in low-pH conditions occurring in the elution of the protein A affinity chromatography step. Additionally, in industrial applications, the affinity step eluate is typically held at low pH to inactivate viruses, however promoting further aggregation. Therefore, it is important to identify pH conditions suitable for virus inactivation on the one hand but to maintain an acceptable aggregate content on the other hand. Furthermore, aggregation may occur during and subsequent to fast neutralization of protein A eluate [13]. With the exception of the above processing steps, the formation of new irreversible aggregates is generally not an issue in the chromatographic steps of the downstream processing of antibodies.

1.1.3 Charge Variants

Monoclonal antibodies typically display charge heterogeneity due to various post-translational modifications [14–16]. The most important ones are deamidation and lysine cleavage. Deamidation introduces negative charges to the mAb molecule by converting an (exposed) amino group into a carboxyl group resulting in acidic charge variants. Deamidation is promoted by storing the mAbs at elevated temperature (e.g., 25 °C) and pH (pH > 7). Lysine cleavage is an enzymatic reaction taking place during the cell culture process. MAbs with C-terminal lysine groups (positive charge) may lose one or both lysine groups due to clipping. For further details on post-translational modifications and the mechanisms for the induction of charge heterogeneity, the reader is referred to the literature [16]. The charge heterogeneity is an important feature of monoclonal antibodies that needs to be taken into account when purifying and analyzing mAbs. It can be modulated using ion-exchange chromatography [17]. However, broad eluting peaks due to charge heterogeneity must not be confused with broad peaks originating from transport resistance or axial dispersion.

1.1.4 Glycoforms

Glycosylation is a major post-translational modification influencing the activity of the monoclonal antibody [16]. However, different glycoforms of intact monoclonal antibodies cannot be resolved using standard chromatographic methods since the difference of the glycan sizes are typically small compared to the size of the mAb (1–3%) and the glycans are not exposed on the outside of the molecule but directed toward the interior of the globular conformation (N-linked glycosylation). Even glycoforms of antibodies with O-linked glycosylation (with charged, sialylated glycans) in the Fab region have not been separated using standard chromatographic techniques to our knowledge. The most common glycans of mAbs do not carry charges at the conditions relevant for chromatography and therefore do not influence charge-based adsorption behavior.

MAb fragments are mostly produced using recombinant microbial expression systems such as *E. coli* where glycosylation machineries have not yet been established in the industry. Thus, mAb fragments from these expression systems are generally not glycosylated. In contrast, other expression systems such as yeast are capable of glycosylation and yeast strains expressing human-like glycosylation patterns have been developed [18].

1.1.5 Process-Related Impurities

There are several types of process-related impurities, ranging from host cell proteins (HCPs) and DNA over endotoxins and viruses to leached ligands such as protein A [11]. Host cell proteins represent a heterogeneous mixture of hundreds of proteins, some of them having very similar adsorptive properties as the mAb leading to co-elution in non-affinity chromatography, e.g., in CEX

chromatography. Due to their lack of Fc regions, HCPs are not captured by protein A while the selectivity of the protein A ligand for the mAb is extremely high, leading to excellent binding of the mAb. However, HCPs may adsorb nonspecifically onto the stationary phase matrix. In addition, data has been presented indicating the association of HCP and mAb, leading to a co-purification of mAb and HCPs. Our observations confirm that this phenomenon is in fact widespread among mAbs. These recent findings highlight the importance of the washing steps in chromatography [19]. DNA also originates from the cell culture. It is reduced by orders of magnitude during the protein A affinity [20] and anion-exchange chromatography steps [21]. Ligand leaching from the columns is the major source of process-related impurities during downstream processing. Especially leached protein A is of concern and needs to be reduced during the subsequent polishing steps. Cation-exchange chromatography usually shows good clearance of leached protein A [20].

1.2 Chromatographic Purification of mAbs

1.2.1 Mode of Operation

Chromatographic modes encountered in mAb and mAb fragment purification vary not only in the functionality of the stationary phase but also in the regimes of relative retention of target and impurities. This is depicted schematically in Fig. 1 in terms of the partition coefficient, which is defined as the ratio of solute concentration in the solid and liquid phase. Furthermore, several processes were developed implementing an interconnection of at least two columns to enhance process performance in comparison with regular batch processing presented here [22]. The experimental design of such processes is described in the literature [23–25].

Saturation Adsorption

Affinity capture steps are typically saturation adsorption processes utilizing the column's dynamic binding capacity (DBC) for retaining the product of interest. Due to mass transfer limitations encountered in mAb purification, the breakthrough curve (BTC) and therefore DBC (e.g., $DBC_{1\%}$ at 1% breakthrough) are a strong function of loading flow rate. Lower velocities result in steeper BTC and higher $DBC_{1\%}$ at the expense of productivity. This can be alleviated increasing the flow rate however decreasing $DBC_{1\%}$. As stationary phases with protein-based affinity ligands such as protein A are very expensive and have limited cyclic lifetime, the low utilization of the static binding capacity (SBC, $DBC_{100\%}$) at increased flow rates results in a strong trade-off with productivity [23]. After washing steps to remove unspecifically bound impurities, elution is generally carried out with a step gradient because resolution fully originates from the stationary phase in these cases [26].

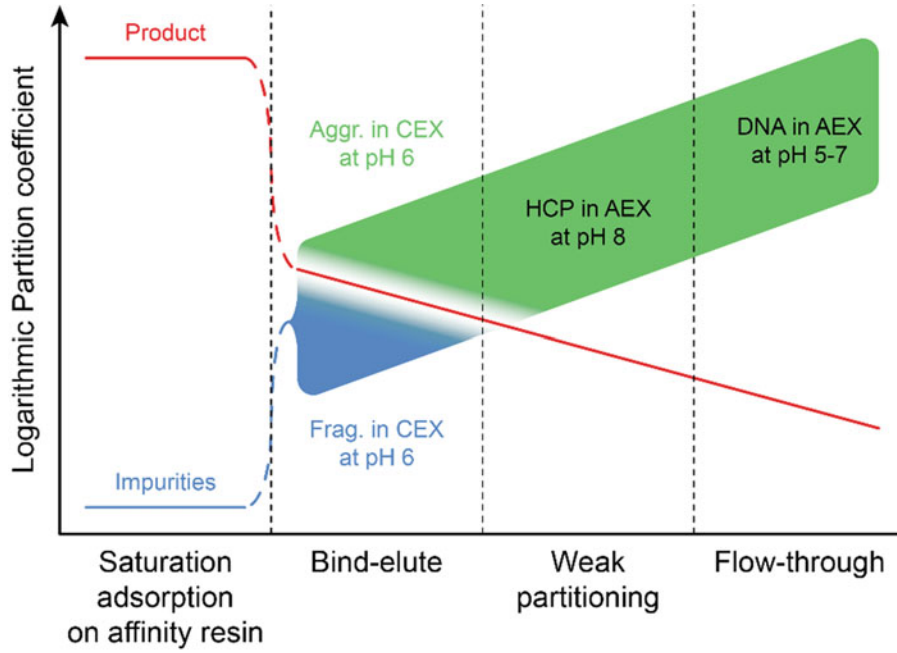

Fig. 1 Schematic diagram of the partition coefficient of product (mAb) and impurities (incl. examples) in different chromatographic modes during loading. Selectivity is highest for affinity chromatography. Ternary separations can be carried out only in bind-elute mode. Weak partitioning and flow-through chromatography work under conditions with little to no retention of the product of interest. Red corresponds to the product and blue (green) to impurities binding less (more) strongly to the stationary phase than the target

Bind-Elute Chromatography

For mAb polishing, at least one bind-elute chromatographic step is generally applied. The majority of the column length is used to resolve different solutes. Therefore, loadings are small compared to the DBC of the stationary phase. The conditions during elution result in different retention of the impurities and the target protein; however, their adsorptive properties are typically very similar resulting in shallow and long linear gradients [26]. Step elution is usually not sufficient to reach satisfying resolutions. Even on modern resins, baseline separation of aggregates and monomer for instance remain unfeasible. Therefore, there is a strong trade-off between either high yields sacrificing purity or high purity at the expense of yield [27].

Flow-Through, Weak Partitioning and Frontal Chromatography

Similar to saturation adsorption, the DBC of the stationary phase is fully utilized in flow-through processes; however, impurities are retained while the target protein remains in the liquid phase. As the product is obtained directly from the feed, which has constant composition, the process can be regarded as isocratic [28]. This allows for very high "loadings" (better: throughput) of the target compound on the stationary phase. A wash step is applied to increase the yield by removing the remaining purified feed from

the void volume of the stationary phase. As the wash buffer does not contain impurities, the equilibrium is shifted toward impurity desorption during this step. For membranes as stationary phases, where diffusion is not rate determining, this is of less importance as practically all mAb containing fluid is flushed out within 1–2 membrane volumes [29]. However, in case of porous resin-based materials, diffusion controls the process requiring longer washing and therefore resulting in increased desorption of bound impurities. Hence, a wash buffer promoting stronger binding conditions than found in the feed is advisable. A separate elution step to obtain the product is not required. Weak partitioning chromatography works similarly to flow-through operation, however the feed pH is adjusted around the target's pI such that the mAb monomer adsorbs only slightly, while aggregates are retained more strongly and can be reduced significantly [28]. As it is typically operated in AEX mode, DNA and acidic HCPs are also removed as in classical flow-through operation.

Frontal chromatography is at the interface between bind-elute and flow-through mode. Both impurities and the product of interest bind to the stationary phase; however, the latter does so only weakly allowing it to be displaced by stronger binding impurities. Therefore, with increasing load on the column, less and less target product is adsorbed on the stationary phase. This allows reaching high yields at increased loadings and productivity. It also results in the possibility to fully utilize the DBC of the stationary phase for impurity adsorption. Due to the partial adsorption of target product, the conditions of the wash step have to be carefully balanced between target desorption and impurity retention in order to further increase the yield without contaminating the product pool.

Continuous Chromatography

Continuous or correctly counter-current chromatography has been developed to overcome limitations encountered in batch operations. As the stationary phase cannot be moved easily against the liquid flow, counter-current processes rely on periodic valve switching changing the position of each column relative to the applied liquid phases [22]. For saturation adsorption, counter-current loading processes were developed (e.g., *n*-column periodic counter-current chromatography (*n*C-PCC), CaptureSMB) to overcome the productivity-capacity utilization trade-off, while simulated moving bed (SMB) and the multi-column counter-current solvent gradient purification (MCSGP) processes were invented to alleviate the purity-yield trade-off encountered in bind-elute chromatography. The reader is referred to the literature for a detailed introduction to the processes [22, 30, 31] and the experimental design [23–25].

1.2.2 Affinity Chromatography

The gold standard in mAb affinity capture is protein A affinity chromatography which is based on the interaction of protein A, immobilized on the stationary phase, with the Fc region of the mAb molecule. The binding of protein A is not equally strong for all immunoglobulins and, in the case of IgG, not equal for all isotypes. An indication about the expected binding strength can be found in [32]. A generally stronger binding to the Fc region is observed by protein G. In particular, protein G is able to bind to IgG3, while protein A is not. Higher binding strength however does not automatically result in higher binding capacities. Also the presence of impurities may influence the binding capacity. In both, protein A and protein G affinity chromatography, the elution is carried out using a low pH buffer. Generally in protein G chromatography, a stronger eluent is required to recover captured antibody from the stationary phase. Thus, protein A chromatography is preferred over protein G chromatography since lower aggregate levels are generally obtained with the former one, resulting in an almost exclusive use of protein A chromatography for antibody capture from cell culture supernatant.

For mAb fragments without an Fc region other affinity-based stationary phases are used. This has not been available until the last few years. Therefore, these stationary phases have been developed only for a relatively short period compared to protein A stationary phases which have been developed for decades. The available κ or λ affinity stationary phase display lower capacities and less chemical resistance compared to protein A/G stationary phases. For instance, for κ-light chain antibody fragments, protein L chromatography is a valid alternative [33].

In order to prepare the harvest for affinity capture, the cells are removed (e.g., by centrifugation) and the supernatant is filtered. Afterward, the clarified supernatant is loaded onto the equilibrated column. After the loading, the column is typically washed with the equilibration buffer. Additional washes, such as a high salt wash or other washes with low concentrations of organic solvents or denaturants, may be included in order to remove impurities that have adsorbed on the stationary phase or the antibody [19]. The elution of the captured antibody is typically done using a step gradient elution with a low pH buffer. The eluate is neutralized either right away or after a hold time (virus inactivation in industrial production). After the antibody elution the column is cleaned. Modern, polymer-based protein A affinity materials may be cleaned routinely with 0.1 M NaOH and may be sanitized using up to 1 M NaOH without a major loss of capacity allowing for running them over hundreds of cycles. Other affinity materials are often not as stable to alkaline treatment. After cleaning, the column is re-equilibrated for the next run or storage.

1.2.3 Ion-Exchange Chromatography

Due to their high pI, mAbs are mostly purified in bind-elute mode using cation-exchange chromatography and in flow-through mode using anion-exchange chromatography. IEX stationary phases are functionalized with either weak or strong acids (CEX) or bases (AEX). The strong forms are fully deprotonated (CEX) or protonated (AEX) at the pH values relevant for the purification of mAbs (ca. pH 4.0–8.5). Most common ligands of strong CEX and AEX materials are sulfonate (denoted S or SO3) and quaternary ammonium (Q) ligands. Weak CEX and AEX stationary phases have pK_A values close to or within the pH range relevant for the purification of mAbs. The most common ligands are carboxylic acids (COO) for CEX and tertiary amines (DEAE, DMAE) for AEX materials. This means that the resins have buffering capacities themselves which lead to (possibly undesired) pH effects upon the change of the ionic strength [34]. With increasing awareness of this sensitivity and the demand for robust processes, the use of weak IEX stationary phases is declining in new process developments.

Cation-Exchange Chromatography

In industrial mAb purification processes, CEX in bind-elute mode (CEX-BE) is very commonly used as second purification step following protein A affinity capture. This combination makes use of the fact that the protein A eluate typically has a low pH, providing conditions that allow for binding of the mAb on the CEX stationary phase. For mAb elution from CEX linear or step gradients are used, typically using salt as a modifier. The buffer systems are dependent on the pH range in which the CEX step is operated. For instance, acetate buffers are used in a range of pH 4.5–5.5 while phosphate buffers are suitable in a range of pH 6.5–7.5. Binding capacities of modern CEX typically exceed 100 mg/mL. However, loadings usually do not exceed 50 g/L as the stationary phase is required to resolve the different solutes during gradient elution. In mAb processing, aggregates and fragments as well as HCPs are typically targeted by the CEX step.

Anion-Exchange Chromatography

The final polishing step in industrial applications is usually an anion-exchange chromatography process operated in flow-through mode (AEX-FT). Conductivity and pH of the solution are the key process parameters for this step defining differential retention of product and impurities. To allow the positively charged antibody to remain in the liquid phase while negatively charged impurities adsorb on the stationary phase, the pH is kept below the mAb's pI. As the pI of DNA and protein A is below typical values of the working pH they are removed in this final processing step. Furthermore, HCP subpopulations can also have a low pI resulting in further HCP reduction.

1.2.4 Size-Exclusion Chromatography

Monoclonal antibodies are large molecules with typically around 150 kDa molecular weight, which suggests separation from small molecular weight impurities by size-exclusion chromatography (SEC). However, SEC processes generally have a low productivity since SEC is not adsorption-based and only a small amount of sample can be loaded. Typically, the feed volume is <4% of the packed bed column volume. Due to its low productivities, SEC is not attractive for large scale processing of mAbs or fragments and was rendered obsolete by the combination of protein A affinity and CEX chromatography. However, it is useful for purification and characterization of proteins in product development where productivity and scalability are not of key importance. In the form of small-scale desalting cartridges (1–5 mL), it is a useful tool for rapid desalting and buffer exchange of mAb samples. Since SEC is not adsorption-based and runs with standard buffers it requires only minimal process development. For mAb purification, it can be used for instance to obtain separate aggregate and monomer pools from protein A eluate [35]. SEC is also used as standard HPLC analytics to determine the aggregate content of mAb samples. Molecules of smaller molecular weight than the mAb are typically resolved worse.

1.2.5 Hydrophobic Interaction Chromatography

In contrast to other adsorption-based chromatography methods, hydrophobic interaction chromatography (HIC) is entropically driven, separating proteins according to their hydrophobicity. In mAb purification, the main purpose for using HIC is the removal of aggregates which are generally more hydrophobic than the monomeric proteins. Adsorption takes place at high salt concentrations (typically 1–1.5 M ammonium sulfate), and low salt concentrations are used for desorption. The high salt concentrations raise the question of waste disposal, which has made HIC unpopular for the purification of mAbs in bind-elute mode, particularly since powerful alternatives, such as multimodal chromatography, have become available.

1.2.6 Multimodal Chromatography

Multimodal chromatography (MMC) is increasingly used for the polishing of mAbs. It typically combines ion-exchange and HIC functionalities with additional hydrogen bonding groups. The purpose of MMC is the removal of residual impurities like HCP, DNA, and aggregates, preferably in flow-through mode. Furthermore, MMC resins usually retain their binding capacities also at high ionic strengths increasing the possible operating ranges with respect to regular IEX. Therefore, they are also often referred to as salt-tolerant. To obtain the best performance, both pH and ionic strength have to be optimized. Being based on polymeric backbones and synthetic ligands, the resins have high chemical resistance also toward cleaning with caustic soda.

1.3 Column Types

Besides the choice of mode of chromatography, also the type of column is important. There are three groups of column types frequently used: packed particles, monoliths, and membranes. The latter two show convective behavior while mass transfer in particles is dominated by pore diffusion or convection depending on the pore size.

For analytical columns usually non-porous particles are used as low capacities are sufficient and mass transfer limitation is smaller with respect to porous particles leading to higher resolution. For preparative chromatography, porous particles are used as the binding capacity is dependent on the surface of the particle. In order to exploit the full capacity, the pore size should be large enough to allow the target protein to diffuse into them. Therefore, the pore size for antibodies should be in the range of 40 nm [36]. Additionally, this results in diffusion limitation in such chromatographic media. To lower diffusion limitation, perfusive materials can be used. In this case, there are two types of pores, small ones to increase the surface area and large ones for convective flow through the particle. The last group of particles have only large pores allowing convective flow, but with a lower surface area. Another important factor is the particle size. Small particles increase the surface area and the resolution of the chromatography. On the other hand, the pressure drop over the column increases the smaller the particles are. Therefore, the particles for preparative chromatography are usually in the size range of 50–100 μm, but if very high resolution is necessary, a smaller particle size can be chosen, at the cost of the pressure drop over the column. In analytical chromatography, the higher backpressure is accepted for the higher resolution. The particle sizes usually used are in the range of 2–20 μm.

Membranes are typically used for flow-through and frontal chromatography, although bind-elute is possible. This is due to the fact that number of theoretical plates and binding capacities are low compared to particle chromatography but they offer a very low pressure drop and therefore enable large flow rates and short process steps. The large pores in the membrane allow for convective flow through it and the rate determining step is not diffusion dependent in this case.

The monoliths have similar properties as membranes: a low pressure drop at high flow rates but a lower capacity. This is due to the large pores in the range of 1–5 μm allowing convective flow inside the monolith. However, scaling of monolith preparation currently limits their application to analytics and sample preparation.

2 Materials

2.1 Columns and Resins

Tables 1 and 2 show an overview of analytical and preparative chromatographic stationary phases suitable for the characterization and purification of monoclonal antibodies. In the analytical case the typical amount of antibody injected is in the order of magnitude of 10–100 μg per mL of packed bed volume while in preparative chromatography the load is typically in the range of 10–100 mg per mL of packed bed volume. The analytical materials presented refer to prepacked columns while for the preparative materials the names of the bulk materials are provided. However, also for the bulk materials, pre-packed columns of various sizes are available from the manufacturer or third-parties. Most generally for production of small amounts of antibodies (milligram to gram range), 0.5–1.0 cm inner diameter columns with 10–15 cm length are sufficient.

2.2 Equipment

It is possible to carry out protein A chromatography using disposable or multi-use cartridges that can be supplied with buffers and feed using a syringe. This procedure is very simple but offers no control of important process parameters, such as the load and the flow velocity and a chromatogram may not be recorded. For reproducible results and proper process development, it is recommended to use an HPLC or a preparative device. Suppliers of HPLC equipment are, for example, Agilent, Waters and Thermo Scientific. Preparative equipment is provided for example by GE Healthcare (ÄKTA series). A preparative system allowing also the exploitation of the advantages of continuous counter-current chromatography is provided by ChromaCon (Contichrom series). All systems feature accurate pumps, a feed supply system (HPLC: autosampler; preparative systems: sample pump), and a monitoring system (HPLC: UV; prep systems: UV, pH, conductivity).

A variety of technical solutions exist to speed up process development. A preliminary stationary phase and buffer screening can be carried out in a 96-well plate format. Equipment for parallelization of single-column batch chromatography is available as well.

2.3 Protein A Affinity Chromatography

2.3.1 Buffers for Protein A Chromatography

The buffer recipes for the method are reported in Table 3. Equilibration buffer is 20 mM sodium phosphate, 150 mM NaCl, pH 7.5, the wash buffer is 20 mM sodium phosphate, 1 M NaCl, pH 7.5, and the elution buffer is 50 mM citrate, pH 3.0. Alternative elution buffers include 50 mM glycine or 50 mM acetate. The pH is adjusted using HCl or NaOH (1 M). Cleaning-in-place (CIP) is carried out with 0.1 M NaOH.

Table 1
Columns for mAb and mAb fragment analysis

Chromatography type	Resin name	Supplier	Mean particle diameter [μm]	Column size (i.D. × L) [mm]
Protein A	Poros A20	Applied Biosystems	20	2.1 × 30
Protein A	Chromolith WP 300 Protein A	Merck KGaA	n/a	4.6 × 25
CIEX (weak)	Propac WCX-10	Thermo Scientific	10	4 × 250
CIEX (strong)	TSKgel SP-STAT	Tosoh	7	4.6 × 100
CIEX (strong)	BioPro SP-F	YMC	5	4.6 × 30
AIEX (strong)	Propax SAX-10	Thermo Scientific	10	4 × 250
AIEX (strong)	BioPro QA-F	YMC	5	4.6 × 30
SEC (<200 kDa)	TSKgel G3000SWxl	Tosoh	5	7.8 × 300
SEC (<200 kDa, also prep.)	Superdex 200 Increase 10/300 GL	GE Healthcare	9	10 × 300
SEC (<75 kDa, also prep.)	Superdex 75 Increase 10/300 GL	GE Healthcare	9	10 × 300
HIC	Propac HIC-10	Thermo Scientific	5	4.6 × 100

Table 2
Stationary phases for preparative purification of mAbs and mAb fragments

Chromatography type	Resin name	Supplier	Mean particle diameter [μm]
Protein A affinity	MabSelect SuRe	GE Healthcare	85
Protein A affinity	Eshmuno A	Merck KGaA	50
Protein A affinity	Amsphere A3	JSR Life Sciences	50
CEX (strong)	Poros 50 HS	Applied Biosystems	50
CEX (strong)	Eshmuno CPX	Merck KGaA	50
CEX (strong)	BioPro SmartSep S10	YMC	10
AEX (strong)	Eshmuno Q	Merck KGaA	85
AEX (strong)	Sartobind Q (Membrane)	Sartorius Stedim	n/a
HIC	Toyopearl Phenyl-650M	Tosoh	65

Table 3
Buffers for protein A chromatography method

Substance [g]	Buffer A (Equilibration)	Buffer B (Wash)	Buffer C (Elution)	Buffer D (CIP)
Composition	20 mM phosphate, 150 mM NaCl, pH 7.5	20 mM phosphate, 1 M NaCl, pH 7.5	50 mM citric acid, pH 3.0	0.1 M NaOH
NaH_2PO_4	0.39	0.36		
Na_2HPO_4	2.37	2.41		
NaCl	8.77	58.44		
Citric acid monohydrate			10.51	
NaOH (solid)				4.0
DI water	1000	1000	1000	1000
Adjust pH to	7.5	7.5	3.0	n/a
Typ. cond. [mS/cm]	18	82	2	n/a

2.3.2 Feed Preparation for Protein A Chromatography

In order to prevent the chromatography column from being fouled it is important to remove cells, cell debris, and other insoluble components from the starting material. A strongly recommended first step is centrifugation. A second required step is filtration (*see* **Note 2**).

2.3.3 Stationary Phases for Protein A Chromatography

The method was tested with MabSelect Sure (GE Healthcare), Eshmuno A (Merck KGaA), and Amsphere A3 (JSR Life Sciences), but it is expected to work for all preparative and analytical protein A stationary phases including cartridges. However, before using the method with other stationary phases, make sure that they are compatible with 0.1 M NaOH as cleaning agent and choose alternative cleaning agents if required.

2.4 Cation-Exchange Chromatography (CEX-BE)

2.4.1 Buffers for CEX-BE

The buffer recipes for the method are reported in Table 4. Equilibration buffer is 25 mM sodium phosphate, pH 6.0 and elution buffer is 25 mM sodium phosphate, 0.5 M NaCl, pH 6.0. The strip buffer is 25 mM sodium phosphate, 1 M NaCl, pH 6.0 and the CIP buffer is 1 M NaOH. The pH is adjusted using HCl or NaOH (1 M).

2.4.2 Feed Preparation for CEX-BE

As a rule of thumb, in order to provide sufficient binding of the mAb on the CEX stationary phase, the pH should be at least 1 unit below the pI of the mAb and the conductivity should be below 5 mS/cm. In order to reduce the ionic strength, the feed may be

Table 4
Buffers for preparative CEX (buffers A-D) and AEX (A, C, D) chromatography methods

Substance [g]	Buffer A (Equilibration)	Buffer B (Elution)	Buffer C (Strip)	Buffer D (CIP)
Composition	25 mM phosphate, pH 6.0	25 mM phosphate, 0.5 M NaCl, pH 6.0	25 mM phosphate, 1 M NaCl, pH 6.0	1 M NaOH
NaH_2PO_4	2.72	2.52	2.54	
Na_2HPO_4	0.33	0.56	0.54	
NaCl		29.22	58.44	
NaOH (solid)				40.0
DI water	1000	1000	1000	1000
Adjust pH to	6.0	6.0	6.0	n/a
Typ. cond. [mS/cm]	2	46	82	n/a

diluted with water, diafiltered against a suitable buffer or desalted using a desalting column (small scale only). An advantage of diafiltration is the possibility to concentrate the feed in order to shorten the loading phase.

2.4.3 Stationary Phases for CEX-BE

The method described here was tested for multiple resins reported in Table 2. However, before using the method with other stationary phases, make sure that they are compatible with 1 M NaOH as cleaning agent.

2.5 Anion-Exchange Chromatography (AEX-FT)

2.5.1 Buffers for AEX-FT

Buffers for AEX depend on the feed conditions. As equilibration and wash buffer, the background composition of the feed is advised (buffer system, pH, conductivity). Similarly, the strip buffer should have the same pH as the feed solution with additional NaCl (1 M). For CIP, 1 M NaOH can be used. As a starting point, buffer A (equilibration/wash) and C (strip) of the CEX method are advised (Table 4).

2.5.2 Feed Preparation for AEX-FT

Feed pH and conductivity define the achievable impurity reduction in AEX-FT. Hence, the pH should generally be at least one unit below the pI of the mAb, and conductivity should not exceed 5 mS/cm. To achieve the target conditions, dilution towards or diafiltration against the desired buffer composition (e.g., buffer A in Table 4) are the methods of choice.

2.5.3 Stationary Phases for AEX-FT

Various stationary phases are available from different suppliers. Due to the low theoretical plate number required in this kind of separation, membranes are well suited for the process. Furthermore, they

do not exhibit mass transfer limitations allowing for fast loading and short wash steps. When using a certain stationary phase, make sure that it is compatible with 1 M NaOH as a cleaning agent.

2.6 Size-Exclusion Chromatography

2.6.1 Buffer for SEC

Size-exclusion chromatography is run isocratic. As a low ionic strength is not relevant, the suggested buffer is 50 mM sodium phosphate, 300 mM NaCl, pH 7.0. The increased salt content also assists in reducing possible interactions of the solute with the stationary phase.

2.6.2 Feed Preparation for SEC

Loading in SEC is limited by the injected volume and should not exceed 4% of the packed bed column volume. For preparative runs, throughput can be increased by using a concentrated feed, which can be obtained by ultra−/diafiltration. Furthermore, the feed should be free of insoluble matter in order to prevent column or pore blocking increasing the column lifetime.

2.6.3 Stationary Phases for SEC

Agarose and silica-based SEC columns are available for mAb analytics and small-scale purification. SEC columns packed with silica-based, small, rigid particles can be operated at higher flow rates and backpressures than columns packed with softer agarose-based material. On the other hand, agarose-based stationary phases can be cleaned with caustic soda while silica-based materials are degraded when treated with caustic and should generally not be operated at pH 8.0 or above. Thus, if silica-based columns are used, it is recommended to use a guard column for protection.

3 Methods

3.1 Protein A Affinity Chromatography

The following protocol describes a generic protein A affinity chromatography capture method for mAbs of IgG subclasses 1, 2 and 4. The method is intended to provide a starting point and has not been optimized.

1. The step duration is given in column volumes (CV), which refers to the total packed bed column volume. As an example, a column of 0.5 cm i.D. and 10 cm length has a column volume of 1 CV = 2 mL.
2. The linear flow velocity u is defined as the ratio of volumetric flow rate Q and the column cross sectional area A ($u = Q/A$). Thus for the above-mentioned column, if Q is 1 mL/min, we obtain $u = 1/0.2$ cm/min = 5 cm/min = 300 cm/h. The reported protein A capture method should be carried out at $u = 300$ cm/h.

3. The method comprises the following steps.

Equilibration	5 CV	100% buffer A	UV auto-zero afterward
Loading		100% feed	Amount depends on target loading
Wash 1	5 CV	100% buffer A	
Wash 2	5 CV	100% buffer B	Reduces HCP content
Wash 3	10 CV	100% buffer A	Reduces cond. at start of elution
Elution	5 CV	100% buffer C	Collect as pool or in fractions
CIP	15 min	100% buffer D	Time-based, flow rate can be halved
Re-equilibration 1	5 CV	100% buffer B	Reduces pH faster
Re-equilibration 2	5 CV	100% buffer A	

4. The feed volume depends on the antibody concentration and the capacity of the stationary phase. The latter is dependent on the feed composition (impurity content) and on the loading flow velocity. For cell culture supernatants with low impurity content, loads of 30–40 mg mAb per mL of column volume can be obtained at a loading flow velocity of 300 cm/h (dynamic binding capacity).
5. Testing a loading capacity of X mg/mL, the amount of column volumes of feed (CV_{feed}) that can be loaded are calculated by $CV_{\text{feed}} = X/c_{\text{feed}}$. Thus in the case of a loading capacity of 30 mg/mL and a feed concentration of $c_{\text{feed}} = 3$ g/L, the load volume is $CV_{\text{feed}} = 10$ CV of feed.
6. After an optional hold at low pH (virus inactivation), the protein A eluate is neutralized in order to avoid formation of aggregates. For neutralization, a strong basic buffer should be used (e.g., 1 M Tris, pH 8.0). After neutralization and sterile filtration, the product is usually stable for days to weeks when stored at 4–8 °C.
7. The column is stored according to the manufacturer's instructions for the stationary phase. Most manufacturers recommend storage in 20% Ethanol at 4–8 °C.

A representative chromatogram from a direct capture of mAb from clarified cell culture supernatant is shown in Fig. 2. *See* **Note 3** for further information on protein A gradient selection and neutralization conditions and Note 4 for antibody storage conditions.

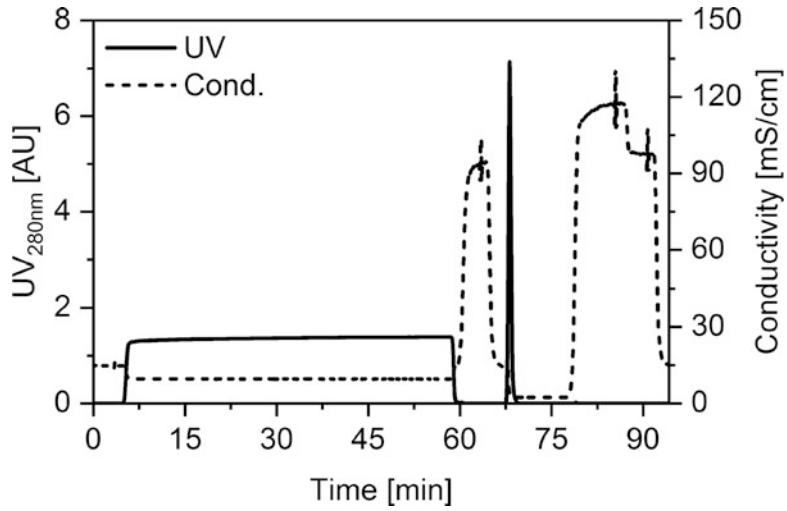

Fig. 2 Chromatogram obtained using a slightly modified version of the preparative protein A affinity method described in this chapter to capture mAb from clarified cell culture supernatant. The stationary phase was MabSelect SuRe prepacked into a column of i.D. 0.5 cm and length 5 cm. The UV signal during the loading step (5–60 min) is due to impurities in the flow-through. The mAb is eluted at about 68 min

3.2 CEX Chromatography (CEX-BE)

The following protocol describes a bind-elute cation-exchange method for purification of mAbs with a pI of 8 or higher. For antibodies with lower pI values (6.5–8), acetate buffers, pH 5.0 (same molarity) may be used.

1. The method uses a linear gradient, which may be used for both analytical and preparative purposes.
2. The step duration is given in column volumes (CV). Refer to the protein A method in Subheading 3.1 for the calculation of the linear flow rate. The reported method should be carried out at $u = 300$ cm/h.
3. The method comprises the following steps.

Equilibration	5 CV	100% buffer A	UV auto-zero afterward
Loading		100% feed	Amount depends on target loading
Wash	5 CV	100% buffer A	
Linear gradient	20 CV	0–100% buffer B	Elution, at least 20 fractions
Strip	5 CV	100% buffer C	Removes strongly bound species
CIP	5 CV	100% buffer D	Cleaning
Re-equilibration 1	5 CV	100% buffer C	Reduces pH faster
Re-equilibration 2	5 CV	100% buffer A	

4. As with protein A affinity chromatography, the feed volume is dependent on the antibody concentration and the capacity of the stationary phase. The latter depends on the feed composition (impurity content) and on the loading flow velocity. Furthermore it is dependent on the pH and the ionic strength of the feed (*see* Subheading 2.4.2).
5. If the mAb is directly captured from clarified cell culture supernatant in a preparative run, generally the ionic strength and the pH need to be adjusted. Cell culture harvest typically has a conductivity of 10–20 mS/cm and a pH value of 7.0–7.5. To achieve reasonable loads of 20–50 mg/mL up to four-fold dilution with deionized water and pH-adjustment to pH < 6.5 may be required. When adjusting the conditions, harvest components may precipitate requiring an additional filtration before loading onto the column. In the worst case, the mAb precipitates and other loading conditions need to be found.
6. It is recommended to use 20 mg/mL as a starting value for the preparative load. If successful, the load may be increased in the following runs. In the case of properly adjusted load conditions in terms of ionic strength and pH (e.g., protein A eluate), loads can exceed 100 mg/mL.
7. In cases where a high product concentration is more important than the product purity, a step gradient (100% B) should be used instead of the linear gradient indicated above. This case has been reported for the purification of λ light chain fragment purification, where the high product concentration was important to increase the output of a subsequent SEC step [37].
8. Typically, the CEX eluate is stable for a couple of days to weeks at sterile conditions if stored at 4–8 °C (*see* **Note 4**).
9. The column is stored according to the manufacturer's instructions for the stationary phase. Most manufacturers recommend storage in 20% Ethanol at 4–8 °C.

3.3 AEX Chromatography (AEX-FT)

1. The following method describes a flow-through anion-exchange method for purification of mAbs with a pI of 8 or higher. For antibodies with lower pI (6.5–8), acetate or citrate buffers, pH 5.0 (same molarity) may be used.
2. The step duration is given in column volumes (CV), but applies equally to membrane volumes (MV). Refer to the protein A method in Subheading 3.1 for the calculation of the linear flow rate. The reported method should be carried out at $u = 300$ cm/h (columns) or $Q = 5$ MV/min (membranes). For membranes, the impact of the flow rate on the onset and shape of the breakthrough is negligible and may therefore be changed freely within the manufacturer's specifications.

3. The method comprises the following steps.

Equilibration	5 CV	100% buffer A	UV auto-zero afterward
Loading		100% feed	Collect as pool or in fractions
Wash	5 CV	100% buffer A	Collect separately
Strip	5 CV	100% buffer C	Removes strongly bound species
CIP	5 CV	100% buffer D	Cleaning
Re-equilibration 1	5 CV	100% buffer C	Reduces pH faster
Re-equilibration 2	5 CV	100% buffer A	

4. As the stationary phase is exclusively used to bind impurities, the feed volume depends on the impurity levels and the capacity of the stationary phase. The latter is in principle dependent on the selected feed pH and conductivity and in the case of columns also on the loading flow rate. For instance, the DNA capacity of the Sartobind Q membrane with 15 layers was shown to be constant at around 8 g/L for pH 4–9 and conductivities below 40 mS/cm [29], which can be attributed to the very low pI of DNA resulting in strong binding even at elevated ionic strength. This behavior was not found for membranes with less layers, and furthermore cannot be expected for HCPs and viruses. Therefore, a fractionated breakthrough (overloading of the stationary phase) curve is suggested to determine a loading that results in sufficient impurity clearance. Typical loadings are in the range of 100–1000 mg/mL stationary phase.
5. The wash step is used to replace the liquid phase in the void volume of the stationary phase thereby increasing the yield. As the replacing buffer will shift the equilibrium toward impurity desorption, it is advised to collect the wash step as a separate fraction not to contaminate the purified product from the loading step.
6. In contrast to the protein A and CEX methods, there is no elution step in this method because the target protein remains in the liquid phase.
7. As for Protein A and CEX chromatography, the product is stable for a couple of days to weeks at sterile conditions if stored at 4–8 °C (*see* **Note 4**).

3.4 SEC for mAb and mAb Fragment Purification

The following method describes a size-exclusion method for the purification of mAbs or mAb fragments.

1. If adsorption of solutes does not occur, resolution on a given stationary phase will only depend on the flow rate, with smaller

values resulting in higher resolution. Typically, linear velocities are below 150 cm/h. For suitable flow rates, please refer to the manufacturer's specifications.

2. The method comprises the following steps

Start-up (only once)	3 CV	Buffer SEC	Slowly ramp up flow rate
Load	≤0.04 CV	Feed	
Elution	2 CV	Buffer SEC	Fractionate

3. Load should not exceed 4% of the column volume in order to achieve a good resolution.
4. The duration of the elution may be shortened toward the end of the last eluting solute.
5. Aggregates and high molecular weight impurities elute before the mAb monomer peak while low molecular weight impurities elute later, often as tail.
6. For the case of mAb fragment purification, affinity chromatography is not as well established and SEC can prove useful, too. Separation of a λ light chain fragment by SEC has been reported in [37].

3.5 Analytics for mAbs and mAb Fragments

The following section very briefly describes the analytics that can be used to test the produced mAb and mAb fragment samples for aggregates, charge isoforms, HCP, leached protein A and DNA, respectively.

3.5.1 Analytical Protein A Chromatography

1. Analytical protein A chromatography is useful for the quantification of mAb in product pools and other fractions.
2. Essentially the same buffers as described in Table 3 can be used.
3. A simplified method comprises the following steps.

Injection		
Wash	5 CV	100% buffer A
Elution	5 CV	100% buffer C
Re-equilibration	10 CV	100% buffer A

4. The method does not include a cleaning step since less and purer sample is loaded onto the column compared to preparative protein A chromatography. However, regular column cleaning is recommended according to the manufacturer's instructions.
5. Detection is done at 280 nm.

6. The detection limit is typically at 5 μg of loaded mAb, corresponding to a concentration 0.05 mg/mL for a 100 μL injection. Try the method first with a load of 10–20 μg.
7. In any case, blank runs should be performed and subtracted from the sample runs.
8. For rapid analytics, the linear flow rate should be maximized, however, remaining within the pressure limits of the column and the equipment. For instance, for the Chromolith WP 300 Protein A column (4.6 × 25 mm, Merck KGaA) a flow rate of 2 mL/min is well suited, which corresponds to a linear flow rate of 720 cm/h.
9. Manufacturers typically provide protocols with their analytical columns, which should be used instead of the generic method above.

3.5.2 Analytical CEX Chromatography

1. Analytical CEX chromatography is useful for the quantification of charge isoforms. It can also be used to determine aggregate and fragment content.
2. Buffers should be replaced by the ones listed in Table 5.
3. Please refer to the description of the preparative CEX method in Subheading 3.2 which is applicable also for analytical purposes.
4. The feed step in the method reported above is replaced by a single injection. Try the method first with an injection of

Table 5
Buffers for SEC chromatography and CEX analytical methods

Substance [g]	Buffer SEC	Buffer CEX A (Equilibration)	Buffer CEX B (Elution)	Buffer CEX C (Strip)
Composition	50 mM sodium phosphate, 300 mM NaCl pH 7.0	20 mM MES, pH 5.5	20 mM MES, 200 mM NaCl, pH 5.5	20 mM MES, 1 M NaCl, pH 5.5
NaH_2PO_4 anh.	1.80			
Na_2HPO_4 anh.	4.97			
MES		3.91	3.91	3.91
NaCl	17.53		11.69	58.44
DI water	1000	1000	1000	1000
Adjust pH to	7.0	5.5	5.5	5.5
Typ. cond. [mS/cm]	32	0.5	20	82

20–40 μg. Typically samples do not need to be adjusted in terms of pH and conductivity.

5. The CIP step can be omitted as less and purer samples are loaded onto the column. However, regular column cleaning is recommended according to the manufacturer's instructions.
6. Detection is done at 280 nm. In case of low injection amounts, detection at 220 nm might also be used.
7. Blank runs should be performed and subtracted from the sample runs.
8. Resolution can be increased by lower flow rates and shallower gradients, both resulting in longer analysis times.

3.5.3 Analytical SEC

1. Analytical SEC chromatography is useful for the quantification of monomers, dimers, and higher order aggregates. Fragments are generally less well resolved and elute as tail of the monomer peak (Fig. 3).
2. The method described in Subheading 3.4 can be used also for analytical purposes.
3. The feed step in the method reported above is replaced by a single injection.
4. Detection is done at 280 nm. In case of low injection amounts, detection at 220 nm might also be used.

3.5.4 HCP-ELISA, Leached Protein A, and DNA-Assay

1. HCP content is quantified using specialized ELISA kits. Suppliers such as Cygnus Technologies cover a broad spectrum of cell lines.

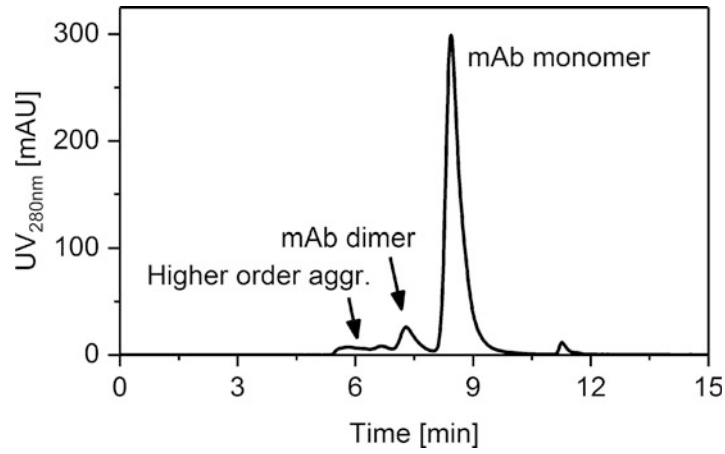

Fig. 3 Size-exclusion chromatogram (TSKgel G3000SWxl) of a protein A eluate of a monoclonal antibody showing high aggregate content

2. Leached protein A is also quantified using specialized ELISAs. Cygnus Technologies supplies kits for quantifying protein A ligands of various manufacturers.
3. DNA quantification is carried out easily using prefabricated, generic kits such as Quant-iT™ dsDNA assay kit (Invitrogen).
4. For all kits, a 96-well plate reader is required for recording the results.

4 Notes

1. *Which purification for which purpose?* Obviously, depending on the purpose of the mAb material produced, different purity requirements persist. The purity specifications for HCP contents are typically <10 ppm for the final product while cell culture supernatants frequently contain 100,000 ppm HCP or more. Figure 4 shows a schematic of a generic downstream process as applied in the industry with the roughly estimated impurity concentrations after each chromatography step. Protein A affinity chromatography generally reduces HCP content by 100–10,000 fold (2–4 logs). For purposes of antibody

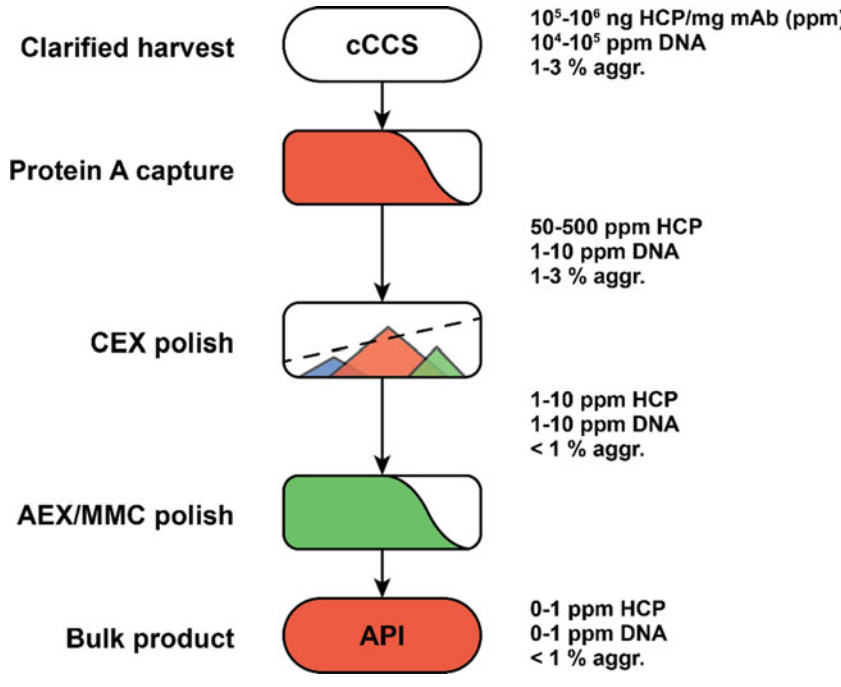

Fig. 4 Chromatographic steps of a generic industrial mAb downstream process. The typical processing mode is schematically shown using the same color code as in Fig. 1. The roughly estimated impurity concentrations after each step are reported on the *right hand side*

characterization (analytical chromatography, SDS page, IEF, MS) this level of purity is generally sufficient. Also if only mg amounts of antibody are available (< 100 mg), purification development cannot be carried out much beyond the capture step. A feasibility study of a downstream process using small-scale columns (1–2 mL column volume) as shown in Fig. 4 requires at least 1 g of mAb. This does not include any scale up or process optimization.

2. *Supernatant filtration*. In order to prevent the chromatography column from being fouled it is important to remove cells, cell debris, and other insoluble components from the starting material. A recommended first step is centrifugation. A second required step is filtration. Depending on the amounts of starting solution to be filtered and the concentration of insoluble components, syringe filters (mL range), disc filters (mL-L range), depth filters (L range), or ultrafiltration (L range) may be used. The filter pore size should be 0.2–0.45 μm. For fast processing in the L range it is recommended to use a peristaltic pump.
3. *Protein A affinity chromatography.*
   (a) Use a linear gradient instead of step gradient if excessive aggregation is observed (> 5% aggregates). The eluate will be less concentrated but the elution conditions are much gentler.
   (b) For most cases in antibody processing, virus inactivation is not relevant and the neutralization buffer may be readily added into the fraction collection containers. However, in the industry, virus clearance is of critical importance in the development of purification processes for drug candidates.
   (c) It is recommended to neutralize the eluate in such way that it can be loaded onto the first polishing step without further treatment. For instance, if the first polishing step is a cation-exchange step, it is recommended to raise the eluate pH to 5–6.
   (d) Protein A eluate neutralization with 1 M or 0.1 M NaOH may lead to irreversible aggregate formation due very high pH values that occur locally at the point of addition of the base in the eluate vessel. For 1 M Tris, pH 8.0 required neutralization buffer volume is typically in the range of 100–200 μL buffer per mL of protein A eluate.
4. *Storage of mAb solutions.* Most antibody solutions are stable for a couple of weeks when kept in the fridge at 4–8 °C in buffers at pH 6.0 with 0.25 mg/mL sodium azide as preservative. Sodium azide can be omitted if sterile filtration (≤0.2 μm) is possible in a sterile environment. Most antibodies are also

freeze-thaw stable but freeze-thawing should not be exaggerated (<3 times) in order to minimize the formation of irreversible aggregates.

Acknowledgments

This work has been supported by the KTI (CTI)-Program of the Swiss Economic Ministry (Project 19190.2 PFIW-IW). The authors declare that they have no conflicts of interest pertaining to the contents of this article.

References

1. Köhler G, Milstein C (1975) Continuous cultures of fused cells secreting antibody of predefined specificity. Nature 256:495–497. https://doi.org/10.1038/256495a0
2. Liu HF, Ma J, Winter C, Bayer R (2010) Recovery and purification process development for monoclonal antibody production. MAbs 2:480–499. https://doi.org/10.4161/mabs.2.5.12645
3. Kelley B (2009) Industrialization of mAb production technology: the bioprocessing industry at a crossroads. MAbs 1:443–452. https://doi.org/10.4161/mabs.1.5.9448
4. Birch JR, Racher AJ (2006) Antibody production. Adv Drug Deliv Rev 58:671–685. https://doi.org/10.1016/j.addr.2005.12.006
5. Kelley B (2007) Very large scale monoclonal antibody purification: the case for conventional unit operations. Biotechnol Prog 23:995–1008. https://doi.org/10.1021/bp070117s
6. Low D, O'Leary R, Pujar NS (2007) Future of antibody purification. J Chromatogr B 848:48–63. https://doi.org/10.1016/j.jchromb.2006.10.033
7. Shukla AA, Hubbard B, Tressel T, Guhan S, Low D (2007) Downstream processing of monoclonal antibodies—application of platform approaches. J Chromatogr B 848:28–39. https://doi.org/10.1016/j.jchromb.2006.09.026
8. Walsh G (2005) Biopharmaceuticals: recent approvals and likely directions. Trends Biotechnol 23:553–558. https://doi.org/10.1016/j.tibtech.2005.07.005
9. Shukla AA, Thömmes J (2010) Recent advances in large-scale production of monoclonal antibodies and related proteins. Trends Biotechnol 28:253–261. https://doi.org/10.1016/j.tibtech.2010.02.001
10. Goyon A, Excoffier M, Janin-Bussat M-C, Bobaly B, Fekete S, Guillarme D, Beck A (2017) Determination of isoelectric points and relative charge variants of 23 therapeutic monoclonal antibodies. J Chromatogr B 1065:119–128. https://doi.org/10.1016/j.jchromb.2017.09.033
11. Carta G, Jungbauer A (2010) Downstream processing of biotechnology products. In: Protein chromatography: Process Development and Scale-Up. Wiley-VCH Verlag GmbH & Co. KGaA, Weinheim, pp 1–55
12. Arosio P, Barolo G, Müller-Späth T, Wu H, Morbidelli M (2011) Aggregation stability of a monoclonal antibody during downstream processing. Pharm Res 28:1884–1894. https://doi.org/10.1007/s11095-011-0416-7
13. Imamura H, Honda S (2016) Kinetics of antibody aggregation at neutral pH and ambient temperatures triggered by temporal exposure to acid. J Phys Chem B 120:9581–9589. https://doi.org/10.1021/acs.jpcb.6b05473
14. Harris RJ, Kabakoff B, Macchi FD, Shen FJ, Kwong M, Andya JD, Shire SJ, Bjork N, Totpal K, Chen AB (2001) Identification of multiple sources of charge heterogeneity in a recombinant antibody. J Chromatogr B Biomed Sci Appl 752:233–245. https://doi.org/10.1016/S0378-4347(00)00548-X
15. Walsh G, Jefferis R (2006) Post-translational modifications in the context of therapeutic proteins. Nat Biotechnol 24:1241–1252. https://doi.org/10.1038/nbt1252
16. Jefferis R (2009) Glycosylation as a strategy to improve antibody-based therapeutics. Nat Rev Drug Discov 8:226

17. Müller-Späth T, Krättli M, Aumann L, Ströhlein G, Morbidelli M (2010) Increasing the activity of monoclonal antibody therapeutics by continuous chromatography (MCSGP). Biotechnol Bioeng 107:652–662. https://doi.org/10.1002/bit.22843
18. Choi B-K, Bobrowicz P, Davidson RC, Hamilton SR, Kung DH, Li H, Miele RG, Nett JH, Wildt S, Gerngross TU (2003) Use of combinatorial genetic libraries to humanize N-linked glycosylation in the yeast Pichia pastoris. Proc Natl Acad Sci 100:5022–5027. https://doi.org/10.1073/pnas.0931263100
19. Shukla AA, Hinckley P (2008) Host cell protein clearance during protein a chromatography: development of an improved column wash Step. Biotechnol Prog 24:1115–1121. https://doi.org/10.1002/btpr.50
20. Steinebach F, Ulmer N, Wolf M, Decker L, Schneider V, Wälchli R, Karst D, Souquet J, Morbidelli M (2017) Design and operation of a continuous integrated monoclonal antibody production process. Biotechnol Prog. https://doi.org/10.1002/btpr.2522
21. Stone MC, Borman J, Ferreira G, Robbins PD (2018) Effects of pH, conductivity, host cell protein, and DNA size distribution on DNA clearance in anion exchange chromatography media. Biotechnol Prog 34:141–149. https://doi.org/10.1002/btpr.2556
22. Steinebach F, Müller-Späth T, Morbidelli M (2016) Continuous counter-current chromatography for the capture and polishing steps in biopharmaceuticals production. Biotechnol J 11:1126–1141. https://doi.org/10.1002/biot.201500354
23. Angarita M, Müller-Späth T, Baur D, Lievrouw R, Lissens G, Morbidelli M (2015) Twin-column CaptureSMB: a novel cyclic process for protein A affinity chromatography. J Chromatogr A 1389:85–95. https://doi.org/10.1016/j.chroma.2015.02.046
24. Steinebach F, Ulmer N, Decker L, Aumann L, Morbidelli M (2017) Experimental design of a twin-column countercurrent gradient purification process. J Chromatogr A 1492:19–26. https://doi.org/10.1016/j.chroma.2017.02.049
25. Vogg S, Wolf MKF, Morbidelli M (2018) Continuous and Integrated Expression and Purification of Recombinant Antibodies. In: Hacker D (ed) Recomb. Protein Expr. Mamm. Cells Methods Protoc. Springer, pp 147–178
26. Carta G, Jungbauer A (2010) Gradient elution chromatography. In: Protein chromatography: Process Development and Scale-Up. Wiley-VCH Verlag GmbH & Co. KGaA, Weinheim, pp 277–308
27. Müller-Späth T, Aumann L, Melter L, Ströhlein G, Morbidelli M (2008) Chromatographic separation of three monoclonal antibody variants using multicolumn countercurrent solvent gradient purification (MCSGP). Biotechnol Bioeng 100:1166–1177. https://doi.org/10.1002/bit.21843
28. Kelley BD, Tobler SA, Brown P, Coffman JL, Godavarti R, Iskra T, Switzer M, Vunnum S (2008) Weak partitioning chromatography for anion exchange purification of monoclonal antibodies. Biotechnol Bioeng 101:553–566. https://doi.org/10.1002/bit.21923
29. Knudsen HL, Fahrner RL, Xu Y, Norling LA, Blank GS (2001) Membrane ion-exchange chromatography for process-scale antibody purification. J Chromatogr A 907:145–154. https://doi.org/10.1016/S0021-9673(00)01041-4
30. Subramanian G (2017) Continuous biomanufacturing: innovative technologies and methods, 1st ed. https://doi.org/10.1002/9783527699902
31. Pfister D, Nicoud L, Morbidelli M (2018) Continuous biopharmaceutical processes. Cambridge University Press
32. GE Healthcare (2007) Antibody purification handbook; Table 3.2
33. Nilson BHK, Solomon A, Björck L, Åkerström B (1992) Protein L from Peptostreptococcus magnus binds to the κ light chain variable domain. J Biol Chem 267:2234–2239
34. Pabst TM, Carta G (2007) pH transitions in cation exchange chromatographic columns containing weak acid groups. J Chromatogr A 1142:19–31. https://doi.org/10.1016/j.chroma.2006.08.066
35. Reck JM, Pabst TM, Hunter AK, Carta G (2017) Separation of antibody monomer-dimer mixtures by frontal analysis. J Chromatogr A 1500:96–104. https://doi.org/10.1016/j.chroma.2017.04.014
36. Carta G, Jungbauer A (2010) Adsorption kinetics. In: Protein chromatography: Process Development and Scale-Up. Wiley-VCH Verlag GmbH & Co. KGaA, Weinheim, pp 161–199
37. Arosio P, Owczarz M, Müller-Späth T, Rognoni P, Beeg M, Wu H, Salmona M, Morbidelli M (2012) In vitro aggregation behavior of a non-amyloidogenic λ light chain dimer deriving from U266 multiple myeloma cells. PLoS One 7:1–12. https://doi.org/10.1371/journal.pone.0033372

Chapter 8

One-Tube Multicolor Flow Cytometry Assay (OTMA) for Comprehensive Immunophenotyping of Peripheral Blood

Anna-Jasmina Donaubauer, Paul F. Rühle, Ina Becker, Rainer Fietkau, Udo S. Gaipl, and Benjamin Frey

Abstract

Recent improvements in the flow cytometry technology allow the determination of the general immune status through the development of multicolor immunofluorescence panels. The one-tube multicolor flow cytometry assay (OTMA) that is presented here identifies 20 different, clinically relevant immune cell subsets and three common activation markers. Thereby, a comprehensive immune status that covers all major immune cells is easily obtained.

The assay is suitable for every common three lasers and 10 color flow cytometer and includes the application of 15 different antibodies. Furthermore, the assay requires only 100 μL of EDTA-treated whole-blood and less than 40 min for sample preparation. By being easily adaptable to individual requirements and by additionally determining absolute cell counts, the assay is well-suited for translational research in clinical trials.

Key words Immunophenotyping, Multicolor flow cytometry, Human whole-blood, One-tube measurement, Immune status, Antibody, Gating strategy, Absolute cell count

1 Introduction

Nowadays, the analysis of the immune status in clinical settings is of great interest, such as for prediction and prognosis [1]. Flow cytometry is one of the most adequate technologies for the determination of individual immunological parameters, because it offers the opportunity to measure multiple parameters at once on a single-cell basis. Several of already existing assays focus solely on a fraction of the immune cells such as on T-cell subsets. On the other hand, modern flow cytometers offer the possibility to differentiate between ten and more colors. Moreover, the availability of specific antibodies and new fluorochromes expanded over the last years [2].

Anna-Jasmina Donaubauer and Paul F. Rühle contributed equally to this work. Udo S. Gaipl and Benjamin Frey contributed equally as senior authors.

Michael Steinitz (ed.), *Human Monoclonal Antibodies: Methods and Protocols*, Methods in Molecular Biology, vol. 1904, https://doi.org/10.1007/978-1-4939-8958-4_8,

These improvements enable new features and advantages such as allowing the analyses of many immune cell subsets and activation state in disease or therapy settings as very rarely only one immune cell type is affected.

The panel presented here enables the determination of the general immune status of the peripheral immune system, covering all major leukocytes (T cells, B cells, natural killer (NK) cells, dendritic cells, monocytes, neutrophils, eosinophils, basophils), as well as 20 immune cell subsets and three activation markers (CD69, CD25, HLA-DR). All analyzed immune cell types are identified by at least one specific surface marker, which is widely accepted and described in the literature. For the detection of those surface markers, 15 different antibodies that are coupled to 10 different fluorochromes are applied. Thereby, the informative content of the panel is extended as more antibodies were used than colors. Antibodies coupled to the same fluorochrome are exclusively used for surface markers that are restricted to a certain immune cell typ. Then, by sticking to a strict gating order, it is possible to differentiate between all 15 antibodies and immune cell types.

The identification of all immune cell types requires only a total of 100 μL of whole-blood. This makes the assay applicable to every routine blood withdrawal. The direct usage of peripheral blood reduces preparation effort and time as well as experimental variations as compared to assays that require a preanalytical isolation of cells such as isolation of peripheral blood mononuclear cells (PBMCs). Moreover, polymorphonuclear cells (PMNs) that have been demonstrated to be a prognostic marker in some tumor entities are not excluded [3]. Finally, immune signatures of the peripheral blood generally have high informative value [4–6].

The OTMA was developed for three lasers and ten color flow cytometer. The measurements were performed on a Gallios flow cytometer (Beckman Coulter) in the standard filter configuration, but the assay is applicable to any other flow cytometer capable of determining at least ten colors.

As this assay offers the screening of the general immune status, one could easily add more staining tubes for further analyses of immune cell subsets. Moreover, the assay is adaptable to individual requirements, as many antibodies can be replaced in order to examine different cell subsets or activation markers. For such individual applications only the pan markers are required for the identification of the major immune cells and must not be replaced. One could easily focus further on, e.g., the identification of B-cell subsets by replacing some markers for antibodies against the surface molecules CD27, CD38, CD5, and CD24 in order to differentiate between pre-naïve, naïve, memory, and transitional B cells [7].

In order to further increase the informative value of the assay, one could include analysis of absolute cell counts, which is especially essential in longitudinal investigations. Leukocyte counts

might vary in different therapy or disease settings and the determination of the absolute cell count is the only way to detect this. Furthermore, the in- or decrease of one cell subset might alter the percentage of other subsets in longitudinal analyses, even though there are no changes in the absolute cell count of those cell subsets.

The following protocol describes the sample preparation as well as the detailed gating strategy for the determination of 20 immune cell subsets and their activation state. Moreover, instructions for the optional analysis of the absolute cell counts, by using the TruCount tube, are included.

2 Materials

Use sterile, ultra-pure water for the preparation of the solutions. All solutions should be stored at 4 °C unless indicated otherwise. Please follow the general waste disposal.

2.1 Solutions

1. Phosphate-buffered saline (PBS): pH 7.4.
2. Solution A (Red blood cell lysing solution): 0.12% formic acid solution (*see* **Note 1**).
3. Solution B (Re-buffering solution): 3.0 g of sodium carbonate, 7.25 g of sodium chloride and 15.55 g of sodium sulfate in 500 mL of water (*see* **Note 2**).

Both solutions (A and B) combined, in the same ratio as they are applied for the sample preparation later, should have a pH value between 6.5 and 7.5 (*see* **Note 3**).

4. Solution C (Leukocyte fixation solution): 1% paraformaldehyde (PFA) in PBS (pH 7.4) (*see* **Notes 4** and **5**).
5. Antibody mix for the determination of the cell types: Master-mix of all the required antibodies. Table 1 lists all the antibodies with the required volume for one blood sample (*see* **Note 6**).
6. TruCount tube antibody mix (optional): Master-mix of all the required antibodies. The antibodies are diluted in PBS (pH 7.4). Table 2 lists all the antibodies and the required amount of PBS for one blood sample (*see* **Note 6**).

2.2 Further Materials

1. EDTA blood collection tube.
2. Polypropylene tubes (5 mL) (*see* **Note 7**).
3. TruCount tube (optional) (BD Biosciences, Heidelberg, Germany).
4. TQ-Prep Workstation (optional) from Beckman Coulter.
5. Three lasers and ten color flow cytometer: The assay was established on a Gallios flow cytometer from Beckman Coulter in the standard filter configuration. The cytometer settings are described in Table 3.

Table 1
Antibody mix

nm	Specificity	Clone	Fluorochrome	Amount [µL]	Vendor	Cat. No.
488	CD28	28.2	BB515	**2.5**	BD Biosciences	564492
	CD16	3G8	PE	**0.1**	BD Biosciences	555407
	CD16	B73.1	PE	**2.5**	BD Biosciences	561313
	CD25	M-A251	PED594	**5.0**	BioLegend	356126
	CD8	HIT8a	PCC5.5	**0.5**	BioLegend	300924
	CD14	M5E2	PCC5.5	**0.5**	BioLegend	301824
	CD19	HIB19	PCC5.5	**0.5**	BD Biosciences	561295
	CD20	2H7	PCC5.5	**0.1**	BD Biosciences	560736
	CD127	MB15-18C9	PEV770	**2.0**	Miltenyi Biotec	130-099-719
638	CD4	RPA-T4	APC	**0.2**	BD Biosciences	555349
	CD123	7G3	APC	**2.0**	BD Biosciences	560087
	CD56	NCAM16.2	APCR700	**2.5**	BD Biosciences	657886
	HLADR	REA332	APCV770	**1.0**	Miltenyi Biotec	130-104-825
405	CD69	FN50	BV421	**5.0**	BD Biosciences	562884
	CD3	UCHT1	KO	**4.0**	Beckman Coulter	B00068

in total: 28.4 µL

Table 2
Antibody mix for the TruCount tube

nm	Specificity	Clone	Fluorochrome	Amount [µL]	Vendor	Cat. No.
488	CD14	M5E2	PCC5.5	**0.5**	BioLegend	301824
	CD19	HIB19	PCC5.5	**0.5**	BD Biosciences	561295
	CD20	2H7	PCC5.5	**0.1**	BD Biosciences	560736
638	CD56	NCAM16.2	APCR700	**2.5**	BD Biosciences	657886
405	CD3	UCHT1	KO	**4.0**	Beckman Coulter	B00068

in total: 7.6 µL; add 12.4 µL PBS

Table 3
Cytometer settings

Laser	Power	Detector	Filter	Range	Voltage	Gain	Fluorochrome
488 nm	22 mW	FSC	--	--	130	7.5	--
		SSC	--	--	90	7.5	--
		FL1	525 BP 40	505 - 545	430	1	BB515
		FL2	575 BP 30	560 - 590	520	1	PE
		FL3	620 BP 30	605 - 635	500	1	PED594
		FL4	695 BP 30	680 - 710	630	1	PCC5.5
		FL5	755 LP	> 755	650	1	PEV770
638 nm	25 mW	FL6	660 BP 20	650 - 670	700	1	APC
		FL7	725 BP 20	715 - 735	600	1	APCR700
		FL8	755 LP	> 755	500	1	APCV770
405 nm	40 mW	FL9	450 BP 50	425 - 475	470	1	BV421
		FL10	550 BP 40	530 - 570	400	1	KO

Abbreviations used for fluorochromes:
BB515: Brilliant Blue 515; **PE**: Phycoerythrin; **PED594**: PE-Dazzle594; **PCC5.5**: PerCP-Cy5.5; **PEV770**: PE-Vio770; **APC**: Allophycocyanin; **APCR700**: APC-R700; **APCV770**: APC-Vio770; **BV421**: Brilliant Violet 421; **KO**: Krome Orang

Abbreviations used for fluorochromes: *BB515* Brilliant Blue 515, *PE* Phycoerythrin, *PED594* PE-Dazzle594, *PCC5.5* PerCP-Cy5.5, *PEV770* PE-Vio770, *APC* Allophycocyanin, *APCR700* APC-R700, *APCV770* APC-Vio770, *BV421* Brilliant Violet 421, *KO* Krome Orang

3 Methods

3.1 Staining Protocol

All procedures are carried out at room temperature unless indicated otherwise.

1. Distribute 100 µL of EDTA-treated peripheral blood into a 5 mL polypropylene tube (*see* **Note 8**).
2. Add the dedicated antibody mix (28.4 µL) for the determination of the cell types directly to the blood sample (*see* **Note 9**) and vortex carefully.
3. If using the TruCount tube, resolve the dry beads at the bottom of the tube by pipetting the TruCount antibody mix (20 µL) directly onto the beads and add 50 µL of the EDTA-treated whole-blood (*see* **Notes 10** and **11**). Do not vortex.
4. Incubate both tubes at room temperature in the dark for 20 min.
5. After the staining, continue immediately with the lysis of the erythrocytes, the re-buffering and the fixation of the

leukocytes. If using a TQ-Prep Workstation, the lysis, the re-buffering and the fixation is an automated process, using the solutions A, B, and C.

These three steps can also be executed manually. Therefore, add 600 μL of solution A to the stained blood sample and vortex for 10 s. Immediately afterward add 265 μL of solution B and vortex for 10 s. Fix the cells by adding 100 μL of solution C and vortex again for 10 s. These steps are also performed for the TruCount tube but to a lesser extent of vortexing to keep the metal retainer in the tube intact.

6. Wash the stained cells twice with 3 mL of PBS: add 3 mL of PBS to the polypropylene tube and centrifuge the tube at 300 × *g* for 5 min. Discard the supernatant and resolve the cell pellet again in 3 mL of PBS and repeat the centrifugation step (*see* **Note 12**). Please consider that the TruCount tube requires no washing steps. Store the TruCount tube at 4 °C until the washing steps are finished.
7. After the second centrifugation step, discard the supernatant and resuspend the cell pellet in a final volume of 200 μL of PBS (*see* **Note 13**).
8. Analyze the samples by flow cytometry.

3.2 Data Analysis

It is essential to keep a strict and detailed gating strategy for the data analysis. The gating procedure can be divided into three main parts. First, the major immune cells are identified by the expression of their pan markers in comparison to their scatter attributes. Second, the major immune cells are divided into subsets by their (co-) expression of antigens. Finally, the expression of activation markers is analyzed on these cell subsets. An overview of all identified cell subsets, as well as their characterization by the specific markers, can be found in Table 4. If desired, the total cell count can be measured by additionally analyzing the TruCount tube.

With every gating step the identified cell subsets are excluded from the next gating step. Consequently, the next input gate contains fewer events with every gating step. The best results are obtained when the more frequent cells are identified initially and subsequently the infrequent ones, as these are enriched with every gating step. Table 5 provides an overview of all required Boolean gates for this gating strategy. This approach also allows the use of different antibodies coupled to the same fluorochrome.

3.2.1 Identification of the Major Immune Cells

The schematic overview of immune cell subsets that are identified with OTMA is depicted in Fig. 1. The major immune cells are displayed following the big black arrows. Except for the examination of the event count (histogram), all analyses are performed by creating dot plots. Unless the expression of two markers is

Table 4
Definition of cell subsets

Cell subset	Definition
Leukocytes	FSC vs. SSC
T cells	CD3+
Cytotoxic T cells (T_C)	CD3+/CD8+/CD4−
TC8hi	CD3+/CD8hi/CD4−
TC8lo	CD3+/CD8lo/CD4−
T helper cells (T_H)	CD3+/CD4+/CD8−
T_{REG}	CD3+/CD4+/CD8−/CD25hi/CD127−/lo
$CD28^-$T cells	CD3+/CD28−
$CD28^-$ TC	CD3+/CD8+/CD4−/CD28−
$CD28^-$ TH	CD3+/CD4+/CD8−/CD28−
DPT	CD3+/CD8+/CD4+
DNT	CD3+/CD4−/CD8−
B cells	CD19+ or CD20+
NK cells	CD3−/CD56+
NK1	CD3−/CD56+/CD16+
NK2	CD3−/CD56hi/CD16−
NK3	CD3−/CD56lo/CD16−
NKT	CD3+/CD56+ or CD3+/CD16+
Neutrophils	SSChi/CD16+
Eosinophils	SSChi/CD16−
Basophils	CD3−/CD14−/(CD16−)/CD19−/CD20−/CD56−/HLADR−/CD123+
Monocytes	CD14+/SSCint
Mo1	CD14+/CD16−
Mo2	CD14hi/CD16+
Mo3	CD14lo/CD16+
Dendritic cells (DCs)	CD3−/CD14−/(CD16−)/CD19−/CD20−/CD56−/HLADR+
mDC	CD3−/CD14−/(CD16−)/CD19−/CD20−/CD56−/HLADR+/CD123−/lo
pDC	CD3−/CD14−/(CD16−)/CD19−/CD20−/CD56−/HLADR+/CD123hi

Table 5
Definition of Boolean gates

Boolean gate	Definition
Rest1	"All Cells" AND (NOT "T cells")
Rest2	Rest1 AND (NOT (Eosinophils OR Neutrophils))
Rest3	Rest2 AND (NOT Monocytes)
Rest4	Rest3 AND (NOT "NK cells")
Rest5	Rest4 AND (NOT "B cells")
Rest6	Rest5 AND (NOT "Dendritic Cells")
Rest7	Rest6 AND (NOT Basophils)

An overview of all Boolean gates required for the identification of all subsets is given. There might be further gates required for transfer of activation markers on the subsets or evaluations of co-expressions

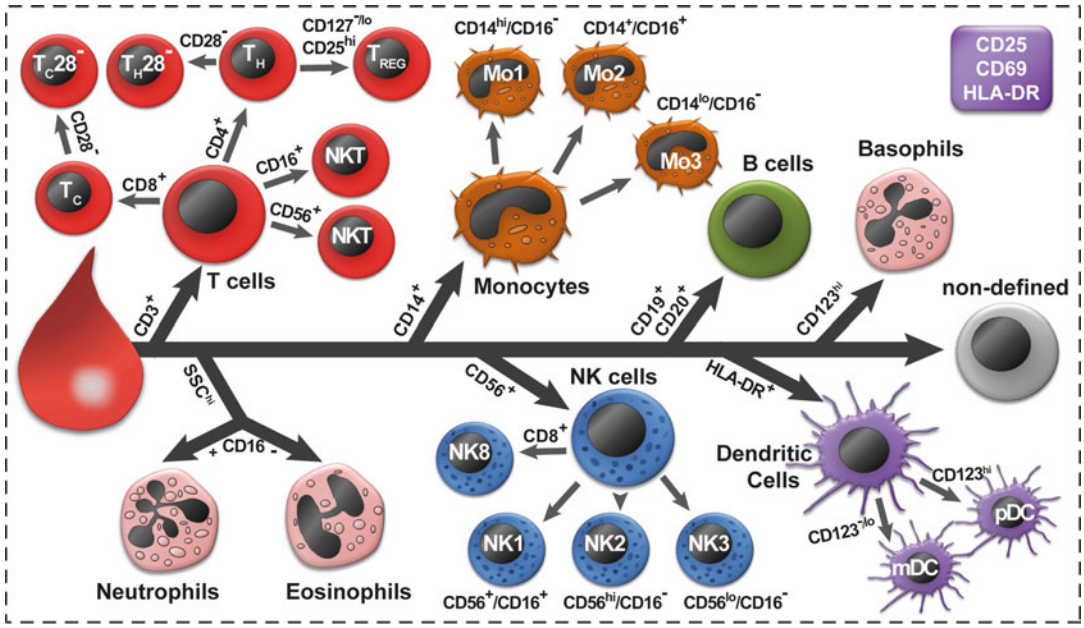

Fig. 1 Schematic overview of the identified immune cell subsets with the one-tube multicolor flow cytometry assay (OTMA)

compared in a plot, all the other plots compare the side scatter (SSC) characteristics with the expression of a single marker.

1. Examine the event count (flow) over time in order to exclude irregularities (e.g., air bubbles) from the analysis.

2. Exclude doublets by investigating the forward scatter (FSC) signal for the peak as well as the time of flight (TOF) characteristics in comparison to the integral attributes (*see* **Note 14**).
3. Define a gate for the leukocytes: Investigate the remaining events for their FSC vs. SSC characteristics. Thereby, define the *all-cells* gate, which represents all leukocytes. The cells from this gate are the input for the following analysis (*see* **Note 15**).
4. Examine the leukocytes (*all-cells* gate) for their surface expression of CD3. Draw a gate around the T cells to define these cells (*T-cells* gate) [8] (*see* **Note 16**).
5. Define a Boolean gate (*rest 1* gate) that covers all cells except the already identified $CD3^+$ T cells.
6. Use the *rest 1* gate as input for the identification of the eosinophils and neutrophils. These cells can be defined through their high SSC characteristics and their differential expression of CD16. Eosinophils are negative for CD16, whereas neutrophils, on the other hand, express CD16 [9]. Draw separate gates around those cell populations (*neutrophils* gate and *eosinophils* gate).
7. Define a new Boolean gate (*rest 2* gate) that covers all cells except the $CD3^+$ T cells, the $CD16^-$eosinophils, and the $CD16^+$ neutrophils. By now, most of the leukocytes are already defined.
8. The cells of *rest 2* are used to define the monocytes in the next step. Monocytes are identified by their CD14 expression [10] and their SSC^{int} characteristics (*see* **Note 17**). Set a gate around the monocytes population (*monocytes* gate).
9. Define a new Boolean gate (*rest 3* gate) which covers all the remaining cells.
10. The remaining cells of gate *rest 3* are now analyzed for their CD56 expression. All the positive cells are defined as NK cells [11]. Draw a gate around these cells (*NK cells* gate) (*see* **Note 18**).
11. Set again a Boolean gate (*rest 4*) which includes all the remaining undefined cells.
12. Examine the cells of *rest 4* for their CD19 and CD20 expression. All cells that are either positive for CD20 and/or CD19 are defined as B cells [12, 13]. Draw a gate around the B cells (*B-cells* gate).
13. Define the Boolean gate *rest 5* that covers all remaining cells.
14. The cells of *rest 5* are now checked for their expression of HLA-DR. The $HLA\text{-}DR^+$ cells that show intermediate SSC characteristics are defined as dendritic cells (DCs) [14] (*see* **Note 19**). Draw a gate covering the dendritic cells (*DCs* gate).

15. Create a Boolean gate (*rest 6*) covering the HLA-DR$^-$ cells.
16. Analyze the cells of *rest 6* for their expression of CD123 (*see* **Note 20**). Draw a gate around the CD123^{hi} cells and define these cells as basophils [15] (*see* **Note 21**).
17. The remaining cells are defined as *rest 7* and are handled as nondefined circulating cells such as macrophages, mast cells, as well as hematopoietic stem and progenitor cells.

3.2.2 Identification of Cell Subsets

After the determination of the major immune cells some of them are further divided into cell subsets by the co-expression of surface markers. The gating strategy is also shown in Fig. 1 and indicated with small gray arrows.

1. The most subsets are distinguished within the T cells. In order to subdivide the T cells, the earlier defined CD3$^+$ T cells are chosen as an input for the analysis. At first the CD4$^+$/CD8$^-$ T helper cells and the CD8$^+$/CD4$^-$ cytotoxic T cells are defined by analyzing those two markers on all the T cells. Draw quadrants into the plot to separate T helper cells (*TH*), T killer cells (*TC*), double negative cells (*DNT*), and double-positive cells (*DPT*) (*see* **Note 22**).
2. In the next step the T helper cells are further subdivided. Therefore, the cells of the *TH* gate are selected as input for the analysis. The cells are analyzed for their CD127 and CD25 expression. Cells that show a CD127$^{-/lo}$ and CD25^{hi} phenotype are defined as regulatory T cells (T_{regs} gate) [16, 17] (*see* **Note 23**).
3. The T cells are also analyzed for their CD28 expression. Again, the cells from the *T-cells* gate are used as input for the analysis. The CD28 gating is most easy to determine when it is analyzed together with the expression of CD25. Set quadrants to distinguish between the different populations. The CD28 expression is then transferred to the T helper cells (*TH*) and the T killer cells (*TC*) by using Boolean gates.
4. Next, the NKT cells are determined even though this subset does not belong to the T cells but these cells express T cell as well as NK cells markers [18–20]. Again, the CD3$^+$ T cells are selected as input for the analysis. The NKT cells are determined by analyzing the expression of CD56 together with the CD16 expression. Draw a gate (*NKT cells*) around all CD16$^+$ and/or CD56$^+$ cells (*see* **Note 24**).
5. The monocytes are also subdivided into three subsets (Mo1–Mo3). The earlier defined *monocytes* gate is used for the analysis. Determine the expression of CD14 and CD16 on the monocytes. Set gates to separate the *Mo1* (CD14$^+$/

CD16$^-$), the *Mo2* (CD14^{hi}/CD16$^+$), and the *Mo3* cells (CD14^{lo}/CD16$^+$) (*see* **Note 25**) [21].

6. Afterward, the NK cells are separated into subtypes, too (NK1–NK3). The cells of the *NK cells* gate were selected for the analysis and their expression of CD56 and CD16 was determined. Draw gates to separate the *NK1* (CD56$^+$/CD16$^+$), the *NK2* (CD56^{hi}/CD16$^-$), and the *NK3* cells (CD56^{lo}/CD16$^-$) [22].
7. We found a notable co-expression of CD8 to HLA-DR on monocytes. Therefore, we suggest evaluating this expression for alterations. Select again the cells of the *monocytes* gate as input and examine the expression of CD8 and HLA-DR. Draw quadrants to separate the cell populations.
8. Finally, the DCs are subdivided into plasmacytoid DCs (pDCs) and myeloid DCs (mDCs). The cells of the *DCs* gate are used as input. DCs are distinguishable by their co-expression of CD123 and CD11c into mDCs (CD11c^{hi}/CD123$^{-/lo}$) and pDCs (CD11c$^-$/CD123^{hi}) [14, 23]. In this panel, the CD123 has been already included for the identification of basophils. We renounced the investigation of CD11c, since after exclusion of all other cells, almost all CD123^{hi} cells were CD11c$^-$ and almost all CD11c$^+$ cells were CD123$^{-/lo}$. Therefore, in order to separate the subtypes, the expression of HLA-DR is plotted against the expression of CD123. Draw gates to separate the CD123$^{-/lo}$ mDCs (*mDCs* gate) and the CD123^{hi} pDCs (*pDCs* gate).

For the B cells, eosinophils, neutrophils, and basophils, no further subgating is performed except the examination of activation markers.

3.2.3 Analyses of the Activation Status

Finally, the activation status of the immune cells is determined. For this purpose, the expression of the activation markers CD69, CD25, and HLA-DR is analyzed in parallel on the major cell types. The gate settings were evaluated by different controls during the assay development. These controls include single stainings of whole-blood, fluorescence minus one (FMO) controls, as well as isotype stainings, which were initialized with the blood of normal healthy donors (NHDs). A description of the controls can be found in the following Figures and Table: Figs. 2, 3, and 4 and Table 6 (*see* **Note 26**). In comparison to the other steps in the data analysis, the analysis of the activation markers does not require such a strict gating strategy (*see* **Notes 27** and **28**). An overview of the expression of the activation markers on the major cell types is provided in Table 7.

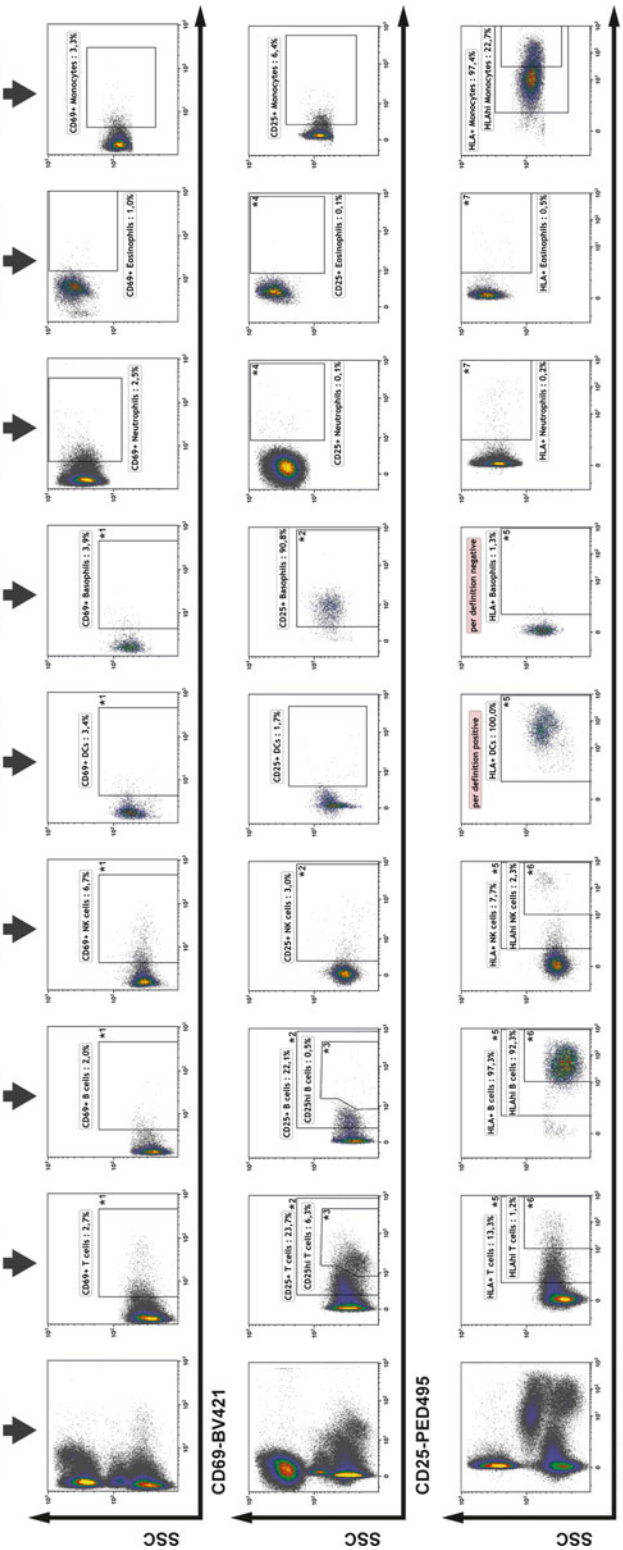

Fig. 2 Gating strategy for activation markers

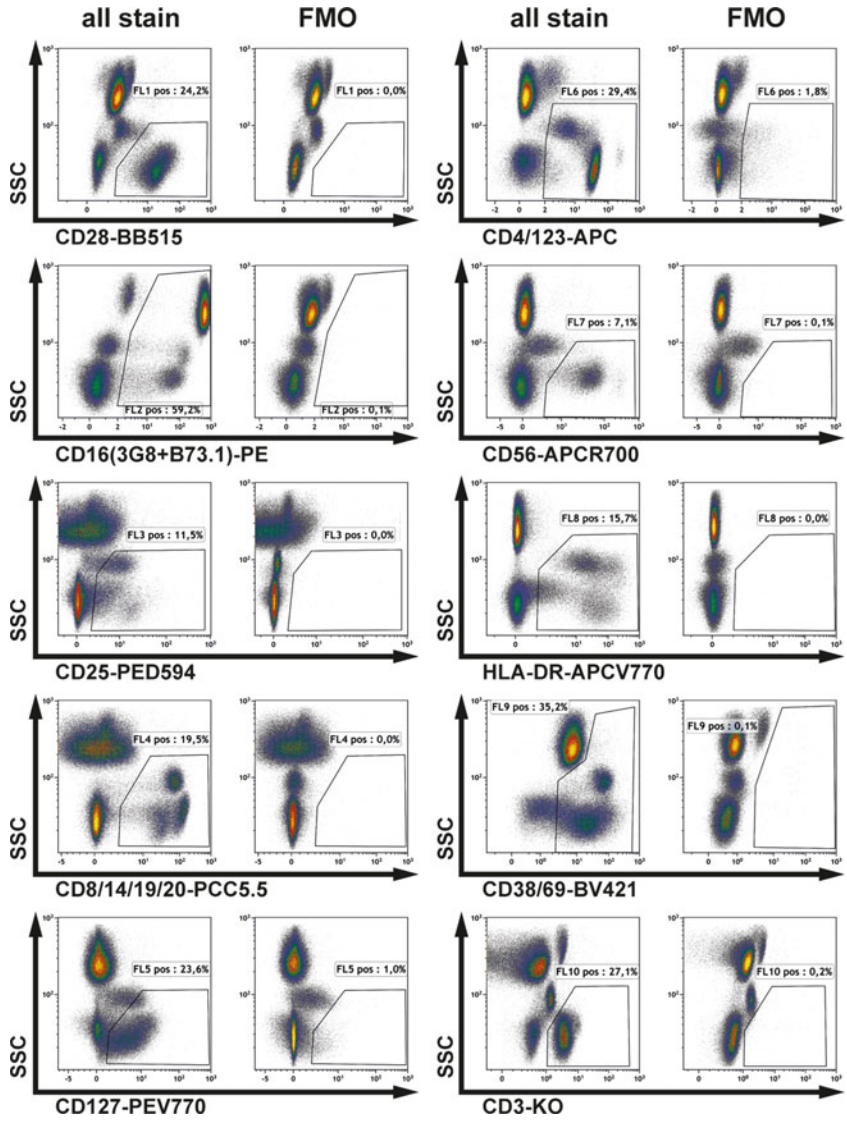

Fig. 3 FMO staining

1. First, the expression of CD25 is evaluated on the different cell types. Examine the expression of the marker on T cells, B cells, NK cells, DCs, basophils, and eosinophils. Create a dot plot for each cell type and use the respective input gate for the analysis. Compare the SSC characteristics with the expression of CD25 for each cell type (*see* **Notes 29** and **30**). Draw gates based on the controls to separate $CD25^+$ cells.
2. The expression of HLA-DR is examined on T cells, B cells, NK cells, DCs, and monocytes. Again, a plot for each cell type is created and the respective input gate is selected for each plot. Compare the SSC characteristics with the expression of

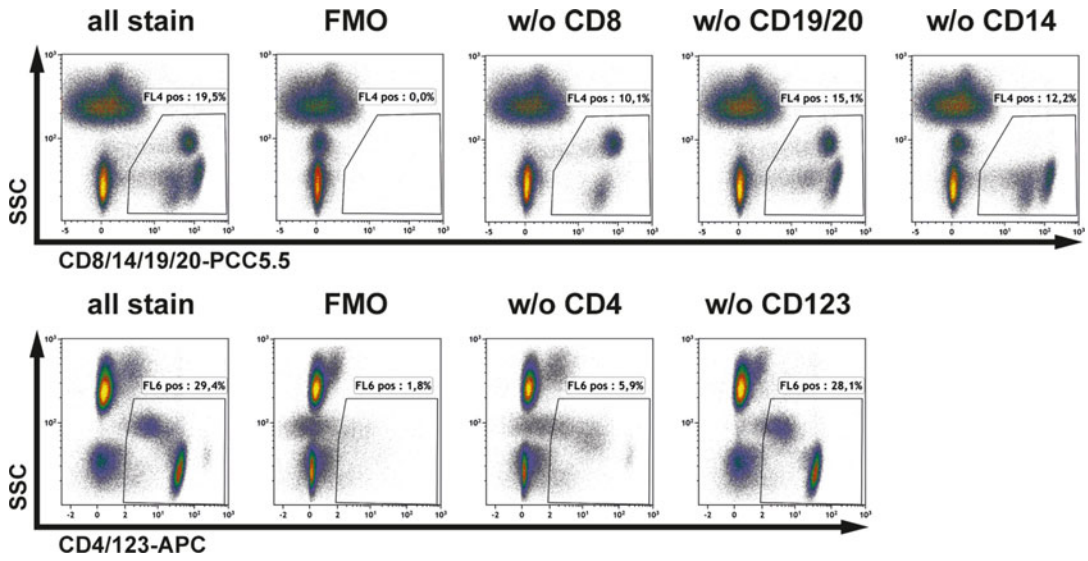

Fig. 4 Evaluation of staining in the PCC5.5 and APC-channel

HLA-DR (*see* **Notes 31** and **32**). Draw gates based on the controls for the HLA-DR$^+$ cells.

3. Finally, the expression of CD69 is analyzed on T cells, B cells, NK cells, DCs, basophils, and neutrophils. As described above, analyze the cells by creating a plot and using the appropriate input gate for each cell type. The SSC characteristics are compared with the expression of CD69. Draw gates based on the controls around the CD69$^+$ cells.

3.2.4 Analysis of the TruCount Tube (Optional)

The determination of absolute cell counts within the panel described above is not allowed. Due to washing steps, there is a subsequent loss of cells. The TruCount tube contains counting beads that allow the determination of absolute cell counts. Thereby, also minor alterations of the leukocytes can be analyzed. Similar as described earlier, it is essential to stick to the gating strategy strictly. Figure 5 provides an overview of the analysis of the TruCount tube.

1. Similar to the panel described above, start the analysis of the TruCount tube by examining the event count over the time in order to exclude irregularities from the analysis.
2. Exclude the doublets from the further analysis by investigating the FSC signal for both the peak and the TOF characteristics in comparison to the integral attributes.
3. The remaining events are analyzed for their FSC vs. SSC characteristics to define the leukocytes. Draw a gate around the leukocyte population (*all cells* gate) (*see* **Note 33**). The counting beads are also detected in this plot. The beads show high

Table 6
Evaluation of isotype staining

Specificity	Fluorochr.	Species	Isotype	Clone	Vendor	Cat. No.	Amount	Evaluation
CD28	BB515	Mouse	IgG1	X40	BD Biosciences	564416	5	No unspecific signals
CD16 (3G8)	PE	Mouse	IgG1	MOPC-21	BD Biosciences	555749	20	No unspecific signals
CD16 (B73.1)	PE	Mouse	IgG1	MOPC-21	BD Biosciences	555749	20	No unspecific signals
CD25	PED594	Mouse	IgG1	MOPC-21	BioLegend	400175	5	*Unspecific signals by monocytes* Excluded in final gating (only monocytes)
CD8	PCC5.5	Mouse	IgG1	MOPC-21	BioLegend	400150	5	Unspecific signals by monocytes Unspecific signal of specific antibody much lower Irrelevant for gating
CD14	PCC5.5	Mouse	IgG2a	G155-178	BD Biosciences	550927	5	Unspecific signals by monocytes Unspecific signal of specific antibody much lower Irrelevant as monocytes express CD14 anyway
CD19	PCC5.5	Mouse	IgG1	MOPC-21	BD Biosciences	555749	20	No unspecific signals
CD20	PCC5.5	Mouse	IgG2b	MPC-11	BioLegend	400338	5	Unspecific signals by monocytes Unspecific signal of specific antibody much lower Irrelevant for gating
CD127	PEV770	Mouse	IgG2a	S43.10	Miltenyi Biotec	130-098-564	10	Unspecific signals by monocytes Irrelevant for gating
CD4	APC	Mouse	IgG1	MOPC-21	BD Biosciences	554681	5	No unspecific signals
CD123	APC	Mouse	IgG2a	G155-178	BD Biosciences	555576	5	No unspecific signals

(continued)

Table 6
(continued)

Specificity	Fluorochr.	Species	Isotype	Clone	Vendor	Cat. No.	Amount	Evaluation
CD56	APCR700	N/A	N/A	N/A	N/A	N/A	N/A	No isotype was available Specific gating was without any problems
HLADR	APCV770	Human	IgG1	REA293	Miltenyi Biotec	130-104-618	10	*Unspecific signals by monocytes* Unspecific signal pf isotype much lower than of specific antibody. Perhaps excluded in final gating (only monocytes)
CD69	BV421	Mouse	IgG1	X40	BD Biosciences	562438	5	No unspecific signals
CD3	KO	Mouse	IgG1	679.1Mc7	Beckman Coulter	A96415	10	No unspecific signals

The isotype staining was performed using blood samples from normal healthy donors (NHDs), which were stained with the according isotype controls applying 100% of the specified test size and were evaluated for unspecific binding capacities. No cells, except monocytes, have shown any unspecific signals. However, this is not a problem since all of these antigens were not investigated on monocytes or they express it anyway (CD14). The only exceptions were the isotypes of the activation markers CD25-PED594 and HLA-DR-APCV770. Here, an evaluation of monocytes expression should be renounced as the expression might not be reliable

Table 7
Expression patterns of activation markers

	CD25		CD69	HLA-DR	
	Positive	High	Positive	Positive	High
T cells	+	+	+	+	+
T_H	+	+	+	+	+
T_C	+	+	+	+	+
B cells	+	+	+	+	+
NK cells	+	–[a]	+	+	+
Basophils	+	–[a]	+	–[b]	–[b]
DCs	+	–[a]	+	–[c]	–[c]
Monocytes	–[d]	–[d]	+	+	+
Neutrophils	+	–[a]	+	+	–[a]
Eosinophils	+	–[a]	+	+	–[a]

[a]Positive expression, but no distinction of high expression pattern
[b]Per definition negative
[c]Per definition positive
[d]Not available as isotype indicated unspecific binding properties

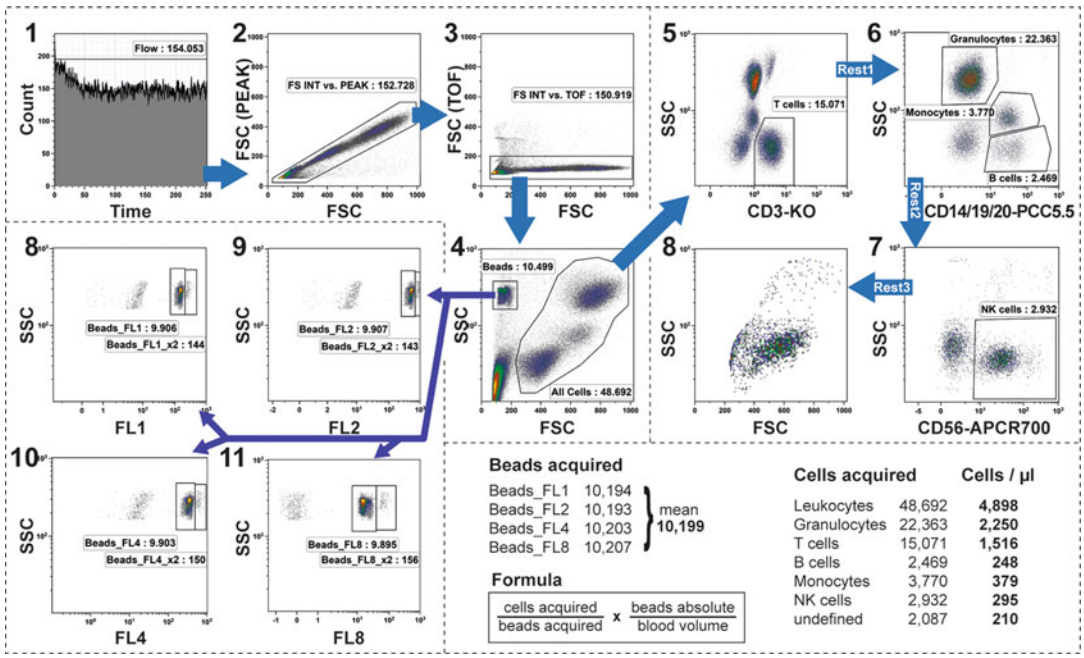

Fig. 5 Determination of the absolute cell count

SSC and low FSC characteristics. Draw a gate around the bead population (*beads* gate) for further analyses.

4. In the next step, the T cells are determined due to their SSC characteristics and the expression of CD3 [8]. Set a gate around the $CD3^+$ T cells.
5. Define a Boolean gate (*rest 1 (CD3−)* gate), covering all remaining undefined leukocytes.
6. Use the cells of *rest 1 (CD3−)* in order to analyze the granulocytes. Plot the SSC values against the expression of CD14/CD19/CD20. Those three markers are all detected in the same fluorescence channel. All cells showing high SSC characteristics are determined as granulocytes. Draw a gate around those SSC^{hi} cells (*granulocytes* gate).
7. Create a new Boolean gate covering the remaining cells (*rest 2 (R1-PMN)* gate).
8. For the determination of the B cells and monocytes the cells of the *rest 2 (R1-PMN)* gate are used as an input. Again, the cells are investigated for their SSC characteristics and the expression of CD14/CD19/CD20. The $CD14^+$ monocytes [10] can be separated from the $CD19^+/CD20^+$ B cells by their higher SSC characteristics. The $CD19^+/CD20^+$ B cells [12, 13] show lower SSC values. Draw separate gates around the monocytes (*monocytes* gate) and the B cells (*B cells* gate).
9. Define a new Boolean gate (*rest 3 (R2-Mo, B)* gate) including the remaining cells.
10. Finally, the counting beads are characterized by their high autofluorescence. They can be detected in the fluorescence channels 1, 2, 4, and 8. Create a plot for each fluorescence channel and plot the SSC characteristics against the respective fluorescence signal. Use the *beads* gate as an input for the analysis. The beads population shows high SSC characteristics, as well as high fluorescence values. Draw gates covering the bead populations in each fluorescence channel (*beads FL1*, *beads FL2*, *beads FL4*, and *beads FL8* gate) (*see* **Notes 34** and **35**).
11. The absolute cell count for the subsets determined in the TruCount tube can be calculated by using just the following formula (*see* **Note 36**):

$$\frac{\text{Cells acquired}}{\text{Beads aquired}} \times \frac{\text{Beads absolute}}{\text{Blood volume}}$$

4 Notes

1. Add 1200 μL of >98% formic acid solution to 1 L of water and mix.
2. Dissolve 3.0 g of sodium carbonate, 7.25 g of sodium chloride, and 15.55 g of sodium sulfate in 500 mL of water. Make sure that the reagents are completely dissolved by mixing the solution thoroughly. Afterward, the solution should be filtered sterile. For this purpose we use the stericup vacuum sterile filter (0.22 μm) from Merck-Millipore. The preparation of solution B requires water-free sodium carbonate. If the water-free chemical is not available, sodium carbonate monohydrate is also suitable. In this case, 3.5 g of sodium carbonate monohydrate are required for the solution.
3. Adjustment of the pH: In order to check the pH value, both solutions are combined in the same ratio as they are applied for the sample preparation later: 2400 μL of solution A with 1060 μL of solution B are combined in a 15 mL tube. The pH value of this solution should range between 6.5 and 7.5. If the pH is too high, use formic acid for adjustments. For a pH below 6.5 use water for further adjustments.
4. We use 166.6 mL of a 4% Roti-Histofix solution (Carl Roth, Germany) and add the appropriate amount of PFA to a fresh and sterile 500 mL PBS bottle.
5. Instead of preparing fresh solutions for every staining, we recommend preparing a stock of solutions A, B, and C which will last for max. 8 weeks. We do not recommend storing these solutions even longer, because they are not long-time stable.
6. The antibody mix for both tubes can be prepared for multiple measurements in advance. We store the antibody mix for up to 4 weeks at 4 °C in lightproof tubes.
7. The altered surface of polypropylene tubes reduces cell loss as the adhering of cells at the tube walls is minimized.
8. Mix the EDTA tube properly by inverting it before starting to allow a consistent distribution of the blood cells.
9. During the staining procedure, blood smears at the tube walls should be avoided. If these smears appear, they must be removed immediately as dry blood smears will occur as dead or unstained cells in the measurement.
10. Before using the TruCount tube check if the beads and the metal retainer are intact and there is no liquid in the tube, otherwise discard it and take a new one. Note the Lot number and bead count of each package for further analysis.

11. For the determination of the absolute cell count, the TruCount tube requires the exact amount of 50 µL of blood. To improve the accuracy, we recommend adding the blood by reverse pipetting. Therefore, the pipette knob is pressed down to the second stop point while the blood is drawn into the pipette tip. When releasing the fluid into the tube only press the pipette knob down to the first stop point.
12. Discard the supernatant by inverting the tube and place the tube upside down onto a paper towel to get rid of excess fluid. Do not invert more than once, otherwise cells can be lost.
13. If you cannot measure the cells directly after staining, store the samples in the dark at 4 °C until the measurement.
14. The doublets are investigated by two approaches because some doublets are only detectable with the one or the other method.
15. All events in the *all cells* gate with lowered FSC values were excluded as dead or dying cells from the gate. In fact, dead cell marker investigations showed most positivity within these lowered FSC events. Therefore we decided not to include a dead cell marker. In general, dead cells are not a problem in fresh blood samples. Moreover, it would occupy another fluorescence channel.
16. We consider starting the analysis with the T-cell identification since the CD3 expression is quite high and therefore easy to determine.
17. The anti CD14 antibody shares its fluorescence signal (PCC5.5) with other antibodies (CD8, CD19, and CD20). Therefore, it is necessary to define only the SSC^{int} cells but not the SSC^{lo} cells as monocytes to exclude false-positive events.
18. Since the NK cells are defined as $CD16^+$ cells like a lot of other cell types, the CD56 expression is additionally monitored. But since this expression is very weak the possibility of obtaining false positives is quite high. Therefore two different exclusion steps can be performed. First, only the $CD56^+$ and/or $CD123^-$ cells are monitored and subsequently all cells with a high SSC are excluded. In the last step the NK cells are defined as $CD56^+$ and/or $CD16^+$ [24].
19. HLA-DR is expressed by many cells and therefore DCs can only be identified after the exclusion of all the other cell types. Therefore, leftover or falsely gated cells may alter the DC frequency. Thus, only HLA-DR^+ cells with intermediate SSC characteristics were considered DCs.
20. Similar to DCs, basophils do not express a pan marker. CD123 is expressed by several cell types and therefore these cells have to be excluded prior to basophil identification [15].

21. Under certain circumstances the CD123 expression can be downregulated [15]. Therefore, there is another gate called *BAS_123low* with a lower CD4/CD123 expression than normal.
22. T cells expressing neither CD4 nor CD8 or cells expressing both markers differ from the classical view of circulating T cells. Nonetheless, we monitor these cells as double-negative or double-positive T cells, because they were observed in all peripheral blood samples. For both cell types an elevation has been connected to progression of autoimmune diseases [25, 26]. Moreover, $CD8^+$ T killer cells can be separated into a $CD8^{hi}$ (*T8hi*) and a smaller $CD8^{lo}$ ($T8^{lo}$) subset because the CD8 expression of T killer cells in contrast to the CD4 expression on T helper cells is lowered in certain subsets [27].
23. If the T_{reg} cells population is not clearly distinguishable from the other $CD4^+$ cells, the expression of the corresponding markers can also be examined on the T killer cells. These cells should not show a clear positive population. Adjust the T_{regs} gate on the level of the T killer cells so that nearly all cells are negative and use this gating for the analysis of the T_{regs} on the level of the $CD4^+$ cells.
24. NKT cells can show differences in the expression of CD4 and CD8 [20]. Therefore, we suggest not only determining the NKT cells on the level of the $CD3^+$ T cells but also on the level of $CD4^+$ T cells and on the level of $CD8^+$ T cells. Therefore, use either the cells of the *TH* or the *TC* gate as input for the analysis of the NKT cells.
25. There is also the possibility of including a fourth group of monocytes called Mo4 or pre DCs, but these cells are very rare in the main gating. They are defined as $CD14^{lo}/CD16^-$ [28].
26. We suggest performing all controls described in order to evaluate the optimal gate settings for the activation markers.
27. Many cells (in this case: T cells, B cells, NK cells, basophils, and DCs) show similar expression patterns. Therefore, we applied the same gate setting for cells, which show the same autofluorescence characteristics.
28. In general, the activation status can be examined on any desired, earlier defined cell subtype to gain further data. Therefore, the respective input gate has to be chosen for the analysis.
29. Additional high expression gates can be defined for the CD25 expression on B cells and T cells to increase the informative content.
30. The expression of CD25 is not evaluated on monocytes due to unspecific binding properties of the isotype staining.

31. An unspecific binding of the HLA-DR antibody could be observed on monocytes. Therefore, the gating should be performed carefully. Nonetheless, we observed similar expression patterns with other antibodies. Consequently, we included the marker for the analysis of the activation status of monocytes because the specific signal was much higher than the unspecific isotype signal.
32. Per definition, B cells, DCs, as well as monocytes express HLA-DR constantly. Thus, this molecule is technically not an activation marker on those cell types. We decided to analyze the HLA-DR expression anyway, as there are fluctuations in the expression in response to several stimuli [29].
33. The preparation of the TruCount tube requires no washing steps. Therefore, more dead cells and cell fragments are detected during the measurement. These cells show low SSC and FSC characteristics and must be excluded from the all cells gate.
34. The counting beads often stick together and appear not only as singlets but also as doublets during the measurement. These doublets show a stronger fluorescence signal than the singlets. Set separate gates for bead singlets and bead doublets in all four fluorescence channels. For the determination of the absolute bead count we multiply the number of the bead doublets by 2 and add it to the number of the bead singlets. This guaranties a more precise absolute bead count.
35. The bead count recorded in all four fluorescence channels should be nearly similar. If the bead count differs strongly, the previous gating steps should be reevaluated.
36. The absolute bead count varies between different lot numbers of the TruCount tubes. Therefore, it is crucial to document the bead count of the used tube.

References

1. Galon J, Angell HK, Bedognetti D, Marincola FM (2013) The continuum of cancer immunosurveillance: prognostic, predictive, and mechanistic signatures. Immunity 39(1):11–26. https://doi.org/10.1016/j.immuni.2013.07.008
2. Chattopadhyay PK, Roederer M (2012) Cytometry: today's technology and tomorrow's horizons. Methods 57(3):251–258. https://doi.org/10.1016/j.ymeth.2012.02.009
3. Moreira A, Leisgang W, Schuler G, Heinzerling L (2017) Eosinophilic count as a biomarker for prognosis of melanoma patients and its importance in the response to immunotherapy. Immunotherapy 9(2):115–121. https://doi.org/10.2217/imt-2016-0138
4. Bjoern J, Brimnes MK, Andersen MH, Thor Straten P, Svane IM (2011) Changes in peripheral blood level of regulatory T cells in patients with malignant melanoma during treatment with dendritic cell vaccination and low-dose IL-2. Scand J Immunol 73(3):222–233. https://doi.org/10.1111/j.1365-3083.2010.02494.x
5. Tokuno KH, Shoichi H, Yoshino S, Yoshida S, Oka M (2009) Increased prevalence of regulatory T-cells in the peripheral blood of patients

with gastrointestinal cancer. Anticancer Res 29 (5):1527–1532

6. Ho CMM, Philip L, Wallace PK, Zhang Y, Fora A, Mellors P, Tario JD, McCarthy BLS, Chen GL, Holstein SA, Balderman SR, Xuefang C, Paiva B, Hahn T (2017) Immune signatures associated with improved progression-free and overall survival for myeloma patients treated with AHSCT. Blood Adv 1(15):1056–1066. https://doi.org/10.1182/bloodadvances.2017005447
7. Shirota Y, Yarboro C, Fischer R, Pham TH, Lipsky P, Illei GG (2013) Impact of anti-interleukin-6 receptor blockade on circulating T and B cell subsets in patients with systemic lupus erythematosus. Ann Rheum Dis 72 (1):118–128. https://doi.org/10.1136/annrheumdis-2012-201310
8. Jarry A, Cerf-Bensussan N, Brousse N, Selz F, Guy-Grand D (1990) Subsets of CD3+ (T cell receptor alp or y/6) and CD3-lymphocytes isolated from normal human gut epithelium display phenotypical features different from their counterparts in peripheral blood. Eur J Immunol 20(5):1097–1103. https://doi.org/10.1002/eji.1830200523
9. Ravetch JV, Bolland S (2001) IgG Fc receptors. Annu Rev Immunol 19:275–290. https://doi.org/10.1146/annurev.immunol.19.1.275
10. Pan T, Zhou T, Li L, Liu Z, Chen Y, Mao E, Li M, Qu H, Liu J (2017) Monocyte programmed death ligand-1 expression is an early marker for predicting infectious complications in acute pancreatitis. Crit Care 21(1):186. https://doi.org/10.1186/s13054-017-1781-3
11. Knudsen JH, Court-payen M, Kjærsgaard E, Christensen NJ (2009) Lymphocyte subset composition in peripheral blood from normal subjects may be influenced by both spleen size and plasma norepinephrine. Scand J Clin Lab Invest 55(7):643–648. https://doi.org/10.3109/00365519509110264
12. Cheadle WG, Pemberton RM, Robinson D, Livingston DH, Rodriguez JL, Polk HC Jr (1993) Lymphocyte subset responses to trauma and sepsis. J Trauma 35(6):844–849
13. Monserrat J, de Pablo R, Diaz-Martin D, Rodriguez-Zapata M, de la Hera A, Prieto A, Alvarez-Mon M (2013) Early alterations of B cells in patients with septic shock. Crit Care 17 (3):R105. https://doi.org/10.1186/cc12750
14. O'Doherty U, Peng M, Gezelter S, Swiggard WJ, Betjes M, Bhardwaj N, Steinman RM (1994) Human blood contains two subsets of dendritic cells, one immunologically mature and the other immature. Immunology 82 (3):487–493
15. Chirumbolo S, Bjorklund G, Vella A (2017) Using a CD45dim/CD123bright/HLA-DRneg phenotyping protocol to gate basophils in FC for airway allergy. CD123 does not decrease. Adv Respir Med 85(4):193–201. https://doi.org/10.5603/ARM.2017.0032
16. Liu W, Putnam AL, Xu-Yu Z, Szot GL, Lee MR, Zhu S, Gottlieb PA, Kapranov P, Gingeras TR, Fazekas de St Groth B, Clayberger C, Soper DM, Ziegler SF, Bluestone JA (2006) CD127 expression inversely correlates with FoxP3 and suppressive function of human CD4+ T reg cells. J Exp Med 203 (7):1701–1711. https://doi.org/10.1084/jem.20060772
17. Seddiki N, Santner-Nanan B, Martinson J, Zaunders J, Sasson S, Landay A, Solomon M, Selby W, Alexander SI, Nanan R, Kelleher A, Fazekas de St Groth B (2006) Expression of interleukin (IL)-2 and IL-7 receptors discriminates between human regulatory and activated T cells. J Exp Med 203(7):1693–1700. https://doi.org/10.1084/jem.20060468
18. Al Omar SY, Marshall E, Middleton D, Christmas SE (2012) Increased numbers but functional defects of CD56+CD3+ cells in lung cancer. Int Immunol 24(7):409–415. https://doi.org/10.1093/intimm/dxr122
19. Bjorkstrom NK, Gonzalez VD, Malmberg KJ, Falconer K, Alaeus A, Nowak G, Jorns C, Ericzon BG, Weiland O, Sandberg JK, Ljunggren HG (2008) Elevated numbers of Fc RIIIA+ (CD16+) effector CD8 T cells with NK cell-like function in chronic hepatitis C virus infection. J Immunol 181(6):4219–4228. https://doi.org/10.4049/jimmunol.181.6.4219
20. Michel JJ, Turesson C, Lemster B, Atkins SR, Iclozan C, Bongartz T, Wasko MC, Matteson EL, Vallejo AN (2007) CD56-expressing T cells that have features of senescence are expanded in rheumatoid arthritis. Arthritis Rheum 56(1):43–57. https://doi.org/10.1002/art.22310
21. Guilliams M, Ginhoux F, Jakubzick C, Naik SH, Onai N, Schraml BU, Segura E, Tussiwand R, Yona S (2014) Dendritic cells, monocytes and macrophages: a unified nomenclature based on ontogeny. Nat Rev Immunol 14(8):571–578. https://doi.org/10.1038/nri3712
22. Montaldo E, Del Zotto G, Della Chiesa M, Mingari MC, Moretta A, De Maria A, Moretta L (2013) Human NK cell receptors/markers: a tool to analyze NK cell development, subsets and function. Cytometry A 83(8):702–713. https://doi.org/10.1002/cyto.a.22302

23. Robinson SP, Patterson S, English N, Davies D, Knight SC, Reid CD (1999) Human peripheral blood contains two distinct lineages of dendritic cells. Eur J Immunol 29 (9):2769–2778. https://doi.org/10.1002/(SICI)1521-4141(199909)29:09<2769::AID-IMMU2769>3.0.CO;2-2
24. Hong HS, Eberhard JM, Keudel P, Bollmann BA, Ahmad F, Ballmaier M, Bhatnagar N, Zielinska-Skowronek M, Schmidt RE, Meyer-Olson D (2010) Phenotypically and functionally distinct subsets contribute to the expansion of CD56-/CD16+ natural killer cells in HIV infection. AIDS 24(12):1823–1834. https://doi.org/10.1097/QAD.0b013e32833b556f
25. Quandt D, Rothe K, Scholz R, Baerwald CW, Wagner U (2014) Peripheral CD4CD8 double positive T cells with a distinct helper cytokine profile are increased in rheumatoid arthritis. PLoS One 9(3):e93293. https://doi.org/10.1371/journal.pone.0093293
26. Crispín JC, Oukka M, Bayliss G, Cohen RA, Van Beek CA, Stillman IE, Kyttaris VC, Juang YT, Tsokos GC (2008) Expanded double negative T cells in patients with systemic lupus erythematosus produce IL-17 and infiltrate the kidneys. J Immunol 181(12):8761–8766
27. Trautmann A, Rückert B, Schmid-Grendelmeier P, Niederer E, Bröcker EB, Blaser K, Akdis CA (2003) Human CD8 T cells of the peripheral blood contain a low CD8 expressing cytotoxic/effector subpopulation. Immunology 108(3):305–312
28. Thomas R, Lipsky PE (1994) Human peripheral blood dendritic cell subsets. Isolation and characterization of precursor and mature antigen-presenting cells. J Immunol 153 (9):4016–4028
29. Holmannova D, Kolackova M, Kunes P, Krejsek J, Mandak J, Andrys C (2016) Impact of cardiac surgery on the expression of CD40, CD80, CD86 and HLA-DR on B cells and monocytes. Perfusion 31(5):391–400. https://doi.org/10.1177/0267659115612905

Chapter 9

Humanization and Simultaneous Optimization of Monoclonal Antibody

Taichi Kuramochi, Tomoyuki Igawa, Hiroyuki Tsunoda, and Kunihiro Hattori

Abstract

Antibody humanization is an essential technology for reducing the potential risk of immunogenicity associated with animal-derived antibodies and has been applied to a majority of the therapeutic antibodies on the market. For developing an antibody molecule as a pharmaceutical at the current biotechnology level, however, other properties also have to be considered in parallel with humanization in antibody generation and optimization. This section describes the critical properties of therapeutic antibodies that should be sufficiently qualified, including immunogenicity, binding affinity, physicochemical stability, expression in host cells and pharmacokinetics, and the basic methodologies of antibody engineering involved. By simultaneously optimizing the antibody molecule in light of these properties, it should prove possible to shorten the research and development period necessary to identify a highly qualified clinical candidate and consequently accelerate the start of the clinical trial.

Key words Humanization, Immunogenicity, Optimization, Protein expression, Stability

1 Introduction

Monoclonal antibody recognizes antigen with high affinity and neutralizes the function of the antigen. In addition, it binds to the antigen-expressing cells and triggers effector functions that eliminate those cells, through antibody-dependent cellular cytotoxicity (ADCC) or complement-dependent cytotoxicity (CDC), via its Fc region. In the area of autoimmune diseases, antibodies that neutralize the function of inflammatory cytokines, such as IL-6 receptor or tumor necrosis factor, have shown significant efficacy in patients with rheumatoid arthritis [1–4] and, in the area of cancer diseases, antibodies that recognize tumor antigens, such as CD52 or CD20, and eliminate the cancer cells that express them by triggering the effector function have shown survival benefit [5, 6]. Because these monoclonal antibodies have shown higher efficacy with fewer side effects than classical small-molecule drugs,

Michael Steinitz (ed.), *Human Monoclonal Antibodies: Methods and Protocols*, Methods in Molecular Biology, vol. 1904, https://doi.org/10.1007/978-1-4939-8958-4_9,

monoclonal antibodies now play an important role in the therapeutic field of various disease areas. As of June 2018, 73 recombinant monoclonal antibodies have been approved by the FDA, and more than 700 new candidates are entering into clinical trials.

Before the recent success of monoclonal antibodies, initial clinical studies of murine monoclonal antibodies obtained from hybridoma technology were hampered by the development of human anti-murine antibody (HAMA) response [7, 8]. As a result of the response, therapeutic murine monoclonal antibodies were cleared so rapidly from the body that efficacy in the clinical trial was limited.

To address these issues of murine-derived monoclonal antibodies, antibody engineering technology has been developed to generate chimeric and humanized antibodies in which the immune response (immunogenicity) against murine-derived monoclonal antibodies is reduced [9, 10]. Mouse-human chimeric antibody, in which the mouse constant region of murine-derived monoclonal antibody was replaced with a human constant region, significantly reduced the risk of immunogenicity. Furthermore, humanized antibody, in which mouse complementarity-determining regions (CDRs) of mouse-human chimeric antibody were grafted into human frameworks, further reduced the risk of immunogenicity while maintaining the therapeutic activity of the murine or chimeric antibody [11]. The method for generating humanized antibody from murine antibody, called CDR-grafting humanization, significantly contributed to the current success of therapeutic monoclonal antibodies [10].

A number of novel technologies have been reported that further reduce the potential immunogenicity of CDR-grafted humanized antibody [12, 13]. Aiming to reduce the potential immunogenicity of framework residues, researchers have used frameworks based on human germline sequences or consensus sequences as acceptor human frameworks rather than human frameworks with somatic mutation (s), which may include effector T-cell epitopes for some individuals [14–16]. Furthermore, aiming to reduce the potential immunogenicity of nonhuman CDRs, grafting specificity-determining residues (SDRs) has been proposed [17–19]. Instead of grafting the entire mouse CDRs into an acceptor human framework, only the SDRs, the minimum CDR residues required for antigen-binding activity, are grafted into the human germline framework. This SDR grafting method results in improved humanness (similarity to human germline sequence) of the humanized antibody and may reduce the number of effector T-cell epitopes in the mouse CDRs, potentially minimizing the risk of immunogenicity of the variable region. However, the exact effects of these additional humanization technologies (germline humanization and SDR grafting) on clinical immunogenicity have not been addressed in clinical.

Since the field of therapeutic monoclonal antibodies has become extremely competitive nowadays, especially against validated antigens, it is necessary to develop highly optimized antibody, not simply humanized antibody [20–23]. Highly optimized humanized antibody would have superior pharmacological properties important for clinical efficacy, such as high antigen-binding activity and long half-life, as well as biophysical properties important for commercial development of the therapeutic antibody, such as stability and expression yield. In order to efficiently generate such highly optimized antibody, it is necessary to consider these pharmacological and biophysical properties during the process of humanization.

A humanization process enabling the generation of highly optimized monoclonal antibody consists of five steps. The first step is to construct a three-dimensional structure model of parental nonhuman antibody by homology modeling. The second step is to select acceptor human frameworks appropriate for their antigen-binding activity, immunogenicity, expression, stability, and pharmacokinetics. The third step is to prepare expression vectors for multiple versions of humanized antibodies. The fourth step is to express and purify the humanized antibodies. The last step is to multidimensionally evaluate the humanized antibodies.

2 Materials

2.1 Selecting a Framework

1. 3D modeling software or web server (Accelrys Inc., CCG (Chemical Computing Group), WAM (Web Antibody Modeling), PIGS (Prediction of ImmunoGlobulin Structure), or Rosetta Antibody Modeling Server (RosettaAntibody).
2. GENETYX (GENETYX CORPORATION).

2.2 Expression and Purification

1. FreeStyle 293 Expression Medium (Thermo Fisher Scientific).
2. 293fectin Transfection Reagent (Thermo Fisher Scientific).
3. MILLEX-GV (0.22 μm or o.45 μm) (Millipore).
4. rProtein A Sepharose™ Fast Flow (GE Healthcare).

2.3 Antigen-Binding Activity

1. Biacore T200 (GE Healthcare).
2. Recombinant proteinA/G (Thermo Scientific).
3. Sensor chip (CM4, GE Healthcare).
4. Biacore T200 Evaluation Software (GE Healthcare).

2.4 DSC (Differential Scanning Calorimetry) Analysis

1. Microcal Capillary DSC system (GE Healthcare UK Ltd).
2. PBS.
3. Origin 7.0 software (OriginLab1 Corporation, Northampton, MA).

2.5 Size Exclusion Chromatography (SEC) Analysis

1. Alliance system (Waters, Milford, MA).
2. TSK gel G3000SWXL column (7.8 × 300 mm).
3. 50 mM sodium phosphate, 300 mM sodium chloride, pH 7.0.

2.6 Pharmacokinetics

1. C57BL/6J normal mice.
2. Anti-human IgG.
3. WinNonlin Professional (version 4.0.1) software (Pharsight).

2.7 Heat Acceleration Study

1. An slide-A-Lyzer™ MINI Dialysis Device, 10 K MWCO, 0.1 mL (Thermo Fisher Scientific).

3 Methods

3.1 Antibody Humanization

1. Constructing a structure model of the parental variable region

   If a crystal structure of the parental nonhuman antibody is not available, construct a homology model using available modeling methods. A number of well-established antibody modeling programs based on homology and conformational searching algorithms have been reported [24–29]. Computer software incorporating these methods is commercially available.

2. Selecting a framework

   Selecting the acceptor human frameworks while considering the four key factors—immunogenicity, antigen binding activity, expression/stability, and pharmacokinetics—is the most important step in obtaining highly optimized humanized antibody. The conventional CDR-grafting method uses single-acceptor human frameworks (frameworks 1, 2, 3, and 4 derived from single-human antibody germline sequence) for grafting parent CDRs and, therefore, it is generally difficult to meet all four key factors. In such cases, each nonhuman framework (frameworks 1, 2, 3, and 4) should be individually humanized by selecting the most appropriate human germline framework for that framework while considering all four key factors (Fig. 1). This approach, called framework shuffling, enables the selection of more desirable human frameworks for generating highly optimized humanized antibody—those that are not only less immunogenic, but also have high stability/expression and longer half-life.

   (a) Align each parental nonhuman antibody framework sequence (heavy chain frameworks 1, 2, 3, and 4 and light chain frameworks 1, 2, 3, and 4) with the human germline framework sequences obtained through the protein database, such as IMGT, V BASE, EMBL, or NCBI (*see* **Notes 1** and **2**).

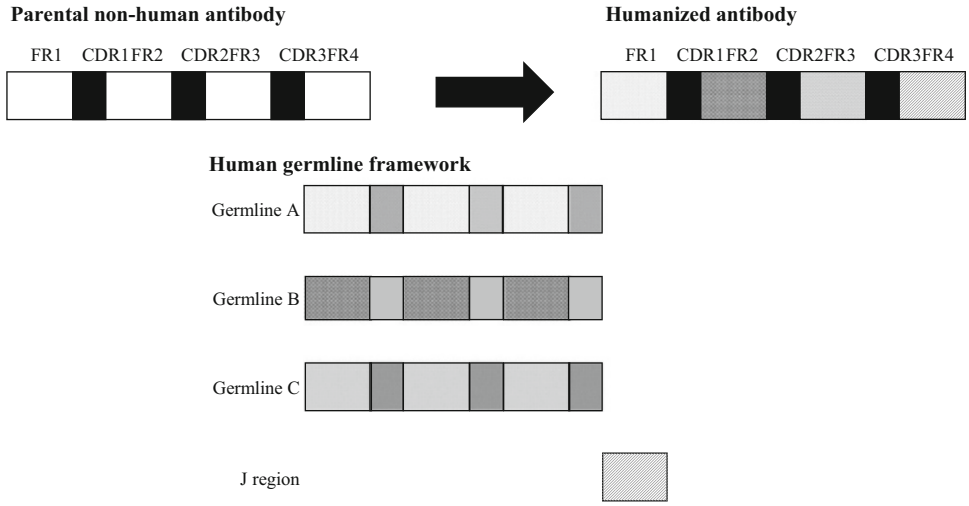

Fig. 1 Selecting the acceptor human framework by framework shuffling. Each acceptor framework is selected from a different germline framework for generating humanized antibody. In this case, humanized antibody is generated by using germline A as framework1, germline B as framework2, germline C as framework3, and J region as framework4

(b) Check the residues comprising the upper hydrophobic core within the immunoglobulin domain: these are located at positions 2, 4, 24, 27, and 29 in framework 1; 69, 71, 78 and 94 in framework 3 of the heavy chain, and at positions 2 and 4 in framework 1; and 64, 66 and 71 in framework 3 of the light chain of the parental nonhuman antibody framework sequence (residue positions are described in Kabat numbering) [30, 31] (Table 1).

(c) As a template for each parental nonhuman antibody framework, choose a human germline framework sequence that completely conserves all the upper hydrophobic core residues. Different human germline sequences can be used for humanizing each framework. This process is most important for maintaining the antigen-binding activity of the humanized antibody (*see* **Note 3**).

(d) In the selected human gemline framework sequences, check the residues in four key structures to generate humanized antibody with high expression and stability. The four key structure residues are as follows: hydrophobic residues that comprise upper and lower hydrophobic cores that are important for packing of the immunoglobulin domain and conformation of framework 1 [32, 33]; hydrophilic core residues that comprise the hydrogen bond network within the immunoglobulin domain;

Table 1
Sequence alignment of key residues of the human consensus VH and VL families

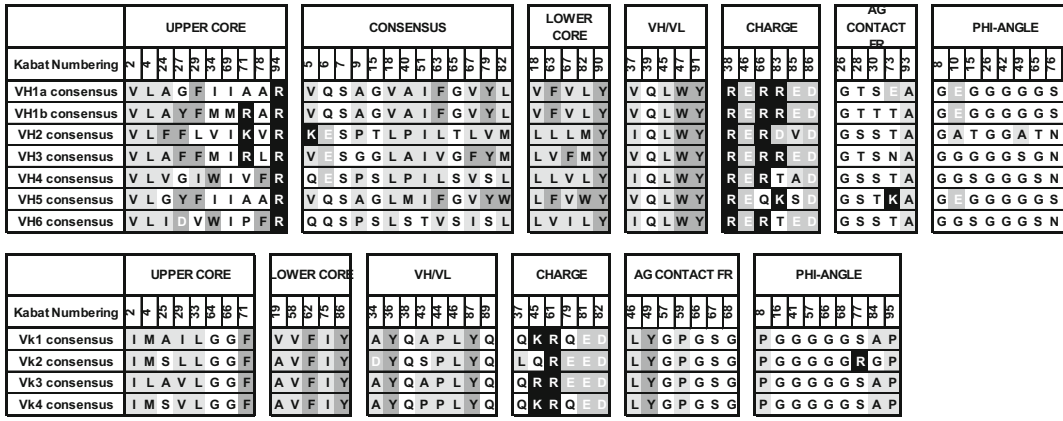

residues in turn structures (phi-angle); and residues located in the VH/VL interface (Table 1).

(e) All the above residues are highly conserved depending on the germline subgroups, especially those in the VH domain. To select appropriate human germline frameworks that are homologous to the parental nonhuman antibody framework, compare consensus residues and a structure model of parental nonhuman antibody with those of the consensus human germline antibodies (Table 1). Considering the similarity of the sequence and the structure, select a human germline framework with the correct residues at the correct positions as a template (*see* **Notes 4–6**).

(f) Determine the amino acid residues in the framework of parental nonhuman antibody which might influence antigen-binding activity. Amino acid residues that potentially influence the antigen-binding activity are summarized in Table 1. Check whether these residues could interact with the antigen by constructing a structure model of the parental nonhuman antibody.

(g) Compare the parental nonhuman antibody framework with the parental nonhuman germline framework with the highest homology, to identify distinctive amino acids in the framework. These distinctive amino acids derived from somatic mutation (s) in the framework might affect the antigen-binding activity.

(h) To generate humanized antibody with a longer half-life, select low isoelectric point (p*I*) frameworks containing larger numbers of Glu and asp residues and smaller numbers of Arg and Lys (*see* **Note 7**).

(i) Check how frequently the selected germline framework sequences are used in humanized antibody. If the frequency is extremely low, it could be immunogenic in some individuals. In such cases, reconsider whether another germline sequence with high frequency could be selected (*see* **Note 8**).

(j) There are no key residues in framework 4, therefore select the human germline sequence with the highest homology in the J region as framework 4.

(k) Compare the sequence of the designed humanized antibody framework with that of the parental nonhuman antibody.

(l) Check all the different amino acids between the designed humanized antibody framework and the parental nonhuman antibody.

(m) Check whether these different amino acids could affect the CDR conformation or antigen-binding activity using a constructed parental nonhuman structure model. Generally, amino acid residues that are exposed on the surface of the antibody and are distant from the CDRs do not affect the antigen-binding activity.

(n) Check whether or not the selected human germline frameworks have potential chemical modification sites, such as a deamidation site (Asn-Gly), an isomerization site (Asp-Gly), a surface exposed methionine residue, and a glycosylation site (Asn-X-Ser/Thr, where X is not Pro).

(o) Check again all the processes from **steps a-n** to confirm that there is no omission.

(p) Finally, select the appropriate human germline frameworks for 1, 2, 3, and 4, considering the stability, immunogenicity (germline frequency), pharmacokinetics (isoelectric point), and other chemical modification motifs (*see* **Notes 9–11**).

(q) Select the human signal sequence that is derived from the germline sequence used in framework 1 of the humanized antibody. The amino acid of the signal sequence can be obtained from the protein database described above (*see* **Note 2**).

3. Designing versions of humanized antibodies

   After designing the amino acid sequence of the variable region of the humanized antibody by connecting selected human germline frameworks with parental nonhuman CDRs, care should be taken on the boundary regions of selected human frameworks and parental nonhuman CDRs. For example, as a result of connecting the human germline framework and the parental nonhuman CDR, a potential deamidation site or glycosylation site might be generated on the boundary region. Presence of such modification sites could affect the commercial development of the humanized antibody. It is also possible to reduce potential immunogenicity by paying attention to the amino acid sequences of the boundary regions of selected human germline frameworks and nonhuman CDRs to increase humanness.

   (a) Design the amino acid sequence of the variable regions of designed humanized antibody by connecting individually selected human germline frameworks 1, 2, 3, and 4 and CDR 1, 2 and 3 of parental nonhuman antibody.

   (b) In the amino acid sequences of the boundary regions between the frameworks and CDRs, check whether a deamidation site (Asn-Gly), isomerization site (Asp-Gly), or glycosylation site (Asn-X-Ser/Thr, where X is not Pro) has been generated or not.

   (c) In the amino acid sequences of the boundary regions between the frameworks and CDRs, check whether designed boundary regions match with corresponding human germline boundary sequences. If they do not match, consider using another human germline framework that can be used as an acceptor framework. For example, Thr-Cys, Ser-Cys, and Asn-Cys are predominant amino acids at positions 22 and 23 of the light chain of the framework. If amino acids at positions 24 and 25 of the light chain of the CDR are Arg-Ser, amino acids at positions 22 and 23 of the framework are generally restricted to either Ser-Cys or Asn-Cys. If the selected framework amino acids at positions 22 and 23 are Thr-Cys, the potential immunogenicity risk of this variable region would be higher than using a framework with Ser-Cys or Asn-Cys at positions 22 and 23. In such cases, consider whether a germline framework with Ser-Cys or Asn-Cys at positions 22 and 23 of the light chain could be selected (*see* **Note 12**).

4. Expressing and purifying humanized antibody

   (a) Design the nucleotide sequences from the amino acid sequences of designed humanized variable regions and synthesize a designed cDNA sequence (*see* **Notes 13** and **14**).

(b) Insert the synthesized cDNA fragments of the full-length heavy and light chains (including signal sequence, humanized variable region sequence, and human constant region sequence) into a mammalian cell expression vector to construct the designed humanized antibody heavy chain and light chain expression vectors, respectively. Confirm the nucleotide sequences of the prepared expression vectors by DNA sequencing.

(c) Transiently express the antibody with FreeStyle 293 expression system.

(d) Centrifuge the culture supernatants to remove cells and filter them through a 0.45 or 0.22 μm filter. Purify the antibody from the obtained culture supernatants by using rProtein A Sepharose™ Fast Flow.

(e) Determine the concentration of the purified antibody by measuring the absorbance at 280 nm using a spectrophotometer and calculating the antibody concentration from the determined values using an absorbance coefficient calculated as previously described.

3.2 Evaluating Humanized Antibody Variants

Evaluating the humanized antibody variants in terms of antigen-binding activity, immunogenicity, pharmacokinetics, thermal stability (melting temperature), and accelerated stability study under elevated temperature is necessary for selecting highly optimized humanized antibody. However, it is not efficient to evaluate all these properties for a large number of generated humanized antibody variants, since some of them might have lower antigen-binding activity than the parental nonhuman antibody. Therefore, evaluating antigen-binding activity, thermal stability, expression level, and aggregation tendency, which are somewhat easy to conduct, is recommended as a primary screening when selecting highly optimized antibody.

1. Antigen-binding activity

   Assess the antigen-binding activity of the humanized antibody variants described above by using Biacore T200.

   (a) Capture purified humanized antibody variants to recombinant proteinA/G immobilized onto a sensor chip by an amino-coupling method.

   (b) Inject appropriate concentrations of the target antigen as an analyte.

   (c) Analyze the obtained sensorgrams by Biacore T200 Evaluation Software, and determine the KD (M) of each humanized antibody variant (*see* **Notes 15** and **16**).

2. DSC (Differential Scanning Calorimetry) analysis

   Assess the thermal stability of humanized antibody variants by measuring the melting temperature (Tm) using Microcal Capillary DSC system.

   (a) Dilute or dialyze the test sample at 0.15 mg/mL concentration into PBS, and use the corresponding buffer as a reference.

   (b) Scan the sample from 20 to 115 °C at a rate of 240 °C/h. Use a filtering period of 8 s and analyze the data using Origin 7.0 software.

   (c) Correct the result of thermograms by subtracting that of the control buffer and determine the Tm of each humanized antibody variant.

3. Expression level analysis

   Assess the expression level of each humanized antibody variant by comparing the concentration of purified antibodies in Subheading 3.1, **step 4**. However, the concentration of purified humanized antibody is affected not only by the expression level but also by the purification efficiency or recovery. If the precise expression levels of antibody variants are needed, antibody concentration in the supernatant should be determined by Biacore or ELISA using human IgG detection system.

4. Size exclusion chromatography (SEC) analysis
   Evaluate the aggregation tendency of humanized antibody variants by SEC using the high-performance liquid chromatography.

   (a) Inject the humanized antibody variants into a TSK gel G3000SWXL column (7.8 × 300 mm) at a flow rate of 0.5 mL/min. Use 50 mM sodium phosphate, 300 mM sodium chloride, pH 7.0 as a mobile phase buffer.

   (b) Detect the eluted humanized antibody variants by UV absorbance at 215 nm.

   (c) Analyze the data and calculate the content of aggregate (%) using Empower2 installed in Alliance system.

3.3 Analyzing Framework Back-Mutation

By selecting the frameworks 1, 2, 3, and 4 that conserve all the upper core and key structure residues, the humanized antibody generally maintains an equivalent antigen-binding activity to parental nonhuman antibody. However, if none of the humanized antibody variants can maintain an antigen-binding activity equivalent to the parental nonhuman antibody, framework back-mutation should be conducted.

1. Shuffle the parent and humanized heavy (VH) and light (VL) chain domains, and analyze the antigen-binding activity to

identify which domain (s) is responsible for the loss of antigen-binding activity (*see* **Note 17**).

(a) Humanized VH/Humanized VL.

(b) Humanized VH/Parent VL.

(c) Parent VH/Humanized VL.

(d) Parent VH/Parent VL.

2. Replace each human germline framework sequence in the VH and/or VL that is responsible for the loss of binding with the sequence from the parental nonhuman framework. Specifically, generate the following (a)-(d) antibodies, in which one of the four human germline frameworks is replaced with the parental nonhuman framework. Analyze the antigen-binding activity of these antibodies, and identify which framework (s) is responsible for the loss of antigen-binding activity.

   (a) pGL FR1_hGL FR2_hGL FR3_hGL FR4.

   (b) hGL FR1_pGL FR2_hGL FR3_hGL FR4.

   (c) hGL FR1_hGL FR2_pGL FR3_hGL FR4.

   (d) hGL FR1_hGL FR2_hGL FR3_pGL FR4.
   (hGL is the selected human germline sequence, and pGL is the parental nonhuman antibody framework).

3. To identify the amino acid residue (s) that is responsible for the loss of antigen-binding activity, compare the amino acid sequence of each human germline framework with that of the parental nonhuman antibody. Check the position of these amino acids using the constructed structure model to determine whether these amino acids should be substituted simultaneously or not. If these different amino acids are in close contact to each other and are expected to affect antigen-binding activity cooperatively, substitute these amino acids simultaneously to those of parental nonhuman antibody. If these amino acids are not in close contact to each other and contribute to the antigen-binding activity independently, substitute these amino acids separately. Determine the antigen-binding activity of these variants as described above.

3.4 Selecting Highly Optimized Humanized Antibody

After obtaining the humanized antibody variants which show comparable antigen-binding activity to that of parental nonhuman antibody, conducting pharmacokinetics and predicting the risk of immunogenicity are recommended as a second screening to select highly optimized humanized antibody.

3.4.1 Pharmacokinetics

1. Administer each humanized antibody variant at an appropriate dose to C57BL/6J normal mice by single intravenous (i.v.) or subcutaneous (s.c.) injection.

2. Collect blood samples from each mouse at an appropriate time after the injection.
3. Determine the concentration of each antibody in mouse plasma using anti-human IgG ELISA.
4. Calculate pharmacokinetic parameters (elimination half-life, clearance, and bioavailability) from the plasma concentration–-time data using non-compartmental analysis of WinNonlin Professional (version 4.0.1) software.

3.4.2 Immunogenicity

1. Predict the number of T-cell epitope (s) which may be present in the humanized antibody using an in silico tool (*see* **Note 18**).
2. To evaluate the potential immunogenicity, perform an HLA-binding assay that measures binding activity of the peptides with MHC class II or an in vitro T-cell assay using the peptides. Peptides for these assays can be selected by in silico prediction. These assays can identify the potential immunogenic peptides in the entire sequence of the humanized antibody.
3. To analyze the potential immunogenicity of whole humanized antibody, perform an in vitro T-cell assay, which detects the T-cell response to humanized antibody by ELISPOT or T-cell proliferation.

3.4.3 Evaluation of Antibody Stability

The stability of an antibody is one of the key factors to consider when selecting a clinical candidate, because chemical degradation of an antibody during the storage period and in plasma could reduce an antibody's binding ability, thus leading to poor efficacy in a future clinical trial. To select an antibody with sufficient stability for therapeutic use, a heat acceleration study is recommended.

1. Heat acceleration study
   (a) Prepare buffer solutions with different pH (*see* **Note 19**).
   (b) Dialyze antibody solution at 5 °C overnight to exchange the buffer with a slide-A-Lyzer™ MINI Dialysis Device, 10K MWCO, 0.1 mL (Thermo Scientific).
   (c) Adjust the concentration of antibody to 1 mg/mL and make enough aliquots of antibody solution for the number of data points (*see* **Note 20**).
   (d) Store one tube at 5 °C, which is taken as the tube for day 0, and the rest of the tubes at 40 °C.
   (e) Collect a tube at each data point and store it at 5 °C until the final data point, at which all the samples can be evaluated together.
   (f) Perform SPR (*see* Subheading 3.2, **step 1**) to analyze the binding ability, SEC (*see* Subheading 3.2, **step 4**), and SDS-PAGE.

2. Antibody engineering to remove a degradation hot spot
   When a heat acceleration study reveals that antigen-binding activity is markedly reduced, removal of the degradation hot spot(s) is an effective way to solve the issue. Or changing to a back-up antibody may be another option, if you have an appropriate one.
   (a) Check if either the heavy or the light chain has a degradation hot spot in its amino acid sequence (*see* **Notes 11** and **21**).
   (b) When a degradation motif is identified in either of the variable regions, substitute an amino acid of the motif with one of the other 18 amino acids (excluding the original amino acid and cysteine) (*see* **Note 22**).
   (c) Express and purify all the antibody variants with the substitutions according to the method shown in Subheading 3.1, **step 4** and perform SPR, DSC, and SEC, as shown in Subheading 3.2, **steps 1**, **2**, and **4**, respectively.
   (d) Select an antibody variant with a comparable binding affinity to the parent antibody (*see* **Note 23**).
   (e) Evaluate the stability of the selected antibody in a heat acceleration study, as described in **step 1**.

3.4.4 Selection of Highly Optimized Humanized Antibody

After obtaining pharmacological and biophysical properties of humanized antibody, these properties should be compared with each other to select the highly optimized humanized antibody. If there is just one highly optimized humanized antibody that has superior pharmacological and biophysical properties compared with all other humanized antibody variants, this can be the clinical candidate. However, such cases are very rare and, in most cases, some properties are superior, but other properties are not. Therefore, the key factors (antigen-binding activity, immunogenicity, stability/expression, and pharmacokinetics) should be prioritized according to the properties required for the humanized antibody. If a subcutaneous formulation is required, stability and pharmacokinetics may have higher priority since a stable, high-concentration formulation needs to be developed. For oncology diseases, immunogenicity might not be the highest priority since the immune response is often compromised in cancer patients.

4 Notes

1. Using human germline frameworks instead of human antibody frameworks with somatic mutation (s) as the acceptor frameworks could reduce the potential immunogenicity of the humanized antibody.

2. The protein database can be accessed through the web addresses of IMGT (http://www.imgt.org/), V BASE (http://vbase.mrc-cpe.cam.ac.uk/), EMBL (http://www.ebi.ac.uk/embl/), or NCBI (http://www.ncbi.nlm.nih.gov/).
3. Upper hydrophobic core residues are key residues for determining CDR structures and strongly affect the antigen-binding activity after CDR grafting. However, human germline sequences that conserve all the upper hydrophobic core residues may not be identified. In such a case, prepare human germline framework sequence variants in which upper hydrophobic core residues are substituted with those of the parental nonhuman framework to enable generation of humanized antibody which maintains an antigen-binding activity equivalent to that of parental nonhuman antibody. After this, check the possibility of back-mutating these substituted amino acid (s) to the germline sequence in order to minimize potential immunogenicity. This approach enables humanization to be completed quickly and allows properties to be optimized through the CDRs and the frameworks simultaneously.
4. Seven VH and seven VL (four of Kappa and three of Lambda) human germline consensus sequences have been generated by sequence homology and the conserved structure residues for each germline sequence have been identified [33].
5. Physicochemical properties of antibodies with these consensus sequences have been evaluated and have revealed that germline families of the heavy chain have a significant effect on the expression and stability of single-chain Fv, and that the VH3 germline family appears to have favorable properties. However, there is a report that CDR grafting into a VH3 germline framework does not necessarily result in stable single-chain Fv [34]. These reports indicate that several factors, including CDR sequences, contribute to the stability of humanized antibodies rather than a single parameter such as germline family.
6. A model structure of each consensus family can be obtained through the PDB database. Accession numbers of each subgroup are as follows: VH1a (1DHA), VH1b (1DHO), VH2 (1DHQ), VH3 (1DHU), VH4 (1DHV), VH5 (1DHW), VH6 (1DHZ), VK1 (1DGX), VK2 (1DH4), VK3 (1DH5), VK4 (1DH6), Vλ1 (1DH7), Vλ2 (1DH8), and Vλ3 (1DH9).
7. Antibody with lower p*I* has longer half-life [35]. Lower p*I* antibody has a more negatively charged antibody surface in plasma, which reduces the nonspecific uptake of the antibody into the cell by electrostatic repulsion between the low pI antibody and negatively charged cell surface.

8. Differences in the frequency of germline usage are reported, and it is known that particular germline frameworks are frequently used in the human antibody repertoire [36]. Since a germline framework with high frequency is considered to be more immune tolerant compared to that with low frequency, humanized antibody with a high-frequency germline framework sequence is expected to be less immunogenic.
9. An appropriate software, like GENETYX, can provide the theoretical isoelectric point of a designed humanized antibody.
10. If none of the framework sequences fulfills all the requirements described above, more than one framework could be selected for humanization. For example, one framework, termed FR1A, conserves the upper hydrophobic core and structure core residues but its p*I* is extremely high, and the second framework, termed FR1B, conserves upper hydrophobic core residues and has a pI but does not conserve structure core residues. In this case, FR1A and FR1B could both be selected as candidate acceptor frameworks.
11. Chemical modifications, such as deamidation, isomerization, succinimide formation, methionine, and tryptophan oxidation, often lead to reduced antigen-binding activity, and might affect immunogenicity, safety, or pharmacokinetics. Such modification sites should be removed before selecting the clinical candidate.
12. The framework sequences selected for humanization could affect the risk of immunogenicity of the boundary regions. Therefore, in silico tools such as Epibase (Lonza Inc.), iTope/TCED (Antitope Ltd.), and EpiMatrix (EpiVax Inc.) [37–41], which can predict the presence of peptide sequences carrying T-cell epitopes, could be used to predict the potential immunogenicity of designed humanized antibody variants. Although these in silico tools are valuable for predicting the risk of immunogenicity, it should be noted that they tend to be over-predictive.
13. Many companies, such as Life Technologies and GenScript USA Inc., provide gene design that considers codon adaptability, mRNA structure, and various cis-elements in transcription and translation. This provides levels of production and gene synthesis that are precise and efficient in comparison to conventional methods of assembly PCR. If your laboratories cannot use these services, nucleotide sequence of human germline framework can be obtained from IMGT, V BASE, EMBL, or NCBI, and cDNA sequence could be synthesized by assembly PCR.

14. If no human constant regions of the heavy and light chains are available in your laboratories, cDNA of the human constant regions also needs to be designed and synthesized.
15. With membrane-bound antigen, the antigen-binding activity of humanized antibody variants can be analyzed by Biacore using the extracellular domain of antigens, or by cell ELISA using a cell line expressing membrane-bound antigen.
16. For Biacore analysis, prepare extracellular domain of antigen with a tag, such as His6 tag. Extracellular domain of antigen is immobilized onto a sensor chip through anti-tag antibody. Inject humanized antibody variants as the analyte and determine the antigen-binding activity. For cell ELISA, prepare an antigen-expressing cell and determine the antigen-binding activity.
17. If the antigen-binding activity of ii is lower than that of iv, the loss of binding activity is caused by the VH domain of humanized antibody. Therefore, use the following process to identify which framework (s) and which amino acid (s) are responsible for the loss of binding activity.
18. These services are commercially available from many companies such as Antitope, Algonomics, Lonza (formerly Algonomics), and Proimmune.
19. It is mandatory to evaluate the stability of an antibody at pH 7.4, which equates to the physiological condition. In addition to that, assessing the stability of an antibody at other pH levels is recommended, such as pH 5.0 and pH 6.0. The pH markedly affects the speed of chemical degradation, so points that are missed in the assay at neutral pH may be identified under acidic conditions. For example, the deamidation rate is faster at neutral pH than at acidic pH, while the isomerization reaction is accelerated in acidic conditions.
20. The target antibody profile should be considered when deciding the data points. For example, when monthly treatment is set as part of the target antibody profile, the stability of the antibody should be tested for at least 1 month.
21. Numerous degradation hot spots have been reported [22], of which the sequence motifs of Asn-Gly (NG) and Asp-Gly (DG) are well known as hot spots for potent deamidation and isomerization, respectively.
22. When the NG motif is identified in a variable region, either N or G should be substituted with another of the 18 amino acids.
23. When several antibody variants retain a comparable binding affinity with the parent antibody, select the best antibody variant by considering other aspects, such as thermal stability, aggregation amount, and expression level.

References

1. Nishimoto N, Kishimoto T (2008) Humanized antihuman IL-6 receptor antibody, tocilizumab. Handb Exp Pharmacol 181:151–160
2. Buch MH, Emery P (2011) New therapies in the management of rheumatoid arthritis. Curr Opin Rheumatol 23:245–251
3. Tanaka T, Kishimoto T (2012) Immunotherapeutic implication of IL-6 blockade. Immunotherapy 4:87–105
4. Breedveld F (2011) The value of early intervention in RA-a window of opportunity. Clin Rheumatol 33:33–39
5. Pangalis GA et al (2001) Campath-1H (anti-CD52) monoclonal antibody therapy in lymphoproliferative disorders. Med Oncol 18:99–107
6. Weiner GJ (2010) Rituximab: mechanism of action. Semin Hematol 47:115–123
7. Schroff RW et al (1985) Human anti-murine immunoglobulin responses in patients receiving monoclonal antibody therapy. Cancer Res 45:879–885
8. Shawler DL et al (1985) Human immune response to multiple injections of murine monoclonal IgG. J Immunol 135:1530–1535
9. Boulianne GL, Hozumi N, Shulman MJ (1984) Production of functional chimaeric mouse/human antibody. Nature 312:643–646
10. Hwang WY, Foote J (2005) Immunogenicity of engineered antibodies. Methods 36:3–10
11. Jones PT et al (1986) Replacing the complementarity-determining regions in a human antibody with those from a mouse. Nature 321:522–525
12. Almagro JC, Fransson J (2008) Humanization of antibodies. Front Biosci 13:1619–1633
13. Wu H, Dall'Acqua WF (2005) Humanized antibodies and their applications. Methods 36:1–2
14. Tan P et al (2002) "Superhumanized" antibodies: reduction of immunogenic potential by complementarity-determining region grafting with human germline sequences: application to an anti-CD28. J Immunol 169:1119–1125
15. Hwang WY et al (2005) Use of human germline genes in a CDR homology-based approach to antibody humanization. Methods 36:35–42
16. Pelat T et al (2008) Germline humanization of a non-human primate antibody that neutralizes the anthrax toxin, by in vitro and in silico engineering. J Mol Biol 384:1400–1407
17. Tamura M et al (2000) Structural correlates of an anticarcinoma antibody: identification of specificity-determining residues (SDRs) and development of a minimally immunogenic antibody variant by retention of SDRs only. J Immunol 164:1432–1441
18. Gonzales NR et al (2004) SDR grafting of a murine antibody using multiple human germline templates to minimize its immunogenicity. Mol Immunol 1:863–872
19. Kashmiri SV et al (2005) SDR grafting—a new approach to antibody humanization. Methods 36:25–34
20. Maloney DG (2012) Anti-CD20 antibody therapy for B-cell lymphomas. N Engl J Med 366:2008–2016
21. Ducancel F, Muller BH (2012) Molecular engineering of antibodies for therapeutic and diagnostic purposes. MAbs 4:445–457
22. Igawa T et al (2011) Engineering the variable region of therapeutic IgG antibodies. MAbs 3:243–252
23. Strohl WR (2009) Optimization of Fc-mediated effector functions of monoclonal antibodies. Curr Opin Biotechnol 20:685–691
24. Greer J (1991) Comparative modeling of homologous proteins. Methods Enzymol 202:239–252
25. Morea V, Lesk AM, Tramontano A (2000) Antibody modeling: implications for engineering and design. Methods 20:267–279
26. Whitelegg NR, Rees AR (2000) WAM: an improved algorithm for modelling antibodies on the WEB. Protein Eng Des Sel 13:819–824
27. Marcatili P, Rosi A, Tramontano A (2008) PIGS: automatic prediction of antibody structures. Bioinformatics 24:1953–1954
28. Sircar A, Kim ET, Gray JJ (2009) RosettaAntibody: antibody variable region homology modeling server. Nucleic Acids Res 37:474–479
29. Almagro JC et al (2011) Antibody modeling assessment. Proteins 79:3050–3066
30. Ewert S, Honegger A, Plückthun A (2004) Stability improvement of antibodies for extracellular and intracellular applications: CDR grafting to stable frameworks and structure-based framework engineering. Methods 34:184–199
31. Ewert S et al (2003) Biophysical properties of human antibody variable domains. J Mol Biol 325:531–553
32. Honegger A, Plückthun A (2001) The influence of the buried glutamine or glutamate residue in position 6 on the structure of immunoglobulin variable domains. J Mol Biol 309:687–699

33. Jung S et al (2001) The importance of framework residues H6, H7 and H10 in antibody heavy chains: experimental evidence for a new structural subclassification of antibody V (H) domains. J Mol Biol 9:701–716
34. Honegger A et al (2009) The influence of the framework core residues on the biophysical properties of immunoglobulin heavy chain variable domains. Protein Eng Des Sel 22:121–134
35. Igawa T et al (2010) Reduced elimination of IgG antibodies by engineering the variable region. Protein Eng Des Sel 23:385–392
36. Glanville J et al (2009) Precise determination of the diversity of a combinatorial antibody library gives insight into the human immunoglobulin repertoire. Proc Natl Acad Sci U S A 106:20216–20221
37. Van WI et al (2007) Immunogenicity screening in protein drug development. Expert Opin Biol Ther 7:405–418
38. Perry LC, Jones TD, Baker MP (2008) New approaches to prediction of immune responses to therapeutic proteins during preclinical development. Drugs R D 9:385–396
39. Bryson CJ, Jones TD, Baker MP (2010) Prediction of immunogenicity of therapeutic proteins: validity of computational tools. BioDrugs 24:1–8
40. Koren E et al (2007) Clinical validation of the "in silico" prediction of immunogenicity of a human recombinant therapeutic protein. Clin Immunol 124:26–32
41. De Groot AS, McMurry J, Moise L (2008) Prediction of immunogenicity: in silico paradigms, ex vivo and in vivo correlates. Curr Opin Pharmacol 8:620–626

Chapter 10

Antibody Fragments Humanization: Beginning with the End in Mind

Nicolas Aubrey and Philippe Billiald

Abstract

Molecular engineering has made possible to reformat monoclonal antibodies into smaller antigen-binding structures like scFvs, diabodies, Fabs with new potential in vivo applications because they do not induce Fc-mediated functions. However, most of these molecules are from rodent origin. As a consequence, they are immunogenic and approval for administration to humans requires prior humanization. Today, there is no well-identified strategy to create recombinant humanized antibody V-domains that preserve the antigen-binding characteristics of the parental antibody associated with high stability and solubility. Here, we propose a strategy that consists in grafting CDRs onto properly chosen human antibody frameworks in order to reduce immunogenicity. A flowchart indicates the way to proceed in order to introduce an internal affinity purification tag while structural refinements are proposed to maintain antigen-binding characteristics. The best humanized candidates are identified through selection steps including in silico analysis, research scale production followed by early functional evaluation, purification assays, aggregation, and stability assessment.

Key words Monoclonal antibody, Therapeutic antibody, Fab, scFv, Protein L, Humanization, CDR grafting

1 Introduction

Antibody fragments often referred to miniaturized antibodies are made of antibody V-domains combined in a variety of ways to form recombinant antigen-binding molecules that fail to induce effector functions as antibody-dependent cell-mediated cytotoxicity or complement-dependent cytotoxicity. Antibody fragments include antigen-binding fragments (Fabs), single-chain variable fragments (scFvs), and "customized" structures such as dual-affinity re-targeting antibodies (DARTs) [1, 2].

Despite the small size and relative lack of complexity of antibody fragments, their development in view of clinical applications often proves troublesome. Nonhuman antibody V-domains not only remain potentially immunogenic but the lack of the Fc moiety

Michael Steinitz (ed.), *Human Monoclonal Antibodies: Methods and Protocols*, Methods in Molecular Biology, vol. 1904, https://doi.org/10.1007/978-1-4939-8958-4_10,

increases the risk of aggregation during production. In addition, the purification process from the cell host culture medium can be hard since antibody fragments do not interact with Protein A resins [3–5].

Today, molecular engineering and reformatting of antibodies derived from murine hybridoma remain the main source of recombinant therapeutic antibody fragments alongside in vitro selection of fully human molecules from antibody phage libraries or in vivo selection from transgenic mice [1]. There are lots of reasons for this including the availability of a near-limitless number of hybridomas secreting high-affinity antibodies directed against almost all antigenic molecules. Visiting the ATCC collection is very interesting from this point of view (www.atcc.org). Creation of recombinant antigen-binding molecules derived from hybridomas through rapid identification, cloning, and expression of the functional V-domains is now a well-standardized process [6]. However, the potential immunogenicity of murine antibody V-domains is a major barrier to injection in humans so that well-stratified strategies are expected for making these molecules more human. At the time of writing, three out of the four Fabs approved by the FDA for therapeutic applications were humanized fragments (idarucizumab, certolizumab, ranibizumab) while the fourth (abciximab) was a first generation antibody fragment produced from a chimeric mouse/human IgG, known to be poorly tolerated [7, 8].

Due to the nature of the antigen-specific binding site, antibody V-domains exhibit unique CDR structure and will always carry the risk of developing anti-idiotype antibodies [9]. However, significant safety gains can be made through humanization of the V-domains frameworks (Fig. 1). This will reduce the risk of hypersensitivity reactions and the generation of anti-drug antibodies (ADA) that can modify pharmacokinetics and contribute to loss of efficacy. Here, the challenge consists in maintaining correct packing of antibody domains and positioning of the CDRs in order to retain full binding properties and high structural stability to avoid the formation of immunogenic aggregates [10].

In this chapter, we propose a guided humanization protocol of antibody V-domains associated with a first line in silico validation and early in vitro assessment of antibody fragment function and stability. Embracing these guidelines as routine procedure should lead to fast generation of antibody-based molecules dedicated to clinical applications [11].

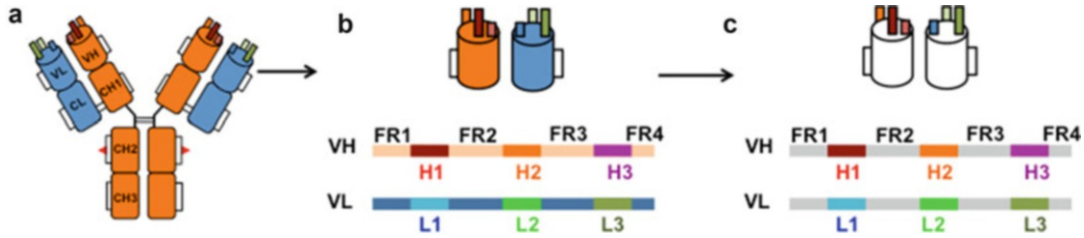

Fig. 1 Nonhuman immunoglobulin G and humanized antibody V-domains. (**a**) Natural nonhuman IgG made of two light chains (blue) and two heavy chains (orange), each organized in domains. (**b**) Fv variable fragment consisting of the variable domains VH and VL. Each variable domain contains three hypervariable loops (CDRs) whose association constitutes the antigen-combining site. In the sequence, CDRs H1 (red), H2 (orange), and H3 (purple) and L1 (blue), L2 (light green), and L3 (forest green) alternate with framework regions (FR) in light orange and dark blue for VH and VL, respectively. (**c**) Humanized Fv fragment. The nonhuman FRs have been substituted for appropriate human FRs (white) prior to additional refinements in order to maintain the topography of the combining site

2 Material

2.1 Data Bases and Web Resources for In Silico Humanization

1. Fully integrated web resources on antibodies including IMGT® (http://www.imgt.org) and the University College of London (UCL) antibodies website (http://www.bioinf.org.uk/abs/) [12–14].
2. Blastp search (http://www.uniprot.org/blast/).
3. PIGSpro: A web server developed at Sapienza university for antibody 3D-modeling (https://cassandra.med.uniroma1.it/pigspro/) [15].
4. MultAlin: A multiple sequence alignment software (http://multalin.toulouse.inra.fr/multalin/multalin.html) [16].
5. ProtParam: An online tool that allows the computation of physical and chemical parameters for a given protein (https://web.expasy.org/protparam/) [17].
6. The HLA peptide-binding prediction software developed at the NIH (https://www-bimas.cit.nih.gov/molbio/hla_bind/) [18].

2.2 Expression and Purification of Recombinant Antibody Fragments

1. Instrumentation: laminar flow hood, CO_2 incubator, centrifuge.
2. Cell host for expression, preferentially CHO.
3. Plasmids for expression will be constructed using basic molecular biology for gene cloning, plasmid propagation and purification.
4. HiTrap Protein L column (GE Healthcare).

2.3 Primary Screening of Humanized Antibody Fragments

1. Instrumentation: PAGE-Electrophoresis equipment.
2. NuPAGE 4–12% Bis-Tris Protein gel.
3. Control antibody fragment: abciximab, Reopro® (Lilly).

2.3.1 SDS-PAGE

2.3.2 ELISA for Antigen-Binding Screening

1. Instrumentation: Microplate spectrophotometer.
2. 96-Wells microtiter plate for ELISA.
3. Protein target.
4. Coating buffer: 50 mM sodium carbonate buffer pH 9.6.
5. Blocking solution: 1% bovine serum albumin in PBS pH 7.4 or equivalent.
6. Washing buffer PBS pH 7.4 containing Tween-20 0.1%.
7. Anti-human IgG (Fab specific)-peroxidase conjugate.
8. Protein L-peroxidase conjugate.
9. Peroxidase substrate: StepTM Ultra TMB-ELISA or equivalent.
10. 2 M H_2SO_4.

2.4 Size-Exclusion Chromatography

1. Instrumentation: AKTA purifier FLPC system or equivalent.
2. Superdex 75 10/300 GL chromatography column or equivalent.
3. Running buffer: PBS pH 7.4.
4. Molecular weight markers for gel filtration chromatography.

2.5 SPR Analysis

1. Instrumentation: Biacore 200 biosensor and BIAevaluation 3.0 software (GE Healthcare).
2. Carboxymethylated dextran CM5 chips, EDC and amine coupling kit (GE Healthcare).
3. Protein target.

2.6 Stability

1. Instrumentation: Thermostated spectrofluorometer (FS5, Edinburgh instrument).
2. Adapted quartz cuvettes.

3 Methods

3.1 Structural Analysis of the Parental Nonhuman V-Domain Templates

The sequence encoding the functional nonhuman antibody V-domains of interest must be available when starting with this protocol (*see* **Note 1**). Then, proceed step by step as indicated hereafter.

1. Numbering and CDR identification: using the DomainGapAlign tool on the IMGT website, input the VL domain sequence (also designated as VL0, hereafter) in FASTA format, the domain type (V), and the source species (*see* **Note 2**). Also, select the graphical representation "IMGT collier de perles." The software will identify the type of light chain (IGK for kappa or IGL for lambda chain). The "Collier de perles" allows us to identify the amino acid residue position using IMGT numbering, the IMGT-frameworks, the IMGT-CDRs, and the anchor residues (Fig. 2a). Save the "one layer collier de perles" (*see* **Note 3**). Proceed in the same way when starting to analyze VH domain sequence (also designated as VH0, hereafter).
2. Canonical classes: Paste the VL0 and VH0 sequences in the canonical class identification tool at UCL (http://bioinf.org.uk/abs/chothia.html) and proceed to the analysis. This will allow you to identify the canonical class type and subclasses (*see* **Note 4**). Save results using autogenerated SDR templates.
3. Degree of humanness: the VL0 and VH0 sequences are successively uploaded in the box of the UCL software (http://bioinf.org.uk/abs/shab/). For each sequence, the software assigns a *Z*-score that correlates with antigenicity (*see* **Note 5**).
4. Packing angle: Input the VL0 and VH0 sequences in the packing angle prediction server at UCL (http://www.bioinf.org.uk/abs/paps/). This server will predict the VH/VL packing angle in a set of structures from the PDB data bank (*see* **Note 6**).
5. 3D-modeling: In case a crystal structure of the antibody is not available, create a 3D-structural model using PIGSpro software [15]. Upload VH0 and VL0 sequences and proceed to modeling in an automatic or manual fashion. The software will display a 3D-model with coloured CDRs and full rotating options. Sequence alignment with the template will be available and PDB file can be downloaded for further inspection with the molecular graphics PyMOL interface.
6. Using IMGT/DomainGapsAlign, identify the closest human germline V-REGION and J REGION alleles for VL0 and VH0. Paste the VL0 protein sequence, select V-domain type and *Homo sapiens* species. Record the percentage of sequence identity with the closest gene and allele sequences from the IMGT domain. Proceed in the same way with VH0.
7. All the data collected here above will be stored and summarized as indicated in Fig. 2.

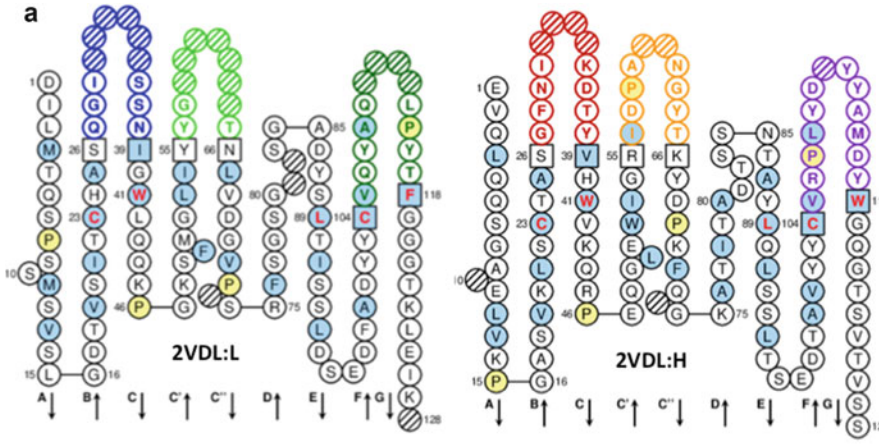

b

	type	Canonical structure	Z-score	p.cent identity with human germline	Packing angle
VL0 (2VDL:L)	IGKV	L1: similar to 2 / 11A L2: 1 / 7A L3: similar to 1/ 9A	-1.5	IGKV1-8*01 **67.0 %** 94 overlap	
VH0 (2VDL:H)	IGHV	H1: 1 / 10A H2: 2 / 10A	-0.9	IGHV1-69-2*01 **65.6 %** 98 overlap	**-42.1**

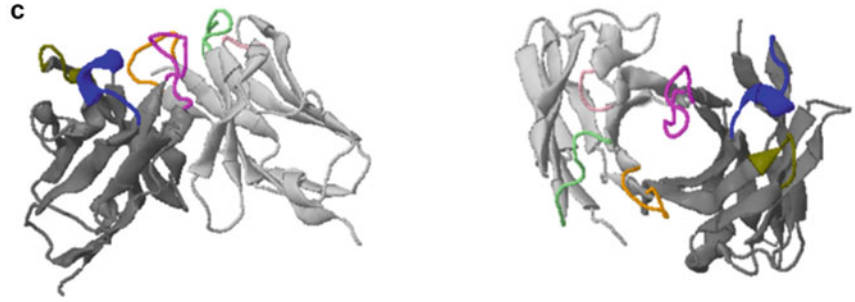

Fig. 2 Structural analysis of nonhuman antibody V-domains to be collected prior to the humanization process (here exemplified with antibody 10E5, abciximab, 2VDL.pdb). (**a**) "Collier de perles" showing the amino acid residues with the IMGT unique numbering. The CDRs L1, L2, and L3 are in blue, light green, and forest green respectively. CDRs H1, H2, and H3 are in red, orange, and purple respectively. The anchor residues are shown in square. (**b**) Main structural features of the nonhuman V-domains. (**c**) 3D-structural model of Fv domains generated using PIGS software. Side view (left) and Top view (right)

3.2 Design of Humanized V-Domains

3.2.1 Identification of Human Framework Acceptors

The antibody humanization process starts with the selection of human framework acceptor regions. We recommend identifying four templates for each nonhuman V-domain according to four independent criteria. In so doing, chances of identifying a lead with optimized properties in terms of immunogenicity and safety, antigen-binding activity, and structural stability at the end of the

whole process are increased. Figure 3 summarizes the stepwise process leading to humanized V-domains.

1. Selection of acceptor frameworks based on criterium 1: *Most similar human germline*.

   Using IMGT/DomainGapsAlign, identify the closest human germline V-REGION and J REGION alleles for VL0. Proceed as in Subheading 3.1, **step 6**. Save the closest gene and allele sequence identity and % identity from the IMGT domain. Cut/paste the sequence into a word editing format. Do the same with VH0.

   The closest human sequences IGKV-J-region or IGLV-J region for VL0 and IGHV-D-J-region for VH0 will be designated hereafter as TL1 and TH1 for human light chain and heavy chain acceptors, respectively.

2. Selection of acceptor frameworks based on criterium 2: *High sequence identity*.

   Using blastp search compare the nonhuman VL0 sequence against the UniProtKB protein sequence database. Paste the sequence in FASTA format and run the search. Then, filter the result by popular organisms (human). Select the sequence with the highest match hit that encodes a functional antibody V-domain. Save the identity code and % of identity. Display the alignment. Download the sequence in Fasta format. Proceed in the same way with VH0.

   These sequences will be designated TL2 and TH2, respectively.

3. Selection of acceptor frameworks based on criterium 3: *Best fit using V-domains from the same human or humanized antibody*.

   Using PIGSpro software, input human TL1 and TH1 sequences. Run a search. Select templates from the same antibody structure even if a different template with a higher sequence identity exists for one or both chains. Ensure this antibody is from human origin or humanized. Save its identification code as in the PDB databank and copy/paste its V-domain sequences (*see* **Note 7**).

   These sequences will be designated as TL3 and TH3, respectively.

4. Selection of acceptor frameworks based on criterium 4: *Fixed framework*.

   At the RCSB-PDB data bank (https://www.rcsb.org), successively download myeloma antibodies REI (1REI) and NEW (7FAB) as human framework acceptor regions for VL0 and VH0, respectively (*see* **Note 8**). Select "sequence" tab and download FASTA file. Here below, these sequences will be designated as TL4 and TH4, respectively.

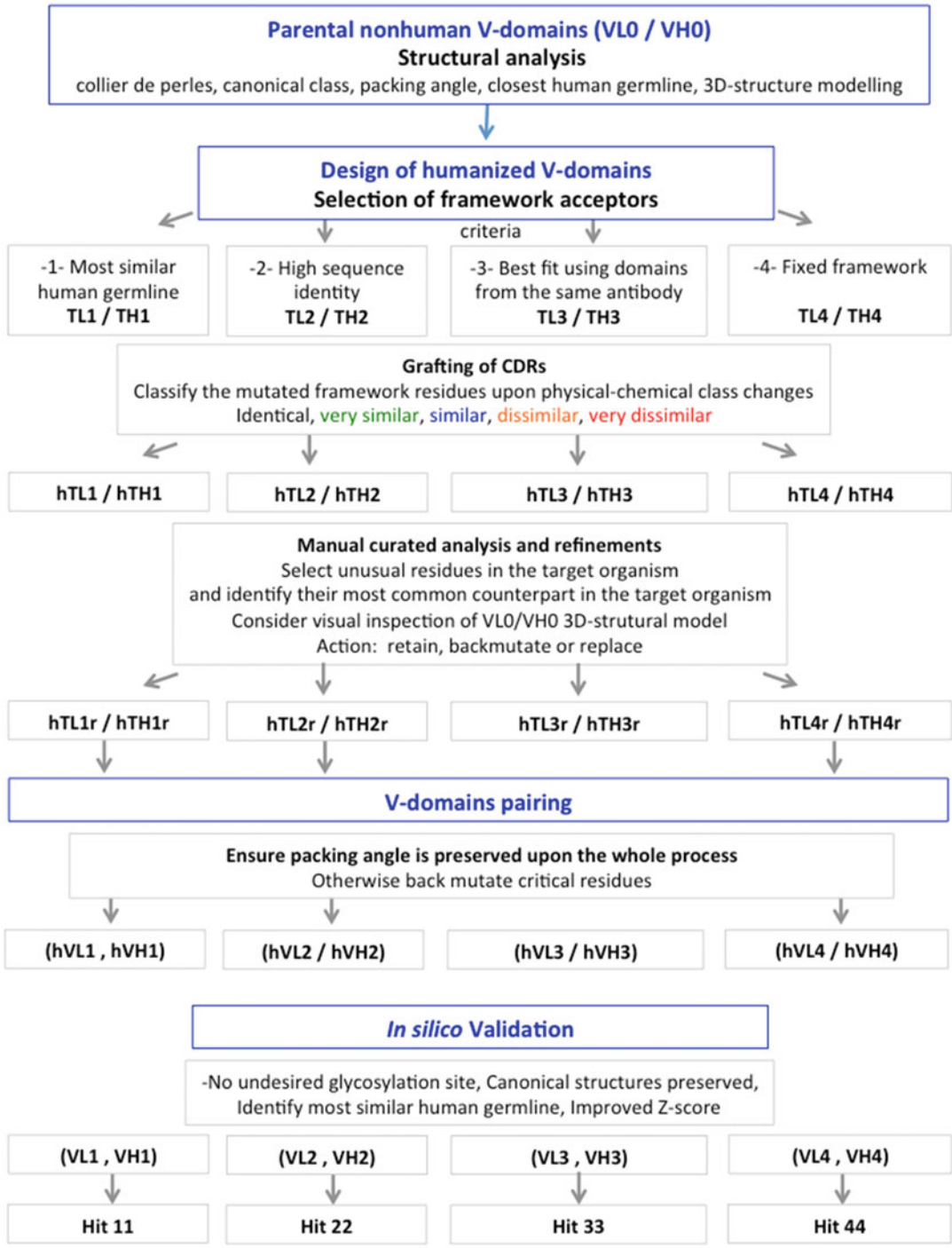

Fig. 3 Flowchart depicting the stepwise process leading to the humanization of nonhuman monoclonal antibody V-domains

3.2.2 Optional: Engineering of a Protein L (PpL)-Binding Site

In case the light chain of the antibody is of kappa type, it may be of interest to graft a protein L (PpL)-binding site for purification. PpL is an alternative to the current IgG purification gold standard (Protein A) and also allows efficient capture of antibody fragments (Fabs and scFvs) which is not the case with Protein A. Here, we suggest conferring PpL-binding ability without affecting humanness.

1. A straightforward strategy consists in using the DIQMTQSPSSLSASVGDRVTITCR N-terminal sequence as a substitute for the L1 to L24 residues of the humanized V-kappa domain (*see* **Note 9**).

3.2.3 Grafting of CDRs

1. Using Multalin online facility, align parental nonhuman light chain sequence (VL0) with acceptor sequences (TL1 to TL4). Select "normal" for the output style. Edit the results as an htlm page and copy/paste in a text editor.
2. Graft the nonhuman CDRs and anchor residues, all identified according to the IMGT nomenclature, on each of the human acceptors. Use the same color code as in "collier de perles" for CDRs and black color for framework residues. Underline residues belonging to CDRs. This leads to 4 humanized VL domains designated as hTL1 to hTL4. Proceeding like this should enable us to preserve original canonical structures.
3. While focusing on the humanized frameworks now, classify each mutated residue according to physico-chemical class changes: Very similar (green), similar (blue), dissimilar (orange), and very dissimilar (red) (*see* **Note 10**). Keep other residues in black.
4. Now considering the parental nonhuman heavy chain sequence (VH0), repeat **steps 1–3**. This leads to four humanized VH domains designated as hTH1 to hTH4.

3.2.4 Manual Curated Analysis and Refinements

1. Using abYsis, analyze one by one the humanized template sequences (*see* **Note 11**). Select "annotate" in the list box. Enter the protein sequence to be analyzed. Proceed in a sequential manner from hTL1 to hTL4 and then from hTH1 to hTH4.
2. Select "humanize" option and pay special attention to the sequence in the second row. Unusual residues in the target organism (human) are shown in red. Now, only consider those residues that are located in the IMGT-frameworks which were identified as different or very different from the original nonhuman sequences when proceeding with Subheading 3.2.3, **step 3** (residues colored in orange or red).
3. Analyze the residues identified in **step 2** one after the other.

First, locate the residue not only within the "collier de perles" but also using the 3D model.

In case the residue is close to one of the CDRs and depending on the structure and size of the antigen targeted, the side chain of the mutated residue may impact the antigen/antibody interaction. For this reason, we suggest to back mutate.

In case the side chain of the residue is exposed on the surface or is buried inside the antibody domain and far from CDRs, maintain the substitution and do not back mutate.

The sequence revised in this way will be designated with the suffix "r" (i.e., hTL1 will lead to hTL1r).

4. Go back to **step 1** with the next sequence. When refinements have been carried out for all sequences, go to the next section.

3.3 V-Domain Pairing

1. Proceed to pairing each humanized VL with its VH partner (hTL1r with hTH1r and so on for hTL2r, hTL3r, and hTL4r).
2. For each paired VL/VH, determine the packing angle value using the UCL facility at http://www.bioinf.org.uk/abs/paps/.
3. For each pair with the exception of (hTL3r, hTH3r), ensure the value observed is identical or close to the one of the VL0/VH0 pair (*see* **Note 12**). In case it is not, proceed to back mutation of residues buried in VL/VH interface. Critical residues are L44, L46, L47, L50, L52, L103 for VL and H38, H47, H50, H68, H70, H103, H120 for VH. Here, it is a priority to back mutate residues which show very dissimilar physico-chemical properties when compared to VL0 and VH0. Inspection of the 3D-model helps to identify additional residues of VL and VH domains that are in close vicinity or in contact (H40, H44).
4. Ensure that the back mutations introduced have restored a packing angle value identical or close to the original one.
5. At the end of this process the humanized V-domains are designated as hVL1 to hVL4 for IGKV or IGLV and hVH1 to hVH4 for IGHV.

3.4 Validation of the Humanized Sequences

Proceed independently for each hVL and hVH humanized sequence.

1. Even if it is unlikely, ensure that no N-linked glycosylation site (Asn-X-Ser/Thr) has been introduced during the process, otherwise back mutate.
2. Ensure that all hVL and all hVH domains differ from each other. Otherwise, go back to initial step.
3. Using the canonical class identification tool at UCL, ensure the nonhuman canonical structures are preserved throughout the

whole process. Otherwise ensure that grafting of IMGT-CDRs and anchor residues was done in an appropriate manner as indicated in Subheading 3.2.3, **step 2**. In case their identity is not preserved in the final sequence, restore.

4. Using the IMGT/DomainGapAlign tool, ensure the % identity with human germline has improved during the process when compared to the nonhuman counterpart (VL0 or VH0). It should be close to or higher than 80%. If this is not the case, leave the sequence behind, go back to Subheading 3.2.1. Using the same criterium, select the next acceptor sequence of the list and run all the process again.
5. Using the humanness assessment facility at UCL (http://www.bioinf.org.uk/abs/shab/), match the sequence against characterized human antibody sequences. Run the search after selecting the targeted database (human light or heavy chain sequences) and the option "overlap the mouse *Z*-score with the query and human sequences." Ensure the quality of humanness has improved in the process. The *Z*-score must have shifted toward a positive value (*see* **Note 5**). In case *Z*-score has not been improved, determine the *Z*-score for each of the intermediate templates generated over the whole humanization process and identify the first one for which *Z*-score has not been improved. Inspect the mutations that have been introduced at that step and proceed either to some back mutation or to mutations as deduced from abYsis suggestions (*see* Subheading 3.2.4, **step 3**) provided they contribute to improve the *Z*-score. In case this is not successful, reconsider whether another acceptor sequence satisfying the original criterium could be selected.
6. Rank 9-mer peptides potentially able to bind HLA class I molecules (https://www-bimas.cit.nih.gov/molbio/hla_bind/). Select a cut point of 90. In case peptides are above the cut point, try to reduce the immunogenic potential by mutating the one or two amino acids responsible for this score. To do that, either back mutate or select one of the most frequent residues displayed at these positions in human antibodies using "humanize" option from the menu at the top of the AbYsis program.
7. Check whether any unusual residue has been introduced over the whole process using the "antibody sequence test" at http://www.bioinf.org.uk/abs/seqtest.html.
8. At the end of the validation process the sequences will be designated as VL1 to VL4 and VH1 to VH4 (*see* **Note 13**).

3.5 Expression of Recombinant Antibody Fragments

In routine, four humanized recombinant antibody fragments will be produced resulting from pairing VL1 with VH1 (hit 11), VL2 with VH2 (hit 22), VL3 with VH3 (hit 33), VL4 with VH4 (hit 44)

(Fig. 3). In addition, each humanized VL can be paired with any of the other humanized VH (for instance VL1 with VH4, leading to hit 14). This will increase the diversity maximizing the chance to identify binders. In this way up to 16 humanized antibody fragments will be synthesized. Whatever the strategy, it is also worth pairing together the murine VL (VL0) and VH (VH0), which will serve as a reference (chimeric recombinant antibody fragment, hit 00).

We suggest producing the recombinant antibody fragments in a Fab format. It is recommended to select CHO cells and a bicistronic vector for expression and secretion but many other efficient expression systems are available (*see* **Note 14**).

3.5.1 Plasmid Construction

1. A cDNA encoding the mammalian leader sequence "MDMRVPAQLLGLLLLWLRGARC" followed by the VL0 fused with homo sapiens Ig kappa constant (IGKC*01) is designed after codon optimization for expression in mammalian cells. Introduce correct unique restriction sites flanking the entire gene. If possible, introduce an additional unique restriction site in the cDNA at the junction of variable and constant domain of each chain to allow potential C-domain shuffling and the construction of other antibody fragments in a straightforward manner.
2. A cDNA encoding the leader sequence "MDWTWRILFLVAAATGAH" followed by the VH0 fused with homo sapiens Ig heavy constant gamma 1 (IGHG1) followed by nine residues (EPKSCDKTH) is designed after codon optimization for expression in mammalian cells. Introduce correct unique restriction sites flanking the entire gene.
3. Order customized synthetic genes encoding the sequence designed here above (**steps 1** and **2**). It is worth here to order genes cloned in a bicistronic vector directly suitable for transient expression (i.e., pBIC-PS, NVH Medicinal, F) using the appropriate cloning sites. This process will lead to expression vector V-00 encoding the chimeric light chain and the chimeric Fd chain.
4. For any of the humanized VL (VL1 to VL4) and VH (VH1 to VH4), proceed as in **steps 1** (for VL) and **2** (for VH). The bicistronic expression vectors designed in this way will be designated as V-11 to V-14, V-21 to V-24, V-31 to V-34, V-41 to V-44 were the first digit designates the humanized VL type and the second digit designates the humanized VH type (*see* **Note 15**).
5. Transform bacteria with each of the plasmids. Grow an overnight culture of bacteria from single colonies harboring the desired plasmid and prepare plasmid DNA using an endotoxin-free plasmid preparation kit.

3.5.2 Transfection and Cell Culture

1. CHO cells are thawed 2 weeks prior to transfection and maintained at $3{\cdot}10^5$ viable cell/mL in complete protein-free medium at 37 °C, 5% CO_2 atmosphere.
2. On the day of transfection, cells are split in a number of flasks corresponding to the expected number of transfections at $10{\cdot}10^5$ viable cells/mL in 30 mL medium.
3. The expression plasmid is introduced into mammalian cells using the transfection reagent according to the manufacturer's instructions and cells are cultured in protein-free medium.
4. Twenty-four hours post transfection, monitor cell viability on a daily basis. Typically, cells should maintain over 80% viability in the first 5 days. When the viability drops significantly (day 6 post-transfection), the cell-free medium is collected after centrifugation ($3000 \times g$), aliquoted and stored at −20 °C.

3.6 Primary Screening of Humanized Fab Fragments

3.6.1 Small-Scale Expression Screening

1. Expression of each variant is analyzed by SDS-PAGE under nonreducing and reducing conditions. 10–20 μL of each cell-free supernatant are loaded. When running samples, always take a positive control (i.e., abciximab, 0.5 μg) and a negative control (supernatant of CHO).
2. Gels are stained with Coomassie blue to visualize protein content.

3.6.2 Functional Screening

1. Antigen-binding activity is analyzed by direct ELISA using plates coated with the antigen (100 μL) at a concentration of 0.5–1 μg/mL in 50 mM $NaHCO_3$ buffer (pH 9.6) at 4 °C overnight. Depending on the antigen, coating conditions may have to be optimized.

   All subsequent steps are performed at room temperature.
2. The plates are blocked with the blocking solution for 1 h. Then the cell-free culture medium (100 μL) is added to the plate at three successive dilutions (1:10, 1:100; 1:1000) in duplicate for 1 h incubation.
3. After washing with Tris-buffered saline containing 0.05% Tween 20, an anti-human IgG (Fab specific)-peroxidase conjugate or PpL-peroxidase conjugate is added to the plate and is incubated for 1 h.
4. After washing the plate, the assay is developed using the peroxidase substrate solution, and development of the color product is terminated by the addition of 0.1 M HCl.
5. The absorbance for each well is measured at 450 nm using a microplate reader. The binding activity of Fab is determined by subtracting the absorbance of background binding from the value obtained with Fab.

6. Hits for which the capacity to bind the antigen is demonstrated both through anti-human IgG and PpL primary binders are selected (*see* **Note 16**).

3.7 Protein L Capture and Product Homogeneity

1. Protein L column (1 mL) equilibrated in PBS pH 7.4 is loaded with up to 20 mL of cell-free supernatant dialyzed against PBS pH 7.4.
2. The column is washed with PBS pH 7.4 until monitoring $A_{280\ nm}$ reaches 0.01 AU.
3. Elute Fab bound to the matrix with 0.1 M Glycine-HCl at pH 2.5 (five column volumes) and collect 500 μL fractions on ice immediately neutralized with Tris 1 M (50 μL).
4. Identify fractions in which the Fab product is eluted by using the $A_{280\ nm}$ absorption.
5. Pool fractions with $A_{280\ nm}$ higher than 0.1 AU and dialyze them against PBS. Centrifuge, check $A_{280\ nm}$, and take an aliquot.
6. Evaluate the purity by SDS-PAGE followed by Coomassie brilliant blue staining under reducing and nonreducing conditions (Fig. 4a).

3.8 SPR Analysis

Humanized variant functionality and off-rate kinetics are analyzed using PpL affinity purified samples.

1. We routinely use CM5 sensor chips and the amine coupling method for immobilization for the antigen to target (Fig. 4b).
2. Fab samples (0, 10, 50, 100, and 500 nm in PBS pH 7.4) are injected at a flow rate of 20 μL/min for 2 min and allowed to dissociate for 3 min, followed by a 5-s regeneration pulse of 10 mM HCl. The binding experiments are performed in triplicate at 25 °C in PBS.
3. Rate constants are calculated using the BIAevaluation 3.0 software. A K_D in the nM range or even lower indicates quite a good affinity.

3.9 Aggregates and Oligomers

1. Dilute the protein samples in PBS pH 7.4 ($A_{280\ nm}$: 0.9 AU) and carry out a UV-vis spectrum from 220 to 350 nm (*see* **Note 17**).
2. Using size-exclusion chromatography (SEC) will allow any multimers to be detected. Equilibrate a Superdex 75 10/300 GL column with PBS pH 7.4 at 0.8 mL/min.
3. Inject 100 μL of PpL-purified Fab ($A_{280\ nm}$: 0.9 AU) at a flow rate of 0.8 mL/min and record the elution with a UV recorder at 280 nm.

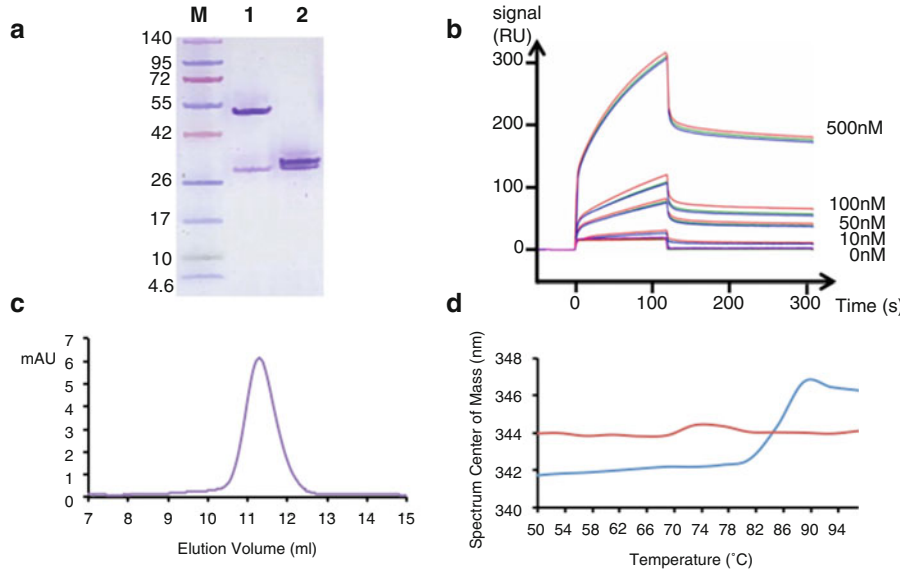

Fig. 4 Typical features of a recombinant humanized Fab analysed after transient expression in CHO cells and Protein L (PpL) capture. (**a**) SDS-PAGE analysis under non-reducing (1) and reducing (2) conditions of proteins eluted from PpL resin. M: molecular weight markers (kDa). (**b**) Interaction of immobilized antigen with purified humanized Fab analysed by SPR at 500, 100, 50, 10 and 0 nM, in triplicate. (**c**) Typical elution profile of PpL-purified humanized Fab after gel filtration on a calibrated Superdex 75 10/300 GL column. (**d**) Unfolding transition is observed by following the variation of the fluorescence spectra center of mass of the Trp fluorescence as a function of temperature. Blue: humanized Fab; Red: reference material (abciximab)

4. When the sample has passed the column, inject a molecular weight standard. Record the UV280nm chromatogram and calibrate (Fig. 4c).

3.10 Thermal Stability

1. Purified Fab solution (0.75 nM in PBS) is placed in a quartz cuvette which is inserted in the thermostated support of the spectrofluorometer with slit widths of 1 and 5 nm for excitation and emission respectively.
2. Excite the sample at 275 nm and record the emission spectra from 310 to 410 nm at increasing temperatures from 25 to 97 °C. For each temperature, four spectra are recorded (Fig. 4d).
3. Identify the wavelength corresponding to Spectrum Center of Mass (nm). Its temperature-dependent evolution makes it possible to determine the Tm of the fragment (*see* **Note 18**).

4 Notes

1. It is worth recording direct evidence that the nonhuman antibody V-sequences identified for the project encode a molecular unit with the desired specificity. Indeed, some hybridomas are not well characterized or express additional variable regions [19, 20]. Starting the process with sequences that do not encode the antibody of interest would be detrimental to the project. Therefore, it is recommended to design, produce, and evaluate antigen-binding properties of a recombinant antibody-fragment made of the original V-domain sequences [6].
2. The IMGT/DomainGapAlign tool allows identifying the closest germline V-REGION and J-REGION alleles for V-domains from any species or from specified species. It allows alignment and identification of amino acid changes as very similar, similar, dissimilar, and very dissimilar. As an option it provides a standardized 2D graphical representation of antibody V-domains primary or secondary structure also called "Collier de perles". The IMGT standards have been approved by the World Health Organization-International Union of Immunological Societies (WHO-IUIS) Nomenclature Committee. They will be used all along this chapter.
3. "Collier de perles" is a graphical 2D representation of antibody V-domains based on the IMGT unique numbering. This representation makes it possible to identify the CDRs and the framework regions according to IMGT unique numbering and nomenclature. Amino acid residues are shown in the one-letter abbreviation. Anchor positions supporting the hypervariable loops are shown in squares. The CDRs are colored in blue, light green, and forest green (L1, L2, and L3 respectively) and in red, orange, and purple for H1, H2, and H3 respectively [21]. Hatched circles correspond to missing positions. Arrows indicate the direction of the beta strands and their designation. IMGT delimitation of antibody CDRs has proven to be more appropriate for preserving antigen-binding after humanization according to the CDR grafting strategy. This can be exemplified with several therapeutic antibodies including alemtuzumab [22, 23]. Correspondence with other nomenclatures (Kabat, Chothia) is available at AbNum (http://www.bioinf.org.uk/abs/abnum/).
4. "Canonical structures" refer to secondary structure characteristics and the main-chain conformations of antibody V-domains. These conformations are determined by the length of the loops and also by the presence of key residues not only in the loops, but in the frameworks that determine the

conformation through their packing, hydrogen bonding, or the ability to assume unusual main-chain conformations [24–26]. The canonical class identification tool at UCL allows identifying classes and subclasses using the autogenerated SDR template with a more accurate identification than when using strict Chothia SDR templates. Although CDR H3 loop is critical for specific antigen-binding activity, H3 conformation has proven unclassifiable and thus the corresponding canonical features will be ignored at this early step.

5. *Z*-score is the result of a complex calculation which takes into account the mean sequence identity of a sequence scored against a set of human sequences [12]. It represents how typical a sequence is in the human repertoire and, in doing so, contributes to prediction of antigenicity. A *Z*-score of zero represents a sequence which shows average similarity to the repertoire of human sequences targeted. Sequences with positive *Z*-scores show higher sequence identity with human sequences while negative *Z*-score have a less typically human character. Over the humanization process, the *Z*-score is expected to increase and reach a value close to, or above 0. On the graphical representation, the *Z*-score of the query sequence is plotted as a vertical line that should have shifted from the murine to the human profile when compared to the nonhuman counterpart. *Z*-score must be seen as a decision aid tool in support of the IMGT/DomainGapAlign analysis. Indeed, some human sequences are less typically human in nature than mouse sequences [27].
6. Preserving antigen-binding activity requires not only correct conformation of the CDRs as indicated in **Note 4**, but also correct position of both polypeptide chains with respect to each other [13]. The VH/VL packing angle usually ranges from −60.8° to −31.0°. Such a variation can have a significant impact on the topography of the combining site. This is the reason why special attention should be paid at the interface positions L44, L46, L47, L50, L52, L103, H38, H47, H50, H68, H70, H103, and H120. Some of these residues interact with each other and mutations may also alter the stability of the functional unit.
7. The "best fit using VH and VL from the same human or humanized antibody" strategy is intended to preserve the packing of the interface between V-domains [13]. The best option is to select the antibody with the closest VH. If several are available, consider the VL in a second phase.

   In some cases, the method may not allow identifying V-domain acceptors from the same antibody. An alternative consists in screening the KEGG drug database for therapeutic antibodies

sequences (http://www.genome.jp/kegg/drug). Usually, antibodies from this database are well characterized in terms of solubility, stability, and expression. However, by proceeding in this way, one must take care not to infringe any existing intellectual property. This strategy was used for the first FDA-approved humanized antibody (daclizumab, Zinbryta®) using Eu human IgG as acceptors [28].

8. The "fixed framework strategy" does not require any database search. It has proven to be successful for several humanized antibodies, the first one being alemtuzumab [22]. Human myeloma proteins NEW and REI are used as templates because their X-ray 3D-structures are available (7FAB.pdb and 1REI.pdb). These molecules are well characterized in terms of stability and expression. However, the fixed framework may require greater number of back mutations to achieve the goal of an active molecule [29].
9. Ninety-five percent of mouse immunoglobulins contain kappa light chain [30]. As a consequence, the vast majority of humanized therapeutic antibodies are made of a kappa chain (IGK) and not a lambda chain (IGL). Protein L (PpL) has a strong affinity for a conformational motif occurring in more than 60% V-kappa chains with no detrimental effect on epitope-paratope interaction. This property makes PpL a valuable tool for affinity capture of antibody fragments and for detection in functional assays such as ELISA. GMP grade PpL resins are now marketed for pharmaceutical development. PpL-binding ability is highly dependent on several residues belonging to V-kappa FR1 and this is the reason why we recommend grafting the DIQMTQSPSSLSASVGDRVTITCR sequence to engineer a PpL-binding site on any antibody fragment. Usually, this sequence does not alter the humanness or the antigen-binding activity [11]. Alternatively, a manual curated analysis and the mutation of a limited number of residues can be considered. For efficient PpL interaction, two residues in IGKV FR1 are critical and must be absolutely preserved: Pro_{L8} and Arg_{L18}. Ser_{L10}, Leu_{L11}, Thr_{L20} are advantageous while Pro_{L12} and Pro_{L15} are deleterious and have to be replaced by Ser and Val, respectively. In addition several other residues contribute to the interaction including residues at position L24 [4].

   In case the antibody light chain belongs to the lambda type and not kappa, do not try to engineer a PpL-binding site. LambdaFabSelect® is an affinity resin binding dedicated to the capture of antibody fragments containing lambda light chain. It should meet the need of an efficient purification system.
10. Amino acid residues differ from each other by their side chain. When undertaking substitution into the sequence, it is worth considering three properties of the residue side-chains:

i. hydroxypathy classes, i.i. volume, and i.i.i. chemical characteristics as indicated in [31] (http://www.imgt.org/IMGTeducation/Aide-memoire/_UK/aminoacids/IMGTclasses.html). Residues belonging to the same group under the three criteria will be considered very similar. Residues sharing two properties out of the three will be similar. Two residues will be considered dissimilar when exhibiting only one common property out of the three. Finally, very dissimilar residues do not have any common properties according to this classification.

11. AbYsis is a web-based antibody research system that provides a user-friendly and flexible server for structural analysis [32]. A list box displays various options including "annotate" for antibody sequence analysis and humanization. A link to the University College of London (UCL) website is also available.
12. (hTL3r, hTH3r) pair has been designed based on the "best fit using VH and VL from the same human or humanized antibody" strategy. One of the main advantages of this strategy is that the packing of the interface is likely to be optimum in terms of structural stability and solubility. For this reason, it is advised to preserve critical residues of hTL3 and hTH3 templates buried in the VH/VL interface.
13. There is no definitive strategy to remove all the immunogenicity related to the sequence. As a first-line analysis, we simply recommend combining the use of computational tools to identify the degree of homology with human germlines and the humanness *Z*-score. Several methods based on HLA-binding motifs have also been developed to identify peptide epitopes. However, these methods tend to over-predict the number of functional epitopes within a given sequence. Immunogenicity will always be present in some antibody molecules [9]. This is due, in part, to the fact that each antibody is selected for a unique epitope specificity and consequently exhibits a unique structure. This is well exemplified by adalimumab, a fully human antibody, that can induce neutralizing antibodies in a subset of patients that varies between 5% and 89% depending on the disease and therapy [33]. When the lead is identified, we suggest validating the whole process by using the Food and Drug Administration (FDA) recognized algorithm EpiMatrix developed at Epivax (Providence, RI) which correlates well with in vivo [34]. In vitro assay using naïve peripheral blood mononuclear cells (PBMC) are not recommended until host cell proteins or endotoxins contaminate the sample of interest [35].
14. Because antibody fragments are usually aglycosylated proteins, a wide range of host cells have been reported, the most popular

being mammalian cells (preferentially HEK or CHO), yeast cells (*Pichia pastoris*), and bacteria (*Escherichia coli*). In order to avoid in vitro refolding which is a long and tedious task, we suggest using host cell expression systems suitable for the secretion of the recombinant antibody fragment into the culture supernatant after selection of appropriate leader sequences. It is beyond the scope of this chapter to detail the construction of these systems and the selection process, but several comprehensive protocols have been reported elsewhere using basic molecular biology and cell culture techniques [36, 37]. As an illustration we report here a transient expression system which was successfully used to select the lead of a humanized anti-thrombotic Fab [11].

15. A more cost-effective but also more time-consuming strategy for synthesis and cloning of expression vector may consist in ordering genes encoding VL1 to VL4 and VH1 to VH4 without constant domain, flanked with unique restriction sites. Genes synthesized in this way will be cloned sequentially into the bicistronic vector in order to encode each of the designed humanized Fabs. Correct V-domain exchange will be confirmed by sequencing of the plasmids prior moving on. Basic molecular biology will be carried out as in [6].
16. Rapid ELISA screening is essential to identify the variants that satisfy both antigen-binding and PpL recognition criteria. The best antigen-binders will first be identified after developing with anti-human Ig-peroxidase conjugate. The signal should be dose-dependent, in the same range as the one observed for the chimeric Fab which is expected to preserve the original murine antibody antigen-binding properties. Among the best antigen-binders identified as above, those leading to a signal at least twice as high as the one observed with the irrelevant Fab (abciximab) when developing with PpL-peroxidase conjugate, will be selected. In the unlikely event that no PpL binders are identified, select the lead among the best antigen-binders. Some alternatives to PpL have been reported for purification of antibody fragments. These include Kappa select® which is a resin coupled with a 14 kDa affinity ligand to Kappa chain constant domain and also CaptureSelect® resin which displays a camelid-derived single-domain antibody fragment of a VHH anti-CH1. Both alternatives will only be valuable for antibody fragments carrying constant domains (Ck or CH_1) such as Fabs, not for scFvs.
17. During the humanization process some hydrophobic spots may have been generated onto the molecule and contribute to the formation of multimeric structures and aggregates with potential adverse effects including immunogenicity and reduced drug efficacy. Monitoring UV-vis spectrum of

PpL-purified Fab and $A_{320\ nm}/A_{280\ nm}$ ratio will allow detecting sub-micron aggregates while nano-aggregates (dimeric and multimeric Fabs) will be identified following SEC-HPLC analysis. These observations will be of interest in view to optimize the formulation and selection of adjuvants for long-term stability and bioactivity [38].

18. Thermal shift fluorescence analysis is a rapid and inexpensive initial method to investigate the stability of a label-free protein. The purified recombinant protein in its folded state is slowly heated to undergo thermal denaturation. Because intrinsic tryptophan fluorescence is very sensitive to protein conformational changes in the local environment, the fluorescence maximum shift and changes in fluorescence intensity are recorded. This allows monitoring unfolding transitions in proteins upon thermal denaturation [39].

    The method can also be used under a wide range of buffer solutions (ionic strength, pH, additives) to identify the best formulation in a high-throughput context.

    This approach is a common alternative to circular dichroism spectroscopy (CD), infrared spectroscopy (IR), and differential scanning calorimetry which require expensive instrumentation.

References

1. Alvarenga LM, De Moura JF, Billiald P (2017) Recombinant antibodies: trends for standardized immunological probes and drugs. In: Current developments in biotechnology and bioengineering. Elsevier Science, Amsterdam, Boston, pp 97–121
2. Nelson AL (2010) Antibody fragments: hope and hype. MAbs 2:77–83
3. Grodzki AC, Berenstein E (2010) Antibody purification: affinity chromatography – protein A and protein G Sepharose. Methods Mol Biol 588:33–41
4. Lakhrif Z, Pugnière M, Henriquet C et al (2016) A method to confer Protein L binding ability to any antibody fragment. MAbs 8:379–388
5. Lebozec K, Jandrot-Perrus M, Avenard G et al (2018) Quality and cost assessment of a recombinant antibody fragment produced from mammalian, yeast and prokaryotic host cells: a case study prior to pharmaceutical development. New Biotechnol 44:31–40
6. Fields C, O'Connell D, Xiao S et al (2013) Creation of recombinant antigen-binding molecules derived from hybridomas secreting specific antibodies. Nat Protoc 8:1125–1148
7. Schuurman J, Parren PW (2016) Editorial overview: special section: new concepts in antibody therapeutics: what's in store for antibody therapy? Curr Opin Immunol 40:vii–xiii
8. Wagner CL, Schantz A, Barnathan E et al (2003) Consequences of immunogenicity to the therapeutic monoclonal antibodies ReoPro and Remicade. Dev Biol 112:37–53
9. Harding FA, Stickler MM, Razo J et al (2010) The immunogenicity of humanized and fully human antibodies. MAbs 2:256–265
10. Moussa EM, Panchal JP, Moorthy BS et al (2016) Immunogenicity of therapeutic protein aggregates. J Pharm Sci 105:417–430
11. Lebozec K, Jandrot-Perrus M, Avenard G et al (2017) Design, development and characterization of ACT017, a humanized Fab that blocks platelet's glycoprotein VI function without causing bleeding risks. MAbs 9:945–958
12. Abhinandan KR, Martin ACR (2007) Analyzing the "degree of humanness" of antibody sequences. J Mol Biol 369:852–862
13. Abhinandan KR, Martin ACR (2010) Analysis and prediction of VH/VL packing in antibodies. Protein Eng Des Sel 23:689–697

14. Lefranc M-P, Ehrenmann F, Ginestoux C et al (2012) Use of IMGT(®) databases and tools for antibody engineering and humanization. Methods Mol Biol 907:3–37
15. Lepore R, Olimpieri PP, Messih MA et al (2017) PIGSPro: prediction of immunoGlobulin structures v2. Nucleic Acids Res 45: W17–W23
16. Corpet F (1988) Multiple sequence alignment with hierarchical clustering. Nucleic Acids Res 16:10881–10890
17. Appel RD, Bairoch A, Hochstrasser DF (1994) A new generation of information retrieval tools for biologists: the example of the ExPASy WWW server. Trends Biochem Sci 19:258–260
18. Parker KC, Bednarek MA, Coligan JE (1994) Scheme for ranking potential HLA-A2 binding peptides based on independent binding of individual peptide side-chains. J Immunol 152:163–175
19. Bradbury A, Plückthun A (2015) Reproducibility: standardize antibodies used in research. Nature 518:27–29
20. Bradbury ARM, Trinklein ND, Thie H et al (2018) When monoclonal antibodies are not monospecific: hybridomas frequently express additional functional variable regions. mAbs 10(4):539–546
21. Ehrenmann F, Lefranc M-P (2011) IMGT/DomainGapAlign: IMGT standardized analysis of amino acid sequences of variable, constant, and groove domains (IG, TR, MH, IgSF, MhSF). Cold Spring Harb Protoc 2011:737–749
22. Riechmann L, Clark M, Waldmann H et al (1988) Reshaping human antibodies for therapy. Nature 332:323–327
23. Lefranc M-P, Pommié C, Ruiz M et al (2003) IMGT unique numbering for immunoglobulin and T cell receptor variable domains and Ig superfamily V-like domains. Dev Comp Immunol 27:55–77
24. Chothia C, Lesk AM, Gherardi E et al (1992) Structural repertoire of the human VH segments. J Mol Biol 227:799–817
25. Chothia C, Lesk AM (1987) Canonical structures for the hypervariable regions of immunoglobulins. J Mol Biol 196:901–917
26. North B, Lehmann A, Dunbrack RL (2011) A new clustering of antibody CDR loop conformations. J Mol Biol 406:228–256
27. Gao SH, Huang K, Tu H et al (2013) Monoclonal antibody humanness score and its applications. BMC Biotechnol 13:55
28. Queen C, Schneider WP, Selick HE et al (1989) A humanized antibody that binds to the interleukin 2 receptor. Proc Natl Acad Sci U S A 86:10029–10033
29. Waldmann H, Hale G (2005) CAMPATH: from concept to clinic. Philos Trans R Soc Lond Ser B Biol Sci 360:1707–1711
30. Woloschak GE, Krco CJ (1987) Regulation of kappa/lambda immunoglobulin light chain expression in normal murine lymphocytes. Mol Immunol 24:751–757
31. Pommié C, Levadoux S, Sabatier R et al (2004) IMGT standardized criteria for statistical analysis of immunoglobulin V-REGION amino acid properties. J Mol Recognit 17:17–32
32. Swindells MB, Porter CT, Couch M et al (2017) abYsis: integrated antibody sequence and structure-management, analysis, and prediction. J Mol Biol 429:356–364
33. Getts DR, Getts MT, McCarthy DP et al (2010) Have we overestimated the benefit of human(ized) antibodies? MAbs 2:682–694
34. De Groot AS, McMurry J, Moise L (2008) Prediction of immunogenicity: in silico paradigms, ex vivo and in vivo correlates. Curr Opin Pharmacol 8:620–626
35. Jawa V, Cousens LP, Awwad M et al (2013) T-cell dependent immunogenicity of protein therapeutics: preclinical assessment and mitigation. Clin Immunol 149:534–555
36. Nettleship JE, Flanagan A, Rahman-Huq N et al (2012) Converting monoclonal antibodies into Fab fragments for transient expression in mammalian cells. In: Hartley JL (ed) Protein expression in mammalian cells. Humana Press, Totowa, NJ, pp 137–159
37. Gupta SK, Shukla P (2017) Microbial platform technology for recombinant antibody fragment production: a review. Crit Rev Microbiol 43:31–42
38. Raynal B, Lenormand P, Baron B et al (2014) Quality assessment and optimization of purified protein samples: why and how? Microb Cell Fact 13:180
39. Callis PR (1997) 1La and 1Lb transitions of tryptophan: applications of theory and experimental observations to fluorescence of proteins. Methods Enzymol 278:113–150

Chapter 11

Antigen-Specific Human Monoclonal Antibodies from Transgenic Mice

Susana Magadán Mompó and África González-Fernández

Abstract

Due to the difficulties found when generating fully human monoclonal antibodies (mAbs) by the traditional method, several efforts have attempted to overcome these problems, with varying levels of success. One approach has been the development of transgenic mice carrying immunoglobulin (Ig) genes in germline configuration. The engineered mouse genome can undergo productive rearrangement in the B-cell population, with the generation of mouse B lymphocytes expressing human Ig (hIg) chains. To avoid the expression of mouse heavy or light chains, the endogenous mouse Ig (mIg) loci must be silenced by gene-targeting techniques. Subsequently, to obtain antigen-specific mAbs, conventional immunization protocols can be followed and the mAb technique used (fusion of activated B cells with mouse myeloma cells, screening, cloning, freezing, and testing) with these animThis chapter summarizes the most common chromatographic mAb andals expressing human Ig genes. This chapter describes the type of transgenic-knockout mice generated for various research groups, provides examples of human mAbs developed by research groups and companies, and includes protocols of immunization, generation, production, and purification of human mAbs from such mice. In addition, it also addresses the problems detected, and includes some of the methods that can be used to analyze functional activities with human mAbs.

Key words Human monoclonal antibodies, Transgenic mice, Immunoglobulin transgenes, Knockout mice, Transloci bearing human Ig genes, Gene targeting, YAC-based human Ig transloci

1 Introduction

Antibodies are one of the main defense mechanisms of vertebrate animals, able to neutralize and destroy pathogens with the help of other components of the immune system. Until the development of monoclonal antibodies (mAbs) in 1975 by Köhler and Milstein [1], antisera containing a mixture of several types of antibodies (polyclonal antibodies) were used for diagnostic or therapeutic purposes. The first evidence that mAbs could have therapeutic potential came in the early 1980s, when a patient (Philip Karr) suffering from a lymphoma showed a clear response to treatment with mouse antibodies directed against the Ig idiotype in his tumor cells [2]. Soon after, several pharmaceutical companies started to

Michael Steinitz (ed.), *Human Monoclonal Antibodies: Methods and Protocols*, Methods in Molecular Biology, vol. 1904, https://doi.org/10.1007/978-1-4939-8958-4_11,

become involved in the production of mAbs directed against different human cell-surface molecules, developing antibodies for the treatment of cancer and autoimmune diseases, as well as against transplant rejection processes. From the first clinical trials, it became clear that murine antibodies could be immunogenic [3]. After several immunizations, patients developed hypersensitivity reactions and anti-murine antibodies were produced (HAMA: human anti-mouse antibodies or HARA: human anti-rat antibodies), thereby reducing the potential of antibodies in human therapy.

Although the use of fully human mAbs could have several advantages compared with the use of murine antibodies (lower immunogenicity, better interaction with human effector systems such as opsonization, binding to Fc receptors, or the same glycosylation pattern), the production of human mAbs has resulted to be more tedious than first thought. There have been several attempts to produce fully human mAbs, which are very well addressed in other chapters of this book. The use of viral infection, fusion with human myeloma cells, and heterohybridomas with mouse myeloma fused to human B cells are just three examples of approaches to produce the tumoral transformation of B cells. The low yields of antibody production, the absence of a stable human myeloma cell line, the instability of the heteromyelomas produced, and the technical problems found during the fusions all led to the search for new alternative methods for obtaining human antibodies in large quantities.

One of these alternatives was the genetic modification of murine antibodies. The genetic structure of Igs with discrete gene domains made their manipulation relatively easy by changing murine sequences to human ones. Chimerization, humanization, CDR grafting, and chain shuffling were the methods used to decrease the antigenicity of the murine antibodies [4], while trying to maintain the affinity and specificity of the original antibodies. Indeed, several chimeric or humanized antibodies have already been approved by the Food and Drug Administration (FDA) of the United States and by the European Medical Agency (EMEA) [5, 6]. However, immune responses to chimeric or humanized antibodies have also been observed in patients, especially in those receiving mAbs for long periods of time due to their chronic processes [7], which reinforced the need to go one step further and obtain fully human antibodies.

The use of phage libraries carrying human Ig genes was one of the techniques that allowed the production of fully human mAbs [8]. The cloning of human Ig coding regions in phage genes (single-chain Fv fragments, scFv) allowed the production of phages libraries with different Ig specificities. In this context, the selection of the antibody with the desired specificity and affinity is carried out by the sequential enrichment of engineered phages against a specific

antigen. This method has numerous advantages, including that no animal immunization is required, any antigen can be used (even when highly toxic) and it has a low cost. Initially, there were some problems when using phage libraries carrying human Ig sequences, among others: low affinity; absence of glycosylation in the antibody fragments; and immunogenicity to some random combinations of heavy and light chains that are not normally found in vivo. Moreover, without the Fc regions, the scFV scFvs do not fulfill certain important effector functions such as antibody-dependent cytotoxicity, complement activation, or induction of phagocytosis, which are essential for some therapies. Although most phage libraries only carry variable Ig regions (single-chain Fv from heavy and light chains), using adequate expression systems (such as the cloning of coding regions for heavy and light chains in mammalian cells), it was possible to produce fully human antibodies, overcoming the problems mentioned above [9, 10].

New expression vectors, the identification of adequate places for the gene integration of the genome, and the development of new methods to grow cells have turned the cell culture system into the most suitable approach for producing high yields of human antibodies. The most frequently used cell lines are those of lymphoid origin, like mouse myelomas (NSO or SP2/0) that are easy to transfect and have a high secretory level, and non-lymphoid cells, such as CHO (from Chinese hamster ovary) or Hela (from human cervical cancer). Differences in the pattern of Ig glycosylation are crucial elements for the immune response that can be generated against such engineered human antibodies. It is known that around 1% of the IgG molecules present in human serum are directed against the epitope α1,3-Gal β1,4-GlcNAc, probably due to their presence in enteric bacteria [11]. Although murine cells can add a terminal α1,3 galactose to the antibodies, making them highly immunogenic [12], human, primate, and CHO cells have lost the enzyme responsible for this type of glycosylation [13]. Some examples of fully human mAbs using phage display are adalimumab (anti-TNFα) against rheumatoid arthritis, Crohn's disease or psoriasis, and ABT-874 against p40 (neutralizing both IL-12 and IL-23) [5, 9].

The introduction of human hematopoietic cells into severe combined immunodeficient (SCID) mice is another approach/ for producing human antibodies. These mice receive human hematopoietic cells (either into fetal tissue or peripheral blood cells) [14, 15] and are immunized to generate fully human mAbs. To produce Trimera mice, conventional animals are totally irradiated to destroy their bone marrow. These mice then receive a bone marrow transplant, obtained from SCID mice, and subsequently human hematopoietic tissue. Following antigen immunization, hybridomas secreting antigen-specific human antibodies can be generated from such treated mice [16]. However, maintenance of

these animals is not easy, as it requires special installations and sterile conditions, while the animals can suffer from agammaglobulinemia, severe lymphopenia, and infections.

In the 1980s, thanks to the development of molecular biology techniques and to the advances in the manipulation of embryonic cells, in microinjections and in the use of several vectors, different models were generated of transgenic mice carrying Ig genes (initially of mouse or rat origin) [17]. The first transgenic mice carried a rearranged mouse Ig transgene, but the expression of the transgene was very poor. New attempts, including rearranged mouse or rat Ig genes entirely under their own control regions, allowed the correct expression of the transgenes. This opened up the possibility for other research groups to introduce more Ig genes into the mouse germline, either in rearranged or in un-rearranged form. The generation of several transgenic mice carrying different types of Ig transgenes has provided, and continues to provide invaluable information about phenomena such as, among others, the following: control of expression of Ig genes; allelic and isotypic exclusion; the rearrangement and somatic hypermutation processes [17–20]; description of regulatory elements; identification of hotspots and cold mutations; and the development of new techniques, such as the use of Peyer's patches B cells to analyze mutations [21–23].

After this success, in the 1990s, some researchers tried to engineer mouse strains by the introduction of human immunoglobulin genes codifying for heavy and light chains into the mouse germline. These transgenic mice carrying un-rearranged sequences of human immunoglobulin genes could potentially now produce B cells expressing human Igs. This was possible because human sequences were shown to be compatible with the mouse factors involved in the rearrangement of Ig genes, class switch, and affinity maturation. The animals could secrete fully human antibodies in their serum with a diverse repertoire, be immunized in a conventional way, and undergo similar processes of selection and maturation to mouse B cells. These strains could now be used to generate mouse hybridomas following the classical approach of producing a large panel of fully human mAbs with high affinity and specificity, against a large repertoire of antigens (pathogens, proteins, or even human tumor cells) [24–26].

As reviewed by Brüggemann [27], transgenic mice were developed using vectors containing different amounts of foreign DNA: miniloci; bacteriophage P1 clones; bacterial chromosomes (BACs); yeast chromosomes (YACs); or human chromosome fragments (HCF). One important question was how many genes (especially of variable regions) should be integrated, following the hypothesis that a larger number of genes could generate a wider repertoire of antibodies. As miniloci or plasmids only integrate low amounts of foreign DNA, artificial chromosomes were used instead to include more genes, containing either heavy or light chain genes (Table 1).

Table 1
Summary of some examples of genetic constructions used to generate transgenic mice and cattle, able to produce fully human Igs

Loci	Human	Size (kb)	Functional V genes	References
IgH[a]				
HuIgH	μ	25	2	[24, 28]
HuIgH[cos]	μ	100	2	[24, 29]
HC1	μ γ1	61	1	[30]
HC2	μ γ1	80	4	[31]
IgH[b]				
J1.3	μ	85	2	[32, 33]
HuIgH	μ	240	5	[34]
YH1	μ	220	5	[35]
YH2	μ γ2	1020	≈40	[36]
hCF(SC20)	μ γ (1–4)	1500	≈40	[37]
IgH[c]				
18hVH-DJ	Chimeric Human VDJ, Mouse C_H	340	18	[38, 39]
39hVH-DJ	Chimeric Human VDJ, Mouse C_H	550	39	[38, 39]
80hVH-DJ	Chimeric Human VDJ, Mouse C_H	940	80	[38, 39]
IgH[d]				
hIGH	Transchromosomic cattle		All	[40, 41]
Igk[a]				
KC1	κ	24	1	[30]
Kco4	κ	43	4	[31]
Loci k[b]				
Yk1	κ	170	2	[34]
HuIgkYAC	κ	300	2	[42]
HucosIgkYAC	κ	1300	≈80	[29]
KCo5	κ	450	≈26	[43]
Yk2	κ	800	≈25	[35]
hCF(2-W23)	κ	3000	≈35	[37]
Loci k[c]				
16hVk-J	Chimeric Human VJ, Mouse Cκ	240	16	[38, 39]
30hVk-J	Chimeric Human VJ, Mouse Cκ	390	30	[38, 39]
40hVk-J	Chimeric Human VJ, Mouse Cκ	480	40	[38, 39]

(continued)

Table 1
(continued)

Loci	Human	Size (kb)	Functional V genes	References
Loci k[d]				
kHAC	κ		All	[40, 41]
LociIg λ[b]				
Yλ	λ	380	15	[44]

[a]Genetic constructions using cosmids (COS)
[b]Genetic constructions using yeast artificial chromosomes (YAC)
[c]Genetic constructions using bacterial artificial chromosome (BAC)
[d]Genetic constructions using human artificial chromosome (HAC)

The amount of DNA incorporated, the number of different V segments, the presence or absence of regulatory elements in those transgenes, or the integration in the genome, all differed from one mouse to another, leading to important differences between the types of transgenic mice [27, 28].

To avoid mouse antibody production, gene targeting on embryonic stem cells was necessary to remove endogenous Ig genes. A mouse unable to secrete μ heavy chain was the pioneer [45] (Table 2) and was, subsequently, used by many groups. Although the normal development of B cells was impaired in these mice without the Cμ membrane exon, the production of endogenous mouse IgA or IgG was observed in these mice. This meant that the generation of new knockout mice lacking J heavy genes was required to avoid gene rearrangement [46]. Mice homozygous for the deletion of J heavy genes presented a complete interruption in B-cell development (no mature B cells were found in bone marrow or in the periphery) and an impaired antibody production. However, the introduction of a complex human immunoglobulin Yeast Artificial Chromosome (YAC) into these mice led to the recovery of the B-cell population [56].

Several knockout mice for κ chains were also generated in the 1990s (Table 2). Although some hybrid antibodies (human heavy with mouse λ chains) were observed in some mice, the inactivation of the λ locus was shown to be not as crucial as that of the κ locus, because over 90% of the mouse antibodies used the κ chain [57]. Recently, a λ knockout mouse has been developed and patented by Drs Brüggemann and Zou, (Table 2), and it can be crossed with other transgenic and knockout mice.

The development of the "final" transgenic mouse producing fully human Igs in the absence of mouse endogenous antibodies is a very complex process, which has required and continues to require, the effort and time of several research groups and companies (Table 3). Once the transgenic and knockout mice are developed,

Table 2
Summary of some knockout (Ko) mice for Ig genes, indicating the genes inactivated and effects on animals

Inactivation	Gene affected	Effects	References
Heavy			
μ MT (−/−)	Ko: mouse Ig μ membrane exon. Stop codon and neo cassette intro the membrane exon of the IgM constant region	Absence of B cells	[45]
JH (−/−)	Ko: mouse JH genes	No detectable mouse IgM or IgG antibodies	[46] GenPharm International. Taconic
Ig D (−/−)	Ko: one exon of the constant region (Cδ3) and exons for the secretory and membrane-spanning part of the protein (δS, δX, δM1, and δM2) (inactivated by insertion of a neomycin resistance gene)	No detectable mouse IgD antibodies	[47]
IgE (−/−)	Ko: homozygous null mutation of the Cε gene	No detectable mouse IgE antibodies	[48]
JH (−/−)	Ko: First exon Joining heavy chain locus	Mouse IgM levels reduced Mouse IgA levels elevated Mouse IgG marginal reduction	[49]
Cμ (−/−)	Ko: truncated rat Cμ	B cell numbers reduced >95%. No detectable rat antibodies	[50]
JH (−/−)	Ko: rat JH segments	B cell numbers reduced >95% No detectable rat antibodies	[50]
Kappa			
κ (−/−)	Ko: Cκ (inactivated by insertion of a neomycin resistance gene)	Increased mouse λ + B cells k rearrangements not completely abolished	[51]
κ (−/−)	Ko: κ (intron enhancer, inactivated by insertion of a neomycin resistance gene)	Increased mouse λ + B cells k rearrangements completely blocked	[52]
κ (+/−) κ (−/−)	Ko: J κ, κ intron enhancer and Cκ exon with a neo cassette	Tenfold more λ + B cells	[53]
κ (−/−)	Ko: Ck by gene targeting	Four main λ are expressed (λ1, 2(V2), 2(Vx), 3)	[54]

(continued)

Table 2
(continued)

Inactivation	Gene affected	Effects	References
κ (−/−)	Ko: Neo cassette in the Ck	Affected serum titers after secondary immunization	[55]
Lambda			
λ (−/−)	Ko: λ locus deleted using LoxP constructs	No λ expression	Bruggemann, M.; Zou, X. Patent number: 20110093961

several crossings of individual mice are necessary to obtain animals with distinct features. Figure 1 shows an example of obtaining a mouse carrying six features: a mouse carrying a human heavy transgene (HuIgH+) is crossed with a mouse lacking endogenous heavy genes (ko moIgH −/−); a human transgenic κ mouse (HuIg κ +) is crossed with a knockout mouse for mouse κ (ko moIg κ −/−); a mouse carrying a human λ (HuIgλ+) transgene, is crossed with a mouse knockout for endogenous λ genes (Ko moko λ −/−). Finally, all these resulting mice must then be crossed to generate a mouse with six features: HuIgH+, HuIgκ+, HuIgλ+, moIgH (−/−), moIgk (−/−), moIgλ (−/−), which is able to produce the human Ig chains included in the transgenes, without the presence of endogenous mouse antibodies (Fig. 1).

The production of human antibodies using several types of transgenic mice has mainly been carried out by companies (Table 3) and by a small number of research groups. The extreme difficulty in generating these mice, their requirements in terms of crossing and special maintenance and, more importantly, the patents protecting most of these mice have restricted the use of this source of human antibodies in research laboratories. Moreover, several problems have been found in certain mice, including a low number of peripheral B cells, the expression of endogenous mouse chains (by aberrant rearrangements or splicing processes), and a lower efficiency in the production of Igs.

Some research groups [27, 28, 34, 60], including our group [61–65], have generated hybridomas from transgenic mice carrying human Ig genes. In our case, two different mouse strains (BAB 4 and BAB 5) developed by Dr. Brüggemann [59] were used. The BAB4 strain (referred to as four-feature mice) carries human IgM, κ transgenes in an inactivated background of mouse heavy and κ chain genes, while the BAB5 strain (referred to as five-feature mice) carries an additional human λ transgene. Both strains produce fully human IgM antibodies [61] with either human κ or λ

Table 3
Examples of mice carrying human Ig genes obtained by crossing

Crossing	Regions affected	Effects	Company/Reference
λ (−/−) × κ (−/−)	Ko: mouse λ and κ chain loci	No production of light chains	[57]
Double inactivated (DI) strain	Ko: mouse JH and Ck regions	Pro-B but no mature B cells	Abgenix. U.S. patent application Ser. No. 07/466,008, filed Jan. 12, 1990
J (−/−) × k (−/−)	Ko: mouse J segment genes (heavy and light chains)	No expression of mouse heavy and kappa chains	Abgenix Patent number: 6673986 Filing date: Mar 15, 1993
Double-Tc/KO mice. Double-Tc/KO(λ1 low/low) strain	Ko: mouse Cμ2, Cμ3-Cμ4, and Mμ1-Mμ2 exons replaced by a neo cassette. Ko: Mouse Ck exon replaced by a neo cassette Animal crossed with CD1 animals homozygous λ1 low	No mouse IgM or IgG on serum No kappa expression Low mouse lambda expression	[58]
BAB4	Tg: human Heavy, human kappa Ko: mouse heavy, mouse kappa	No mouse IgM on serum No kappa expression	[59]
BAB5	Tg: human Heavy, kappa, lamba Ko: mouse heavy, kappa	No mouse IgM on serum No kappa expression	[59]
Medarex's HuMAb Mouse (TM)	Tg: human heavy, kappa Ko: mouse heavy, kappa	Human Igs, Mouse antibody producing genes inactivated	Medarex
KHK's TC Mouse™	Tg: two human chromosome fragments containing the Ig heavy chain locus and the human kappa locus (unstable)	Human Igs	Kyowa Kirin company
KM Mouse™	Crossing KHK's TC mouse with Medarex's HuMAb Mouse Tg Tg: human heavy, human kappa Ko: mouse heavy, mouse kappa	Majority of human Ig subclasses (IgG1, 2, 3, 4, IgA)	Medarex-Kyowa Kirin companies
KM Mouse™ × λHAC KM Mouse™	Tg: human lambda light chain	Human lambda expression	Kyowa Kirin company

(continued)

Table 3
(continued)

Crossing	Regions affected	Effects	Company/Reference
XenoMouse I Strain	Tg: Human IgMκ antibodies Ko: mouse JH and Ck regions	Reduced number of B cells	[34]
XenoMouse IIa Strain:	Similar to Xenomouse I, but additional γ2 and mouse 3′enhancer on cis	Normal B cells	Abgenix
L6 strain	Tg: human heavy and kappa light chains Ko: double inactivated mouse background (L6)	Normal B cells	Abgenix
Xenomouse strain	Tg. Human V, D, Cμ, Cδ, Cγ1, γ2, γ3, α, ε Tg: human Vκ, Jκ, Cκ Ko: mouse H (J segment genes), Cκ deleted	Human Igs	Abgenix
Kymouse™	Human Heavy, κ and λ loci Kymouse HK™ (Ig H and Ig κ) Kymouse HL™ (Ig H and Ig λ) Kymouse HKL™ (Ig H, Ig κ and Ig λ) Kymouse KO (Knockout mouse Ig κ)	Human Igs	Kymab
Crescendo transgenic platform	Engineered human Ig H analogous to H chain antibodies produced naturally in llamas	Human Igs with only heavy chains	Crescendo Biologics

Tg transgenic, *ko* knockout, *Ig* immunoglobulin, *Ref* references

chains; few antibodies carrying endogenous mouse lambda were found, even though the animals did not have the λ locus inactivated. Several mouse hybridomas secreting human IgM antibodies have been produced from these animals [61–64]. We have shown that the rearrangement of only one human IGVH gene was sufficient to generate a wide repertoire of antigen-specific antibody responses in these mice [63]. Other authors have indicated that a reduced V repertoire has important consequences on T-independent antigen responses [66].

We were able to generate human monoclonal antibodies with several specificities from BAB4 and BAB5 mice, such as those directed against human CD69 [62], human class II MHC molecules [64], or human leucocytes [65], which could potentially be used in human therapy. Hybridomas-secreting human Ig antibodies have also been developed by other groups, generating mAbs directed against tetanus toxin, IgE, progesterone, human CD4,

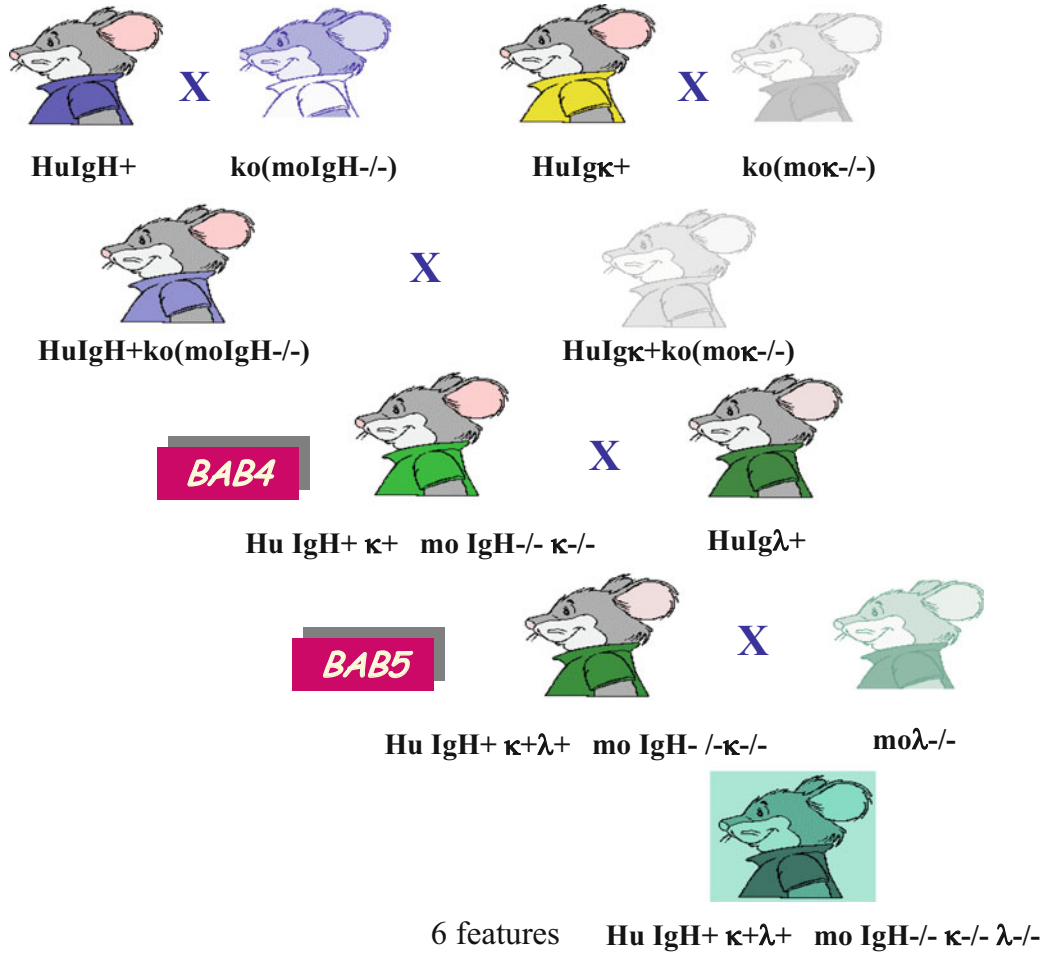

Fig. 1 Examples of mouse crosses to generate transgenic mice carrying four features (like BAB4 mice), five features (like BAB5 mice), or six features. *HulgH+, Hulgκ+, and Hulgλ+: transgenic mouse carrying human heavy, kappa, and lambda genes ko (molgH−/−, molgκ−/−, molgλ−/−): knockout for mouse heavy, kappa, and lambda genes*

EGFR, IL-8, L-selectin, GCSF, etc., [27], or even more recently against the HIV gp140 antigen [60].

Several companies have engineered mice to produce fully human antibodies in vivo, and they have developed specific mAbs for human therapy (some of them already approved and many more in clinical trials) (Tables 4 and 5). Examples of companies are:

Bristol-Myers Squibb (http://www.bms.com) has the UltimMab platform developed by Medarex which consists of a transgenic mouse strain capable of producing multiple high-affinity human sequence IgGκ mAbs [31, 67]. The light-chain transgene is partly derived from a yeast artificial chromosome encompassing nearly half of the human Vκ region, while the heavy-chain transgene encodes for human μ and γ1 constant regions. Over 30 antibody

Table 4
Summary of FDA approved fully human monoclonal antibodies derived from four transgenic technologies

Antibody	Trade name	Company	Antigen	Main indication	Approval
Alirocumab[a]	PRALUENT	Regeneron, Sanofi	PCSK9	Hypercholesterolemia	2015
Bezlotoxumab[b]	ZINPLAVA	Merck	Toxin B	*Clostridium Difficile* Infection	2017
Brodalumab[c]	SILIQ	Abgenix, Amgen, Astra Zeneca, KHK, Valeant	IL-17RA	Psoriais	2017
Canakinumab[b]	ILARIS	Medarex, Novartis	IL-1β	Cryopyrin-associated periodic syndrome	2009
Daratumumab[b]	DARZALEX	Medarex, Genmab, Janssen Biotech	CD38	Multiple Myeloma	2015
Denosumab[c]	PROLIA	Abgenix, Amgen	RANKL	Postmenopausal osteoporosis	2010
Dupilumab[a]	DUPIXENT	Regeneron, Sanofi	IL-4Rα	Atopic dermatitis	2017
Durvalumab[c]	IMFINZI	Medimmune/ AstraZeneca	PDL-1 inhibitor	Urothelial carcinoma	2017
Evolocumab[c]	REPATHA	Amgen	PCSK9	Hypercholesterolemia hyperlipidemia	2015
Golimumab[b]	SIMPONI	Medarex, Centocor Ortho, Janssen Biotech	TNF-α	Rheumatoid arthritis/psoriatic arthritis and ankylosing spondylitis	2009
Ipilimumab[b]	YERVOY	Medarex	CTLA4	Melanoma	2011
Nivolumab[b]	OPDIVO	BMS, Medarex, Ono	PD-1	Lung cancer	2015
Ofatumumab[d]	ARZERRA	Genmab, GSK, Novartis	CD20	Chronic lymphocytic leukemia	2009
Olaratumab[b]	LARTRUVO	ImClone Systems, Medarex	PDGFRA	Soft tissue sarcoma	2016
Panitumumab[c]	VECTIBIX	Abgenix, Amgen	EGFR	Colorectal cancer	2006
Sarilumab[a]	KEVZARA	Regeneron, Sanofi	IL-6R	Rheumatoid arthritis	2017
Secukinumab[c]	CONSENTYX	Novartis	IL-17	Psoriasis, psoriatic arthritis and ankylosing spondylitis	2015

(continued)

Table 4 (continued)

Antibody	Trade name	Company	Antigen	Main indication	Approval
Ustekinumab[b]	STELARA	Centocor Ortho, Medarex	IL-12	Psoriaris, multiple sclerosis	2009

Transgenic lines used: [a]Murphy et al. [38]; [b]Lonberg et al. [31]; [c]Mendez et al. [35]; [d]Fishwild et al. [43]

compounds have been derived via the UltiMabTechnology, eight mAbs have already been approved (Table 4), while others are on clinical trials (Table 5).

Amgen, who acquired Abgenix with its Xenomouse technology (http://www.amgen.com); The XenoMouse strains include most of the variable region repertoire in germline-configured human IgH and Igk loci, the genes for Cμ, Cδ and either Cγ1, Cγ2, or Cγ4, as well as the cis elements required for their function [35, 68]. The IgH and Igk transgenes were bred onto a genetic background deficient in the production of murine Ig, and the mice developed a diverse primary immune repertoire similar to that from adult humans [68]. The immunization of these mice, followed by conventional hybridoma technology, has allowed, until now, the generation and approval of six fully human mAbs: Brodalumab, Denosumab, Durvalumab, Evolocumab, Panitumumab and Secukinumab, and many others currently on clinical trials (Tables 4 and 5).

The Regeneron company (https://www.regeneron.com) has developed the VelocImmune mice technology, which allows the generation of fully human antibodies in two steps: (1) Conventional hybridoma cells are generated from transgenic animals carrying the entire human Ig heavy and κ light chain variable repertoire. As these animals contain all their mouse constant regions, the obtained hybridomas secrete chimeric mAbs (human-mouse) against the immunizing antigen. (2) The mouse constant region is replaced in those hybrid cells by its human counterpart through genetic engineering and further insertion into mammalian cell lines [38, 39]. Using this technology, the company has developed three FDA approved fully human monoclonal antibodies (Alirocumab, Dupilumab, and Sarilumab) (Table 4), and others at different phases of clinical trials [69], some of them in collaboration with the company Sanofi (Table 5).

Kirin Brewery Company (http://www.kirin.co.jp) has the TransChromo mouse platform (TC Mouse™). The mice have incorporated the entire human immunoglobulin (hIg) loci, expressing a fully diverse repertoire of hIgs, including all the subclasses of

Table 5
Summary of fully human monoclonal antibodies derived from transgenic technology in several phases of clinical trials

Antibody	Company[a]	Antigen	Main indication	Clinical trials[a]
Phases 2/3				
Bimagrumab	Morphosys, Novartis	ActRIIB	Inclusion body myositis	Phase 2/3
Burosumab	KHK, Ultragenyx	FGF23	X-linked hypophosphatemia	Phase 3
Erenumab	Amgen, Novartis	CGRP R	Migraine	Phase 3
Fasinumab	Regeneron, Sanofi	NGF	Chronic low back pain	Phase 3
Figitumumab	Amgen, Pfizer, Schering-Plough	IGF-1R	Lung cancer	Phase 3. Discontinued
Fulranumab	Amgen, J&J, Takeda	NGF	Ostheoarthritis pain	Phase 3. Discontinued
Patritumab	Amgen, Daiichi Sankyo, U3 Pharma	HER3	Lung cancer	Phase 3. Discontinued
Rilotumumab	Amgen	HGF/SF	Gastric cancer	Phase 3
Tabalumab	AME, Lilly	BAFF	Lupus	Phase 3. Discontinued
Tremelimumab	Amgen, Medimmune, Pfizer	CTLA4	Melanoma, small cell lung cancer and prostate cancer	Phase 3
Zalutumumab	Genmab	EGFR	Head and neck cancer	Phase 3. Discontinued
Zanolimumab	Genmab, TenX	CD4	Cutaneous T-cell lymphoma, rheumatoid arthritis, psoriasis, melanoma	Phase 3
Phases 1/2				
ABX-IL8	Abgenix, Amgen	IL-8	Inhibition of angiogenesis, tumor growth	Phase 2
ABX-PTH	Abgenix	PTH	Secondary hyperparathyroidism	Phase 1
AGS-1C4D4	Agensys	PSCA	Prostate cancer	Phase 2
AMG 108	Amgen, Medarex	IL-1R1	Rheumatoid arthritis	Phase 2
AMG 714	Amgen, Genmab	IL-15	Celiac disease	Phase 2
AMG 811	Amgen, Medarex	IFN-γ	Lupus	Phase 1
Bleselumab	Astellas, KHK	CD40	Kidney transplant rejection	Phase 2
Conatumumab	Amgen, Millennium	Death receptor 5	Several tumors	Phase 1/2
Crotedumab	Regeneron	GCGR	Diabetes	Phase 1

(continued)

Table 5
(continued)

Antibody	Company[a]	Antigen	Main indication	Clinical trials[a]
Eldelumab	Medarex	IP-10	Ulcerative colitis	Phase 2
Enoticumab	Regeneron, Sanofi	DLL4	Solid tumors	Phase 1
Evinacumab	Bayer, Regeneron	ANGPTL3	Dyslipidemia	Phase 2
Hgs004	HGS	CCR5	HIV infection	Phase 1
Icrucumab	ImClone	FLT1	Tumors	Phase 2
Inclacumab	Genmab, Roche	P-selectin	Atherosclerotic cardiovascular diseases	Phase 2
Intetumumab	Centocor Ortho	Integrin αV	Tumors	Phase 1/2
Iratumumab	Medarex	CD30	Lymphoma, non-Hodgkin disease	Discontinued
Krn330	KHK	A33	Colorectal cancer	Phase 1/2
Lucatumumab	Novartis, Xoma	CD40	Follicular lymphoma	Discontinued
Mdx-1105	Medarex	PD-L1	Tumors	Phase 1/2
Mdx-1342	Medarex	CD19	Chronic lymphocytic leukemia	Phase 1
Mdx-1401	BioWa, Medarex	CD30	Malignant lymphoma	Phase 1
Mdx-1411	Medarex	CD70	Chronic Lymphocytic Leukemia or Mantle Cell Lymphoma	Phase 1
Medi-3617	AstraZeneca, Medimmune	Angiopoietin 2	Tumors	Phase 1
Medi-570	Medimmune	ICOS	Lupus	Phase 1
Nesvacumab	Regeneron, Sanofi	Angiopoietin 2	Solid tumors	Phase 2
Oxelumab	Genentech, Roche	OX40L	Asthma	Phase 2
Pamrevlumab	FibroGen	CTGF	Idiopathic pulmonary fibrosis	Phase 2
Prezalumab	Amgen, Medimmune	B7RP-1	Sjogren's syndrome	Phase 2
Regn1154	Regeneron	Undisclosed	Undisclosed by the company	Phase 1
Regn1400	Regeneron	HER3	Tumors	Phase 1
Regn3500	Regeneron, Sanofi	IL-33	Asthma	Phase 1
Regn3918	Regeneron	C5	Paroxysmal nocturnal hemoglobinuria	Phase 1
Selicrelumab	Amgen, Pfizer, VLST	CD40	Solid tumors	Phase 1

(continued)

Table 5
(continued)

Antibody	Company[a]	Antigen	Main indication	Clinical trials[a]
Sifalimumab	Medimmune	IFN-α	SLE, dermatomyositis, and polymyositis	Phase 2
Tezepelumab	Amgen, AstraZeneca	TSLP	Asthma	Phase 2
Tovetumab	Medimmune	PDGFRA	Tumors	Discontinued
Trevogrumab	Regeneron, Sanofi	Myostatin	Muscular atrophy/ Musculoskeletal disorders	Phase 2
Ulocuplumab	Medarex	CXCR4	Leukemia, solid tumors, Waldenstrom's macroglobulinaemia	Phase 1/2
Urelumab	BMS	4-1BB	Non-Hodgkin's lymphoma; Solid tumours	Phase 2
Varlilumab	Celldex	CD27	Malignant melanoma; Solid tumours Renal cell carcinoma	Phase 1/2
Preclinical				
HuMax-cMet	Genmab	cMet	Solid tumors	Preclinical
CE-355621	Amgen, Pfizer	cMet	Solid tumors	Preclinical
Regeneron patent anti-CD20	Regeneron	CD20	B cell lymphoma	Preclinical
KHK patent anti-Thrombopoietin Receptor	KHK, Kirin Pharma	TPO receptor	Thrombocytopenia	Preclinical
Zymogenetics patent anti-IL-21	Zymogenetics, Novo Nordisk	IL-21	Autoimmune and inflammatory diseases	Preclinical
Millennium patent anti-B7-H4	Abgenix, Millennium	B7-H4	Breast cancer	Preclinical
Japan Tobacco patent anti-ICOS	Japan Tobacco	ICOS	Oncology, transplants and autoimmune diseases	Preclinical
Genentech patent anti-TrkC	Genentech	TrkC	Peripheral neuropathy	Preclinical
Celldex patent anti-B11	Celldex	B11	Tumors	Preclinical
Regeneron patent anti-CD48	Regeneron	CD48	Allergy; inflammation	Preclinical
U.Massachusetts patent anti-SOD1	U.Massachusetts	SOD1	Amyotrophic lateral sclerosis	Preclinical

(continued)

Table 5
(continued)

Antibody	Company[a]	Antigen	Main indication	Clinical trials[a]
Regeneron patent anti-TL1A	Regeneron	TL1A	Inflammatory bowel disease; other autoimmune diseases	Preclinical
IPH5401	Innate, Novo Nordisk	C5aR	Rheumatoid arthritis	Phase I / Preclinical in oncology
Novo Nordisk patent anti-OSCAR	Novo Nordisk	OSCAR	Autoimmune inflammatory diseases	Preclinical
Regeneron patent anti-TIE-2	Regeneron	TIE-2	Block angiogenesis	Preclinical
Regeneron patent anti-ASIC1	Regeneron	ASIC1	Pain	Preclinical
Regeneron patent anti-HLA-B27	Regeneron	HLA-B27	Ankylosing spondylitis and other spondyloarthropathies	Preclinical
Regeneron patent anti-PROKR1	Regeneron	PROKR1	Tumors, pain	Preclinical
Regeneron patent anti-GREM1	Regeneron	Gremlin 1	Fibrosis and cancer	Preclinical
Regeneron patent anti-LEPR	Regeneron	LEPR	Lipodystrophies; leptin deficiency	Preclinical

[a]Observation: Commercialization by companies and the state of clinical trials can change during time. It has been compiled from various sources (http://adisinsight.springer.com/search; https://es.wikipedia.org; https://patents.google.com; https://lifescivc.com/2017/05/human-antibody-discovery-mice-phage; Refs. 5, 27

IgGs (IgG1–G4). Immunization of the TC Mouse with human antigens led to obtaining hybridoma clones expressing fully human antibodies specific for the target human antigen. However, due to the instability of the Ig kappa locus-bearing HCF2, the efficiency of hybridoma production was less than one-tenth of that observed in normal mice [70]. This problem was solved by crossing these mice with the Medarex-YAC transgenic mice, generating the KM Mouse, which performed as well as normal mice regarding efficiency of hybridoma production.

Trianni (http://trianni.com) has developed the TRIANNI mouse. The animals carry immunoglobulin loci containing human variable domain exons within the context of remaining mouse sequences. The company indicates that this approach guarantees efficient expression of the full human antibody repertoire, but maintains the natural immune response of the wild-type mouse.

The current portfolio of fully human mAbs on clinical trials derived from transgenic mice (Table 5) or from other types of technologies [5] is very large, indicating the current high level of interest in them by the pharmaceutical industry. Together with new

technologies being developed for the generation of human mAbs [71–73], companies such as Kymab (with a new platform called kymouse™), Crescendo Biologics (with its triple knockout mice lacking mouse H, κ and λ genes) [74], Creative Biolabs (Magic™ Human Antibody Discovery Platform using transgenic mice/rats), Merus (MeMo™, transgenic mouse carrying single light chain), Technology™ (FHA mice), Harbour Biomed (transgenic mice platform), Ablexis, Wuxi Pharma and Open Monoclonal technology (Omni Rat platform with transgenic rats), Sangamo Biosciences, and many others, have been dedicating particular attention and efforts to transgenic and knock-out rodents, for their use in the generation of therapeutic human mAbs [75]. It is expected that, in the near future, new human mAbs will be generated from these platforms, and approved by the regulatory agencies for several human diseases.

The generation of human mAbs from transgenic mice will now be described in detail. Firstly, the immunization protocols will be presented, followed by the generation of hybridomas, screening of the antibody-secreting hybridomas, and further antibody purification. In addition, the problems detected and the potential functional studies to be performed in vitro and in vivo with the antibodies are included.

2 Materials

2.1 Immunization

Adjuvants: several adjuvants can be used, such as Complete and Incomplete Freund's Adjuvants (CFA, IFA), Ribi Adjuvant System, and Aluminium Hydroxide.

2.2 Fusion

1. Murine myeloma cell lines Sp2/0 or NSO. Other mouse hybridoma fusion partners are listed in the American Type Culture Collection (www.atcc.org).
2. Splenocytes from immunized transgenic mice carrying human Ig genes.
3. Media: Roswell Park Memorial Institute (RPMI-1640) or Dulbecco Modified Eagle's Minimal Essential Medium (DMEM), supplemented with 5–20% fetal calf serum (FCS), 4 mM L-glutamine, 1 mM sodium pyruvate, nonessential amino acids, 50 U penicillin, 50 μg streptomycin.
4. Hybridoma-grade dimethyl sulfoxide (DMSO) for cryopreservation.
5. Hypoxanthine–Aminopterin–Thymidine (HAT) and hypoxanthine–thymidine (HT) for hybridoma selection.
6. Polyethylene glycol solution (PEG) 50% (w/v).

7. 4% Trypan blue solution, made with phosphate-buffered saline (PBS) for counting viable cells.
8. Erythrocytes lysis solution; 0.1 Methylene Violet 6B in 0.21% citric acid in saline.

2.3 Screening by ELISA or by Flow Cytometry

2.3.1 Buffers

1. Phosphate-buffered saline (PBS); 0.01 M sodium phosphate dibasic 0.15 M sodium chloride.
2. PBS-BSA buffer; PBS, 0.7 g/L BSA, 1.0 g/L sodium azide, in deionized water, pH to 7.4.
3. Washing buffer; PBS, 0.01% Tween 20, pH 7.4.
4. Blocking buffer; PBS with 5% nonfat dry milk, or with 5% FCS, or with 2% BSA.
5. Citrate buffer; prepare two solutions, 0.1 M citric acid and 0.1 M sodium citrate, and combine them to get a pH of 4.3.
6. Stop solution; 0.1 M citric acid with 0.01% sodium azide.

2.3.2 Substrate

1. Freshly prepared horseradish peroxidase substrate (ABTS, 2,2′-Azinobis[3-ethylbenzothiazoline-6-sulfonic acid]) diluted in 0.1 M citrate buffer (pH 4.3) with 1 μl H_2O_2/5 ml at a final ABTS concentration of 0.3 mg/ml.

2.3.3 Secondary Antibodies

1. Goat or rabbit Igs conjugated with enzymes (ELISA) or fluorochromes (flow cytometry) directed against human immunoglobulin heavy and/or light chains.

2.4 Immunoglobulin Sequencing

1. Total RNA isolation kit.
2. Reverse transcriptase.
3. Standard PCR reagents (Taq polymerase, dNTPs, primers, thermo tubes, agarose, ethidium bromide).
4. Sequencing kit.

2.5 Antibody Purification

1. Protein A, Protein G, Protein L, and pre-packed ready-to-use columns.

2.6 Complement Activation

1. Human serum as source of complement or commercial human complement.
2. Lyophilized rabbit complement.
3. 20 μg/ml propidium iodide in PBS.

2.7 Purification Using Protein A/G/L

1. Conjugation of ligand to CNBr activated Sepharose-4B.
2. Coupling buffer; 0.1 M $NaHCO_3$, 0.5 M NaCl, pH 8.3.
3. Washing buffers: (a) 0.1 M sodium acetate, 0.5 M NaCl, adjust with acetic acid to pH 4.0, and (b) 0.1 M Tris, 0.5 NaCl, adjust with HCl to pH 8.

2.8 Equipment and Laboratory Ware

1. Cell culture laboratory including: laminar flow hood, CO_2 incubator, fridges (−20 and −80 °C), liquid nitrogen container, inverted and standard microscopes, 37 °C water bath, refrigerated centrifuges. Sterile pipettes, sterile 24-well and 96-well plates, tissue culture flasks, 15 and 50 ml conical tubes, hemocytometers, sterile scissors and forceps.
2. Equipment for screening tests: ELISA reader, Flow Cytometer.
3. DNA Sequencing: PCR-thermocycler, sequencer.

3 Methods

3.1 Immunization

Protocols for mice immunization vary widely according to the antigen used (*see* **Note 1**). In general, the immunogen is prepared with an adjuvant, and injected several times (2–3 times or more) at regular intervals (after 3–4 weeks). The titer of specific human antibodies in mouse serum should be at least 1/1000 by ELISA.

3.1.1 Immunogen Preparation

When the antigen is a soluble protein, Alum can be used as adjuvant.

1. Mix 1 ml of 1 mg/ml protein with 1 ml of a solution 5% Alum ($KAl(SO_4)_2{\cdot}12H_2O$) in sterile distilled water.
2. Add 4 M NaOH, drop by drop, to adjust the pH to 6.5. A white precipitate appears. Centrifuge 5 min, 1000 × *g*. Discard the supernatant, wash the precipitate in sterile PBS and, finally, add PBS to reach the desired concentration.

Intact (tumor, primary, or peripheral blood) cells are highly immunogenic and do not usually require adjuvants. Nevertheless, our experience with transgenic mice suggests that the use of Freund's adjuvants improves the immune response.

1. Wash the target cells with PBS followed by centrifugation. Add PBS and count the cells using Trypan blue in a Neubauer chamber. Prepare 5×10^6–1×10^7 cells in 250 μl of sterile PBS.
2. Add an equal volume of Freund's adjuvant and mix thoroughly to get a thick white emulsion. A 1 ml syringe or a vortex can be used.

Small molecules, such as peptides or oligosaccharides with low molecular weight, are not usually immunogenic (called haptens) and they have to be attached covalently to a carrier (a protein or other compounds). The most common carriers are keyhole limpet hemocyanin (KLH), bovine serum albumin (BSA), and ovalbumin (OVA) (*see* **Note 2**).

1. Add 5 mg of peptide to 5 mg of KLH dissolved in 1 ml of 50 mM sodium borate buffer pH 8. Slowly add 1 ml freshly prepared 1% glutaraldehyde solution with gentle mixing at room temperature (RT). Incubate for 2 h at RT rotating gently.
2. Add 0.25 ml of 1 M glycine to bind unreacted aldehyde groups. Dialyze the reaction mixture overnight at 4 °C against PBS. Prepare the immunogen immediately with Alum or Freund's adjuvant as indicated above.

3.1.2 Animals, Route, and Schedule of Inoculation

1. At least five mice (6–12 weeks old) per immunogen should be used. The first immunization is usually by intraperitoneal (ip) inoculation, and it is common to use "complete" adjuvants containing heat-killed bacteria such as *Mycobacterium tuberculosis* in Complete Freund's Adjuvant (CFA), or *Bordetella pertusis* in Alum.
2. Three to four weeks later, the animals are immunized again, but now with incomplete adjuvants (without bacteria) by ip injection. After 10 days, the presence of antigen-specific human antibodies can be detected in serum. Blood can be obtained by mandibular vein puncture or by tail nicking. In both cases, anesthesia is not required. After collection, blood is maintained at 37 °C for 1 h and then at 4 °C for several hours or overnight. After centrifugation at 10,000 × *g* for 10 min, serum is collected, aliquoted, and can be maintained at −20 °C for long periods of time.
3. Sera from immunized mice are tested by indirect ELISA (using specific antigen) or by flow cytometry (on target cells) (*see* later). If the human antibody levels in mice are not sufficient, repeat the ip immunization 2–3 weeks later, until the required levels are reached.
4. Choose the desired animal (more than one can be used per fusion). Three days before fusion, immunize it again by intravenous (iv) injection without adjuvant. The amount of antigen to be injected in the final boost could be around 25 μg of protein/hapten-carrier or 5×10^6 cells resuspended in sterile PBS or in saline.

3.1.3 Serum Titration by ELISA

This protocol is useful when the antigen used for immunization is a soluble protein or a hapten.

1. Dilute the antigen in PBS at a final protein concentration of 1–10 μg/ml. Coat the wells of a 96-well ELISA plate with 50 μl of the antigen and incubate for 2 h at room temperature (RT), or 4 °C overnight. The incubation time, type of buffer, antigen concentration, and the type of plate to be used may require some optimization.

2. Remove the coating solution and wash the plate three times by filling the wells with 200 µl PBS. Flick the plate over a sink to be sure that all the solution is removed. Dry by blotting onto tissue paper.
3. Block the remaining protein-binding sites by adding 200 µl of blocking buffer per well. Incubate overnight at 4 °C or for at least 2 h at RT. If the plate is to be stored at 4 °C, add sodium 0.01% azide and then it can be stored for 2 months.
4. Wash the plate twice with washing buffer. Add 50 µl per well of diluted serum in blocking buffer. Test serial dilutions of the supernatants, for example from 1/250 to 1/10,000. Incubate for 1–2 h at 37 °C, or overnight at 4 °C.
5. Wash the plate three times with washing buffer. Add to each well 50 µl of enzyme labeled antibodies directed against human immunoglobulins (HuIgs). Goat or Rabbit anti-HuIgs can be used coupled to horseradish peroxidase diluted in PBS-1% BSA, following the commercial indications, and incubate for 1 h at RT or at 37 °C.
6. Wash the plate three times with washing buffer. Add 50 µl/well of freshly prepared ABTS, the horseradish peroxidase substrate, incubate at room temperature for 5–20 min, depending on the rate of color development. Stop the reaction by adding stop solution and read the absorbance at 405 nm in an ELISA reader.

3.1.4 Serum Titration by Flow Cytometry

1. Target cells (3×10^5) are incubated at 4 °C for 30–45 min with PBS alone or with serial dilutions of serum (from 1/10 to 1/1000 or more).
2. Wash twice with PBS by spinning in a microfuge. Stain cells with 50 µl of diluted FITC-rabbit anti-HuIgs reagent at 4 °C for 20 min. Dilutions will depend on the original concentration; follow commercial indications or prepare several dilutions to standardize the immunofluorescence technique.
3. The stained cells are washed twice with PBS and the cellular fluorescence is measured using a Flow cytometer. Fluorescence can be analyzed several days later, if the cells are fixed with 0.1% formaldehyde in PBS at 4 °C.

3.2 Hybridoma Production

1. When human transgenic mice are used as a source of B lymphocytes, the protocol for obtaining hybridomas does not differ significantly from those previously described [76, 77], in which the myeloma and spleen cells are fused using polyethylene glycol (PEG). It is very important to work under sterile conditions when producing and growing hybridomas. Regarding cells, a healthy myeloma cell line is required (we recommend

Sp2/0), as well as spleen cells from immunized transgenic mouse (*see* **Note 3**).

2. A week before cell fusion, the myeloma cell culture should be started in a suitable medium (DMEM or RPMI-1640, antibiotics and 5% FCS). Cells must have high viability (>95%) and a density of ≅2–5 × 10^6 cells/ml. Cell density can be controlled by periodic monitoring of cell growth, including daily visualization under an inverted microscope and cell counting (using Trypan blue stain and a Neubauer chamber, or an automatic cell counter).
3. Kill the mouse by cervical dislocation and immerse it in 70% ethanol. From this step, all work must be carried out under a laminar flow hood in sterile conditions. Tear the superficial skin and make a small incision in the left abdominal side. Take the spleen with a forceps and release it by cutting the mesentery.
4. Prepare a spleen single-cell suspension in culture medium (RPMI-1640, 10% FCS) at 4 °C. Transfer the suspension to a sterile 15 ml tube and harvest by centrifugation (200 × *g*, 5 min at 4 °C). Add medium without FCS to the pellet and count the cells. To remove the erythrocytes in the counting sample, use erythrocyte lysis solution. Keep the tube with the single-cell suspension at 4 °C.
5. The myeloma cells (Sp2/0) are maintained in culture for approximately 1 week and then transferred to sterile tubes and centrifuged (at 200 × *g* for 5 min at 4 °C). The pellets are added to a single tube and suspended in culture medium without FCS. Count the cells using Trypan blue.
6. In a sterile 50 ml conical tube, mix spleen and myeloma cells in a 3:1 (spleen: myeloma) proportion. Fill the tube with serum-free medium and spin at 200 × *g* for 5 min at RT. Discard the supernatant, be sure to eliminate all medium, because it is very important to maintain the concentration of PEG (the fusion agent).
7. Place the tube in a 37 °C water bath (continue working under a laminar flow hood). Add slowly (drop by drop) 1 ml of 37 °C pre-warmed PEG with a glass pipette, and stir the mixture with the pipette. After adding all PEG, continue stirring for 2 min.
8. With the same pipette, add drop by drop a total of 10 ml of serum-free pre-warmed medium, and continue stirring. Finally, add drop by drop a total of 12 ml of serum-free pre-warmed medium, but now without stirring. Keep the tube at 37 °C in a water bath for 20–30 min.
9. Spin at 162 × *g* for 5 min and then resuspend the cells in media with 20% FCS and 1× HAT. Distribute the cells into 24-flat-bottom well plates (four plates are usually used per fusion, each

one at a different concentration). The plates have to be kept, with minimal manipulation, in an incubator (at 37 °C with 5% CO_2) for approximately 1–2 weeks. Monitor the clone growth under an inverted microscope.

3.3 Selection of Cell Colonies

If the fusion is successful, several round colonies appear in each well. When the colony is sufficiently large, it is possible to pick it up under an inverted magnifier and transfer it to an individual well in a 96-well plate.

1. To perform this pre-cloning, examine 24-well plates on an inverted stereo microscope (low magnification) and delimit with a marker the position of the colony. Pick up individual colonies under the inverted stereo microscope using a micropipette (volume 10 μl) and transfer each colony into an individual well on a previously prepared 96-well plate with 190 μl of medium (20% FCS and 1× HAT). Check daily, replacing 50% of the well volume with new media and finally, before cloning, test the antibody production by the screening method.
2. The hybridoma can be adapted to grow in normal medium (without HAT), either before or after cloning. In this process, usually a high proportion of cells do not survive. Strict monitoring of cell growth and viability is required during the adaptation phase. Furthermore, secretion levels should also be assessed, as they can change during adaptation. For 5–7 days, substitute HAT for HT medium, changing 25% of medium daily. When the cells are stable in HT medium, proceed in the same way, but now changing to normal medium. During these steps, always keep cryopreserved cells as backup. Cells growing in HAT or HT media (at least two vials of each) and in media alone (at least six vials of each) are cryopreserved using the standard procedure in a freshly prepared mixture of 90–95% FCS and 5–10% tissue–culture–grade DMSO, with at least 10^6 viable cells per cryovial. Cells can be maintained in a liquid nitrogen container at –196 °C for long periods of time.

3.4 Hybridoma Cloning by Limiting Dilution

There are several methods for hybridoma cloning, such as the use of agar or cell separation by FACS, but here the limiting dilution procedure, a simple and quick method, is described.

1. Prior to cloning, count hybridoma cells using a Neubauer chamber and dilute them to the correct concentration. In a flat-bottom 96-well plate, add 2000 cells (in 200 μl) into each well of the first left column. Add 100 μl medium to the remaining wells, using a multichannel pipette. With the same pipette, perform serial dilutions (1/2) by transferring 100 μl from the first left column to the second, mix and transfer 100 μl from the second column to the third and so on, until the last right

column (column 12). Fill the wells with medium until a final volume of 200 µl.

2. Analyze under an inverted microscope if individual cells have been added into the last right columns, and keep the plates in the incubator with 5% CO_2 at 37 °C. Leave cells growing for 5–7 days, checking daily, and identify with a marker the wells that have a single-cell clone.
3. Test the supernatant of these wells, by the previously chosen screening method, to find out if the cells produce the desired antibody. Select 3–5 of the best colonies, expand and freeze them.
4. To have stable cells, every hybridoma requires at least 2–3 consecutive rounds of recloning. Even highly selected hybridoma cells need to be periodically retested to confirm their specificity and to be recloned, to avoid the overgrowing of hybridomas that have lost their secretion capacity (*see* **Note 4**).

3.5 Selection of Positive Clones

One of the most important aspects is the correct choice of a screening assay to determine the presence of specific antibodies in the supernatants (*see* **Note 5**). The screening assay should be set up well before carrying out the fusion, using the serum of the immunized mice as a source of antigen-specific antibodies, and serum from non-immunized animals as well as medium as negative controls.

3.6 Characterization of Human Antibodies

Before introducing the human mAbs obtained in clinical assays or from a commercial supplier, they must be thoroughly characterized. This process includes not only determining the isotype or immunochemical properties of the mAb, but also its functional activities (*see* **Notes 6–9**).

3.6.1 Isotype Determination

Knowledge of the antibody class/subclass and the type of light chain of the antibody structure makes it possible to focus the strategy of purification and to predict its effector functions, such as complement activation, antibody-dependent cell cytotoxicity (ADCC), and induction of phagocytosis. There are several available assays for determining the type of immunoglobulin heavy and light chains, although the easiest way is to adapt the screening assay (indirect ELISA or Flow cytometry), using secondary antibodies directed against specific classes or subclasses of human immunoglobulins (*see* **Note 10**). Similarly, it is possible to modify the ELISA for the quantification of the antibody secreted, using a sandwich ELISA in which the plate is coated with rabbit or goat immunoglobulins directed against human antibodies, and with commercial human serum to perform the standard curve.

3.6.2 DNA Sequence

The primary structure or the amino acid sequence of our human mAb may be deduced from DNA sequencing (*see* **Note 11**). Any of the different tools offered by the International Immuno-GeneTics (IMGT) information system [78] can be used to align the obtained Ig sequences with human germinal sequences, to determine the VDJ and VJ junctions, and also to deduce the secondary and tertiary structure.

1. Isolate RNA from 2.5×10^6 hybridoma cells using RNeasy mini kit.
2. Obtain first-strand cDNA by incubating the RNA with human immunoglobulin constant region-specific primer (there is a tool on the IMGT website, www.imgt.org, to find the specific primer for each human isotype) and SuperScript III RT. The retrotranscription is performed following the manufacturer's instructions.
3. Amplify the rearranged V–J and V–D–J regions by PCR using between 2 and 5 μl of cDNA, in the presence of 2 mM $MgCl_2$, 0.1 mM dNTPs, 3 U of Taq polymerase, in a total volume of 50 μl. Use 0.25 μM of human VH or VL sense primers, in combination with JH or JL specific antisense primers (visit the IMGT website, www.imgt.org, to find the specific primer for each human segment).
4. To obtain a good product, 30 cycles are sufficient: 30 s denaturation (94 °C), 1 min annealing (depends on the primer sequences), and 1 min elongation (72 °C). Before adding the enzyme, the samples are preheated at 94 °C for 2 min, and the final cycle is completed by 10 min elongation at 72 °C. The PCR products are analyzed on a 1.5% agarose gel and are then ready for sequencing.

3.6.3 Effector Functions: Complement-Dependent Cytotoxicity Assay

The mechanisms of action of the mAbs produced should be studied by in vitro and in vivo assays. These assays should include tests to evaluate the ability for complement binding and activation, Fc receptor binding, ADCC, and possible cytotoxic effects, even if these properties are not required for the purpose of the particular human mAb being used.

1. The ability of a human mAb to activate complement can be analyzed by Flow cytometry. A total of 5×10^5 target cells are incubated for 30 min at 4 °C with 250 μl medium alone (as negative control), or 250 μl hybridoma supernatant, or an isotype control (a human mAb that does not recognize our target cell).
2. Wash cells twice by spinning and incubate them at 37 °C for 30 min with 250 μl rabbit complement diluted 1:2 in medium,

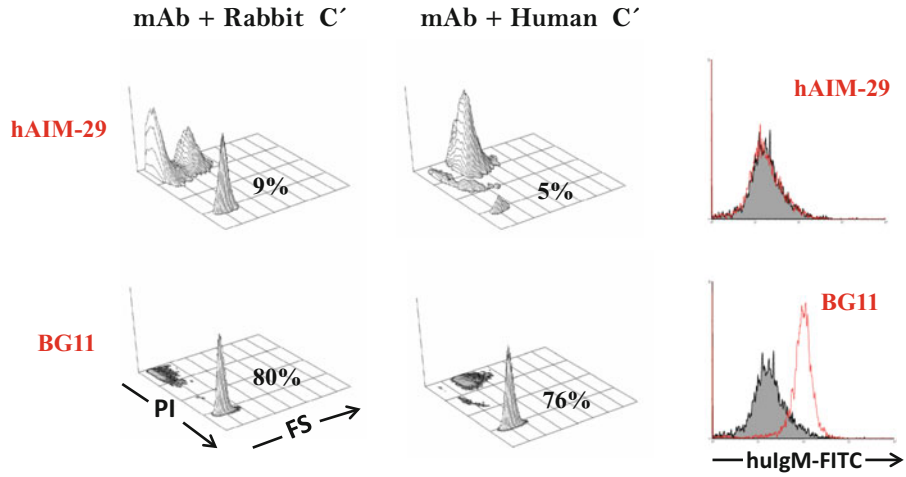

Fig. 2 Complement activation by human mAbs. Target cells (Hmy-22, a tumor B-cell line) were incubated with rabbit or human complement (C′) in the presence of hAIM-29 (human IgM mAb anti-human CD69) or BG11 (human IgM mAb anti-human B cells). The viability of the cells was tested by the incorporation of propidium iodide (PI) by flow cytometry analysis. The panels at the extreme right of the figure show how target cells were stained with hAIM-29 and BG11 human mAbs, followed by FITC-conjugated anti-human IgM (red line)

human complement, or human serum as a source of complement.

3. Add 5 μl of propidium iodide (20 μg/ml) and analyze death cells by Flow cytometry for propidium iodide staining (Fig. 2).

3.7 Purification of Antibodies

Antibody purification is required to concentrate the mAb for in vivo studies or if it is to be labeled with fluorochromes, biotin, or enzymes. Human mAbs can be purified by several methods, including ammonium sulfate precipitation, affinity chromatography, gel filtration, or a combination of techniques for obtaining an efficient purification ratio. The choice of the technique depends on the type of antibody, as well as on the initial concentration, and the purity is enhanced if the hybridoma is previously adapted to a reduced or free serum medium.

When the concentration of the antibody is low, for example in hybridoma supernatants, affinity chromatography is the most suitable purification method. The affinity ligands are usually attached to sepharose/agarose gel beads or to membranes, such as proteins with high affinity to the Fc portion of different antibody classes (Protein G/A or specific antibodies directed against some isotypes), or to the light chains (Protein L or specific antibodies directed against light chains), or to the specific antigen recognized by our human mAb. Among these, the most frequently used are protein G or A, as the specific antigens are not always easily obtained in large quantities and at high purity (*see* **Notes 12–14**).

Table 6
Protein A/G/L characteristics for human moAb purification[a]

	Human antibody	Binding capacity	Binding buffer pH	Elution buffer pH
Prot A	$IgG_{1,2,4}$; IgA; IgM	IgG, strong IgA and IgM, weak	0.1 M phosphate, 0.15 M NaCl pH 7.2–8	0.1 M Glycine–HCl pH 4
Prot G	All IgG	Strong	0.1 M phosphate pH 5–6	0.1 M Glycine–HCl pH 2.5
Prot L	All classes with kappa light chain[b]	Medium	0.1 M phosphate, 0.15 M NaCl pH 7.2–8	0.1 M Glycine–HCl pH 2.5

[a]This is general information. You can find differences that depend on the product. Please read the technical brochure carefully
[b]The protein L binds human kappa chains, which have a V segment belonging to the I, III, or IV family [79]

3.7.1 Purification Using Protein A/G/L

1. Centrifuge the human mAb supernatant at 20,000 × *g*, 4 °C and filter through a 0.45 μm filter. Dilute the sample in binding buffer and ensure that the pH is similar to that of the binding buffer (*see* Table 6).
2. Pre-warm the Protein A/G/L-Agarose resin or Sepharose gel, and the diluted sample and buffers at RT. Then, add 2–4 ml to a disposable polystyrene column and allow time to ensure proper packing.
3. Equilibrate the column by adding 5–10 volumes of binding buffer (*see* Table 6), allowing the buffer to drain through the column.
4. Carefully add the diluted hybridoma supernatant into the column, avoiding that the total amount of Ig applied to the column is higher than 80% of the total capacity of the column.
5. By saving the flow-through, the non-bound antibody can be recovered and examined by antibody-specific assays.
6. After passing the sample, wash the column with 10–15 volumes of binding buffer, and collect aliquots in which the non-bound antibody can be recovered.
7. Release bound human antibodies using 5–10 ml of elution buffer (*see* Table 6) and collecting 0.5-1 ml aliquots in tubes, into which 100 μl 1 M phosphate buffer at pH 7.5–9 had been added earlier.
8. The presence of Igs in the collected tubes is monitored by measuring the absorbance in a spectrophotometer at 280 nm. When the absorbance of two or three consecutive fractions is 0, the column can be regenerated.

9. Wash the column with 6 volumes of elution buffer and monitor the presence of protein in the collected fractions. Finally, add 5 ml of water with 0.02% sodium azide and store the column at 4 °C.
10. The eluted samples should be dialyzed to exchange the buffer compatible with the techniques that are going to be applied to a particular human mAb (*see* **Note 12**).

3.7.2 Purification Using Other Immobilized Ligand Columns

If the antigen recognized by the particular human mAb being used is available in large quantities or the antibodies being used are directed against HuIgs, the purification can be performed by affinity chromatography using a column in which these ligands are bound.

1. CNBr-activated Sepharose 4B is probably the most widely used matrix, which is commercially available and ready to use.
2. The amount of CNBr-activated Sepharose 4B to be used depends on the ligand quantity. In general, 1 g resin has to be weighed for 3.5 ml of gel, bearing in mind that 1 ml of gel is required per each 5–10 mg of protein to be linked. If the ligand has a very low molecular weight, 2 mg/ml of gel can be used.
3. Before starting the coating with the ligand (antigen or antibody), it should be verified that it is pure and that it has previously been dialyzed against the coupling buffer (0.1 M $NaHCO_3$, pH 8.3, 0.5 M NaCl). After dialysis, determine the protein concentration. A final concentration of 2–8 mg/ml is required. If necessary, concentrate the ligand by Amicon or by Centricon filtration.
4. Rehydrate the CNBr-Sepharose gel in 1 mM HCl for 15 min at RT. Do not use a magnetic stirrer. Pour the gel into a bottle top vacuum filter, and wash the gel with 1 mM HCl (200 ml/g resin). Take care that the gel does not dry. Resuspend the gel in 1–2 ml of coupling buffer and mix with the dialyzed ligand in a 15 ml or 50 ml tube. Complete with coupling buffer. Rotate the tube for 1–2 h at RT or overnight at 4 °C. To control the coupling, remove supernatant aliquots and measure the optical density at 280 nm.
5. When the coupling is over 90%, wash the gel with at least 5 gel volumes of coupling buffer in a bottle top vacuum filter, and proceed to block the remaining active groups by holding the resin for 2 h at RT in 0.1 M Tris–HCl pH 8.
6. Spin out the resin at 400 × *g* for 5 min. Remove the supernatant and wash the resin by centrifugation, alternating three times the following with washing buffers I and II (*see* Subheading 2). Finally, the resin is resuspended in PBS, 0.1% sodium azide, and stored at 4 °C.

7. To purify the human mAb, pour the gel into a polysterene disposable column and wash with PBS. Apply the sample (previously filtered through a 0.45 μm filter) and proceed to the elution as indicated earlier for the protein A/G/L affinity columns. To assess the most suitable buffer, different elution buffers (with different pH and ionic strength) have to be tested. The presence of Igs can also be monitored by measuring the absorbance at 280 nm.
8. Wash the column with PBS until the elution liquid is at pH 7.4. Store the column in PBS containing 0.1% azide.

3.8 Production (Medium Scale) with CELLine System

In the past, the production of mAb on a small-medium scale was performed by injecting the hybridoma cells into the peritoneal cavity of a mouse previously primed with pristane. This method prompts ethical questions due to the pain and distress caused in these animals, and many countries have imposed new laws that prohibit or limit the use of animals for expanding hybridomas. Alternatively, different in vitro mAb production systems can be used that are based on hollow fiber, suspension growth, or double membrane technology [80]. In all cases, a reasonable investment in staff and equipment is required. This section includes a detailed description of our experience using CELLine-CL350 systems distributed by Integra Bioscience for growing hybridomas producing human mAbs. CELLine is a multichamber system based on membrane technology, in which hybridoma cells are maintained in a 15 ml cultivation chamber, and are separated from the nutrient compartment by a semi-permeable membrane. Small molecules pass across the membrane, but the antibodies are retained in the cell growth chamber.

1. Culture medium (DMEM or RPMI-1640, 10% FCS) and nutrient medium (DMEM or RPMI-1640) must be warmed to 37 °C. It is important to wet the semi-permeable membrane prior to the inoculation of cells. Add 10 ml of nutrient medium into the nutrient chamber and let the semi-permeable membrane equilibrate for at least 5 min. Selective access to the nutrient and cultivation chambers is possible through separate compartments closed by independent caps.
2. Hybridoma cells should have a cellular viability higher than 95%; around 8×10^6 viable cells in 5 ml culture medium are needed. Open the cell compartment and inoculate the hybridoma cells by inserting the pipette into the silicone cone, trying to avoid bubbles. Close the cell chamber cap.
3. Add 340 ml of nutrient medium into its compartment and close the cap. Place the CELLine into the incubator (5% CO_2, 37 °C) and monitore hybridoma growth, particularly when using this system for the first time to grow hybridomas.

Each cell culture has its own growth characteristics. After 72 h, take an aliquot and test for cell viability and antibody level, using the chosen screening method.

4. Five to seven days later (depending on the hybridoma growth), nutrient media must be discarded and changed, and the antibodies contained in the cell compartment are then recovered. With a 10 ml serological pipette, carefully mix the cells up and down and aspirate the cell suspension, which could be more than 5 ml, due to osmotic flux.
5. Centrifuge the tube for 5 min at 300 × *g*, then take the supernatant and filter it through a 0.22 μm filter. The antibody level should be tested (by ELISA or flow cytometry) and purified by affinity chromatography, or frozen at −20 °C.
6. The cell pellet is resuspended with nutrient media, and 20% of these cells are mixed with 4 ml of warmed culture medium and inoculated again into the culture chamber. Add 350 ml of fresh nutrient medium into its compartment, and place the CELLine system into the incubator until the next harvest, approximately every 5–7 days. If the sterility barrier is not breached and the system is handled carefully, the culture can be maintained for several months (*see* **Note 15**).

3.9 High-Throughput Sequencing for Human Antibody Discovery

The recent methods of high-throughput sequencing and bioinformatics, applied to the immunoglobulin repertoire sequencing (Ig-seq), are being very useful for getting a deeply understanding of the B-cell-mediated immune responses, but also for new monoclonal antibody discovery [81]. In this sense, inferring antigen specificity by combining large-scale sequencing data and bioinformatics offers several advantages over standard hybridoma screening methods (*see* **Notes 16 and 17**). For example, Ig-seq delivers a more comprehensive picture of the total (or particular B-cell subsets) clonal repertoire landscape, thereby revealing somatic variants that may offer improved biophysical proprieties. In addition, the identification of antibodies by in silico methods reduces the cost and time consuming of the previous techniques (hybridoma production, cloning, screening, etc.).

Ig-Seq has already been applied in humanized mouse strains to validate that most of antibody transcripts are of human origin [74] and monitor the maturation pathway of specific antibodies in transgenic mice immunized with HIV immunogens [82]. In addition, different approaches for isolation of monoclonal antibodies directly from mice have been developed. In the first study published by Reddy et al. [83], the VH and VL repertoire analysis revealed that, 7 days after secondary immunization, the antibody repertoire encoded by murine bone marrow plasma B cells becomes highly polarized. To identify antigen-specific antibodies, they paired VH and VL genes based on their relative rank frequency and they were

expressed as scFvs. Thus, antibodies with nanomolar affinity for antigen were obtained. In further studies, similar strategies were used to identify antigen-binding splenic clonotypes. Furthermore, single-cell sequencing protocols to obtain VH and VL chain pairings have also been employed for antibody discovery from mice and humans [84, 85]. Thus, maybe in few years the protocols shown in this chapter will be adapted to this new technology (*see* **Note 18**).

4 Notes

1. As the immune response in transgenic mice may be lower than in conventional mice, repeated immunizations may be required. The use of a good adjuvant to potentiate antigen immunogenicity and analysis of serum 7–15 days after second immunization are both strongly recommended.
2. When haptens are conjugated to carrier proteins, it should be remembered that mice would produce antibodies to the carrier protein, as well as to the hapten. It is important to design a screening test that is useful for discriminating between hapten-specific and carrier-specific antibodies. For example, if KLH is to be used as a carrier, the hapten should also be linked to BSA or OVA by the same coupling method, and this complex should be used to assess anti-hapten antibody titers. Alternatively, special activated microplates can be used for covalent immobilization of peptides, carbohydrates, etc.
3. Numerous mouse myeloma cells have been successfully used for the generation of hybridomas. However, the most widely used cell lines are NSO/1 and Sp2/O, both descendants of MOPC-21. Neither of these cell lines produces endogenous Igs and they can both be selected using HAT (due to their defect in an essential biosynthetic pathway).
4. Stability of the hybridoma can be a problem, which may require continuous cloning-freezing-thawing. Even when growing well, the hybridoma quite frequently stops the production of antibodies. Therefore, a routine-screening process is required. Thawing the hybridoma cells in wells with a layer of mouse spleen or thymic cells can sometimes help.
5. There is frequently a low yield of antibodies using conventional hybridoma media. Growing cells at high concentrations can partially resolve this problem.
6. Regarding mAb characterization, the analysis of carbohydrate content must not be forgotten. In general, antibodies are mainly glycosylated within the Fc region and, depending on the expression system, the glycosylation pattern of the mAbs can be modified, principally mannosylation, galactosylation,

fucosylation, and sialylation. Knowing the glycosylation level is important, because these residues can affect the effector functions, immunogenicity, and half-life of therapeutic mAbs in the human body.

7. It is important to verify if the human mAbs show cross-reactivity with other human tissues. This cross-reactivity can be determined using immunohistochemical procedures.
8. In vivo assays with human antibodies in animal models are difficult to perform, due to the immunogenicity reactions. To obtain a situation comparable to a human being, immunosuppressed animals should be used, after previously receiving transplanted human bone marrow cells.
9. Absence of mouse J chain in human Igs. Conventional mouse IgM and IgA incorporate a mouse J chain in their structure, showing characteristic pentameric or dimeric forms, respectively. In the absence of the J chain, monomeric and hexameric forms of IgM should be expected, but not pentameric forms. Using Western blot, we investigated if the mouse J chain was present in an IgM mAb generated from a BAB4 mouse. J chain was not detected, indicating that these antibodies could be expressed and secreted in its absence.
10. Problems with some immunological methods. When human antibodies are directed against human cells, a high level of background can be found if using secondary antibodies (labeled antibodies directed to human immunoglobulins) in certain techniques, such as immunofluorescence (flow cytometry, confocal) or histochemistry using human tissues. The background is mainly found in human B cells and macrophages, and at the tissue interstices.
11. There is a limited repertoire of antibodies, due to the low number of V genes integrated in the genome. It is not a real problem if the work is undertaken with T-dependent antigens. The use of only one VH gene can be sufficient to generate a variety of antibodies, thanks to other sources of variability (light chains, rearrangement, mutations) [63].
12. For purification of human IgG antibodies, Protein G is the most suitable regardless of the type of subclass (Protein A could be also used, except for human IgG3 subclass). However, in some cases, the pH used for the optimal Protein G binding (pH $\cong$ 5) and/or elution (pH 2.5) can alter the antigen binding or the biological activity of the human mAb. In such situations, Protein A may be a better alternative, as pH 7–8 is the optimum for Protein A binding, while the elution can be performed at pH 3–6.
13. The main problem comes when the objective is to purify other isotypes (IgM or IgA) because these ligands have shown a low

affinity to Protein A/G. One option can be Protein L. This is an immunoglobulin-binding protein isolated from the bacteria *Peptostreptococcus magnus*, which binds certain kappa variable segments (families I, II, and III) without interfering with antigen binding [79].

14. Different production of heavy and light chains. An overproduction of light chains, but not of the whole antibody, is frequently found. For a correct quantification of antibody production, one should test for the presence of the heavy chain. Overproduction of light chains can also affect the purification of antibodies when Protein L is used, resulting in a low yield of antibody purification.
15. The half-life of human IgM is very short (3–4 days). Therefore, it is strongly recommended to use genetic engineering techniques to change the isotype of IgM antibodies to IgGs.
16. If transgenic mice carrying human Ig genes are still producing endogenous mouse Igs, the yield of human antibody production can be lower due to competition with the endogenous Igs. The best animal model is the one that does not produce endogenous Igs.
17. Availability. The majority of animal models producing human Igs are not readily available to the scientific community, because of the patents protecting this technology. As mentioned earlier, several companies are now developing fully human mAbs using this technology.
18. Alternatives to the generation of conventional hybridomas could come from strategies like those developed by Neoclone Biotechnology. The technology includes the in vitro culture of selected splenocytes (from immunized mice) with cytokines and low levels of antigen (Ag). This reactivation process yields affinity-matured, class-switched B cells. NeoClone has already developed and commercialized a murine mAb technology and is currently testing a novel hu-mAb technology using therapeutically relevant cancer Ags. The protocols include the use of human peripheral blood in a SCID mouse model, and later on animals are immunized with Ag-pulsed dendritic cells (DC). Activated spleen or lymph node B cells are cultured in vitro with cytokines. Then, the antigen specific cells are sorted, followed by the sequencing of their heavy and light Ig chains. The genes coding for those chains are cloned into antibody expression vectors. This method has several advantages: the developed mAbs are fully human (from human cells), it does not require patient immunization, and it is possible to reactive the cells in vitro several times to increase the affinity.

Acknowledgments

Financial support from the Xunta de Galicia (CINBIO, Centro singular de investigación de Galicia 2016-2019 ref. ED431G/02 and grupo de referencia competitiva ref. ED431C 2016041) and the European Union (European Regional Development Fund—ERDF) is gratefully acknowledged. S. Magadán has also received funding from People Programme (Marie Curie Actions) of the European Union's Seventh Framework Programme (FP7/2007-2013) under REA grant agreement n° 600391.

References

1. Köhler G, Milstein C (1975) Continuous cultures of fused cells secreting antibody of predefined specificity. Nature 256:495–497
2. Miller RA, Maloney DG, Warnke R, Levy R (1982) Treatment of B-cell lymphoma with monoclonal anti-idiotype antibody. N Engl J Med 306:517–522
3. Stas P, Pletinckx J, Gansemans Y, Lasters I (2009) Immunogenicity assessment of antibody therapeutics. In: Melvyn Little ATA (ed) Recombinant antibodies for immunotherapy. Cambridge University Press, Cambridge
4. Lo BKC (2005) Protein therapeutics: mouse, humanized and human antibodies. In: Walker JM, Rapley R (eds) Medical methods handbook. Springer, New York, pp 429–446
5. Arruebo M, Vilaboa N, Sáez Gutierrez B, Lambea J, Tres A, Valladares M, González-Fernández A (2011) Assessment of the evolution of cancer treatment therapies. Cancers 3:3279–3330
6. Elbakri A, Nelson PN, Abu Odeh RO (2010) The state of antibody therapy. Hum Immunol 71:1243–1250
7. Hansel TT, Kropshofer H, Singer T, Mitchell JA, George AJT (2010) The safety and side effects of monoclonal antibodies. Nat Rev Drug Discov 9:325–338
8. Chester KA, Begent RH, Robson L, Keep P, Pedley RB, Boden JA et al (1994) Phage libraries for generation of clinically useful antibodies. Lancet 343:455–456
9. Lonberg N (2008) Fully human antibodies from transgenic mouse and phage display platforms. Curr Opin Immunol 20:450–459
10. Bratkovic T (2010) Progress in phage display: evolution of the technique and its application. Cell Mol Life Sci 67:749–767
11. Hamadeh RM, Jarvis GA, Galili U, Mandrell RE, Zhou P, Griffiss JM (1992) Human natural anti-Gal IgG regulates alternative complement pathway activation on bacterial surfaces. J Clin Invest 89:1223–1235
12. Sheeley D, Merrill B, Taylor L (1997) Characterization of monoclonal antibody glycosylation: comparison of expression systems and identification of terminal alpha-linked galactose. Anal Biochem 247:102–110
13. Borrebaeck CK, Malmborg AC, Ohlin M (1993) Does endogenous glycosylation prevent the use of mouse monoclonal antibodies as cancer therapeutics? Immunol Today 14:477–479
14. Kamel-Reid S, Letarte M, Doedens M, Greaves A, Murdoch B, Grunberger T et al (1991) Bone marrow from children in relapse with pre-B acute lymphoblastic leukemia proliferates and disseminates rapidly in scid mice. Blood 78:2973–2981
15. McCune JM (1996) Development and applications of the SCID-hu mouse model. Semin Immunol 8:187–196
16. Eren R, Lubin I, Terkieltaub D, Ben-Moshe O, Zauberman A, Uhlmann R et al (1998) Human monoclonal antibodies specific to hepatitis B virus generated in a human/mouse radiation chimera: the Trimera system. Immunology 93:154–161
17. Storb U (1987) Transgenic mice with immunoglobulin genes. Annu Rev Immunol 5:151–174
18. Brinster RL, Ritchie KA, Hammer RE, O'Brien RL, Arp B, Storb U (1983) Expression of a microinjected immunoglobulin gene in the spleen of transgenic mice. Nature 306:332–336

19. Rusconi S, Köhler G (1985) Transmission and expression of a specific pair of rearranged immunoglobulin mu and kappa genes in a transgenic mouse line. Nature 314:330–334
20. Grosschedl R, Weaver D, Baltimore D, Costantini F (1984) Introduction of a mu immunoglobulin gene into the mouse germ line: specific expression in lymphoid cells and synthesis of functional antibody. Cell 38:647–658
21. González-Fernández A, Milstein C (1993) Analysis of somatic hypermutation in mouse Peyer's patches using immunoglobulin kappa light-chain transgenes. Proc Natl Acad Sci U S A 90:9862–9866
22. Betz AG, Milstein C, González-Fernández A, Pannell R, Larson T, Neuberger MS (1994) Elements regulating somatic hypermutation of an immunoglobulin kappa gene: critical role for the intron enhancer/matrix attachment region. Cell 77:239–248
23. Yélamos J, Klix N, Goyenechea B, Lozano F, Chui YL, González-Fernández A, Pannell R, Neuberger MS, Milstein C (1995) Targeting of non-Ig sequences in place of the V segment by somatic hypermutation. Nature 376:225–229
24. Wagner S, Popov A, Davies S, Xian J, Neuberger M, Brüggemann M (1994) The diversity of antigen-specific monoclonal antibodies from transgenic mice bearing human immunoglobulin gene miniloci. Eur J Immunol 24:2672–2681
25. Brüggemann M, Taussig MJ (1997) Production of human antibody repertoires in transgenic mice. Curr Opin Biotechnol 8:455–458
26. Jakobovits A, Green LL, Hardy MC, Maynard-Currie CE, Tsuda H, Louie DM et al (1995) Production of antigen-specific human antibodies from mice engineered with human heavy and light chain YACs. Ann N Y Acad Sci 764:525–535
27. Brüggemann M, Osborn MJ, Ma B, Hayre J, Avis S, Lundstrom B, Buelow R (2015) Human antibody production in transgenic mice. Arch Immunol Ther Exp 63:101–108
28. Brüggemann M, Caskey HM, Teale C, Waldmann H, Williams GT, Surani MA et al (1989) A repertoire of monoclonal antibodies with human heavy chains from transgenic mice. Proc Natl Acad Sci U S A 86:6709–6713
29. Zou X, Xian J, Davies N, Popov A, Brüggemann M (1996) Dominant expression of a 1.3 Mb human Ig kappa locus replacing mouse light chain production. FASEB J 10:1227–1232
30. Taylor L, Carmack C, Schramm S, Mashayekh R, Higgins K, Kuo C et al (1992) A transgenic mouse that expresses a diversity of human sequence heavy and light chain immunoglobulins. Nucleic Acids Res 20:6287–6295
31. Lonberg N, Taylor LD, Harding FA, Trounstine M, Higgins KM, Schramm SR et al (1994) Antigen-specific human antibodies from mice comprising four distinct genetic modifications. Nature 368:856–859
32. Brüggemann M, Neuberger MS (1996) Strategies for expressing human antibody repertoires in transgenic mice. Immunol Today 17:391–397
33. Wagner SD, Gross G, Cook GP, Davies SL, Neuberger MS (1996) Antibody expression from the core region of the human IgH locus reconstructed in transgenic mice using bacteriophage P1 clones. Genomics 35:405–414
34. Green LL, Hardy MC, Maynard-Currie CE, Tsuda H, Louie DM, Mendez MJ et al (1994) Antigen-specific human monoclonal antibodies from mice engineered with human Ig heavy and light chain YACs. Nat Genet 7:13–21
35. Mendez M, Green L, Corvalan JR, Jia X, Maynard-Currie C, Yang X et al (1997) Functional transplant of megabase human immunoglobulin loci recapitulates human antibody response in mice. Nat Genet 15:146–156
36. Jakobovits A (1998) Production and selection of antigen-specific fully human monoclonal antibodies from mice engineered with human Ig loci. Adv Drug Deliv Rev 31(1–2):33–42
37. Tomizuka K, Yoshida H, Uejima H, Kugoh H, Sato K, Ohguma A et al (1997) Functional expression and germline transmission of a human chromosome fragment in chimaeric mice. Nat Genet 16:133–143
38. Murphy AJ, Macdonald LE, Stevens S et al (2014) Mice with megabase humanization of their immunoglobulin genes generate antibodies as efficiently as normal mice. Proc Natl Acad Sci U S A 111:5153–5158
39. Macdonald LE, Karow M, Stevens S, Auerbach W, Poueymirou WT, Yasenchak J, Frendewey D, Valenzuela DM, Giallourakis CC, Alt FW, Yancopoulos GD, Murphy AJ (2014) Precise and in situ genetic humanization of 6 Mb of mouse immunoglobulin genes. Proc Natl Acad Sci U S A 111:5147–5552
40. Sano A, Matsushita H, Wu H, Jiao JA, Kasinathan P, Sullivan EJ, Wang Z, Kuroiwa Y (2013) Physiological level production of antigen-specific human immunoglobulin in cloned transchromosomic cattle. PLoS One 8: e78119
41. Matsushita H, Sano A, Wu H, Jiao JA, Kasinathan P, Sullivan EJ, Wang Z, Kuroiwa Y

(2014) Triple immunoglobulin gene knockout transchromosomic cattle: bovine lambda cluster deletion and its effect on fully human polyclonal antibody production. PLoS One 9: e90383

42. Davies NP, Rosewell IR, Richardson JC, Cook GP, Neuberger MS, Brownstein BH, Norris ML, Brüggemann M (1993) Creation of mice expressing human antibody light chains by introduction of a yeast artificial chromosome containing the core region of the human immunoglobulin kappa locus. Biotechnology (N Y) 11:911–914
43. Fishwild DM, O'Donnell SL, Bengoechea T, Hudson DV, Harding F, Bernhard SL et al (1996) High-avidity human IgG kappa monoclonal antibodies from a novel strain of minilocus transgenic mice. Nat Biotechnol 14:845–851
44. Popov A, Zou X, Xian J, Nicholson I, Brüggemann M (1999) A human immunoglobulin lambda locus is similarly well expressed in mice and humans. J Exp Med 189:1611–1620
45. Kitamura D, Roes J, Kühn R, Rajewsky K (1991) A B cell-deficient mouse by targeted disruption of the membrane exon of the immunoglobulin mu chain gene. Nature 350:423–426
46. Chen J, Trounstine M, Alt FW, Young F, Kurahara C, Loring JF et al (1993) Immunoglobulin gene rearrangement in B cell deficient mice generated by targeted deletion of the JH locus. Int Immunol 5:647–656
47. Nitschke L, Kosco M, Köhler G, Lamers M (1993) Immunoglobulin D-deficient mice can mount normal immune responses to thymus-independent and -dependent antigens. Proc Natl Acad Sci U S A 90:1887–1891
48. Oettgen H, Martin T, Wynshaw-Boris A, Deng C, Drazen J, Leder P (1994) Active anaphylaxis in IgE-deficient mice. Nature 370:367–370
49. Erlandsson L, Andersson K, Sigvardsson M, Lycke N, Leanderson T (1998) Mice with an inactivated joining chain locus have perturbed IgM secretion. Eur J Immunol 28:2355–2365
50. Ménoret S, Iscache AL, Tesson L, Rémy S, Usal C, Osborn MJ, Cost GJ, Brüggemann M, Buelow R, Anegon I (2010) Characterization of Immunoglobulin heavy chain knockout rats. Eur J Immunol 40:2932–2941
51. Zou Y, Takeda S, Rajewsky K (1993) Gene targeting in the Ig kappa locus: efficient generation of lambda chain-expressing B cells, independent of gene rearrangements in Ig kappa. EMBO J 12:811–820
52. Takeda S, Zou YR, Bluethmann H, Kitamura D, Muller U, Rajewsky K (1993) Deletion of the immunoglobulin kappa chain intron enhancer abolishes kappa chain gene rearrangement in cis but not lambda chain gene rearrangement in trans. EMBO J 12:2329–2336
53. Chen J, Trounstine M, Kurahara C, Young F, Kuo CC, Xu Y et al (1993) B cell development in mice that lack one or both immunoglobulin kappa light chain genes. EMBO J 12:821–830
54. Sanchez P, Drapier AM, Cohen-Tannoudji M, Colucci E, Babinet C, Cazenave PA (1994) Compartmentalization of lambda subtype expression in the B cell repertoire of mice with a disrupted or normal C kappa gene segment. Int Immunol 6:711–719
55. Zou X, Xian J, Popov AV, Rosewell IR, Müller M, Brüggemann M (1995) Subtle differences in antibody responses and hypermutation of lambda light chains in mice with a disrupted chi constant region. Eur J Immunol 25:2154–2162
56. Green LL, Jakobovits A (1998) Regulation of B cell development by variable gene complexity in mice reconstituted with human immunoglobulin yeast artificial chromosomes. J Exp Med 188:483–495
57. Zou X, Piper T, Smith J, Allen N, Xian J, Brüggemann M (2003) Block in development at the pre-B-II to immature B cell stage in mice without Ig kappa and Ig lambda light chain. J Immunol 170:1354–1361
58. Tomizuka K, Shinohara T, Yoshida H, Uejima H, Ohguma A, Tanaka S et al (2000) Double trans-chromosomic mice: maintenance of two individual human chromosome fragments containing Ig heavy and kappa loci and expression of fully human antibodies. Proc Natl Acad Sci U S A 97:722–727
59. Nicholson I, Zou X, Popov A, Cook G, Corps E, Humphries S et al (1999) Antibody repertoires of four- and five-feature translocus mice carrying human immunoglobulin heavy chain and kappa and lambda light chain yeast artificial chromosomes. J Immunol 163:6898–6906
60. Pruzina S, Williams G, Kaneva G, Davies S, Martín-López A, Brüggemann M et al (2011) Human monoclonal antibodies to HIV-1 gp140 from mice bearing YAC-based human immunoglobulin transloci. Protein Eng Des Sel 24:791–799
61. Magadán S, Valladares M, Suarez E, Sanjuán I, Molina A, Ayling C et al (2002) Production of antigen-specific human monoclonal antibodies: comparison of mice carrying IgH/kappa

or IgH/kappa/lambda transloci. Biotechniques 33:680–684

62. Molina A, Valladares M, Sancho D, Viedma F, Sanjuan I, Gambón F, Sánchez-Madrid F, González-Fernández A (2003) The use of transgenic mice for the production of a human monoclonal antibody specific for human CD69 antigen. J Immunol Methods 2823:147–158
63. Suárez E, Magadán S, Sanjuán I, Valladares M, Molina A, Gambón F, Díaz-Espada F, González-Fernández A (2006) Rearrangement of only one human IGHV gene is sufficient to generate a wide repertoire of antigen specific antibody responses in transgenic mice. Mol Immunol 43:1827–1835
64. Díaz B, Sanjuan I, Gambón F, Loureiro C, Magadán S, González-Fernández A (2009) Generation of a human IgM monoclonal antibody directed against HLA class II molecules: a potential agent in the treatment of haematological malignancies. Cancer Immunol Immunother 58:351–360
65. Magadán S, Sanjuán I, Valladares M et al (2004) A new potential therapeutic agent against B cell malignancies. In: 12th annual international congress of immunology/4th annual conference of the Federation-of-Clinical-Immunology-Societies (FOCIS). Medimond International Proceedings, Montreal, Canada, pp 409–422
66. Xu J, Davis M (2000) Diversity in the CDR3 region of V(H) is sufficient for most antibody specificities. Immunity 13:37–45
67. Lonberg N (2008) Human monoclonal antibodies from transgenic mice. Handb Exp Pharmacol 181:69–97
68. Green L (1999) Antibody engineering via genetic engineering of the mouse: XenoMouse strains are a vehicle for the facile generation of therapeutic human monoclonal antibodies. J Immunol Methods 231:11–23
69. Spits H (2014) New models of human immunity. Nat Biotechnol 32:335–336
70. Ishida I, Tomizuka K, Yoshida H, Tahara T, Takahashi N, Ohguma A et al (2002) Production of human monoclonal and polyclonal antibodies in TransChromo animals. Cloning Stem Cells 4:91–102
71. Chen WC, Murawsky CM (2018) Strategies for generating diverse antibody repertoires using transgenic animals expressing human antibodies. Front Immunol 9:460
72. Beck A, Wurch T, Bailly C, Corvaia N (2010) Strategies and challenges for the next generation of therapeutic antibodies. Nat Rev Immunol 10:345–352
73. Green LL (2014) Transgenic mouse strains as platforms for the successful discovery and development of human therapeutic monoclonal antibodies. Curr Drug Discov Technol 11:74–84
74. Lee EC, Liang Q, Ali H, Bayliss L, Beasley A, Bloomfield-Gerdes T, Bonoli L, Brown R, Campbell J, Carpenter A, Chalk S, Davis A, England N, Fane-Dremucheva A, Franz B, Germaschewski V, Holmes H, Holmes S, Kirby I, Kosmac M, Legent A, Lui H, Manin A, O'Leary S, Paterson J, Sciarrillo R, Speak A, Spensberger D, Tuffery L, Waddell N, Wang W, Wells S, Wong V, Wood A, Owen MJ, Friedrich GA, Bradley A (2014) Complete humanization of the mouse immunoglobulin loci enables efficient therapeutic antibody discovery. Nat Biotechnol 32:356–363
75. Osborn MJ, Ma B, Avis S et al (2013) High-affinity IgG antibodies develop naturally in Ig-knockout rats carrying germline human IgH/Igkappa/Iglambda loci bearing the rat CH region. J Immunol 190:1481–1490
76. Galfrè G, Howe S, Milstein C, Butcher G, Howard J (1977) Antibodies to major histocompatibility antigens produced by hybrid cell lines. Nature 266:550–552
77. Galfrè G, Milstein C (1981) Preparation of monoclonal antibodies: strategies and procedures. Methods Enzymol 3:3–46
78. Lefranc M (2003) IMGT, the international ImMunoGeneTics database. Nucleic Acids Res 31:307–310
79. Nilson B, Lögdberg L, Kastern W, Björck L, Akerström B (1993) Purification of antibodies using protein L-binding framework structures in the light chain variable domain. J Immunol Methods 164:33–40
80. Dewar V, Voet P, Denamur F, Smal J (2005) Industrial implementation of in vitro production of monoclonal antibodies. ILAR J 46:307–313
81. Parola C, Neumeier D, Reddy ST (2018) Integrating high-throughput screening and sequencing for monoclonal antibody discovery and engineering. Immunology 153:31–41
82. Briney B, Sok D, Jardine JG, Kulp DW, Skog P, Menis S, Jacak R, Kalyuzhniy O, de Val N et al (2016) Tailored immunogens direct affinity maturation toward HIV neutralizing antibodies. Cell 166:1459–1470
83. Reddy ST, Ge X, Miklos AE, Hughes RA, Kang SH, Hoi KH, Chrysostomou C, Hunicke-Smith SP, Iverson BL, Tucker PW, Ellington AD, Georgiou G (2010) Monoclonal antibodies isolated without screening by analyzing

the variable-gene repertoire of plasma cells. Nat Biotechnol 28:965–969

84. Wang B, Kluwe CA, Lungu OI, DeKosky BJ, Kerr SA, Johnson EL, Jung J, Rezigh AB, Carroll SM, Reyes AN, Bentz JR, Villanueva I, Altman AL, Davey RA, Ellington AD, Georgiou G (2015) Facile discovery of a diverse panel of anti-Ebola virus antibodies by immune repertoire mining. Sci Rep 5:13926
85. Wang B, Lee CH, Johnson EL, Kluwe CA, Cunningham JC, Tanno H et al (2016) Discovery of high affinity anti-ricin antibodies by B cell receptor sequencing and by yeast display of combinatorial VH:VL libraries from immunized animals. MAbs 8:1035–1044

Chapter 12

Refining the Quality of Monoclonal Antibodies: Grafting Unique Peptide-Binding Site in the Fab Framework

Jeremy D. King and John C. Williams

Abstract

Monoclonal antibodies (mAbs) are a major therapeutic modality. Grafting the meditope binding site onto mAbs, also known as meditope-enabling, can extend the usefulness of mAbs by providing an additional protein-protein interaction surface without altering the stability or antigen binding. We have previously used this site for attaching dyes, cytotoxic drugs, and entire proteins. Here, we provide a simple protocol for meditope-enabling mAbs, and verifying meditope and antigen binding using flow cytometry (FACS).

Key words Meditope, Antibody-drug conjugate, Bispecific antibody

1 Introduction

Antibodies are the largest class of therapeutic molecules and one of the most important tools in the biosciences [1]. Their utility can be extended through the addition of new proteins or small molecules, such as dyes [2, 3]. One technology for such additions is the meditope platform [4]. The meditope is a 12 amino acid, cyclic peptide that binds to the cavity between the light and heavy chains of cetuximab. The binding site is unique to cetuximab, and completely absent from human antibodies [4]. However, we have successfully grafted the binding site onto several human monoclonal antibodies, including trastuzumab [4, 5]. Once engineered, meditope-binding site acts effectively as a unique and highly specific but innocuous receptor site on the mAb. As such, there are multiple applications made available with this technology [6, 7].

For instance, it is possible to use the technology for pre-targeted imaging. Here, meditope-enabled mAbs targeting a specific antigen is administered to the patient. Over time, the mAb accumulates at the site of disease and clears the blood stream (typically 2 days). At that point, it is possible to add the meditope functionalized with DOTA and a radionuclide. The radiolabeled

Michael Steinitz (ed.), *Human Monoclonal Antibodies: Methods and Protocols*, Methods in Molecular Biology, vol. 1904,
https://doi.org/10.1007/978-1-4939-8958-4_12,

meditope can rapidly accumulate at the disease site decorated with meditope-enabled mAb. Unbound material is rapidly filtered and excreted. Imaging of the disease can occur as soon as 2 h. Two significant advantages to this approach are: (1) the radionuclide undergoes fewer half-lives, thus there is more signal and (2) as the radio-labeled meditope is rapidly cleared, there is less background as well as less radiation exposure for the patient. The increase in signal and the decrease in background significantly improve the overall image quality. Initial studies using the meditope for pre-targeted imaging are very promising. Other applications include drug delivery, clustering through multivalent meditopes, and the creation of multispecific immune engagers.

Herein, we provide a detailed approach to meditope-enable and characterize any antibody, give the sequence is known.

2 Materials

2.1 Grafting

1. Sequence Alignment Software.

2.2 Verification

1. Alexa647-Ac-CQFDLSTRRLQCGGSK meditope (*see* **Note 1**).
2. Dye labeled secondary antibody for flow cytometry (*see* **Note 2**).
3. A flow cytometer capable of two color detection (*see* **Note 3**).
4. Washing buffer (1× PSB with 1% BSA).

3 Methods

3.1 Grafting

1. Locate the amino acid sequence of the antibody of interest (*see* **Note 4**).
2. Download the fasta sequence for cetuximab (PDB ID 4gw1, DOI: https://doi.org/10.2210/pdb4GW1/pdb), meditope-enabled trastuzumab (PDB ID 4hjg, DOI: https://doi.org/10.2210/pdb4HJG/pdb), and parental trastuzumab (PDB ID 4hkz, DOI: https://doi.org/10.2210/pdb4HKZ/pdb) from https://www.rcsb.org/. For all PDBs, the light chain is chain A, and the heavy chain is chain B.
3. In your alignment software, import the light chains from your antibody of interest, cetuximab, meditope-enabled trastuzumab, and parental trastuzumab (Fig. 1).
4. Align the sequences using clustalW.
5. Locate and substitute the following positions in your antibody of interest (Table 1).
6. Export your meditope-enabled light chain.

Fig. 1 Sequence alignment comparing trastuzumab, me-trastuzumab, and cetuximab. The meditope site was originally derived from cetuximab

Table 1
Light chain mutations

Trastuzumab number	Substitution
LC S9	I
LC S10	L
LC K39	R
LC P40	T
LC G41	N
LC K42	G
LC A43	S
LC K45	R
LC F83	E (*see* **Note 5**)
LC T85	D
LC Q100	A

7. In your alignment software, import the heavy chains from your antibody of interest, cetuximab, meditope-enabled trastuzumab, and trastuzumab.
8. Align the sequences using clustalW.

Table 2
Heavy chain mutations

Trastuzumab number	Substitution
HC A40	S
HC V93	I

9. Locate and substitute the following positions in your antibody of interest (Table 2).
10. Export your meditope-enabled heavy chain.
11. Synthesize codon-optimized DNA with substituted amino acid sequences or introduce substitutions into existing vector through mutagenesis (*see* **Note 6**).

3.2 Verification of Binding by FACS

1. 5×10^6 cells expressing the target antigen are grown prior to FACS (*see* **Note 7**).
2. On the day of FACS, 5×10^6 cells are brought to final volume of 1 mL in washing buffer. Cells are then washed by centrifuging at $300 \times g$ for 5 min, removing the supernatant, and resuspending with fresh washing buffer. This wash is repeated twice.
3. Split the cells into five tubes of 200 μL, corresponding to 1×10^6 cells per tube. Label the tubes (1) parental antibody, (2) meditope-enabled antibody (memAb), (3) meditope alone, (4) secondary alone, and (5) untreated.
4. To the parental antibody sample, add the original parental antibody to a final concentration of 100 nM. To the memAb sample, add the memAb to a final concentration of 100 nM. The other three samples are not treated at this time.
5. Incubate all samples on ice for 30 min.
6. Wash the samples with washing buffer as above to remove unbound antibodies.
7. Add the fluorescently labeled secondary antibody, according to the manufacturer's guidelines, to the parental, memAb, and secondary alone control samples.
8. Add the fluorescently labeled meditope to a final concentration of 50 nM to the memAb and meditope control samples.
9. Incubate all samples on ice for 30 min.
10. Wash the samples with washing buffer as above to remove unbound meditope and antibodies.
11. Perform flow cytometry on all five samples recording the fluorescence channels for both the meditope and secondary antibody dyes.

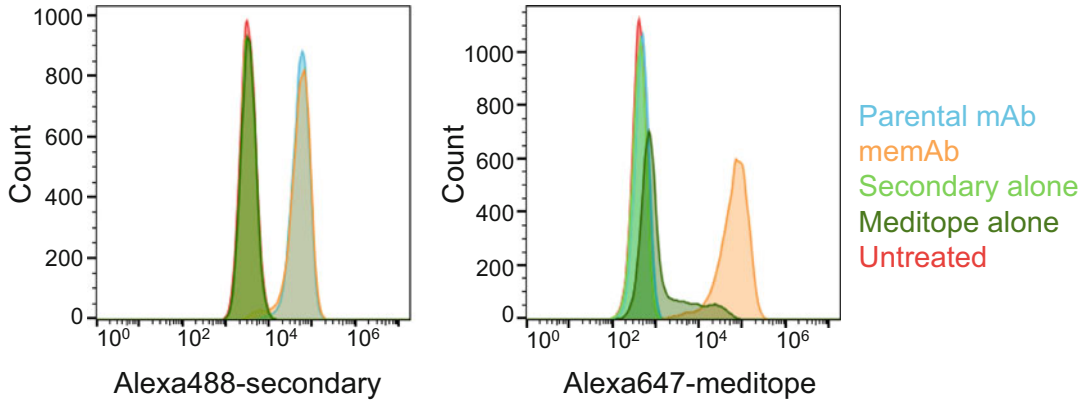

Fig. 2 FACS-binding analysis of memAb. By comparing the binding of the Alexa488, anti-Fc secondary between the parental mAb and memAb, we can see that antigen binding is not altered by meditope-enabling. From Alexa647-meditope sample, we can see that only in the presence of the memAb will the meditope bind to the target cells, indicating specific meditope-memAb interactions. Slight nonspecific binding the Alexa647-meditope to the cells is observed, likely from the sticky nature of Alexa647. In the above experiment, the parental mAb is trastuzumab and memAb is me-trastuzumab

12. The parental mAb should show binding to the target cells. The memAb sample should show the same binding to the target cells as the parental mAb when comparing labeling using the secondary antibody. The memAb sample should also show signal from the meditope, indicating meditope binding. The control samples (secondary alone, meditope alone, and untreated) should not show any labeling. Weak nonspecific binding is sometimes observed from the Alexa647-meditope (Fig. 2).

4 Notes

1. We normally use N-terminally acetylated CQFDLSTRRLQ CGGSK as a starting peptide, and conjugate Alexa647 to the terminal lysine through NHS chemistry (e.g., Cat. # A37573, ThermoFisher). This can readily be purchased from peptide synthesis companies.
2. We use F(ab′)2-Goat anti-Human IgG Fc Secondary Antibody, Alexa Fluor 488 (Cat. # H10120, ThermoFisher). Depending on your species and Fc, you will need to pick an appropriate secondary.
3. The dye combination for the meditope and secondary must be compatible for two color FACS on your FACS machine. Alternative dyes can be used on either the meditope or secondary. We prefer to keep Alexa647 on the meditope as we have seen less nonspecific binding with this dye compared to Alexa488.

4. This procedure has been successfully tested on κ-LC antibodies based on 4d5 (trastuzumab) constant region framework.
5. In our original memAb grafting, we replaced position 83 with isoleucine. After additional optimization, we have switched position 83 to glutamic acid. The affinity improves from 1000 to 20 nM with this substitution [8].
6. The affinity for meditope in meditope-enabled antibodies varies slightly from antibody to antibody [5].
7. We recommend FACS as an initial verification for meditope and antigen binding. It is generally relatively easy to find a cell line expressing the target antigen. We recommend further verification of memAb properties using size-exclusion chromatography and surface plasmon resonance (SPR). We routinely mix memAb with equimolar concentrations Alexa647-meditope, and run the mixture on a size-exclusion column. If the meditope binds, it will co-elute with the memAb. If the antigen is available or can be produced, we will test antigen binding using SPR. To date, every memAb tested has had indistinguishable binding from the parental mAb.

References

1. Strebhardt K, Ullrich A (2008) Paul Ehrlich's magic bullet concept: 100 years of progress. Nat. Rev. Cancer 8:473. https://doi.org/10.1038/nrc2394
2. Brinkmann U, Kontermann RE (2017) The making of bispecific antibodies. MAbs 9 (2):182–212. https://doi.org/10.1080/19420862.2016.1268307
3. Schumacher D, Hackenberger CPR, Leonhardt H et al (2016) Current status: site-specific antibody drug conjugates. J Clin Immunol 36 (1):100–107. https://doi.org/10.1007/s10875-016-0265-6
4. Donaldson JM, Zer C, Avery KN et al (2013) Identification and grafting of a unique peptide-binding site in the Fab framework of monoclonal antibodies. Proc Natl Acad Sci U S A 110 (43):17456–17461. https://doi.org/10.1073/pnas.1307309110
5. Zer C, Avery KN, Meyer K et al (2017) Engineering a high-affinity peptide binding site into the anti-CEA mAb M5A. Protein Eng Des Sel 30(6):409–417. https://doi.org/10.1093/protein/gzx016
6. King JD, Ma Y, Kuo Y-C et al (2018) Template-catalyzed, disulfide conjugation of monoclonal antibodies using a natural amino acid tag. Bioconjug Chem 29(6):2074–2081. https://doi.org/10.1021/acs.bioconjchem.8b00284
7. van Rosmalen M, Ni Y, Vervoort DFM et al (2018) Dual-color bioluminescent sensor proteins for therapeutic drug monitoring of antitumor antibodies. Anal Chem 90(5):3592–3599. https://doi.org/10.1021/acs.analchem.8b00041
8. Bzymek KP, Puckett JW, Zer C et al (2018) Mechanically interlocked functionalization of monoclonal antibodies. Nat Commun 9 (1):1580. https://doi.org/10.1038/s41467-018-03976-5

Chapter 13

Basic Procedures for Detection and Cytotoxicity of Chimeric Antigen Receptors

Keichiro Mihara, Tetsumi Yoshida, and Joyeeta Bhattacharyya

Abstract

Chimeric antigen receptors against CD19 (anti-CD19-CAR) are widely recognized and used by not only researchers associated with immunology, molecular biology, and cell biology but also physicians to treat B-cell malignancies. Anti-CD19-CAR is currently clinically available as one of the therapeutic modalities for refractory acute B-cell-typed lymphoblastic leukemia (B-ALL) patients. However, to detect CAR on the cell surface and investigate the efficacy of CAR-T cells, there are numerous experimental modalities including flow cytometry, the Cr-releasing assay, immunoblot, and immunostaining. We have chosen several techniques, which are necessary and sufficient as well as reliable and reproducible to detect and assess the killing effect of CAR-T cells. Here, we describe protocols for basic experiments and procedures for the detection of CAR on transduced cells and in in vitro coculture experiments to assess cytotoxicity using CAR-T cells.

Key words CD19, CD38, Flow cytometry, Autolysis, CAR, Antibody capping

1 Introduction

We developed chimeric antigen receptors against CD19 (anti-CD19-CAR) about two decades ago [1], and they are now widely recognized and used by not only researchers associated with immunology, molecular biology, and cell biology but also physicians to treat B-cell malignancies. Since Grupp et al. and Porter et al. reported that T cells bearing anti-CD19-CAR (anti-CD19-CAR T cells) were markedly effective in patients with relapsed/refractory acute B-cell-typed lymphoblastic leukemia (B-ALL) as well as refractory chronic lymphoid leukemia [2, 3], CAR-T cells have become well known. Thus, anti-CD19-CAR is currently clinically available as one of the therapeutic modalities for refractory B-ALL patients. However, to detect CAR on the cell surface and investigate the efficacy of CAR-T cells, there are numerous experimental modalities including flow cytometry, the Cr-releasing assay, immunoblot, and immunostaining. We have chosen several techniques, which are necessary and sufficient as well as reliable and

Michael Steinitz (ed.), *Human Monoclonal Antibodies: Methods and Protocols*, Methods in Molecular Biology, vol. 1904,
https://doi.org/10.1007/978-1-4939-8958-4_13,

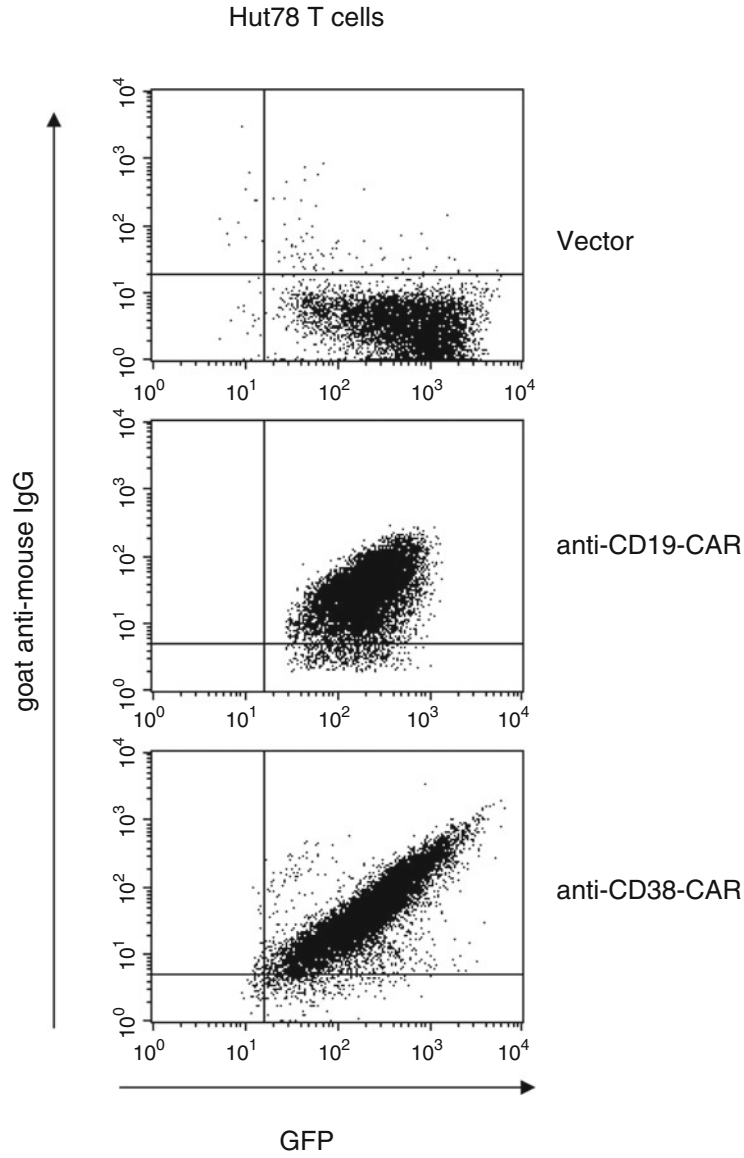

Fig. 1 Expression of anti-CD19- or anti-CD38 CAR on T cells. Expression of anti-CD19- or anti-CD38-CAR on Hut78 T cells. Both the anti-CD19- and anti-CD38-CAR, which reacted with GAM Ab-biotin that was bound by SA-PerCP, and green fluorescent protein (GFP) as an internal marker were co-expressed on the surface of Hut78 T cells. (Reproduced from ref. 5 with permission from Willy)

reproducible to detect and assess the killing effect of CAR-T cells. We preferably use flow cytometry to detect surface CAR on T cells (Fig. 1), which is easy, swift, and reliable [4–10]. For the evaluation of cytotoxicity with CAR-T cells, flow cytometry is desirable, because necrosis and apoptosis can be differentially discriminated and further investigation can be performed (Figs. 2 and 3).

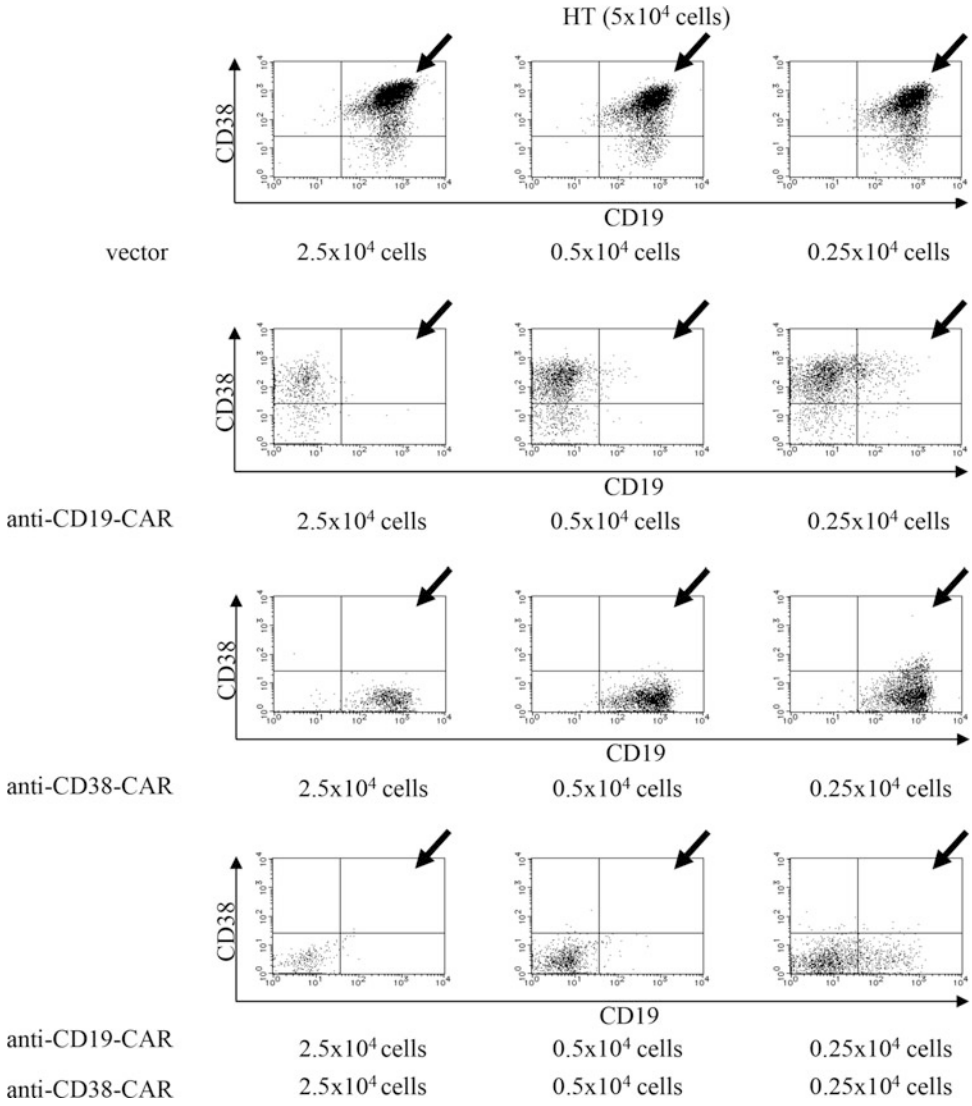

Fig. 2 Cytotoxicity of Hut78 T cells with anti-CD19- and/or anti-CD38-CAR against HT cells. HT cells (5×10^4) were cocultured with CD19- and/or CD38-specific Hut78 T cells for 4 days at various ratios of target to effector cells (2.5×10^4, 0.5×10^4, and 0.25×10^4). T cells with anti-CD19- and/or anti-CD38-CAR killed HT cells effectively. Viable HT cells are in the quadrant indicated by arrowheads. (Reproduced from ref. 5 with permission from Willy)

Accordingly, protocols used in basic experiments and procedures for the detection of CAR on transduced cells and in in vitro coculture experiments to assess cytotoxicity using CAR-T cells are indicated in this chapter. Furthermore, in the case of surface molecules targeted by CAR on activated T cells, capping with antibody to an identical antigen that CAR recognizes is a prerequisite for transduced T-cell survival. Trouble-shooting is briefly described as well.

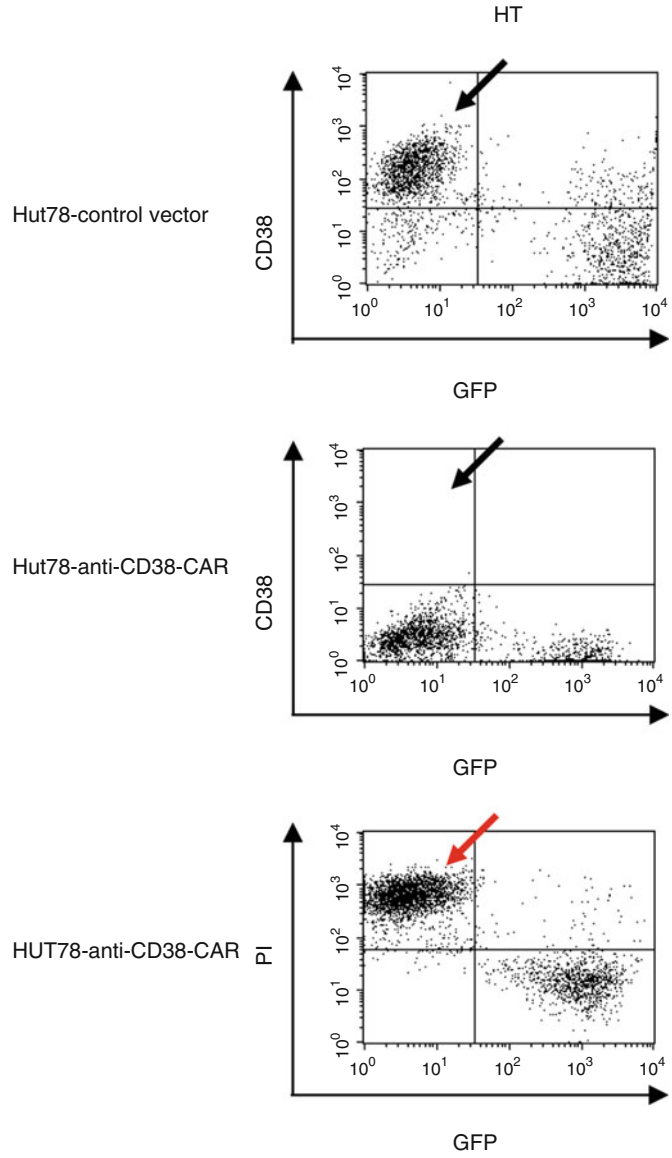

Fig. 3 Incorporation of PI dye into HT cells cocultured with anti-CD38-CAR T cells. HT cells were examined after 4 days of culture with Hut78 T cells transduced with vector alone at an effector: target ratio of 0.5: 1 (as indicated by black arrows in the upper panel) and with anti-CD38-CAR (middle panel). After 4 days of culturing HT cells with Hut78 T cells bearing the anti-CD38-CAR, PI dye was incorporated into these HT cells co-incubated with Hut78 cells expressing the anti-CD38-CAR, showing that the HT cells had not lost the expression of CD38 but were dead (as indicated by red arrows in the lower panel). (Reproduced from ref. 4 with permission from Wolters Kluwer Health)

2 Materials

Prepare all solutions and reagents of analytical grade. Prepare and store them at room temperature unless indicated otherwise. Faithfully follow institutional regulations.

2.1 Culture of T Cells Transduced In Vitro

1. RPMI-1640 medium supplemented with 10% heat-inactivated fetal calf serum (FCS), supplemented with L-glutamine (2 mM), penicillin (100 U/mL), and streptomycin (100 μg/mL).
2. Human recombinant Interleukin-2 (IL-2).
3. Culture flasks and 15 mL polystyrene tubes.
4. Falcon tubes for flow cytometer.

2.2 Antibodies and Solutions for Immunostaining

1. Goat anti-mouse (Fab′)2 polyclonal antibody conjugated to biotin (abbreviated as GAM Ab-biotin) (*see* **Note 1**).
2. Streptavidin conjugated to peridinin chlorophyll protein (PerCP) (abbreviated as SA-PerCP) (*see* **Note 2**).
3. Anti-CD19 antibody conjugated with phycoerythrin (PE) (*see* **Note 3**).
4. Phosphate-buffered saline, pH 7.4 (PBS): 0.01 M phosphate buffer, 0.0027 M potassium chloride, and 0.137 M sodium chloride, pH 7.4.

2.3 Cells Transduced

1. CD19 (as well as CD38)-positive HT cells, which are derived from diffuse large B-cell lymphoma.
2. T cells transduced with CAR (e.g., anti-CD19-CAR) as well as T cells with control vector.

2.4 Flow Cytometry

1. Flow cytometer (e.g., FACS Canto II or Calibur) (Becton Dickinson).
2. Setup beads and controls (Becton Dickinson).
3. Sheeth fluid (Becton Dickinson).

3 Methods

Carry out all procedures at room temperature unless otherwise specified.

3.1 Staining and Detection of CAR on T Cells

1. Incubate transduced T cells at 37 °C in 5% CO_2–95% air in RPMI-1640 medium, 10% heat-inactivated FCS, and L-glutamine in the presence of IL-2 (20–200 IU/mL) in a 25 cm^2 flask. Replace medium including IL-2 every 3–5 days (*see* **Note 4**).

2. Wash cells bearing CAR with PBS three times and then directly add 20 μL of GAM Ab-biotin to the pellet in a Falcon tube. Incubate it for 30 min on ice and then wash cells with PBS three times. Directly add 20 μL of SA-PerCP to cells in the tube.
3. Wash cells with PBS three times. Then, suspend cells in 1 mL of PBS. Cells are subjected to flow cytometry for the detection of CAR. Cover tubes including stained cells with aluminum foil to protect from light to maintain the intensity of fluorescence. This procedure is not necessary in the case of fluorescein isothiocyanate (FITC).
4. Prepare a flow cytometer (e.g., FACS Canto II) to detect multicolored fluorescent dye.
5. Run the sample following standardizing with setup beads as well as control beads. Then, analyze the data obtained (*see* **Note 5**).

3.2 Specific Cytotoxicity of Anti-CD19-CAR T Cells with HT Cells ($CD19^+$ Cells) in Coculture Experiments

1. Wash HT cells and anti-CD19-CAR T cells or vector-transduced T cells with PBS three times. Initially, put HT cells into 96 or 48-well plates at the indicated cell numbers (~1×10^5 cells/well for 96-well plate) (*see* **Note 6**).
2. Put transduced T cells into identical well plates, where HT cells are placed depending on effector target ratios.
3. Incubate at 37 °C in 5% CO_2–95% air for 72–96 h.
4. Harvest incubated cells from wells (*see* **Note 7**).
5. Wash cells with PBS three times.
6. Directly put 20 μL of anti-CD19 antibody-PE into a falcon tube.
7. Place it at 4 °C for 30 min.
8. Wash cells with PBS three times.
9. Prepare a cell slurry in 1 mL of PBS.
10. Subject cells to flow cytometry for the detection of HT cells.
11. Calculate HT cells included in the harvested sample (*see* **Notes 8** and **9**).

4 Notes

1. Although GAM-Ab directly conjugated with fluorescent dye can also be used for the detection of CAR, the intensity of the fluorosignal is quite weak even though any fluorescent dye is used. Accordingly, the streptavidin-biotin system is strongly recommended.

2. Any other fluorescent dye from PerCP could be used for immunostaining depending on the fluorescent reference of the vector or surface molecule.
3. Any other fluorescent dye from PE could be used for immunostaining depending on the fluorescent reference of the vector or surface molecule. Furthermore, it is necessary to select an appropriate antibody with an identical epitope of the antigen that CAR-T cells recognize. Anti-CD38-CAR T cells target CD38, so choose anti-CD38 monoclonal antibody, that reacts with the epitope of CD38, which anti-CD38-CAR T cells can recognize.
4. Ignore this step if CAR on T cells is directly detected. As IL-2 causes cell death through activation, cells are desirably cultured within 2 weeks. When a surface molecule is targeted by CAR on activated T cells, capping with an antibody with an identical antigen that CAR recognizes is a prerequisite for transduced T-cell survival. In the case of CD38, since CD38 is expressed on activated T cells prior to transduction, the rate of recovery of T cells with anti-CD38-CAR is quite low compared with that of vector-transduced T cells due to apoptosis caused by the interaction of anti-CD38-CAR with the CD38 molecule. Accordingly, the addition of an anti-CD38 antibody can increase the yield of viable transduced T cells by blocking the auto-lytic reaction. To increase the number of T cells with anti-CD38-CAR and maintain the viability of the cells, we replaced the medium containing the anti-CD38 antibody purified from the hybridoma, from which scFV of anti-CD38-CAR originated (0.15 mg/mL) and IL-2 (200 IU/mL) every 4–5 days until 14 days post-transduction. Hut78 T cells do not have CD38. These were described previously [4–10].
5. When a fluorescent dye other than PE is used for staining, choose the most appropriate laser and filter depending on the fluorescence.
6. Never put too many cells into wells, or they might be killed because of overgrowth.
7. As cells are sticky at the bottom edge in the well, mechanically detach them with a sharp pipette tip using a circular motion.
8. Specific cytotoxicity is evaluated using the formula (B-A)/B where A is the number of $CD19^+$ HT cells after incubation with anti-CD19-CAR-expressing T cells, and B is the number of $CD19^+$ HT cells after incubation with vector-transduced T cells.
9. Make a note of the running time to count 10,000 cells.

Acknowledgment

This work was supported by a Japanese Grant-in-Aid for Science Research.

References

1. Imai C, Mihara K, Andreansky M, Nicholson IC, Pui CH, Geiger TL et al (2004) Chimeric receptors with 4-1BB signaling capacity provoke potent cytotoxicity against acute lymphoblastic leukemia. Leukemia 18:676–684
2. Grupp SA, Kalos M, Barrett D, Aplenc R, Porter DL, Rheingold SR et al (2013) Chimeric antigen receptor-modified T cells for acute lymphoid leukemia. N Engl J Med 368:1509–1518
3. Porter DL, Levine BL, Kalos M, Bagg A, June CH (2011) Chimeric antigen receptor-modified T cells in chronic lymphoid leukemia. N Engl J Med 365:725–733
4. Mihara K, Yanagihara K, Takigahira M, Imai C, Kitanaka A, Takihara Y et al (2009) Activated T-cell-mediated immunotherapy with a chimeric receptor against CD38 in B-cell non-Hodgkin lymphoma. J Immunother 32:737–743
5. Mihara K, Yanagihara K, Takigahira M, Kitanaka A, Imai C, Bhattacharyya J et al (2010) Synergistic and persistent effect of T-cell immunotherapy with anti-CD19 or anti-CD38 chimeric receptor in conjunction with rituximab on B-cell non-Hodgkin lymphoma. Br J Haematol 151:37–46
6. Mihara K, Bhattacharyya J, Kitanaka A, Yanagihara K, Kubo T, Takei Y et al (2012) T-cell immunotherapy with a chimeric receptor against CD38 is effective in eliminating myeloma cells. Leukemia 26:365–367
7. Bhattacharyya J, Mihara K, Kitanaka A, Yanagihara K, Kubo T, Takei Y et al (2012) T-cell immunotherapy with a chimeric receptor against CD38 is effective in eradicating chemotherapy-resistant B-cell lymphoma cells overexpressing survivin induced by BMI-1. Blood Cancer J 2:e75
8. Mihara K, Yoshida T, Ishida S, Takei Y, Kitanaka A, Shimoda K et al (2016) All-trans retinoic acid and interferon-α increase CD38 expression on adult T-cell leukemia cells and sensitize them to T cells bearing anti-CD38 chimeric antigen receptors. Blood Cancer J 6: e421
9. Yoshida T, Mihara K, Takei Y, Yanagihara K, Kubo T, Bhattacharyya J et al (2017) All-trans retinoic acid enhances cytotoxic effect of T cells with an anti-CD38 chimeric antigen receptor in acute myeloid leukemia. Clin Transl Immunology 5:e116
10. Mihara K, Yoshida T, Takei Y, Sasaki N, Takihara Y, Kuroda J et al (2017) T cells bearing anti-CD19 and/or anti-CD38 chimeric antigen receptors effectively abrogate primary double-hit lymphoma cells. J Hematol Oncol 10:116

Chapter 14

Rapid Chimerization of Antibodies

Koji Hashimoto, Kohei Kurosawa, Hidetaka Seo, and Kunihiro Ohta

Abstract

We previously developed the in vitro method to generate monoclonal antibodies (mAbs) from libraries constructed with chicken B-cell line DT40 (referred to as the "ADLib system"). As the wild-type DT40 cells express immunoglobulin M (IgM), the original ADLib system provides monoclonal antibodies in chicken IgM format. For the therapeutic, diagnostic, and research purposes, the Fc regions of IgMs should be exchanged to other classes and species, for example human or murine IgG. However, the Fc engineering by conventional bioengineering process is laborious and takes plenty of time. Here, we developed a method to enable the seamless replacement of the Fc regions of antibodies generated by the ADLib system, using recombination-mediated cassette exchange (RMCE). In this system, two Cre recombinase recognition sites were inserted into the IgM's Fc region of the DT40 genome, allowing the exchange of the Fc region to the sequences of interest by co-transfection of a donor sequence and a Cre recombinase expression vector. We describe the detailed protocol of the technology: how to construct the RMCE host strains, select mAbs by the ADLib system, and exchange their Fc regions to generate chimeric mAbs.

Keywords Chimeric antibody, Fc engineering, Monoclonal antibody library, DT40 cell, ADLib system, Recombination-mediated cassette exchange (RMCE), Cre recombinase, Trichostatin A (TSA)

1 Introduction

The recent successes in the field of therapeutic antibodies are based on the advances in antibody engineering technologies. One of the most important technologies is Fc engineering, which can provide multiple functions to mAbs such as the toxicity by site-specific drug conjugation, enhanced binding activity to Fc receptors resulting in the improved ADCC (antibody-dependent cellular cytotoxicity) activity, or enhanced CDC (complement-dependent cytotoxicity) activity. In a conventional Fc engineering, chimeric antibodies can be generated by fairly straightforward genetic engineering; by joining the immunoglobulin (Ig) variable regions of a selected mouse hybridoma to human Ig constant regions, and be used as such or as a first stage toward further humanization [1, 2]. However, this process involves multiple steps including time-consuming genetic manipulation that has to be performed for each selected

Michael Steinitz (ed.), *Human Monoclonal Antibodies: Methods and Protocols*, Methods in Molecular Biology, vol. 1904,
https://doi.org/10.1007/978-1-4939-8958-4_14,

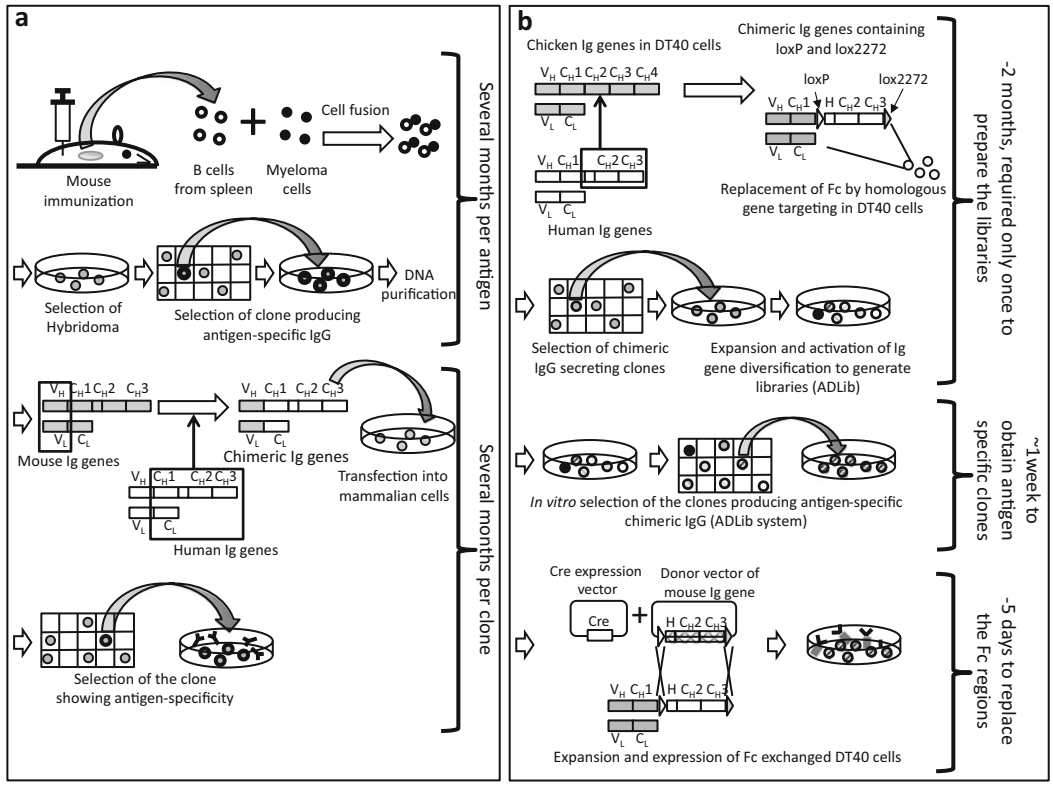

Fig. 1 (**a**) Schematic diagram of the conventional method to generate mAbs and the chimerized antibodies. First, the spleen containing B cells from an immunized mouse is collected. The B cells are fused with myeloma cells to construct hybridoma and isolate clones producing antigen-specific IgGs. The DNA sequences coding mouse V_H and V_L are then isolated from the clones, as well as the DNA sequences coding human immunoglobulin constant regions from human cells. Mouse/human chimeric genes are constructed by genetic engineering and transfected into mammalian cells specialized to protein expression. Chimeric antibodies are finally obtained from the selected clone showing antigen-specificity [7–9]. (**b**) Schematic diagram of the method for RMCE-based generation of chimeric IgGs. DT40 strains producing membrane-bound and secreted form human chimeric IgGs flanked by loxP and lox2272 are constructed by gene targeting. The immunoglobulin variable genes of the transformed clones producing human chimeric IgGs are diversified by treatment with TSA to generate cell libraries displaying repertoires of antibodies. Diversified libraries can be stocked for repeated later use by freezing the cells. The cells producing the antigen-specific antibodies of interest are screened and selected using antigen-conjugated magnetic beads. The selected clones are expanded and the Fc regions can be exchanged to mouse IgG by RMCE. IgGs are recovered in the form of culture supernatant

antigen-specific clone as illustrated in Fig. 1a. Chimerization by using mammalian culture cells can also induce a loss of mAb expression or specificity, so that repeated selection rounds of compatible candidate clones can be required until finding the most suitable one. We previously developed the in vitro cell-based technology referred to as the "ADLib (Autonomously Diversifying Library) system," which allows the rapid screening and isolation of DT40 cells expressing antigen-specific mAbs (in about one week starting from the B-cell clone selection from the cell surface mAb display library diversified by Trichostatn A (TSA), a histone

deacetylase inhibitor) [3, 4]. Although the ADLib system generates mAbs rapidly in vitro, one of the disadvantages is that DT40 cells express chicken IgMs. Generally, IgMs are less preferred than IgGs because IgGs are much easier to be purified and more widely used in the therapeutic, diagnostic and research field than IgMs. In our previous reports, we successfully inserted the coding sequence of the human IgG's Fc region to the chicken IgM heavy-chain locus of DT40 cells by gene targeting to generate the chicken-human chimeric IgG expressing cells [5]. However, as the targeting rate of DT40's Fc region is very low (less than 1%), this method was not suitable for the simultaneous chimerization of multiple mAbs obtained by the ADLib system. To overcome this disadvantage, we have developed a method to efficiently exchange the Fc regions of antibodies by using RMCE based on the Cre/loxP system [6]. The RMCE-based strategy is composed of two steps (Fig. 2a). First, human IgG1-Fc placed between loxP and lox2272, a loxP mutant 2272 which has been reported to recombine with an identical mutant, but not with the wild-type loxP, is integrated to the Fc region of DT40 cells by the conventional gene-targeting method driven by the endogenous homologous recombination machinery (Fig. 2b). Second is RMCE-based exchange of human IgG1-Fc region to any other sequence of interest inserted between loxP and lox2272 (Fig. 2c). With this strategy, any Fc sequence of interest can be integrated to DT40 antibodies, either before or after isolation of specific mAbs by the ADLib system. By combining this method with the ADLib system (Fig. 3), we can directly select and test multiple antigen-specific human chimeric antibody candidates for antigens of interest in minimal time, followed by the exchange of Fc region by RMCE to various sequences including IgGs of other species or functional peptides (e.g., toxic peptides, fluorescence proteins, etc.). This method could therefore remarkably reduce the process time and labor spent and prompt to develop valuable Fc engineered mAbs for various purposes, as shown in Fig. 1b by comparison to the traditional method of Fig. 1a. The present protocol describes each important step of the complete process including the genetic construction of the RMCE host cells for library generation, the selection of antigen-specific candidate clones by applying the ADLib system, and the exchange of Fc region by RMCE.

2 Materials

2.1 Cell Culture

IMDM, GultaMAX Supplement.
Fetal bovine serum.
Chicken serum.
Penicillin.
Streptomycin.
2-Mercaptoethanol.

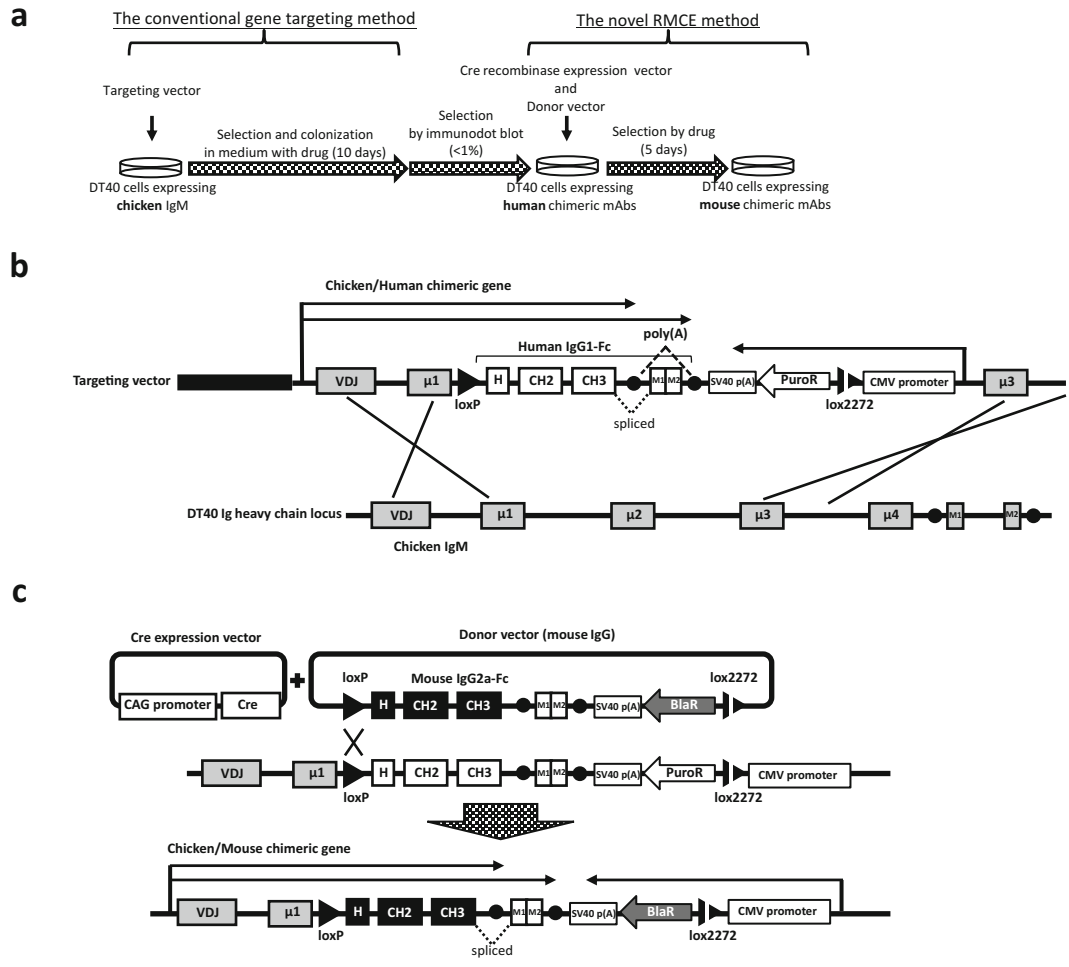

Fig. 2 (**a**) Experimental outline of the generation of chimeric antibodies. The endogenous chicken IgM-Fc region was replaced with human IgG1-Fc cassette by the conventional targeted integration method. Human IgG1-Fc was switched to mouse IgG2a-Fc by RMCE. (**b**) Scheme for the development of RMCE host strains. The targeting vector was designed to target the chicken IgM Fc region at Ig heavy chain locus. The targeting vector contains human IgG1-Fc and puromycin resistance gene in the opposite orientation. LoxP and lox2272 were placed upstream of human IgG1-Fc and between CMV promoter and cDNA of puromycin resistance gene of the targeting vector, respectively. The transmembrane domains of human IgG (M1 and M2) and a polyA signal were inserted downstream of human IgG1-Fc and its polyA to simultaneously express both membrane-bound and secreted version of chimeric antibodies by alternative splicing. (**c**) Scheme for the RMCE strategy. Cre recombinase expression vector and the donor vector including the mouse IgG2a-Fc gene and a promoter-less blasticidin resistance gene were co-transfected, and DT40 cells properly replaced by its human IgG1-Fc with mouse IgG2a-Fc were selected by the addition of blasticidin

2.2 Transfection for Gene Targeting

Wild-type DT40 cells.
Phenol/chloroform.
Phosphate buffer saline (PBS).
Electroporator (GenePulser).

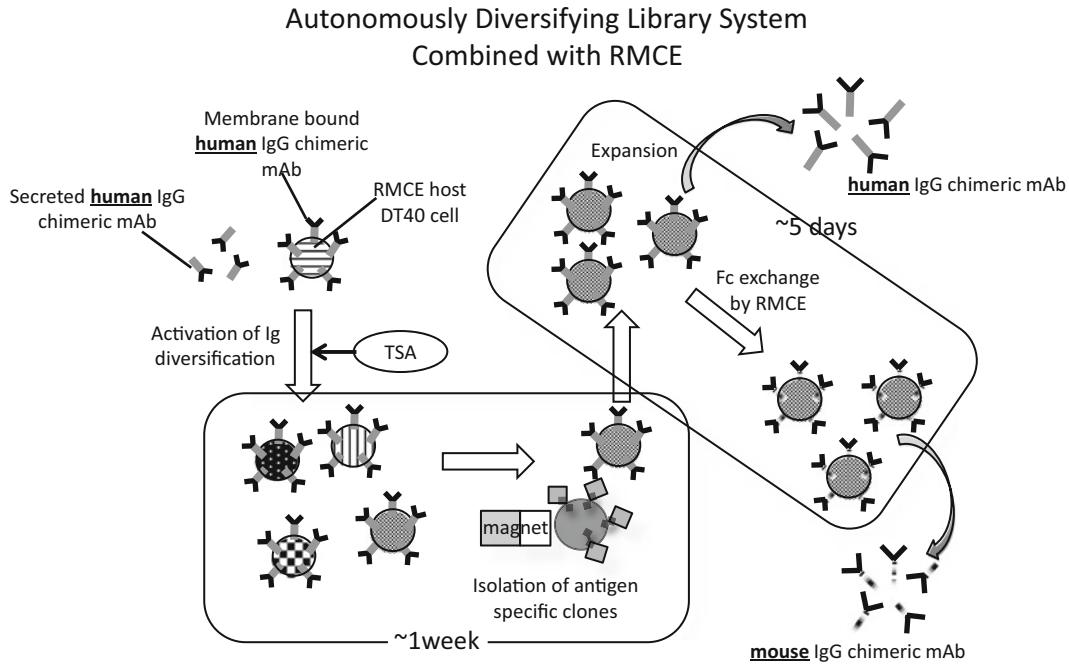

Fig. 3 Schematic diagram of the ADLib system using the RMCE host DT40 cells expressing human IgG chimeric mAbs. The DT40 cells producing antigen-specific mAbs are selected using antibody-conjugated magnetic beads. The selected cells are expanded followed by the exchange of Fc region by RMCE to express mouse IgG chimeric mAbs

Electroporation cuvette (0.4 cm).
96-Well flat-bottom microtiter plate.

2.3 Immunodot Blot

Nitrocellulose membrane.
TBST: TBS, 0.05% Tween 20.
Skim Milk.
Horseradish Peroxidase (HRP)-conjugated anti-human IgG antibody.
ECL reagent.
Image visualizer.

2.4 mAb Selection by the ADLib System

Trichostatin A (TSA).
Magnetic beads (Dynal Tosylactivated M280 Dynabeads).
Magnetic stand (Dynal MPC-S).
Buffer A: 0.1 M Na-Phosphate buffer, pH 7.4.
Buffer B: PBS, 0.1% BSA, pH 7.4.
Buffer C: 0.2 M Tris–HCl, 0.1% BSA, pH 8.5.
Sodium azide.
Selection buffer: PBS, 1% BSA.

2.5 ELISA

U-shaped bottom maxisorp immunoplate.
PBST: PBS, 0.05% Tween 20.
HRP substrate (DAKO TMB+ Substrate-Chromogen).

0.5 M H_2SO_4.
Microplate reader.
Horseradish Peroxidase (HRP)-conjugated anti-human IgG antibody.

2.6 Transfection for Fc Engineering

Cre recombinase expression vector.
Electroporator (Lonza Nucleofector 2b).
Cell Line Nucleofector Kit T (including Electroporation cuvette, Solution T and Supplement 1).

2.7 Antibiotics and Final Concentrations for DT40 Selection

Puromycin (0.5 μg/ml).
Blasticidin (25 μg/ml).
L-Histidinol dihydrochloride (450 μg/ml).
Zeocin (1600 μg/ml).

3 Methods

3.1 Construction of the Targeting Vector for RMCE Host Strains

1. Prepare the synthetic sequence of human IgG1-Fc gene. Amplify the ~2 kb region from 340 bp upstream of the 5′ end of hinge region to the membrane domains by PCR using human genomic DNA as a template. When amplifying, delete the intron sequence between exon M1 and M2 for membrane-bound domain.
2. Prepare an antibiotic resistance marker gene (e.g., puromycin resistance marker (PuroR) in Fig. 2b) driven by the CMV promoter and terminated by SV40 polyA site. When amplifying, lox2272 site is inserted between the antibiotic resistance marker gene and the CMV promoter.
3. Clone human IgG1-Fc gene and the antibiotic resistant marker gene to the appropriate vector so that they are the opposite orientation to each other. When cloning, loxP site is integrated upstream of human IgG-Fc gene.
4. Amplify about 1.3 kb of the region upstream of the second exon of the chicken IgM heavy chain locus using genomic DNA from DT40 as a PCR template. Clone the PCR fragment to the upstream of human IgG-Fc gene of **step 3** as one homologous sequence for gene targeting.
5. Amplify about 4.2 kb of the region downstream of the second exon of the chicken IgM heavy chain locus using genomic DNA from DT40 as a PCR template. Clone the PCR fragment to the downstream of the CMV promoter gene of **step 4** as the other homologous sequence for gene targeting.

3.2 Cell Culture

Culture DT40 cells in "IMDM, GultaMAX Supplement" supplemented with 10% fetal bovine serum, 1% chicken serum, 50 U/ml penicillin-50 μg/ml streptomycin, and 55 μM 2-mercaptoethanol

at 39.5 °C in 5% CO_2 incubator. Change the medium every 1 or 2 days to maintain the cell density between $2 \times 10^5 \sim 2 \times 10^6$ cells/ml.

3.3 Construction of RMCE Host Strains

1. Linearize 40 μg of the targeting vector plasmid with an appropriate restriction enzyme, which can introduce a single cut in vector segments.
2. Purify the DNA segments with phenol/chloroform, followed by ethanol precipitation.
3. Resuspend the DNA pellet in 800 μl of sterilized PBS and keep it on ice.
4. Harvest 1×10^7 DT40 cells and wash them in ice-cold PBS.
5. Add the DNA solution into the cell suspension and transfer to the electroporation cuvette.
6. Incubate the cuvette on ice for 10 min.
7. Perform electroporation using Gene Pulser at 25 μF and 550 V.
8. Chill the cuvette on ice quickly and stand for 10 min.
9. Transfer the cells in 20 ml medium and incubate at 37 °C and 5% CO_2 for 24 h.
10. The cells are then harvested and resuspended into 80 ml of the medium containing an antibiotic (e.g., puromycin in Fig. 2b).
11. Dispense the cell suspension into four 96-well plates (200 μl in each well).
12. Incubate at 39.5 °C and 5% CO_2. Drug resistant colonies are visible after approximately 6 days.

3.4 Screening of RMCE Host Strains

The RMCE host strains are screened by immunodot blot using the culture supernatants of the candidate clones with anti-human IgG-Fc antibody because the targeted clones secrete chimeric human antibodies.

1. Spot 2 μl of culture supernatant from each well containing a single colony onto a nitrocellulose membrane.
2. Block the membrane in TBST containing 5% skim milk at room temperature for 1 h.
3. Wash the membrane twice in TBST for 5 min.
4. Incubate with HRP-conjugated anti-human IgG-Fc antibody dissolved in TBST containing 0.1% skim milk for 1 h.
5. Wash the membrane five times in TBST (15 min × 1, 5 min × 4).
6. Incubate with ECL reagent for 1 min and detect the signals by image visualizer.

7. Transfer the colonies corresponding to dots with positive signals to fresh culture medium and expand the cells.
8. (Option) Verify the correct insertion of the construct by RT-PCR, FACS, immunoblot etc. [6].

3.5 Preparation of Diversified DT40 Cell Libraries [4]

The RMCE host strains are treated with Trichostatin A (TSA, at final concentration of 8.3–10 nM) for approximately 4–8 weeks. The cell density should be lower than ~2 × 10^6 cells/ml. The TSA-containing medium should be changed every day (*see* **Note 1**).

3.6 Preparation of Antigen-Conjugated Magnetic Beads [4]

1. Add 200 μl of Tosylactivated M280 Dynabeads into a 1.5 ml tube. Place the tube on Dynal MPC-S for 2 min.
2. Discard the supernatant and detach the tube from Dynal MPC-S.
3. Resuspend the beads in 400 μl of buffer A containing 0.3 mg/ml of the antigen of interest.
4. Incubate at 37 °C for 16 h with gentle rotation.
5. Insert the tube on Dynal MPC-S for 2 min.
6. Discard the supernatant and remove the tube from Dynal MPC-S.
7. Resuspend the beads in 400 μl of buffer B and set the tube on Dynal MPC-S for 2 min.
8. Discard the supernatant and detach the tube from Dynal MPC-S.
9. Resuspend the beads in 400 μl of buffer C and incubate at 37 °C for 4 h.
10. Set the tube on Dynal MPC-S for 2 min.
11. Discard the supernatant and detach the tube from Dynal MPC-S.
12. Resuspend the beads in 400 μl of buffer B containing 0.02% sodium azide. Note that antigen-conjugated beads should be prepared prior to the selection described below.

3.7 Selection of Cells Using Magnetic Beads [4]

1. Harvest 1 × 10^8 cells of the diversified library in Subheading 3.5.
2. Wash the cells twice in 5 ml of selection buffer.
3. Resuspend the cells in 1 ml of selection buffer.
4. The cells are transferred into 1.5 ml tube and collected by centrifugation.
5. During centrifugation, prepare the magnetic beads solution.
   (a) Add 5 μl of the antigen-conjugated magnetic beads suspension into 1 ml of selection buffer in a 1.5 ml tube. Resuspend the cells by gentle pipetting.

(b) Set the tube on Dynal MPC-S for 2 min.

(c) Discard the supernatant and detach the tube from Dynal MPC-S.

(d) Resuspend the beads in 1 ml of selection buffer.

(e) Repeat **steps (b)–(d)** once again.

6. Mix the cell pellet from **step 4** in the beads suspension from **step 5** in 1.5-ml tube.
7. Incubate at 4 °C with gentle rotation for 30 min.
8. Spin down the liquid briefly and set the tube on Dynal MPC-S for 2 min.
9. Discard the supernatant and detach the tube from Dynal MPC-S.
10. Suspend the pellet in 1 ml of selection buffer by gentle pipetting.
11. Repeat **steps 8–10** four times to wash the pellet.
12. During **step 11**, prepare 30 ml of pre-warmed medium in 50 ml tube.
13. Place the tube on Dynal MPC-S for 2 min and discard the supernatant.
14. Resuspend the pellet by gentle pipetting in 0.5 ml of selection buffer.
15. Add the suspension to the medium prepared in **step 12** and mix well by pipetting.
16. Dispense the cells into 96-well plates (300 μl in each well).
17. Incubate at 39.5 °C and 5% CO_2. Colonies are visible after approximately 6 days (*see* **Note 2**).

3.8 Screening of the mAb-Expressing Clones [4]

1. Add 100 μl of PBS containing 5 μg/ml of antigen into the wells of 96-well immunoplates. In addition, prepare another protein as a reference negative control to eliminate clones producing antibodies with nonspecific binding.
2. Incubate at 4 °C overnight.
3. Discard the solution. The plate is then blocked with 200 μl of PBS containing 1% BSA.
4. Incubate at room temperature for 30 min.
5. Discard the solution.
6. Wash three times with 200 μl of PBST.
7. Add 100 μl of the culture supernatant from the cells expanded in 96-well plates.
8. Incubate at room temperature for 1 h.

9. Discard the supernatants and wash five times with 200 μl of PBST.
10. Add 100 μl of PBS containing 1% BSA with HRP-conjugated anti-human IgG-Fc antibody.
11. Incubate at room temperature for 1 h.
12. Discard the contents.
13. Wash five times with 200 μl of PBST.
14. Add 100 μl of TMB+ and incubate at room temperature for ~3 min.
15. Add 100 μl of 0.5 M H_2SO_4 to stop the reaction. The reaction should be terminated before reaching a plateau.
16. Measure the optical density at 450 nm with a microplate reader.
17. Subtract the background signal of the medium from the signals of each well in the plates.
18. Calculate the antigen/negative control ratios.
19. Select clones that exhibit a high ratio (e.g., >10) and expand them for the Fc engineering in Subheading 3.9.

3.9 Fc Engineering by RMCE

1. Construct a donor vector for RMCE. The donor vector should contain the following genes: loxP site, the sequence of the interest, SV40 polyA site, and a promoter-less antibiotic resistance marker gene (e.g., blasticidin resistance marker (BlaR) in Fig. 2c) placed in the opposite orientation and lox2272 site.
2. Mix Solution T and Supplement 1 in the ratio 45:10.
3. Add 0.8 μg of Cre recombinase expression vector and 7.2 μg of the donor vector to 100 μl of the solution above.
4. Harvest 1×10^7 cells of the clone selected in Subheading 3.8. Discard the supernatant completely so that the transfection solution is not diluted.
5. Resuspend the cells with the solution in **step 3** and transfer to the electroporation cuvette (*see* **Note 3**).
6. Perform transfection by Nucleofector 2b using program B-23.
7. Transfer the cell in the 20 ml pre-warmed medium immediately and incubate at 39.5 °C and 5% CO_2 for 24 h (*see* **Note 4**).
8. Add an antibiotic (e.g., blasticidin in Fig. 2c) directly to the culture medium and incubate further. If you go well, the cell density becomes around 10^6 cells/ml in 4 days (*see* **Note 5**).
9. (Option) Examine the exchange of Fc region by FACS, ELISA, immunoblot etc. [6].

3.10 (Option) Fc Engineering Followed by mAb Selection with the ADLib System

In the protocol above, mAbs are selected first by the ADLib system, and then Fc regions are switched. Meanwhile, this protocol is flexible enough to generate Fc-engineered mAbs in the reverse process: (1) switching Fcs as described in Subheading 3.9 prior to the mAb selection, (2) performing the ADLib system described in Subheadings 3.5–3.8. This approach might be useful when you decided which formats are preferable before the antibody selection.

4 Notes

1. Be careful not to let the cell density become too low. The growth rate gets slow in the medium containing TSA (approximately half speed than usual).
2. If too many colonies appear (>100 per plate), the cell number for selection can be reduced (e.g., 1×10^7 cells).
3. Resuspend cells gently. Since the transfection solution is toxic, so vigorous pipetting may result in low efficiency and take more time to obtain Fc-engineered cells.
4. First, add 500 μl of pre-warmed medium to the cuvette immediately for minimizing the damage of the cell. Then gently transfer all the culture to the fresh media.
5. Even if the transfection efficiency is low for some reason, you can obtain Fc-engineered cells within at least 7 days due to the rapid growth rate of DT40 cells (doubling time is ~8 h).

References

1. Liu AY, Robinson RR, Murray DE Jr, Ledbetter HA (1987) Production of a mouse-human chimeric monoclonal antibody to CD20 with potent Fc-dependent biologic activity. J Immunol 139:3521–3526
2. Morrison SL, Johnson MJ, Herzenberg LA, Oi VT (1984) Chimeric human antibody molecules: mouse antigen-binding domains with human constant region domains. Proc Natl Acad Sci U S A 81:6851–6855
3. Seo H, Masuoka M, Murofushi H, Takeda S, Shibata T, Ohta K (2005) Rapid generation of specific antibodies by enhanced homologous recombination. Nat Biotechnol 23:731–735
4. Seo H, Hashimoto S, Tsuchiya K, Lin W, Shibata T, Ohta K (2006) An ex vivo method for rapid generation of monoclonal antibodies (ADLib system). Nat Protoc 1:1502–1506
5. Lin W, Kurosawa K, Murayama A, Kagaya E, Ohta K (2011) B-cell display-based one-step method to generate chimeric human IgG monoclonal antibodies. Nucleic Acids Res 39:e14. https://doi.org/10.1093/nar/gkq1122
6. Hashimoto K, Kurosawa K, Murayama A, Seo H, Ohta K (2016) B cell-based seamless engineering of antibody Fc domains. PLoS One 11:1–22
7. de St. Groth SF, Scheidegger D (1980) Production of monoclonal antibodies: strategy and tactics. J Immunol Methods 35:1–21. https://doi.org/10.1016/0022-1759(80)90146-5
8. Köhler G, Milstein C (1975) Continuous cultures of fused cells secreting antibody of predefined specificity. Nature 256:495–497
9. Köhler G, Milstein C (1976) Derivation of specific antibody-producing tissue culture and tumor lines by cell fusion. Eur J Immunol 6:511–519

Chapter 15

Phage Display Technology for Human Monoclonal Antibodies

Marco Dal Ferro, Serena Rizzo, Emanuela Rizzo, Francesca Marano, Immacolata Luisi, Olga Tarasiuk, and Daniele Sblattero

Abstract

During the last 20 years in vitro technologies opened powerful routes to combine the generation of large libraries together with fast selection and screening procedures to identify lead candidates. One of the most successful methods is based on the use of filamentous phages. Functional Antibodies (Abs) fragments can be displayed on the surface of phages by fusing the coding sequence of the antibody variable (V) regions to the phage minor coat protein pIII. By creating large libraries, antibodies with affinities comparable to those obtained using traditional hybridoma technology can be isolated by a series of cycles of selection on the antigen of interest. In this system, antibody genes can be recovered simultaneously with selection and can be easily further engineered, for example by increasing their affinity to levels unobtainable in the immune system, or by modulating their specificity and their effector functions (by recloning into a full-length immunoglobulin scaffold). This chapter describes the basic protocols for antibody library construction and selection of binder with desired specificity.

Key words Phage display, Antigens, Monoclonal antibody, High-throughput, scFv

1 Introduction

Traditional methods to generate monoclonal antibodies rely on the immunization of laboratory animals and the subsequent immortalization and selection of specific hybridoma cells. The process is laborious, requires costly animal houses and its efficacy depends on the ability of the immune system to mount a humoral productive response to the potential antigens. The advent of recombinant DNA technology has brought in the field new potentialities allowing to recapitulate in vitro the complete process of antibody production and selection, by-passing immunization, animal handling, and the laborious process of clone isolation. The great advantage of in vitro methods is the possibility of coupling together the cloning of functional antibody fragments, their selection, and finally the isolation of the positive antibodies coding genes. in vitro methods

Michael Steinitz (ed.), *Human Monoclonal Antibodies: Methods and Protocols*, Methods in Molecular Biology, vol. 1904, https://doi.org/10.1007/978-1-4939-8958-4_15,

allow identifying antibodies with high-throughput potential, speed, and flexibility: antibodies can be selected and their affinities and specificities can be precisely tailored according to the needs. Phage [1, 2] and yeast display [3, 4] are the commonest methods for this purpose.

In 1985, G.P. Smith [5] first introduced the concept of displaying exogenous proteins on the surface of M13 phages, showing the potentials of building phage libraries displaying large repertoires of different proteins. Antibody display libraries have been the most successful application of this concept [6]. The basic idea behind the display technology is that once a large library of antibodies is created, those with desirable properties can be selected. A phage displaying a specific antibody on its surface can be isolated for its binding property to a target ligand starting from a collection of billions of phages displaying different antibodies. Since the phage displayed protein gene is present in the phage genome, the selection of a virus allows the concomitant recovery of the corresponding antibody gene. Once isolated genetic details are easily identified by DNA sequencing and the sequence could be used for subsequent applications (*see* Fig. 1).

To carry out this procedure a few essential steps are required.

First, a library containing the antibody DNA sequences is created. Antibody diversity is restricted to the variable regions (VH and VL) and these gene fragments are inserted into a specific vector in frame with the sequence encoding the phage protein pIII. Once assembled, the phage particle will expose the functional antibody fragment fused to the amino terminus of the minor coat protein III. In the creation of an antibody library several different choices can be made: a) which form of antibody fragment to use; b) the source of V regions repertoire. In general, successful approaches have employed either the single-chain fragment variables (scFv) [7] format, consisting in a VL and VH regions linked by a flexible linker, or the Fab (Fragment antigen-binding) format, in which VH-CH1 and VL-CL associate non-covalently [8].

Natural V region repertoires can be recovered by RT-PCR amplification starting from lymphocytes which may or may not have undergone antigen stimulation. Such V genes are amplified using primers which recognize the 5′ end of the V genes and the 3′ end of the J genes [9]. These naïve libraries turned out to be robust sources of antibodies potentially against any target [10–12], including those poorly antigenic in animals. As an alternative, synthetic antibody libraries have been created by introducing diversity artificially using oligonucleotides into frameworks with desirable properties [13–15]. To generate diversity, completely degenerate oligonucleotides were used [16], although recently it has been found that diversity restricted to only few amino acids can provide antibodies with similar high affinities [17].

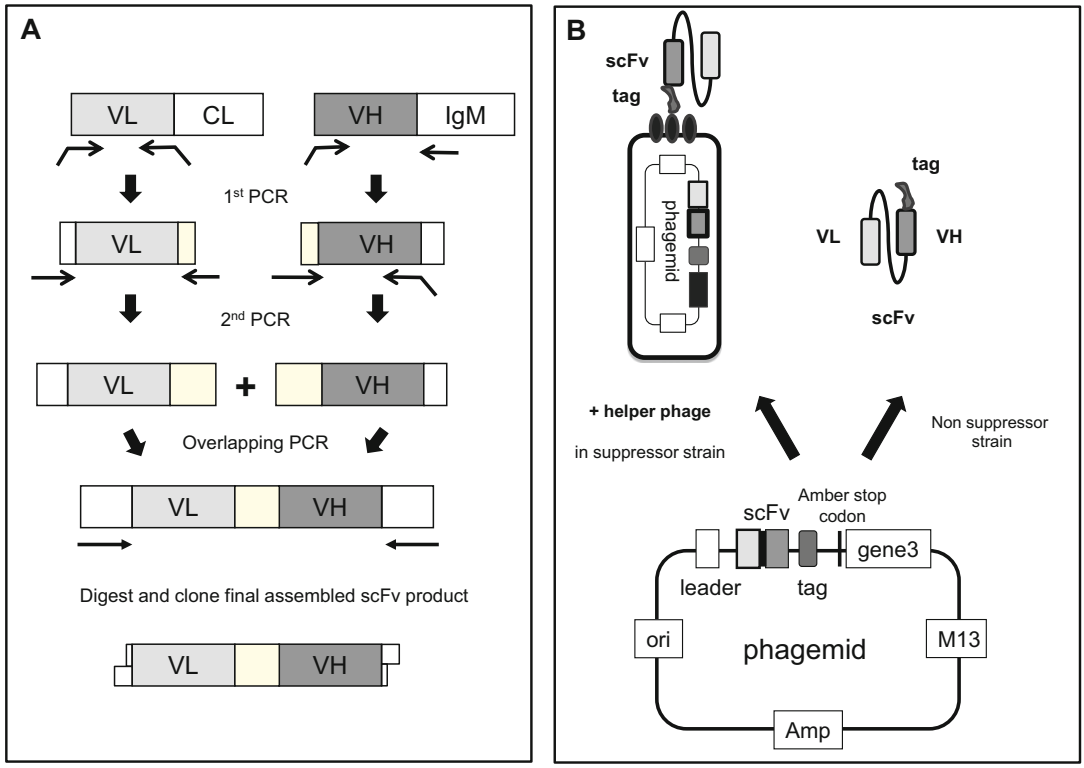

Fig. 1 (**a**) PCR assembly of V genes into a scFv format. (**b**) Schematic of a phagemid display vector with phage or soluble scFv production scheme

Before proceding to selection the clonal diversity of the library, either naïve or synthetic, needs to be assessed. Next generation sequencing is now routinely used to measure diversity and to validate the design of displayed libraries [18].

Once a library is created, the enrichment of antigen-specific phage antibodies is carried out by "phage panning", using immobilized [19] or labeled antigens [20].

In this process, the antigen of interest is directly immobilized on a solid support, such as microplate wells or is coupled to magnetic beads. The phage particles are then added to allow the binding of phages displaying appropriate antibody. After extensive washing to remove all nonspecifically bound material, phages displaying specific antibodies are retained while low affinity or unspecific phages are washed away. The selection procedure is repeated two to five rounds usually decreasing antigen concentration and increasing stringency of washing steps, leading to the isolation of phages expressing the desired antibodies (i.e., those that bind the antigen of interest). Bound phages are then eluted from the target antigen and used to infect bacteria for binding analysis. The possibility of performing successive rounds of selection allows the isolation of binders present in very low number in a population of

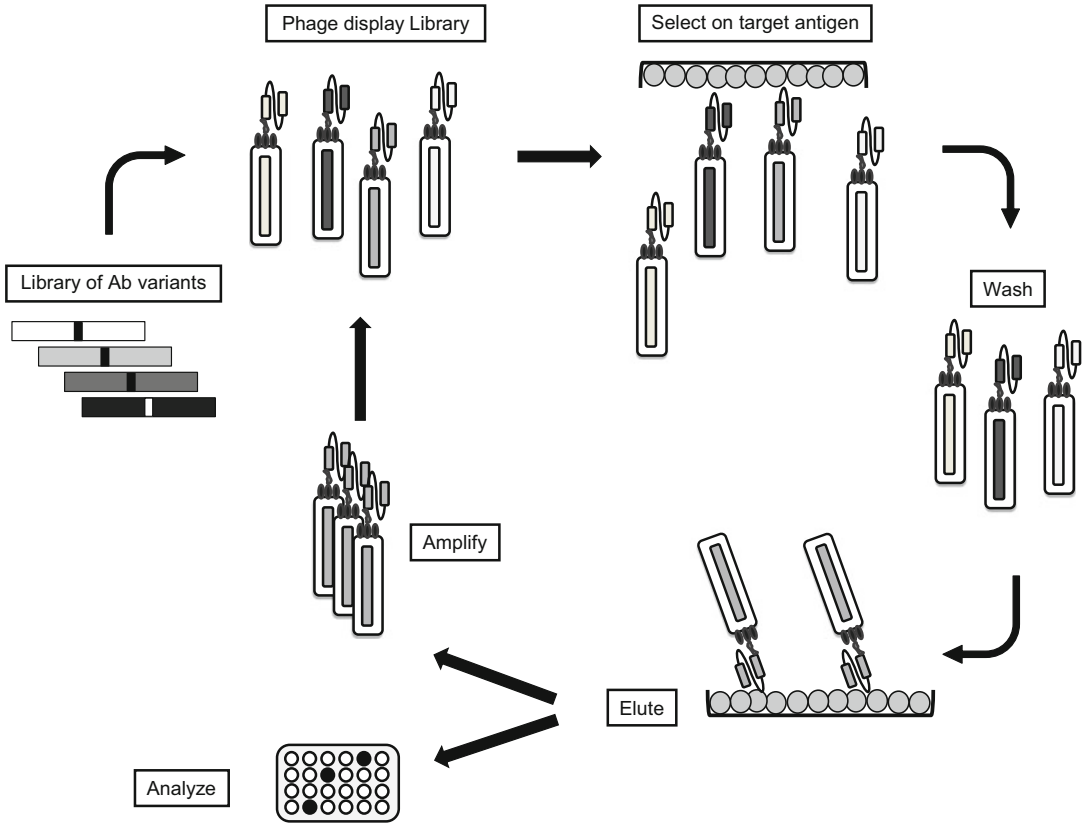

Fig. 2 Phage display selection cycle. Up to five rounds of selection over a specific target are performed; in each round, unreactive clones are removed, and reactive clones are amplified. Positive clones are successively isolated and identified by DNA sequencing

billions of different phages. A typical selection round is illustrated in Fig. 2.

At the end, specific antibodies for a given antigen are identified through an ELISA screening within several random clones. At this point, as antibody genes are directly identified by sequencing they can be subjected to downstream genetic engineering, for instance to increase affinity (through the generation of mutated antibodies secondary libraries) and/or to build full-length immunoglobulin with the desired effector functions.

2 Materials

2.1 Construction of Antibody Libraries

1. Bacterial strain used is *Escherichia coli* DH5αF′ *[F′/endA1 hsd17(rK_mKþ) supE44 thi-1 recA1gyrA (Nalr) relA1 _(lac-ZYA-argF) U169 deoR (F80dlacD-(lacZ)M15)].*
2. Ficoll-Paque PLUS (GE Healthcare).

3. Plasmid DNA is prepared using a commercial Miniprep kit, following the instructions of the manufacturer.
4. Stock solutions of antibiotics are prepared by dissolving kanamycin at 50 mg/mL in water and ampicillin at 100 mg/mL in water. Kanamycin and ampicillin stocks are filtered with 0.22 μm filter device and stored at −20 °C. Repeated freeze and thaw of ampicillin is avoided, and aliquots are prepared for single use.
5. 2×TY (2× Tryptone Yeast) liquid broth is prepared adding 16 g bacto-tryptone, 10 g bacto-yeast, and 5 g NaCl to 1 L of ddH_2O. Final pH 7.0. Agar plates are prepared by adding 1.5% bacto-agar to 2×TY broth. Make up to 1 L with distilled water, autoclave and allow to cool to 55 °C. At this temperature antibiotics and glucose can be added, prior to pouring into plates.
6. Glycerol molecular biology grade, (60% v/v), autoclaved.
7. All restriction endonucleases, T4 DNA ligase and buffers are purchased from New England Biolabs. All cloning steps are performed according to the manufacturer's suggestions and to standard molecular biology procedures.
8. Commercial Gel Extraction Kit and PCR Clean-Up Kit are used for purification of DNA from agarose gel and restriction reaction mixtures, respectively, following the instructions of the manufacturer.
9. Commercial DNA clean and concentrator kit is used to purify and concentrate the ligation mixture, following the instructions of the manufacturer (*see* **Note 1**).
10. High-efficiency Electrocompetent Cells for Phage Display are used for transformations. 25 μL aliquot is used for transformation of 1–2 μL of purified DNA, using 1 mm gap cuvette (*see* **Note 2**).

2.2 Phage Production and Titration

1. Helper phage M13KO7.
2. Solution for precipitation of phages: 20% (w/v) polyethylene glycol (PEG) 6000 and 2.5 M NaCl. The solution is filtered through a 0.22 μm filter before use, store at room temperature.
3. PBS: 8 g NaCl, 0.2 g KCl, 1.44 g Na_2HPO_4 and 0.24 g KH_2PO_4 in 1 L H_2O, final pH 7.4.
4. 20% glucose: filtered with 0.22 μm filter device and stored at room temperature.
5. 2×TYAG (2×TY Ampicillin Glucose): add 100 μg/mL ampicillin and 1% of glucose to 2×TY liquid broth.
6. 2×TYAK (2×TY Ampicillin Kanamycin): add 100 μg/mL ampicillin and 50 μg/mL kanamycin to 2×TY liquid broth.

2.3 Phage Selection to Immobilized Antigen

1. Immuno MaxiSorp Tubes.
2. Antigen of interest dissolved in either carbonate buffer (pH 9.6) or PBS at a concentration of 1–100 μg/mL.
3. Carbonate buffer: mix 0.1 M Na_2CO_3 and 0.1 M $NaHCO_3$ until pH 9.6. 0.1 M Na_2CO_3, 10.6 g Na_2CO_3/L H_2O; 0.1 M $NaHCO_3$ 8.4 g $NaHCO_3$/L H_2O.
4. PBS-Tween-20: add 1 mL of Tween-20 per liter of PBS.
5. 2% MPBS: 2 g nonfat milk powder/100 mL PBS.
6. 4% MPBS: 4 g nonfat milk powder/100 mL PBS.
7. 100 mM triethylamine (TEA): 140 μL triethylamine/10 mL H_2O. Prepare fresh; pH 12.

2.4 Immuno-precipitation with Magnetic Beads

1. Biotinylated antigen, 100–500 nM, best done using a commercial kit.
2. Streptavidin-coupled Dynabeads M-280 (Invitrogen).
3. Small magnets designed for fitting of 1.5–2 mL tubes.
4. 100 mM triethylamine: 140 μL triethylamine/10 mL H_2O. Prepare fresh; pH 12.
5. 1 mM DTT (1,4-Dithiothreitol).

2.5 Phage ELISA

1. Antigen: 1–100 μg/mL dissolved in either carbonate buffer or PBS.
2. For antigen immobilization done by absorption to MaxiSorp 96-well plates.
3. Anti-phage mAb horseradish peroxidase (HRP)-conjugated used at a final dilution of 1:5000 (GE Healthcare).
4. TMB (3,3′,5,5′-tetramethylbenzidine) ready-to-use, premixed solution for colorimetric HRP-based ELISA detection.
5. 2 N sulfuric acid: 55.6 mL 97% sulfuric acid dilute up to 1 L H_2O.

2.6 Soluble ELISA

1. Antigen: 1–100 μg/mL dissolved in either carbonate buffer or PBS.
2. MaxiSorp 96-well plates for antigen immobilization by absorption.
3. Monoclonal antibody anti-immunoaffinity tag (e.g., 9E10 anti-myc, anti HIS6, anti V5) for the detection of soluble scFv.
4. Horseradish peroxidase (HRP)-conjugated anti-mouse IgG.
5. 3,3′,5,5′-Tetramethylbenzidine ready-to-use, premixed solution for colorimetric HRP-based ELISA detection.
6. 2 N sulfuric acid: 55.6 mL 97% sulfuric acid dilute up to 1 L H_2O.

3 Methods

3.1 V Genes Amplification from Peripheral Blood Lymphocytes

A library with the maximum antibody diversity could be generated by amplifying naturally rearranged V genes. There are two requirements: the availability of peripheral blood lymphocytes (PBLs) from several non-immunized donors and a set of PCR primers able to amplify all known VH, Vκ, and Vλ gene sequences [9, 21].

1. Samples of human PBLs are purified by density gradient centrifugation on Ficoll Paque PLUS and are used as starting material (*see* **Note 3**).
2. Total RNA is prepared by using a commercial kit. The quality of the RNA preparation must be checked on an appropriate gel.
3. cDNA is synthesized using reverse transcriptase and random hexamer primers starting with 1 μg of total RNA in a final volume of 20 μL following instructions provided.
4. VH genes are amplified by PCRs and a reaction should be carried out for each individual VH-Back primer (as described in [9]) in order to amplify even rarely occurring VH genes. VH back primers are paired with an IgM constant-region primer.

   Reactions are performed using 1 μL of cDNA as template, with a High-Fidelity DNA polymerase, in a volume of 50 μL. Cycling parameters are 98 °C for 10 s (denaturation), 65 °C for 30 s (annealing), and 72 °C for 30 s (extension) for 31 cycles. All 50 μL are loaded on a 1.5% agarose gel and purified using a purification kit.
5. Vλ and Vk genes are similarly amplified (using individual VL-back primers with the mix of VL-for primers) from random primed cDNA with the same cycling parameters. All 50 μL are loaded on a 1.5% agarose gel and purified using a purification kit.
6. Pull through PCR of amplified V regions. V regions amplified from cDNA are re-amplified to increase the amount available for cloning as well as to add extra DNA sequences (e.g., restrictions sites) at each end. As the starting template is a PCR fragment this amplification tends to be extremely efficient. VH (and VL) purified genes are pooled equally and re-amplified using external primers (*see* Fig. 1b) in 50 μL reaction volume using 5 ng of purified VH (other parameters as above). All 50 μL are loaded on a 1.5% agarose gel and purified.
7. The scFv library is generated by mixing equal amounts (5–50 ng) of VH and VL genes and performing a two-step overlapping PCR, essentially as described in [22]: 8 cycles of PCR without primers followed by 25 cycles in the presence of external primers. Cycling parameters are 98 °C for 10 s

(denaturation), 60 °C for 30 s (annealing), and 72 °C for 30 s (extension). At least five assembly reaction of 50 μL should be set up and product purified on a 1.5% agarose gel.

3.2 Ligation and Electroporation of ScFv Library

In general, the diversity of a library is limited by the amount of vector/insert used and by the transformation efficiency of bacteria. The largest libraries require hundreds of electroporations to generate the required diversity (*see* **Note 4**).

1. Both phagemid cloning vector pDAN5 [12] and purified scFv fragments are sequentially digested, with BssHII restriction endonuclease for 2 h at 50 °C and then with NheI for 4 h at 37 °C. Efficient digestion with both enzymes is crucial to avoid self-ligation of the vector. Vector is loaded on an agarose gel and gel purified using a purification kit. scFv inserts are purified using clean up kit.
2. Ligation reaction is prepared as follows: double-digested and purified vector 2–5 μg, double digested and purified scFv 1–2.5 μg (phagemid:insert molar ratio of 1:3); T4 DNA ligase; 1× DNA ligase buffer. Incubate reactions at 2 h at 22 °C and then at 16 °C overnight (*see* **Note 5**).
3. Clean up and concentrate ligation using a commercial kit.
4. Elute the DNA in ultrapure H_2O.
5. The ligation mix is electroporated into Electrocompetent Cells. The number of total electroporation should be determined calculating the number of transformants obtained with a single electroporation (*see* **Note 6**).
6. Transformations are pooled and plated on 2×TYAG 15 cm plates and grow O/N at 25–28 °C to obtain a primary library. Make dilutions to estimate library diversity.
7. The next day colonies are scraped up in 2×TY 20% glycerol and frozen down in 1 mL aliquots and some small working aliquots of 100 μL.

3.3 Rescuing Phagemid Particles from Libraries

Growth of phagemid libraries requires the use of helper phage, which provides all the other proteins needed to produce the phage particles. The helper phage has a disabled or weaker packaging signal than that of the phagemid vector and provides all the proteins required for phagemid replication, ssDNA production, and packaging. The different clones of the library have very different effects on bacterial growth rates, therefore library amplification should be minimized to prevent bias toward the least toxic clones.

1. The starting culture should contain at least ten times more clones than the original library diversity but should not exceed OD 600_{nm} 0.05. For most rescues, the inoculum is therefore

30–300 μL of the glycerol stock (or concentrated solution of bacteria scraped from plate). The inoculum should be placed in an appropriate volume of 2×TYAG in a sterile flask 5–10 times bigger than the culture volume.

2. Grow with shaking (250 rpm) for 1.5–2.5 h at 37 °C, to an OD 600_{nm} of 0.5. Check the OD regularly so as not to overgrow the cells (once reached this OD, cells are into the mid-log phase and they express the F-pilus for infection) (*see* **Note 7**).
3. When an OD 600_{nm} of 0.5 is reached, add a 20-fold excess of helper phage (consider culture concentration as 5×10^8 cells/mL). Leave at 37 °C for 45 min, standing with occasional shaking.
4. Spin the cells for 15 min at 4000 × *g*. When bacteria need to be kept vital, they should be spun no greater than 4000 × *g*. When they are to be removed to collect supernatant, higher g forces can be used.
5. Discard the supernatant.
6. Dissolve the bacterial pellet in a volume five times greater than the initial culture volume of 2×TYAK. Grow shaking (250 rpm) overnight at 28 °C, using enough flasks to ensure that the flask volume is five times greater than the culture volume.
7. The following day bacteria are centrifuged at 6000–12,000 × *g* for 25 min at 4 °C. the supernatant, containing phages, is collected and subjected to PEG precipitation.

3.4 PEG Precipitation of Phagemid Particles

The concentration of phage or phagemid particles in the supernatant of culture medium is usually 10^{11-12} per mL. It is often useful to remove bacterial debris and concentrate phages. This is best done by PEG precipitation. The addition of polyethylene glycol (average molecular weight 6000) to a final concentration of 1–4% (w/v) results in the precipitation of essentially all phage particles. Particles are dissolved in PBS and re-centrifuged to remove bacteria, prior to a second PEG precipitation and filter sterilization, if desired.

1. Add 1/5 volume of PEG/NaCl solution to the cleared supernatant (e.g., 20–80 mL), mix well, and leave for 30–60 min on ice. Successful precipitation can usually be seen after few minutes as haziness.
2. Spin down at 4500 × *g* for 15 min at 4 °C; discard the supernatant. The pellet should be white. If it is brown, this is usually due to contamination with bacteria, and the PEG precipitation should be repeated.
3. Dissolve phage pellet in 1/10 original volume with PBS.

4. Spin in microcentrifuge (10 min, max speed) to remove the remaining bacteria, a small brown pellet could be visible. Transfer the supernatant to a new tube.
5. **Steps 1–4** can be repeated for added purity (double PEG precipitation), and especially if the first PEG precipitate is brown, and should always be done for prolonged storage of phage preparations. In this case add 1/5 PEG solution to the supernatant; leave on ice for 10–20 min; haziness should be seen immediately. Spin phage down (5 min, max speed), remove the supernatant carefully, and dissolve the pellet in PBS 1/50 of the original volume with a 1 mL filter-tip. Remove bacteria again by spinning (2 min, max speed).
6. The phages are now ready for selection. The standard titer after double precipitation should be about $2–10 \times 10^{13}$ phages/mL. Although phages can be stored at 4 °C without much loss of titer the displayed antibodies will proteolytically be removed by contaminating proteases, so they should be used within a few days (*see* **Note 8**).

3.5 Phage Titration into E. coli

Phagemid concentration should be titrated both before the selection as well as after (i.e., eluted phages). *E. coli* expressing F-pili are infected by phagemid and after appropriate dilution plated into 2×TY agar plates with the appropriate antibiotic. Only those cells that have been infected, thus acquiring the antibiotic resistance, will form colonies after O/N growth.

1. Make serial 10- to 100-fold dilutions of the phagemid solution in 2×TY medium to final volume of 1 mL (i.e., 10 μL into 990 μL (10^{-2}); 10 μL of this into 990 μL (10^{-4}) etc.). For accurate titrations make ten-fold rather than 100-fold dilutions steps around the relevant dilutions. Use new sterile tips for pipetting each titration step, otherwise the titration is inaccurate. For phagemid stocks after PEG precipitation ($10^{12–13}$ phages/mL) go down to 10^{-10}; for phagemid eluates ($10^{6–8}$ phages/mL at round 1–2 of selections) go down to 10^{-6}.
2. Add 10 μL of the diluted phages to 1 mL of exponentially growing *E. coli* (OD $600_{nm} = 0.5$). Incubate without shaking at 37 °C for 45 min.
3. Plate 100 μL of each dilution onto 2×TYAG plates and incubate O/N at 28 °C.
4. As a control, uninfected *E. coli* should be plated and grown on a separate plate with ampicillin. Colonies grown on this plate indicate a possible contamination, indicating inadequate sterile techniques.
5. Next day, count the number of colonies and calculate the phage titer. Titer is expressed as number of phages/μL.

3.6 Selection of Phage Antibodies to an Antigen Immobilized on Plastic Surfaces

While many different plastic surfaces are suitable for selections, Immuno MaxiSorp Tubes have become the standard. They have a high capacity (600 ng/cm^2) and have yielded many specific antibodies from several different antibody libraries. Surfaces can be coated with antigen in a variety of ways, the most common is direct adsorption to a plastic surface where it is non-covalently associated via electrostatic and van-der-Waals interactions. Usually, antigen is coated at 1–10 μg/mL and conditions that work for ELISA are likely to work for selection. Nonfat powdered milk is the standard blocking reagent. Tween 20 0.1–0.5% can also be added to all incubation to reduce nonspecific or polyreactive binders. After antigen coating the phagemid library is incubated in direct contact with plastic surface. Washes are then performed and in principle nonbinding phages are washed away while specific phages will be retained and late rescued by infection. In practice, this cannot be carried out in a single cycle, but requires several rounds of binding, washing, elution, and amplification. In general, 2–4 cycles are usually required.

1. Add 1 mL antigen (usually concentrated 10 μg/mL) to a 75 mm × 12 mm Immuno Tube. Leave O/N at 4 °C (or 1 h at 37 °C). Next day, wash 3× with PBS (simply pour solution in and pour out again immediately).
2. Block the Immuno Tube by adding 2% MPBS to the rim. Seal the tube with parafilm and leave for 30 min-2 h at room temperature. Meanwhile, preblock PEG-concentrated phage (1–5 × 10^{12} phages) in a final volume of 1 mL with 2% MPBS (*see* **Note 9**).
3. Wash the Immuno Tube 2× with PBS-Tween-20 and 2× with PBS and transfer phage-mix (**step 2**) to Immuno Tube and cover tube with parafilm. Incubate for 30 min on a rotator and then for 1.5 h standing at room temperature.
4. Wash tubes ten times with PBS-Tween-20, then ten times with PBS (*see* **Note 10**). Each washing step is performed by pouring buffer in and out immediately (*see* **Note 11**).
5. Elute phages from tube by adding 1 mL 100 mM triethylamine. Cover tube with fresh parafilm (this prevents cross contamination) and rotate the tube for 10 min on an under and over turntable. Do not increase elution time as phage viability decreases.
6. Transfer the solution into an Eppendorf tube with 0.5 mL of 1.0 M Tris–HCl, pH 7.4 and mix by inversion. It is necessary to neutralize the phage eluate immediately after elution.
7. Transfer phage mix into ice or store at 4 °C.
8. Titrate the phage in DH5αF′ cells to determine the output.

9. Re-infect the selected phages in DH5αF′ cells and harvest phages (*see* Subheading 3.3).
10. Start a new round of selection.
11. An alternative method to elute selected phages from the immunotube includes adding 1 mL of bacteria at OD 600_{nm} 0.5 (*see* **Note 12**) and leave the tube at 37 °C for 30–45 min with occasional shacking. In this case bacteria are plated directly on 2 cm × 15 cm 2×TY agar plates added with ampicillin and incubated O/N at 28 °C.

3.7 Selection of Phage Antibodies Using Biotinylated Antigen and Streptavidin-Paramagnetic Beads

An alternative to select antibodies bound to plastic plates is to select the antibodies in solution. This solves problems related to antigens that change conformation when directly coated onto solid surfaces. Furthermore, affinity selections are more straightforward with this method allowing a precise control of the interaction between the phage particle and the antigen that takes place in solution. The antigen is labeled by biotinylation (using kits that are sold by many companies) and incubated with the phage antibody library, after both have been appropriately blocked. Once interaction between the two has occurred the complex can be retrieved by using magnetic beads coated with streptavidin. Specificity is achieved by washing the beads several times. Phages are eluted from the beads with either acid or alkaline solution.

1. Phage preparation (corresponding to 10^{12} phages) is saturated to a final concentration of 2% MPBS in 500 μL volume. 100 μL of streptavidin-magnetic beads are added to select streptavidin-binding phage. Solution is equilibrated on rotator at room temperature for 60 min.
2. Remove the streptavidin-binding phage by drawing the beads to one side using a magnet and remove the supernatant.
3. Add biotinylated antigen (100–500 nM) to the equilibrated phage mix.
4. Incubate on a rotator at room temperature for 30 min–1 h.
5. While incubating the phage wash 100–200 μL streptavidin-magnetic beads with PBS and resuspend in 2% MPBS on a rotator at room temperature for 30 min–1 h.
6. Draw equilibrated beads to one side with magnet, remove buffer and resuspend beads with phage-antigen mix, and incubate on a rotator at room temperature for 15 min (*see* **Note 13**).
7. Place tubes in magnetic rack and wait until all beads are bound to the magnetic site (30 s). Wash the beads from the cap by tipping the rack upside down and back again.
8. Leave tubes in the rack for 1–2 min then aspirate the supernatant carefully, leaving the beads on the side of the tube.

9. Wash the beads carefully six times with 0.75 mL PBS-Tween-20.
10. Wash the beads four times with 0.75 mL PBS.
11. Elute phage from beads with 500 μL 100 mM TEA for 10 min maximum.
12. Transfer the solution to an Eppendorf tube containing 250 μL Tris–HCl, pH 7.4 and mix by inversion. It is necessary to neutralize the phage eluate immediately after elution.
13. Use an aliquot of the selected phages to re-infect in DH5αF′ cells for another round of selection, repeating all steps above.
14. Store the remaining beads or eluate at 4 °C as a backup.
15. Bound phages could be eluted by mixing the beads with 1 mL of *E. coli* DH5αF′, at OD 600_{nm} 0.5, at 37 °C, for 45 min, with occasional shaking (*see* **Note 12**). In this case bacteria are plated on 2 × 15 cm 2×TY agar plates added with ampicillin and grown O/N at 28 °C.

3.8 Library Amplification After Selection

1. In the case of Immuno Tube selection mix 5 mL of DH5αF′ cell with 0.5 mL of phage eluate (*see* **Note 14**) in a 50 mL tube. The eluate must be diluted at least ten-fold (for toxicity reasons) if TEA has been used for elution.
2. For soluble biotinylated antigen selections mix 1 mL of *E. coli* with 100–200 μL of phage eluate (*see* **Note 14**).
3. Incubate at 37 °C for 30 min with occasional shacking.
4. Plate out samples on 2 × 15 cm 2×TYAG plates. For later rounds of selection, one plate is sufficient, as diversity is reduced.
5. Grow the plates O/N at 28 °C. Growth at higher temperatures may lead to loss of some antibody clones.
6. After overnight growth add 2 mL of 2×TY into 2 × 15 cm plates and scrape the bacteria off using a sterile spreader.
7. Transfer the cells into a tube and make a homogeneous suspension by pipetting up and down with a sterile pipette.
8. Add sterile glycerol to 20% final concentration and immediately store at −80 °C samples into a Cryotube in at least three aliquots.
9. Rescue phages from library according to protocol 3.3.

3.9 Growing Phage Clones in Microtiter Plates for ELISA Testing

After two or three rounds of selection, individual colonies from the selection are tested for antigen binding by ELISA. A microtiter-well system can be used for individual phage preparation. The principle involving growth, helper phage infection, and phage production is the same as that for the library, but it is applied to single clones in the 96-well plate format. Care must be taken to prevent cross-

contamination between wells; both growth and ELISA controls should be included on the master plates.

1. Put 100 μL of 2×TYAG into each well of a round-bottomed 96-well plate. Inoculate a single colony in each well by touching the top of a colony with an autoclaved toothpick or sterile plastic tip. Grow with shaking (250 rpm) overnight at 30 °C (*see* **Note 15**). There is no need for specific holder designed for microtiter plates, this could be inserted within a plastic box cushioned with foam, tightly taped and placed as far as possible from the ventilator to avoid evaporation (*see* **Note 16**).
2. Next day, use a 96-well sterile transfer device or pipet to inoculate 2 μL per well from this plate to a round-bottomed 96-well containing 120 μL 2×TYAG per well. Grow to OD 600_{nm} 0.5 (around 2.5 h), at 37 °C, shaking.
3. To each well add 50 μL 2×TYAG containing 1×10^9 pfu helper phage. The ratio of phage to bacterium should be about 20:1. Stand 45 min at 37 °C.
4. After the incubation, spin at 500 × *g* (faster will crack the plates) for 20 min; then remove the supernatant with a multichannel pipette or suction device.
5. Resuspend the bacterial pellet in 120 μL 2×TYAK. Glucose is omitted in this step. Grow overnight 28 °C, shaking.
6. Next day, spin at 500 × *g* for 10 min and use 50 μL supernatant per well for phage ELISA.

3.10 Phage ELISA

1. Coat plate with 100 μL per well of protein antigen used for selections. Coating antigen is usually prepared in PBS (occasionally in carbonate buffer). Leave O/N at 4 °C or at 37 °C for 2 h. This is dependent upon the specific antigen and should be tested if possible (*see* **Note 17**).
2. Discard the antigen solution, rinse wells twice with PBS, and block with 120 μL per well of 2% MPBS, for at least 45 min at room temperature.
3. Wash wells twice with PBS.
4. Add 50 μL 4% MPBS and 50 μL culture supernatant containing the phage antibodies to the appropriate wells, mix carefully. Leave approximately 1.5 h at room temperature with mild shaking.
5. Discard solution, wash out wells 3× with PBS-Tween-20 and 3× with PBS.
6. Add 100 μL diluted HRP-conjugated mouse anti-phage mAb. Use the dilution indicated by the manufacturer. Incubate for 1 h at room temperature.
7. Discard solution and wash wells 3× with PBS-Tween-20 and 3× with PBS.

8. Dispense 100 μL TMB solution per well, leave at room temperature in the dark for 5–20 min (sometimes longer).
9. Quench by adding 42 μL stop solution 2 N H_2SO_4.
10. Read at 450 nm.

3.11 Growing Soluble Fragments in Microtiter Plates

An alternative to using phagemids for ELISAs is to use antibody soluble fragments. The phagemid vector usually carries an amber stop codon between the gene coding for the scFv and the geneIII; therefore, the gene coding for the scFv fragment is transcribed and soluble fragments are produced. The antibody leaks into the supernatant that could be directly used as primary antibody source.

1. Put 100 μL of 2×TYAG into each well of a 96-well round-bottomed plate. Inoculate a single colony in each well by touching the top of a colony with an autoclaved toothpick or sterile plastic tip. Grow with shaking (250 rpm) overnight at 30 °C (*see* **Note 15**). There is no need for specific holder designed for microtiter plates, this could be inserted within a plastic box cushioned with foam, tightly taped and placed as far as possible from the ventilator to avoid evaporation (*see* **Note 16**).
2. Next day, use a 96-well sterile transfer device or pipette to inoculate 2 μL per well from this plate to a 96-well round-bottomed plate containing 100 μL 2×TYA, 0.1% glucose per well. Grow at 37 °C, shaking, until OD 600_{nm} is approximately 0.6 (about 2–3 h).
3. Add 50 μL 2×TYA, 1.5 mM IPTG (final concentration 0.5 mM IPTG). Continue shaking at 25–28 °C O/N.
4. Next day, spin at 500 × *g* for 10 min and use 50 μL supernatant in ELISA.

3.12 Soluble Fragment ELISA in Microtiter Plates

Soluble scFv can be tested for antigen-binding activity on ELISA plates coated directly with antigens. Detection is done by a sandwich assay involving anti-tag antibody and a secondary enzyme-conjugated antibody.

1. Coat plate with 100 μL per well of protein antigen used for selections. Coating antigen is prepared in PBS (occasionally in carbonate buffer). Leave overnight at 4 °C or at 37 °C for 1 h. This is dependent upon the particular antigen and it should be tested if possible.
2. Discard the antigen solution and rinse wells twice with PBS and block with 120 μL per well of 2% MPBS, for at least 45 min at room temperature.
3. Wash wells twice with PBS.

4. Add 50 μL 4% MPBS to all wells and then add 50 μL culture supernatant containing soluble antibody fragment to the appropriate wells. Leave 1.5 h at room temperature with mild shaking.
5. Discard solution, wash out wells 3× with PBS-Tween-20 and 3× with PBS.
6. Pipette 100 μL of anti-tag antibody, at the appropriate dilution, in 2% MPBS into each well. Incubate at room temperature for 1 h.
7. Discard antibody, wash out wells with 3× with PBS-Tween-20 and 3× with PBS.
8. Add 100 μL of diluted anti-mouse-HRP (horseradish peroxidase), or anti-mouse-AP (alkaline phosphatase), labeled secondary antibody to each well. Incubate for 1 h at room temperature.
9. Discard second antibody, and wash wells 3× with PBS-Tween-20 and 3× with PBS.
10. To develop with TMB: dispense 100 μL TMB solution per well, leave at room temperature in the dark for 10–30 min (sometimes longer). Quench by adding 42 μL stop solution 2 N H_2SO_4.
11. Read at 450 nm.

3.13 PCR Amplification and Fingerprinting of Selected Clones

After positive clones have been identified, it is important to determine how many different antibodies have been selected.

A simple and fast method involves the use of PCR to amplify the scFv regions and then to digest the DNA samples with a frequently cutting restriction enzyme, such as BstNI or HaeIII. The digested DNA fragments are separated on an agarose gel and the various clones are characterized by their own DNA fragment patterns.

1. Make up a PCR-Mastermix with 20 μL per clone. Use forward and back primers mapping external to the 5′ and 3′ end of the scFv insert.
2. Aliquot 20 μL of the Mastermix into 0.5 mL tubes, or into 96-well PCR microplates.
3. Add 0.5–1 μL of culture taken from the master plate into PCR reaction (excess bacteria in the PCR reaction can cause inhibition).
4. Heat to 95 °C for 10 min using the PCR-block. This is needed to break open the bacteria and release the template DNA. Perform 30 cycles of denaturation, annealing and elongation steps using the temperature and incubation times indicated on the DNA Taq Polymerase datasheet (*see* **Note 18**).

5. Check 2 μL of the PCR reaction on a 1.5% agarose-gel. This will indicate how many clones lack the insert.
6. Make up a fingerprinting-Mastermix and add 15 μL to each PCR tube.

   Mastermix is as follows: BstNI buffer (10×) 3 μL, Water 11.6 μL, BstNI (10 U/μL) 0.2 μL.
7. Digest samples at 60 °C for 2–3 h.
8. Load on a 3% agarose gel, run and compare the banding patterns of individual clones on a UV transilluminator.

4 Notes

1. Electroporation of pure DNA strongly increases transformation efficiency: we recommend cleaning and concentrating the ligation mixture using the DNA Clean & Concentrator™-5 kit from Zymo Research. This kit allows purifying and concentrating up to 5 μg of ligation mixture in a final volume of 6 μL of water.
2. Electrocompetent cells can be produced in-house or purchased from several manufacturers. The use of high-efficiency cells (above 5×10^9 transformants per μg of DNA) is recommended to obtain high number of transformants. To generate large libraries we suggest the use of TG1 Electrocompetent Cells from Lucigen (above 10^{10} transformants per μg of DNA), following the instructions of the manufacturer.
3. Blood samples should be processed as soon as these are taken from the donor. Prolonged storage on ice or at 4 °C results in the isolation of degraded RNA.
4. Large libraries are constructed by maximizing the efficiency of all reactions and protocols. Small decrease in the performances of protocols at any of these steps will easily lead to the production of libraries 10- to 100-fold smaller than expected. Optimized steps must include RNA extraction, PCR amplification, restriction enzymes digestion, ligation, and purification. For an efficient ligation, DNA fragments and vector must be fully cut, with no or little degradation; most of the vectors are re-ligated after a partial cutting.
5. The ligation should be done using high-concentration T4 DNA ligase enzyme O/N. Overnight ligations give best results compared with few hours at room temperature. Clean up of the large-scale ligation and resuspension in water is essential, as high concentration of DNA is required without presence of any salts in solution, since the presence of contaminants leads to a dramatic decrease in the electroporation transformation efficiency.

6. To obtain high transformation efficiency, work as quickly as possible throughout the whole protocol, cells must be kept in a cold environment.
7. During the infection of F′ bacteria with phagemid, it is important to ensure that the bacteria are expressing the pilus. At the time of infection, bacteria should be in log-phase growth, with an OD 600_{nm} around 0.5. This value could not be simply obtained by diluting bacteria grown to saturation (i.e., OD 600_{nm} 2.0). Bacteria should always be kept at 37 °C before infection, as the pilus is lost after 2–3 min at room temperature. It is therefore strongly suggested to prepare in advance all reagents before removing the bacteria from the shaker, and to perform all steps quickly, without allowing the temperature to decrease.
8. For selection steps, it is strongly suggested to use freshly prepared phages, and to store them at 4 °C for no longer than 1 day. Alternatively, phages could be purified by CsCl gradient centrifugation: in this case they are stable for years if stored at −80 °C.
9. This blocking step is suggested to reduce background binding and should be performed in all selection rounds.
10. Sometimes, antigen "stickiness" is a problem, in which case polyreactive clones may be selected from the repertoire. In that case inclusion of Tween-20 (0.05–0.1%) in all incubation steps (in selection itself, in all washes and blocking steps) may help to remove these binders, reduce the background, and favor the specific ones.
11. According to most experimental protocols, the stringency of the washing steps should increase with the selection rounds. We use the following procedure: tubes are washed 15 times with PBS-Tween-20 (0.05–0.1%) and 15 times with PBS, to remove unbound phages, for the first round of selection. For the second round, ten washes with PBS-Tween-20 (0.05–0.1%) are followed by 10 min washing in rotation with PBS, followed by ten more PBS washes.
12. It is important that bacterial culture has the correct OD 600_{nm} for the elution step at the end of the selection. It is therefore necessary to start bacterial growth early enough so that at the end of the experiment (about 3 h) bacteria are in log-phase growth with an OD 600_{nm} in the 0.3–0.6 range. It is suggested to grow bacteria in several tubes (only 1 mL is required for a single elution) inoculating different starting amounts of bacteria, and choose the tube with the OD 600_{nm} closest to 0.5 for the final elution step.
13. Incubation with slow and constant rotation is required, since the beads quickly form deposits on the bottom of the tube.

14. It is advisable to use no more than half of the selected phages for amplification, since in the event of an error, one can always return and repeat the amplification.
15. This plate will be the "master plate" with the primary selected clones that are not infected by helper phage. Care should be taken to avoid contamination or mislabeling of the plate.
16. Growth conditions in microtiter plates (speed, temperature, and position of the plate in the incubator) should be tested during the first time growth.
17. The antigen can be recovered after coating for further use if needed. In this case overnight incubation at 4 °C is recommended.
18. The PCR reactions performed on the positive selected clones have the purpose to check the full-length of the scFv. Therefore, a High-Fidelity DNA Taq Polymerase is not required and whatever Polymerase can be used.

References

1. Marks JD, Hoogenboom HR, Bonnert TP, McCafferty J, Griffiths AD, Winter G (1991) By-passing immunization. Human antibodies from V-gene libraries displayed on phage. J Mol Biol 222:581–597
2. Scott JK, Smith GP (1990) Searching for peptide ligands with an epitope library. Science 249:386–390
3. Boder ET, Midelfort KS, Wittrup KD (2000) Directed evolution of antibody fragments with monovalent femtomolar antigen-binding affinity. Proc Natl Acad Sci U S A 97:10701–10705
4. Boder ET, Wittrup KD (1997) Yeast surface dispay for screening combinatorial polypeptide libraries. Nat Biotechnol 15:553–557
5. Smith GP (1985) Filamentous fusion phage: novel expression vectors that display cloned antigens on the virion surface. Science 228:1315–1317
6. Bradbury A, Velappan N, Verzillo V, Ovecka M, Chasteen L, Sblattero D, Marzari R, Lou J, Siegel R, Pavlik P (2003) Antibodies in proteomics I: generating antibodies. Trends Biotechnol 21:275–281
7. McCafferty J, Griffiths AD, Winter G, Chiswell DJ (1990) Phage antibodies: filamentous phage displaying antibody variable domains. Nature 348:552–554
8. Hoogenboom HR, Griffiths AD, Johnson KS, Chiswell DJ, Hudson P, Winter G (1991) Multi-subunit proteins on the surface of filamentous phage: methodologies for displaying antibody (Fab) heavy and light chains. Nucleic Acids Res 19:4133–4137
9. Sblattero D, Bradbury A (1998) A definitive set of oligonucleotide primers for amplifying human V regions. Immunotechnology 3:271–278
10. Marks JD, Griffiths AD, Malmqvist M, Clackson T, Bye JM, Winter G (1992) By-passing immunization: building high affinity human antibodies by chain shuffling. Biotechnology 10:779–783
11. Vaughan TJ, Williams AJ, Pritchard K, Osbourn JK, Pope AR, Earnshaw JC, McCafferty J, Hodits RA, Wilton J, Johnson KS (1996) Human antibodies with sub-nanomolar affinities isolated from a large non-immunized phage display library [see comments]. Nat Biotechnol 14:309–314
12. Sblattero D, Bradbury A (2000) Exploiting recombination in single bacteria to make large phage antibody libraries. Nat Biotechnol 18:75–80
13. Hoogenboom HR, Winter G (1992) By-passing immunisation. Human antibodies from synthetic repertoires of germline VH gene segments rearranged in vitro. J Mol Biol 227:381–388
14. Prassler J, Thiel S, Pracht C, Polzer A, Peters S, Bauer M, Nörenberg S, Stark Y, Kölln J, Popp A, Urlinger S, Enzelberger M (2011) HuCAL PLATINUM, a synthetic fab library optimized for sequence diversity and superior

performance in mammalian expression systems. J Mol Biol 413:261–278

15. Weber M, Bujak E, Putelli A, Villa A, Matasci M, Gualandi L, Hemmerle T, Wulhfard S, Neri D (2014) A highly functional synthetic phage display library containing over 40 billion human antibody clones. PLoS One. https://doi.org/10.1371/journal.pone.0100000
16. Krebs B, Rauchenberger R, Reiffert S, Rothe C, Tesar M, Thomassen E, Cao M, Dreier T, Fischer D, Hoss A, Inge L, Knappik A, Marget M, Pack P, Meng XQ, Schier R, Sohlemann P, Winter J, Wolle J, Kretzschmar T (2001) High-throughput generation and engineering of recombinant human antibodies. J Immunol Methods 254:67–84
17. Fellouse FA, Esaki K, Birtalan S, Raptis D, Cancasci VJ, Koide A, Jhurani P, Vasser M, Wiesmann C, Kossiakoff AA, Koide S, Sidhu SS (2007) High-throughput generation of synthetic antibodies from highly functional minimalist phage-displayed libraries. J Mol Biol 373:924–940
18. Rouet R, Jackson KJL, Langley DB, Christ D (2018) Next-generation sequencing of antibody display repertoires. Front Immunol. https://doi.org/10.3389/fimmu.2018.00118
19. Bradbury A, Velappan N, Verzillo V, Ovecka M, Chasteen L, Sblattero D, Marzari R, Lou J, Siegel R, Pavlik P (2003) Antibodies in proteomics II: screening, high-throughput characterization and downstream applications. Trends Biotechnol 21:312–317
20. Di Niro R, Sulic AM, Mignone F, D'Angelo S, Bordoni R, Iacono M, Marzari R, Gaiotto T, Lavric M, Bradbury AR, Biancone L, Zevin-Sonkin D, De Bellis G, Santoro C, Sblattero D (2010) Rapid interactome profiling by massive sequencing. Nucleic Acids Res 38:e110
21. Lim TS, Mollova S, Rubelt F, Sievert V, Dubel S, Lehrach H, Konthur Z (2010) V-gene amplification revisited – an optimised procedure for amplification of rearranged human antibody genes of different isotypes. New Biotechnol 27:108–117
22. Krebber A, Bornhauser S, Burmester J, Honeggar A, Willuda J, Bosshard HR, Pluckthun A (1997) Reliable cloning of functional antibody variable domains from hybridomas and spleen cell repertoires employing a reengineered phage display system. J Immunol Methods 201:35–55

Chapter 16

Recombinant Antibody Selections by Combining Phage and Yeast Display

Fortunato Ferrara, Maria Felicia Soluri, and Daniele Sblattero

Abstract

In vitro display technologies have put together the generation of large antibody libraries with selection and screening procedures to identify lead candidates. Phage display antibody libraries allow selecting and identifying binders for a variety of antigens. Nonetheless, the procedure is limited by the possibility to quantitatively follow the enrichment during selection cycles and tune up the clones for specific binding proprieties (i.e., affinity). Yeast display allows the expression of thousands of copies of the antibody on each cell, simultaneously carrying the plasmid encoding that antibody, moreover the selection parameters can be accurately controlled by flow cytometry-based analysis and sorting.

The combination of phage and yeast display takes advantage of both platforms by starting with a vast number of antibodies in the phage display selections followed by the precise sorting of the clones specifically recognizing the target of interest.

In the present chapter, we illustrate protocols to generate and enrich - using fluorescence-activated cell sorting (FACS) - yeast display antibody libraries, using selection outputs obtained from phage antibody display libraries as starting material. The present methods can be easily applicable for the identification of monoclonal antibodies with desired binding properties.

Key words Phage antibody display, Yeast surface antibody display, FACS, Antigens, Monoclonal antibody, High-throughput, scFv

1 Introduction

The display of recombinant antibodies on the surface of microorganisms such as phage and yeast cells has been developed and largely used to generate and select recombinant antibodies with specific affinity for a wide range of targets of interest [1–6]. Very large libraries can be generated, displayed, and screened using phage antibody display-based selections, but it has revealed cumbersome to fine-tune the selections when trying to isolate antibody with specific binding properties. Selecting using phage display is a "black-box" process where, until the screening of individual phage clones, there is little or no evidence about the quality of the ongoing selections. An approach to address these limitations is to

Michael Steinitz (ed.), *Human Monoclonal Antibodies: Methods and Protocols*, Methods in Molecular Biology, vol. 1904, https://doi.org/10.1007/978-1-4939-8958-4_16,

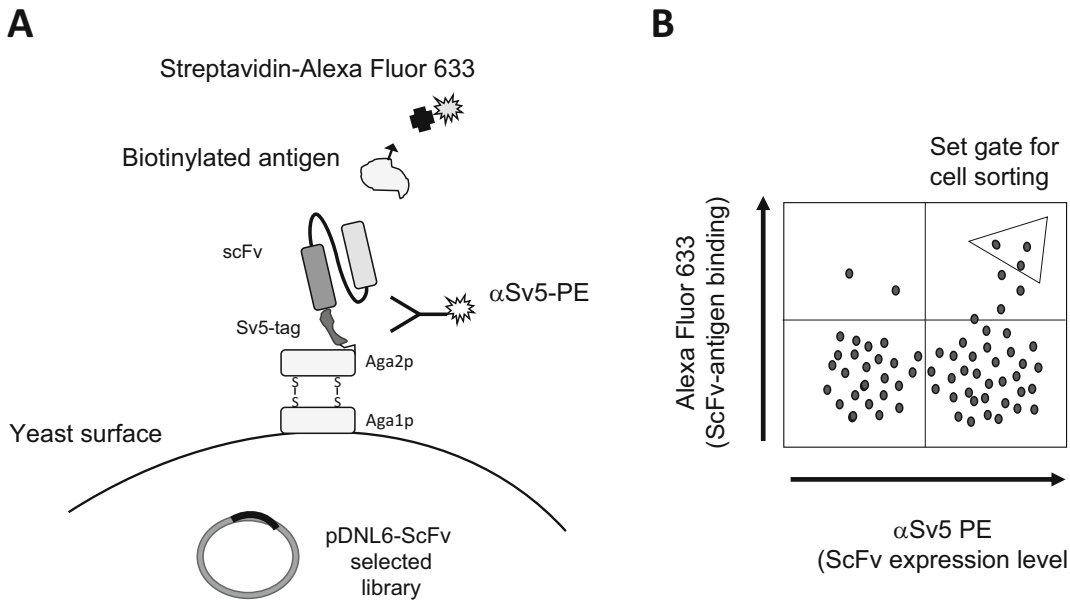

Fig. 1 Schematic representation of the scFv yeast surface display and selection strategy. Antibodies are first selected against a biotinylated antigen by phage display, after which the whole selection output is cloned into a yeast display vector (pDNL6-scFv) using homologous recombination, and expressed on the yeast surface. The display of the antibody can be detected using a fluorescently conjugated anti-tag (SV5) antibody, while the bound protein can be detected by utilizing fluorescently conjugated streptavidin (Streptavidin-Alexa Fluor 633) (**a**). By flow cytometry, it is possible to identify clones resulting positive for both fluorescent signals (expression of the antibody and binding to the antigen), and to sort this population (**b**)

generate yeast antibody libraries starting from pre-enriched phage antibody display outputs selected on the target of interest.

Yeast has found large use as a host cell in genetic engineering since its ability to fold and glycosylate heterologous eukaryotic proteins, a characteristic that it is not achievable in the more tradition prokaryotic-based systems, like phage display.

In particular, *Saccharomyces cerevisiae* has been exploited to display on its surface different eukaryotic proteins: at the beginning, about 20 years ago, it was developed for the evolution of proteins in vitro [7], but the possibility to display protein was quickly exploited as a rapid method to identify protein-protein interaction, in particular to select antibody libraries against targets of interest, and to determine the epitope of antibodies [3], being the field of human antibody engineering the most profitable protein engineering research field (Fig. 1).

Compared to prokaryotic-based display systems, yeast display has two extraordinary advantages: (1) as a unicellular eukaryote, yeast favors the expression and folding of eukaryotic proteins, a key aspect in the field of human antibody engineering that has encountered massive difficulties in phage display systems because of missfolding issues; (2) using labeled target antigens, yeast antibody

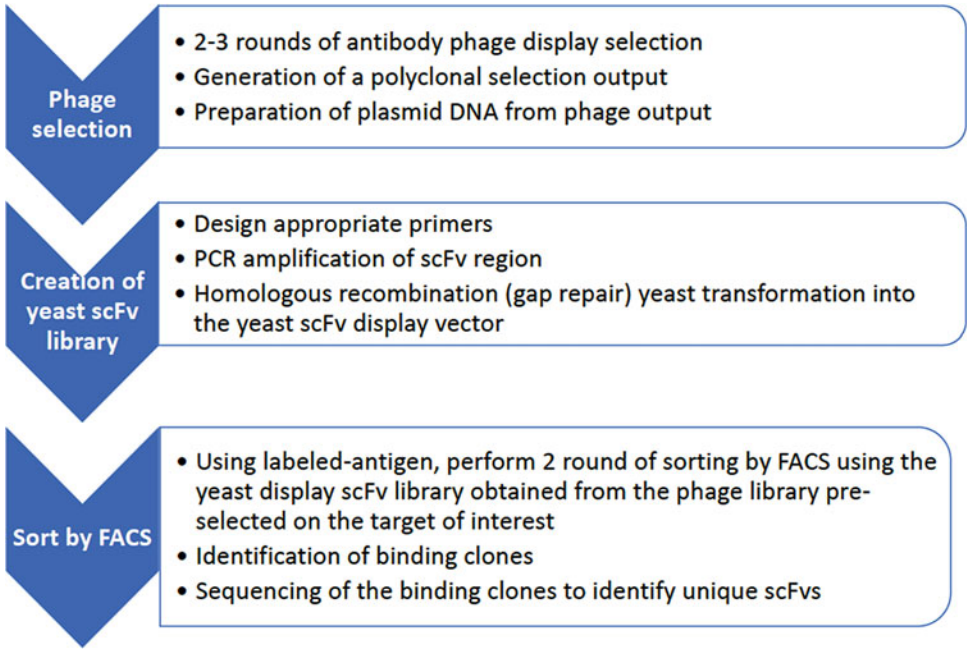

Fig. 2 Flow chart of the selection strategy combining both phage and yeast antibody display. A naïve phage antibody display library undergoes two/three rounds of selection on an antigen of interest. The enriched polyclonal population, plasmid DNA from the last selection output is purified and used to amplify the scFv genes with primers design to add gap-repair based to allow the yeast transformation through homologous recombination (*see* the text for more details). The obtained yeast antibody library is analyzed and enriched by sorting against labeled antigens to identify specific binders

display libraries can be coupled with FACS to tailor the selection toward high affinity antibodies that specifically bind to the target of interest [3].

Moreover, the combination of yeast antibody display and FACS allows highly controlled and real-time selection steps that can enable a fine discrimination of clones exhibiting different properties such as affinity or stability, and it even allows easily obtaining binders able to discriminate between highly homologous antigens [8, 9], features that can be obtained more effectively than phage display.

In the present chapter, we explain protocols for the creation and selection of yeast single-chain variable fragments (scFv) display libraries (Fig. 2).

We describe the different steps required by the whole procedure (Fig. 3): (1) yeast scFv library generation, starting from pre-enriched phage scFv display selection outputs and made by exploiting the homologous recombination gap repair cloning, (2) FACS-based enrichment of target antigen-binding clones from the obtained libraries, and (3) screening and sequencing analysis.

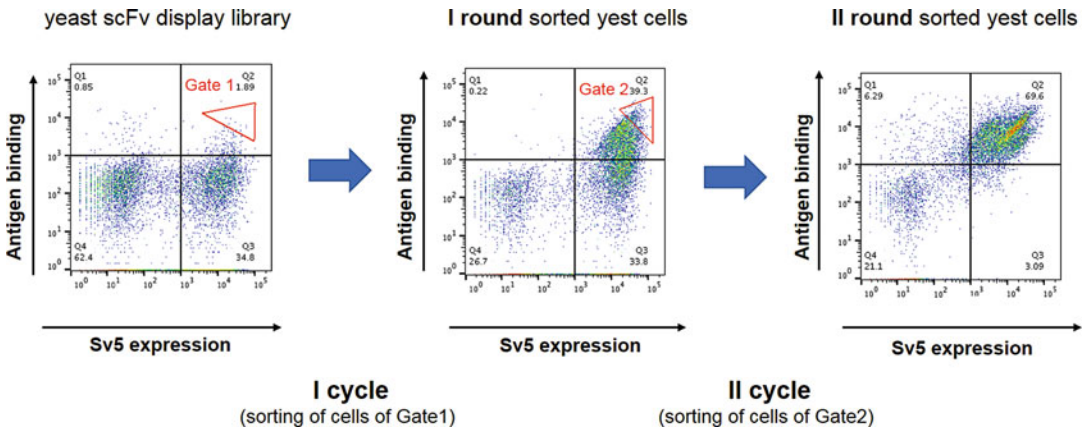

Fig. 3 Illustration of a yeast surface scFv display library selection on a target of interest by FACS. A polyclonal scFv population was obtained after phage display selection and subcloned into the yeast scFv display library. After induction, the yeast scFv display library was incubated with biotinylated antigen and underwent flow cytometry-based sorting as described in the methods. Antigen-binding scFv clones were enriched with two rounds of FACS. The horizontal axis shows the level of display of the SV5 tag, while the vertical axis represents the antigen-binding activity. The red triangles represent the gates used to sort the yeast populations for each round. Numbers indicate the percentage of cells falling into each quadrant according to their positivity for PE and/or Alexa Fluor 633. Percentage of cells into Q2 (double positive) increases after each sorting cycle indicating the goodness of enrichment of antigen-binding scFv clones

2 Materials

Prepare all solutions using ultrapure water and analytical grade reagent. Unless indicated otherwise, prepare and store all reagents at room temperature (RT).

2.1 Creation of Phage-Derived scFv Display Yeast Library

1. ScFv-antibody phage display selection outputs (*see* **Note 1**).
2. 2×TY (2× Tryptone Yeast) media: 16 g tryptone, 10 g yeast extract, 5 g NaCl, bring volume to 1 L with distillated H_2O, adjust pH to 7.0, and sterilize by autoclaving.
3. 1000× carbenicillin: 1 g of carbenicillin, add water to 10 mL and store aliquots at −20 °C.
4. Plasmid DNA is prepared using a commercial Miniprep kit, following the instructions of the manufacturer.
5. Primers for gap repair transfer of scFvs from phage vector to yeast display vector (*see* **Note 2**):

   pDantopDNL6 Forward:

   5′ TCTGGTGGTGGTGGTTCTGCTAGAGGCGCGGCAG CAAGCGGCGCGCATGCC 3′.

   pDantopDNL6 Reverse:

   5′ ATCCAGGCCCAGCAGTGGGTTTGGGATTGGTTTGCC 3′.

6. 10× PCR buffer: 200 mM Tris–HCl, 100 mM $MgCl_2$, 100 mM KCl, 1% Triton X-100, pH 8.8, filter sterilize.
7. 50 mM $MgSO_4$ solution.
8. dNTPs 10 mM each.
9. Taq polymerase.
10. *S. cerevisiae* strain EBY100 (MATa GAL1-AGA1::URA3 ura3-52 trp1 leu2Δ1 his3Δ200 pep4::HIS3 prb1Δ1.6R can1 GAL).
11. pDNL6 [10] or suitable yeast display vector.
12. BssHII and NheI restriction enzymes (*see* **Note 3**).
13. YPD (Yeast Extract-Peptone-Dextrose): 10 g of yeast extract, 20 g of bacteriological peptone, 20 g dextrose, bring volume to 1 L with ddH_2O, and filter sterilize with 0.22 μm filter units.
14. Yeast Transformation Buffer: 100 mM lithium acetate, 10 mM Tris–HCl, pH 7.6, and 1 mM EDTA.
15. Yeast Plate Buffer: 40% PEG, 100 mM lithium acetate, 10 mM Tris–HCl, pH 7.5, 1 mM EDTA.
16. Deoxyribonucleic Acid from Salmon Testes, 10 mg/mL.
17. DMSO.
18. Selective Growth media = SD-CAA: 5 g/L casamino acids (−ade, −ura, −trp), 20 g/L dextrose, 1.7 g/L YNB (Yeast Nitrogen Base) w/out ammonium sulfate and amino acids, 5.3 g/L ammonium sulfate, 10.19 g/L Na_2HPO_4-$7H_2O$, 8.56 g/L NaH_2PO_4-H_2, and filter sterilize with 0.22 μm filter units.
19. For YPD plate, prepare the YPD solution and add 20 g/L of agar. For SD-CAA plates, prepare the SD-CAA solution without the casamino acids and the dextrose, bring the volume to 900 mL with ddH_2O autoclave to sterilize, let the agar cool until it is cold enough to touch and add the casamino acids and the dextrose. Bring the volume to 1 L with ddH_2O, mix and poor into plates and allow to become solid at RT. Store the plates at 4 °C (*see* **Note 4**).
20. Yeast Washing Buffer: PBS supplemented with 2 mM EDTA and 0.5% BSA.

2.2 Selection of Target-Specific Clones by FACS

1. scFv-antibody yeast library generated in the previous section.
2. Selective scFv induction media = SG/R-CAA: Same as selective media except substitute the following sugars for dextrose: 20 g/L galactose, 20 g/L raffinose, 1 g/L dextrose, and filter sterilize with 0.22 μm filter units.
3. Yeast Wash Buffer: PBS supplemented with 2 mM EDTA and 0.5% BSA.

4. Biotinylated or fluorescently labeled target molecules (*see* **Note 5**).
5. Mouse anti-SV5-PE (*see* **Note 6**).
6. Streptavidin-Alexa Fluor 633.

2.3 Screening and Sequencing of Binding Clones

1. pDNL6 specific primers for sequencing (*see* **Note 7**)
   pDNL6 Forward:
   5′ TAGATACCCATACGACGTTC 3′.
   pDNL6 Reverse:
   5′ GTACGAGCTAAAAGTACAGTG 3′.

3 Methods

Methods described here below require the availability of a phage display library previously selected on recombinant antigen. The methods also assumed the availability of biotinylated or fluorescently labeled target antigen. Briefly, a naïve antibody library is enriched for binders to an antigen of interest by phage display, afterward the entire output of the phage antibody selection can be screened by yeast display and fined tuned by FACS.

3.1 Amplification of scFv Genes from Phage Antibody and Yeast Display Vector Preparation

scFvs need to be amplified from the phage output to add nucleotides at both PCR product ends to allow homologous recombination with a linearized yeast display vector.

1. To recover the scFv genes prepare DNA minipreps from the final output cycle of phage selection. Miniprep will be used as PCR template using standard methods, to specifically amplify the scFv sequences.
2. Set up the PCR reactions using the PCR buffer described in Subheading 3 and 3.5 μL of 50 mM $MgSO_4$ for a 50 μL reaction (*see* **Note 8**). Use the pDantopDNL6 Forward and pDantopDNL6 Reverse primers (*see* **Note 2**) and 0.1–1 ng of the scFv phage display library selection output plasmid miniprep as template for 50 μL reaction. Set up the following PCR conditions: initial denaturation: 94 °C for 2 min followed by 25 cycles: 94 °C for 30 s, 78 °C for 1 min and a final elongation step at 72 °C for 10 min. Set up enough reactions to generate 2 μg of PCR product.
3. Check the PCR reactions by running them on a 1.5% agarose gel. Cut out bands (approximately 800 bp) with a clean razor blade, and isolate PCR products using a gel isolation kit following the manufacturer's protocols (we suggest the one provided by Qiagen). Elute in ddH_2O and measure concentration by spectrophotometer. Be sure to reach at least 1.5/2 μg of purified product.
4. Digest 5 μg of yeast vector pDNL6 with BssHII and NheI. Run the digested plasmid on 0.75% agarose gel, cut out the vector

band (~6000 bp) with clean razor blade, and isolate fragment using a gel isolation kit following the manufacturer's protocols. Elute in ddH_2O and measure concentration by spectrophotometer. Be sure to reach at least 1.5/2 μg of purified vector.

3.2 Preparation of Yeast Competent Cells

The generation of the yeast library requires the introduction of the PCR products and the digested yeast display vector into yeast via transformation of yeast cells through chemical methods. Key aspects of efficient yeast transformation consist in starting out with high-quality competent yeast cells and this paragraph will describe how to achieve good quality competent cells for the generation of pre-enriched yeast antibody display libraries.

1. Inoculate one colony of EBY100 yeast strain from a YPD plate into a 10 mL YPD culture medium and grow overnight at 30 °C with shaking at 250 rpm in a 250 mL baffled flask. Culture should reach stationary phase ($OD_{600} > 2$).
2. Dilute culture into 100 mL YPD medium (with 100 μL Kan) in a 500 mL sterile baffled flask with a starting OD_{600} of approx. 0.5. Grow with shaking 3–6 h at 30 °C so that the culture is at an OD_{600} around 1.5. Harvest cells by centrifugation for 10 min at 3000 × *g* in 2 × 50 mL conical tubes.
3. Discard the supernatant and resuspend in 50 mL autoclaved ddH_2O.
4. Consolidate to a single 50 mL tube and centrifuge again.
5. Discard the supernatant and resuspend in 1 mL of Yeast Transformation Buffer.
6. Store at 4 °C, best to use immediately (*see* **Note 9**).

3.3 Transformation of Yeast Competent Cells

The exogenous DNA (plasmid and PCR products) is introduced into the yeast cells by transformation. Thanks to the homology of the nucleotides present at the ends of the PCR products and at the extremity of the linearized yeast display plasmid, taking advantage of the gap repair system of the yeast cell, circular vectors containing the scFvs sequences are generated.

1. Aliquot 10 μg of 10 mg/mL salmon testes DNA for each transformation performed in a 1.5 mL tube.
2. Add 500 ng of digested vector and 1.5 μg of PCR product (insert) to tube.
3. Add 100 μL competent cells and vortex.
4. Add 600 μL of Yeast Plate Buffer and vortex (*see* **Note 10**).
5. Incubate for 30 min at 30 °C with shaking.
6. Add DMSO, 10% of the total volume.
7. Heat shock for 15 min at 42 °C in a water bath.
8. Spin 5 s in micro-centrifuge and remove the supernatant. Do not spin longer as it will become hard to resuspend cells.

9. Resuspend in 1 mL of ddH_2O.
10. Plate 2 μL of cell suspension (dilute it in 1000 μL of SD/CAA or water) on SD/CAA plates. This will give the possibility of calculating the size of the library.
11. Place the rest of the transformed cells into 25 mL selective SD/CAA (Kanamycin + Tetracycline) liquid media and grow 2–3 days at 30 °C until colonies appear on the plate. To freeze aliquots, spin down the liquid culture at 3000 × *g* 5 min and resuspend it in 500 μL of sterile 80% glycerol and 2 mL of SD/CAA liquid media, pipet 1 mL aliquots into cryotubes and store at −80 °C.

3.4 Induction and Analysis of the Yeast Antibody Display Library

The scFvs are expressed and displayed on the surface of the yeast cells thanks to the induction of a promoter responding to the presence of galactose in the media. Before the actual sorting it is a good procedure to check the quality of the generated yeast library.

1. Starting from the 25 mL culture (which should have reached saturation $OD_{600} > 4$), prepare a 10 mL culture at $OD_{600}0.5$ in SG/R-CAA and grow at 20 °C with shaking overnight. The induced library can be stored for several weeks at 4 °C.
2. Check the success of the induction of the yeast library by flow cytofluorimetry using the mouse anti-SV5-PE antibody only. Spin down 100 μL of the induced library at 10,000 × *g* for 30 s and wash by adding 1 mL of Yeast Wash Buffer and spin down again.
3. Resuspend cells in 100 μL PBS and add a 1:2000 solution of mouse anti-SV5-PE antibody (1 mg/mL) and vortex. Incubate at 4 °C (optional with rotation) for 30 min. Wash with 1 mL of Yeast Wash Buffer, spin down at 10,000 × *g* for 30 s, and finally resuspend in 1 mL of PBS and place on ice.
4. Analyze the cells by flow cytofluorimetry. At least 30% of the population should be SV5-positive (*see* **Note 11**). The induced library is now ready for FACS selection experiments.

3.5 Yeast Sorting by FACS

Using a fluorescence-activated cell sorter is possible to fine tune, with desired binding proprieties (i.e., high affinity), the selection procedure of the population of pre-enriched scFvs displayed on yeast.

1. Check the OD_{600} of the induced library (by diluting 1:10) to determine cell density. For the first round of sorting, add 1–2 × 10^6 yeast cells to five 1.5 mL tubes and wash them twice with 1 mL of Yeast Wash Buffer.
2. Resuspend the cells in 100 μL PBS containing 200, 100, 10, 1, and 0 nM of biotinylated target antigen (*see* **Note 12**). Incubate for 30 min at 25 °C. Wash each of the incubations twice with Yeast Wash Buffer and incubate with 100 μL of PBS

solution containing 1:2000 diluted anti-SV5-PE (1 μg/μL) and 1:400 Streptavidin-Alexa Fluor 633 (1 μg/μL) (detectable with the laser for Allophycocyanin APC) (*see* **Note 13**) for 30 min on ice. Wash the cells twice with Yeast Wash Buffer and resuspend each reaction in 1 mL PBS. Keep the cells on ice in the dark until sorting.

3. Analyze the yeast population by FACS. Compare the populations stained with the different antigen concentrations to the negative control with no antigen to check for nonspecific binders. If the purpose of the experiment is to look for high affinity binders, the population incubated with the lowest concentration of target antigen, which still gives a significant signal higher than the one obtained with the negative control, should be used for the sorting. If the goal is to find a broad number of different scFvs recognizing the target, a higher concentration incubation should be sorted to increase the diversity. The chosen stringency can be also modulated by the placement of the sort gate, although we recommend not to be too stringent in the first round of sorting. We usually sort between 10,000 and 20,000 events (*see* **Note 14**) directly into 1 mL of SD-CAA media.
4. Dilute the sorted population in 10 mL of SD-CAA media and grow at 30 °C with 250 rpm shaking for 48 h. The culture should reach saturation ($OD_{600} > 5$).
5. To induce the first sorting output, dilute the saturated culture at OD_{600} 0.5 in fresh SD-CAA media and let it recover for 1–2 h at 30 °C with 250 rpm shaking. Spin the culture at 3000 × *g* for 5 min and resuspend the pellet in 10 mL of SG/R-CAA media and grow at 20 °C for 16–20 h. The remaining sorted culture in SD-CAA media can be used to prepare glycerol freezer stocks to be stored at −80 °C.
6. Wash approximately 1–2 × 10^6 cells from the induced first-round output with Yeast Wash Buffer. Set up control and selection incubations using the biotinylated target antigen in the same manner as the first round and incubate for 30 min at 25 °C. If higher affinity antibodies are desired, the target antigen concentration can be lowered.
7. Wash the cells twice with Yeast Wash Buffer and incubate with 100 μL of PBS solution containing 1:2000 diluted anti-SV5-PE and 1:400 Streptavidin-Alexa Fluor 633 for 30 min on ice. Wash the cells twice with Yeast Wash Buffer and resuspend each reaction in 1 mL PBS. Keep the cells on ice in the dark until sorting.
8. Analyze the stained yeast by FACS and compare the signal from the different target antigen concentrations to the negative control with no target antigen. Choose the incubation with

the amount of antigen that matches the experimental goal (i.e., diversity of the binding scFvs VS high affinity binders). Analyze the cells from the chosen target antigen selection incubation and sort PE and APC positive cells into a collection tube containing 1 mL of SD-CAA. If the analyzed yeast population has achieved a satisfactory binding population it is possible to plate the sorted cells on several large SD-CAA plates. Generally, the colonies are visible on the plates after 2 or 3 days of incubation at 30 °C, and it is recommended to pick individual colonies, using sterile toothpicks, from the plate with lower colony density (i.e., 500 cells/plate) and to inoculate them in 1 mL/well of SD-CAA + Kanamycin + Tetracycline in 96-DeepWell plates.

9. If another sorting step is necessary dilute the sorted population in 10 mL of SD-CAA media and grow at 30 °C with 250 rpm shaking for 48 h and induce it by first diluting the saturated culture at OD_{600} 0.5 in fresh SD-CAA media and let it recover for 1–2 h at 30 °C with 250 rpm shaking, then, after spinning the culture at 3000 × *g* for 5 min, resuspend the pellet in 10 mL of SG/R-CAA media down and grow at 20 °C for 16–20 h. The rest of the culture in SD-CAA media can be used to prepare a glycerol freezer stock of the second sort and stored at −80 °C.

   As previously described for the previous rounds, prepare incubations of different concentrations of the biotinylated antigen. The incubation with a secondary detection reagent (Neutravidin-APC conjugated) different from the one used in the previous round is recommended to analyze and sort, proceeding as described before. Plate the sorted cells on one or several large SD-CAA plates. If the intention is to screen individual clones from this sort output, some plates can be seeded at a lower density (500 cells/plate) for screening by picking individual colonies and inoculate them in 1 mL of SD-CAA + Kanamycin + Tetracycline in 96-DeepWell plates. After the colonies have grown, make a glycerol freezer stock of the remaining culture obtained after the third-round sort output as described previously (*see* **Note 15**).

3.6 Screening of Individual Clones for Antigen Binding

To identify individual clones worth to be submitted to sequencing analysis, single clones are tested by flow cytometry for their binding activity to the target of interest.

1. Grow the colonies picked and inoculated in 1 mL of SD-CAA in deep well plates at 30 °C with shaking (300 rpm) for at least 16 h. The estimated OD_{600} should be around 5. Transfer 120 μL of this overnight culture into the new 96-DeepWell-plate containing 480 μL of SG/R-CAA + Kanamycin and

Tetracycline. Grow with shaking (300 rpm) for 18–24 h at 20 °C to induce the expression of scFv.

2. Add 120 µL of 80% glycerol to each well in **step 1** and store the plate at −80 °C. This is the master plate.
3. Use the induced yeast culture from **step 2** for binding analysis by FACS.
4. Aliquot 50 µL containing 2×10^6 cells into 96-well V/U-bottom plates and add 50 µL of biotinylated target antigen solutions with given concentrations (based on the concentration used for the final sort) into each well.
5. Incubate for 1 h overnight at 4 °C with rocking.
6. Wash cells twice with 200 µL of Yeast Wash Buffer.
7. Resuspend cells in 100 µL of PBS containing 1:2000 dilution of biotinylated anti-SV5-PE mAb and 1:400 streptavidin-APC. Incubate for 1 h at 4 °C.
8. Wash three times with Wash Buffer and eventually resuspend in 200 µL PBS.
   Measure cell fluorescence by FACS able to automatically analyze 96 samples using the PE channel and APC channels.

3.7 Sanger Sequencing of Individual Clones (See Note 16)

1. From the 96DeepWell plate containing SD-CAA media, plate small patches of binding clones (5–10 µL) on SD-CAA plates and incubate for 1–2 days at 30 °C (until the colonies are visible on the plate).
2. The scFv sequences of the binding clones can be determined by colony PCR followed by sequencing of the PCR products (*see* **Note 17**). From each plated colony, scrape yeast with a 5 µL loop and spread in the bottom part of a PCR tube. Cap the tube and microwave on high power for 2 min. Prepare a PCR master mix as follows: 10× of standard PCR buffer, dNTPs at a final concentration of 200 µM each, 1 µL of Taq, pDNL6 Forward and pDNL6 Reverse primers at a final concentration of 0.5 µM each and H_2O up to 25 µL/reaction. Add 25 µL of PCR mix in each tube containing microwaved yeast cells and run the following PCR cycle: 95 °C for 3 min followed by 30 cycles: 95 °C for 30 s, 55 °C for 30 s 72 °C for 1 min, and a final elongation step at 72 °C for 10 min (*see* **Note 18**).
3. Run the PCR reactions on an agarose gel, excise bands (should be approximately 1000 bp) with a clean razor blade, and purify using the Qiagen gel isolation kit or other suitable protocols. Sequence the purified PCR products using the pDNL6 Forward and pDNL6 Reverse primers.

4 Notes

1. We have used polyclonal phage scFv display selection outputs selected on recombinant protein target antigens as starting material for making yeast scFv display libraries. Our protocols are developed for phage scFv display libraries in the phagemid vector [5]. Protocols for the generation and use of phage scFv display libraries to enrich on purified target antigens have been described previously [8, 10].
2. The primers were designed to be compatible with the phagemid vector pDan5 [5] and the pDNL6 [10] yeast display vector. If different vectors are planned to be used, new primers will need to be designed. Part of the primers should allow the gap repair cloning, that in yeast works when 20–40 base pairs of homology with the linearized yeast vector are included into each primer. The remaining part of the primers must ensure that the scFv is amplified in frame from the phage display vector.
3. BssHII and NheI restriction sites are present in the pDNL6 yeast display vector (as well as in the pDan5 phage display vector). If a different vector is used, different enzymes may be necessary, and the key aspect is that the sites chosen to linearize the vector must be compatible with the homologous recombination primers.
4. We suggest adding Kanamycin (1000× solution 50 mg/mL in water) and Tetracycline (1000× solution 12 mg/mL in 70% ethanol) to all the yeast media solutions to prevent bacteria growth. The yeast is unaffected by the antibiotics.
5. We usually use biotinylated recombinant proteins as target. EZ-Link-NHS-LC-LC-Biotin is generally used to biotinylate purified recombinant proteins. We suggest performing some sort of quality control on the labeled target antigen.
6. We generally directly conjugate anti-SV5 mouse antibody with phycoerythrin (PE) using the Lightning-Link® R-Phycoerythrin (R-PE) kit from Innova Bioscience.
7. Different primers may be designed if a vector other than pDNL6 is used.
8. Standard PCR protocol with commercially available PCR buffer can be followed, we found the described method faster.
9. It is recommended to use freshly prepared competent cells for cloning the selection outputs. Cells can be kept a 4 °C for a week and be used for plasmid miniprep transformations.

10. It is possible to buy all the premade solutions for the yeast transformation from Sigma-Aldrich: Yeast Transformation Kit product code YEAST1.
11. The described protocol generates a C-terminal SV5 epitope tag on the scFv displayed on yeast. A display-negative population is always present after induction when analyzed by FACS, and the maximum induction will vary from experiment to experiment.
12. A range of concentrations has been provided based on our experience that usually covers most libraries generated from phage scFv display selection outputs. This range may need to be adjusted depending on the binding activity of different libraries.
13. Other fluorophore combinations can be used to match the capabilities of the available FACS instrument.
14. After two rounds of phage selection we have usually an output of 10^5 to 10^6, so with 10^6 to 10^7 yeast cells we cover $10\times$ the diversity and considering that we usually sort 1% of the yeast population on our first round of sorting we found that 10,000–20,000 events are enough to compromise between diversity and affinity, although the number of stained yeast cells and of sorted events can be modulated based on the experimental needs.
15. We have found that usually two or three rounds of sorting provide sufficient enrichment for monoclonal screening. More rounds of sorting can be performed with the risk to greatly reduce the diversity of the output.
16. There are companies that can directly sequence yeast colonies growing on an agar plate. The direct Sanger sequencing of yeast colony can be quite expensive.
17. As alternative, the plasmids can be rescued into bacteria, miniprepped, and sequenced. A protocol for this has been previously described [8].
18. Although the microwave method usually is successful, yeast colony PCR can be temperamental. Yeast minipreps followed by plasmid rescue into bacteria, miniprepping, and sequencing is an alternative method (*see* **Note 17**). The further advantage of this method is that it provides the plasmid containing the scFv, which can be used in downstream procedures such as PCR or cloning.

References

1. Clackson T et al (1991) Making antibody fragments using phage display libraries. Nature 352 (6336):624–628
2. Winter G et al (1994) Making antibodies by phage display technology. Annu Rev Immunol 12:433–455
3. Feldhaus MJ et al (2003) Flow-cytometric isolation of human antibodies from a nonimmune Saccharomyces cerevisiae surface display library. Nat Biotechnol 21(2):163–170
4. Boder ET, Wittrup KD (1997) Yeast surface display for screening combinatorial polypeptide libraries. Nat Biotechnol 15(6):553–557
5. Sblattero D, Bradbury A (2000) Exploiting recombination in single bacteria to make large phage antibody libraries. Nat Biotechnol 18 (1):75–80
6. Bradbury AR et al (2011) Beyond natural antibodies: the power of in vitro display technologies. Nat Biotechnol 29(3):245–254
7. Gera N, Hussain M, Rao BM (2013) Protein selection using yeast surface display. Methods 60(1):15–26
8. Ferrara F et al (2015) Recombinant renewable polyclonal antibodies. MAbs 7(1):32–41
9. D'Angelo S et al (2018) Selection of phage-displayed accessible recombinant targeted antibodies (SPARTA): methodology and applications. JCI Insight 3(9)
10. Ferrara F et al (2012) Using phage and yeast display to select hundreds of monoclonal antibodies: application to antigen 85, a tuberculosis biomarker. PLoS One 7(11):e49535

Chapter 17

Epitope Mapping via Phage Display from Single-Gene Libraries

Viola Fühner, Philip Alexander Heine, Kilian Johannes Carl Zilkens, Doris Meier, Kristian Daniel Ralph Roth, Gustavo Marçal Schmidt Garcia Moreira, Michael Hust, and Giulio Russo

Abstract

Antibodies are widely used in a large variety of research applications, for diagnostics and therapy of numerous diseases, primarily cancer and autoimmune diseases. Antibodies are binding specifically to target structures (antigens). The antigen-binding properties are not only dependent on the antibody sequence, but also on the discrete antigen region recognized by the antibody (epitope). Knowing the epitope is valuable information for the improvement of diagnostic assays or therapeutic antibodies, as well as to understand the immune response of a vaccine. While huge progress has been made in the pipelines for the generation and functional characterization of antibodies, the available technologies for epitope mapping are still lacking effectiveness in terms of time and effort. Also, no technique available offers the absolute guarantee of succeeding. Thus, research to develop and improve epitope mapping techniques is still an active field. Phage display from random peptide libraries or single-gene libraries are currently among the most exploited methods for epitope mapping. The first is based on the generation of mimotopes and it is fastened to the need of high-throughput sequencing and complex bioinformatic analysis. The second provides original epitope sequences without requiring complex analysis or expensive techniques, but depends on further investigation to define the functional amino acids within the epitope. In this book chapter, we describe how to perform epitope mapping by antigen fragment phage display from single-gene antigen libraries and how to construct these types of libraries. Thus, we also provide figures and analysis to demonstrate the actual potential of this technique and to prove the necessity of certain procedural steps.

Key words Phage display, Epitope mapping, Antigen fragments, Protein fragments, Panning

1 Introduction

The key molecules of the adaptive immune system are antibodies (Abs), which are involved in the binding of potentially harmful structures, called antigens (Ags) [1, 2]. These antigens can have different compositions (e.g., lipids, carbohydrates, etc.), but are mainly constituted by pathogen-derived proteins. In the presence of autoimmune diseases or certain types of cancer, self-antigens can

Michael Steinitz (ed.), *Human Monoclonal Antibodies: Methods and Protocols*, Methods in Molecular Biology, vol. 1904, https://doi.org/10.1007/978-1-4939-8958-4_17,

also be targeted by the immune system [3, 4]. The success of the cellular and humoral immune responses depends on the characteristics of the antibody-antigen interaction, which in turn depend on the antibody-binding region (paratope) and the discrete region of the antigen that is bound by the antibody (epitope). This particular antigenic region is characterized as a close cluster of surface accessible amino acids [5, 6]. Epitopes are commonly classified as linear or conformational. A linear epitope is constituted by consecutive amino acids on the protein sequence (usually 4–15 amino acids) and is therefore always continuous. A conformational epitope contains amino acids that are in close proximity on the tertiary structure of the antigen, but not obligatorily on its primary structure. Consequently, conformational epitopes are often, but not necessarily always, discontinuous [7, 8].

In the past few decades, the use of monoclonal antibodies (mAbs) for therapy against infectious diseases, cancer, or autoimmune diseases vastly increased [9] and with it the need for epitope determination techniques. Knowing the epitopes or targets of neutralizing or protective antibodies raised against pathogens or toxins is valuable information for vaccine development [10–12] and also for the development of mAbs against this target as a therapeutic molecules [13, 14]. In cancer immunotherapy, epitope characterization in early phase of antibody development is crucial, because of cancer escape mechanisms based on the occurrence of mutations that disrupt the binding of the therapeutic mAb to its target. Finally, epitope determination is not only crucial to enhance the efficacy of diagnostics, therapeutics, or vaccines [15, 16], but also to understand immune responses [17].

The most used techniques for epitope mapping are site-directed mutagenesis of the antigen [18], high-throughput mutagenesis [19], array-based oligopeptide scanning [20], peptide phage display [21], and X-ray co-crystallography [22, 23]. Even though it is not applicable to every antigen, X-ray co-crystallography is considered the gold standard for epitope mapping. It is the most effective method for the determination of conformational epitopes and unique in providing information on the Ab-Ag interaction at atomic level. Unfortunately, this method is also time consuming, highly laborious, and difficult, which drastically limits its applicability, especially when several mAbs need to be characterized or for basic research applications. Site-directed mutagenesis can be considered the best alternative to X-ray co-crystallography for functional epitope characterization, but it is not applicable timewise in the absence of preliminary information on the epitope region localization. The high-throughput mutagenesis approach tries to overcome this limitation, since it is based on an antigen library containing mutations on every position of a certain target [19]. Nevertheless, it is difficult to find a system to display and screen any desired antigen and it is laborious to discriminate

between mutations that affect the antibody binding (epitope region) and those that impair the folding of the overall antigen, unspecifically destroying the binding. Array-based oligopeptide scanning overtakes any other method in terms of usability, but it is also very expensive and associated with a low success rate for the mapping of conformational epitopes. The absence of a one-for-all approach leads to the search for new alternatives, such as bioinformatics analysis [24] or adaptation of other procedures (e.g., H/De-exchange mass spectrometry) [25, 26].

Phage display technology, currently one of the leading technologies for the generation of mAbs for therapy, diagnostic, and basic research [9, 27, 28], has already been used to display peptides or protein fragments [29–31] to map the response to vaccine or for the identification of novel diagnostic biomarkers [32].

Main advantage of this technique is that both phenotype (protein on phage surface) and genotype (protein coding sequence inside the phage capsid) are coupled in the same system. This enables easy retrieval of genetic information of phage displayed proteins or peptides, after selection from highly diverse libraries (theoretically up to 10^{11} different clones) [33, 34] by panning. Phage display has also been adopted for epitope mapping. Its use is based on two main strategies, defined by the type of library employed: peptide phage display from synthetic peptide libraries, or antigen fragment display from single-gene libraries [35]. In the first approach, short peptides (6–12 amino acids) with random sequences are displayed and used to perform panning on the studied mAb. Since the peptides are random and not related to the actual target, many positive hits need to be sequenced to generate statistically reliable data. Therefore, this approach necessarily requires next generation sequencing and advanced tools for bioinformatic analysis of the different peptide sequences [36], especially to rule out false-positive results. Also, depending on the peptide length, the nominal diversity of the library cannot always be reached because of physical limitations in the library size; complex design and library characterization is required to overcome this problem [37]. On the other hand, the use of single-gene libraries drastically reduces the risk of false-positive results since the displayed antigen fragments belong to the antigen gene and are not random. This also reduces the number of positive hit sequences needed to identify the epitope region and so the complexity of the data analysis. If more information is needed on the actual contribution of each amino acid to the interaction with the antibody, site-directed mutagenesis can be easily combined with this antigen fragment phage display approach [38] after the identification of the epitope region.

Since most of the conformational epitopes are discontinuous, this limits their display on short peptides. This limitation may be partially overtaken by the use of single-gene libraries that allow the

display of antigen fragments of various lengths (from empirical data: 18–128 amino acids), in a system that is known to allow the folding of complex molecules like antibodies and that has already been used for the mapping of conformational epitopes [39]. In this chapter, we describe an optimized protocol for epitope mapping, using single-gene libraries of prokaryotic or eukaryotic antigens.

2 Materials

2.1 Enzymes, Kits, and Antibodies

1. Phusion DNA polymerase + buffer 5× (New England BioLabs inc. (NEB)).
2. *Taq* DNA polymerase + buffer 5× (Promega).
3. *Pme*I endonuclease + cut smart buffer (NEB).
4. Calf intestine phosphatase (CIP) (NEB).
5. T4 ligase + buffer (Promega).
6. Trypsin (1 mg/mL stock).
7. Gel and PCR purification kit (Macherey-Nagel).
8. Fast DNA End Repair kit (Thermo Fisher Scientific).
9. Antibody of interest, preferably solubilized in PBS without any additives.
10. Unrelated antibody (CTR-Ab), preferably solubilized in PBS without any additives.
11. Anti-M13 phage (pVIII) antibody HRP-conjugated GE27-9421-01 (GE Healthcare).
12. Anti-M13 phage (pVIII) antibody 61097 (Progen).

2.2 DNA and Oligonucleotides

1. Primers for gene amplification (designed by the researcher).
2. Primers (forward and reverse) annealing to the phagemid 5′ and 3′ of the cloning site (designed by researcher).
3. DNA of the Antigen (either genomic DNA/cDNA or Plasmid).
4. Phagemid (pHORF3 [32] is used in this protocol).
5. dNTP mix (10 mM each).

2.3 Media and Supplements

1. SOC medium pH 7.0: 2% (w/v) tryptone, 0.5% (w/v) yeast extract, 0.05% (w/v) NaCl, 20 mM Mg solution, 20 mM glucose (sterilize magnesium and glucose separatetely, add solutions after autoclavation).
2. 2×TY medium: 1.6% (w/v) tryptone, 1% (w/v) yeast extract, 0.5% (w/v) NaCl.
3. Glycerol.

4. 2×TY-glycerol: 1.6% (w/v) tryptone, 1% (w/v) yeast extract, 0.5% (w/v) NaCl, 16% (v/v) glycerin.
5. 2 M Glucose (autoclaved).
6. Ampicillin (100 mg/mL stock).
7. 2×TY-GA: 2×TY, 100 mM glucose, 100 μg/mL ampicillin.
8. Agar-agar.
9. 2×TY-GA agar plates: 2×TY-GA, 1.5% (w/v) agar-agar.
10. Kanamycin (50 mg/mL stock).
11. 2×TY-AK: 2×TY, 100 μg/mL ampicillin, 50 μg/mL kanamycin.
12. Tetracyclin (20 mg/mL stock).
13. 2×TY-T: 2×TY, 20 μg/mL tetracycline.

2.4 Buffer and Solutions

1. TAE-buffer 50×: 2 M Tris–HCl, 1 M acetic acid, 0.05 M EDTA, pH 8.0.
2. Agarose 1.5% (w/v) in 1× TAE-buffer.
3. Polyethylenglycol-Sodium Chloride (PEG-NaCl) solution: 20% (w/v) PEG 6000, 2.5 M NaCl.
4. Phage dilution buffer (PDB) pH 7.5: 10 mM Tris–HCl, 20 mM NaCl, 2 mM EDTA.
5. Phosphate buffered saline (PBS) pH 7.4: 8.0 g NaCl, 0.2 g KCl, 1.44 g $Na_2HPO_4.2H_2O$, 0.24 g KH_2PO_4 in 1 L.
6. PBS-T (PBS, Tween 20 0.05% (v/v)).
7. Panning block (skimmed milk powder 1% (w/v), bovine serum albumine (BSA) 1% (w/v) in PBS-T).
8. Blocking buffer: 2% MPBS-T (skimmed milk powder 2% (w/v) in PBS-T).
9. TMB-A: 50 mM citric acid, 30 mM potassium citrate, pH 4.1.
10. TMB-B: 90% (v/v) ethanol, 10% (v/v) acetone; 10 mM tetramethylbenzidine; 1 mL 30% H_2O_2.
11. TMB solution: mix 19 parts of TMB-A with 1 part of TMB-B directly prior to use.
12. 1 N H_2SO_4.

2.5 Bacteria and Phage

1. *E. coli* TOP10 F′ (Thermo Fisher Scientific), genotype: F′ {*lac*Iq, Tn*10*(TetR)} *mcr*A Δ(*mrr-hsd*RMS-*mcr*BC) Φ80*lac* ZΔM15 Δ*lac*X74 *rec*A1 *ara*D139 Δ(*ara leu*) 7697 *gal*U *gal*K *rps*L (StrR) *end*A1 *nup*G.
2. *E. coli* XL1-Blue MRF′ (Agilent), genotype: Δ(*mcrA*)*183* Δ(*mcrCB-hsdSMR-mrr*)*173 endA1 supE44 thi-1 recA1 gyrA96 relA1 lac* [F′ *pro*AB *lac*I^qZΔM15 Tn10 (Tet^r)].

3. *E. coli* TG1 (Lucigen), genotype: [F′ *traD36 proAB lacIqZ* ΔM15] *supE thi-1* Δ(*lac-proAB*) Δ(*mcrB-hsdSM*)5(*rK–mK–*).
4. Hyperphage (M13K07ΔgIII) for oligovalent display (Progen).
5. Helperphage wt M13K07 (for optional second panning round).

2.6 Electronic Devices

1. NanoDrop spectrophotometer (Thermo Fisher Scientific).
2. Sonicator Bioruptor® Plus Sonication System (Diagenode).
3. MicroPulser Electroporator (Bio-Rad).
4. Thermo shaker compact (Eppendorf).
5. Power supply Amersham Bioscience EPS 310 (GE Healthcare).
6. Agarose gel chamber Peqlab PerfectBlue™ (VWR International).
7. −80 °C freezer.
8. Incubator for shake flasks, e.g., Multitron Standard (Infors HT).
9. Spectrophotometer with 600-nm wavelenght, e.g., Libra S11 (Biochrom).
10. Sorval Centrifuge RC5B Plus, rotor GS-3 and SS-34 (Thermo Fisher Scientific).
11. Refrigerated centrifuge for 15 and 50 mL tubes and plates; e.g., centrifuge 5810 R (Eppendorf).
12. Columbus Pro plate washer (Tecan, Männedorf, Switzerland).
13. VorTemp 56 incubator (Labnet).
14. EL405 plate washer (BioTek Instruments).
15. ELISA plate reader with 450 and 620 nm filter, e.g., Tecan sunrise (Tecan).

2.7 Lab Eqiupment, Consumables, and Miscellaneous

1. Pipette tips, 10, 20, 100, and 1000 μL.
2. Filtered pipette tips, 10, 20, 100, and 1000 μL, e.g., TipOne (StarLab International).
3. Amicon® Ultra-0.5 mL Centrifugal Filters Ultracel®-30K (Millipore).
4. 0.45 μm filter with celluloseacetate-membrane.
5. 1.5 mL reaction tubes.
6. 2 mL cryovials (Sarstedt AG & Co. KG).
7. 50 and 15 mL tubes, e.g., CentriStar (Corning).
8. 100 and 500 mL glass shake flasks.
9. GS-3 centrifugation bottles (Thermo Fisher Scientific).
10. SS-34 centrifugation tube (Thermo Fisher Scientific).
11. Gene Pulser® electroporation cuvetts 0.1 cm (Bio-Rad).

12. 1 mL cuvettes (Sarstedt AG & Co. KG).
13. Drigalsky spatula (VWR International).
14. 10 cm Petri dishes.
15. 24.5 × 24.5 × 2.5 cm plates.
16. 96-well U-shaped polypropylene plate, e.g., greiner bio-one (Greiner bio-one).
17. 24-deep well plate.
18. 96-well Costar® ELISA plate (Corning).
19. Liquid Nitrogen.

3 Methods

3.1 Gene Amplification, Fragmentation, and End-Repair

1. Design primers specific for the gene of interest.
2. Amplify the gene using polymerase chain reaction in duplicates (Table 1).
3. Run an agarose gel to check the amplification (band size, PCR side products, etc.).
4. Mix the two PCR reactions and purify using NucleoSpin Gel and PCR clean-up kit (Macherey-Nagel), eluting the DNA in 50 μL Milli-Q water.
5. Quantify the eluted DNA using a spectrophotometer and prepare the sample for the DNA fragmentation: 1 μg DNA in 100 μL Milli-Q water.
6. Fragment the DNA using the Bioruptor® Plus Sonication System (Diagenode) according to the manufacturer's protocol for the generation of 150 bp long fragments. Briefly, use 70 sonication cycles of 30 s "on" alternate by 30 s "off" at low power intensity all at 4 °C in water bath (*see* **Note 1**).
7. Run a 1.5% agarose gel loading 5 μL of the sample to check the actual size of the fragments (*see* **Note 2**).
8. Concentrate the fragments using Amicon Ultra-0.5 mL Centrifugal Filters Ultracel-30K (Millipore) following the manufacturer's instructions.
9. Measure the DNA concentration.
10. Repair the ends of the fragmented DNA using Fast DNA End Repair kit (Thermo Scientific) according to the manufacturer's instructions (Table 2).
11. Incubate the reaction at 20 °C for 15 min (do not let it stand longer) and purify using the NucleoSpin Gel and PCR clean-up kit (Macherey-Nagel). Elute in 20 μL Milli-Q water.

Table 1
PCR reaction

DNA (50 ng/μL plasmid, or 200 ng/μL genome)	1 μL
dNTP mix (10 mM each)	1 μL
HF buffer 5×	10 μL
Primer forward + reverse (10 μM each)	2.5 μL + 2.5 μL
Phusion® DNA polymerase (2 U/μL)	0.5 μL
H_2O Milli-Q	32.5 μL
Total volume	50 μL

Table 2
DNA-ends repair reaction (*see* Note 18)

Fragmented DNA (final amount 0.8–1 μg)	*X* μL
10× end repair reaction mix	5 μL
End repair enzyme mix	2.5 μL
H_2O Milli-Q	*Up to 50 μL*

3.2 Phagemid-Fragment Ligation and Library Construction

1. The preparation of the phagemid varies with the kind of phage display method used. In this protocol pHORF3 is used that allows blunt end cloning of the fragmented DNA in fusion to the pIII gene (gIII) (*see* **Note 3**). Perform plasmid digestion as described in Table 3.
2. Incubate the reaction for 2 h at 37 °C, then add 1 μL of calf-intestinal alkalyne phosphatase (10 U/μL, NEB), and further incubate for 1 h.
3. Purify the digested vector using the NucleoSpin Gel and PCR clean-up kit (Macherey-Nagel). Elute in 20 μL Milli-Q water.
4. Perform ligation reaction for 16 h at 16 °C with a molar ration of 1:10 (vector:insert) (Table 4).
5. Inactivate the ligation for 10 min at 65 °C and clean the reaction using Amicon® Ultra-0.5 mL Centrifugal Filters Ultracel®-30K (Millipore). Briefly, add 400 μL of Milli-Q water in the reaction and centrifuge (5 min, 14,000 × *g*). Repeat this washing step three times before collecting the final volume as instructed by the manufacturer.
6. Mix 5 μL of the purified ligation with 25 μL electrocompetent *E. coli* TOP10F′ (Thermo Scientific) in a 0.2 mL tube, transfer the volume into a 0.1 mm cuvette, then keep it on ice for 1 min prior to electroporation.

Table 3
Phagemid restriction digestion

Phagemid (total 5 μg)	*X* μL
Buffer CutSmart 10× (NEB)	2 μL
*Pme*I (10 U/μL, NEB)	1 μL
H_2O Milli-Q	*Up to 20 μL*

Table 4
Gene fragments ligation into phagemid

Digested ≈4-kb phagemid (total 1 μg)	*X* μL
Gene fragment average 200 bp (total 0.5 μg)[a]	*Y* μL
T4 DNA ligase buffer 10× (Promega)	10 μL
T4 DNA ligase (3 U/μL, Promega)	3.5 μL
H_2O Milli-Q	*Up to 100 μL*

[a]In this example, the considered average size of the fragments is ≈200 bp and thus ≈0.5 μg DNA should be added to obtain a molar ration of 1:10 (vector:insert)

7. Transform bacteria by electroporation (Ω; 1.8 kV; pulse ≈5 ms long) and immediately add 1 mL of SOC medium pre-warmed at 37 °C.
8. Transfer the cells into a 1.5 mL tube and incubate at 37 °C for 1 h at 600 rpm in a thermo mixer.
9. Take 10 μL of transformed bacteria and make ten-fold dilutions until 10^{-5} in 2×YT.
10. Plate 50 μL of the dilution 10^{-3} and 100 μL of the dilution 10^{-5} onto 2×YT-GA agar 10 cm plates and grow it overnight at 37 °C.
11. Plate the remaining ≈990 μL of the transformation onto a 24.5 × 24.5 × 2.5 cm plate with 2×YT-GA agar and incubate at 37 °C for 16 h.
12. Count colonies on the 10 cm plates (*see* **Note 4**).
13. Add 20 mL of 2×YT-glycerol 16% to the 24.5 × 24.5 × 2.5 cm plate and incubate on a rocker for 10 min.
14. Carefully scrape off the cells with a drigalski spatula and prepare aliquots of 1 mL in cryovials.
15. Immerse the cryovials into liquid nitrogen and wait for 5 min. Then, carefully take the tubes with protection gloves and store them at −80 °C.

Table 5
Colony PCR reaction

dNTP mix	0.2 µL
$MgCl_2$ 25 mM	0.8 µL
GoTaq® Flexi Buffer 5×	2 µL
Primer forward + reverse (10 mM each)	0.5 µL + 0.5 µL
GoTaq® DNA polymerase (5 U/µL)	0.05 µL
H_2O Milli-Q	5.95 µL
Total volume	*10 µL*

3.3 Library Quality Control and Packaging

1. From the 10 cm plates used for the determination of transformation rate (*see* Subheading 3.2, **step 12**), take at least 20 colonies to perform a colony PCR (Table 5). As negative control, use the empty phagemid as template for one of PCR reaction (*see* **Note 5**).
2. To check the size of each fragment, prepare a 1.5% agarose gel, load the samples, and separate DNA fragments by electrophoresis at 80 V for 1 h to increase the resolution (*see* **Note 6**).
3. Determine the insert rate of your library by calculating the percentage of positive clones (those that have larger amplicons compared to the negative control). If the insert rate is much below 80%, consider repeating previous steps, mainly the phagemid preparation or ligation.
4. Inoculate 200 mL of 2×YT-GA in a 500 mL shake flask with 200–500 µL of the library glycerol stock preparation (*see* Subheading 3.2, **step 15**).
5. Incubate the shake flask at 37 °C, 250 rpm until $OD_{600} \approx 0.5$. Transfer 25 mL ($\approx 1.25 \times 10^{10}$ cells) of the culture to a 50 mL tube and infect cells with 2.5×10^{11} CFU (MOI 1:20) of Hyperphage (M13K07ΔgIII).
6. Incubate the tube for 30 min at 37 °C without shaking, then 30 min at 37 °C and 250 PRM.
7. Centrifuge the tube at 3220 × *g*, 10 min, RT. Discard the supernatant, suspend the cells in 10 mL of 2×YT-AK, and transfer them into a 500 mL shake flask containing 190 mL of the same medium. Incubate the flask at 30 °C, 250 rpm for 20-24 h.
8. Transfer the culture to a 500 mL centrifuge tube and centrifuge at 10,000 × *g*, 10 min, 4 °C. If the supernatant is still turbid repeat centrifugation. Collect the supernatant and add 1/5 volume (≈40 mL) of PEG-NaCl solution. Incubate the tube at 4 °C on ice overnight. In parallel, inoculate 25 mL of 2×YT-T with *E. coli* XL1-Blue MRF′ into a 100 mL shake flask and incubate at 37 °C, 250 rpm, overnight.

9. Centrifuge the tube containing the supernatant with PEG-NaCl at 10,000 × *g*, 1 h, 4 °C. Discard the supernatant.
10. Suspend the phage containing pellet in 10 mL of ice-cold PBS and transfer them to a 50 mL centrifuge tube.
11. To remove residual bacteria debris, centrifuge the suspension 20,000 × *g*, 10 min, 4 °C and collect the supernatant.
12. Filter the suspension through a 0.45 μm filter and transfer it to another 50 mL centrifuge tube.
13. Add 1/5 volume (≈2 mL) of PEG-NaCl solution and incubate for 30 min on ice. Mix every 5 min.
14. Centrifuge the suspension 20,000 × *g*, 30 min, 4 °C, then discard the supernatant.
15. Suspend the pellet in 1 mL of PBS, transfer to a 1.5 mL tube, and centrifuge 16,000 × *g*, 30 min, 4 °C.
16. Transfer the supernatant into a cryovial and store it at 4 °C for further use.
17. Use the *E. coli* XL1-Blue MRF′ culture, to inoculate 25 mL 2×YT-T in a 100 mL shake flask. Prepare the new bacterial culture to obtain an initial $OD_{600} \approx 0.1$ and incubate at 37 °C and 250 rpm, until $OD_{600} \approx 0.5$.
18. Take 10 μL of the phage suspension and make tenfold dilutions until 10^{-9} in PBS.
19. Prepare four 1.5 mL tubes with 50 μL of *E. coli* XL1-Blue MRF′ cells in each and transfer 10 μL of the last four phage dilutions to each tube (these will be dilutions 10^{-8}, 10^{-9}, 10^{-10}, 10^{-11} on the plate).
20. Incubate the tubes at 37 °C for 30 min without shaking.
21. Divide one 2×YT-GA agar plate into four parts and spot three droplets (10 μL each) per dilution, one dilution per every part. Let the droplets dry under the biological cabinet for ≈5 min and incubate the plate at 37 °C for 16 h.
22. Divide another 2×YT-GA agar plate into two parts and spread the remaining volume (≈30 μL) of the two intermediate dilutions (10^{-9} and 10^{-10}).
23. Count the colonies on countable droplets and calculate the titer as CFU/mL: arithmetic mean of the colonies from 3 droplets multiplied per 6 (spotting dilution factor) and per the titering dilution factor. This quality measurement is called "library titer" (*see* **Note 7**).
24. From the other plate, pick at least 20 colonies and send them for sequencing for quality control (*see* **Note 8**). Align all the "in-frame correct antigen fragments" onto the target gene to

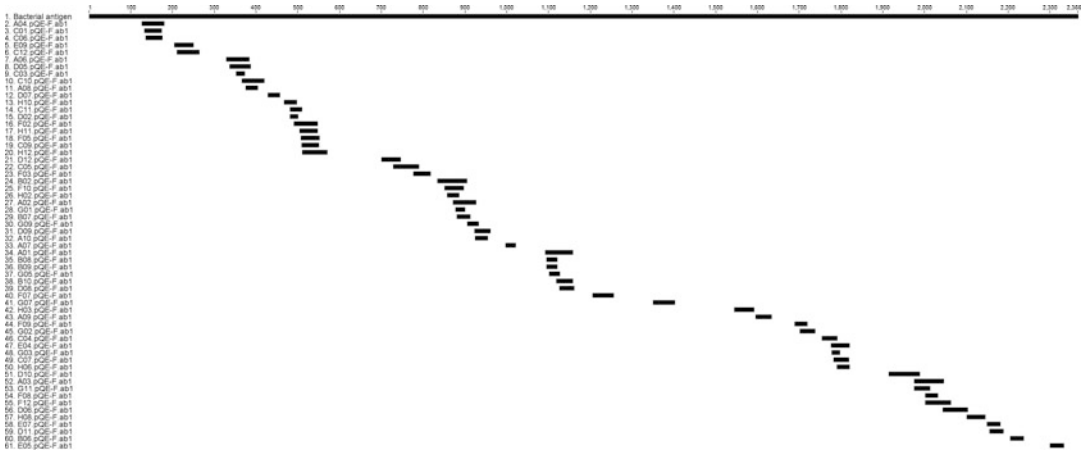

Fig. 1 Antigen fragments distribution and gene coverage after antigen fragment library packaging. Of 93 sequenced library clones, 60 were encoding "in-frame correct antigen fragments" (64.5%). From the alignment of these clones onto the target antigen sequence an antigen coverage of 55% was calculated. Several fragments corresponding to non-covered regions in the alignment were isolated during the different antigen fragment panning campaigns. This finding confirms that the presence of gaps in the alignment is caused by the limited number of sequenced library clones and not by a bias in the fragmentation or library generation procedure

confirm that the fragment distribution is homogeneous and estimate the gene coverage. Sequence more clones only if a more accurate estimation of the coverage is required (*see* Fig. 1).

3.4 Antigen Panning

1. Coat 1 well of a 96-well ELISA plate with 0.5–1.5 μg of purified monoclonal antibody diluted in 150 μL of PBS (recommended well A1, called "panning well"). This is the antibody we intend to map the epitope from (*see* **Note 9**).
2. Coat another well (recommended well A3, called negative selection well) with 0.5-1.5 μg of an unrelated antibody (CTR-Ab) diluted in 150 μL PBS. Use a CTR-Ab of the same isotype and format of the one coated in the panning well.
3. After 1 h incubation at RT, discard the antibody solutions and add 300 μL of Panning Block solution in both coated wells and incubate the plate at 4 °C overnight. In parallel, inoculate 25 mL of 2×YT-T in a 100 mL shake flask with *E. coli* XL1-Blue MRF′ and incubate overnight at 37 °C and 250 rpm.
4. On the next day, wash the coated microtiter plate wells 3× with PBS-T using an ELISA washer (*see* **Note 10**).
5. In the negative selection well add $\approx 1 \times 10^9$ (library diversity should be covered at least 50×) phage of the antigen fragment library into 150 μL of Panning Block solution (*see* Fig. 2, step 1).

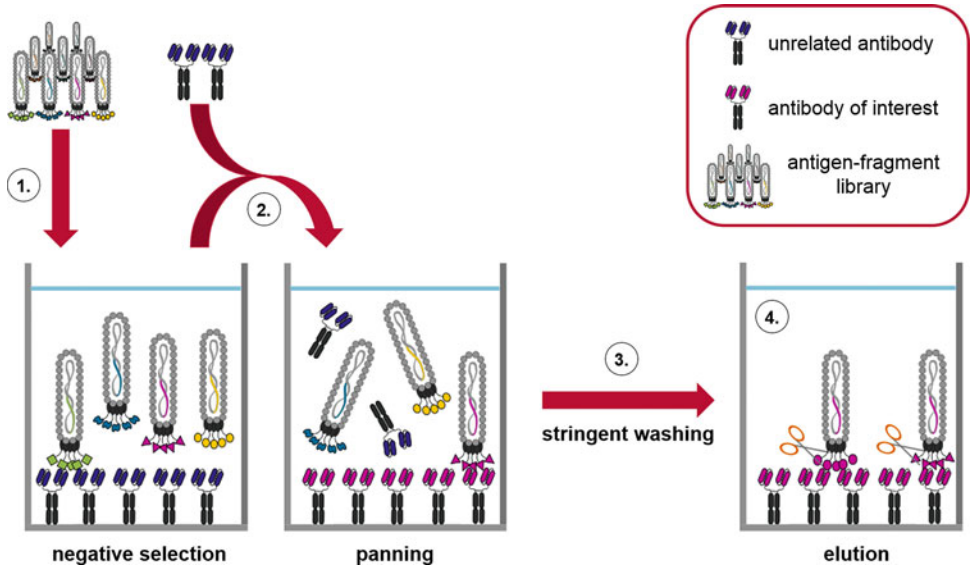

Fig. 2 Schematic view of the antigen fragment panning procedure. (1) The cross-reactive antigen fragments are negatively selected from the antigen-fragment library via preincubation on a coated unrelated CTR-antibody. (2) Afterwards, the preincubated library is transferred into the panning well onto the target antibody for selection. In this step, large excess of soluble unrelated CTR-antibody is added for competition to further reduce the selection of cross-reactive fragments. (3) After incubation, unbound antigen fragment phage particles are removed by stringent washing. (4) Phage encoding antigen fragments that bound to the coated antibody are eluted with trypsin

In the panning well, add 150 µL of Panning Block solution and incubate the plate 30 min at room temperature.

6. Empty the panning well and transfer in it the antigen fragment phage library from the negative selection well (*see* Fig. 2, step 2). Add in the panning well 1 µg of soluble CTR-Ab (*see* Fig. 2, step 2) necessary for competition (*see* **Note 11**). Incubate for 1.5 h at RT.
7. After 1 h, inoculate 25 mL 2×YT-T with 300 µL of the *E. coli* XL1-Blue MRF′ overnight culture (initial OD_{600} should be 0.08–0.1), incubate at 37 °C, 250 rpm for ≈1.5 h or until $OD_{600} \approx 0.5$ and use on **step 12**. While the cells are growing perform **steps 9–11**.
8. Remove the library from the panning well and perform harsh and extensive washing of the well (*see* Fig. 2, step 3) to remove unbound phage (*see* **Note 12**).
9. Elute the binding phage by adding 160 µL of 10 µg/mL Trypsin diluted in PBS for 30 min at 37 °C (*see* Fig. 2, step 4).
10. Store 140 µL of eluted phage as backup. For long-term storage add 20% glycerol and deposit at −80 °C. Storage up to several weeks is also possible without addition of glycerol at 4 °C. These phage can be used for an optional 2nd panning round (*see* Subheading 3.7).

11. Use 10 µL of eluted phage to infect 50 µL *E. coli* XL1-Blue MRF′ at $OD_{600} \approx 0.5$, incubate for 30 min at 37 °C without shaking. With 10 additional µL of eluted phage make a 10- and 100-fold dilution in PBS. Use 10 µL of each dilution for infection as described above.
12. Completely plate the dilutions onto different 2×YT-GA agar 10 cm plates and incubate at 37 °C overnight (*see* **Note 13**).
13. On the next day, count the colonies and infer the titer of eluted phage. Afterwards, store the plates at 4 °C for a few days or start directly with monoclonal phage production and screening (*see* Subheading 3.5).

3.5 Monoclonal Phage Production and Screening

1. Add 150 µL of 2×YT-GA to each well of a 96-well U-bottom propylene plate.
2. Use 200 µL pipette tips to pick 94 colonies (optional 46 from each panning round) from the plates described on the last step of the previous part. In the same plate, include two wells (H6 and H12) with medium only and one well (H9) with a colony to produce a non-related phage for production control.
3. Cover the plate (this will be called "Master plate") with a breathable membrane and incubate at 37 °C, 800 rpm overnight in a Labnet Vortemp56 incubator (*see* **Note 14**).
4. In another 96-well U-shaped propylene plate, add 150 µL/well of 2×YT-GA and transfer 10 µL of the previously grown plate to this new one. Store the Master plate at 4 °C and incubate the new one at 37 °C, 800 rpm for 1.5-2 h (this will be called "production plate").
5. Dilute purified Hyperphage (M13K07ΔgIII) in 2×YT to a concentration of 1×10^{10} CFU/mL and add 10 µL of this solution to each well of the 96-well plate (3.3×10^9 CFU/well).
6. Incubate for 30 min at 37 °C without shaking, followed by 30 min at 37 °C, 800 rpm.
7. Centrifuge the plate 3200 × *g* for 10 min at RT, remove the supernatant by quickly inverting the plate over a laboratory waste disposal, and add 150 µL/well of 2×YT-AK.
8. Incubate the plate overnight at 30 °C and 800 rpm.
9. Coat the wells of a Costar® ELISA plate with 100 ng antibody in 100 µL PBS at 4 °C overnight and a negative control plate with an unrelated antibody, preferably the same as used for competition (coat wells H6 and H9 with α-pVIII antibody (Progen 61097)).
10. Discard the supernatant and block the wells with 250 µL blocking buffer for 1 h at RT.

11. Pellet bacteria of the production plate at 3200 × *g* for 10 min at RT.
12. Wash ELISA plates three times with H_2O 0.05% Tween20 (v/v). Add 75 µL blocking buffer per well and mix with 25 µL supernatant of the corresponding well of the production plate. In well H6, add 1×10^{10} cfu of Hyperphage (M13K07ΔgIII) as a positive control.
13. Incubate the ELISA plate for 2 h at RT.
14. Wash ELISA plates three times with H_2O 0.05% Tween20 (v/v) and incubate with 100 µL/well secondary α-pVIII-HRP antibody (GE 27-9421-01; diluted 1:40,000 in blocking buffer) 45 min at RT.
15. Wash ELISA plates three times with H_2O 0.05% Tween20 (v/v) and develop with 100 µL/well TMB substrate solution.
16. Stop reaction with 100 µL/well 1 N sulfuric acid.
17. Measure absorption at 450 nm (reference measurement at 620 nm) (*see* **Note 15**).

3.6 Identification and Sequencing of Positive Hits and Epitope Determination

1. In screening ELISA each clone has been tested in one well for binding to the studied antibody and in another well for cross-reactive binding to the CTR-Ab. Divide the ELISA signal of the first by the signal of the second plate to determine the signal-to-noise ratio.
2. Afterwards, select the clones specific to the studied Ab according to their signal-to-noise ratio. Consider as specific only clones that fulfill the following three conditions: (1) signal-to-noise ratio higher than 5; (2) absolute signal from studied Ab well at least three times higher than the media control well; (3) absolute signal from CTR-Ab well comparable, but not higher than the media control well. When only condition 3 is verified, the clone can be considered "nonbinding"; when only condition 2 is verified and the signal-to-noise ratio is close to 1, the clone can be considered "crossreactive" (*see* Fig. 3).
3. Divide the positive clones in three categories: signal to noise comprised between 5 and 10, between 10 and 20, or higher than 20. Select at least 4 clones per each category (*see* **Note 16**).
4. Take the Master plate stored on Subheading 3.5, **step 3** and use it as a source of the selected clones to prepare DNA for sequencing.
5. After sequencing, exclude the sequences containing frameshifts or stop codons, but be aware that these clones might still be expressed in *E. coli* production system (*see* **Note 17**).
6. Translate the remaining sequences to obtain the corresponding amino acid sequence (*see* Fig. 4a).

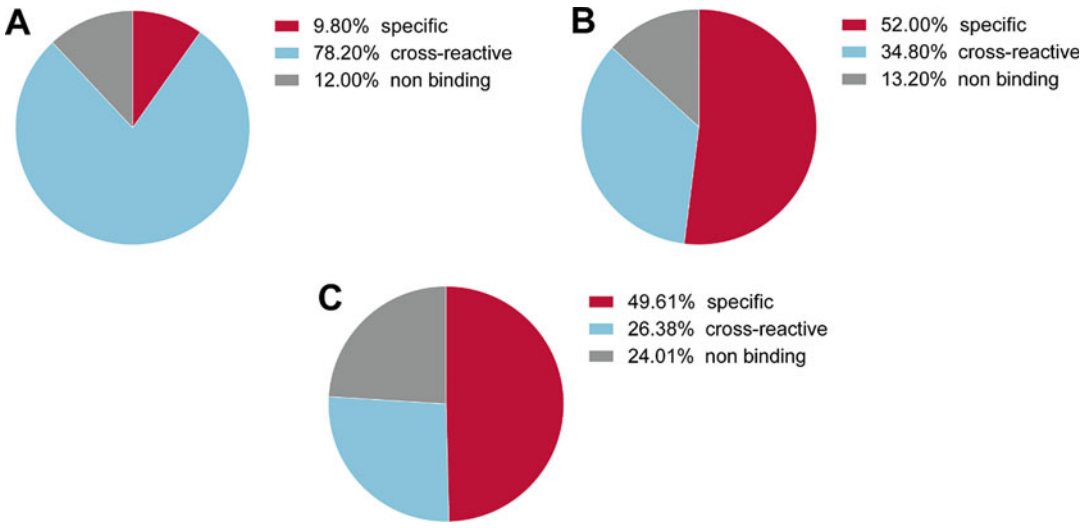

Fig. 3 Panning efficiency shown in Screening ELISA. (**a**) Screening ELISA result after panning without soluble competition. The majority of screened clones (>75%) are cross-reactive, as they bind to the unrelated antibody as much as to the target antibody. Consequently, the percentage of specific hits is very low (<10%). (**b**) Screening ELISA result after panning on the same target Ab of (**a**) but with soluble competition. The relative amount of specific binders is drastically increased, while the percentage of cross-reactive binders is significantly reduced. (**c**) Screening ELISA results from antigen panning with soluble competition on 15 different target mAbs (scFv-Fc format)

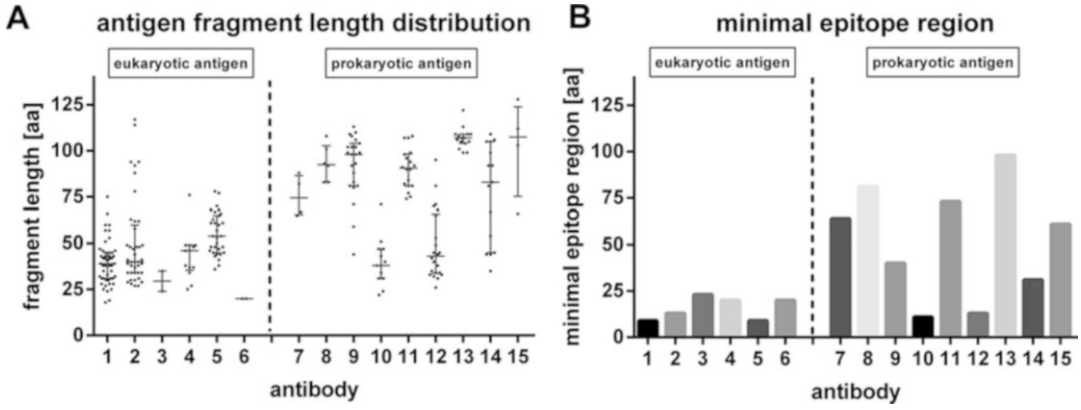

Fig. 4 Length distribution of epitope-containing fragments and minimal epitope length for 15 different mAbs (scFv-Fc format). (**a**) Epitope containing fragments length distribution. Shown is the length of fragments, with median and quartiles. Each dot represents an individual fragment which contributed to define the epitope. For both, eukaryotic and prokaryotic antigens, very short (<20 aa) as well as very long (>100 aa) fragments have been isolated. (**b**) The minimal epitope-binding region generated by the alignment of the epitope-containing isolated fragments. The epitope region length correlates with the average length of the fragments that define the epitope more than their number. Indirectly, the length distribution contributes to the definition of the type of epitope bound by an antibody (continuous or discontinuous) and the definition of the shortest sequence capable of recreating it

7. Align all the amino acid sequences, e.g., with ClustalOmega tool (EBI, http://www.ebi.ac.uk/Tools/msa/clustalo) to identify the minimum overlapping region that contains the epitope (*see* Fig. 4b and **Note 18**).

3.7 Phage Amplification and Panning Round 2 (Optional Step; See Note 15)

1. Inoculate 25 mL of 2×YT in a 100 mL shake flask with *E. coli* TG1 and incubate overnight at 37 °C, 250 rpm.
2. On the next day, inoculate 300 μL of the *E. coli* TG1 overnight culture in 25 mL 2×YT (initial $OD_{600} = 0.08–0.1$), incubate at 37 °C, 250 rpm for ≈1.5 h until $OD_{600} \approx 0.5$.
3. When the desired OD is reached, add 1 mL of *E. coli* TG1 culture into a well of a 24-deep well plate. Then, infect the culture with 60 μL of eluted phage from **step 11** and incubate for 30 min at 37 °C without shaking followed by 30 min at 37 °C and 500 rpm.
4. Centrifuge the plate 2500 × *g* for 10 min at RT. Discard the supernatant, add 5 mL of pre-warmed 2×YT-GA, and incubate at 37 °C under 500 rpm for 30 min until $OD_{600} \approx 0.5$ is reached. Then, add Helperphage M13K07 ($\approx 5 \times 10^{10}$ total, MOI 1:20) for 30 min at 37 °C without shaking. Then, incubate for 30 min at 37 °C and 500 rpm. If polyvalent display is desired Hyperphage M13K07ΔgIII can be used.
5. Centrifuge the plate 2500 × *g* for 10 min at RT. Remove the supernatant completely (be careful with the pellet). Add 5 mL 2×YT-AK, suspend the pellet and incubate at 30 °C and 500 rpm overnight.
6. For the next panning round, coat the studied antibody and the CTR-antibody in a 96-well ELISA according to **steps 1** and **2**. Moreover, inoculate 2×YT-T with *E. coli* XL1-Blue MRF′ the same way as described in **step 3**.
7. On the next day, centrifuge the 24-well plate (3220 × *g*, 10 min, RT) and collect the production supernatant in a 15 mL tube.
8. Mix 50 μL of the antigen fragment phage production supernatant with 100 μL of Panning block solution and store the rest at 4 °C.
9. Perform the second panning round identically to panning round 1 (Subheading 3.4) with one exception: instead of the library, use the amplified phage (*see* the previous step).

4 Notes

1. A sonication protocol, set to produce in average 150 bp fragments, will realistically provide fragments of a size distribution

in the range of ca. 60–300 bp, corresponding to 20–100 amino acids. The broad size distribution is crucial since the nature of the epitope investigated often is unknown. Conformational epitopes, which depend on the original protein folding, cannot be recreated with short antigen fragments, while in case of linear epitopes the shorter fragments facilitate higher epitope resolution. It is also possible to generate two libraries for the same gene, one of short fragments and one of larger fragments. When the type of epitope is known, fragment size can be adjusted according to the specific needs. Please consider DNA fragments longer than 300–400 bp may result in antigen fragments that are rarely displayed on phage and might get lost in the library packaging step.

2. Fragmented DNA appears on the gel as a smear with a concentrated band on the expected size defined by the fragmentation protocol. If the fragmented DNA is not concentrated on the expected size, a higher number of sonication cycles or an optimization of the sample preparation and sonication protocol might be considered.
3. This protocol is written based on the pHORF3 system originally generated for ORFeome display [32]. This phagemid allows cloning of fragments in a blunt *Pme*I restriction site upstream the gIII. This way, fragments that are in-frame will be expressed in fusion with pIII, so that the protein fragment corresponding to the cloned fragment will be displayed on the surface of the phage particles.
4. The expected amount of CFU should be 10^6–10^8. This is statistically way above the number of clones necessary to cover the gene length. For example, a 1200 bp long gene would need approximately 2102 cloned fragments of 150 bp to be completely covered when walking one nucleotide upstream at a time. The number "N" of fragments needed to cover the gene is obtained with the following formula:

$$N = 2x(a - b + 1)$$

where "a" is the size of the gene and "b" is the average size of the fragmented DNA. The factor two takes into account that the cloning was performed with random insert orientation. The value "1" refers to the fragments offset. This formula is just to guide the researcher in a simple manner. For a more accurate estimation of the number of fragments required to cover the gene of interest please refer to Connor et al. [40]. Indeed, gene coverage can be estimated only after library packaging (*see* **Note 8** and Fig. 1).

5. The pair of oligonucleotide primers used for colony PCR (including negative control) depends on the phagemid system

used. However, regardless the phagemid used, it is recommended to have primers annealing on the phagemid backbone and approximately 110 bp distant from the restriction site used for cloning. This way, the negative control will have a size of about 250 bp and all the positive clones should be above this size. Primers annealing far from the insert will produce long amplicons for the empty vector and consequently reduce the capability to differentiate between negative and positive clones when the latter carries a short insert.

6. To discriminate between empty vector and short inserts a high-resolution electrophoresis is essential. Initially, it is possible to optimize the running and imaging conditions to detect small size differences between the fragments, i.e., increase agarose gel concentration, or running with lower voltage. Nevertheless, the optimal evaluation of the amplicon size is done with capillary electrophoresis (e.g., using QIAxcel Advanced System, QIAGEN, Hilden, Germany).
7. The expected titer is 10^{10}–10^{12} CFU/mL. If the titer is much below this value, consider repeating the phage production (**steps 4–16**).
8. The data obtained from sequencing provides first information about the library in regards of insert rate, insert length, and insert length distribution. Since blunt end cloning after random DNA fragmentation was used to generate the library, expect that statistically only 1/18 clones (5.56%) will carry a plasmid coding for a correct target fragment fused in-frame to pIII. This is due to random gene orientation, random insert length (has to be $3 \times n + 1$ to be in-frame with pIII), and random reading frame of the original gene. Due to Hyperphage (M13K07ΔgIII) packaging an ORF enrichment is expected [41, 42]. The percentage of "in-frame correct antigen fragments" should be higher than 60%. When less than 60% is reached, consider repeating packaging or even library cloning.
9. Normally, coating of antibodies directly onto the ELISA plate surface is unproblematic. Nevertheless, for some antibodies the activity might be considerably reduced or even eliminated after immobilization on the plastic surface. In this case, coat the plate for 1 h at RT with 100 µL/well of an capture antibody directed against the Fc part of the studied mAb diluted in PBS to 2–4 µg/mL, then block by adding 300 µL/well of blocking buffer for 30 min prior to adding the mAb. It is important to consider the relative amount of BSA or other stabilizers present in the antibody preparation, which may affect the coating!
10. The washing should be performed with an ELISA washer (e.g., TECAN Columbus Plus) to increase stringency and reproducibility. To remove antigen or blocking solutions wash 3× with

PBS-T ("standard washing protocol" for TECAN washer). If no ELISA washer is available, wash manually 3× with PBS-T.

11. Because of the intrinsic nature of the library, also antigen fragments that are normally buried inside the protein will be displayed. Many of the amino acid patches that are needed for protein-protein interfaces, rather than protein-solvent interfaces, are known for their tendency to unspecifically bind other proteins and are therefore considered "sticky" [43]. To reduce the selection of unwanted crossreactive antigen fragments, it is important to include the competition with an unrelated antibody (*see* also Figs. 2 and 3). For the same reason, the preincubation step is used.
12. After binding of antibody phage, stringent washing is required. This washing step should be performed with an ELISA washer. Wash 10× with PBS-T ("stringent bottom washing protocol" in case of TECAN washer). If no ELISA washer is available, for stringent off-rate selection increase the number of washing steps up to 50 times.
13. Considering that the number of phage containing the epitope can be highly variable depending on the type of epitope to map and the success of the selection, there is no optimal dilution that can be systematically adopted as standard. The protocol suggests a plating dilution that is more likely to give the researcher enough colonies to start a screening, which is at least 92 isolated colonies. However, if the plates have too few or too much colonies, the spreading step should be repeated using a lower or a higher dilution from the material stored at 4 °C.
14. The growth of colonies in the 96-well U-shaped polypropylene plate can also be done for only 6 h. We suggest incubating the bacterial cells overnight to ensure higher final density and lower OD_{600} clone-to-clone variation.
15. When the number of specific clones after screening ELISA is lower than 3%, we suggest screening further clones (number depending on percent of specific clones in initial screening). Alternatively, the whole antigen fragment panning can be repeated. To limit the selection of undesired hits, it is favorable to use more stringent washing conditions and increase the amount of CTR-competing Ab and the duration of the competition. It may help to add the competing antibody after the stringent washing for one hour and then repeat the washing prior trypsin elution. If this does not lead to better results, it is possible to amplify the phage eluted after the first panning round and proceed with a second round. The advantage of using a second round is the enrichment of pre-selected clones from the first round. Nevertheless, if in the screening after

panning round 1 only few specific clones were detected, one can assume that the majority of eluted phage present cross-reactive or nonbinding antigen fragments. For this reason, even in case of a second panning round it is important to ameliorate the washing and competition steps as described at the beginning of this note to do not overamplify these unwanted clones.

16. In case the number of specific hits is particularly high, it is possible to reduce the number of candidates for sequencing determining first the antigen fragment length as described in Subheading 3.3, **steps 1** and **2**. For a better resolution of the mapping, sequence the shortest fragments. Also, with this approach, it is possible to distinguish among different fragments so to avoid redundant sequencing results.
17. To avoid misinterpretations, it is important to exclude sequences containing frameshifts and stop codons from data evaluation. Nevertheless, the capability of *E. coli* to read quadruplets may lead to the selection of sequences that are not cloned in-frame between signal sequence and gIII, but may effectively translate into a functional antigen fragment specific for the antibody of interest. Also, in this analysis it should be considered that *E. coli* XL1-Blue MRF′ can read-through Amber and, to a lower extent, also Opal and Ochre stop codons [44, 45].
18. If the result is not satisfactory because the found epitope is too long according to the researcher needs, we suggest sequencing more clones to increase the mapping resolution. Also, in this case it may be appropriate to preliminarily determine the fragment length via PCR (*see* **Note 16**). When this does not help, it may be required to design a new library having different fragment size distributions or to adopt a different epitope mapping approach.

Acknowledgments

We thank CNPq for providing the scholarship of GMSGM (process 204693/2014-4). V.F. was funded by the Federal State of Lower Saxony, Niedersächsisches Vorab (VWZN2889/3215/3266). This chapter is a completely revised and updated version of [46].

References

1. Heesters BA, van der Poel CE, Das A, Carroll MC (2016) Antigen presentation to B cells. Trends Immunol. https://doi.org/10.1016/j.it.2016.10.003
2. Gunn BM, Alter G (2016) Modulating antibody functionality in infectious disease and vaccination. Trends Mol Med. https://doi.org/10.1016/j.molmed.2016.09.002

3. Soliman C, Yuriev E, Ramsland PA (2016) Antibody recognition of aberrant glycosylation on the surface of cancer cells. Curr Opin Struct Biol 44:1–8. https://doi.org/10.1016/j.sbi.2016.10.009
4. Rock KL, Reits E, Neefjes J (2016) Present yourself! By MHC class I and MHC class II molecules. Trends Immunol. https://doi.org/10.1016/j.it.2016.08.010
5. Sela-Culang I, Kunik V, Ofran Y (2013) The structural basis of antibody-antigen recognition. Front Immunol 4:302. https://doi.org/10.3389/fimmu.2013.00302
6. Kaur H, Salunke DM (2015) Antibody promiscuity: understanding the paradigm shift in antigen recognition. IUBMB Life 67:498–505. https://doi.org/10.1002/iub.1397
7. Kringelum JV, Nielsen M, Padkjær SB, Lund O (2013) Structural analysis of B-cell epitopes in antibody:protein complexes. Mol Immunol 53:24–34. https://doi.org/10.1016/j.molimm.2012.06.001
8. Gupta S, Ansari HR, Gautam A et al (2013) Identification of B-cell epitopes in an antigen for inducing specific class of antibodies. Biol Direct 8:27. https://doi.org/10.1186/1745-6150-8-27
9. Frenzel A, Schirrmann T, Hust M (2016) Phage display-derived human antibodies in clinical development and therapy. MAbs 8:1177–1194. https://doi.org/10.1080/19420862.2016.1212149
10. Cherryholmes GA, Stanton SE, Disis ML (2015) Current methods of epitope identification for cancer vaccine design. Vaccine 33:7408–7414. https://doi.org/10.1016/j.vaccine.2015.06.116
11. Lanzavecchia A, Frühwirth A, Perez L, Corti D (2016) Antibody-guided vaccine design: identification of protective epitopes. Curr Opin Immunol 41:62–67. https://doi.org/10.1016/j.coi.2016.06.001
12. Aghebati-Maleki L, Bakhshinejad B, Baradaran B et al (2016) Phage display as a promising approach for vaccine development. J Biomed Sci 23:66. https://doi.org/10.1186/s12929-016-0285-9
13. Pin E, Henjes F, Hong M-G et al (2016) Identification of a novel autoimmune peptide epitope of prostein in prostate cancer. J Proteome Res. https://doi.org/10.1021/acs.jproteome.6b00620
14. Miethe S, Rasetti-Escargueil C, Liu Y et al (2014) Development of neutralizing scFv-Fc against botulinum neurotoxin A light chain from a macaque immune library. MAbs 6:446–459. https://doi.org/10.4161/mabs.27773
15. Mendonça M, Moreira GMSG, Conceição FR et al (2016) Fructose 1,6-bisphosphate aldolase, a novel immunogenic surface protein on Listeria species. PLoS One 11:e0160544. https://doi.org/10.1371/journal.pone.0160544
16. Jiang X, Totrov M, Li W et al (2016) Rationally designed immunogens targeting HIV-1 gp120 V1V2 induce distinct conformation-specific antibody responses in rabbits. J Virol 90 (24):11007–11019. https://doi.org/10.1128/JVI.01409-16
17. He W, Tan GS, Mullarkey CE et al (2016) Epitope specificity plays a critical role in regulating antibody-dependent cell-mediated cytotoxicity against influenza A virus. Proc Natl Acad Sci 113:11931–11936. https://doi.org/10.1073/pnas.1609316113
18. Benjamin P (1996) Site-directed mutagenesis in epitope mapping. Methods 9:508–515
19. Davidson E, Doranz BJ (2014) A high-throughput shotgun mutagenesis approach to mapping B-cell antibody epitopes. Immunology 143:13–20. https://doi.org/10.1111/imm.12323
20. Vernet T, Choulier L, Nominé Y et al (2015) Spot peptide arrays and SPR measurements: throughput and quantification in antibody selectivity studies. J Mol Recognit 28:635–644. https://doi.org/10.1002/jmr.2477
21. Wen X, Sun J, Wang X et al (2015) Identification of a novel linear epitope on the NS1 protein of avian influenza virus. BMC Microbiol 15:168. https://doi.org/10.1186/s12866-015-0507-4
22. Augustin T, Cehlar O, Skrabana R et al (2015) Unravelling viral camouflage: approaches to the study and characterization of conformational epitopes. Acta Virol 59:103–116. https://doi.org/10.4149/av_2015_02_103
23. Malito E, Carfi A, Bottomley MJ (2015) Protein crystallography in vaccine research and development. Int J Mol Sci 16:13106–13140. https://doi.org/10.3390/ijms160613106
24. Gershoni JM, Roitburd-Berman A, Siman-Tov DD et al (2007) Epitope mapping: the first step in developing epitope-based vaccines. BioDrugs 21:145–156
25. Gallagher ES, Hudgens JW (2016) Mapping protein-ligand interactions with proteolytic fragmentation, hydrogen/deuterium exchange-mass spectrometry. Methods Enzymol 566:357–404. https://doi.org/10.1016/bs.mie.2015.08.010

26. Prądzińska M, Behrendt I, Astorga-Wells J et al (2016) Application of amide hydrogen/deuterium exchange mass spectrometry for epitope mapping in human cystatin C. Amino Acids. https://doi.org/10.1007/s00726-016-2316-y
27. Schirrmann T, Meyer T, Schütte M et al (2011) Phage display for the generation of antibodies for proteome research, diagnostics and therapy. Molecules 16:412–426. https://doi.org/10.3390/molecules16010412
28. Kuhn P, Fühner V, Unkauf T et al (2016) Recombinant antibodies for diagnostics and therapy against pathogens and toxins generated by phage display. Proteomics Clin Appl 10:922–948. https://doi.org/10.1002/prca.201600002
29. Hust M, Meysing M, Schirrmann T et al (2006) Enrichment of open reading frames presented on bacteriophage M13 using hyperphage. BioTechniques 41:335–342
30. Zantow J, Just S, Lagkouvardos I et al (2016) Mining gut microbiome oligopeptides by functional metaproteome display. Sci Rep 6:34337. https://doi.org/10.1038/srep34337
31. Wu C-H, Liu I-J, Lu R-M, Wu H-C (2016) Advancement and applications of peptide phage display technology in biomedical science. J Biomed Sci 23:8. https://doi.org/10.1186/s12929-016-0223-x
32. Kügler J, Zantow J, Meyer T, Hust M (2013) Oligopeptide m13 phage display in pathogen research. Viruses 5:2531–2545. https://doi.org/10.3390/v5102531
33. Kügler J, Wilke S, Meier D et al (2015) Generation and analysis of the improved human HAL9/10 antibody phage display libraries. BMC Biotechnol 15:10. https://doi.org/10.1186/s12896-015-0125-0
34. Lloyd C, Lowe D, Edwards B et al (2009) Modelling the human immune response: performance of a 10^{11} human antibody repertoire against a broad panel of therapeutically relevant antigens. Protein Eng Des Sel 22:159–168. https://doi.org/10.1093/protein/gzn058
35. Rowley MJ, O'Connor K, Wijeyewickrema L (2004) Phage display for epitope determination: a paradigm for identifying receptor-ligand interactions. Biotechnol Annu Rev 10:151–188. https://doi.org/10.1016/S1387-2656(04)10006-9
36. Ibsen KN, Daugherty PS (2017) Prediction of antibody structural epitopes via random peptide library screening and next generation sequencing. J Immunol Methods 451:28–36. https://doi.org/10.1016/j.jim.2017.08.004
37. Sieber T, Hare E, Hofmann H, Trepel M (2015) Biomathematical description of synthetic peptide libraries. PLoS One 10(6):e0129200. https://doi.org/10.1371/journal.pone.0129200
38. Rojas G, Tundidor Y, Infante YC (2014) High throughput functional epitope mapping: revisiting phage display platform to scan target antigen surface. MAbs 6:1368–1378. https://doi.org/10.4161/mabs.36144
39. Cariccio VL, Domina M, Benfatto S et al (2016) Phage display revisited: epitope mapping of a monoclonal antibody directed against Neisseria meningitidis adhesin A using the PROFILER technology. MAbs 8:741–750. https://doi.org/10.1080/19420862.2016.1158371
40. Connor DO, Zantow J, Hust M et al (2016) Identification of novel immunogenic proteins of Neisseria gonorrhoeae by phage display. PLoS One 11(2):e0148986. https://doi.org/10.1371/journal.pone.0148986
41. Rondot S, Koch J, Breitling F, Dübel S (2001) A helper phage to improve single-chain antibody presentation in phage display. Nat Biotechnol 19:75–78. https://doi.org/10.1038/83567
42. Soltes G, Hust M, Ng KKY, Bansal A et al (2007) On the influence of vector design on antibody phage display. J Biotechnol 127:626–637. https://doi.org/10.1016/j.jbiotec.2006.08.015
43. Levy ED, De S, Teichmann SA (2012) Cellular crowding imposes global constraints on the chemistry and evolution of proteomes. Proc Natl Acad Sci U S A 109(50):20461–20466. https://doi.org/10.1073/pnas.1209312109
44. Singaravelan B, Roshini BR, Munavar MH (2010) Evidence that the supE44 mutation of Escherichia coli is an amber suppressor allele of glnX and that it also suppresses ochre and opal nonsense mutations. J Bacteriol 192(22):6039–6044. https://doi.org/10.1128/JB.00474-10
45. O'Donoghue P, Prat L, Heinemann IU et al (2012) Near-cognate suppression of amber, opal and quadruplet codons competes with aminoacyl-tRNAPyl for genetic code expansion. FEBS Lett 586(21):3931–3937. https://doi.org/10.1016/j.febslet.2012.09.033
46. Moreira GMSG, Fühner V, Hust M (2018) Epitope mapping by phage display. Methods Mol Biol 1701:497–518. https://doi.org/10.1007/978-1-4939-7447-4_28

Chapter 18

A High-Throughput Magnetic Nanoparticle-Based Semi-Automated Antibody Phage Display Biopanning

Angela Chiew Wen Ch'ng, Azimah Ahmad, Zoltán Konthur, and Theam Soon Lim

Abstract

Panning is a common process used for antibody selection from phage antibody libraries. There are several methods developed for a similar purpose, namely streptavidin mass spectrometry immunoassay (MSIA™) Disposable Automation Research Tips, magnetic beads, polystyrene immunotubes, and microtiter plate. The advantage of using a magnetic particle processor system is the ability to carry out phage display panning against multiple target antigens simultaneously in parallel. The system carries out the panning procedure using magnetic nanoparticles in microtiter plates. The entire incubation, wash, and elution process is then automated in this setup. The system also allows customization for the introduction of different panning stringencies. The nature of the biopanning process coupled with the limitation of the system means that minimal human intervention is required for the infection and phage packaging stage. However, the process still allows for rapid and reproducible antibody generation to be carried out.

Key words Panning, Antibody library, Monoclonal antibodies, Phage display, Semi-automated, Magnetic nanoparticles

1 Introduction

Phage display is an in-vitro selection technology that is synonymous with monoclonal antibody generation. When it was first introduced by George Smith in 1985, peptides were the only molecules that were being presented on phage [1–3]. Since then, the application of phage display has expanded to include multiple antibody fragments and other immunological molecules like T-cell receptors and protein scaffolds. Before the advent of phage display, monoclonal antibodies were produced by means of hybridoma technology. A major bottleneck associated with the use of hybridoma method for antibody generation was the need to use animal hosts resulting in animal derived antibodies that has a high immunogenicity risk in humans [2, 4]. Another consideration is the time required to obtain antibodies as immunization of the host animal and screening may

Michael Steinitz (ed.), *Human Monoclonal Antibodies: Methods and Protocols*, Methods in Molecular Biology, vol. 1904, https://doi.org/10.1007/978-1-4939-8958-4_18,

result in months of work. These issues can be circumvented with the use of phage display technology to generate and identify human monoclonal antibodies.

The phage display panning process resembles the traditional gold panning process. Biopanning involves the sieving process of a targeted antibody toward a particular antigen by affinity-based separation [3]. The process first involves the immobilization of the target antigen onto a solid surface such as magnetic beads, column matrices, polystyrene tube, or microtiter plate. The major difference between different solid surfaces is the binding capacity, which may vary due to the surface area and condition. In general, the antigen will be coated on the solid surface using a coating buffer or phosphate buffered saline (PBS) [5]. Then, the excess free surface is blocked to avoid any nonspecific binding. This is done prior to the introduction of antibody phage preparation for binding. Post incubation, a series of washes are done with a wash buffer to remove weak and unspecific binders. Then, the leftover bound phage is rescued by infecting suitable *Escherichia coli* host for the next round of panning [2, 6–8]. However, some precautionary step must be taken to avoid the enrichment of unspecific binders, which are normally the plastic binders and blocking agent binders [9]. The process is normally repeated between three to five times to achieve good enrichment of clones.

In the antibody panning process, there are several parameters that have to be considered for optimal selection, namely (1) target antigen and its immobilization strategy, (2) antibody library quality/repertoire (frequency of antigen-specific antibody), (3) binding conditions, (4) washing conditions, and (5) elution strategy [10–13] (Fig. 1a). In this chapter, the antigens are immobilized on streptavidin-conjugated magnetic beads before antibody selection. As a comparison, magnetic beads have a higher surface area to volume ratio, which increases the binding surface area allowing for more biotinylated antigens to be presented during panning [13]. In addition to that, the use of streptavidin-biotin interaction allows for a more easy and rapid antigen presentation on the solid phase in a unidirectional manner. The application of the streptavidin-biotin interaction allows the immobilization process to be more specific as compared to general absorption to polystyrene surfaces [14]. The streptavidin magnetic beads can also aid in reducing the purification step of the target antigen as it can be applied for the purification of biotinylated target antigen from a crude preparation with great specificity [15]. The optimal condition for the conjugation will make sure the magnetic bead is covered by the biotinylated antigen [16]. Optimization of the binding, washing, and elution steps during panning can be done using several different strategies in order to obtain the best candidate [17].

The basic requirement for antibody phage display panning experiments is the availability of a good quality antibody library.

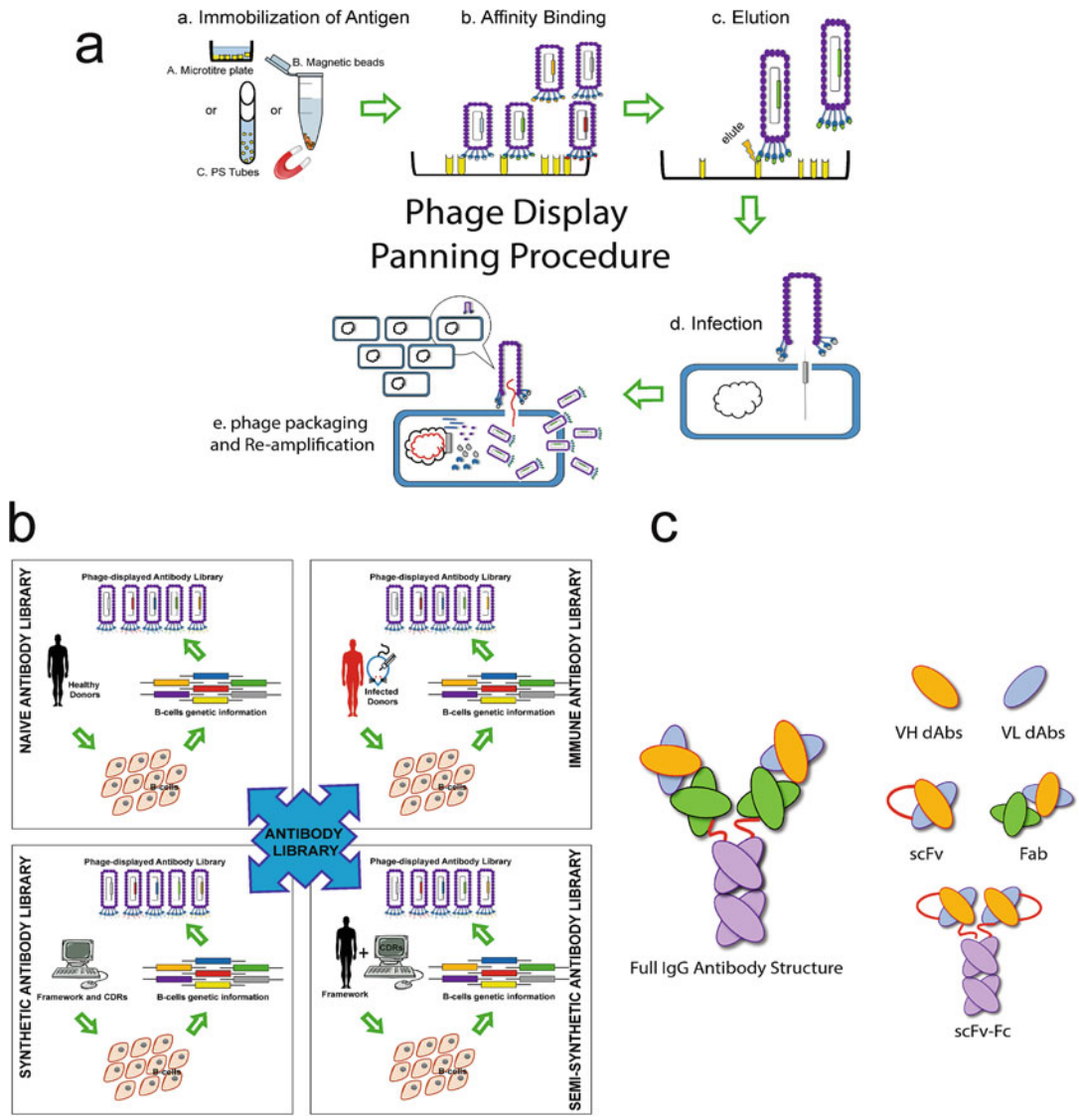

Fig. 1 The phage display antibody selection with (**a**) the general phage display panning procedure (including immobilization, binding, elution, infection, and re-amplification process) by using (**b**) the different types of antibody phage library, either naïve, immune, synthetic, or semi-synthetic antibody library which could be found in (**c**) different antibody formats such as scFv, Fab, and dAbs

This is highly dependent on the nature of the human antibody sequences or repertoire found in the host. There are various types of antibody libraries that have been reported over the years. Antibody libraries are mainly classified as naïve, immune, semi-synthetic, and synthetic antibody libraries [11] (Fig. 1b). The main difference between these libraries is the origin of the repertoire that is available. This is mainly influenced by the health condition of the donors as well as the immunologic response of

the host which contributes to the diversity of the repertoire [18]. Normally, the antibody repertoire of a naïve antibody library ("one pot" library) is derived from healthy individuals [19]. On the other hand, immune libraries represent a collection of antibody sequences from disease-infected donors. The immunologic and genetic variations between different individuals can impact the variability or diversity of the antibody sequences. The immune repertoire is generally a reflection of the natural response to the infection that results in a skewed repertoire. On the other hand, the repertoire of semi-synthetic and synthetic libraries are chemically synthesized either with a modular consensus framework and randomized complementary determining regions (CDRs) or using many different V-gene frameworks [20, 21]. The differences between the antibody libraries are illustrated in Fig. 1b [3]. In order to get strong and specific binders, affinity binding and washing steps play a critical role [17].

The demand for monoclonal human antibodies by phage display has been increasing over the years due to its promising results and application in the pharmaceutical industry [22]. Thus, automated systems can aid in improving the panning efficiency for an increased rate of production to meet the demands of the market. Magnetic particle processors were originally designed for DNA purification applications and have been expanded to carry out phage display panning for antibody selection [23]. The use of an automation system can help to speed up the selection process as it allows high-throughput sample handling of up to 96 different antigens simultaneously with minimal human intervention. This can help reduce human error during the antibody selection process and increase reproducibility in the process.

The design of process pipelines for an automated system is challenging in terms of cost and compatibility. There are several key stages involved in antibody selection procedures which are panning, infection, propagation, colony picking, and ELISA evaluations. The setup for a fully automated pipeline for every stage of work without human intervention is principally possible with the machines available today. However, the cost will be incredibly expensive for majority of research laboratories. Thus, the need for full automation is very much dependent on the scope and timeline of the project pursued besides the financial resources [13]. In order to introduce automation at a reasonable cost to improve the panning process, introduction of automation just for the panning process would be sufficient as it is the most critical stage.

This chapter uses a pin-based magnetic particle processor to automate the panning procedure. The system enables the handling of 96 antigens with a 96 magnetic pinhead, corresponding to the positions of a 96-well microtiter plate. The processor can accommodate up to eight 96 wells microtiter plates that are filled with different buffers for washing and incubation purpose (Fig. 2a and Table 1).

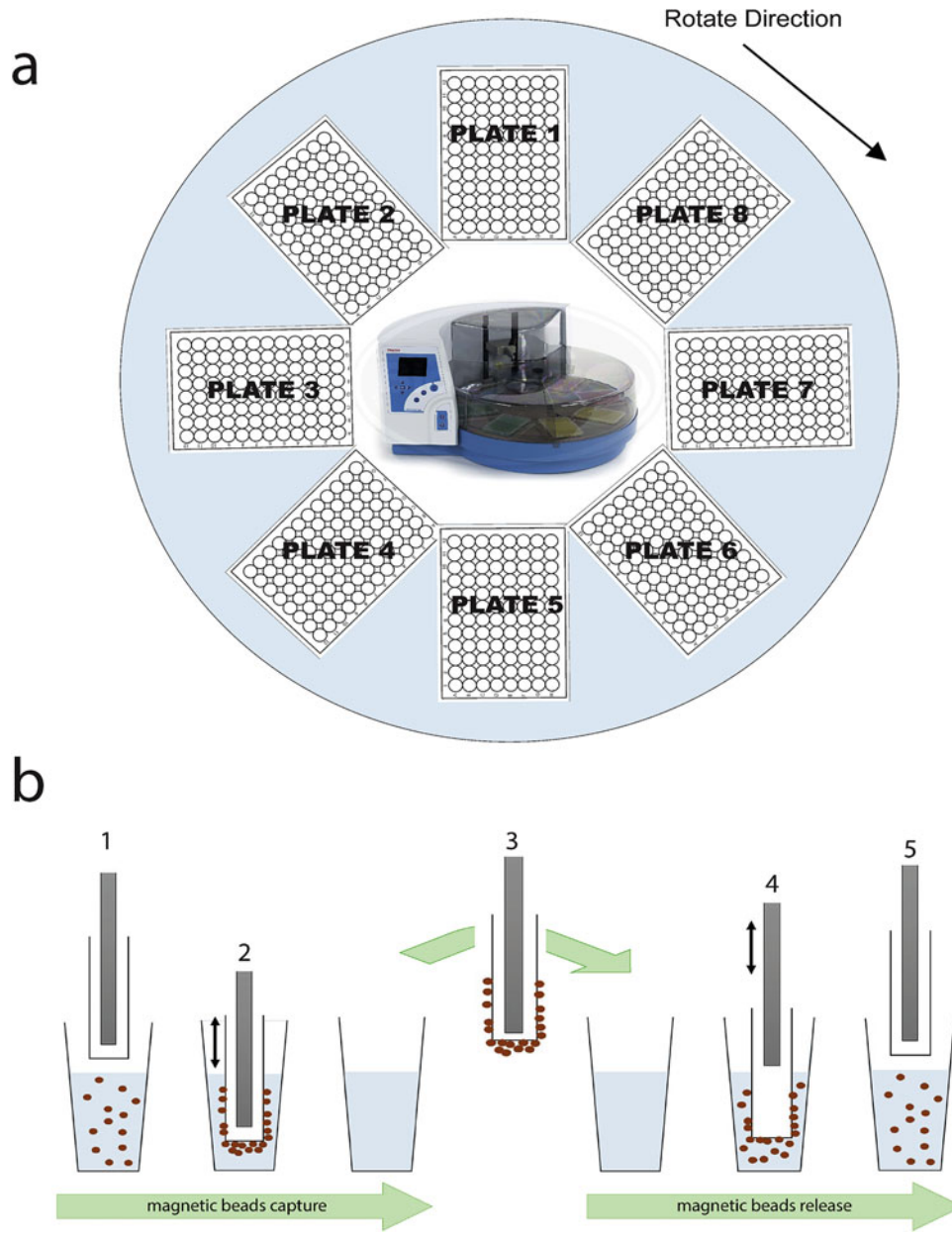

Fig. 2 The design of the Kingfisher Flex magnetic particle processor. (**a**) Rotating plate platform of a Kingfisher Flex magnetic particle processor. The magnetic head is at a fixed loading position. The beads are recovered from one plate to another new plate by rotating the plate holder table clockwise. (**b**) The operating mode of magnetic particle processors. (1) The plastic cap covered rod-shaped magnet moves into a solution containing suspended magnetic beads. (1) The magnet moving up and down with beads attracted to the cover, and (3) transfer the beads to a new solution by moving the covered magnet to the next position. (4) Magnet is released from the cap to allow the beads to suspend in solution. (5) Both magnet head and plastic covers are raised to the starting position to proceed to the next stage of the process

Table 1
Overview of plate position for automated magnetic bead-based panning procedure on a kingfisher Flex

Plate no.	Panning round 1	Panning round 2	Panning round 3	Panning round 4
1	Bead plate	Bead plate	Bead plate	Bead plate
2	Wash plate	Wash plate	Wash plate	Wash plate
3	Phage plate	Phage plate	Phage plate	Phage plate
4	Wash plate 1	Wash plate 1	Wash plate 1	Wash plate 1
5	Release plate/*E. coli* TG1 culture plate	Wash plate 2	Wash plate 2	Wash plate 2
6	–	Release plate/*E. coli* TG1 culture plate	Wash plate 3	Wash plate 3
7	–	–	Release plate/*E. coli* TG1 culture plate	Wash plate 4
8	–	–	–	Release plate/*E. coli* TG1 culture plate
Total time	~140 min	~150 min	~160 min	~170 min

The plastic covered-rod shaped magnets play the role of transferring the magnetic particles from **step 1** to the last step of panning by a sequence of capture and release motions (Fig. 2b), which is normally done by manual pipetting. By doing this, no labor force is needed for the transferring process between steps allowing independent process running. The capture and release movements during the incubation and transfer are software driven and all the parameters such as time, position, frequency, and strength of shaking movements can be customized. The precision of the processor control allows for a more reproducible process at each step of the phage display selection protocol for as many as 96 parallel selections. The benefit of using a magnetic bead-based selection instead of a microtiter plate-based selection scheme is the background reduction of unspecific binders to the surface. This is achieved by the transfer of a minimal volume of magnetic particles from vessel to vessel [13].

The magnetic bead-based panning procedure is generally carried out using a magnetic particle processor for up to four rounds of selection (Table 1). Standardization of panning parameters such as washing conditions and incubation times allows all panning procedures to be well controlled and replicated (Table 2). Although the method allows automation of the panning process, however human intervention is needed for some stages, such as preparation of microtiter plates, infection of the bacterial host, and starting the

Table 2
Automated magnetic bead-based panning round 4 procedure for Kingfisher Flex

Plate no.	Plate name	Procedure	Volume (μL)	Time (min)
1	Bead plate	Blocking of antigen-conjugated and control magnetic beads with PTM	200	60
2	Wash plate	Wash of magnetic beads in PBST	200	60
3	Phage plate	Incubation of magnetic beads in antibody phage library/antibody phage stock of the selection rounds	200	10
4	Wash plate 1	Wash 1 of magnetic beads in PBST	200	10
5	Wash plate 2	Wash 2 of magnetic beads in PBST	200	10
6	Wash plate 3	Wash 3 of magnetic beads in PBST	200	10
7	Wash plate 4	Wash 4 of magnetic beads in PBST	200	10
8	Release plate/*E. coli* TG1 culture plate	Waiting plate for magnetic beads which will be replaced by *E. coli* TG1 culture when it is ready for infection	200	[a]
Total time				170

[a]At this stage, 10 μL bead-bound phage solution will be collected for titration. The infection process takes place outside Kingfisher Flex Instrument at 37 °C incubator

packaging process by superinfection with a helper phage. A standard operating procedure (SOP) to adapt all biological processes into a 96-well microtiter plate format requires some manipulation by hand. The whole protocol streamlines the bead loading, phage selection, phage amplification, and phage ELISAs processes to confirm the binding activity in microtiter plate format. Analysis of clonal enrichment and clone identification is carried out with two stages of ELISA. The first ELISA is carried out at polyclonal level (Fig. 3 and Table 3), in which the amplified phage of the selection rounds is tested against the antigen targets using a magnetic bead-based ELISA protocol. The second ELISA involves random selection of 92 clones from the selection rounds (refer to the results of the polyclonal ELISA) and subsequent analysis for binding by either phage ELISA or soluble recombinant protein ELISA [12] (Fig. 4).

This protocol is an improved version of the method published in [13].

2 Materials

2.1 Loading of Magnetic Beads

1. Dynabeads™ M-280 Streptavidin (Invitrogen Dynal AS) (*see* **Note 1**).

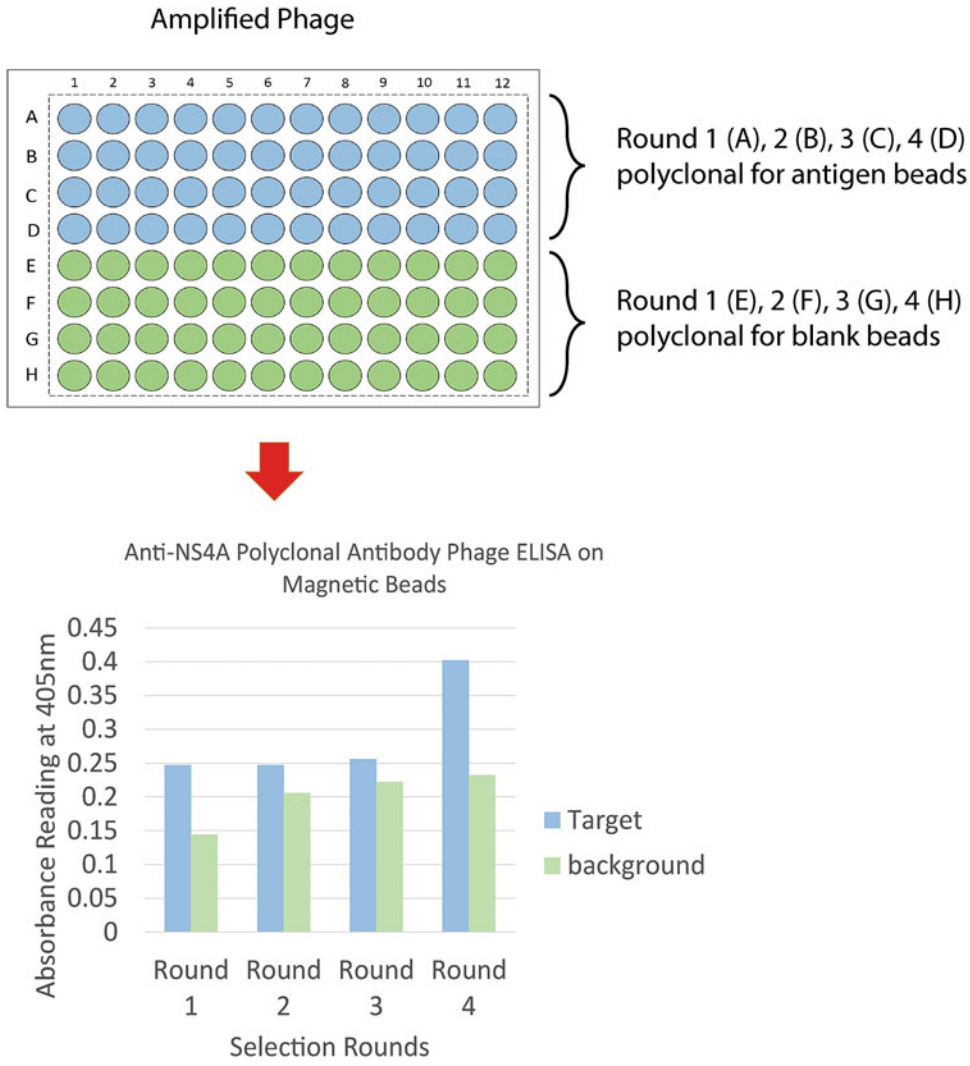

Fig. 3 The typical polyclonal antibody phage ELISA by using magnetic beads. The upper figure shows the plate layout for the selection of 12 different targets. For each selection, the phage stock solutions are split and pipetted into the positions A–D and E–H of the same column, respectively. All steps of the ELISA are performed in a 96-well magnetic particle processor. The bottom figure shows the typical graph plot for the enrichment of specifically binding antibody phage during four rounds of selection on NS4A. Specific enrichment is seen in round 4

2. Phosphate-buffered saline (PBS): 8 g/L NaCl, 0.2 g/L KCL, 1.44 g/L $Na_2HPO_4{\cdot}2H_2O$ and 0.24 g/L KH_2PO_4, pH 7.4 (*see* **Notes 2** and **3**).
3. Phosphate-buffered saline Tween (PBST): PBS and 0.1% Tween-20.

Table 3
Automated magnetic bead-based polyclonal antibody ELISA protocol for Kingfisher Flex

Plate no.	Plate name	Procedure	Volume (μL)	Time (min)
1	Bead plate	Blocking of antigen-conjugated and control magnetic beads with PTM	200	60
2	Wash plate	Wash of magnetic beads in PBST	200	10
3	Phage plate	Incubation of magnetic beads in antibody phage library/ antibody phage stock of the selection rounds	200	60
4	Wash plate 1	Wash 1 of magnetic beads in PBST	200	20
5	M13 Antibody Plate	Incubation of antigen-conjugated and control beads with anti-M13 HRP (1:5000) in PTM	200	60
6	Wash plate 2	Wash 3 of magnetic beads in PBST	200	10
7	Substrate plate	Incubation of magnetic beads in ABTS	200	30[a]
8	–	–	–	–
Total time				170

The magnetic beads must be removed before measuring the absorbance in plate reader
[a]At this stage, the ABTS incubation takes place at microplate shaker at room temperature

2.2 Semi-Automated Panning Using a Magnetic Particle Processor

1. *E. coli* TG1 genotype: *supE thi-1 Δ (lac-proAB) Δ (mcrB-hsdSM) 5 (rK– mK–) [F′ traD36 proAB lacIq ZΔM15]* (*see* **Notes 4** and **5**).
2. KingFisher 96 KF microplate (PP) (Thermo Scientific™) (*see* **Note 3**).
3. KingFisher Flex 96 tip comb for KF magnets (PP) (Thermo Scientific™) (*see* **Note 3**).
4. Aera Seal breathable sealing film (Sigma-Aldrich, Taufkirchen) (*see* **Note 6**).
5. Phosphate-buffered Saline (PBS): 8 g/L NaCl, 0.2 g/L KCL, 1.44 g/L $Na_2HPO_4{\cdot}2H_2O$ and 0.24 g/L KH_2PO_4, pH 7.4 (*see* **Notes 2** and **3**).
6. Phosphate-buffered saline Tween (PBST): PBS and 0.1% Tween-20 (*see* **Note 2**).
7. 2YT medium: 1.6% (w/v) tryptone, 1% (w/v) yeast extract, and 0.5% NaCl, pH 7.0 (*see* **Notes 2** and **3**).
8. 10× Amp/Glu solution: 100 μg/mL ampicillin, and 2% (w/v) glucose in 2YT medium (*see* **Note 2**).

2.3 Packaging of Phagemids

1. M13K07 Helper-phage (New England BioLabs) (*see* **Note 7**).
2. Nunc™ 96-Well Filter Plates (Thermo Fisher Scientific).

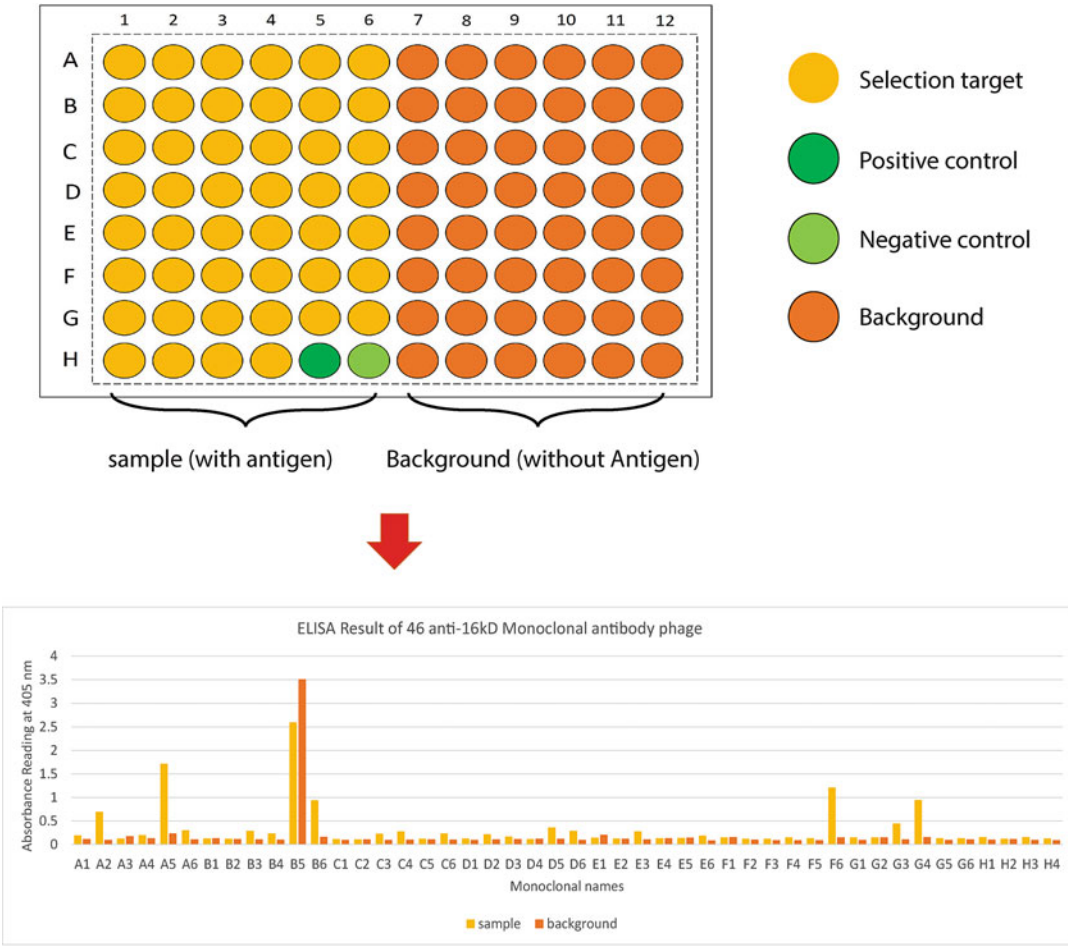

Fig. 4 The typical ELISA design for 46 monoclonal antibody phage. On the top figure shows the plate layout for target antigen coating. The monoclonal antibody phage of the plate positions A1–H6 (or A7–H12, respectively) are added to each half of the Assay plate. The bottom figure shows the results for 46 anti-16kd antibody phage ELISA. All clones with a >tenfold signal-to-background ratio are considered positive. In this case, only four clones (A5, B6, F6, and G4) show an $OD_{405nm} > 1.0$

3. 2YT-AG-2: 2YT medium containing 100 μg/mL ampicillin, 2% (w/v) glucose (*see* **Note 2**).
4. 2YT-AKG: 2YT medium containing 100 μg/mL ampicillin, 60 μg/mL kanamycin, 0.1% (w/v) glucose (*see* **Note 2**).
5. Glycerol solution: 80% (v/v) glycerol in distilled water, then autoclave (*see* **Notes 2** and **3**).

2.4 Titration of Phage Particles

1. 2YT-AG agar plates: 2YT medium containing 100 μg/mL ampicillin, 2% (w/v) glucose and 1.5% (w/v) agar-agar (*see* **Note 3**).
2. 2YT-KG agar plates: 2YT medium containing 60 μg/mL kanamycin and 1.5% (w/v) agar-agar (*see* **Note 2**).

2.5 Magnetic Particle ELISA of Polyclonal Antibody Phage

1. KingFisher 96 KF microplate (PP) (Thermo Scientific™) (*see* **Note 3**).
2. KingFisher Flex 96 tip comb for KF magnets (PP) (Thermo Scientific™) (*see* **Note 3**).
3. Anti-M13 Horseradish Peroxidase (HRP)-conjugated monoclonal antibody (*see* **Note 2**).
4. ABTS developing solution: 10 mg tablet ABTS in 5 mL of 50 mM Citric Acid, 5 mL of 50 mM Trisodium Citrate and 10 μL H_2O_2. Store in the dark (*see* **Note 8**).

2.6 Production of Phage Monoclonal Antibody Fragments in Microtiter Plates

1. Nunc™ 96-Well Polystyrene Round Bottom Microwell Plates (Thermo Scientific).
2. *E. coli* TG1 genotype: *supE thi-1 Δ (lac-proAB) Δ (mcrB-hsdSM) 5 (rK− mK−) [F′ traD36 proAB lacIq ZΔM15]* (*see* **Notes 4** and **5**).
3. 2YT-AG-2: 2YT medium containing 100 μg/mL ampicillin, 2% (w/v) glucose (*see* **Note 2**).
4. M13K07 Helper-phage (New England BioLabs) (*see* **Note 7**).
5. 2YT-AKG: 2YT medium containing 100 μg/mL ampicillin, 60 μg/mL Kanamycin, 0.1% (w/v) glucose (*see* **Note 2**).

2.7 ELISA of Phage Monoclonal Antibody Fragments in Microtiter Plates

1. 96-well Polystyrene Flat-bottom Microplates (Greiner Bio-One, Frickenhausen).
2. Bovine Serum Albumin (BSA): 10 mg/mL stock solution in PBS (*see* **Note 2**).
3. Anti-M13 Horseradish Peroxidase (HRP)-conjugated monoclonal antibody (*see* **Note 2**).
4. ABTS developing solution: 10 mg tablet ABTS in 5 mL of 50 mM Citric Acid, 5 mL of 50 mM Trisodium Citrate and 10 μL H_2O_2. Store in the dark (*see* **Note 8**).

3 Methods

The key advantage of the semi-automated phage display panning protocol is the ability to carry out selections for 96 different target antigens in parallel (*see* **Notes 9** and **10**). This method also minimizes the risk of human error during the panning process with minimal human intervention when compared with the conventional panning protocol. Prior to the panning process, the antibody library has to be packaged according to standard protocols for the library. This will be dependent on the type of antibody library being used for panning. The protocol can be applied for antibodies with different formats ranging from single chain fragment variable (scFv), Fragment Antibody (Fab), to domain antibodies (dAb)

(*see* **Note 11**) (Fig. 1c). The standard protocol outlined allows for sample handling to become straightforward and easy (*see* **Notes 12** and **13**) (Tables 1 and 2). The protocol is designed as a semi-automated alternative for high-throughput antibody screening by phage display.

3.1 Loading of Magnetic Beads

1. Take 1 mg (roughly 100 μL) of Dynabeads™ M-280 Streptavidin magnetic beads into a 2 mL fresh microcentrifuge tube and wash 5 min for three times with 1.5 mL PBST at room temperature (RT). At the same time, dissolve (a) 100–200 μg of biotinylated protein antigen or (b) 1–2 μg biotinylated peptide target in 1 mL PBS. Then, discard the wash solution and resuspend the magnetic beads with 1 mL antigen/target solution. Incubate the mixture overnight (o/n) at 4 °C or 1 h at RT on a rotator (*see* **Notes 1**, **11**, and **14**).
2. Mount the microcentrifuge tube to a magnet rack to remove the antigen solution. Wash the magnetic beads by resuspending the beads with 1.5 mL PBST. Repeat the step for three times (*see* **Notes 1** and **14**).
3. Mount the microcentrifuge tube to a magnet rack and discard the wash solution. Finally, resuspend the magnetic beads with 200 μL PBS and store *antigen-loaded bead stock* at 4 °C until use (*see* **Notes 1**, **14** and **15**).

3.2 Semi-Automated Panning on Magnetic Particle Processor

In order to simplify the protocol, this particular protocol is designed for simultaneous selection on 12 antigens, arranged from position A1 to A12 in a 96-well microtiter plate in the magnetic particle processor. The protocol is also described for use with the Kingfisher Flex (Thermo Fisher Scientific, Finland) system. The number of plates and working steps for each panning round is summarized in Table 1, whereas the detailed parameters for the fourth panning round are summarized in Table 2. Although the protocol is described for 12 antigens, lesser number of target antigen selection can still be performed by removing the microtiter plate positions accordingly.

1. Culture a single clone of *E. coli* TG1 in 5 mL of 2YT o/n at 37 °C with shaking at 200 rpm, the day before phage display panning. At the same time, a 5 mL maxibinding polystyrene (PS) immunotube was blocked with 5 mL of PBST-Milk (PTM) o/n at 4 °C and seal with parafilm (*see* **Note 4**).
2. The blocked immunotube was first washed with PBST before pre-incubation of the unselected antibody phage library. In a 5 mL PS tube, add 20 μL of unconjugated Dynabead M-280 Streptavidin to 100 μL of 1×10^{10}–1×10^{11} phage particles in 100 μL PTM and incubate for 1–2 h at RT (*see* **Notes 16** and **17**). Then separate the beads from the antibody library

preparation. The antibody library preparation is then incubated in the blocked immunotube and rotated for 1 h at RT.

3. Arranging *bead plate (Plate no. 1)*. Fill the positions A1–A12 of a 96-well V-bottom PP (PP) microtiter plate (KingFisher 96 KF microplate (PP)) with 180 µL PTM. Add 20 µL of the corresponding *antigen-loaded bead stocks* for each antigen to the specified position, namely beads with antigen 1 to positions A1, beads of antigen 2 to positions A2, and so on (total of 12 antigens in this case) (*see* **Notes 2**, **3**, **13**, and **18**). For the first round of panning, continue with step 4. For the following selection rounds, continue with **step 5**.
4. Arrange *phage-plate* (*Plate no. 3 as shown in* Fig. 2a and Table 1) *for the first round*. Fill positions A1–A12 of a 96-well V-bottom PP microtiter plate with 200 µL of the antibody phage library solution after removing the magnetic beads with the help of a magnetic stand. The following rounds of panning will continue with **step 6** (*see* **Notes 2–4** and **18**).
5. Arrange *phage-plate for subsequent rounds* and fill positions A1–A12 of a 96-well V-bottom PP microtiter plate with 100 µL PTM. Add 100 µL of the amplified phage solutions of the previous round according to the same antigen order in positions A1–A12 (*see* **Notes 2–4** and **18)**.
6. Prepare *wash plate* (*plate no. 2, 4, 5, 6 as shown in* Fig. 2a and Table 1) and fill positions A1–A12 of a 96-well V-bottom PP microtiter plates with 200 µL PBST (*see* **Notes 2, 3** and **19**).
7. Prepare *release plate* (*Plate no. 5, 6, 7 as shown in* Fig. 2a and Table 1) and fill positions A1–A12 of a 96-well V-bottom PP microtiter plates with 200 µL PBS (*see* **Notes 2, 3** and **20**). The *release plate* will be replaced later by the *E. coli TG1 culture plate*.
8. Place the plates in the Kingfisher Flex plate holder table according to the plate numbering in Fig. 2a and Table 1 and start the magnetic bead-based panning program. The magnetic beads should then move from plate to plate according to the program.
9. Inoculate 5 mL 2YT in a 50 mL Falcon tube with 50 µL of a fresh o/n *E. coli* TG1 culture at 37 °C and 200 rpm shaking until OD_{600} ~ 0.5 is reached. This can be done when there is about 105 min left in the program run (*see* **Notes 4** and **21**). When the *E. coli* TG1 reaches OD_{600} ~ 0.5, replace *the release plate* with *E. coli TG1 culture plate*.
10. Incubate the beads in each plate. The beads should be kept in suspension by moving plastic tips up and down in the wells at either medium or fast speed (30–50 mm/s) during incubation (Fig. 2b). Before the panning program has finished, prepare

E. coli TG1 culture plate and fill positions A1–A12 of a 96-well U-bottom PP microtiter plate with 200 µL of *E. coli* TG1 culture. Place the *E. coli TG1 culture plate* to replace the release plate in Kingfisher Flex instrument before the program finish. By doing so, the beads will be released static in the *E. coli TG1 culture plate* (*see* **Notes 4** and **20**).

11. Take out the *selection stock plate* from the Kingfisher Flex instrument, cover with a plastic lid and incubate for 30 min at 37 °C, static (*see* **Notes 22–24**).
12. Remove the beads (*see* **Note 17**) and add 20 µL 10× Amp/Glu solution. The plate is then sealed with breathable sealing film (*see* **Note 6**). Then, the plate was incubated in a microplate shaker for 2 h at 37 °C and 1400 rpm (*see* **Note 25**).
13. Then, proceed to Packaging of Phage Particles protocol (Subheading 3.3).

3.3 Packaging of Phage Particles

The steps described in this section are continued from the semi-automated selection protocol in Subheading 3.2.

1. Collect *selection stock plate* from the microplate shaker. Then, 200 µL of pre-warmed (37 °C) 2YT-AG medium is added to the culture, mix thoroughly before transferring 200 µL into a 96-well filtration plate (*see* **Notes 2** and **25**).
2. Seal the *selection stock plate* again with breathable sealing film and continue incubation in a microplate shaker o/n at 37 °C shaking at 1200 rpm (*see* **Notes 6** and **25**).
3. Add 10 µL M13K07 helper phage stock (10^{11} cfu/mL) which is equivalent to 10^{9} helper phage particles to the filtration plate and incubate stationary for 30 min at 37 °C (*see* **Notes 4**, **26**, and **27**).
4. Filter the bacterial culture by centrifuge microtiter plate for 15 min at 2560.3 × *g* (swing out rotor). Discard the supernatant with remaining M13K07 helperphage.
5. Resuspend bacteria in 220 µL pre-warmed 2YT-AKG (30 °C) and transfer to a fresh 96-well U-bottom PP microtiter plate. Seal *phage production plate* with breathable sealing film and incubate in a microplate shaker overnight at 30 °C shaking at 1400 rpm (*see* **Notes 6** and **17**).
6. The next day, add 160 µL of autoclaved 80% glycerol solution to *selection stock plate*. Then, mix and store as glycerol stock at −80 °C (*see* **Note 4**).
7. Pellet down the bacteria in *phage production plate* by centrifugation 15 min at 2560.3 × *g* (swing out rotor). Transfer the supernatant carefully without disturbing the pellet to a 96-well filtration plate (*see* **Notes 4** and **22–24**).

8. Place filtration plate on the top of a new 96-well U-bottom PP microtiter plate and fix with sticky tape.
9. Filter antibody presenting phage particles to remove possible contaminating *E. coli* TG1 cells by centrifugation for 2–5 min at 936.3 × *g*. Store the filtrate and discard bacteria pellets and used filtration plate (*see* **Notes 4** and **22**–**24**).
10. Add 50 μL PBS to each well of the *phage stock plate* and mix thoroughly. Use 100 μL for the next round of selection whereas use 10 μL for phage titration.

3.4 Titration of Phage Particles

1. Inoculate 5 mL of 2YT in a 50 mL falcon tube with a single clone of *E. coli* TG1 from an agar plate and grow o/n at 37 °C and 200 rpm (*see* **Notes 4** and **21**).
2. Inoculate 10 mL 2YT in a 50 mL falcon tube with 100 μL of o/n *E. coli* TG1 culture and grow at 37 °C and 200 rpm until OD_{600} ~ 0.5 (*see* **Notes 4** and **21**).
3. Make 1:10 serial dilutions of phage suspension in PBS (*see* **Notes 21**–**24** and **27**).
4. Infect 100 μL of *E. coli* TG1 to phage dilutions and incubate for 30 min at 37 °C without shaking (*see* **Notes 4** and **21**).
5. Mix infected *E. coli* TG1 cultures and plate out 10 μL droplets of each dilution series on a single 2YT-AG and 2YT-K agar plates per enriched library. Incubate plates top down o/n at 37 °C after the droplets are dried (*see* **Notes 23**, **24**, and **27**).

3.5 ELISA of Polyclonal Antibody Phage

The ELISA protocol in the Kingfisher Flex is summarized in Table 3 with a proposed layout shown in Fig. 3.

1. Arrange *bead plate*. Fill each position of a 96-well V-bottom PP microtiter plate with 180 μL PTM and add 20 μL (roughly 10–20 μg) of *antigen-loaded bead stock* according to plate layout. Then, add magnetic beads of antigen 1 to positions A1–D1, beads of antigen 2 to positions A2–D2, and so on (*see* **Notes 4**, **13**, and **18**).
2. Use empty beads as a negative control. Take 1 mg (roughly 100 μL) of Dynabeads™ M-280 Streptavidin magnetic beads in 2 mL fresh microcentrifuge tube and wash 5 min for three times with 1.5 mL PBST at room temperature (RT). Discard last wash solution and resuspend in 200 μL. Add 20 μL to positions E1–H12 (*see* **Notes 14** and **17**).
3. Arrange *phage plate*. Fill each position of a 96-well V-bottom PP microtiter plate with 150 μL PTM. Add 50 μL of phage solution from the phage stock plates of the individual rounds to plate according to layout. Add phage stocks of selection rounds 1–4 on antigen 1 to position A1–D1 and E1–H1 respectively. Add

phage stocks of selection rounds 1–4 on antigen 2 to position A2–D2 and E2–H2 respectively and so on (*see* **Note 4**).

4. Prepare three *wash plates* and fill 96-well V-bottom PP microtiter plates with 200 μL PBST (*see* **Notes 2** and **19**).
5. Prepare *antibody plate*. Fill 96-well V-bottom PP microtiter plates with 200 μL mouse monoclonal anti-M13 HRP-conjugated-PTM solution (1:5000) (*see* **Notes 2** and **19**).
6. Place the plates in the Kingfisher Flex plate holder table and start magnetic bead-based ELISA program. The program should be set to move magnetic beads from plate to plate and incubate the beads in each plate (Fig. 2a). During all incubations, the beads should be kept in suspension by moving plastic tips up and down in the wells at fast and medium speed (30–50 mm/s) (*see* **Note 19**).
7. While ELISA program is running, prepare the *substrate plate*. Dissolve one ABTS tablet (10 mg) in 10 mL substrate buffer. Shortly after the antibody plate incubation step in the ELISA process is finished, add 10 μL hydrogen peroxide to substrate solution and pipette 200 μL to each well of a 96-well polystyrene microtiter plates and place plate in Kingfisher Flex (*see* **Notes 8** and **20**).
8. Once beads are incubated in the substrate and color developed for 20 min, remove beads from the substrate manually (*see* **Notes 8** and **20**).
9. Take out *substrate plate* from the Kingfisher Flex plate holder table and measure substrate-specific extinction at 405 nm in a plate reader machine (*see* **Notes 8** and **20**).
10. For each individual selection target, evaluate enrichment by plotting the obtained values for antigen-loaded and control beads of each phage selection rounds next to each other (Fig. 3) (*see* **Notes 23** and **28**).

3.6 Production of Phage Monoclonal Antibody Fragments in Microtiter Plates

For monoclonal antibody fragment, individual clones were picked. Each of the individual colonies represents an antibody fragment (*see* **Note 29**).

1. Inoculate 5 mL of 2YT in a 15 mL PP tube with a single clone of *E. coli* TG1 from an agar plate and grow shaking o/n at 37 °C and 200 rpm (*see* **Note 4**).
2. Inoculate 5 mL 2YT in a 50 mL PP tube with 50 μL of o/n *E. coli* TG1 culture and incubate shaking at 37 °C and 200 rpm until OD_{600} ~ 0.4–0.5 (*see* **Note 4**).
3. Meanwhile, prepare a 1:10 dilution series of the desired panning round from the corresponding phage stock plate by adding 10 μL phage to 90 μL PBS (*see* **Notes 4**, **21**, **22**, and **26**).

4. Add 100 µL of *E. coli* TG1 cell (OD_{600} ~ 0.4–0.5) to phage dilutions 10^{-5}–10^{-8} and incubate for 1 h at 37 °C (*see* **Note 4**).
5. Mix infected *E. coli* cultures and plate out 100 µL of each dilution series on a 2YT-AG agar plate. Once dried, incubate plates top-down at 37 °C o/n (*see* **Notes 4**, **21**, **22**, and **26**).
6. Pick 92 clones into 96-well U-bottom PP microtiter plate filled with 200 µL 2YT-AG (*see* **Notes 4**, **21**, and **30**).
7. Leave positions H5, H6, H11, and H12 empty for controls. Seal *mother plate* with breathable sealing film and incubate in a microplate shaker o/n at 37 °C and 1400 rpm (*see* **Notes 6** and **27**).
8. Next day, inoculate fresh 96-well U-bottom PP microtiter plate containing 180 µL 2YT-AG with 20 µL of the o/n culture and incubate *daughter plate* for 2 h at 37 °C and 1400 rpm (*see* **Notes 6** and **27**).
9. Add 150 µL glycerol solution to each well of the *mother plate* and store as glycerol stock −80 °C (*see* **Note 27**).
10. Add 10 µL M13K07 helper phage stock (10^{11} cfu/mL) which is equivalent to 10^9 helper phage particles to the each well of the *daughter plate* and incubate stationary for 1 h at 37 °C (*see* **Notes 4**, **26**, and **27**).
11. Filter the bacterial culture by centrifuging microtiter plate for 15 min at 2560.3 × *g* (swing out rotor). Discard the supernatant with remaining M13K07 helperphage.
12. Resuspend bacteria in 220 µL pre-warmed 2YT-AKG (30 °C) and transfer to a fresh 96-well U-bottom PP microtiter plate. Seal *daughter plate* with breathable sealing film and incubate in a microplate shaker o/n at 30 °C shaking at 1400 rpm (*see* **Notes 6** and **17**).
13. Pellet down the bacteria in *daughter plate* by centrifugation 15 min at 2560.3 × *g* (swing out rotor). Transfer the supernatant carefully without disturbing the pellet to a 96-well filtration plate (*see* **Notes 4** and **22**–**24**).
14. Place filtration plate on the top of a new 96-well U-bottom PP microtiter plate and fix with sticky tape.
15. Filter antibody presenting phage particles to remove possible contaminating *E. coli* TG1 cells by centrifugation for 2–5 min at 936.3 × *g*. Store the filtrate and discard bacteria pellets and used filtration plate (*see* **Notes 4** and **22**–**24**).
16. Transfer monoclonal antibody phage containing culture supernatant into fresh 96-well U-bottom PP microtiter plate and store until further use at 4 °C. Discard the pellet-containing plate (*see* **Note 27**).

3.7 ELISA of Phage Monoclonal Antibody Fragments in Microtiter Plates

Two ELISA plates are needed for 92 colonies of soluble monoclonal antibody fragments. 46 individual clones in which A1–H6 are the antigen coated whereas the other half (A7–H12) are the background in which no antigen or BSA coated on wells as negative controls. The individual clones will be evaluated on the binding affinity to target antigen and unspecific binding toward the background (PTM, plastic binders, or blank phage). The proposed layout is shown in Fig. 4.

1. To analyze the antigen specificity of the phage antibody fragment, coat half of a polystyrene (PS) 96-well microtiter plate (positions A1–H6) by transferring (a) 1–2 μg protein antigen in 100 μL PBS or (b) 10–20 ng peptide antigen in 100 μL PBS to each well. At the same time, coat the other half of the plate (positions A7–H12) with 100 μL/well of an appropriate negative control, such as Bovine Serum Albumin (10 μg/mL in PBS) or PTM and incubate microtiter plate o/n at 4 °C (*see* **Notes 2**, **3**, and **27**).
2. Discard coating solution and wash all wells two times for 5 min by completely filling them with PBST (*see* **Note 19**).
3. Block all wells by completely filling them with 300 μL of PTM and incubate for 1 h at RT, 600 rpm (*see* **Notes 27** and **31**).
4. Discard blocking solution and wash all wells three times for 5 min by completely filling them with PBST (*see* **Note 19**).
5. Fill each well with 50 μL PTM and 50 μL phage antibody fragment solution of the respective 46 clones to each half of the plate (containing target antigen and a negative control, respectively) and incubate for 1 h at RT, 600 rpm (*see* **Notes 27** and **32**).
6. Discard phage antibody fragment solution and wash wells three times for 5 min by completely filling them with PBST (*see* **Note 19**).
7. Add 100 μL of mouse monoclonal anti-M13 HRP-conjugated-PTM solution (1:5000 in PTM) to each well and incubate for 1 h at RT, 600 rpm (*see* **Note 27**).
8. Discard mouse monoclonal anti-M13 HRP-conjugated-PTM solution (1:5000 in PTM). Then, wash the wells three times with PBST and two times with PBS (*see* **Note 27**).
9. Meanwhile, prepare substrate by dissolving two ABTS tablet (10 mg) in 20 mL substrate buffer. Immediately prior use, add 20 μL hydrogen peroxide to the substrate solution (*see* **Note 8**).
10. Finally, add 100 μL of substrate to each well and allow developing for 5–30 min at RT in the dark (*see* **Notes 8** and **27**).

11. Read substrate-specific extinction at 405 nm in a plate reader (*see* **Notes 8** and **28**).
12. Plot the obtained values for antigen and negative control protein for each soluble monoclonal antibody fragment next to each other and identify positive candidates with an acceptable signal-to-background ratio (Fig. 4) (*see* **Note 28**).

Semi-automated magnetic bead-based selection allows for easy in-vitro selection of specific antibodies by the physical interaction between the antibody on the phage particle, with an immobilized target antigen. The panning protocol can be optimized with different parameters such as incubation time, speed of motion, number, and volume of washing step. Figure 3 shows a typical ELISA result highlighting the enrichment patterns of antibody phage selection for four round whereas Fig. 4 shows the typical second stage selection via monoclonal ELISA. Normally, the phage clones were chosen from either the third or fourth round of amplified phage, depending on the result of polyclonal ELISA. Several clones from each pooled phage indicate the binding of the phage to the respective antigen.

In short, semi-automated bead-based antibody selection protocol is more efficient as compared to manual method. This is because it allows up to 96 phage display selection in one round with high surface area on beads compared to plates. This method can be performed in solution using streptavidin magnetic beads coupled with an automated bead processor. Furthermore, bead-based ELISA screening can allow for detection of antigens normally difficult to assess using conventional ELISA.

4 Notes

1. Dynabeads M-280 Streptavidin are magnetic beads designed and optimized for usage in Kingfisher Flex, especially for protein. There are many other different Dyanabeads, including M-270 for DNA and RNA conjugation. Other than that, some improvement had been done for the Dynabeads series with MyOne Streptavidin C1 and MyOne Streptavidin T1 having a much smaller bead size which has a higher binding capacity to DNA/RNA as compared to M-design. Dynabeads MyOne Streptavidin C1 are also suited for short biotinylated antigens, such as peptides of hydrophilic nature. Other than Dynabeads, many other streptavidin magnetic beads from different manufacturers can be optimized and applied in Kingfisher Flex, such as Chemicell SiMAG Streptavidin Magnetic beads and Merck Millipore PureProteome™ Streptavidin Magnetic Beads.

2. It is advised to aliquot all the reagents, buffers, and solutions in small tubes, which can be discarded after single use to prevent cross-contaminant during the experiment [12, 13].
3. The plastic ware and buffers involved in the semi-automated panning must be free of contamination. Thus, it is advised to use new buffers and plastic ware for every round of panning to prevent cross contamination. If reuse of plastic is necessary, plastic ware should be treated with UV-light for 20 min every time before reuse.
4. Filter tips should be used throughout all the experiment involving phage particle which will contaminate the pipette as well as culturing *E. coli* TG1.
5. Besides TG1, there are several other *E. coli* strains that can be used to re-amplify the phagemid with the help of helper phage, as long as the genotype of the *E. coli* contains the F′ episome such as *E. coli* XL1 Blue, SS320, ER2738, and so on [24, 25]. The F-episome is needed for the production F-pili necessary for the infection process by M13 phage.
6. The breathable sealing film can be replaced by a cellophane tape which is considered a cheap alternative having the same function as the breathable sealing film, in terms of contamination prevention and gas permeability. However, cellophane tape tends to trap vapor after long-term incubation due to a slightly poorer gas permeability as compare to the breathable sealing film without affecting the growth of bacteria.
7. Besides M13KO7, hyperphage is another choice of helper phage which increases the presentation efficiency on the phage particle for about 400-fold by enforced oligovalent antibody display on every phage particle. The enrichment of blank helper phage can be reduced by using hyperphage due to the loss of the functional pIII gene. In other words, the source of pIII in phage assembly is mainly encoded by the phagemid-encoded pIII-antibody fusion [26].
8. Other than ABTS, TMB (3, 3′, 5, 5′-Tetramethylbenzidine) can be used as substrates for detection purposes [12, 13].
9. The four different selection of antibodies methods, including (a) immobilization to the 96-well microtiter plates; (b) Immobilization to immunopins in a 96-well format; (c) Immobilization onto membranes from 2D-gels [27]; or (d) Immobilization onto magnetic particles using a magnetic particle processor containing 96 magnetic pins [28, 29].
10. The larger surface area increases the protein accessibility to the phage particles with less steric hindrance. The incorporation of automation during the panning process is to ensure a more

robust, efficient, and reproducible result on the antibody selection [12].

11. The target molecule for automated panning can be of natural source, recombinant proteins or synthetic compounds, especially different types of antibody library [13, 28, 30].
12. The semi-automated robot benefits the panning method by using magnetic nanoparticles to help the conjugation of target proteins on the large surface beads for downstream complexes separation by magnetic force [31]. The use of magnetic nanoparticles in panning allows proteins to bind more effectively on the surface of nanoparticles as compared to a larger solid phase like polystyrene microtiter plates or immunotubes [12].
13. The semi-automated protocols are robust and effective as they utilize a magnetic particle processor and successfully in generating mAbs against various antigens simultaneously [12, 13].
14. The washing can be done either on rotator or pipette aspiration.
15. The conjugation of protein or peptide can be validated before it is being applied to Kingfisher flex machine for biopanning process by SDS PAGE and concentration checking on before and after binding.
16. The PP immunotube was first blocked with blocking agent, such as PTM or BSA to allow the blocking agent to bind onto the wall, which later will be used to eliminate the blocking agent (PTM/BSA) and plastic phage binders. Immunotubes were used instead of Microtiter plate (MTP) depending on the volume of unspecific phage binder elimination from the phage library. In other words, Immunotube will bind more unspecific binders to lower the chances of unspecific binding during affinity binding between antigen and phage library.
17. Magnetic beads were removed or discarded with the help of magnetic stand or 2 min centrifugation at 936.3 $\times g$ to collect the beads at the bottom of the tubes. Then, transfer carefully the antibody phage to the phage-plate.
18. One of the main problems associated with the conversion from conventional methods to a semi-automated platform is the tedious preparation process required for antigen conjugation. However, the availability of various chemical and enzymatic conjugation methods has made the transition from conventional methods to semi-automated platforms easier [32, 33].
19. The washing procedure is increasing by panning round to remove unspecific antibody binders whereas the automated processor help to reduce human error as skill mastered varied most of the time [12].

20. Loading of released beads into the next plate (*E. coli* TG1 culture or ABTS) can be done manually without the Kingfisher Flex during infection.
21. To examine for contamination, it is recommended to spot blank *E. coli* TG1 and PBS on 2YT-GA and 2YT-K agar plate on each round of panning [12, 13].
22. The rescued and amplified phage can be estimated by titrating 10 μL of each dilution on a 2YT-GA and 2YT-K agar plate. Then, plates were incubated top-down o/n at 37 °C [12, 13].
23. The successful enrichment for eluted phage usually is 10^3–10^5 phage per well after the first panning round and increases two to three orders in magnitude per each additional panning round whereas the amplified phage will have a titer of about 10^{12}–10^{14} phage/mL. On an average, phage preparations in microtiter plates (200 μL culture volume) produce 10^{10}–10^{11} c.f.u. as compared with the c.f.u. values obtained on 2YT-AG and 2YT-K agar plates for each phage library. The helper phage genome containing population should be a minimum of 4–5 orders of magnitude smaller than the antibody fragment containing phagemid population [12, 13]. Formula to calculate the colony forming unit, c.f.u. = number of colonies × dilution factor × 100.
24. Some of the eluted phage from each panning round will be stored at −80 °C for future reference when there is any repeat on panning for specific panning round required to avoid wasting of time for start from the beginning [12, 13].
25. The subculturing and packaging process can be done either with the 2 mL microcentrifuge tube in a thermomixer at 37 °C, 800 rpm for 2 h or in 96-well U-bottom PP plate in Plate Shaker-Thermostat (Biosan, Latvia).
26. The amount of helper phage that is needed for packaging process is highly dependent on the rescued phage from the selection. Too much of helper phage raised the background problem. For high background on amplified phage, researchers should consider decreasing the amount of phage for packaging.
27. Eight-channel micro-pipettes are advised to be used in order to avoid pipetting errors [12, 13].
28. The actual affinity binding between the antibody phage and antigen is reflected by the difference between the sample and background absorbance reading at 405 nm. The background indicates unspecific binders (such as milk binding or plastic binder) and blank helper phage.
29. The monoclonal antibodies can either be selected or validated on ELISA by using soluble antibody fragments. The soluble antibody fragment can be produced via 1 mM IPTG induction.

30. The problem of cross contamination normally occurs during the colony picking from a dense plate. To avoid that, serial dilution must be done before plating out the output clones on an agar plate [12, 13, 34].
31. The purpose of blocking the wells with PTM is to prevent the phage or soluble protein of antibody bind to the maxi-binding wells of PS microplate. This will lead to false-positive reading.
32. The incubation for binding affinity can be done at 37 °C, 600 rpm (micro-plate shaker) for 2 h for optimal results.

Acknowledgments

The authors would like to acknowledge the support from the Malaysian Ministry of Education under the Higher Institution Centre of Excellence (HICoE) Grant (Grant no. 311/CIPPM/44001005).

References

1. Rami A et al (2017) An overview on application of phage display technique in immunological studies. Asian Pacific J Trop Biomed 7(7):599–602. https://doi.org/10.1016/j.apjtb.2017.06.001
2. Frenzel A et al (2016) Phage display-derived human antibodies in clinical development and therapy. MAbs 8(7):1177–1194. https://doi.org/10.1080/19420862.2016.1212149
3. Hust M, Dübel S (2004) Mating antibody phage display with proteomics. Trends Biotechnol 22(1):8–14. https://doi.org/10.1016/j.tibtech.2003.10.011
4. R Strohl W (2014) Antibody discovery: sourcing of monoclonal antibody variable domains. Curr Drug Discov Technol 11(1):3–19
5. Zhuang G et al (2001) A kinetic model for a biopanning process considering antigen desorption and effective antigen concentration on a solid phase. J Biosci Bioeng 91(5):474–481. https://doi.org/10.1016/S1389-1723(01)80276-0
6. Rudnick SI et al (2011) Influence of affinity and antigen internalization on the uptake and penetration of anti-HER2 antibodies in solid tumors. Cancer Res 71(6):2250–2259. https://doi.org/10.1158/0008-5472.can-10-2277
7. Giordano RJ et al (2001) Biopanning and rapid analysis of selective interactive ligands. Nat Med 7(11):1249–1253. https://doi.org/10.1038/nm1101-1249
8. Chin CF et al (2016) Application of streptavidin mass spectrometric immunoassay tips for immunoaffinity based antibody phage display panning. J Microbiol Methods 120:6–14. https://doi.org/10.1016/j.mimet.2015.11.007
9. Hakami AR et al (2015) Non-ionic detergents facilitate non-specific binding of M13 bacteriophage to polystyrene surfaces. J Virol Methods 221:1–8. https://doi.org/10.1016/j.jviromet.2015.04.023
10. Elgundi Z et al (2016) The state-of-play and future of antibody therapeutics. Adv Drug Deliv Rev 122:2–19. https://doi.org/10.1016/j.addr.2016.11.004
11. Ch'ng ACW et al (2016) Phage display-derived antibodies: application of recombinant antibodies for diagnostics. In: Saxena SK (ed) Proof and concepts in rapid diagnostic tests and technologies. InTech, London, pp 107–135
12. Ch'ng ACW et al (2018) Magnetic nanoparticle-based semi-automated panning for high-throughput antibody selection. In: Hust M, Lim TS (eds) Phage display: methods and protocols. Springer, New York, NY, pp 301–319. https://doi.org/10.1007/978-1-4939-7447-4_16
13. Konthur Z et al (2010) Semi-automated magnetic bead-based antibody selection from phage display libraries. In: Kontermann R, Dübel S (eds) Antibody engineering. Springer, Berlin, pp 267–287. https://doi.org/10.1007/978-3-642-01144-3_18

14. Jamshaid T et al (2016) Magnetic particles: from preparation to lab-on-a-chip, biosensors, microsystems and microfluidics applications. TrAC Trends Anal Chem 79:344–362. https://doi.org/10.1016/j.trac.2015.10.022
15. Tayapiwatana C et al (2006) A novel approach using streptavidin magnetic bead-sorted in vivo biotinylated survivin for monoclonal antibody production. J Immunol Methods 317:1):1–1) 11. https://doi.org/10.1016/j.jim.2006.07.024
16. Hien TBD et al (2012) Potential application of antibody-mimicking peptides identified by phage display in immuno-magnetic separation of an antigen. J Biotechnol 161(3):213–220. https://doi.org/10.1016/j.jbiotec.2012.06.039
17. Lim BN et al (2014) Principles and application of antibody libraries for infectious diseases. Biotechnol Lett 36(12):2381–2392. https://doi.org/10.1007/s10529-014-1635-x
18. Georgiou G et al (2014) The promise and challenge of high-throughput sequencing of the antibody repertoire. Nat Biotechnol 32:158–168. https://doi.org/10.1038/nbt.2782
19. Romao E et al (2016) Identification of useful nanobodies by phage display of immune single domain libraries derived from camelid heavy chain antibodies. Curr Pharm Des 22 (43):6500–6518
20. Knappik A et al (2000) Fully synthetic human combinatorial antibody libraries (HuCAL) based on modular consensus frameworks and CDRs randomized with trinucleotides 1. J Mol Biol 296(1):57–86. https://doi.org/10.1006/jmbi.1999.3444
21. Carmen S, Jermutus L (2002) Concepts in antibody phage display. Brief Funct Genomics 1(2):189–203. https://doi.org/10.1093/bfgp/1.2.189
22. Rosenberg AS, Sauna ZE (2017) Immunogenicity assessment during the development of protein therapeutics. J Pharm Pharmacol 70 (5):584–594. https://doi.org/10.1111/jphp.12810
23. Fang X et al (2007) Automation of nucleic acid isolation on KingFisher magnetic particle processors. J Assoc Lab Autom 12(4):195–201. https://doi.org/10.1016/j.jala.2007.05.001
24. Hanes J et al (2000) Picomolar affinity antibodies from a fully synthetic naive library selected and evolved by ribosome display. Nat Biotechnol 18:1287–1292. https://doi.org/10.1038/82407
25. Hallborn J, Carlsson R (2002) Automated screening procedure for high-throughput generation of antibody fragments. BioTechniques 33:S30–S37
26. Schwenk JM et al (2007) Determination of binding specificities in highly multiplexed bead-based assays for antibody proteomics. Mol Cell Proteomics 6(1):125–132. https://doi.org/10.1074/mcp.T600035-MCP200
27. Behrens CR, Liu B (2014) Methods for site-specific drug conjugation to antibodies. MAbs 6(1):46–53. https://doi.org/10.4161/mabs.26632
28. Ta HT et al (2012) Enzymatic antibody tagging: toward a universal biocompatible targeting tool. Trends Cardiovasc Med 22 (4):105–111. https://doi.org/10.1016/j.tcm.2012.07.004
29. Liu B et al (2002) Towards proteome-wide production of monoclonal antibody by phage display. J Mol Biol 315(5):1063–1073. https://doi.org/10.1006/jmbi.2001.5276
30. Walter G et al (2001) High-throughput screening of surface displayed gene products. Comb Chem High Throughput Screen 4 (2):193–205. https://doi.org/10.2174/1386207013331228
31. Turunen L et al (2009) Automated panning and screening procedure on microplates for antibody generation from phage display libraries. J Biomol Screen 14(3):282–293. https://doi.org/10.1177/1087057108330113
32. Rondot S et al (2001) A helper phage to improve single-chain antibody presentation in phage display. Nat Biotechnol 19(1):75–78. https://doi.org/10.1038/83567
33. Smeal SW et al (2017) Simulation of the M13 life cycle I: assembly of a genetically-structured deterministic chemical kinetic simulation. Virology 500:259–274. https://doi.org/10.1016/j.virol.2016.08.017
34. Nakano K et al (2017) E. coli mismatch repair enhances AT-to-GC mutagenesis caused by alkylating agents. Mutat Res 815:22–27. https://doi.org/10.1016/j.mrgentox.2017.02.001

Chapter 19

A Binding Potency Assay for Pritumumab and Ecto-Domain Vimentin

Ivan Babic, Santosh Kesari, and Mark C. Glassy

Abstract

Pritumumab, a natural human IgG1kappa mAb, was isolated from the regional lymph node of a patient with cervical cancer. This antibody has been reported to bind the cytoskeletal protein vimentin, and to cell surface expressed vimentin referred to as ecto-domain vimentin (EDV). Here, we report details of the development of a potency of binding assay for pritumumab as a prerequisite before pursuing clinical trials. The enzyme linked immunosorbent assay (ELISA) to detect antibody-binding antigen can serve as a potency assay for release of manufactured samples to be used in clinical studies. Several layers of controls for this assay along with suitability testing for reagents and components of the assay must be developed before the assay can be incorporated for stability testing and release of manufatured samples.

Key words Pritumumab, Ecto-domain vimentin, Enzyme linked immunosorbent assay (ELISA), Potency assay, Investigational new drug (IND), Good laboratory practices (GLP)

1 Introduction

1.1 Pritumumab Antibody

Pritumumab, a natural human IgG1kappa mAb, was originally developed by the fusion of B-lymphocytes from a lymph node of a patient with cervical cancer with the UC-729-6 human fusion partner [1] and has shown promise in the clinic for brain cancer patients [2, 3]. The critical thinking behind the development of pritumumab is based on the intelligence of the natural human immune response in generating an anti-cancer response [4]. The center of this anti-cancer immune response is using the regional draining lymph node as a drug discovery tool [5, 6]. The clinical work with pritumumab, through a Phase II setting with Japanese brain cancer patients, was done with the hybridoma-derived antibody [2, 3]. Of the 249 patients who were treated with the mAb, 126 were evaluated for safety and 74 were evaluated for efficacy. Pritumumab demonstrated therapeutic benefit and this data has been summarized elsewhere [3]. Evaluation of the efficacy of pritumumab indicated that 14.8% of glioblastoma patients, 26.8% of malignant astrocytoma patients,

Michael Steinitz (ed.), *Human Monoclonal Antibodies: Methods and Protocols*, Methods in Molecular Biology, vol. 1904, https://doi.org/10.1007/978-1-4939-8958-4_19,

and 44.4% of astrocytoma patients benefited from therapy [3]. Importantly, no major adverse drug effects were seen and no severe host reaction to the administered antibody was observed making long-term repetitive treatment reasonable. For commercial applications a more economically manufactured version was made based on the preferred Chinese Hamster Ovary (CHO) cell line [7]. By all tests the pritumumab made in CHO is identical to the original hybridoma mAb and is therefore a biosimilar [7]. The antigen recognized by pritumumab is an altered form of vimentin that is expressed on the cell surface and called ecto-domain vimentin (EDV; refs. 2, 8–10). EDV cell surface expression is restricted to solid tumors [2, 7]. The epitope recognized by pritumumab is a non-helical region of the rod area of EDV (Pellecchia and Glassy, manuscript in prepartion). The original clinical work done with the hybridoma-derived pritumumab was a low-dose trial of either one or two milligrams once or twice a week [2, 11, 12]. To repeat and extend the treatment protocol to include higher doses an Investigational New Drug (IND) application was filed with the United States Food and Drug Administration (FDA). To support the further planned clinical trial work the FDA requested a potency assay be developed for pritumumab under Good Laboratory Practice (GLP). The pupose of this report is to describe the details of the development of this potency assay.

1.2 Vimentin the Target of Pritumumab

Normal vimentin is a type III intermediate filament (IF) protein that is found in the cytoskeleton of mesenchymal cells [13–16]. Among its many functions vimentin also plays a significant role in supporting and anchoring the position of the organelles in the cytosol [16–19]. Vimentin is attached to the nucleus, endoplasmic reticulum, and mitochondria, either laterally or terminally. Vimentin comprises part of the cytoskeleton, is involved in intracellular transport, and is a highly developmentally-regulated proten [18]. Because of this, vimentin is often used as a marker of mesenchymally-derived cells or cells undergoing an epithelial-to-mesenchymal transition (EMT) during both normal development and metastatic progression [18, 20–22]. Additionally, the level of vimentin expression highly correlates with tumor aggressiveness, recurrence, and poor prognosis [13, 14, 18]. In its native state vimentin is primarily helical dimers and tetramers [13]. Vimentin has also been independently shown to be expressed on the cell surface [21–24], though it is unclear what form is expressed, as well as secreted [25–27]. In tumor cells normal vimentin expression is upregulated which may contribute to the cancer state. Some malignant state traits attributed to vimentin include a stem cell marker associated with malignancy [21]. Highly malignant tumor cells were positive for vimentin via 14-3-3ε over expression [28]. Vimentin is a scaffold protein in invadosomes of the invasive cancer cells [29] and forms a complex with Hsp90

in geldanamycin-induced apoptosis [30]. Vimentin-beclin-14-3-3 complex participates in the regulation of autophagy [31]. Inhibition of vimentin expression attenuates wound healing [32]. Peptides involved in tumor angiogenesis bind to vimentin [33]. Vimentin is the ligand to Dectin-1 as an innate immunity receptor [34] and cooperates with NOD2 also in conjunction with innate immunity [35]. Overexpression of vimentin occurs with tumor heterogeneity via cellular coalescence [36]. In total, these tumor traits are reflections of vimentin modification, modulation, and alteration by specialized epigentic events consisting of (a) citrullination at arginine residue in autoimmune recognition by T cells [37, 38], (b) palmitoylation of cytoskeleton associated protein in anti-proliferative signaling [39], (c) phosphorylation regarding the state of mitotic furrow conjunction with cytokinesis [40], and (d) sumoylation in cell migration of glioma [41]. Networks of vimentin with actin and tubulin assemblies elicit dynamic cytoskeletal integrative signaling between the cellular plasma membrane and nucleus to adapt to quick microenvironmental changes for maintaining epithelial homeostasis [13]. The antigen/epitope of EDV located in the C2 domain of vimentin may be an intermolecular dissociation/association of filament formation (fasciculation) [42, 43]. In this regard the interaction between EDV and p34Ag is quite relevant in fasciculation of vimentin. Taken together with these vimentin relating cellular responses, it could be considered that the vimentin network behaves as a hub and spoke for the various kind of regulators, cofactors, modulator molecules, and chaperone molecules which vimentin sequesters and expels to manipulate the functions of critical factors even in tumorigenesis. In the malignant cell, EDV was recognized by pritumumab on the special vesicular protrusions of the plasma membrane in terms of Vimentin-Exposing Ectosome (VEE) during the G2/M-cell cycle [42]. Thus, it is not difficult to imagine VEEs play important roles in cancer stem cell survival and prolificity through communication with the T-niche [38]. The function of VEE for the presentation of EDV to the immune effector cells for the immune response is an interesting issue of antigen presentation regarding tumor cell-mediated immune tolerance that relates to negative host immune response in patients with progressive disease.

An ideal tumor antigen target would have certain criteria [44]. The antigen should be tumor restricted or conserved across a wide range of tumor types and preferably expressed on the cell surface available for immune attack. To escape immunoediting the antigen should have no known biological function and therefore not subjective to mutational pressure. The antigen should not be shed nor internalized after antibody binding so once bound on the cell surface the antibody-antigen complex would stimulate an immune response. In total, it appears that the immune profile of EDV makes it now ready for prime time. Based on the specificity profile along with the above criteria EDV appears to be a relavent biomarker for the focus an immunotherapy program.

1.3 Potency Assay–GLP Criteria

In nonclinical research, good laboratory practice or GLP specifically refers to a quality uniform system of controls to ensure the uniformity, consistency, reliability, reproducibility, quality, and integrity of chemical (including pharmaceuticals) nonclinical safety tests. For clinical trials with new biomolecules it is essential that GLP procedures are strictly adhered to so the data can be better understood and interpreted. The assay described here meets all of these criteria.

An objective of this study is to develop a GLP-based enzyme immuno-assay (EIA) for pritumumab using commercial sources of recombinant human vimentin [45, 46]. In addition, to satisfy the FDA requirements for a GLP method an EIA protocol was developed to monitor the potency and specificity of pritumumab for clinical trials. It should be noted that all of the steps and procedures described here are equally applicable to other antibodies being prepared for the clinic [47].

2 Materials

2.1 Antibodies and Conjugates

1. Pritumumab antibody; both the Drug Substance (DS) and Clinical reference standards.
2. InVivoMAb Human IgG1 isotype Control; Control human IgG1 antibody (BioXCell).
3. Mouse anti-human IgG HRP conjugate; Mouse anti-Human IgG Fc Secondary Antibody, HRP conjugate (ThermoFisher).

2.2 Sandwich ELISA

1. PathScan Total Vimentin Sandwich ELISA Kit; Vimentin ELISA Kit (Cell Signaling Technology).

2.3 Capture Antigen

1. Human Vimentin/VIM Protein (His Tag); Recombinant human vimentin with carboxy terminal poly-histidine tag (SINO Biological).

2.4 Detection Reagents and Wash Buffers

1. Ultra TMB solution; 1-Step Ultra TMB-Elisa (ThermoFisher Scientific).
2. Phosphate Buffered Saline (PBS) was buffer (Corning).

2.5 Plates and Plate Reader

1. 96-well plate (Greiner).
2. Round-bottom 96-well plate (Costar).
3. 96-well plate reader; Read absorbance OD450 nm; model is PolarStar Omega 96-well plate reader.

3 Methods

1. Remove the ELISA plate from the PathScan Total Vimentin Sandwich ELISA Kit (*see* **Note 1**) and place the plate with microstrips at room temperature for 15 min. After the

microwell strips have reached room temperature, break off the required number of microwells, or just use the whole 96-well plate. Unused microwells should be resealed and stored at 4 °C immediately.

2. Recombinant Human Vimentin (His Tag) (Sino Biological, Cat#10028-H08B) (*see* **Note 2**) (Use two vials of 50 μg per 96-well plate. Reconstitute each vial with 200 μl of sterile water to get stock solution of 0.25 mg/ml). Add the 400 μl from the two vials to 10 ml PBS to get 10 μg/ml human vimentin ready for capture.
3. Recombinant Human Vimentin is diluted to 10 μg/ml with PBS as described above in **step 1**.
4. Add 100 μl of diluted Human Vimentin to the wells. Cover and incubate the plate for 2 h at room temperature (*see* **Note 3**).
5. Wash wells:
   (a) Discard plate contents into a receptacle.
   (b) Wash three times with PBS, 200 μl each time for each well (*see* **Note 4**).
   (c) For each wash, strike plates on fresh towels hard enough to remove the residual solution in each well, but do not allow wells to completely dry at any time.
6. Will run triplicates for each Antibody test. Make up concentrations of Pritumumab and Isotype control in PBS as shown below. Typically, this is started after 1.5 h of adding human vimentin to plates. The highest dilution is prepared by pipetting from the antibody stock and then serial dilutions made from that stock. The dilutions are prepared in eppendorf tubes first then transfered to a round-bottom 96-well plate for transfer to wells with a multichannel micropipette (*see* **Note 5**). Once dilutions are ready add 100 μl of Pritumumab antibody or the Isotype Control IgG1 to each well. Cover and incubate the plate at room temperature for 1 h. Make sure to run duplicates of each concentration (although preferably run triplicates).

Final concentrations of Pritumumab and Isotype Control (in PBS) to test:

1.	200 μg/ml	(20 μl of Pritumumab Ab +980 μl PBS)
2.	100 μg/ml	(500 μl from **step 1** + 500 μl PBS)
3.	40 μg/ml	(400 μl from **step 2** + 600 μl PBS)
4.	20 μg/ml	(500 μl from **step 3** + 500 μl PBS)
5.	10 μg/ml	(500 μl from **step 4** + 500 μl PBS)
6.	1 μg/ml	(100 μl from **step 5** + 900 μl PBS)
7.	0.1 μg/ml	(100 μl from **step 6** + 900 μl PBS)
8.	No Ab	

7. Repeat wash procedure (**step 4**).
8. Add 100 μl of diluted (1:150 in PBS) mouse anti-human HRP-Linked secondary antibody to each well. Cover and incubate the plate for 45 min at room temperature (*see* **Note 6**).
9. Repeat wash procedure (**step 4**). Then do two more wash steps each for 5 min at room temperature on shaker (gentle shaking) (*see* **Note 7**).
10. Add 100 μl of 1-Step Ultra TMB-Elisa to each well. Incubate the plate for 15 min at room temperature with gentle tapping for the 15 min to help with color development (*see* **Note 8**).
11. Add 100 μl of STOP Solution to each well. Mix gently by pipetting up/down. Transfer 200 μl to the Greiner 96-well plate and read absorbance immediately (*see* **Note 9**). Initial color of positive reaction is blue, which changes to yellow upon addition of STOP Solution.
12. Read absorbance at 450 nm on the PolarStar Omega 96-well plate reader (*see* **Note 10**).
13. For the analysis: subtract out the No Ab control (well 8 result) from wells of corresponding strip (i.e., wells 1–8 of same strip), then plot graph using GraphPad Prism (v5), transform concentrations on *X* axis to Log10 scale and perform nonlinear curve fit using Log agonist vs. variable response four parameter logistic (4PL) regression, set constraints: bottom = 0. This will generate EC50 values (*see* **Notes 11** and **12**).

4 Notes

1. Cell Signaling Technology markets a Vimentin Sandwich ELISA kit, which can be modified for use with Pritumumab. The ELISA plate provided with this kit has mouse anti-vimentin monoclonal antibody (mAb) immobilized on the surface of the plate. Using this commercial plate provides consisitency in terms of materials for the assay. The ELISA plate is used to capture vimentin, the target of Pritumumab. Also, a commercial source of recombinant human vimentin offers the best option for consistency of the assay. Commercial suppliers of recombinant human vimentin were tested and observed that the best binding was using human vimentin from Sino Biological Inc. Additionally, the FDA requires suitability testing to be performed as demonstration that the assay materials and protocol are consistent over time, between different analysts, and between different locations. Such suitability testing is required if purchasing new reagents for the assay, training new personal (analysts) to perform the assay, or relocation of laboratory or change in environment different from initial assay development.

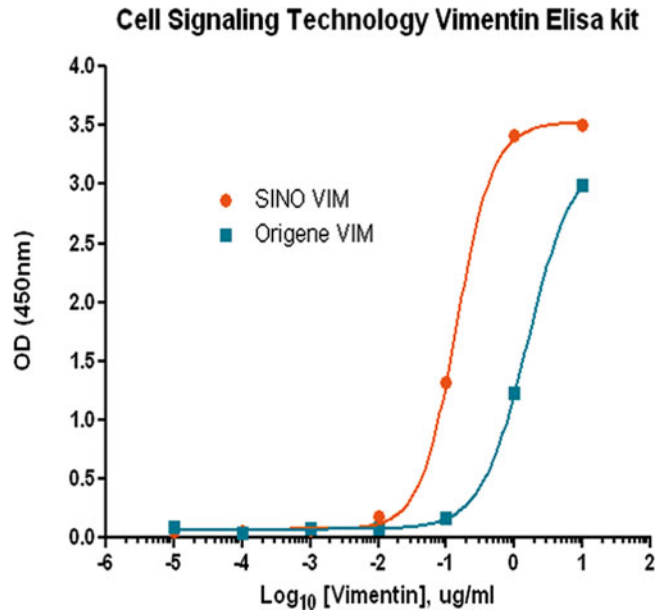

Fig. 1 Testing different sources of recombinant human vimentin with pritumumab in the Cell SignalingTechnology vimentin sandwich ELISA assay. Recombinant human vimentin purchased from SINO Biological and from Origene were compared for binding to pritumumab after capture on the Cell Signaling Technology vimentin Sandwich ELISA plate. Pritumumab shows better binding to SINO Biological human vimentin

2. Determine which commercially available source of vimentin works best in the ELISA assay and determine the concentration to use and the time of capture. It is important that the vimentin target saturates the ELISA plate and that it is recognized by the pritumumab antibody. This requires testing different sources of human vimentin, testing different concentrations, and testing capture time. As an example, Fig. 1 shows an initial test of two sources of human vimentin: one from Sino Biological and one from Origene. Testing both at the same concentration shows pritumumab binds better to vimentin from Sino Biological. The concentration of vimentin to test ranged from 100 ng/ml to 100 μg/ml, and the time of capture was kept short to allow the assay to be performed in a few hours. Times tested were between 30 min to 4 h. The ideal concentration for the human vimentin to saturate the ELISA plate was determined to be 10 μg/ml capture for 2 h at room temperature.
3. To develop the assay for Pritumumab important controls are needed: (a) human isotype control IgG1 as a negative control for binding to vimentin, (b) use bovine serum albumin (BSA) instead of vimentin as a control for specificity of Pritumumab for vimentin, and (c) no target captured as a control for non-specific binding to the plate itself. Upon demonstration that the ELISA plate captures human vimentin which can be bound

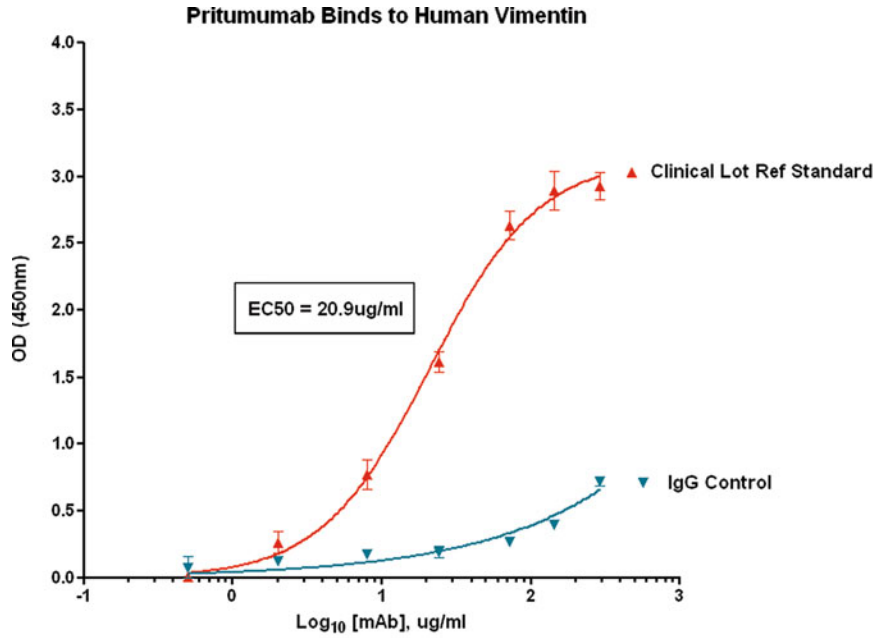

Fig. 2 Pritumumab drug substance (DS) Clinical Lot Reference Standard but not IgG1 control binds vimentin. The antibody pritumumab or isotype control antibody was tested for binding to vimentin in ELISA potency of binding assay. Pritumumab, but not the isotype control antibody, showed significant binding to capture human vimentin

by the pritumumab mAb it is necessary to develop controls as demonstration of specificity of binding. First, a negative control antibody is required to demonstrate that pritumumab antibody binding is specific to the target. Figure 2 shows a representative example where clinical lot pritumumab was tested along with an isotype control antibody in binding to captured human vimentin in the ELISA assay. Only at concentrations above 100 μg/ml does the control antibody start binding nonspecifically in the assay. Pritumumab starts to bind at much lower concentrations and reaches saturation of binding at about 100 μg/ml. This demonstrates that pritumumab binds specifically to the target. However, it is necessary to demonstrate specificity of binding by comparing pritumumab binding in the absence of captured target or in the presence of irrelevant protein capture (for example bovine serum albumin, BSA). Figure 3 shows that pritumumab only binds when human vimentin is captured on the ELISA plate.

4. Perform wash steps in a consistent manner throughout the protocol to minimize error bars. This involves always adding the wash buffer starting on the same side for each wash.
5. Performing dilutions in eppendorf tubes instead of microplate directly minimizes pipetting errors.

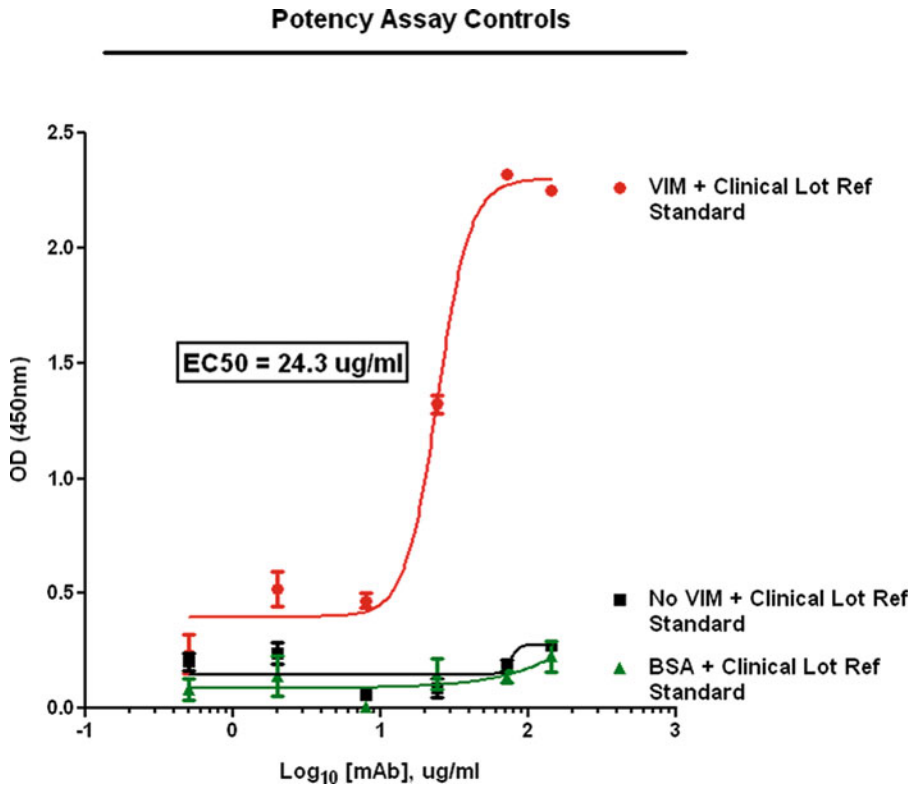

Fig. 3 Pritumumab clinical lot reference standard binds specifically to vimentin. Vimentin, bovine serum albumin, or just PBS control were captured on ELISA plate coated with mAb to vimentin. Pritumumab clinical lot reference standard was then added and only bound in the presence of captured recombinant human vimentin

6. Incubation can be between 30 min and 1 h. Important to be consistent with time for each assay.
7. Gentle tapping of the plate by hand can be done if there is no shaker available that fits the plates.
8. Color development typically occurs within the first 5 min and can be stopped once the deep blue color is observed. If 15 min incubation is not enough then can leave for 30 min.
9. From start to finish the assay takes 4 h as outlined.
10. Make sure to read absorbance right away. The signal does degrade over time.
11. Once a potency assay has been developed there are FDA required suitability criteria to be incorporated as demonstration that the reagents and components of the assay are functioning or operating as decsribred for the potency assay. We incorporated the rabbit anti-vimentin antibody supplied with the Vimentin ELISA Sandwich Assay kit. This is used to demonstrate that, first, the human vimentin can saturate the plate at

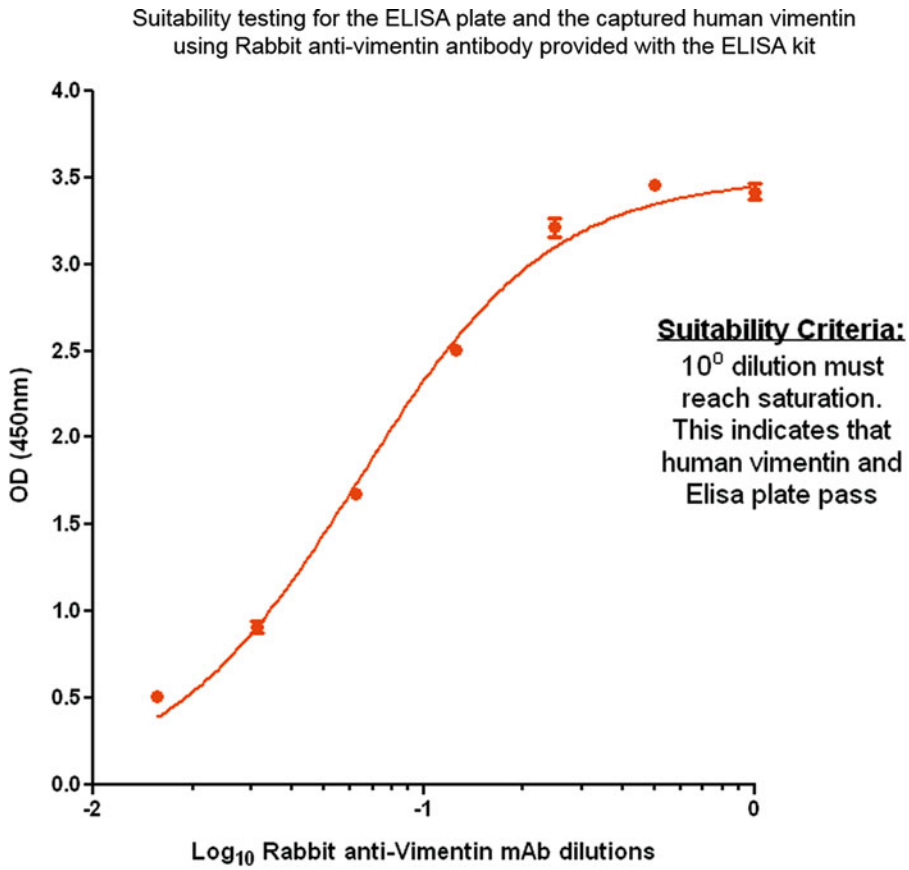

Fig. 4 Suitability testing of components of the ELISA potency assay. Recombinant human vimentin was captured on ELISA plate coated with mouse mAb to vimentin and followed by incubation with dose titration of Rabbit anti-vimentin antibody provided with the Cell Signaling Technology Sandwich ELISA. At 10° dilution the antibody saturates demonstrating suitability of both the capture method and the recombinant human vimentin for testing pritumumab potency of binding

a defined concentration and that it can be recognized by the rabbit antibody. This assay is to be incorporated as a control in cases where potency of manufactured pritumumab fails or when new reagents or plate reader is used, or if analysts performing the experiment are changed, or when the assay is relocated to a new facility. Figure 4 shows suitability testing and criteria for pritumumab potency assay.

12. The potency assay should explicitly define acceptance criteria for future manufactured samples of pritumumab. This criteria provides a quality control for manufactured samples of the antibody. Figure 5a, b demonstrate that the toxicology (tox) lot and clinical lot of pritumumab perform similar in the potency assay and acceptance criteria could then be determined. Once acceptance criteria are defined repeatability of the assay is demonstrated by comparing different vials of the

a

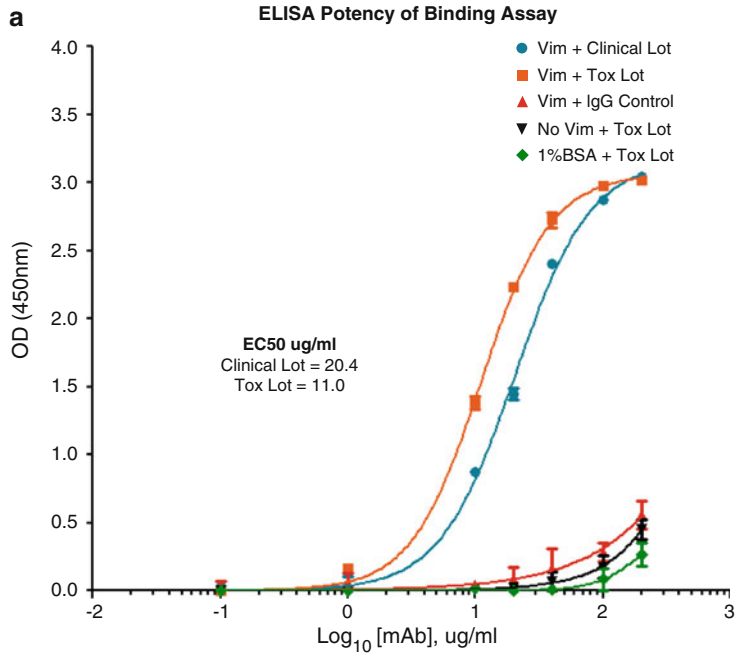

b

	Clinical Lot	Tox Lot	IgG Control	No Vim + Tox Lot	1%BSA + Tox Lot
log(agonist) vs. response -- Variable slope (four parameters)			Ambiguous	Ambiguous	
Best-fit values					
Bottom	= 0.0	= 0.0	= 0.0	= 0.0	= 0.0
Top	3.171	3.063	~ 182.1	~ 109.3	0.5330
LogEC50	1.311	1.042	~ 5.409	~ 4.161	2.300
HillSlope	1.467	1.589	0.8110	1.282	2.452
EC50	20.45	11.02	~ 256318	~ 14483	199.4
Span	= 3.171	= 3.063	= 182.1	= 109.3	= 0.5330
Std. Error					
Top	0.08036	0.03773	~ 97910	~ 35289	2.143
LogEC50	0.02483	0.01380	~ 291.5	~ 111.1	1.423
HillSlope	0.1226	0.1034	0.7424	0.9502	4.562
95% Confidence Intervals					
Top	2.994 to 3.348	2.980 to 3.147	(Very wide)	(Very wide)	-4.184 to 5.250
LogEC50	1.256 to 1.365	1.012 to 1.072	(Very wide)	(Very wide)	-0.8332 to 5.433
HillSlope	1.197 to 1.737	1.361 to 1.816	-0.8231 to 2.445	-0.8096 to 3.373	-7.590 to 12.49
EC50	18.03 to 23.19	10.27 to 11.81	(Very wide)	(Very wide)	0.1468 to 270799
Goodness of Fit					
Degrees of Freedom	11	11	11	11	11
R square	0.9955	0.9982	0.7861	0.9005	0.7935
Absolute Sum of Squares	0.08461	0.03695	0.1145	0.03591	0.03045
Sy.x	0.08770	0.05796	0.1020	0.05713	0.05262
Constraints					
Bottom	Bottom = 0.0	Bottom = 0.0	Bottom = 0.0	Bottom = 0.0	Bottom = 0.0
Number of points					
Analyzed	14	14	14	14	14

Acceptance Criteria:
Expected $Log_{10}EC50$ = 1.2552 with Std. Dev. $Log_{10}EC50$ ±0.3
This provides a range of $Log_{10}EC50$ = 0.9552 to 1.5552
Corresponds to an EC50 range of 9.0 ug/ml to 35.9 ug/ml

Fig. 5 Control testing for the ELISA Potency Assay. (**a**) Nonlinear regression curve fitting showing that no vimentin or bovine serum albumin (BSA) controls confirm specificity of pritumumab for captured vimentin in the ELISA assay. Both the pritumumab tox lot and clinical lot perform similarly in the assay. (**b**) Table of values from the nonlinear curve fitting used for acceptance criteria Log10 EC50 determination for the antibody pritumumab in the ELISA assay

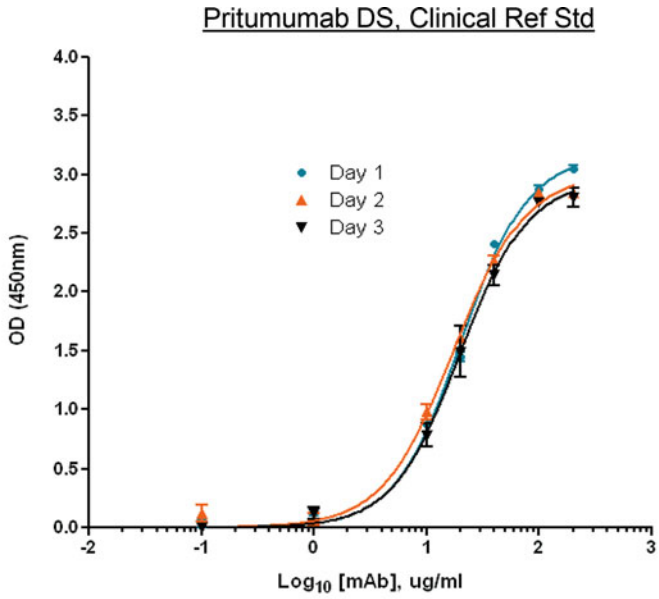

		Mean EC50 (ug/ml)	SD	SEM	Intra-Assay CV	Inter-Assay CV
Clinical Lot Reference Standard	Test 1 (Day 1)	20.45	1.4973	1.0588	7.32%	8.08%
	Test 2 (Day 2)	17.52	1.5095	1.0674	8.62%	
	Test 3 (Day 3)	19.91	1.5467	1.0937	7.77%	

Fig. 6 Nonlinear Regression curve fitting to establish EC50 (ug/ml) for Pritumumab drug substance (DS), Clinical Reference Standard. The intra-assay and inter-assay % coefficient of variance was determined for the ELISA potency of binding assay from three independent experiments performed on three separate days. Shown is the curve fitting for each trial (top) and the results table with mean EC50, standard deviation (SD), and standard error of the mean (SEM) (bottom)

same source of the antibody and comparing the assay performed in at least three independent runs. This is used to determine the percent intra- and inter-assay variance which should not exceed 10% (Fig. 6). Successful completion of these stages of assay development then allows for the assay to be used for stability testing. This involves testing samples stored under different conditions (5 °C, −20 °C, or −70 °C) for different lengths of time (6 months, 12 months, 18 months, 24 months, etc.). Performing the potency assay for pritumumab on samples stored for 12 months at different temperatures demonstrates that, first, all the samples pass the acceptance criteria, and second, that storage at either −20 °C or −70 °C are likely best conditions for this antibody (Fig. 7).

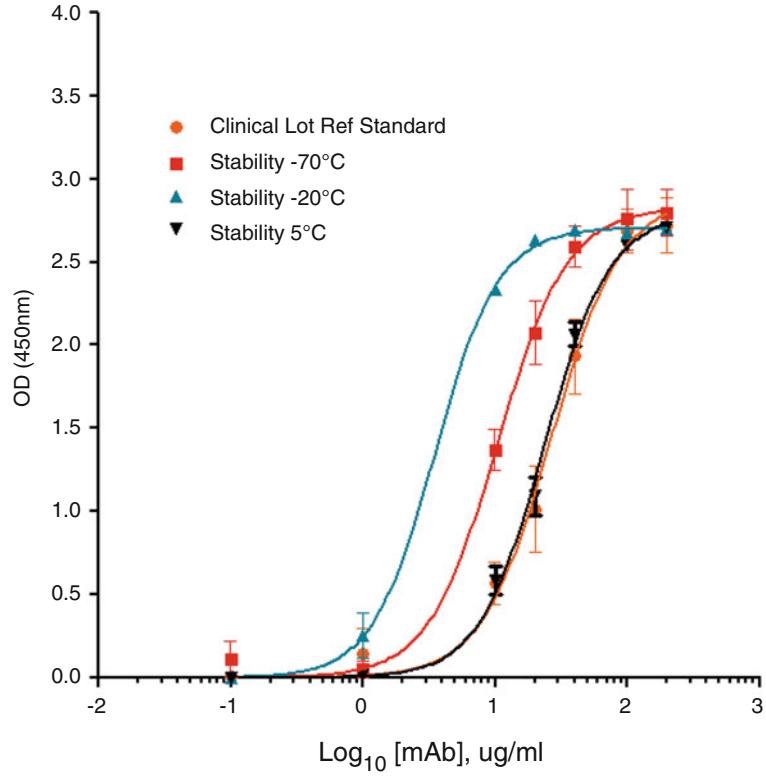

EC50	Clinical Lot Ref Standard	Stability -70°C	Stability -20°C	Stability 5°C
(ug/ml)	26.67	10.48	3.509	23.63

Fig. 7 Testing of stability samples of pritumumab antibody in the potency of binding ELSIA assay. The ELISA potency assay was used to test the Clinical Lot Ref standard with 12 month stability samples held at $\leq -70\ ^{\circ}C$, $-20\ ^{\circ}C$, and $5\ ^{\circ}C$. The results demonstrate that all the stability samples had EC50 values equal to or less (i.e., lower EC50 indicative of higher binding affinity) than the clinical lot reference standard

References

1. Glassy MC, Handley HH, Hagiwara H, Royston I (1983) UC 729-6, a human lymphoblastoid B cell line useful for generating antibody secreting human-human hybridomas. Proc Natl Acad Sci U S A 80:6327–6331
2. Glassy MC, Hagiwara H (2009) Summary analysis of the pre-clinical and clinical results of brain tumor patients treated with pritumumab. Hum Antibodies 18:127–137
3. Babic I, Nurmammadov E, Yenugonda V, Juarez T, Nomura N, Pingle SC, MC G, Kesari S (2017) Pritumumab, the first therapeutic antibody for glioma patients. Hum Antibodies 26:95–101
4. Glassy MC, Gupta R (2013) Technical and ethical limitations in making human monoclonal antibodies, chapter 2. In: Steinitz M (ed) Springer protocols, Methods in molecular biology, vol 1060. Humana Press, New York, pp 9–30
5. Glassy MC, McKnight ME (1993) A novel drug discovery programme utilizing the human immune response. Curr Opin Investig Drugs 2:853–858
6. Glassy MC, McKnight ME (1994) Pharming the human lymph node. Expert Opin Investig Drugs 3:1057

7. Gupta R, York D, Kotlan B, Bleck G, Glassy E, Glassy M (2013) Use of the Gpex® system to increase production of Pritumumab in a CHO cell line. J Bioprocess Technol Photon 98:318–326
8. Aotsuka Y, Hagiwara H (1988) Identification of a malignant cell associated antigen recognized by a human monoclonal antibody. Eur J Cancer 24(5):829–838
9. Kokunai T, Tamaki N, Matsumoto S (1990) Antigen related to cell proliferation in malignant gliomas recognized by a human monoclonal antibody. J Neurosurg 73(6):901–908
10. Hagiwara H, Aotsuka Y, Yamamoto Y, Miyahara J, Mitoh Y (2001) Determination of the antigen/epitope that is recognized by human monoclonal antibody CLN-IgG. Hum Antibodies 10:77–82
11. AV H, Glassy MC (2017) Idiotypic antibody network regarding malignant cell regression in the brain tumor patients treated with the natural human monoclonal antibody, Pritumumab. Integr Canc Biol Res 1:003
12. Kokunai T (2002) Anti-TA226 human monoclonal antibody (ACA-11) against glioma. Nihon Rinsho 60(1):100–106
13. Fuchs E, Weber K (1994) Intermediate filaments: structure, dynamics, function, and disease. Annu Rev Biochem 63:345–382
14. Ivaska J, Pallari HM, Nevo J, Eriksson JE (2007) Novel functions of vimentin in cell adhesion, migration, and signaling. Exp Cell Res 313:2050–2062
15. Chernyatina AA, Nicolet S, Aebi U, Hermann H, Strelkov SK (2012) Atomic structure of the vimentin central a-helical domain and its implications for intermediate filament assembly. Proc Natl Acad Sci 109:13620–13625
16. Apostolou E, Hochdlinger K (2013) Chromatin dynamics during cellular reprogramming. Nature 502:462–469
17. Franke WW, Franke WW, Appelhans B, Schmid E, Freudenstein C, Osborn M, Weber K (1979) Identification and characterization of epithelial cells in mammalian tissues by immunofluorescence microscopy using antibodies to prekeratin. Differentiation 15(1):7–25
18. Mendez MG, Kojima S, Goldman RD (2010) Vimentin induces changes in cell shape, motility, and adhesion during the epithelial to mesenchymal transition. FASEB J 24 (6):1838–1851
19. Lang SH, Hyde C, Reid IN, Hitchcock IS, Hart CA, Gordon Bryden AA, Villette JM, Stower MJ, Maitiand NJ (2002) Enhanced expression of vimentin in motile prostate cell lines and in poorly differentiated and metastatic prostate carcinoma. Prostate 52(4):253–263
20. Hugo H, Ackland ML, Blick T, Lawrence MG, Clements JA, Williams ED, Thompson EW (2007) Epithelial--mesenchymal and mesenchymal--epithelial transitions in carcinoma progression. J Cell Physiol 213(2):374–383
21. Mitra A, Satelli A, Xia XQ, Xia CJ, Mishra L, Li SL (2015) Cell-surface vimentin: a mislocalized protein for isolating csVimentin(+) CD133(-) novel stem-like hepatocellular carcinoma cells expressing EMT markers. Int J Cancer 137(2):491–496
22. Satelli A, Li S (2011) Vimentin in cancer and its potential as a molecular target for cancer therapy. Cell Mol Life Sci 68(18):3033–3046
23. Weidle UH, Maisel D, Klostermann S, Schiller C, Weiss EH (2011) Intracellular proteins displayed on the surface of tumor cells as targets for therapeutic intervention with antibody-related agents. Cancer Genomics Proteomics 8(2):49–63
24. Li H, Meng QH, Noh H, Somaiah N, Torres KE, Xia X, Batth IS, Joseph CP, Liu M, Wang R, Li S (2018) Cell-surface vimentin-positive macrophage-like circulating tumor cells as a novel biomarker of metastatic gastrointestinal stromal tumors. Oncoimmunology 7 (5):e1420450. https://doi.org/10.1080/2162402X.2017.1420450. eCollection 2018
25. Mor-Vaknin N, Punturieri A, Sitwala K, Markovitz DM (2003) Vimentin is secreted by activated macrophages. Nat Cell Biol 5:59–63
26. Pall T, Pink A, Kasak L, Turkina M, Anderson W, Valkna A, Kogerman P (2011) Soluble CD44 interacts with intermediate filament protein vimentin on endothelial cell surface. PLoS One 6:e29305
27. Satelli A, Hu J, Xia X, Li S (2016) Potential function of exogenous vimentin on the activation of Wnt signaling pathway in cancer cells. J Cancer 7:1824–1832
28. Liu TA, Jan YJ, Ko BS, Liang SM, Chen SC, Wang J, Hsu C, Wu YM, Liou J-Y (2013) 14-3-3ε overexpression contributes to epithelial-mesenchymal transition of hepatocellular carcinoma. PLoS One 8:e57968
29. Sutoh-Yoneyama M, Hatakeyama S, Habuchi T, Inoue T, Nakamura T, Funyu T, Wiche G, Oyama C, Tsuboi S (2014) Vimentin intermediate filament and plectin provide a scaffold for invadopodia, faciliating cancer cell invasion and extravasation for metastasis. Eur J Cell Biol 93:157–169
30. Zhang MH, Lee JS, Kim HJ, Jin DI, Kim JI, Lee KJ, Seo JS (2006) HSP90 protects apoptotic cleavage of vimentin in geldanamycin-

induced apoptosis. Mol Cell Biochem 281:111–121

31. Wang RC, Wei Y, An Z, Zou Z, Xiao G, Bhagat G, White M, Reichelt J, Levine B (2012) Akt-mediated regulation of autophagy and tumorigenesis through beclin 1 phosphorylation. Science 338:956–959
32. Rogel MR, Soni PN, Troken JR, Sitikov A, Trejo HE, Ridge KM (2011) Vimentin is sufficient and required for wound repair and remodeling in alveolar epithelial cells. FASEB J 25:3873–3883
33. Glaser-Gaby L, Raiter A, Battler A, Hardy B (2011) Endothelial cell surface vimentin binding peptide induces angiogenesis under hypoxic/ischemic conditions. Microvasc Res 82:221–226
34. Thiagarajan PS, Yakubenko VP, Elsori DH, Yadav SP, Willard B, Tan CD, Rodoriguez ER, Febbraio M, Cathcart MK (2013) Vimentin is an endogenous ligand for the pattern recognition receptor Dectin-1. Cardiovasc Res 99:494–504
35. Henderson P, Wilson DC, Satsangi J, Stevens C (2012) A role for vimentin in chrohns disease. Autophagy 8:1695–1696
36. Ambrose J, Livitz M, Wessels D, Kuhl S, Lusche DF, Scherer A, Voss E, Soll DR (2015) Mediated coalescence: a possible mechanism for tumor cellular heterogeneity. Am J Cancer Res 5:3485–3504
37. Brentvill VA, Metheringham RL, Gunn B, Symonds P, Daniels I, Gijon M, Cook K, Xue W, Durrant LG (2016) Citrullinated vimentin presented on MHC-II in tumor cells is a target for CD4+ T-cell-mediated antitumor immunity. Cancer Res 76:548–560
38. Bay-Jensen AC, Karsdal MA, Vassiliadis E, Wichuk S, Marcher-Mikkelsen K, Lories R, Christiansen C, Maksymowych WP (2013) Circulating citrullinated vimentin fragments reflect disease burden in ankylosing spondylitis and have prognostic capacity for radiographic progression. Arthritis Rheum 65:972–980
39. Planey SL, Keay SK, Zhang CO, Zacharias DA (2009) Palimitoylation of cytoskeleton associated protein 4 by DHHC2 regulates antiproliferative factor-mediated signaling. Am Soci Cell Biol 20:1456–1463
40. Yasui Y, Goto H, Matsui S, Manser E, Lim L, Nagata K, Inagaki M (2001) Protein kinase required for segregation of vimentin filaments in mitotic process. Oncogene 20:2868–2876
41. Wang L, Zhang J, Banerjee S, Barnes L, Sajja V, Liu Y, Guo B, Du Y, Agarmal MK, Wald DN, Wang Q, Yang J (2010) Sumoylation of vimentin354 is associated with PIAS3 inhibition of glioma cell migration. Oncotarget 1:620–627
42. Hugwil AV (2015) Antigenicity of the tumor-associated antigen vimentin epitope on ectosomes of brain tumor cell. Int J Cancer Res Dev 1:7–13
43. Da Q, Behymer M, Correa JI, Vijayan V, Cruz MA (2014) Platelet adhesion involves a novel interaction between vimentin and von Willebrand factor under high shear stress. Blood 123:2715–2721
44. Glassy MC, Koda K (2002) The nature of an ideal therapeutic human antibody. Expert Opin Biol Ther 2:1–2
45. Lowery J, Guo M, Weitz DA, Kuezmarski E, Goldman RD (2016) Methods for determining the cellular function of vimentin intermidiate filaments. Methods Enzymol 568:391–421
46. Lam FW, Da Q, Guillory B, Cruz MA (2018) Recombinant human vimentin binds to P-selectin and blocks neutrophil capture and rolling on platelets and entothelium. J Immunol 200:1718–1726
47. Mukerjee S, McKnight M, Glassy M (1998) Immnoscreening protocols for the identification of clinically useful antibodies and antigens. Expert Opin Investig Drugs 7:373–389

Chapter 20

A Method to Detect the Binding of Hyper-Glycosylated Fragment Crystallizable (Fc) Region of Human IgG1 to Glycan Receptors

Patricia Blundell and Richard Pleass

Abstract

Engineering the fragment crystallizable (Fc) of human IgG can bring improved effector functions to monoclonal antibodies and Fc-fusion-based medicines and vaccines. Such Fc-effector functions are largely controlled by posttranslational modifications (PTMs) within the Fc, including the addition of glycans that introduce structural and functional heterogeneity to this class of therapeutic. Here, we describe a detailed method to allow the detection of hyper-sialylated Fcs to glycan receptors that will facilitate the future development of new mAbs and Fc-fragment therapies and vaccines.

Key words IgG, Glycans, Glycosylation, Fc-receptors, ADCC, ADCP, CDC, Effector function, Therapeutic antibodies

1 Introduction

Immunoglobulin G (IgG) antibodies are glycosylated at asparagine 297 (Asn-297) of the unique N-linked sequon located within the Fc [1, 2]. The Fc glycans attached at Asn-297 are typically biantennary complex types, exhibiting high levels of fucosylation of the core GlcNAc residue, partial galactosylation, and bisecting GlcNAc, and of these structures less than 20% are sialylated [3]. The low levels of branching and terminal structures, such as sialic acid, are a consequence of constraints imposed on Asn-297 glycan processing by the Fc protein backbone [4, 5].

The composition of glycans attached at Asn-297 significantly effects Fc-mediated interactions with different receptors [3], and multiple lines of evidence have shown that glycosylation is critical to driving either the anti- or pro-inflammatory capability of IgG [6]. Glycosylation of Asn-297 in the Fc is thus essential for interactions with type 1 receptors (Fcγ) and type 2 receptors (glycan dependent) and is also necessary for driving interactions with the

Michael Steinitz (ed.), *Human Monoclonal Antibodies: Methods and Protocols*, Methods in Molecular Biology, vol. 1904, https://doi.org/10.1007/978-1-4939-8958-4_20,

complement cascade [1]. Although protocols are essentially well described for detecting interactions with type I Fcγ-receptors, detailed protocols for the detection of such reagents to type 2 glycan receptors are less commonly described in the literature.

In humans, infusion of Fc-fragments is sufficient to ameliorate idiopathic thrombocytopenic purpura (ITP) in children, demonstrating the therapeutic utility of the Fc in vivo [7]. The anti-inflammatory property of the Fc is lost after deglycosylation of IgG, and a small population of IgG-bearing sialylated Fcs has been identified as making a significant contribution to the control of inflammation in animal models [8–10]. Higher levels of sialylation also lead to longer serum retention times [11, 12], and studies in humans and mice have shown that influx and efflux of IgG into the central nervous system (CNS) is glycan and sialic acid dependent [13–15]. Consequently, IgG-Fc sialylation has emerged as an important but controversial concept for regulating anti-inflammatory activity of antibodies and Fc-fragments [6].

Methods to enhance the sialylation of the Fc have largely focused on modifications to Asn-297 attached glycans [8, 16]. We have previously shown how Asn-297 limited approaches can be overcome through the introduction of additional N-linked glycosylation sites into a limited number of exposed areas within the IgG1-Fc fragment [17]. For example, insertion of a N-terminal hinge-distal glycan site (N221) significantly increases sialylation allowing engagement with glycan-receptors not previously known to bind the Fc [17]. By adding a cysteine-silenced 18 amino-acid C-terminal extension containing an additional N-linked site (N563), further glycan complexity can also be brought to the IgG1-Fc (Fig. 1).

We provide a detailed protocol for the detection of glycan modified IgG1-Fc fragments containing one, two or three additional N-linked glycans to glycan receptors by enzyme-linked immunosorbent assays (ELISA).

2 Materials

Coating buffer: 0.05 M carbonate-bicarbonate solution, pH 9.6.

Incubation and wash buffer: TMS solution (20 mM Tris–HCl, 150 mM NaCl, 2 mM $CaCl_2$, 2 mM $MgCl_2$).

Blocking buffer: TMS solution containing 5% bovine serum albumin.

Developing solution: Sigmafast p-Nitrophenyl phosphate tablet dissolved in Tris-buffer solution provided.

Glycan receptors: 50 μg lyophilized histidine-tagged recombinant Siglec-1 (R&D Systems) or Siglec-4/MAG (Sinobiologicals) were reconstituted to 100 μg/ml with ddH_2O.

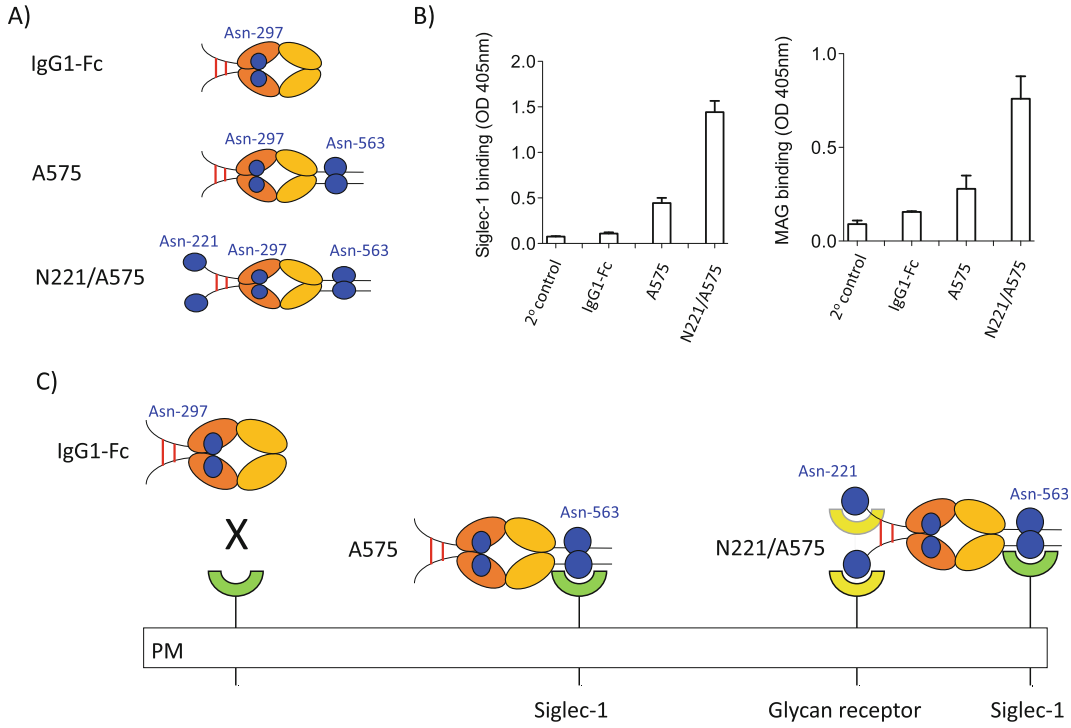

Fig. 1 Detection of hyper-sialylated Fc-fragment binding to glycan receptors by ELISA. (**a**) Fc-fragments containing one, two, or three N-linked attachment sites together with methods for determining their glycan composition by HILIC-UPLC analysis have been described previously [17]. (**b**) Fc-fragments containing three N-linked glycans (N221/A575) bind more strongly to both Siglec-1 and Siglec-4 (myelin-associated glycoprotein), than Fc-fragments only containing two (A575) or one N-linked sugar (IgG1-Fc control). Error bars represent standard deviations around the mean value, $n = 3$ independent experiments. (**c**) In contrast with the Asn-297 glycan, which is largely buried within the Fc cavity, both Asn-221 and Asn-563 are located at the N- and C-terminal tips of the Fc and, as our data show, would therefore be more accessible for posttranslational modifications by glycan-modifying enzymes that permit A575 and N221/A575 to bind more strongly to sialic-acid dependent receptors [17]

Detecting antibodies: Affinity purified alkaline-phosphatase conjugated F(ab′)$_2$ fragment goat anti-human IgG Fcγ-fragment specific from Jackson Immuno Research or Invitrogen.

1. Precision pipettors and disposable tips to deliver 10–1000 µl.
2. A multi-channel pipette is desirable for large assays.
3. Graduated 100 ml and 1 l cylinders for buffers.
4. Rocking platform.
5. Microplate reader capable of measuring absorbance at 405 nm wavelength.
6. Microplate washer.
7. Data analysis and graphing software.

3 Methods (*See* Notes 1 and 2)

1. Nunc microtiter plates are coated down with recombinant glycan receptors (*see* **Note 1**), typically 100 μl per well at 2–10 μg/ml in carbonate-bicarbonate coating buffer pH 9 and incubated in a fridge overnight at 4 °C.
2. The following day plates are washed five times with excess TSM incubation buffer (1–5 min incubation between washes), prior to blocking for 2 h in 150 μl per well of blocking buffer.
3. Plates are then washed as before.
4. Adding Fc-fragments, the plate is gently tapped onto some tissue paper to empty all remaining liquid from all the wells. Into duplicate wells, 100 μl of varying concentrations of Fc-fragments in incubation buffer are added (*see* **Note 2**). We typically titrate by doubling dilution down the plate Fc-fragments from 50 to 0 μg/ml. Receptors are allowed to bind Fc-fragments overnight at 4 °C.
5. The following day plates are washed five times with excess TSM incubation buffer (1–5 min incubation between washes), prior to the addition of 100 μl per well of alkaline-phosphatase conjugated $F(ab')_2$ goat anti-human IgG Fcγ-fragment-specific detection antibody diluted 1 in 500 in TMS buffer. Glycosylated Fc-fragments bound to glycan receptors are allowed to bind the conjugated antibody for 1 h at room temperature on a rocking platform.
6. Plates are washed as above and developed for 5–15 min with 100 μl/well of developing solution.
7. Read plates at 405 nm wavelength using a LT-4500 microplate absorbance reader (Labtech), and the data plotted with GraphPad Prism (Fig. 1).

4 Notes

1. We have found that this protocol is amenable to the study of many other glycan receptors. However, from our experience we advise determining background binding of the detecting antibody to each glycan receptor first, as the Fab domains within the alkaline-phosphatase conjugated detecting antibody can themselves be glycosylated [18]. For example, we have seen direct binding of both the Jackson and Invitrogen $F(ab')_2$ detecting reagents to Siglec-5, CLEC-1B and DC-SIGNR [17]. Preliminary removal of $F(ab')_2$ associated glycans with glycosidases, e.g., PNGase F (New England Biologicals) may therefore be required for the study of certain receptors.

2. This protocol works equally well for Fc-fragments and Fab'$_2$ fragments (both available from Jackson Immuno Research) that have previously been digested with commercially available glycosidases, e.g., PNGase F, Endo H or neuraminidase. For example, Siglec-5 binding above is lost after neuraminidase treatment.

References

1. Czajkowsky DM, Hu J, Shao Z et al (2012) Fc-fusion proteins: new developments and future perspectives. EMBO Mol Med 4:1015–1028
2. Lund J, Takahashi N, Pound JD et al (1996) Multiple interactions of IgG with its core oligosaccharide can modulate recognition by complement and human Fcy receptor I and influence the synthesis of its oligosaccharide chains. J Immunol 157:4963–4969
3. Dalziel M, Crispin M, Scanlan CN et al (2014) Emerging principles for the therapeutic exploitation of glycosylation. Science 343:1235681. https://doi.org/10.1126/science.1235681
4. Frank M, Walker RC, Lanzilotta WN et al (2014) Immunoglobulin G1 Fc domain motions: implications for Fc engineering. J Mol Biol 426:1799–1811
5. Subedi GP, Hanson QM, Barb AW (2014) Restricted motion of the conserved immunoglobulin G1 N-glycan is essential for efficient Fc g RIIIa binding. Structure 22:1478–1488
6. Schwab I, Nimmerjahn F (2013) Intravenous immunoglobulin therapy: how does IgG modulate the immune system? Nat Rev Immunol 13:176–189
7. Debre M, Bonnet MC, Fridman WH et al (1993) Infusion of Fc gamma fragments for treatment of children with acute immune thrombocytopenic purpura. Lancet 342:945–949
8. Washburn N, Schwab I, Ortiz D et al (2015) Controlled tetra-Fc sialylation of IVIg results in a drug candidate with consistent enhanced anti-inflammatory activity. Proc Natl Acad Sci U S A 112:E1297–E1306
9. Anthony RM, Kobayashi T, Wermeling F et al (2011) Intravenous gammaglobulin suppresses inflammation through a novel T(H)2 pathway: commentary. Nature 475:110–113
10. Anthony RM, Wermeling F, Karlsson MCI et al (2008) Identification of a receptor required for the anti-inflammatory activity of IVIG. Proc Natl Acad Sci U S A 105:19571–19578
11. Liu L (2015) Antibody glycosylation and its impact on the pharmacokinetics and pharmacodynamics of monoclonal antibodies and Fc-fusion proteins. J Pharm Sci 104:1866–1884
12. Li H, Sethuraman N, Stadheim TA et al (2006) Optimization of humanized IgGs in glycoengineered Pichia pastoris. Nat Biotechnol 24:210–215
13. St-Amour I, Pare I, Alata W et al (2013) Brain bioavailability of human intravenous immunoglobulin and its transport through the murine blood–brain barrier. J Cereb Blood Flow Metab 33:1983–1992
14. Finke JM, Ayres KR, Brisbin RP et al (2017) Antibody blood-brain barrier efflux is modulated by glycan modification. Biochim Biophys Acta 1861:2228–2239
15. Zhang G, Lopez PHH, Li CY et al (2004) Anti-ganglioside antibody-mediated neuronal cytotoxicity and its protection by intravenous immunoglobulin: implications for immune neuropathies. Brain 127:1085–1100
16. Fiebiger BM, Maamary J, Pincetic A et al (2015) Protection in antibody- and T cell-mediated autoimmune diseases by antiinflammatory IgG Fcs requires type II FcRs. Proc Natl Acad Sci 112:E2385–E2394. https://doi.org/10.1073/pnas.1505292112
17. Blundell PA, Le NPL, Allen J et al (2017) Engineering the fragment crystallizable (Fc) region of human IgG1 multimers and monomers to fine-tune interactions with sialic acid-dependent receptors. J Biol Chem 292:12994–13007
18. van de Bovenkamp FS, Hafkenscheid L, Rispens T et al (2016) The emerging importance of IgG Fab glycosylation in immunity. J Immunol 196:1435–1441

Chapter 21

A Cell-Based Reporter Assay Measuring the Activation of Fc Gamma Receptors Induced by Therapeutic Monoclonal Antibodies

Michihiko Aoyama, Minoru Tada, and Akiko Ishii-Watabe

Abstract

Fc gamma receptors (FcγRs) are expressed on the surface of various immune cells, and the interactions between FcγRs and the Fc region of immunoglobulin G are involved in the activation of immune cells by antigen-bound antibodies. Fc-mediated immune-cell activations are related to both the efficacy and the safety of therapeutic monoclonal antibodies. It is indispensable to elucidate the Fc-mediated functions in the development of therapeutic monoclonal antibodies. Here, we describe a cell-based assay using FcγR-expressing reporter cell lines that can be used to evaluate the human FcγR-activation properties of therapeutic monoclonal antibodies by a rapid and simple procedure.

Key words Cell-based reporter assay, Fc gamma receptor, Effector function, Therapeutic monoclonal antibody, Antibody Fc region

1 Introduction

The Fc region of immunoglobulin G (IgG) is recognized by Fc gamma receptors (FcγRs) on the surface of various immune cells, and the interactions between FcγRs and the Fc region induce the activation of immune cells [1]. The activation of FcγRs plays a critical role in antibody effector functions including antibody-dependent cellular cytotoxicity (ADCC), which is one of the most important mechanisms of action of therapeutic monoclonal antibodies (mAbs) targeting tumor cells [2]. Fc engineering technologies by amino acid substitutions [3–5] or glycoform modifications [6–8] that are intended to enhance the binding of mAbs to FcγRs have been advanced for tumor-targeting therapeutic mAbs. However, a concern is that FcγR-mediated activations of immune cells are related to immune-mediated adverse reactions such as infusion reactions [9–11]. Thus, the evaluation of FcγR-activation

Michael Steinitz (ed.), *Human Monoclonal Antibodies: Methods and Protocols*, Methods in Molecular Biology, vol. 1904, https://doi.org/10.1007/978-1-4939-8958-4_21,

properties of mAbs is critical for assessing the efficacy and safety profiles of therapeutic mAbs, especially novel Fc-engineered mAbs.

The human FcγR family consists of four types of activating FcγRs (FcγRI, FcγRIIa, FcγRIIIa, and FcγRIIIb) and an inhibitory FcγR (FcγRIIb). Human FcγRs have different structures, binding affinities, and specificity to each human IgG subclass, and their expression profiles in immune cells differ from each other [1, 12]. Because the characteristics of the members of the FcγR family differ greatly between humans and other mammals, it is difficult to extrapolate the results of nonclinical studies using experimental animals to clinical studies. Therefore, human primary cells (e.g., human peripheral blood mononuclear cells [hPBMCs] or natural killer [NK] cells for ADCC) are generally used for the cell-based assays evaluating the Fc-mediated functions of therapeutic mAbs. The use of human primary cells provides advantages in that (1) the cells are available from multiple donors (which enables the evaluation of the inter-individual variability of responses), (2) various immune cells are included, and (3) the cells' responses are expected to be closer to physiological conditions. However, there are also disadvantages of using human primary cells; e.g., poor reproducibility, complicated handling, ethical issues when using cells from volunteers, and the high cost of using commercially available PBMCs.

To overcome these disadvantages, cell-based assays using FcγR-expressing reporter cell lines have been developed and used as a surrogate for ADCC or antibody-dependent cellular phagocytosis (ADCP) assays [13, 14]. In these assays, antigen-expressing target cells and FcγR-expressing reporter cells are cocultured in the presence of mAbs, and the activation of FcγRs by antigen-bound mAbs can be measured as reporter gene activity. An assay using FcγR-expressing reporter cell lines has advantages in that the activation of a specific type of FcγRs expressing on the reporter cells can be simply evaluated with high reproducibility and robustness.

We recently developed a cell-based FcγR reporter assay that does not use target cells for the evaluation of FcγR-activation properties independently of the antigen-binding properties of mAbs or antigen-expression levels in target cells. In this assay, FcγR-expressing reporter cells are cultured in a 96-well plate where mAbs are captured on the plate by immobilized Protein L (Figs. 1 and 2). Our study demonstrated that (1) the FcγRIIIa-activation properties of Fc-engineered mAbs measured by this method were correlated with the release of inflammatory cytokines and chemokines from hPBMCs [15], and (2) our new assay is a promising tool for evaluating and predicting the activation of human immune cells by an antibody Fc region.

In this chapter, we provide the protocol of our cell-based FcγR reporter assay along with the Protein L-immobilized method and important details for performing the assay successfully.

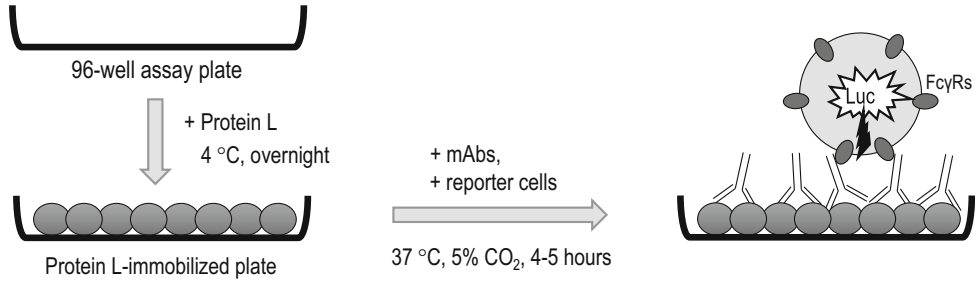

Fig. 1 Overview of the assay. Protein L solution is added to the wells of a 96-well assay plate. The plate is incubated at 4 °C overnight to immobilize Protein L at the well surface. After the solution is removed, mAbs and reporter cells are added to each well and incubated for 4–5 h at 37 °C in 5% CO_2. The mAbs are captured by immobilized Protein L in a constant orientation which may mimic the antigen-bound form. The reporter cells are activated via the crosslinking of the FcγRs by the Fc region of the mAbs, resulting in the expression of NFAT-driven luciferase reporter

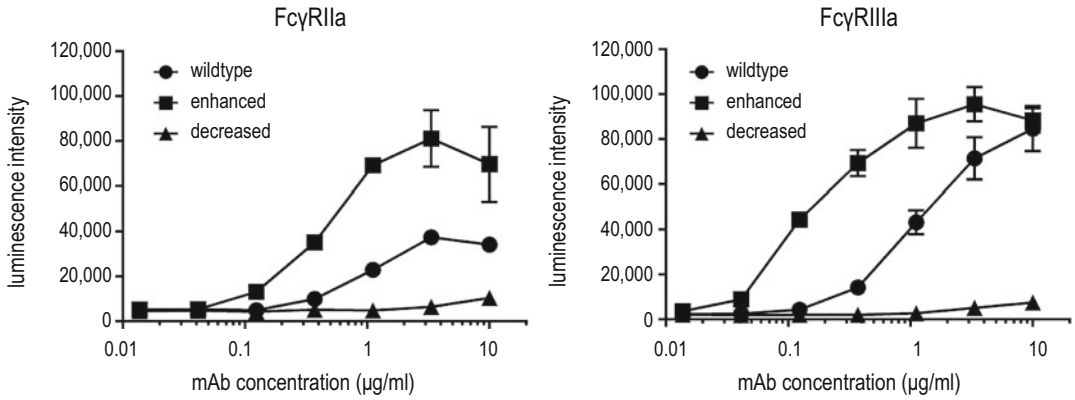

Fig. 2 FcγR-activation properties of Fc-engineered anti-CD20 mAbs. FcγRIIa and FcγRIIIa activation properties of anti-CD20 mAbs were measured by the cell-based FcγR reporter assay with the Protein L-immobilized method. The reporter cells, Jurkat/FcγRIIa/NFAT-Luc or Jurkat/FcγRIIIa/NFAT-Luc, were cultured in the presence of serially diluted anti-CD20 mAbs on the Protein L-immobilized plate for 4 h. The differences in FcγR activation properties among three anti-CD20 mAbs with different FcγR-binding affinities were detected by this method: the "enhanced" mutant with G236A/S239D/I332E substitutions which binds FcγRIIa and FcγRIIIa with higher affinity than the wild type showed a greatly enhanced activation of FcγRIIa and FcγRIIIa compared to the wild type, and the "decreased" mutant with L234A/L235A substitutions which hardly binds FcγRs showed a remarkably decreased activation of FcγRIIa and FcγRIIIa. The data are mean ± SEM ($n = 3$)

2 Materials

1. FcγR-expressing reporter cells: Jurkat cells stably expressing NFAT-driven luciferase reporter gene and human FcγRIIa (Jurkat/FcγRIIa/NFAT-Luc) or FcγRIIIa (Jurkat/FcγRIIIa/NFAT-Luc) were established in our laboratory [14, 15].
2. Cell culture medium: RPMI1640 medium supplemented with 10% heat-inactivated fetal bovine serum (FBS).

3. Phosphate-buffered saline (PBS).
4. To make 20 μg/mL of Protein L solution: Dissolve 1 mg of recombinant Protein L in 500 μL of PBS and store at −20 °C. Dilute 50 μL of stocked Protein L solution with 5 mL of PBS before use.
5. The 96-well Maxisorp plate: F16 Black MAXISORP FLUORONUNC CERT (Thermo).
6. Plate seal.
7. Opti-MEM I Reduced Serum Medium (Thermo).
8. Luciferase assay reagent: Thaw ONE-Glo™ Luciferase Assay Buffer and ONE-Glo™ Luciferase Assay Substrate, which are the components of ONE-Glo™ Luciferase Assay System (Promega), at room temperature and mix just before the luciferase assay.
9. The 96-well plate for luminescence measurement: OptiPlate-96 White (PerkinElmer).
10. Plate reader for performing luminescence measurement.

3 Methods

3.1 Preparation of FcγR-Expressing Reporter Cells

1. Culture FcγR-expressing reporter cells with cell culture medium at 37 °C in 5% CO_2 (*see* **Note 1**).
2. On the day of the assay, harvest the cells by centrifuging at 250 × *g* for 5 min and resuspend the cells with Opti-MEM I Reduced Serum Medium (*see* **Note 2**).
3. Count the number of viable cells and adjust the cell density at 1.1×10^6 cells/mL in Opti-MEM I Reduced Serum Medium (*see* **Note 3**).

3.2 Preparation of the Protein L-Immobilized Assay Plate

1. One day before the assay, add 50 μL of 20 μg/mL Protein L solution to each well of a 96-well Maxisorp plate and seal the plate (*see* **Notes 4** and **5**).
2. Incubate the plate at 4 °C overnight to immobilize the Protein L on the surface of the wells.
3. Discard the Protein L solution and wash each well with 100 μL of sterile PBS (*see* **Note 6**).

3.3 Assay

1. Prepare serially diluted mAb solution in sterile PBS (*see* **Notes 7–9**).
2. Seed 90 μL of 1.1×10^6 cells/mL suspension of FcγR-expressing reporter cells in each well of the Protein L-immobilized assay plate (approx. 1×10^5 cells/well).

3. Add 10 μL of the serially diluted mAb solution to each well, and seal the plate.
4. Incubate the plate for 4–5 h at 37 °C, 5% CO_2.
5. After the incubation, add 100 μL of Luciferase assay reagent and mix well by pipetting to completely lyse the cells (*see* **Notes 10** and **11**).
6. Transfer 150 μL of the mixture to another 96-well plate for luminescence measurement.
7. Measure luminescence by using a plate reader.
8. Plot the luminescence intensity against the logarithm concentration of the mAbs.

4 Notes

1. Maintain the cells to keep the cell density at 0.3–1.5 × 10^6 cells/mL.
2. The presence of bovine IgGs from FBS in the assay mixture may interfere with the binding between the FcγRs and mAbs. The cells should be suspended in serum-free medium.
3. Confirm that the viability of the cells is >80% by the trypan blue exclusion method or a similar method.
4. The direct immobilization of the mAbs to a polystyrene plate is one of the most well-characterized methods for evaluating the mAb-induced cytokine release from human PMBCs or whole blood, and this method has been used for evaluating the agonistic activities of mAbs to immune-cell surface antigens [16]. However, we found that the direct immobilization method could not detect a difference in FcγR activation properties of Fc-engineered mAbs. We suspected that mAbs directly immobilized on the plate surface are non-physiologically presented in a random orientation which does not reflect the antigen-bound form of mAbs. The mAbs-capturing method using immobilized Protein L has an advantage in that mAbs are captured in a constant orientation which may mimic the antigen-bound form, because Protein L binds a specific region in light chains of mAbs (Fig. 1).
5. The bottom of the wells should be fully covered with Protein L solution, because a heterogeneous immobilization of Protein L may induce variability among the wells.
6. Residual Protein L in solution may inhibit the capturing of mAbs to the plate. When discarding the Protein L solution and PBS in the washing step, remove the solution completely by aspiration or by beating the plate against thick paper towel.

Be careful not to leave the plate in the dry condition for long time.

7. Because Protein L binds to kappa light chain but not to lambda light chain, mAbs with lambda light chain cannot be used in this assay.
8. The concentration of the mAb solution prepared in this step should be tenfold the final concentration in the assay.
9. The dose-response relationship in this assay sometimes shows a bell-shaped curve. Thus, we strongly recommend designing the assay so that appropriate dose-response curves can be obtained. An assay with a single dose or a few dose levels may result in a misinterpretation of the estimation of FcγR-mediated biological activities of the mAb.
10. Luciferase assay reagent should be equilibrated to room temperature before adding it to the cells.
11. The number of repeats in the pipetting should be kept constant between the wells.

References

1. Nimmerjahn F, Ravetch JV (2008) Fcgamma receptors as regulators of immune responses. Nat Rev Immunol 8(1):34–47. https://doi.org/10.1038/nri2206
2. Weiner LM, Surana R, Wang S (2010) Monoclonal antibodies: versatile platforms for cancer immunotherapy. Nat Rev Immunol 10 (5):317–327. https://doi.org/10.1038/nri2744
3. Shields RL, Namenuk AK, Hong K, Meng YG, Rae J, Briggs J, Xie D, Lai J, Stadlen A, Li B, Fox JA, Presta LG (2001) High resolution mapping of the binding site on human IgG1 for Fc gamma RI, Fc gamma RII, Fc gamma RIII, and FcRn and design of IgG1 variants with improved binding to the Fc gamma R. J Biol Chem 276(9):6591–6604. https://doi.org/10.1074/jbc.M009483200
4. Lazar GA, Dang W, Karki S, Vafa O, Peng JS, Hyun L, Chan C, Chung HS, Eivazi A, Yoder SC, Vielmetter J, Carmichael DF, Hayes RJ, Dahiyat BI (2006) Engineered antibody Fc variants with enhanced effector function. Proc Natl Acad Sci U S A 103(11):4005–4010. https://doi.org/10.1073/pnas.0508123103
5. Strohl WR (2009) Optimization of Fc-mediated effector functions of monoclonal antibodies. Curr Opin Biotechnol 20 (6):685–691. https://doi.org/10.1016/j.copbio.2009.10.011
6. Iida S, Misaka H, Inoue M, Shibata M, Nakano R, Yamane-Ohnuki N, Wakitani M, Yano K, Shitara K, Satoh M (2006) Nonfucosylated therapeutic IgG1 antibody can evade the inhibitory effect of serum immunoglobulin G on antibody-dependent cellular cytotoxicity through its high binding to FcgammaRIIIa. Clin Cancer Res 12(9):2879–2887. https://doi.org/10.1158/1078-0432.CCR-05-2619
7. Thomann M, Schlothauer T, Dashivets T, Malik S, Avenal C, Bulau P, Ruger P, Reusch D (2015) In vitro glycoengineering of IgG1 and its effect on Fc receptor binding and ADCC activity. PLoS One 10(8):e0134949. https://doi.org/10.1371/journal.pone.0134949
8. Dekkers G, Treffers L, Plomp R, Bentlage AEH, de Boer M, Koeleman CAM, Lissenberg-Thunnissen SN, Visser R, Brouwer M, Mok JY, Matlung H, van den Berg TK, van Esch WJE, Kuijpers TW, Wouters D, Rispens T, Wuhrer M, Vidarsson G (2017) Decoding the human immunoglobulin G-glycan repertoire reveals a spectrum of Fc-receptor- and complement-mediated-effector activities. Front Immunol 8:877. https://doi.org/10.3389/fimmu.2017.00877
9. Pichler WJ (2006) Adverse side-effects to biological agents. Allergy 61(8):912–920. https://doi.org/10.1111/j.1398-9995.2006.01058.x
10. Okuyama A, Nagasawa H, Suzuki K, Kameda H, Kondo H, Amano K, Takeuchi T (2011) Fcgamma receptor IIIb polymorphism

and use of glucocorticoids at baseline are associated with infusion reactions to infliximab in patients with rheumatoid arthritis. Ann Rheum Dis 70(2):299–304. https://doi.org/10.1136/ard.2010.136283

11. Jonsson F, Mancardi DA, Zhao W, Kita Y, Iannascoli B, Khun H, van Rooijen N, Shimizu T, Schwartz LB, Daeron M, Bruhns P (2012) Human FcgammaRIIA induces anaphylactic and allergic reactions. Blood 119 (11):2533–2544. https://doi.org/10.1182/blood-2011-07-367334
12. Rosales C (2017) Fcgamma receptor heterogeneity in leukocyte functional responses. Front Immunol 8:280. https://doi.org/10.3389/fimmu.2017.00280
13. Parekh BS, Berger E, Sibley S, Cahya S, Xiao L, LaCerte MA, Vaillancourt P, Wooden S, Gately D (2012) Development and validation of an antibody-dependent cell-mediated cytotoxicity-reporter gene assay. MAbs 4 (3):310–318. https://doi.org/10.4161/mabs.19873
14. Tada M, Ishii-Watabe A, Suzuki T, Kawasaki N (2014) Development of a cell-based assay measuring the activation of FcgammaRIIa for the characterization of therapeutic monoclonal antibodies. PLoS One 9(4):e95787. https://doi.org/10.1371/journal.pone.0095787
15. Takakura M, Tada M, Ishii-Watabe A (2017) Development of cell-based assay for predictively evaluating the FcgammaR-mediated human immune cell activation by therapeutic monoclonal antibodies. Biochem Biophys Res Commun 485(1):189–194. https://doi.org/10.1016/j.bbrc.2017.02.050
16. Findlay L, Eastwood D, Stebbings R, Sharp G, Mistry Y, Ball C, Hood J, Thorpe R, Poole S (2010) Improved in vitro methods to predict the in vivo toxicity in man of therapeutic monoclonal antibodies including TGN1412. J Immunol Methods 352(1–2):1–12. https://doi.org/10.1016/j.jim.2009.10.013

Chapter 22

"BIClonals": Production of Bispecific Antibodies in IgG Format in Transiently Transfected Mammalian Cells

Dana Litvak-Greenfeld, Lilach Vaks, Stav Dror, Limor Nahary, and Itai Benhar

Abstract

Bispecific antibodies (bsAbs) are antibodies with two binding sites directed at different antigens, enabling therapeutic strategies not possible with conventional monoclonal antibodies (mAbs). Since bispecific antibodies are regarded as promising therapeutic agents, many different bispecific design modalities have been evaluated. Many of these are based on antibody fragments or on inclusion of non-antibody components. For some therapeutic applications, full-size, native IgG-like bsAbs may be the optimal format.

To prepare bsAbs in IgG format, two challenges should be met. One is that each heavy chain will only pair with the heavy chain of the second specificity and that heavy chain homodimerization will be prevented. The second is that each heavy chain will only pair with the light chain of its own specificity and that pairing with the light chain of the second specificity will be prevented. The first solution to the first criterion (known as knobs into holes, KIH) was presented in 1996 by Genentech and additional solutions were presented more recently. However, until recently, out of >120 published formats, only a handful of solutions for the second criterion that make it possible to produce a bispecific IgG by a single expressing cell were suggested.

Here, we present a protocol for preparing bsAbs in IgG format in transfected mammalian cells. For heavy chain dimerization we use KIH while as a solution for the second challenge—correct pairing of heavy and light chains of bispecific IgGs we present our "BIClonals" technology; an engineered (artificial) disulfide bond between the antibodies' variable domains that asymmetrically replaces the natural disulfide bond between CH1 and CL.

During our studies of bsAbs we found that H-L chain pairing seems to be driven by V_H-V_L interfacial interactions that differ between different antibodies; hence, there is no single optimal solution for effective and precise assembly of bispecific IgGs that suits every antibody sequence, making it necessary to carefully evaluate the optimal solution for each new antibody.

Key words CDR, Complementarity-determining region, dsFv, Disulfide-stabilized Fv fragment, H, An IgG heavy chain, KIH, Knobs-into-holes, L, An IgG light chain, mAb, Monoclonal antibody, V_H, Variable domain of the heavy chain, V_L, Variable domain of the light chain

Dana Litvak-Greenfeld and Lilach Vaks contributed equally to this work.

Michael Steinitz (ed.), *Human Monoclonal Antibodies: Methods and Protocols*, Methods in Molecular Biology, vol. 1904, https://doi.org/10.1007/978-1-4939-8958-4_22,

1 Introduction

Therapeutic monoclonal antibodies (mAbs) are the leading class of biopharmaceutical (biologics) that offer exciting opportunities to the biomedical and biotechnological communities [1, 2]. While mAbs are a symmetric immunoglobulin with two identical heavy chains, each covalently bound to one of two identical light chains, bsAbs are non-symmetric, have two different heavy chains, each bound to a different light chain. Consequently, mAbs are bivalent and monospecific while bsAbs are monovalent and bind two different antigens (or epitopes) [3, 4]. As such, bsAbs offer unique opportunities that may overcome some limitations of existing therapeutic mAbs such as co-clustering of cell-surface receptors or targeting immune effector cells to kill cancer cells [5, 6].

There are many designs and formats of bsAbs, the number of which now exceeds 120 [7, 8]. Many of the bsAb designs involve linking small monospecific antibody fragments in tandem [9]. Although such small fragments are currently leading the clinical development of bsAbs, they have some limitations (that are inherent for small antibody fragments) in stability, solubility, and pharmacokinetic properties [3, 10]. Thus, it is expected that bsAbs of the IgG format will increasingly become more common [6, 11–13]. Existing approaches for producing native IgG-like bsAbs also have limitations. Some solutions involve using two different heavy chains with a common light chain [14]. Other solutions involve assembling half antibodies in vitro to be combined later to an IgG format, and other solutions involve extensive engineering of the Fab arm interface [15], or require non-natural crossing over of heavy and light chains [13]. Antibodies with different variable domain sequences assemble with varying efficiency when expressed as bsAbs, and the choice of the optimal design is not a trivial mission [7]. We present the "BIClonals" technology as a rapid and simple approach for production of bsAbs of IgG format.

To efficiently produce a bsAb in a native IgG format, two challenges should be met; one is that each heavy chain will only pair with the heavy chain of the other specificity (H-H heterodimerization) and that homodimerization will be inhibited. The second is that in the Fab arm interface, it is required that each heavy chain will only pair with its cognate light chain and will not pair with the light chain of the other specificity.

Here, we present a protocol for the production of bsAbs in IgG format in transiently-transfected mammalian cells. According to our design, H-H heterodimerization is facilitated by the KIH approach [14], while for correct H-L pairing we use our "BIClonals" approach [16], for the efficient engineering of the Fab arm interface of bispecific IgGs. Our design involves eliminating in one

of the Fab arms the native disulfide bond between the heavy and light chain and replacing it with an artificial disulfide bond between interfacial positions of the V_H and V_L domains. The second Fab arm is not modified (wild-type, WT). Our "BIClonals" design was found to work with murine, humanized, and human variable domains and both with (κ) and Lambda (λ) light chains. So far, we produced only antibodies of the human IgG1 heavy chain isotype. It minimally deviates from a native IgG format as, in addition to the six point mutations in CH3 required for KIH, it involves only four point mutations in the Fab arm interface of one side of the bispecific IgG.

2 Materials (See Note 1)

2.1 General Buffers and Reagents

1. Phosphate-buffered saline (PBS): 8 g NaCl, 0.2 g KCI, 1.44 g NaH_2PO_4, 0.24 g KH_2PO_4 per 1 l, pH 7.4. (Merck & co., Inc.).
2. Phosphate buffer for column loading: NaH_2PO_4 0.2 M Na_2HPO_4 0.2 M mix at 20:80 ratio to obtain pH 7.4. Dilute ×20 into the filtered conditioned media before loading the affinity columns.
3. MabSelect Elution buffer: 0.1 M citric acid, pH 3.5.
4. KappaSelect Elution buffer: 0.1 M glycine buffer, pH 2.5–3.0.
5. LambdaSelect Elution buffer 0.1 M acetate buffer, pH 3.5.
6. MabSelect/KappaSelect/LambdaSelect Neutralization buffer: 1.5 M Tris–HCl pH 8.8, 150mM NaCl.

2.2 Bacteria Growth Media and Antibiotics

These may be purchased from any supplier of common bacterial growth medium components or pre-prepared media. In our lab we use products of Becton-Dickinson.

1. LB: 10 g Bacto-Tryptone, 5 g Yeast extract, 10 g NaCl/l water. Sterilized by autoclaving. To prepare solid media, add Bacto-agar to the final concentration of 1.8% to the solutions. Following autoclaving and cooling to about 50 °C, supplement the media with 0.4% Glucose and antibiotics and pour the plates.
2. Ampicillin (Roche Diagnostics): Stock solution: 100 mg/ml in water. Store at −20 °C. Recommended working concentration 200 μg/ml.
3. D(+)-Glucose CAS-No: 50-99-7 Merck. Make 40% solution and filter-sterilize using a 0.22 μm filter.
4. Glycerol (Merck). For easy pipetting, prepare an 80% solution and sterilize by autoclaving.

2.3 Construction of pcDNA3.4 Expression Vectors

The expression of a bispecific IgG requires co-introduction of four plasmids into the transfected cells, one for each heavy chain and one for each light chain.

1. The plasmid vectors are based on the CMV promoter-controlled pcDNA3.4 vectors that are provided as the "Antibody Expressing Positive Control Vector" part of the Life Technologies Expi293™ kit for transient transfection-based expression. Sequences of antibody heavy and light chains are cloned into separate vectors as described in the Subheading 3 (*see* **Note 2**).
2. Primers

   CMV-seq-FOR 5′ CTCTAGCGAATTCCCTCTAGACAC.
   CMV-seq-REV 5′ GTAATCCAGAGGTTGATTGTCG.
3. Gibson assembly mix (New England Biolabs).
4. *Dpn*I restriction enzyme (required to digest vector fragments during Gibson assembly) (New England Biolabs): Required for elimination of vector DNA during Gibson assembly.
5. ZymoClean Gel Extraction kit for the isolation of DNA fragments for Gibson assembly.
6. Thermo Scientific Phusion Green High-Fidelity DNA Polymerase. For amplifying DNA fragments required for Gibson assembly of plasmid vectors.
7. Bacteria strains: *E coli* DH5α strain or XL-1 blue (GibcoBRL, Life Technologies (http://www.lifetechnologies.com)) chemically or electro-competent, used for cloning.
8. Ampicillin antibiotic solution (*see* Subheading 2.2).
9. Bacterial growth media: LB (*see* Subheading 2.2).
10. Invitrogen PureLink™ HiPure Plasmid Miniprep Kit (provides highly pure DNA which in our hands works very well in DNA sequencing and in transfection).
11. Electroporation Cuvettes 2 mm Cat no—EP-102 cell projects.
12. Electroporator.

2.4 Expi293™ Kit

The Expi293™ Expression System is a major advance in transient expression technology for rapid and ultra-high-yield protein production from mammalian cells. This, or a similar high-yield transient transection system for HEK293 cells, should be used according to the instructions of the supplier.

2.5 SDS-PAGE Electrophoresis and Immunoblotting

1. Any commercially available SDS/PAGE mini-gel system, including electrophoresis apparatus, blotting apparatus, Sample buffer (reducing and non-reducing), Running buffer, and Blotting buffer. We use the BIO-RAD system. You may

purchase ready-to-use gels (10% or 4–20% gradient) or prepare your own gels.

2. Thermo Scientific GelCode Blue™ Stain Reagent.
3. Nitrocellulose transfer membranes for immunoblotting.
4. HRP-conjugated antibodies:
   (a) Peroxidase AffiniPure Goat Anti-Human IgG (H+L).
   (b) HRP-conjugated Goat anti-Human Kappa Light Chain Secondary Antibody.
   (c) HRP-conjugated Goat anti-Human Lambda Light Chain Secondary Antibody.
5. SuperSignal West Pico Chemiluminescent Substrate (Thermo Scientific).
6. X-ray film for Western blots or a suitable CCD camera-based imaging system.

2.6 Purification of bsAbs Using Affinity Chromatography (See Note 3)

1. MabSelect 1 ml column (GE, gelifesciences Or Blossombio).
2. KappaSelect 1 ml column (GE, Gelifesciences).
3. LambdaSelect 1 ml column (GE Gelifesciences).
4. PD-10 desalting columns for buffer exchange (Sigmaaldrich) (*see* **Note 14**).
5. For dialysis: SnakeSkin-Pleated Dialysis tubing (10 kDa cutoff) supplied by Pierce (now Thermo Scientific).
6. For concentration (when required) Centricon (10 kDa cutoff).

3 Methods

The protocol described below provides the description the construction of plasmid vectors, transient transfection of mammalian cells, analysis of bsAb assembly by SDS/PAGE and immunoblotting, and purification of the bsAbs from the conditioned media. This is a rapid protocol—once you have purified the plasmid DNAs, you can purify several mgs of your bsAbs in less than 2 weeks.

3.1 Construction of pcDNA3.4 Plasmids for Expression of Antibody Heavy and Light Chains

The pcDNA3.4 plasmid vectors described herein are for the expression of a bsAb where one arm has a Kappa light chain and is engineered at the Fab arm while the second arm has a Lambda light chain and is not engineered at the Fab arm. Heavy chain heterodimerization is facilitated by "knobs-into-holes" mutations in the CH3 domains of the two heavy chains [14] (*see* **Notes 4** and **5**). The scheme of the antibody chains that are assembled to a bsAb is shown in Fig. 1. To prepare the set of four plasmids required to produce a bsAb, carry out the following cloning steps. The sequences of the heavy and light chains of the model antibodies are shown in Table 1.

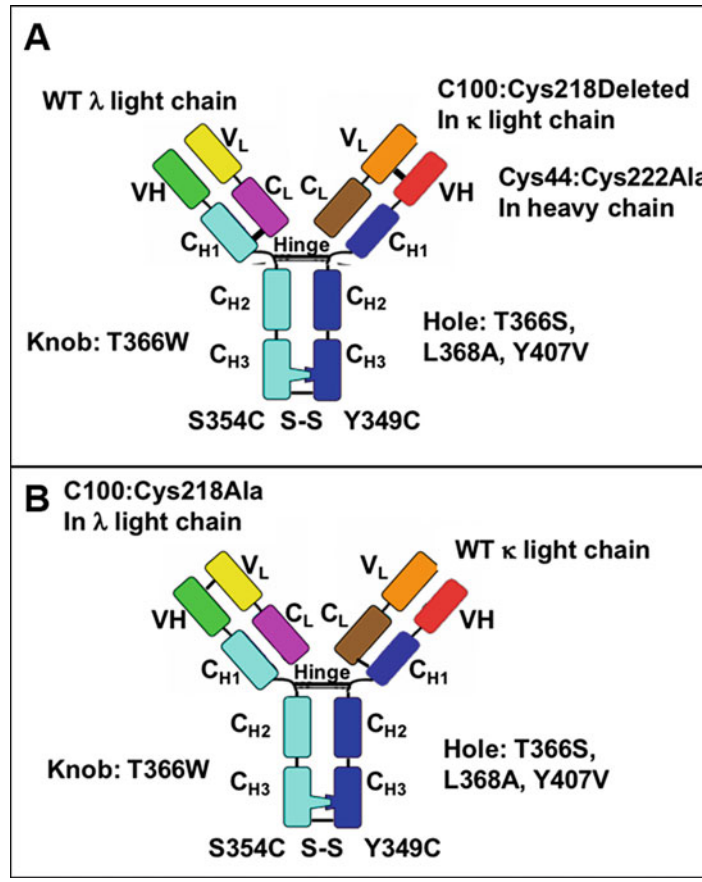

Fig. 1 Schematic representation of bsAbs prepared according to the BIClonals design principles. (**a**) A bsAb with a Kappa light chain in the engineered Fab arm and a Lambda light chain in the WT Fab arm. (**b**) A bsAb with a Lambda light chain in the engineered Fab arm and a Kappa light chain in the WT Fab arm. Heavy chain heterodimerization if provided by the KIH approach [14]

1. First of all, you need to obtain the four prototype plasmids (*see* Fig. 2). After designing them, we suggest ordering them from a certified DNA synthesis company.
2. To prepare the heavy chain vector for the antibody with the engineered Fab arm, use Gibson assembly [17] to replace the V_H of the prototype Knob vector (here it is named **pcDNA3.4-Avastin-VH-(C44)-CH1(C22A)-CH3 (Knob)**) with the V_H of your antibody—carrying the C44 mutation (*see* **Note 6**).
3. To prepare the light chain vector for the antibody with the engineered Fab arm, use Gibson assembly [17] to replace the

Table 1
DNA and amino acid sequences of engineered antibody sequences

Antibody: name and description	DNA sequence	Amino acids sequence
Leader sequence for heavy chain	ATGGAGACTGGGCTGCGCTGGCTTCTCCTG GTCGCTGTGCTCAAAGGTGTCCAGTGT	METGLRWLLLVAVLKGVQC
Anti VEGF antibody Avastin: (IgG1-Kappa) VH domain **G44C** mutation	GAAGTGCAGCTGGTGGAATCCGGCGGAGGC CTGGTGCAGCCTGGCGGCTCTCTGAGACTG TCTTGCGCCGCCTCCGGCTACACCTTCACC AACTACGGCATGAACTGGGTCCGACAGGCC CCTGGCAAG**TGC**CTGGAATGGGTCGGATGG ATCAACACCTACACCGGCGAGCCCACCTAC GCCGCCGACTTCAAGCGGCGGTTCACCTTC TCCCTGGACACCTCCAAGTCCACCGCCTAC CTGCAGATGAACTCCCTGCGGGCCGAGGAC ACCGCCGTGTACTACTGCGCCAAGTACCCC CACTACTACGGCTCCTCCCACTGGTACTTC GACGTGTGGGGCCAGGGCACCCTGGTCACC GTGTCATCT	EVQLVESGGGLVQPGGSLRL SCAASGYTFTNYGMNWVRQA PGK**C**LEWVGWINTYTGEPTY AADFKRRFTFSLDTSKSTAY LQMNSLRAEDTAVYYCAKYP HYYGSSHWYFDVWGQGTLVT VSS (in the WT VH, position 44 is Gly)
Avastin: CH1 and hinge domain with **C222A** mutation	GCTAGCACCAAGGGCCCATCGGTCTTCCCC CTGGCACCCTCCTCCAAGAGCACCTCTGGG GGCACAGCGGCCCTGGGCTGCCTGGTCAAG GACTACTTCCCCGAACCGGTGACGGTGTCG TGGAACTCAGGCGCCCTGACCAGCGGCGTG CACACCTTCCCGGCTGTCCTACAGTCCTCA GGACTCTACTCCCTCAGCAGCGTGGTGACC GTGCCCTCCAGCAGCTTGGGCACCCAGACC TACATCTGCAACGTGAATCACAAGCCCAGC AACACCAAGGTGGACAAGAGAGTTGAGCCC AAATCT**GCC**GACAAAACTCACACATGCCCA CCGTGCCCA	ASTKGPSVFPLAPSSKSTSG GTAALGCLVKDYFPEPVTVS WNSGALTSGVHTFPAVLQSS GLYSLSSVVTVPSSSLGTQT YICNVNHKPSNTKVDKRVEP KS**A**DKTHTCPPCP
Avastin: CH2 domain **(WT)**	GCACCTGAACTCCTGGGGGGACCGTCAGTC TTCCTCTTCCCCCCAAAACCCAAGGACACC CTCATGATCTCCCGGACCCCTGAGGTCACA TGCGTGGTGGTGGACGTGAGCCACGAAGAC CCTGAGGTCAAGTTCAACTGGTACGTGGAC GGCGTGGAGGTGCATAATGCCAAGACAAAG CCGCGGGAGGAGCAGTACAACAGCACGTAC CGTGTGGTCAGCGTCCTCACCGTCCTGCAC CAGGACTGGCTGAATGGCAAGGAGTACAAG TGCAAGGTCTCCAACAAAGCCCTCCCAGCC CCCATCGAGAAAACCATCTCCAAAGCCAAA	APELLGGPSVFLFPPKPKDT LMISRTPEVTCVVVDVSHED PEVKFNWYVDGVEVHNAKTK PREEQYNSTYRVVSVLTVLH QDWLNGKEYKCKVSNKALPA PIEKTISKAK
Avastin: CH3 domain with **T366W** and **S354C** (knob) mutations	GGGCAGCCCCGAGAACCACAGGTGTACACC CTGCCCCCA**TGC**CGGGAGGAGATGACCAAG AACCAGGTCAGCCTG**TGG**TGCCTGGTCAAA GGCTTCTATCCCAGCGACATCGCCGTGGAG TGGGAGAGCAATGGGCAGCCGGAGAACAAC TACAAGACCACGCCTCCCGTGCTGGACTCC GACGGCTCCTTCTTCCTCTATAGCAAGCTC	GQPREPQVYTLPP**C**REEMTK NQVSL**W**CLVKGFYPSDIAVE WESNGQPENNYKTTPPVLDS DGSFFLYSKLTVDKSRWQQG NVFSCSVMHEALHNHYTQKS LSLSPGK

(continued)

Table 1
(continued)

Antibody: name and description	DNA sequence	Amino acids sequence
	ACCGTGGACAAGAGCAGGTGGCAGCAGGGG AACGTCTTCTCATGCTCCGTGATGCATGAG GCTCTGCACAACCACTACACGCAGAAGAGC CTCTCCCTGTCCCCGGGTAAA	
Leader sequence for light chain	ATGGACACGAGGGCCCCCACTCAGCTGCTG GGGCTCCTACTGCTCTGGCTCCCAGGTGCC AGATGTGCC	MDTRAPTQLLGLLLLWLPGA RCA
Avastin: V-Kappa domain with **Q100C** mutation	GACATCCAGATGACCCAGTCCCCCTCCAGC CTGTCCGCCTCCGTGGGCGACAGAGTGACC ATCACCTGTTCCGCCAGCCAGGACATCTCC AACTACCTGAACTGGTATCAGCAGAAGCCC GGCAAGGCCCCCAAGGTGCTGATCTACTTC ACCAGCTCCCTGCACTCCGGCGTGCCCTCC AGATTCTCCGGCTCTGGCTCCGGCACCGAC TTCACCCTGACCATCTCCAGCCTGCAGCCC GAGGACTTCGCCACCTACTACTGCCAGCAG TACTCCACCGTGCCCTGGACCTTCGGC**TGC** GGCACCAAGGTGGAAATCAAG	HMDIQMTQSPSSLSASVGDR VTITCSASQDISNYLNWYQQ KPGKAPKVLIYFTSSLHSGV PSRFSGSGSGTDFTLTISSL QPEDFATYYCQQYSTVPWTF G**c**GTKVEIK (in the WT V-Kappa, position 100 is Gln)
Avastin: C-Kappa domain with **C214 deleted** mutation (it is the last codon of the WT C-kappa)	CGTACGGTGGCTGCACCATCTGTCTTCATC TTCCCGCCATCTGATGAGCAGTTGAAATCT GGAACTGCCTCTGTTGTGTGCCTGCTGAAT AACTTCTATCCCAGAGAGGCCAAAGTACAG TGGAAGGTGGATAACGCCCTCCAATCGGGT AACTCCCAGGAGAGTGTCACAGAGCAGGAC AGCAAGGACAGCACCTACAGCCTCAGCAGC ACCCTGACGCTGAGCAAAGCAGACTACGAG AAACACAAAGTCTACGCCTGCGAAGTCACC CATCAGGGCCTGAGCTCGCCCGTCACAAAG AGCTTCAACAGGGGAGAG	RTVAAPSVFIFPPSDEQLKS GTASVVCLLNNFYPREAKVQ WKVDNALQSGNSQESVTEQD SKDSTYSLSSTLTLSKADYE KHKVYACEVTHQGLSSPVTK SFNRGE
Anti Ang2 antibody Lc06: (IgG1-Lambda) VH domain **(WT)**	CAGGTCCAGCTGGTGGAATCTGGCGCCGAA GTGAAGAAACCTGGCGCCTCCGTGAAGGTG TCCTGCAAGGCCTCCGGCTACACCTTCACC GGCTACTACATGCACTGGGTCCGACAGGCC CCAGGCCAGGGCCTGGAATGGATGGGCTGG ATCAACCCCAACTCCGGCGGCACCAACTAC GCCCAGAAATTCCAGGGCAGAGTGACCATG ACCCGGGACACCTCCATCTCCACCGCCTAC ATGGAACTGTCCCGGCTGCGGAGCGACGAC ACCGCCGTGTACTACTGCGCCCGGTCCCCC AACCCCTACTACTACGACTCCAGCGGCTAC TACTACCCTGGCGCCTTCGACATCTGGGGC CAGGGCACAATGGTCACCGTGTCCTCT	QVQLVESGAEVKKPGASVKV SCKASGYTFTGYYMHWVRQA PGQGLEWMGWINPNSGGTNY AQKFQGRVTMTRDTSISTAY MELSRLRSDDTAVYYCARSP NPYYYDSSGYYYPGAFDIWG QGTMVTVSS
Lc06: CH1 CH1 and hinge domain **(WT)**	GCTAGCACCAAGGGCCCATCGGTCTTCCCC CTGGCACCCTCCTCCAAGAGCACCTCTGGG GGCACAGCGGCCCTGGGCTGCCTGGTCAAG	ASTKGPSVFPLAPSSKSTSG GTAALGCLVKDYFPEPVTVS WNSGALTSGVHTFPAVLQSS

(continued)

Table 1
(continued)

Antibody: name and description	DNA sequence	Amino acids sequence
	GACTACTTCCCCGAACCGGTGACGGTGTCG TGGAACTCAGGCGCCCTGACCAGCGGCGTG CACACCTTCCCGGCTGTCCTACAGTCCTCA GGACTCTACTCCCTCAGCAGCGTGGTGACC GTGCCCTCCAGCAGCTTGGGCACCCAGACC TACATCTGCAACGTGAATCACAAGCCCAGC AACACCAAGGTGGACAAGAAAGTTGAGCCC AAATCTTGTGACAAAACTCACACATGCCCA CCGTGCCCA	GLYSLSSVVTVPSSSLGTQT YICNVNHKPSNTKVDKKVEP KSCDKTHTCPPCP
Lc06: CH2 domain **(WT)**	GCACCTGAACTCCTGGGGGGACCGTCAGTC TTCCTCTTCCCCCCAAAACCCAAGGACACC CTCATGATCTCCCGGACCCCTGAGGTCACA TGCGTGGTGGTGGACGTGAGCCACGAAGAC CCTGAGGTCAAGTTCAACTGGTACGTGGAC GGCGTGGAGGTGCATAATGCCAAGACAAAG CCGCGGGAGGAGCAGTACAACAGCACGTAC CGTGTGGTCAGCGTCCTCACCGTCCTGCAC CAGGACTGGCTGAATGGCAAGGAGTACAAG TGCAAGGTCTCCAACAAAGCCCTCCCAGCC CCCATCGAGAAAACCATCTCCAAAGCCAAA	APELLGGPSVFLFPPKPKDT LMISRTPEVTCVVVDVSHED PEVKFNWYVDGVEVHNAKTK PREEQYNSTYRVVSVLTVLH QDWLNGKEYKCKVSNKALPA PIEKTISKAK
Lc02: CH3 domain with **T366S, L368A, Y470V** and **Y349C** (hole) mutations	GGGCAGCCCCGAGAACCACAGGTG**TGC**ACC CTGCCCCCATCCCGGGAGGAGATGACCAAG AACCAGGTCAGCCTG**AGC**TGC**GCG**GTCAAA GGCTTCTATCCCAGCGACATCGCCGTGGAG TGGGAGAGCAATGGGCAGCCGGAGAACAAC TACAAGACCACGCCTCCCGTGCTGGACTCC GACGGCTCCTTCTTCCTC**GTT**AGCAAGCTC ACCGTGGACAAGAGCAGGTGGCAGCAGGGG AACGTCTTCTCATGCTCCGTGATGCATGAG GCTCTGCACAACCACTACACGCAGAAGAGC CTCTCCCTGTCCCCGGGTAAA	GQPREPQV**C**TLPPSREEMTK NQVSL**S**C**A**VKGFYPSDIAVE WESNGQPENNYKTTPPVLDS DGSFFL**V**SKLTVDKSRWQQG NVFSCSVMHEALHNHYTQKS LSLSPGK
LC06 V-Lambda **(WT)**	CAGCCCGGCCTGACCCAGCCCCCTTCCGTG TCTGTGGCTCCTGGCCAGACCGCCAGAATC ACCTGTGGCGGCAACAACATCGGCTCCAAG TCCGTGCACTGGTATCAGCAGAAGCCCGGC CAGGCCCCCGTGCTGGTGGTGTACGACGAC TCCGACCGGCCCTCTGGCATCCCTGAGCGG TTCTCCGGCTCCAACAGCGGCAACACCGCC ACCCTGACCATCTCCAGAGTGGAAGCCGGC GACGAGGCCGACTACTACTGCCAGGTCTGG GACTCCTCCTCCGACCACTACGTGTTCGGC ACCGGCACCAAAGTGACCGTCCTA	QPGLTQPPSVSVAPGQTARI TCGGNNIGSKSVHWYQQKPG QAPVLVVYDDSDRPSGIPER FSGSNSGNTATLTISRVEAG DEADYYCQVWDSSSDHYVFG TGTKVTVL
LC06 C-Lambda **(WT)**	GGTCAGCCCAAGGCTGCCCCCTCGGTCACT CTGTTCCCGCCCTCCTCTGAGGAGCTTCAA GCCAACAAGGCCACACTGGTGTGTCTCATA	GQPKAAPSVTLFPPSSEELQ ANKATLVCLISDFYPGAVTV AWKADSSPVKAGVETTTPSK

(continued)

Table 1
(continued)

Antibody: name and description	DNA sequence	Amino acids sequence
	AGTGACTTCTACCCGGGAGCCGTGACAGTG GCCTGGAAGGCAGATAGCAGCCCCGTCAAG GCGGGAGTGGAGACCACCACACCCTCCAAA CAAAGCAACAACAAGTACGCGGCCAGCAGC TATCTGAGCCTGACGCCTGAGCAGTGGAAG TCCCACAGAAGCTACAGCTGCCAGGTCACG CATGAAGGGAGCACCGTGGAGAAGACAGTG GCCCCTGCAGAATGTTCTTAA	QSNNKYAASSYLSLTPEQWK SHRSYSCQVTHEGSTVEKTV APAECS

Engineered mutations are highlighted in **bold**. The DNA sequences shown here were optimized for expression in mammalian cells. The leader sequence of the heavy chain is suitable for the two heavy chain plasmids and so is the leader sequence of the light chain

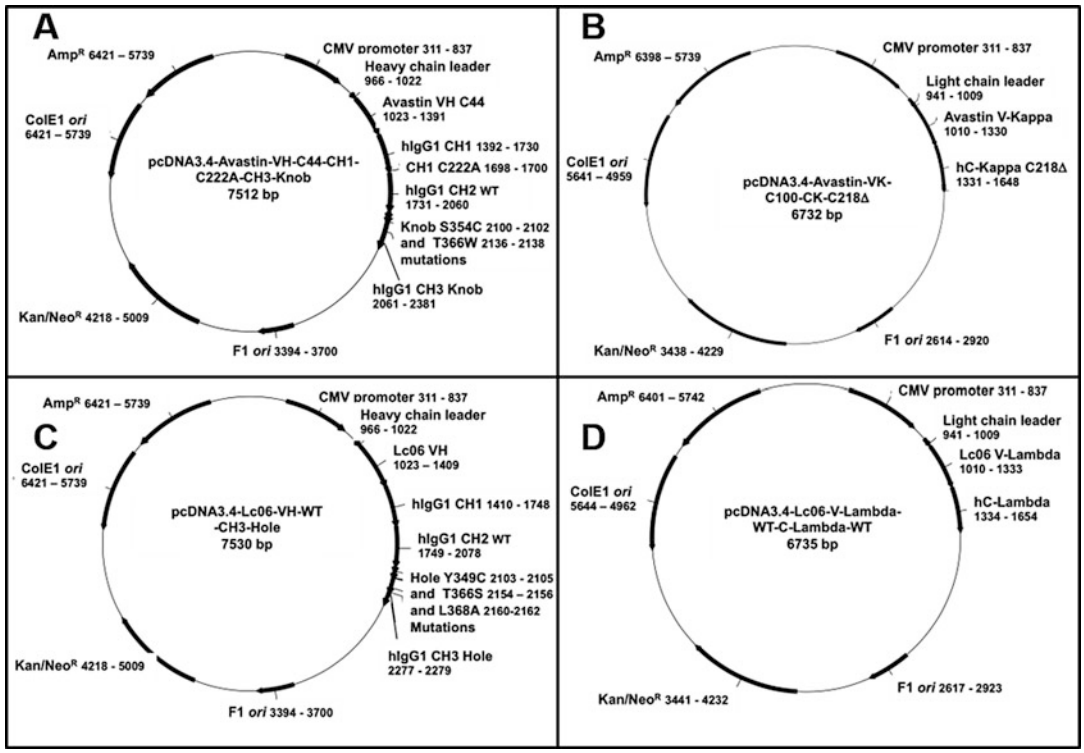

Fig. 2 Maps of pcDNA3.4-based plasmids for expression of bsAbs in transfected mammalian cells. Plasmids **pcDNA3.4-Avastin-VH-(C44)-CH1(C22A)-CH3**d (**a**), and **pcDNA3.4-Avastin-V-Kappa(C100)-C-Kappa (C218DEL)** (**b**) are for the expression of the antibody with the engineered Fab arm. Plasmids **pcDNA3.4-Lc06-VH-CH3 (Hole)** (**c**) **and pcDNA3.4-Lc06-V-Lambda-C-Lambda** are for the expression of the antibody with the WT Fab arm. All four plasmids are ampicillin-resistance carrying *colE1* replicon-based medium copy number plasmids. The expression cassette is controlled by the strong CMV promoter and is comprised of an immunoglobulin leader sequence for secretion followed by the (**a**) Avastin V_H C44, CH1 C222A, CH2 WT, CH3 Knob (sequence 1 in Appendix). (**b**) Avastin V-Kappa C100, C-Kappa with C2018 deleted (sequence 2 in Appendix). (**c**) Lc06 V_H WT, CH1 WT, CH2 WT, CH3 Hole (sequence 3 in Appendix). (**d**) Lc06 V-Lambda WT, C-Lambda WT (sequence 4 in Appendix)

Vκ or Vλ of the prototype light chain vector with the Vκ or Vλ of your antibody—carrying the C100 mutation (*see* **Notes 6** and **7**).

4. To prepare the heavy chain vector for the antibody with the WT Fab arm, use Gibson assembly [17] to replace the V_H of the prototype Hole vector (here it is named **pcDNA3.4-Lc06-VH-CH3 (Hole)**) with the V_H of your antibody.
5. To prepare the light chain vector for the antibody with the WT Fab arm, use Gibson assembly [17] to replace the Vκ or Vλ of the prototype light chain vector (here it is named **pcDNA3.4-Lc06-V-Lambda-C-Lambda**) with the Vκ or Vλ of your antibody (*see* **Note 8**).
6. When the Gibson assembly reaction has been completed, transform chemically competent cells of an *E. coli* strain suitable for cloning with half of the DNA. Store the other half at −20 °C. Plate the transformed bacteria on LB + Ampicillin agar plate and keep in a 37 °C overnight (16–20 h). If no colonies appear the next day, use the electroporation method with the remaining Gibson assembly reaction.
7. Pick single, well-isolated colonies into PCR mix with two primers designed, one for the vector and one for the insert. Additionally, seed each of those colonies as a patch on an LB + Ampicillin plate. Use 25 cycle PCR program with the appropriate annealing temperature according to the primers Tm.
8. Pick positive colonies into 5 ml of LB + Ampicillin. Grow overnight shaking 250 RPM at 37 °C.
9. Next day, use 3 ml of each culture for a DNA miniprep and the remaining 2 ml for preparing glycerol stocks (*see* **Note 9**).
10. After the construction of each new plasmid, it should be verified by sequencing using the CMV-seq-FOR and CMV-seq-REV primers (*see* **Note 10**).

3.2 Expression of bsAbs Using the Expi293™ Transient Transfection System

The workflow with the Expi293TM kit is basically according to the instructions of the supplier. Here are a few important points:

1. Transfect 75×10^6 Expi293™ cells (*see* **Note 11**) using 3.75 μg from each heavy chain and 11.25 μg from each light chain plasmid (*see* **Note 12**). Place the cells in a 125 ml disposable shake flask for growing cells in suspension.
2. Grow in a CO_2 incubator set at 37 °C 8% CO_2 shaking at 150 RPM.
3. 20 hour post transfections add the enhancers (which are part of the Expi293™ kit) and continue growing. This is Day 1.

4. Assay conditioned media on day 4 and day 7 by SDS/PAGE electrophoresis. Usually, the bsAbs are purified from day 7 post transfection.

3.3 Analysis of bsAbs Assembly by SDS/PAGE and Immunoblotting

This step is carried out to evaluate the extent of correct full-size assembly of the bispecific IgG, which leads to a decision whether to apply a single affinity chromatography step or two affinity chromatography steps for purification.

1. Carry out SDS/polyacrylamide gel electrophoresis of proteins according to Laemmli [18]. To 100 μl of conditioned medium, add 25 μl of 5× Sample Buffer. Boil the samples for 3 min prior to the loading onto a 10% gel (or 4–20% gradient gel). Run samples under nonreducing as well as under reducing conditions. Load 20 μl/lane for a gel to be stained and 5–10 μl/lane for a gel that will be used for immunoblotting.
2. Run the mini-gel at 150 V until the blue dye migrates to the bottom of the gel.
3. Carefully remove the gel from the cassette and wash the gel three time, 10 min each in 200 ml of distilled water.
4. Stain the gels with GelCode blue® solution or a similar SDS/PAGE stain solution. Do **NOT** stain gels that are to be used for immunoblotting.
5. **Western Blot (immunoblot) analysis** (*see* **Note 13**): Electrotransfer the proteins that were resolved by SDS-PAGE onto a nitrocellulose membrane.
6. Block the membrane for at least 1 h at 37 °C in 50 ml PBS containing 5% nonfat milk powder at room temperature with slow agitation.
7. Wash the membrane once with PBS followed by incubation HRP-conjugated goat-anti-human (H + L) secondary antibodies (or with HRP-conjugated anti-Kappa or with anti-Lambda secondary antibodies).
8. Wash three time with 200 ml of PBST (PBS containing 0.05% Tween 20) for 15 min each wash and one wash with 200 ml of PBS, develop the nitrocellulose filter with the SuperSignal West Pico Chemiluminescent Substrate (Thermo Scientific) as recommended by the supplier.

3.4 Purification of bsAbs Using Affinity Chromatography Columns

Following is a description of how to purify bsAbs from the conditioned medium of transfected Expi293™ cells using a single (MAbSelect) chromatography step (*see* **Notes 14** and **15**).

1. Collect the conditioned medium into a 50 ml conical tube and remove cells by centrifugation for 10 min, 10000 × *g*., 4 °C. Filter the cell-free conditioned medium using a 0.45 μm syringe filter.

2. To the 30 ml filtered conditioned medium add 1.5 ml 0.2 M Phosphate buffer pH 7.4.
3. Load a 1 ml MabSelect column at a flow rate of 0.5 ml/min (this is the flow rate throughout the loading and purification process) (*see* **Note 14**).
4. Wash the column with 10 column volumes of PBS.
5. Elute the column with **Elution buffer**. Immediately neutralize by adding 1/5 volumes of Neutralization buffer and mix by vortexing.
6. Buffer-exchange the purified bsAb using a PD10 column (*see* **Note 16**). When required, concentrate the purified bsAb using a centrifugal concentration device with 10 kDa cutoff.
7. Analyze fractions on 10% polyacrylamide gel under nonreducing and reducing conditions, loading 3–5 μg protein/lane (*see* Fig. 3).
8. Store the bsAb at a final concentration 1.5 mg/ml (10 μM) at 4 °C. For prolonged storage (longer than 1–2 weeks) store in small aliquots at −80 °C (*see* **Note 17**).

4 Notes

1. In the list of Materials (Subheading 2) we provide the names of vendors from which we currently purchase reagents. We do not by any means endorse these particular vendors. We encourage the users to use vendors of their choice. When using commercial kits and chromatography media, they should be used according to the instructions provided by the supplier.
2. The plasmids described herein can be prepared by ordering synthetic DNA fragments and cloning them into plasmid existing in your lab (as suggested in Appendix). Complete plasmids can be ordered from a number of vendors. In general, we recommend ordering synthetic genes with optimization for the expression organism over PCR amplification from the antibody vector that was used in the antibody discovery step. In addition, we prefer restriction-free cloning, such as Gibson assembly [17] over restriction-based cloning.
3. Selection of the suitable affinity column for the purification of the bsAbs depends on the extent of complete assembly of a full-size IgG. bsAsb that are assembled efficiently should be purified by a single chromatography step (such as MabSelect or KappaSelect, *see* Fig. 3). Antibodies that assembly in-efficiently should be purified by sequential KappaSelect-LambdaSelect chromatography (when one antibody has a Kappa light chain and the second has a Lambda light chain) or by a single affinity

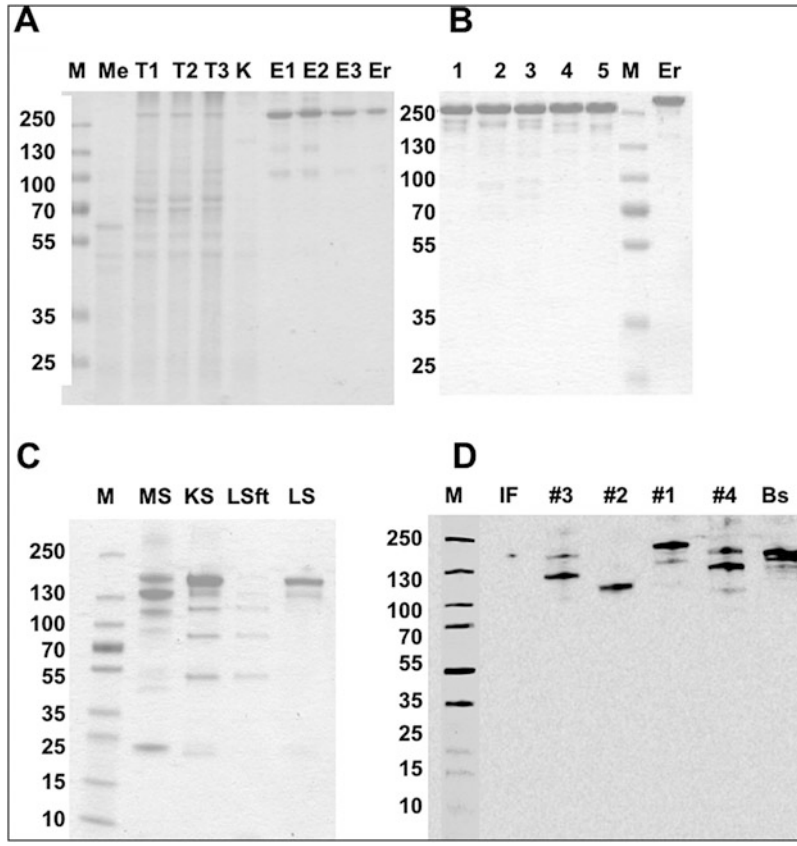

Fig. 3 SDS-PAGE and immunoblot analysis of bsAbs expressed in Expi293™ cells. The four pcDNA3.4-based plasmid vectors were used for transfect Expi293TM cells. 20 μl of conditioned media or about 3 μg of each of the purified proteins were separated on a 10% SDS-PAGE under nonreducing conditions and visualized using GelCode Blue™ staining (**a**, **b,** and **c**). The MW sizes are in kDa. (**a**) Example of a bsAb that assembles efficiently and thus was purified by a single (in this case KappaSelect) affinity chromatography step. Three independent transfections were used to produce this bsAb. Me, conditioned medium of untransfected cells; T1, T2, T3 are day 7 conditioned media from three transfections. K, KappaSelect unbound fraction; E1, E2, E3 are the bsAbs eluted from the KappaSelect column. *Er* erbitux (a commercial IgG used as a full-size IgG protein marker). (**b**) Five different bsAbs (numbered 1–5) that were purified by a single MabSelect affinity chromatography step. *Er* erbitux (a commercial IgG used as a full-size IgG protein marker). (**c**) An extreme example of a bsAb that assembles poorly and thus was purified by a three (in this case MabSelect followed by KappaSelect followed by LambdaSelect) affinity chromatography steps. *M* MW marker, *MS* eluate from the MabSelect column, *KS* eluate from the KappaSelect column, *LSft* the unbound fraction after loading a LambdaSelect column. *LS* eluate from the LambdaSelect column. (**d**) Example of an immunoblot used to analyze conditioned medium of several bsAb. Detection was with an HRP-conjugated goat anti-human (H+L) secondary antibody. *IF* infliximab (a commercial IgG used as a full-size IgG protein marker); #3, #2, #1 are four mAbs with partial efficiency of assembly. *Bs* a bsAb with good efficiency of assembly

chromatography step followed by Cation-exchange when they have two Kappa or two Lambda light chains. We describe using 1 ml bed-volume columns, but larger capacity columns may be used for purifying antibodies from larger volumes of conditioned media.

4. Different antibody sequences express with different efficiency in transfected mammalian cells. This is a challenge for mAb production in general and even more so for a bsAbs, where four recombinant polypeptide chains are co-expressed by each cell. Therefore, it is difficult to predict which Fab arm should be engineered to provide optimal assembly of a full size IgG. Therefore, we recommend that for every new bsAb, the two options for engineering one Fab arm on one of the originating mAbs or of the second arm should be attempted. Since heavy chain heterodimerization is orthogonal to heavy-light chain pairing, it does not matter if the engineered Fab arm is on the Knob or on the Hole heavy chain.
5. The "BIClonals" technology is under patent protection [16]. Plasmid vectors similar to the ones described in this chapter may be obtained from the authors upon request under a materials transfer agreement.
6. Concerning the insertion of cysteine mutations into antibody variable domains, note the position numbers are not sequential but, rather, correspond to the position according to the Kabat numbering scheme [19]. For example, V_H position 44 is position 49 according to IMGT:

   Use the following guidelines:

For V_H, position 44 (Kabat numbering scheme [19]) is the 9th position of framework 2. In almost all cases it is followed by the sequence **LEW** (in human and mouse V_H genes).

For V-Kappa and V-Lambda, position 100 (Kabat numbering scheme [19]) is the 3rd position of framework 4. In almost all cases it follows the sequence **FG** (in human and mouse).

7. For a plasmid for an engineered Fab arm with a **Kappa** light chain, use a design similar to that of **pcDNA3.4-Avastin-V-Kappa(C100)-C-kappa(C218DEL)** (*see* Appendix). For a plasmid with an engineered Fab arm with a **Lambda** light, mutate Vλ position 100 to cysteine and mutate the cysteine located in the penultimate position of Cλ to alanine (it is position 126 in IMGT: and is followed by a serine at the last position of Cλ in humans and serine or leucine in mice) (*see* Table 1).
8. The prototype WT light chain plasmid **pcDNA3.4-Lc06-V-Lambda-C-Lambda** shown in Appendix if for expression of a

Lambda light chain. When you want to express a WT Kappa light chain, you can back mutate plasmid **pcDNA3.4-Avastin-V-Kappa(C100)-C-kappa(C218DEL)**, restoring glutamine at Vκ position 100 and **adding** a lysine codon at the last position of the Cκ domain.

9. To prepare a glycerol stock from an *E. coli* culture, add 0.5 ml of a sterile 80% glycerol solution to the 2 ml culture, mix by vortex, and dispense into two 2 ml freezing tubes that should be clearly labeled and stored at −80 °C.
10. Always verify each plasmid received from another scientist by DNA sequencing.
11. Expi293^{TM} cells are grown in 125 ml shake flasks rotating at 150 RPM in a CO_2 incubator held at 8% CO_2. The cells provide maximal yield after they have been passaged for five times before transfection.
12. A 3:1 light chain vector: heavy chain vector ratio in the transfection provides in most cases better yield than 1:1 ratio. This is true for mAbs in general. For bsAbs, further optimization of the vector DNA ratio used in the transfection may be required when there is a large difference in the expression levels of the four participating antibody chains.
13. In most cases, the extent of correct assembly of a full-size bispecific IgG can be evaluated from a stained SDS/PAGE gel. When in doubt, proceed to immunoblotting. This is where anti Kappa or anti Lambda light chains secondary antibodies can be useful, as they help you identify the missing chain in partially assembled IgGs.
14. The bsAbs can be purified by a single chromatography step or by two affinity chromatography steps. The choice of the purification workflow is dependent on the extent of correct full-size IgG assembly (*see* Fig. 3).
15. When two affinity chromatography steps are required, we recommend using KappaSelect as the first step. The eluate from the KappaSelect column is buffer-exchanged to PBS using a PD-10 column and immediately loaded onto a LambdaSelect column. KappaSelect and LambdaSelect columns should be used according to the instructions of the manufacturer (*see* Subheading 2.6).
16. Instead of buffer exchange using a PD-10 desalting column, the bsAb can be dialyzed against 1000 volumes of PBS for 24 h at 4 °C in a large beaker with stirring using snakeskin or similar dialysis tubing with 10,000 kDa cutoff. We recommend desalting as dialysis may be prone to protein losses due to aggregation.

17. From a single transfection, 30 ml of conditioned medium may yield from as little as 0.5 mg purified IgG (for bsAbs with suboptimal full-size assembly that require two affinity chromatography steps) and up to about 5 mg (for bsAbs with optimal full-size assembly that require a single affinity chromatography step). This is sufficient for affinity, specificity, and stability assays and for FACS an immune-staining of cells and tissues. From a good expresser, several transfections can be used to obtain sufficient bsAb for a small animal model experiment. When larger quantities are required, the same plasmid vectors may be used to establish stable cell lines. How to do that is not in the scope of this chapter.

Acknowledgments

Studies of bispecific antibodies at the Authors' lab were supported in part by The Israel Science Foundation (Grant no. 591/13), by a research grant from the Israel Cancer Research fund (ICRF), by a grant from the Israeli National Nanotechnology Initiative (INNI), Focal Technology Area (FTA) program: Nanomedicine for Personalized Theranostics, by The Leona M. and Harry B. Helmsley Nanotechnology Research Fund and by Varda and Boaz Dotan Research Center in Hemato-oncology affiliated to CBRC at Tel-Aviv University. We are grateful to members of the Benhar Lab for their contributions in optimizing the BIClonals technology.

Appendix: Sequences of Plasmids (Complete Sequences May Be Obtained from the Authors Upon Request)

Below are instructions for designing the set of plasmids required for expression of the Avastin-LC06 bsAb presented here as an example. To create your own bsAbs, replace the variable domains with those of your own antibodies. The plasmid sequences shown here have human gamma1 constant domains (one carrying the Knob mutations and one carrying the "Hole" mutations), a human Kappa light chain that has an engineered Fab arm and a human Lambda light chain which is WT in the Fab arm.

The sequence of plasmid **pcDNA3.1** is available at: https://www.ncbi.nlm.nih.gov/nuccore/EF550208.1

1. **To create pcDNA3.4-Avastin-VH-(C44)-CH1(C22A)-CH3 (Knob) (an expression vector for the human heavy light chain with the C44 mutation in VH, and C222A mutation in CH1 and Knob mutations in CH3)**, insert the

following sequence between coordinates 819 to 2908 of **pcDNA3.1**.

The resulting **pcDNA3.4-Avastin-VH-(C44)-CH1 (C22A)-CH3 (Hole)** carries the cloned V_H-C_H of the therapeutic monoclonal anti VEGF antibody Avastin (Bevacizumab). This is the heavy chain plasmid with the engineered Fab arm.

In the sequence below, the secretion leader sequence ORF spans positions 147–203. The V_H ORF spans position 204–572. The heavy chain CH1-CH3 domains including the STOP codon span positions 573–1565.

GTTTAGTGAACCGTCAGATCGCCTGGAGACGCCATC
CACGCTGTTTTGACCTCCATAGAAGACACCGGGACC
GATCCAGCCTCCGGACTCTAGAGGATCGAACCCTTG
GATCTCTAGCGAATTCCCTCTAGACACAGACGCTCAC
CATGGAGACTGGGCTGCGCTGGCTTCTCCTGGTCGC
TGTGCTCAAAGGTGTCCAGTGTGAAGTGCAGCTGGT
GGAATCCGGCGGAGGCCTGGTGCAGCCTGGCGGCT
CTCTGAGACTGTCTTGCGCCGCCTCCGGCTACACCT
TCACCAACTACGGCATGAACTGGGTCCGACAGGCCC
CTGGCAAGTGCCTGGAATGGGTCGGATGGATCAACA
CCTACACCGGCGAGCCCACCTACGCCGCCGACTTCA
AGCGGCGGTTCACCTTCTCCCTGGACACCTCCAAGT
CCACCGCCTACCTGCAGATGAACTCCCTGCGGGCCG
AGGACACCGCCGTGTACTACTGCGCCAAGTACCCCC
ACTACTACGGCTCCTCCCACTGGTACTTCGACGTGT
GGGGCCAGGGCACCCTGGTCACCGTGTCATCTGCT
AGCACCAAGGGCCCATCGGTCTTCCCCCTGGCACC
CTCCTCCAAGAGCACCTCTGGGGGCACAGCGGCCC
TGGGCTGCCTGGTCAAGGACTACTTCCCCGAACCGG
TGACGGTGTCGTGGAACTCAGGCGCCCTGACCAGCG
GCGTGCACACCTTCCCGGCTGTCCTACAGTCCTCAG
GACTCTACTCCCTCAGCAGCGTGGTGACCGTGCCCT
CCAGCAGCTTGGGCACCCAGACCTACATCTGCAACG
TGAATCACAAGCCCAGCAACACCAAGGTGGACAAGA
GAGTTGAGCCCAAATCTGCCGACAAAACTCACACATG
CCCACCGTGCCCAGCACCTGAACTCCTGGGGGGACC
GTCAGTCTTCCTCTTCCCCCCAAAACCCAAGGACAC
CCTCATGATCTCCCGGACCCCTGAGGTCACATGCGT
GGTGGTGGACGTGAGCCACGAAGACCCTGAGGTCA
AGTTCAACTGGTACGTGGACGGCGTGGAGGTGCATA
ATGCCAAGACAAAGCCGCGGGAGGAGCAGTACAACA
GCACGTACCGTGTGGTCAGCGTCCTCACCGTCCTG
CACCAGGACTGGCTGAATGGCAAGGAGTACAAGTGC
AAGGTCTCCAACAAAGCCCTCCCAGCCCCCATCGAG
AAAACCATCTCCAAAGCCAAAGGGCAGCCCCGAGAA
CCACAGGTGTACACCCTGCCCCCATGCCGGGAGGAG

ATGACCAAGAACCAGGTCAGCCTGTGGTGCCTGGTC
AAAGGCTTCTATCCCAGCGACATCGCCGTGGAGTGG
GAGAGCAATGGGCAGCCGGAGAACAACTACAAGACC
ACGCCTCCCGTGCTGGACTCCGACGGCTCCTTCTT
CCTCTATAGCAAGCTCACCGTGGACAAGAGCAGGTG
GCAGCAGGGGAACGTCTTCTCATGCTCCGTGATGCA
TGAGGCTCTGCACAACCACTACACGCAGAAGAGCCT
CTCCCTGTCCCCGGGTAAAtgAGCGGCCGCTCGAGG
CCGGCAAGGCCGGATCCCCCGACCTCGACAAGGGT
TCGATCCCTACCGGTTAGTAATGAGTTTGATATCTCG
ACAATCAACCTCTGGATTACAAAATTTGTGAAAGATT
GACTGGTATTCTTAACTATGTTGCTCCTTTTACGCTA
TGTGGATACGCTGCTTTAATGCCTTTGTATCATGCT
ATTGCTTCCCGTATGGCTTTCATTTTCTCCTCCTTG
TATAAATCCTGGTTGCTGTCTCTTTATGAGGAGTTG
TGGCCCGTTGTCAGGCAACGTGGCGTGGTGTGCAC
TGTGTTTGCTGACGCAACCCCCACTGGTTGGGGCA
TTGCCACCACCTGTCAGCTCCTTTCCGGGACTTTCG
CTTTCCCCCTCCCTATTGCCACGGCGGAACTCATCG
CCGCCTGCCTTGCCCGCTGCTGGACAGGGGCTCGG
CTGTTGGGCACTGACAATTCCGTGGTGTTGTCGGG
GAAGCTGACGTCCTTTCCATGGCTGCTCGCCTGTG
TTGCCACCTGGATTCTGCGCGGGACGTCCTTCTGC
TACGTCCCTTCGGCCCTCAATCCAGCGGACCTTCCT
TCCCGCGGCCTGCTGCCGGCTCTGCGGCCTCTTCC
GCGTCTTCGCCTTCGCCCTCAGACGAGTCGGATCT
CCCTTTGGGCCGCCTCCCCGCCTGGAAACGGGGGA
GGCTAACTGAAACACGGAAGGAGACAATACCGGAAG
GAACCCGCGCTATGACGGCAATAAAAAGACAGAATA
AAACGCACGGGTGTTGGGTCGTTTGTTCATAAACGC
GGGGTTCGGTCCCAGGGCTGGCACTCTGTCGATAC
CCCACCGAGACCCCATTGGGGCCAATACGCCCGCG
TTTCTTCCTTTTCCCCACCCCACCCCCCAAGTTCGG
GTGAAGGCCCAGGGCTCGCAGCCAACGTCGGGGCG
GCAGGCCCTGCCATAGCAGATCTGCGC

2. **To create pcDNA3.4-Avastin-V-Kappa(C100)-C-Kappa (C218DEL) (an expression vector for the human Kappa light chain with the C100 mutation in V-kappa and C218DEL mutation in C-Kappa)**, insert the following sequence between coordinates 819–2907 of **pcDNA3.1**.

   The resulting **pcDNA3.4-Avastin-V-Kappa(C100)-C-Kappa(C218DEL)** carries the cloned Vκ-Cκ is of the therapeutic monoclonal anti VEGF antibody Avastin (Bevacizumab). This is the light chain plasmid with the engineered Fab arm.

   In the sequence below, the secretion leader sequence ORF spans positions 122–190. The Kappa light chain ORF including the STOP codon spans positions 191–832.

GTTTAGTGAACCGTCAGATCGCCTGGAGACGCCATC
CACGCTGTTTTGACCTCCATAGAAGACACCGGGACC
GATCCAGCCTCCGGACTCTAGAGGATCGAACCCTTA
GGCAGGACCCAGCATGGACACGAGGGCCCCCACTCA
GCTGCTGGGGCTCCTACTGCTCTGGCTCCCAGGTG
CCAGATGTGCCGACATCCAGATGACCCAGTCCCCC
TCCAGCCTGTCCGCCTCCGTGGGCGACAGAGTGAC
CATCACCTGTTCCGCCAGCCAGGACATCTCCAACTA
CCTGAACTGGTATCAGCAGAAGCCCGGCAAGGCCC
CCAAGGTGCTGATCTACTTCACCAGCTCCCTGCAC
TCCGGCGTGCCCTCCAGATTCTCCGGCTCTGGCTC
CGGCACCGACTTCACCCTGACCATCTCCAGCCTGC
AGCCCGAGGACTTCGCCACCTACTACTGCCAGCAG
TCTCCACCGTGCCCTGGACCTTCGGCTGCGGCACC
AAGGTGGAAATCAAGCGTACGGTGGCTGCACCATC
TGTCTTCATCTTCCCGCCATCTGATGAGCAGTTGA
AATCTGGAACTGCCTCTGTTGTGTGCCTGCTGAATA
ACTTCTATCCCAGAGAGGCCAAAGTACAGTGGAAGG
TGGATAACGCCCTCCAATCGGGTAACTCCCAGGAG
AGTGTCACAGAGCAGGACAGCAAGGACAGCACCTAC
AGCCTCAGCAGCACCCTGACGCTGAGCAAAGCAGAC
TACGAGAAACACAAAGTCTACGCCTGCGAAGTCACC
CATCAGGGCCTGAGCTCGCCCGTCACAAAGAGCTT
CAACAGGGGAGAGTAAGGGTTCGATCCCTACCGGTT
AGTAATGAGTTTAAACTCGACAATCAACCTCTGGATT
ACAAAATTTGTGAAAGATTGACTGGTATTCTTAACTA
TGTTGCTCCTTTTACGCTATGTGGATACGCTGCTTT
AATGCCTTTGTATCATGCTATTGCTTCCCGTATGGCT
TTCATTTTCTCCTCCTTGTATAAATCCTGGTTGCTGT
CTCTTTATGAGGAGTTGTGGCCCGTTGTCAGGCAAC
GTGGCGTGGTGTGCACTGTGTTTGCTGACGCAACC
CCCACTGGTTGGGGCATTGCCACCACCTGTCAGCT
CCTTTCCGGGACTTTCGCTTTCCCCCTCCCTATTGC
CACGGCGGAACTCATCGCCGCCTGCCTTGCCCGCT
GCTGGACAGGGGCTCGGCTGTTGGGCACTGACAAT
TCCGTGGTGTTGTCGGGGAAGCTGACGTCCTTTCC
ATGGCTGCTCGCCTGTGTTGCCACCTGGATTCTGC
GCGGGACGTCCTTCTGCTACGTCCCTTCGGCCCTC
AATCCAGCGGACCTTCCTTCCCGCGGCCTGCTGCC
GGCTCTGCGGCCTCTTCCGCGTCTTCGCCTTCGCC
CTCAGACGAGTCGGATCTCCCTTTGGGCCGCCTCC
CCGCCTGGAAACGGGGGAGGCTAACTGAAACACGG
AAGGAGACAATACCGGAAGGAACCCGCGCTATGACG
GCAATAAAAAGACAGAATAAAACGCACGGGTGTTGG
GTCGTTTGTTCATAAACGCGGGGTTCGGTCCCAGG
GCTGGCACTCTGTCGATACCCCACCGAGACCCCAT
TGGGGCCAATACGCCCGCGTTTCTTCCTTTTCCCC
ACCCCACCCCCCAAGTTCGGGTGAAGGCCCAGGGC

TCGCAGCCAACGTCGGGGCGGCAGGCCCTGCCATA
GCAGATCTGCG

3. **To create pcDNA3.4-Lc06-VH-CH3 (Hole) (an expression vector for the human heavy light chain with WT Fab arm and Hole mutations in CH3)**, insert the following sequence between coordinates 819–2918 of **pcDNA3.1**.

   The resulting **pcDNA3.4-Lc06-VH-CH3 (Hole)** carries the cloned V_H-CH of the monoclonal anti Ang2 antibody Lc06 [13]. This is the heavy chain plasmid with a WT Fab arm. In the sequence below, the secretion leader sequence ORF spans positions 147–203. The V_H ORF spans position 204–590. The heavy chain CH1–CH3 domains including the STOP codon span positions 591–1583.

   GTTTAGTGAACCGTCAGATCGCCTGGAGACGCCATC
CACGCTGTTTTGACCTCCATAGAAGACACCGGGACC
GATCCAGCCTCCGGACTCTAGAGGATCGAACCCTT
GGATCTCTAGCGAATTCCCTCTAGACACAGACGCTC
ACCATGGAGACTGGGCTGCGCTGGCTTCTCCTGGT
CGCTGTGCTCAAAGGTGTCCAGTGTCAGGTCCAGC
TGGTGGAATCTGGCGCCGAAGTGAAGAAACCTGGC
GCCTCCGTGAAGGTGTCCTGCAAGGCCTCCGGCTA
CACCTTCACCGGCTACTACATGCACTGGGTCCGACA
GGCCCCAGGCCAGGGCCTGGAATGGATGGGCTGGA
TCAACCCCAACTCCGGCGGCACCAACTACGCCCAGA
AATTCCAGGGCAGAGTGACCATGACCCGGGACACCT
CCATCTCCACCGCCTACATGGAACTGTCCCGGCTGC
GGAGCGACGACACCGCCGTGTACTACTGCGCCCGG
TCCCCCAACCCCTACTACTACGACTCCAGCGGCTAC
TACTACCCTGGCGCCTTCGACATCTGGGGCCAGGG
CACAATGGTCACCGTGTCCTCTGCTAGCACCAAGGG
CCCATCGGTCTTCCCCCTGGCACCCTCCTCCAAGAG
CACCTCTGGGGGCACAGCGGCCCTGGGCTGCCTGG
TCAAGGACTACTTCCCCGAACCGGTGACGGTGTCGT
GGAACTCAGGCGCCCTGACCAGCGGCGTGCACACC
TTCCCGGCTGTCCTACAGTCCTCAGGACTCTACTCC
CTCAGCAGCGTGGTGACCGTGCCCTCCAGCAGCTT
GGGCACCCAGACCTACATCTGCAACGTGAATCACAA
GCCCAGCAACACCAAGGTGGACAAGAAAGTTGAGCC
CAAATCTTGTGACAAAACTCACACATGCCCACCGTG
CCCAGCACCTGAACTCCTGGGGGGACCGTCAGTCT
TCCTCTTCCCCCCAAAACCCAAGGACACCCTCATGA
TCTCCCGGACCCCTGAGGTCACATGCGTGGTGGTG
GACGTGAGCCACGAAGACCCTGAGGTCAAGTTCAA
CTGGTACGTGGACGGCGTGGAGGTGCATAATGCCA
AGACAAAGCCGCGGGAGGAGCAGTACAACAGCACG
TACCGTGTGGTCAGCGTCCTCACCGTCCTGCACCA
GGACTGGCTGAATGGCAAGGAGTACAAGTGCAAGG

TCTCCAACAAAGCCCTCCCAGCCCCCATCGAGAAAA
CCATCTCCAAAGCCAAAGGGCAGCCCCGAGAACCA
CAGGTGTGCACCCTGCCCCCATCCCGGGAGGAGAT
GACCAAGAACCAGGTCAGCCTGAGCTGCGCGGTCA
AAGGCTTCTATCCCAGCGACATCGCCGTGGAGTGG
GAGAGCAATGGGCAGCCGGAGAACAACTACAAGACC
ACGCCTCCCGTGCTGGACTCCGACGGCTCCTTCTT
CCTCGTTAGCAAGCTCACCGTGGACAAGAGCAGGT
GGCAGCAGGGGAACGTCTTCTCATGCTCCGTGATG
CATGAGGCTCTGCACAACCACTACACGCAGAAGAGC
CTCTCCCTGTCCCCGGGTAAAtgAGCGGCCGCTCGA
GGCCGGCAAGGCCGGATCCCCCGACCTCGACAAGG
GTTCGATCCCTACCGGTTAGTAATGAGTTTGATATCT
CGACAATCAACCTCTGGATTACAAAATTTGTGAAAGA
TTGACTGGTATTCTTAACTATGTTGCTCCTTTTACGC
TATGTGGATACGCTGCTTTAATGCCTTTGTATCATGC
TATTGCTTCCCGTATGGCTTTCATTTTCTCCTCCTTG
TATAAATCCTGGTTGCTGTCTCTTTATGAGGAGTTGT
GGCCCGTTGTCAGGCAACGTGGCGTGGTGTGCACT
GTGTTTGCTGACGCAACCCCCACTGGTTGGGGCAT
TGCCACCACCTGTCAGCTCCTTTCCGGGACTTTCGC
TTTCCCCCTCCCTATTGCCACGGCGGAACTCATCGC
CGCCTGCCTTGCCCGCTGCTGGACAGGGGCTCGGC
TGTTGGGCACTGACAATTCCGTGGTGTTGTCGGGG
AAGCTGACGTCCTTTCCATGGCTGCTCGCCTGTGTT
GCCACCTGGATTCTGCGCGGGACGTCCTTCTGCTA
CGTCCCTTCGGCCCTCAATCCAGCGGACCTTCCTTC
CCGCGGCCTGCTGCCGGCTCTGCGGCCTCTTCCGC
GTCTTCGCCTTCGCCCTCAGACGAGTCGGATCTCC
CTTTGGGCCGCCTCCCCGCCTGGAAACGGGGGAGG
CTAACTGAAACACGGAAGGAGACAATACCGGAAGGA
ACCCGCGCTATGACGGCAATAAAAAGACAGAATAAA
ACGCACGGGTGTTGGGTCGTTTGTTCATAAACGCG
GGGTTCGGTCCCAGGGCTGGCACTCTGTCGATACC
CCACCGAGACCCCATTGGGGCCAATACGCCCGCGT
TTCTTCCTTTTCCCCACCCCACCCCCCAAGTTCGGG
TGAAGGCCCAGGGCTCGCAGCCAACGTCGGGGCGG
CAGGCCCTGCCATAGCAGATCTGCGC

4. **To create pcDNA3.4-Lc06-V-Lambda-C-Lambda (an expression vector for the WT human Lambda light chain)**, insert the following sequence between coordinates 819–2907 of **pcDNA3.1**.

   The resulting **pcDNA3.4-Lc06-V-Lambda-C-Lambda** carries the cloned Vλ–Cλ of the monoclonal anti Ang2 antibody Lc06 [13]. This is the light chain plasmid with a WT Fab arm.

In the sequence below, the secretion leader sequence ORF spans positions 122–190. The Lambda light chain ORF including the STOP codon spans positions 191–835.

GTTTAGTGAACCGTCAGATCGCCTGGAGACGCCATC
CACGCTGTTTTGACCTCCATAGAAGACACCGGGACC
GATCCAGCCTCCGGACTCTAGAGGATCGAACCCTTA
GGCAGGACCCAGCATGGACACGAGGGCCCCCACTC
AGCTGCTGGGGCTCCTACTGCTCTGGCTCCCAGGT
GCCAGATGTGCCCAGCCCGGCCTGACCCAGCCCCC
TTCCGTGTCTGTGGCTCCTGGCCAGACCGCCAGAA
TCACCTGTGGCGGCAACAACATCGGCTCCAAGTCCG
TGCACTGGTATCAGCAGAAGCCCGGCCAGGCCCCCG
TGCTGGTGGTGTACGACGACTCCGACCGGCCCTCTG
GCATCCCTGAGCGGTTCTCCGGCTCCAACAGCGGCA
ACACCGCCACCCTGACCATCTCCAGAGTGGAAGCCG
GCGACGAGGCCGACTACTACTGCCAGGTCTGGGACT
CCTCCTCCGACCACTACGTGTTCGGCACCGGCACCA
AAGTGACCGTCCTAGGTCAGCCCAAGGCTGCCCCCT
CGGTCACTCTGTTCCCGCCCTCCTCTGAGGAGCTTC
AAGCCAACAAGGCCACACTGGTGTGTCTCATAAGTG
ACTTCTACCCGGGAGCCGTGACAGTGGCCTGGAAG
GCAGATAGCAGCCCCGTCAAGGCGGGAGTGGAGAC
CACCACACCCTCCAAACAAAGCAACAACAAGTACGC
GGCCAGCAGCTATCTGAGCCTGACGCCTGAGCAGT
GGAAGTCCCACAGAAGCTACAGCTGCCAGGTCACG
CATGAAGGGAGCACCGTGGAGAAGACAGTGGCCCC
TGCAGAATGTTCTTAATAAGGGTTCGATCCCTACCG
GTTAGTAATGAGTTTAAACTCGACAATCAACCTCTGG
ATTACAAAATTTGTGAAAGATTGACTGGTATTCTTAA
CTATGTTGCTCCTTTTACGCTATGTGGATACGCTGC
TTTAATGCCTTTGTATCATGCTATTGCTTCCCGTATG
GCTTTCATTTTCTCCTCCTTGTATAAATCCTGGTTGC
TGTCTCTTTATGAGGAGTTGTGGCCCGTTGTCAGGC
AACGTGGCGTGGTGTGCACTGTGTTTGCTGACGCA
ACCCCCACTGGTTGGGGCATTGCCACCACCTGTCA
GCTCCTTTCCGGGACTTTCGCTTTCCCCCTCCCTAT
TGCCACGGCGGAACTCATCGCCGCCTGCCTTGCCC
GCTGCTGGACAGGGGCTCGGCTGTTGGGCACTGAC
AATTCCGTGGTGTTGTCGGGGAAGCTGACGTCCTTT
CCATGGCTGCTCGCCTGTGTTGCCACCTGGATTCTG
CGCGGGACGTCCTTCTGCTACGTCCCTTCGGCCCTC
AATCCAGCGGACCTTCCTTCCCGCGGCCTGCTGCCG
GCTCTGCGGCCTCTTCCGCGTCTTCGCCTTCGCCCT
CAGACGAGTCGGATCTCCCTTTGGGCCGCCTCCCCG
CCTGGAAACGGGGGAGGCTAACTGAAACACGGAAG
GAGACAATACCGGAAGGAACCCGCGCTATGACGGC
AATAAAAAGACAGAATAAAACGCACGGGTGTTGGGT
CGTTTGTTCATAAACGCGGGGTTCGGTCCCAGGGC

TGGCACTCTGTCGATACCCCACCGAGACCCCATTG
GGGCCAATACGCCCGCGTTTCTTCCTTTTCCCCAC
CCCACCCCCCAAGTTCGGGTGAAGGCCCAGGGCTC
GCAGCCAACGTCGGGGCGGCAGGCCCTGCCATAGC
AGATCTGCGC

References

1. Kaplon H, Reichert JM (2018) Antibodies to watch in 2018. mAbs 10:183–203
2. Nelson AL, Dhimolea E, Reichert JM (2010) Development trends for human monoclonal antibody therapeutics. Nat Rev Drug Discov 9:767–774
3. Kontermann R (2012) Dual targeting strategies with bispecific antibodies. mAbs 4:182–197
4. Riethmuller G (2012) Symmetry breaking: bispecific antibodies, the beginnings, and 50 years on. Cancer Immun 12:12–18
5. Jost C, Plückthun A (2014) Engineered proteins with desired specificity: darpins, other alternative scaffolds and bispecific IgGs. Curr Opin Struct Biol 27C:102–112
6. Krah S, Sellmann C, Rhiel L, Schroter C, Dickgiesser S, Beck J, Zielonka S, Toleikis L, Hock B, Kolmar H et al (2017) Engineering bispecific antibodies with defined chain pairing. N Biotechnol 39:167–173
7. Brinkmann U, Kontermann RE (2017) The making of bispecific antibodies. mAbs 9:182–212
8. Fischer N, Leger O (2007) Bispecific antibodies: molecules that enable novel therapeutic strategies. Pathobiology 74:3–14
9. Rader C (2011) Darts take aim at bites. Blood 117:4403–4404
10. Demarest SJ, Glaser SM (2008) Antibody therapeutics, antibody engineering, and the merits of protein stability. Curr Opin Drug Discov Devel 11:675–687
11. Dong J, Sereno A, Snyder WB, Miller BR, Tamraz S, Doern A, Favis M, Wu X, Tran H, Langley E et al (2011) Stable IgG-like bispecific antibodies directed toward the type I insulin-like growth factor receptor demonstrate enhanced ligand blockade and anti-tumor activity. J Biol Chem 286:4703–4717
12. Klein C, Sustmann C, Thomas M, Stubenrauch K, Croasdale R, Schanzer J, Brinkmann U, Kettenberger H, Regula JT, Schaefer W (2012) Progress in overcoming the chain association issue in bispecific heterodimeric IgG antibodies. mAbs 4:653–663
13. Schaefer W, Regula JT, Bahner M, Schanzer J, Croasdale R, Durr H, Gassner C, Georges G, Kettenberger H, Imhof-Jung S et al (2011) Immunoglobulin domain crossover as a generic approach for the production of bispecific IgG antibodies. Proc Natl Acad Sci U S A 108:11187–11192
14. Merchant AM, Zhu Z, Yuan JQ, Goddard A, Adams CW, Presta LG, Carter P (1998) An efficient route to human bispecific IgG. Nat Biotechnol 16:677–681
15. Lewis SM, Wu X, Pustilnik A, Sereno A, Huang F, Rick HL, Guntas G, Leaver-Fay A, Smith EM, Ho C et al (2014) Generation of bispecific IgG antibodies by structure-based design of an orthogonal Fab interface. Nat Biotechnol 32:191–198
16. Benhar I, Vaks L. Bi- and monospecific, asymmetric antibodies and methods of generating the same. US patent number US 9,624,291 b2 issued Apr. 18, 2017. Priority date Mar. 15, 2012
17. Gibson DG, Young L, Chuang RY, Venter JC, Hutchison CA 3rd, Smith HO (2009) Enzymatic assembly of DNA molecules up to several hundred kilobases. Nat Methods 6:343–345
18. Laemmli UK (1970) Cleavage of structural proteins during the assembly of the head of bacteriophage T4. Nature 227:680–685
19. Kabat EA, Wu TT (1991) Identical V region amino acid sequences and segments of sequences in antibodies of different specificities. Relative contributions of V_H and V_L genes, minigenes, and complementarity-determining regions to binding of antibody-combining sites. J Immunol 147:1709–1719

Chapter 23

Production of Stabilized Antibody Fragments in the *E. coli* Bacterial Cytoplasm and in Transiently Transfected Mammalian Cells

Racheli Birnboim-Perach, Yehudit Grinberg, Lilach Vaks, Limor Nahary, and Itai Benhar

Abstract

Monoclonal antibodies (mAbs) are currently the fastest growing class of therapeutic proteins. Parallel to full-length IgG format the development of recombinant technologies provided the production of smaller recombinant antibody variants. The single-chain variable fragment (scFv) antibody is a minimal form of functional antibody comprised of the variable domains of immunoglobulin light and heavy chains connected by a flexible linker. In most cases, scFvs are expressed in the periplasm bacterium *E. coli*. The production of soluble scFvs is more effective in quantity, however, under the reducing conditions of the *E. coli* bacterial cytoplasm it is inefficient because of the inability of the disulfide bonds to form. Hence, scFvs are either secreted to the periplasm as soluble proteins or expressed in the cytoplasm as insoluble inclusion bodies and recovered by refolding. The cytoplasmic expression of scFvs as a C-terminal fusion to maltose-binding protein (MBP) provided the high-level production of stable, soluble, and functional fusion protein. The below protocol provides the detailed description of MBP-scFv production in *E. coli* utilizing two expression systems: pMALc-TNN and pMALc-NHNN. Although the MBP tag does not disrupt the most of antibody activities, the MBP-TNN-scFv product can be cleaved by Tobacco Etch Virus (TEV) protease in order to obtain untagged scFv.

The second protocol is for efficient production of Fab antibody fragments as MBP fusion proteins secreted by transiently transfected mammalian cells. While transient transfection is a fast and effective way of obtaining several mgs of antibody for initial screening and validation of antibodies, some antibody sequences express poorly or not at all. For such antibodies, fusion to MBP provides an effective approach for solving the expression problem.

Key words Single chain variable fragment (scFv), Fab, Monoclonal antibody (mAb), Maltose-binding protein (MBP), Tobacco Etch Virus (TEV) protease

Racheli Birnboim-Perach and Yehudit Grinberg contributed equally to this work.

Michael Steinitz (ed.), *Human Monoclonal Antibodies: Methods and Protocols*, Methods in Molecular Biology, vol. 1904, https://doi.org/10.1007/978-1-4939-8958-4_23,

1 Introduction

Monoclonal antibodies (mAbs) are currently the fastest growing class of therapeutic proteins and represent one third of the total number of proteins used for therapy of various diseases in developed countries [1]. The production of fully human mAbs using transgenic mice [2, 3], human hybridomas [4], or *Escherichia coli* (*E. coli*) bacteria [5] permits an almost unlimited antibody supply for clinical and research applications. The development of recombinant technologies provided the production of recombinant antibody variants based on different forms of variable domains [6]. The commonly used single-chain variable fragment (scFv) antibodies are a minimal form of functional antibodies comprising of only the variable domains of the immunoglobulin heavy and light chain connected by a short flexible peptide linker [7]. In contrast to the bivalent stable 150 kDa IgG molecule, the smaller 25 kDa scFv is monovalent and upon intravenous injection possesses a short serum half-life of only a few hours [8]. Furthermore, due to its small size, the scFv is considered to have better tumor penetration compared to IgG due to its diffusion properties, making it more suitable tool in anticancer therapy and imaging [9, 10]. A recombinant scFv can be produced in a variety of different systems ranging from bacteria to mammalian cells. However, the reducing environment of the bacterial cytoplasm inhibits the formation of the intradomain disulfide bonds within the scFv or another antibody-based molecule. The common solution for that is secretion of the scFv to the bacterial periplasm where the oxidizing conditions facilitate the formation of the disulfide bonds [11]. As an alternative that allows exceptionally high level of expression, we suggested the expression of the recombinant scFvs as a C-terminal fusion with the *E. coli* maltose-binding protein (MBP) that stabilized the scFv and provided the efficient functional expression in the cell cytoplasm as a soluble, active form [12]. For most cases, the presence of MBP does not have any negative effect on the majority of antibody properties. Moreover, MBP-scFv fusion protein demonstrated higher stability and functionality in vitro than unfused scFv produced in *E. coli* cytoplasm [12]. In addition, MBP can be used as a tag for affinity purification of the recombinant antibody. However, the immunogenicity of the bacterial MBP does not allow applying MBP-fusion antibodies in animal and human research in vivo. Therefore, after MBP served its purpose of allowing efficient expression and purification it should be removed. To facilitate that we introduced the tobacco etch virus (TEV) protease cleavage site between the MBP and the scFv. TEV protease is a 27 kDa catalytic domain of the Nuclear Inclusion a protein (NIa) that recognizes and cleaves specific amino acid consensus sequence (ENLYFQS) leaving only an N-terminal Serine as

an N-terminal extension of the scFv [13]. Thus, the released scFv fragment does not contain an immunogenic tag making it suitable for in vivo application.

The second part of this chapter is a protocol for producing MBP-fused Fab fragments in transfected mammalian cells. Fabs are used frequently in antibody discovery, such as from Fab phage display libraries [14, 15]. Fabs can be produced by bacterial expression and also in transfected mammalian cells [16, 17]. Previously, we described that fusion of scFvs to MBP boosts their production not only in *E. coli*, but also in transfected mammalian cells [18]. We found that antibody expression level (IgGs and Fabs) varies a lot between antibodies of different sequences, and some antibodies express very poorly or not at all. Fusion of MBP to one or both heavy and light chains significantly improved expression.

In this chapter, we describe two different approaches for production of MBP-fused single-chain antibodies in *E. coli* bacteria and one protocol for production of MBP-fused Fabs in transiently transfected HEK293 cells that include:

1. Expression using plasmid pMALc-TNN scFv that encodes the MBP-scFv fusion construct with a TEV protease cleavage site between the fused proteins (Fig. 1a). This provides the opportunity to express the scFv as a soluble protein in the cytoplasmic

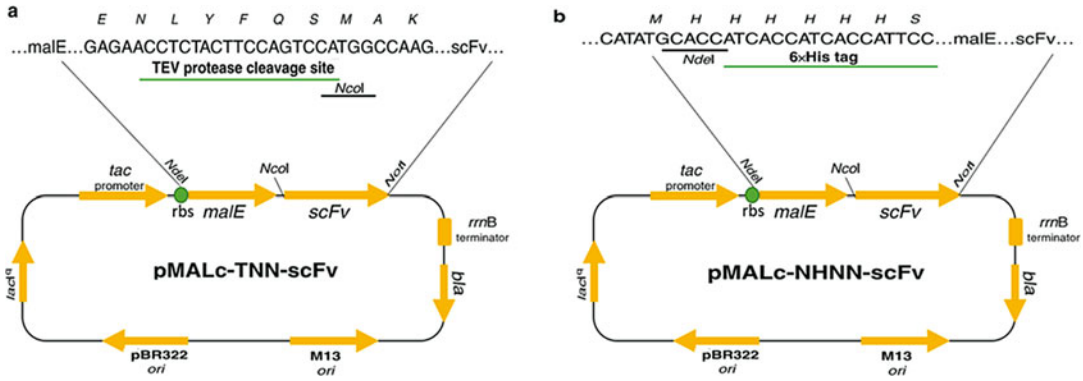

Fig. 1 Maps of pMALc plasmids for cytoplasmic expression of MBP-scFvs in *E. coli*. Plasmids pMALc-TNN (**a**) and pMALc-NHNN (**b**) are ampicillin-resistance carrying *colE1* replicon-based medium copy number plasmids. The plasmids were designed for expression of scFvs, fused to the C-terminus of MBP in the *E. coli* cytoplasm, in a soluble and active form under control of an IPTG-induced *tac* promoter. pMALc allows the cloning of scFv of interest as *NcoI-NotI* fragments to create an open reading frame which codes for a fusion between the cloned scFv and the C-terminus of MBP. (**a**) pMALc-TNN plasmid contains the TEV protease recognition site between MBP and scFv that provides the opportunity for controlled release of the single-chain antibody protein fragment from its MBP tag. (**b**). pMALc-NHNN plasmid encodes 6×His tag at N-terminus of MBP-scFv construct. The resulted fusion protein can be purified using either MBP or 6×His tag, or sequential purification steps using both tags. *MalE* maltose-binding protein (MBP), Bla beta-lactamase. Complete sequences are available from the authors upon request

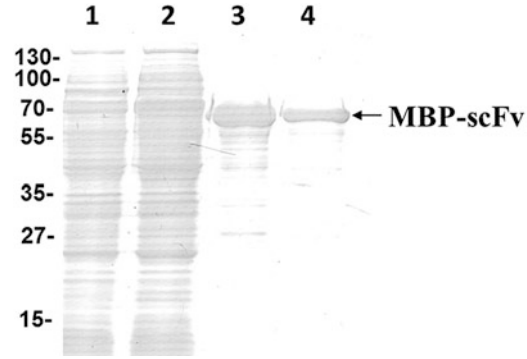

Fig. 2 Analysis of 6×His-tag-MBP-scFv expression and purification by SDS-PAGE. pMALc-NHNN-scFv vector was used for transformation to *E. coli* Rosetta BL-21 bacteria. The culture was induced for protein expression using IPTG followed by protein purification from soluble cytoplasmic fraction. Protein sample were separated on an SDS 12% polyacrylamide gel and visualized using Coomassie blue staining. Lane 1: uninduced soluble fraction; lane 2: induced soluble fraction of 6×His-tag-MBP-scFv; lane 3: amylose resin purified 6×His-tag-MBP-scFv; lane 4: Ni-NTA purified 6×His-tag-MBP-scFv (previously purified on amylose resin)

fraction, purify it on an amylose resin column, cleave the antibody from its tag and obtain the purified scFv.

2. Expression using plasmid pMALc-NHNN-scFv that encodes a 6His-tag-MBP-scFv fusion construct that enables the purification of the protein on either Ni-NTA or amylose purification columns (*see* **Note 1**). Moreover, a sequential purification by both columns can be used (Figs. 1b and 2). Although there is no TEV protease cleavage site to remove the tag in this construct, the presence of maltose binding protein for the majority of the cases does not have any influence on the antibody's binding properties. In addition, the presence of maltose-binding protein can be useful for rapid screening of a large number of scFvs (*see* **Notes 2** and **3**).
3. Expression of Fabs using two plasmids pcDNA3.4-Fd and pcDNA3.4-L that encode the MBP-heavy and for a Kappa light chain of the Fab in Expi293^{TM} cells. The plasmid DNAs are introduced into the cells by transient transfection and the Fabs are purified from conditioned media 4–6 days post transfection by HisTrap chromatography.

2 Materials (*See* Note 4)

2.1 Construction of pMALc-scFv of Interest

1. Plasmid vectors: pMALc-TNN or pMALc-NHNN vector fragments (*see* **Note 5**) previously digested with *Nco*I and *Not*I restriction enzymes (*see* **Note 6**).

2. Single-chain fragment of antibody of interest (*see* **Note 7**).
3. Primers: *Nco*l-scFv-For (5′-tatataCCATGGcc-scFv sequence-3′) and *Not*l-scFv-Rev (5′-tatataGCGGCCGCTTA-scFv sequence-3′) (*see* **Note 8**) for amplification of the scFv. Primer malc6-scq (5′-gacgcgcagactaattcgagc-3′) can be used for sequencing of the insert cloned in either plasmid.
4. PCR Master Mix 2xReddy Mix™ (Abgene (http://www.abgene.com)) for amplification of scFv fragment.
5. PCR cleanup kit.
6. Restriction enzymes: *Nco*l and *Not*l (New England Biolabs (http://www.neb.com)).
7. T4 DNA ligase (New England Biolabs (http://www.neb.com)).
8. Bacteria strains: *E coli* DH5α strain or XL-1 blue (GibcoBRL, Life Technologies) is used for cloning.
9. Ampicillin antibiotic (see Subheading 2.7).
10. Growth media: Yeast extract-tryptone ×2 (2×YT) (*see* Subheading 2.8).

2.2 Expression Using Plasmid pMALc-NHNN/TNN-scFv

1. Plasmid vectors: pMALc-TNN scFv or pMALc-NHNN-scFv (*see* **Note 5**).
2. Bacteria strain: *E. coli* Rosetta BL-21 (Novagen, now EMD4Bioscences).
3. Antibiotics: ampicillin, chloramphenicol (*see* Subheading 2.7).
4. Luria Bertani (LB) growth media (*see* Subheading 2.8).
5. Isopropyl β-D-1-thiogalactopyranoside (IPTG): use 0.5 mM for scFv overexpression (*see* Subheading 2.7).

2.3 Purification of pMALc-NHNN-scFv on a Nickel-NTA Column (See Note 9)

1. Binding buffer: 50 mM NaH_2PO_4, 0.3 M NaCl, 10 mM imidazole, adjust to pH 8.0. PBS + 0.1% Triton X-100 + 10 mM imidazole may be used instead. Filter or sterilize by autoclaving (All reagents were purchased from Merck & Co., Inc.).
2. Sonication device: ultrasonic liquid processor. Optionally, cell disruption by a French press apparatus can be used.
3. Ni-NTA agarose beads (Invitrogen, http://tools.invitrogen.com/content/sfs/manuals/ ninta_system_man.pdf).
4. 10 mL gravity-flow polypropylene columns (pierce, now Thermo Scientific).
5. Imidazole (0.5 M in PBS) for washing and elution of His tagged protein from the column (Merck & Co., Inc.).
6. For dialysis: SnakeSkin-Pleated Dialysis tubing (10 kDa cutoff) supplied by Pierce (now Thermo Scientific).

2.4 Purification on an Amylose Resin Column (See Note 10)

1. Phosphate-buffered saline (PBS) (*see* Subheading 2.7) + 0.5 % Triton X-100 detergent (Sigma).
2. Sonication device: ultrasonic liquid processor.
3. Amylose resin (New England Biolabs (http://www.neb.com)).
4. 10 mL gravity flow polypropylene columns (Pierce, now Thermo Scientific).
5. For elution: 20 mM maltose in PBS. Maltose was purchased from Sigma). For PBS preparation *see* Subheading 2.7.

2.5 Expression and Purification of TEV Protease (See Note 11)

The TEV protease is commercially available from several vendors (such as Invitrogen (http://www.invitrogen.com)). We use plasmid pRK508-TEV [19] for the expression of MBP-TEV protease fusion that can be later purified on amylose column.

1. Plasmid vectors pRK508-TEV (*see* **Note 11**).
2. Bacterial strain: *E. coli* Rosetta BL-21 (Novagen, now EMD4-Bioscicnccs: http://www.emdmillipore.com/life-science-research).
3. Antibiotics: ampicillin, chloramphenicol (*see* Subheading 2.7).
4. Luria-Bertani (LB) growth media (*see* Subheading 2.8).
5. Isopropyl β-D-1-thiogalactopyranoside (IPTG): use 0.5 mM for overexpression (*see* Subheading 2.7).
6. Phosphate-buffered saline (PBS) (*see* Subheading 2.7) + 0.5 % Triton X-100 detergent (Sigma).
7. Sonication device: ultrasonic liquid processor.
8. Amylose resin (New England Biolabs).
9. 10 mL gravity-flow polypropylene columns (Pierce, now Thermo Scientific).
10. For elution: 20 mM maltose in PBS. Maltose was purchased from Sigma). For PBS preparation *see* Subheading 2.8.

2.6 Cleavage with TEV Protease and Purification of scFv Fragment

1. TEV reaction buffer×20: 1 M Tris–HCI (pH 8.0), 10 mM EDTA (Merck & Co., Inc.).
2. 0.1 M DTT in sterile water (Sigma).
3. Amylose resin (New England Biolabs) (http://www.neb.com).
4. 10 mL gravity flow polypropylene columns (Pierce, now Thermo Scientific).

2.7 General Buffers and Reagents

1. Phosphate-buffered saline (PBS): 8 g NaCl, 0.2 g KCI, 1.44 g NaH_2PO_4, 0.24 g KH_2PO_4 per 1 L, pH 7.4. (The reagents were purchased from Merck & co., Inc.)
2. Chloramphenicol (Sigma): 34 mg/mL in 100% ethanol. Store at −20 °C.

3. Ampicillin (Roche Diagnostics (http://www.roche.com)): 100 mg/mL in water. Store at −20 °C.
4. Isopropyl β-D-l-thiogalactopyranoside (IPTG) (Bio Lab LTD. (http://www.biolab-chemicals.com)): 1 M in sterile double distilled (MilliQ) water (SDDW) stored in 1 mL aliquots at −20 °C.

2.8 Bacteria Growth Media and Buffers

These may be purchased from any supplier of common bacterial growth medium components or pre-prepared media. In our lab we use products of Becton-Dickinson (http://www.bd.com/).

1. 2×YT: 16 g Bacto-Tryptone, 10 g Yeast extract, 5 g NaCl/L water.
2. LB: 10 g Bacto-Tryptone, 5 g Yeast extract, 10 g NaCl/L water.

To prepare solid media, Bacto-agar at the final concentration of 1.8% was added to the solutions. Following the autoclaving, the media were supplemented with 0.4% glucose and antibiotics. The final concentrations of the antibiotics used in this study were as follows: ampicillin: 100 μg/mL, chloramphenicol: 34 μg/mL.

2.9 pcDNA3.4 Plasmids for Expression of Antibody Heavy and Light Chains in Mammalian Cells

1. These plasmids are based on the CMV promoter-controlled pcDNA3.4 vectors that are provided as the "Antibody Expressing Positive Control Vector" part of the Life Technologies Expi293™ kit for transient transfection based expression). Sequences of antibody heavy and light chains are cloned into separate vectors as described in the Subheading 3.
2. Primers (*see* **Note 12**): (lower case—overlap with the target vector template; upper case—MBP):

   MBP_Ldr_IgH-For- 5′ ctcaaaggtgtccagtgtAAAACTGAAGAAGGTAAAC.

   MBP_Ldr_IgH-Rev- 5′ ctcctcaagcttcacttcGGCCATGGTACTGAATTC.

   IFX_VH-For- 5′ GAAGTGAAGCTTGAGGAG.

   Neo-Rev- 5′ GCCAACGCTATGTCCTGATAGC.

   Neo-For- 5′ GCTATCAGGACATAGCGTTGGC.

   Gibson-VH-Rev- 5′ ACACTGGACACCTTTGAGCACAGC.

   CMV-seq – 5′ TGGGCGGTAGGCGTGTACGG.
3. Gibson assembly mix (New England Biolabs).
4. *Dpn*I restriction enzyme (New England Biolabs).
5. ZymoClean Gel Extraction kit (https://www.zymoresearch.eu/).

2.10 Expi293™ Kit

The Expi293™ transient Expression System is a major advance in transient expression technology for rapid and ultra-high-yield protein production from mammalian cells. This, or a similar high-yield transient transection system for HEK293 cells, should be used according to the instructions of the supplier.

2.11 Purification of MBP-Fab on a HisTrap Column

1. Phosphate buffer for HisTrap loading: NaH_2PO_4 0.2 M Na_2HPO_4 0.2 M mix at 20:80 ratio to obtain pH 7.4. Dilute ×20 into the filtered conditioned media before loading the HisTrap column.
2. Phosphate-buffered saline (PBS) (*see* Subheading 2.7) (Sigma).
3. HisTrap 1 mL column (GE).
4. Imidazole (0.5 M in PBS) for washing and elution of His-tagged proteins from the column (Merck & Co., Inc).
5. PD-10 desalting columns for buffer exchange) (*see* **Note 22**).
6. For dialysis: SnakeSkin-Pleated Dialysis tubing (10 kDa cutoff) supplied by Pierce (now Thermo Scientific).

3 Methods

The protocol described below provides the description of scFv production process. The expression of single-chain antibody fragment as MBP-fusions improves its stability and solubility and results in higher production yield of MBP-scFv in an *E. coli* expression system. Besides its "chaperon-like" activity, MBP serves for affinity purification of the scFv construct on amylose resin column. In addition, the pMALc-NHNN vector contains the N-terminal 6×His-tag fused to the MBP-scFv construct for possible purification by Ni-NTA column chromatography. The pMALc-TNN plasmid is used to express MBP-scFv containing TEV protease cleavage site separating the scFv from MBP-tag. Although commercial versions of TEV protease are available [Invitrogen (http://www.invitrogen.com)], we describe the expression of MBP-TEV construct in *E. coli* for digestion of the MBP-scFv fusion protein. The main advantage of using “home-made” MBP-TEV protein is the fact that un-tagged scFv will not be trapped by amylose resin, thus can be easily separated from other reaction component.

3.1 Construction of pMALc-scFv of Interest

The pMALc vectors can be used for expression of scFv originated from any organism if the codon usage in *E. coli* bacteria was taken under consideration (*see* **Note 10**). In spite of the differences between pMALc-TNN and pMALc-NHNN described above, the cloning procedure of single-chain antibody fragment for both vectors is identical.

1. The single-chain antibody of interest (designated as scFv) should be amplified by PCR using *Nco*I-scFv-For and *Not*I-scFv-Rev primers (*see* Subheading 2.1). The PCR reaction conditions are: 95 °C for 5 min; 30 cycles of: 94 °C for 30 s, 55 °C for 1 min, 72 °C for 1 min; and a final extension of 72 °C for 5 min. The final reaction volume is 50 μL.
2. Purify the resulted PCR product using a PCR cleanup kit (*see* **Note 11**).
3. Digest the purified PCR fragment with *Not*I and *Nco*I restriction enzymes for 1–1.5 h at 37 °C followed by gel extraction or PCR cleanup.
4. Clone the digested scFv insert to previously *Nco*I/*Not*I digested pMALc vector by standard ligation procedure and transform it into *E. coli* DH5α competent cells.
5. The success of the cloning should be verified by sequencing using the malc6-seq primer.

3.2 Expression of pMALc-NHNN/TNN-scFv

The expression procedure for pMALc-NHNN-scFv and pMAIc-TNN-scFv is identical.

1. Transform Rosetta BL-21 competent cells with pMALc-NHNN/TNN-scFv vector and plate the transformed cells on a 2×YT-agar plate containing: 100 μg/mL ampicillin and 34 μg/mL chloramphenicol. Leave for 16 h at 37 °C until colonics of transformed bacteria are clearly visible.
2. Inoculate 500 mL of LB + 100 μg/mL ampicillin in a 2 L Erlenmeyer flask with pooled colonies scraped off the plate.
3. Grow shaking (250 rpm) at 37 °C to an OD 600 nm (optical density) = 0.6–0.8 (about 3 h).
4. For induction add IPTG to the culture to 0.5 mM final concentration.
5. Continue culture growth for 20 h at 30 °C shaking (250 rpm).
6. Spin down the cells by centrifugation at 8000 × *g* at 4 °C for 30 min. For centrifugation we use RC5C Sorvall centrifuge GSA rotor (Thermo Scientific).
7. It is possible to store the cell pellet at −80 °C for up to several weeks. Alternatively, you can immediately proceed to the cell lysis and protein purification steps.

3.3 Purification of 6×His-MBP-scFv on a Nickel-NTA Column

As was mentioned above, the pMALc-NHNN-scFv construct contains a 6×His-tag that enables the purification of the MBP-scFvs by Nickel-NTA chromatography. It is highly recommended to evaluate the protein concentration and efficiency of induction prior to purification step by SDS-PAGE.

1. Resuspend the cell pellet in cold 1/5 volume (of the induced culture) of binding buffer or in PBS + 0.1% Triton X-100 (*see* Subheading 2.3).
2. Lyse by sonication on ice.
3. Centrifuge at 18,500 × *g* for 30 min at 4 °C to remove the insoluble fraction of the cell lysate. For centrifugation we use 5810R centrifuge (Eppendorf).
4. Transfer the soluble fraction to a clean 50 mL tube and keep it on ice.
5. Prepare the Ni-NTA agarose beads according to vendor's recommendations and wash them with binding buffer. Place them in a gravity column.
6. Load the cell extract and collect flow through by gravity flow (*see* **Note 13**).
7. Wash the column with 50 mL of binding buffer or with PBS + 10 mM imidazole.
8. Elute the MBP-scFv fusion protein with 0.5 M imidazole in PBS. Collect ten fractions (2 mL each) and pool protein containing fractions.
9. Analyze the purified MBP-scFv by SDS/PAGE (as shown in Fig. 2).
10. Perform two-step dialysis against PBS at 4 °C using at least 100 volumes of the combined eluate fractions for each dialysis.
11. Store the protein at a final concentration 1 mg/mL at 4 °C. For prolonged storage (longer than 1–2 weeks) store in small aliquots at −80 °C.

3.4 Purification of 6× His-MBP-scFv and MBP-scFv on an Amylose Resin Column

Both plasmid vectors, pMALc-NHNN-scFv and pMALc-TNN-scFv, enable the production of MBP-fused proteins that can be later purified on amylose resin column chromatography. We recommend the evaluation of the protein concentration and efficiency of induction prior to purification step by SDS-PAGE.

1. Resuspend the cell pellet in 1/5 volume of cold PBS + 0.1 % Triton X-100.
2. Sonicate on ice until complete lysis is reached.
3. Spin 30 min 18,500 × *g* at 4 °C to remove the insoluble fraction of the cell lysate. For centrifugation we use 5810R centrifuge (Eppendorf).
4. Save the soluble fraction and keep it on ice.
5. Prepare the amylose resin column according to vendor's recommendations and wash the beads with PBS.
6. Load the cell extract on the column and collect flow through by gravity flow (*see* **Note 12**).

7. Wash the column with 50 mL PBS.
8. Elute the protein with 20 mM maltose in PBS. Collect 2 mL fractions and pool protein containing fractions.
9. Analyze the purified MBP-scFv by SDS/PAGE (as shown in Fig. 2).
10. Keep the purified protein at a final concentration of 1 mg/mL at 4 °C. For prolonged storage (longer than 1–2 weeks) store in small aliquots at −80 °C. No dialysis step is required.

3.5 Expression and Purification of TEV Protease

The TEV protease is expressed as MBP-fusion and purified on amylose column similar to MBP-scFv purification described in Subheadings 3.2 and 3.4.

1. Transform Rosetta BL-21 competent cells with pRK508-TEV vector and plate the transformed cells on a 2×YT-agar plate containing 100 μg/mL ampicillin and 34 μg/mL chloramphenicol. Leave for 16 h at 37 °C until colonies are clearly visible.
2. Collect the bacteria colonies into 500 mL LB containing 100 μg/mL ampicillin.
3. Grow shaking (250 rpm) at 37 °C to an OD 600 nm = 0.6–0.8.
4. Induce the culture by adding IPTG to a final concentration of 1 mM.
5. Continue shaking 20 h at 16 °C (250 rpm).
6. Harvest the cells by centrifugation at 8000 × *g* for 30 min. For centrifugation we use RC5C Sorvall centrifuge GSA rotor (Thermo Scientific).
7. It is possible to store the cells pellet at −80 °C for several weeks or immediately continue to purification steps.
8. Resuspend the cell pellet in cold 1/5 volume of PBS + 0.1% Triton X-100.
9. Perform sonication on ice until complete lysis is achieved.
10. Centrifuge at 18,500 × *g* for 30 min at 4 °C to remove the insoluble fraction of the cell lysate. For centrifugation we use 5810R centrifuge (Eppendorf).
11. Transfer the soluble fraction to a clean tube and keep on ice.
12. Prepare the amylose resin column and wash the beads with PBS.
13. Load the cell extract (*see* **Note 12**).
14. Wash the column with 50 mL PBS.
15. Elute the protein with 20 mM maltose in PBS. Collect ten fractions (2 mL each) and pool protein containing fractions.

16. Store the purified MBP-TEV protease at a final concentration of 1 mg/mL stored in small aliquots at −80 °C. No dialysis step is required.

3.6 Cutting the MBP-TNN-scFv with TEV Protease and Purification of the scFv Fragment

The purification of the untagged scFv is based on the fact that both the TEV protease and the uncleaved MBP-scFv fusion protein are fused to MBP and can be trapped by an amylose column. The cleaved scFv will not bind to the column and will accumulate in the flow through (unbound) fraction. Since amylose does not always provide a highly purified fusion protein as a single purification step (Fig. 3), for a higher level of protein purity we recommend performing sequential purification steps using size-exclusion chromatography after Amylose resin purification (*see* **Note 14**).

1. Add the following to the microcentrifuge tube:
   (a) 100 μg amylose purified MBP-scFv.
   (b) 37.5 μL TEV reaction buffer ×20.
   (c) 10 μL MBP-TEV (stock concentration 1 mg/mL).
   (d) 7.5 μL 0.1 M DTT.
   (e) Sterile deionized water up to 750 μL.

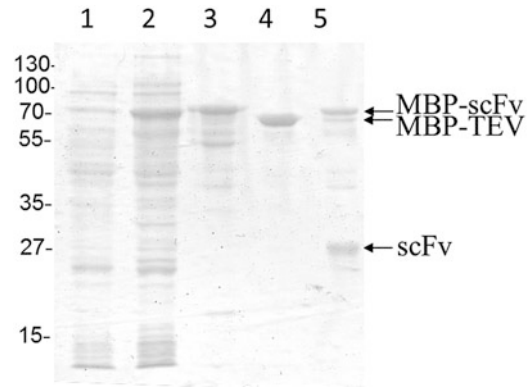

Fig. 3 Analysis of scFv expression and purification using pMALc-TNN expression system by SDS-PAGE. pMALc-TNN-scFv vector was used for transformation to *E. coli* Rosetta BL-21 bacteria. The culture was induced for protein expression using IPTG followed by protein purification from soluble cytoplasmic fraction. The amylose purified MBP-scFv fusion protein was cleaved with TEV protease that released the scFv from the MBP tag TEV protease that was used in this work was produced in *E. coli* Rosetta BL-21 bacteria as MBP fusion and purified in amylose resin. The purification of untagged scFv was provided by loading on amylose resin column and collection of unbound fraction. Protein samples were separated on an SDS 12% polyacrylamide gel and visualized using Coomassie blue staining. Lane 1: uninduced fraction; lane 2: induced MBP-TNN-scFv; lane 3: amylose purified MBP-TNN-scFv; lane 4: amylose purified MBP-TEV; lane 5: amylose (partially) purified untagged scFv (*see* **Note 14**)

2. Incubate at 16 °C overnight (*see* **Notes 15** and **16**).
3. Prepare the amylose resin column and wash the beads with PBS (*see* **Notes 17** and **18**).
4. Load the protein mixture and collect the flow through.
5. Determine the scFv concentration in the flow-through fraction.
6. Analyze the purified MBP-scFv by SDS/PAGE (as shown in Fig. 3).
7. Store the protein at 4 °C. For prolonged storage (longer than 1 week) store in small aliquots at −80 °C.

3.7 Construction of pcDNA3.4-MBP-Fd-His and pcDNA3.4-Kappa Expression Vectors (Fig. 4)

The pcDNA3.4 plasmid vector is available from several sources. The vectors described here are based on existing vectors we constructed for the expression of antibody heavy and light chains in mammalian cells. Here, we describe a vector designed for the expression of an antibody Fd fragment to which MBP was fused between the secretion signal peptide to the beginning of the VH ORF. The light chain vector is an ordinary vector for antibody Kappa light chain expression. If required, MBP can be fused to the Kappa light chain following similar steps to the ones described herein for the heavy chain.

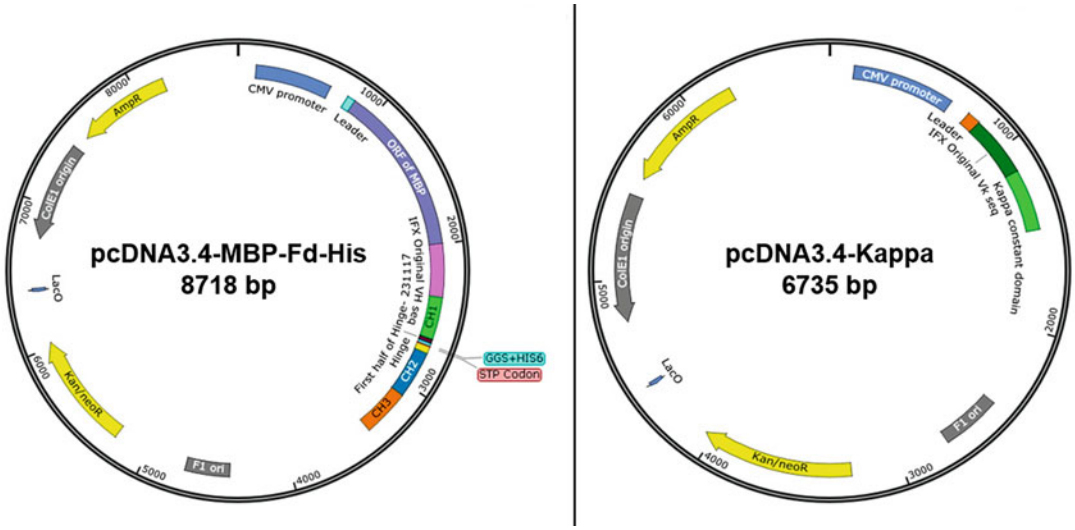

Fig. 4 Maps of pcDNA3.4-based plasmids for expression of MBP-Fab in transfected mammalian cells. Plasmids pcDNA3.4-MBP-Fd (**a**) and pcDNA3.4-L (**b**) are ampicillin-resistance carrying *colE1* replicon-based medium copy number plasmids. The expression cassette is controlled by the strong CMV promoter and is comprised of an immunoglobulin leader sequence for secretion followed by the (**a**) the Fd (VH+CH1) ORF followed by a short Gly-Gly-Ser linker followed by a His tag (sequence 4 in Appendix). (**b**) a Kappa light chain (sequence 5 in Appendix). Complete sequences are available from the authors upon request

The construction of pcDNA3.4 expression vectors for antibody heavy and light chains is by standard DNA cloning procedures and will not be presented in detail here. The sequence of the pcDNA3.4-Fd-His vector for expression of an antibody Fd domain with a C-terminal His tag is sequence 3 in Appendix.

1. PCR amplify the MBP ORF using Phusion high-fidelity thermostable DNA polymerase (New England Biolabs) with pMALc plasmid DNA as template and the primers MBP_Ldr_IgH and MBP_Ldr_IgH-Rev.
2. PCR amplify 2 vector fragments required for Gibson assembly using pcDNA3.4-IgH-Fd-IFX-6H as template with the following primers:

   Reaction 1: (F.1- From IFX toward Neo^R).

   IFX_VH-For- 5′ GAAGTGAAGCTTGAGGAG with Neo-Rev.

   Reaction 2: (From Neo^R to the leader sequence).

   Neo-For and Gibson-VH-Rev primers.
3. Digest the vector fragments in the same tube with *Dpn*I (in Cutsmart restriction buffer (New England Biolabs) to get rid of template DNA. 0.5 μL of enzyme is used for 50 μL reaction which is incubated for 1–2 h at 37 °C (no longer than 2 h).
4. Following digestion separate all fragments (including insert) on 1% preparative agarose gel and purify the DNA fragments using ZymoClean Gel Extraction kit.
5. Carry out a 3-fragment Gibson assembly using Gibson mix (New England Biolabs) according to the instructions of the supplier. Use 25 ng of each vector fragment and 100 ng of MBP. Incubate for 1 h at 50 °C. Following incubation, Transform the DNA into chemically competent *E. coli* DH5α or XL-1 blue. Plate on LB + Ampicillin agar plates to obtain well-isolated single colonies.
6. On the next day, carry out colony PCR on colonies using the up-mentioned MBP_Ldr_IgH-Rev and CMV-Seq primers. Separate the PCR products on a 1.5% agarose gel.
7. Grow 3 mL cultures of from positive clones in LB + ampicillin for 20 h 37 °C.
8. Purify plasmid DNA from each culture using a miniprep kit (Invitrogen) and verify by Sanger sequencing with CMV-Seq as a sequencing primer.

3.8 Expression of MBP-Fab by Transient Transfection of Expi293™ Cells

The workflow with the Expi293TM kit is basically according to the instructions of the supplier. Here are a few important points:

1. Transfect 75×10^6 $Expi293^{TM}$ cells (*see* **Note 19**) using 10 μg pcDNA3.4-Fd-His plasmid and 20 μg pcDNA3.4-Kappa

plasmid (*see* **Note 20**). Place the cells in a 125 mL ventilated shake flask.

2. Grow in a CO_2 incubator set at 37 °C 8% CO_2 shaking at 150 rpm.
3. 20 h post transfections add the enhancers (which are part of the Expi293™ kit) and continue growing. This is Day 1.
4. Assay conditioned on day 5 and day 7 by SDS/PAGE electrophoresis. Usually, the MBP-Fab is purified from day 7 post transfection.

3.9 Purification of MBP-Fab on a HisTrap Column (See Note 21)

1. Collect the conditioned medium into a 50 mL conical tube and remove cells by centrifugation for 10 min, 10,000 × *g*, 4 °C. Filter the cell-free conditioned medium using a 0.45 μm syringe filter.
2. To the 30 mL filtered conditioned medium add 1.5 mL 0.2 M Phosphate buffer pH 7.4 and bring to 5 mM Imidazole.
3. Load a 1 mL HisTrap column at 0.5 mL/min (this is the flow rate throughout the loading and purification process) (*see* **Note 21**).
4. Wash the column with 5 column volumes of PBS + 10 mM Imidazole.
5. Elute the column with PBS + 100 mM Imidazole. Analyze fractions on 12% polyacrylamide gel under nonreducing as reducing conditions, loading 3–5 μg protein/lane (*see* Fig. 5).

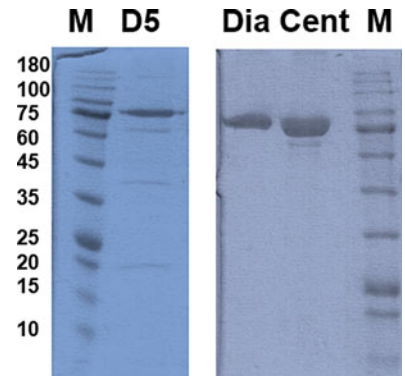

Fig. 5 SDS-PAGE analysis of MBP-Fab expression and purification in Expi293™ cells. pcDNA3.4-MP-Fd-His and pcDNA3.4-Kappa vectors were used for transfect Expi293™ cells. The MW sizes are in kDa. *M*, MW marker; D5, conditioned medium collected 5 days post transfection (20 μL conditioned media loaded); *Dia* dialyzed MBP-Fab after HisTrap purification (3 μg protein loaded). *Cent* concentrated MBP-Fab ready for storage (5 μg protein loaded)

6. Buffer-exchange the purified MBP-Fab using a PD10 column (*see* **Note 22**). When required concentrate using a centrifugal concentration device with 10 kDa cutoff.
7. Store the MBP-Fab at a final concentration 1 mg/mL at 4 °C. For prolonged storage (longer than 1–2 weeks) store in small aliquots at −80 °C.

4 Notes

1. For efficient purification of MBP fused proteins on amylose resin, it is important to ensure high levels of the induced proteins within the total soluble fraction (20–30%). In cases of low induction levels, we recommend preparing the scFv gene by total gene synthesis with optimization for expression in *E. coli*.
2. The presence of fused MBP does not influence scFv protein characteristics. On the other hand, the high immunogenicity of MBP is problematic in terms of its application in animal or human studies for determination of antibody pharmacokinetics, distribution, or therapeutic efficacy.
3. In the protocol, we recommend using sequential chromatography on amylose and Ni-NTA columns. A single-step purification, while in many cases is sufficient for preliminary analysis, rarely provides highly purified proteins. When using pMALc-TNN-scFv that does not contain a built-in 6×His-tag, the user is advised to append one by PCR to the 3′ end of the scFv-coding DNA. Alternatively, a 6×His-tag may be appended to the 5′ end of the MBP coding sequence as presented in the example of the pMALc-NHNN-scFv plasmid. pMALc plasmids are available from New-England Biolabs (NEB)). NEB plasmids may be used instead of the plasmids described herein, in which case, they should be used according to the instructions of the supplier, or NEB plasmids can be modified to become identical to the plasmids described herein (*see* Appendix). We prefer digesting MBP fusion proteins with TEV protease over the Xa protease suitable for NEB pMALc plasmids.
4. In the list of Materials (Subheading 2) we provide the names of vendors from which we currently purchase reagents. We do not by any means endorse these particular vendors. Whenever possible we provide the URLs of the vendor sites. We encourage the users to use vendors of their choice.
5. The vectors should be purified by miniprep kit. The pMALc plasmid concentration is commonly low: 50–150 ng/μL. Do not continue to a digestion step with plasmid concentration lower than 30 ng/μL.

6. The restriction enzyme *Not*I digests linear DNA better than circular DNA. For a successful digestion, we recommend incubating the uncut plasmid with *Nco*I for 1 h at 37 °C and afterward adding *Not*I for an additional 1 h incubation. No DNA cleanup procedure between the enzymes is required.
7. For the construction of scFv from full-length IgG, *see* [20]. In general, we recommend ordering synthetic genes with optimization for the expression organism over PCR amplification from the antibody vector that was used in the antibody discovery step. In addition, we nowadays prefer restriction-free cloning, such as Gibson assembly [21].
8. For the construction of *Nco*I-scFv-For primer use the 18 initial nucleotides of the antibody of interest (no ATG start codon is needed) following the sequence described in Subheading 2.1. For the construction of *Not*I-scFv-Rev primer use the reverse complement C-terminal sequence of scFv follow the sequence described in Subheading 2.1 (no stop codon is needed).
9. Recently we switched from gravity-flow Ni-NTA agarose to HisTrap columns (GE, https://www.gelifesciences.com/en/ke/shop/chromatography/resins/affinity-tagged-protein/histrap-ff-p-00251). Those should be used according to the recommendations of the supplier.
10. Recently we switched from gravity-flow Amylose resin to MBP-Trap columns (GE, https://www.gelifesciences.com/en/bd/shop/chromatography/resins/affinity-tagged-protein/mbptrap-hp-p-00306). Those should be used according to the recommendations of the supplier.
11. Plasmid pRK508-TEV for the expression of the TEV protease was kindly provided by Dr. David Waugh, Macromolecular Crystallography Laboratory, National Cancer Institute at Frederick, MD, USA. TEV protease is also commercially available, for example from Sigma). When purchased, it should be used according to the recommendations of the supplier.
12. The template for which these primers are suitable is pcDNA3.4-Fd-His in which the Fd domain of the therapeutic antibody Infliximab is cloned. It is sequence 3 in Appendix. When other antibodies are cloned, the primers should suit these templates.
13. The low expression levels of the desired protein can be explained by deficiency of a particular aminoacyl tRNA in *E. coli* strain for a particular codon in antibody sequence. The problem can be solved by gene optimization technique or by using the special *E. coli* strains for protein expression.

14. Unless mentioned otherwise, standard protocols of the commercially obtained kits should be used during cloning and purification processes.
15. Although TEV protease is maximally active at 34 °C, we recommend performing the prolonged incubation at 16 °C to ensure the stability of cleaved scFv.
16. To ensure the cleavage efficiency, analyze the protein mixture following the incubation with TEV protease by SDS-PAGE electrophoresis.
17. In the presented protocol we describe the protein purification using gravity-flow columns. For purification using FPLC pump using for example MBPTrap columns (GE Healthcare (http://www.gehealthcarc.com)), loading at 1 mL/min is preferable.
18. We recommend carrying out size-exclusion chromatography not just a polishing step after TEV protease-mediated removal of MBP but also on intact MBP-scFvs. This is important for two reasons: one is that amylose affinity chromatography does not always provide high purity of MBP fusion proteins (Fig. 3). The second reason; in some cases, MBP-based fusion proteins have been shown to form soluble oligomers (also called "soluble aggregates") [22–24]. Although not common, this may occur with MBP-scFvs too (our unpublished observations). To make sure you obtain reliable functional data of your antibodies you should make sure you are working with soluble monomers with a MW of about 65–70 kDa. Size-exclusion chromatography should be carried out using for example a Superdex 200 column (GE Healthcare (http://www.gehealthcare.com)) according to the recommendations of the supplier.
19. Expi293^{TM} cells are grown in 125 mL shake flasks rotating at 150 rpm in a CO_2 incubator held at 8% CO_2. The cells provide maximal yield after they have been passaged for 6 times before transfection.
20. A 2:1 light chain vector: heavy chain vector ratio in the transfection provides in most cases better yield than 1:1 ratio.
21. It is possible to purify MBP-Fabs using KappaSelect or LambdaSelect affinity columns (https://www.gelifesciences.co.jp/catalog/pdf/Kappaselect_LamdaFabSelect.pdf)—according to the light chain the Fab has. We prefer HisTrap purification because it does not involve exposure of the Fab to acidic pH (as is done with the affinity columns) which may be detrimental to the stability of the Fab.
22. Instead of buffer exchange using a PD-10 desalting column, the MBP-Fab can be dialyzed against 1000 volumes of PBS for 24 h at 4 °C using snakeskin or similar dialysis tubing with 10,000 kDa cutoff.

Appendix: Sequences of Plasmids (Complete Sequences Are Available from the Authors Upon Request)

The sequence of **pMALc2** from NEB is available at: https://international.neb.com/-/media/nebus/page-images/tools-and-resources/interactive-tools/dna-sequences-and-maps/text-documents/pmalc2gbk.txt?la=en

1. **pMALc-TNN-scFv35** (the cloned scFv is an anti HCV NS3 protease scFv that was earlier described [25]. To create **pMALc-TNN-scFv35**, insert the following sequence between coordinates 2676 to 2727 of **pMALc2**. In the sequence below, the scFv (including the C-terminal His tag and Myc tag) is cloned between positions 31 to 847.

   tccGAGaacCTCtacTTCcagTccatggccGAGGTC-
   CAGCTGCA
   GCAATCTGGAGCAGAGCTTGTGAGGTCAGGGGCCT
   CAGTCAAGTTGTCCTGCACAGCTTCTGGCTTCAACA
   TTAAAGACTACTATATGCACTGGGTGAAGCAGAGGC
   CTGAACAGGGCCTGGAGTGGATTGGATGGATTGATC
   CTGAGAATGGTGATACTGAATACACTCAGAAGTTCAA
   GGGCAAGGCCACATTGACTGCAGATAAATCCCCCAG
   CACAGCCTACATGCAACTGAGCAGCCTGACATCTGA
   GGACTCTGCAGTCTATTACTGTGCAAGAATTACTAC
   GGATTACTACTTTGACTACTGGGGCCAAGGCACCAC
   GCTCACCGTCTCCTCGggaggtggtggatccggcggtggcggttct
   ggtggaggtggatctGATGTTGTGATGACCCAAACTCCACT
   CTCCCTGCCTGTCAGTCTTGGAGATCAAGCCTCCA
   TCTCTTGCAGATCTAGTCAGAGCCTTGTACATAGTAA
   TGGAAACACCTATTTAGAATGGTACCTGCAGAAACCA
   GGCCAGTCTCCAAAGCTCCTGATCTACAAAGTTTCC
   AACCGATTTTCTGGGGTCCCAGACAGGTTCAGTGGC
   AGTGGATCAGGGACAGATTTCACACTCAAGATCAGC
   AGAGTGGAGGCTGAGGATCTGGGAGTTTATTTCTGC
   TCTCAAAGTACACATGTTCCTCTCACGTTCGGTGCT
   GGGACCAAACTGGAGATCAAACGGgcggccgcACATCA
   TCATCACCATCACGGGGCCGCAGAACAAAAACTCATc
   TCAGAAGAGGATCTGAATggggccgcaT

2. **To create pMALc-NHNN-scFv35** (the cloned scFv is an anti HCV NS3 protease scFv that was described in [25]. To create **pMALc-NHNN-scFv35**, insert the following sequence between coordinates 1524 to 2723 of pMALc2. In the sequence below, there is a His tag before the MBP ORF is between positions 7 to 24. The scFv (including the C-terminal

His tag and Myc tag) is cloned between positions 1186 to 1950.

catatgCACCATCACCATCACCATtccggcAAAACTGAAGAA
GGTAAACTGGTAATCTGGATTAACGGCGATAAAGGCT
ATAACGGTCTCGCTGAAGTCGGTAAGAAATTCGAGAA
AGATACCGGAATTAAAGTCACCGTTGAGCATCCGGAT
AAACTGGAAGAGAAATTCCCACAGGTTGCGGCAACT
GGCGATGGCCCTGACATTATCTTCTGGGCACACGAC
CGCTTTGGTGGCTACGCTCAATCTGGCCTGTTGGCT
GAAATCACCCCGGACAAAGCGTTCCAGGACAAGCTG
TATCCGTTTACCTGGGATGCCGTACGTTACAACGGC
AAGCTGATTGCTTACCCGATCGCTGTTGAAGCGTTA
TCGCTGATTTATAACAAAGATCTGCTGCCGAACCCG
CCAAAAACCTGGGAAGAGATCCCGGCGCTGGATAAA
GAACTGAAAGCGAAAGGTAAGAGCGCGCTGATGTTC
AACCTGCAAGAACCGTACTTCACCTGGCCGCTGATT
GCTGCTGACGGGGGTTATGCGTTCAAGTATGAAAAC
GGCAAGTACGACATTAAAGACGTGGGCGTGGATAAC
GCTGGCGCGAAAGCGGGTCTGACCTTCCTGGTTGA
CCTGATTAAAAACAAACACATGAATGCAGACACCGAT
TACTCCATCGCAGAAGCTGCCTTTAATAAAGGCGAA
ACAGCGATGACCATCAACGGCCCGTGGGCATGGTC
CAACATCGACACCAGCAAAGTGAATTATGGTGTAAC
GGTACTGCCGACCTTCAAGGGTCAACCATCCAAACC
GTTCGTTGGCGTGCTGAGCGCAGGTATTAACGCCG
CCAGTCCGAACAAAGAGCTGGCGAAAGAGTTCCTCG
AAAACTATCTGCTGACTGATGAAGGTCTGGAAGCGG
TTAATAAAGACAAACCGCTGGGTGCCGTAGCGCTGA
AGTCTTACGAGGAAGAGTTGGCGAAAGATCCACGTA
TTGCCGCCAcTatggAAAACGCCCAGAAAGGTGAAATC
ATGCCGAACATCCCGCAGATGTCCGCTTTCTGGTAT
GCCGTGCGTACTGCGGTGATCAACGCCGCCAGCGG
TCGTCAGACTGTCGATGAAGCCCTGAAAGACGCGCA
GACTAATTCGAGCTCggtaccgtcctctctcgtgatcgagggtaggcct
gaattcagtaccatggccGAGGTCCAGCTGCAGCAATCTGGA
GCAGAGCTTGTGAGGTCAGGGGCCTCAGTCAAGTT
GTCCTGCACAGCTTCTGGCTTCAACATTAAAGACTA
CTATATGCACTGGGTGAAGCAGAGGCCTGAACAGGG
CCTGGAGTGGATTGGATGGATTGATCCTGAGAATGG
TGATACTGAATACACTCAGAAGTTCAAGGGCAAGGC
CACATTGACTGCAGATAAATCCCCCAGCACAGCCTA
CATGCAACTGAGCAGCCTGACATCTGAGGACTCTGC
AGTCTATTACTGTGCAAGAATTACTACGGATTACTAC
TTTGACTACTGGGGCCAAGGCACCACGCTCACCGTC
TCCTCGggaggtggtggatccggcggtggcggttctggtggaggtggatct
GATGTTGTGATGACCCAAACTCCACTCTCCCTGCCT
GTCAGTCTTGGAGATCAAGCCTCCATCTCTTGCAGA

TCTAGTCAGAGCCTTGTACATAGTAATGGAAACACCT
ATTTAGAATGGTACCTGCAGAAACCAGGCCAGTCTC
CAAAGCTCCTGATCTACAAAGTTTCCAACCGATTTTC
TGGGGTCCCAGACAGGTTCAGTGGCAGTGGATCAG
GGACAGATTTCACACTCAAGATCAGCAGAGTGGAGG
CTGAGGATCTGGGAGTTTATTTCTGCTCTCAAAGTA
CACATGTTCCTCTCACGTTCGGTGCTGGGACCAAAC
TGGAGATCAAACGGgcggccgcagactacaaggact

The sequence of plasmid **pcDNA3.1** is available at: https://www.ncbi.nlm.nih.gov/nuccore/EF550208.1

3. **To create pcDNA3.4-Fd-His (an expression vector for an antibody Fd domain with a C-terminal His tag)**, insert the following sequence between coordinates 820 to 2912 of **pcDNA3.1**. (The resulting **pcDNA3.4-Fd-His** carries the cloned VH-CH1 is of the therapeutic monoclonal anti TNFα antibody Infliximab). In the sequence below, the secretion leader sequence ORF spans positions 147 to 203. The Fd (VH +CH1) (including a C-terminal His tag and stop codon) spans positions 204 to 911. In the sequence shown herein, the His tag and stop codon were inserted between the end of the human Gamma1 CH1 to the hinge region (spanning positions 882 to 908). Upon removal of the sequence spanning positions 882 to 911, a full human IgG1 heavy chain ORF will be restored.

GTTTAGTGAACCGTCAGATCGCCTGGAGACGCCATC
CACGCTGTTTTGACCTCCATAGAAGACACCGGGACC
GATCCAGCCTCCGGACTCTAGAGGATCGAACCCTTG
GATCTCTAGCGAATTCCCTCTAGACACAGACGCTCA
CCATGGAGACTGGGCTGCGCTGGCTTCTCCTGGTC
GCTGTGCTCAAAGGTGTCCAGTGTGAAGTGAAGCTT
GAGGAGTCTGGAGGAGGCTTGGTGCAACCTGGAGG
ATCCATGAAACTCTCCTGTGTTGCCTCTGGATTCAT
TTTCAGTAACCACTGGATGAACTGGGTCCGCCAGTC
TCCAGAGAAGGGGCTTGAGTGGGTTGCTGAAATTAG
ATCAAAATCTATTAATTCTGCAACACATTATGCGGAG
TCTGTGAAAGGGAGGTTCACCATCTCAAGAGATGAT
TCCAAAAGTGCTGTGTACCTGCAAATGACCGACTTA
AGAACTGAAGACACTGGCGTTTATTACTGTTCCAGG
AATTACTACGGTAGTACCTACGACTACTGGGGCCAA
GGCACCACTCTCACAGTGTCCTCCgctAGCaccaagggcc
catcggtcTTCCCCCTGGCACCCTCCTCCAAGAGCACCT
CTGGGGGCACAGCGGCCCTGGGCTGCCTGGTCAAG
GACTACTTCCCCGAACCGGTGACGGTGTCGTGGAA
CTCAGGCGCCCTGACCAGCGGCGTGCACACCTTCC
CGGCTGTCCTACAGTCCTCAGGACTCTACTCCCTCA
GCAGCGTGGTGACCGTGCCCTCCAGCAGCTTGGGC
ACCCAGACCTACATCTGCAACGTGAATCACAAGCCC
AGCAACACCAAGGTGGACAAGAGAGTTGAGCCCAAA

TCTTGTGACAAAACTggcggctcccatcaccatcaccatcacTGAGA
GCCCAAATCTTGtGACAAAACTCACACATGCCCACCG
TGCCCAGCACCTGAACTCCTGGGGGGACCGT-
CAGTC
TTCCTCTTCCCCCCAAAACCCAAGGACACCCTCATG
ATCTCCCGGACCCCTGAGGTCACATGCGTGGTGGT
GGACGTGAGCCACGAAGACCCTGAGGTCAAGTTCA
ACTGGTACGTGGACGGCGTGGAGGTGCATAATGCC
AAGACAAAGCCGCGGGAGGAGCAGTACAACAGCAC
GTACCGTGTGGTCAGCGTCCTCACCGTCCTGCACC
AGGACTGGCTGAATGGCAAGGAGTACAAGTGCAAGG
TCTCCAACAAAGCCCTCCCAGCCCCCATCGAGAAAa
CCATCtCCAAAGCCAAAGGGCAGCCCCGAGAACCAC
AGGTGTACACCCTGCCCCCATCCCGGGATGAGCTG
ACCAAGAACCAGGTCAGCCTGACCTGCCTGGTCAAA
GGCTTCTATCCCAGCGACATCGCCGTGGAGTGGGA
GAGCAATGGGCAGCCGGAGAACAACTACAAGACCAC
ACCTCCCGTGCTGGACTCCGACGGCTCCTTCTTCC
TCTACAGCAAGCTCACCGTGGACAAGAGCAGGTGG
CAGCAGGGGAACGTCTTCTCATGCTCCGTGATGCA
TGAGGCTCTGCACAACCACTACAcGCAGAAGAGCCT
CTCCCTGTCCCCGGGTAAAtgAGCGGCCGCTCGAGG
CCGGCAAGGCCGGATCCCCCGACCTCGACAAGGGT
TCGATCCCTACCGGTTAGTAATGAGTTTGATATCTCG
ACAATCAACCTCTGGATTACAAAATTTGTGAAAGATT
GACTGGTATTCTTAACTATGTTGCTCCTTTTACGCTA
TGTGGATACGCTGCTTTAATGCCTTTGTATCATGCT
ATTGCTTCCCGTATGGCTTTCATTTTCTCCTCCTTG
TATAAATCCTGGTTGCTGTCTCTTTATGAGGAGTTG
TGGCCCGTTGTCAGGCAACGTGGCGTGGTGTGCAC
TGTGTTTGCTGACGCAACCCCCACTGGTTGGGGCA
TTGCCACCACCTGTCAGCTCCTTTCCGGGACTTTCG
CTTTCCCCCTCCCTATTGCCACGGCGGAACTCATCG
CCGCCTGCCTTGCCCGCTGCTGGACAGGGGCTCGG
CTGTTGGGCACTGACAATTCCGTGGTGTTGTCGGG
GAAGCTGACGTCCTTTCCATGGCTGCTCGCCTGTG
TTGCCACCTGGATTCTGCGCGGGACGTCCTTCTGC
TACGTCCCTTCGGCCCTCAATCCAGCGGACCTTCCT
TCCCGCGGCCTGCTGCCGGCTCTGCGGCCTCTTCC
GCGTCTTCGCCTTCGCCCTCAGACGAGTCGGATCTC
CCTTTGGGCCGCCTCCCCGCCTGGAAACGGGGGAG
GCTAACTGAAACACGGAAGGAGACAATACCGGAAGG
AACCCGCGCTATGACGGCAATAAAAAGACAGAATAAA
ACGCACGGGTGTTGGGTCGTTTGTTCATAAACGCGG
GGTTCGGTCCCAGGGCTGGCACTCTGTCGATACCCC
ACCGAGACCCCATTGGGGCCAATACGCCCGCGTTTC
TTCCTTTTCCCCACCCCACCCCCCAAGTTCGGGTGA
AGGCCCAGGGCTCGCAGCCAACGTCGGGGCGGCAG

GCCCTGCCATAGCAGATCTGCGCAGCTGGGGCTCT
AGGGGGTATCCCCACGCGCC

4. **To create pcDNA3.4-MBP-Fd-His** insert the following sequence between positions 837 to 840 of **pcDNA3.4-Fd-His**. (the cloned VH-CH1 is of the therapeutic monoclonal anti TNFα antibody Infliximab). In the sequence below is the MBP ORF.

AAAACTGAAGAAGGTAAACTGGTAATCTGGATTAACG
GCGATAAAGGCTATAACGGTCTCGCTGAAGTCGGTA
AGAAATTCGAGAAAGATACCGGAATTAAAGTCACCGT
TGAGCATCCGGATAAACTGGAAGAGAAATTCCCACA
GGTTGCGGCAACTGGCGATGGCCCTGACATTATCTT
CTGGGCACACGACCGCTTTGGTGGCTACGCTCAATC
TGGCCTGTTGGCTGAAATCACCCCGGACAAAGCGTT
CCAGGACAAGCTGTATCCGTTTACCTGGGATGCCGT
ACGTTACAACGGCAAGCTGATTGCTTACCCGATCGC
TGTTGAAGCGTTATCGCTGATTTATAACAAAGATCTG
CTGCCGAACCCGCCAAAAACCTGGGAAGAGATCCCG
GCGCTGGATAAAGAACTGAAAGCGAAAGGTAAGAGC
GCGCTGATGTTCAACCTGCAAGAACCGTACTTCACC
TGGCCGCTGATTGCTGCTGACGGGGGTTATGCGTT
CAAGTATGAAAACGGCAAGTACGACATTAAAGACGT
GGGCGTGGATAACGCTGGCGCGAAAGCGGGTCTGA
CCTTCCTGGTTGACCTGATTAAAAACAAACACATGAA
TGCAGACACCGATTACTCCATCGCAGAAGCTGCCTT
TAATAAAGGCGAAACAGCGATGACCATCAACGGCCC
GTGGGCATGGTCCAACATCGACACCAGCAAAGTGAA
TTATGGTGTAACGGTACTGCCGACCTTCAAGGGTCA
ACCATCCAAACCGTTCGTTGGCGTGCTGAGCGCAG
GTATTAACGCCGCCAGTCCGAACAAAGAGCTGGCG
AAAGAGTTCCTCGAAAACTATCTGCTGACTGATGAA
GGTCTGGAAGCGGTTAATAAAGACAAACCGCTGGGT
GCCGTAGCGCTGAAGTCTTACGAGGAAGAGTTGGC
GAAAGATCCACGTATTGCCGCCAcTatggAAAACGCCC
AGAAAGGTGAAATCATGCCGAACATCCCGCAGATGT
CCGCTTTCTGGTATGCCGTGCGTACTGCGGTGATC
AACGCCGCCAGCGGTCGTCAGACTGTCGATGAAGC
CCTGAAAGACGCGCAGACTAATTCGAGCTCggtaccgtc
ctctctcgtgatcgagggtaggcctgaattcagtaccatggcc

5. **To create pcDNA3.4-IFX-Kappa** (an expression vector for a Kappa light chain. The cloned Kappa light chain is of the chimeric therapeutic monoclonal anti TNFα antibody Infliximab) insert the following sequence between position 819 to 2907 of pcDNA3.1 In the sequence below, the secretion leader sequence ORF spans positions 122 to 190. The Kappa light chain (mouse Vκ + human Cκ) spans positions 191 to 832.

GTTTAGTGAACCGTCAGATCGCCTGGAGACGCCATC
CACGCTGTTTTGACCTCCATAGAAGACACCGGGACC
GATCCAGCCTCCGGACTCTAGAGGATCGAACCCTTA
GGCAGGACCCAGCATGGACACGAGGGCCCCCACTC
AGCTGCTGGGGCTCCTACTGCTCTGGCTCCCAGGT
GCCAGATGTGCCGACATCTTGCTGACTCAGTCTCCA
GCCATCCTGTCTGTGAGTCCAGGAGAAAGAGTCAGT
TTCTCCTGCAGGGCCAGTCAGTTCGTTGGCTCAAG
CATCCACTGGTATCAGCAAAGAACAAATGGTTCTCC
AAGGCTTCTCATAAAGTATGCTTCTGAGTCTATGTC
TGGGATCCCTTCCAGGTTTAGTGGCAGTGGATCAG
GGACAGATTTTACTCTTAGCATCAACACTGTGGAGT
CTGAAGATATTGCAGATTATTACTGTCAAGAAAGTCA
TAGCTGGCCATTCACGTTCGGCTCGGGGACAAATTT
GGAAGTAAAACGCACGGTGGCTGCACCATCTGTCTT
CATCTTCCCGCCATCTGATGAGCAGTTGAAATCTGG
AACTGCCTCTGTTGTGTGCCTGCTGAATAACTTCTA
TCCCAGAGAGGCCAAAGTACAGTGGAAGGTGGATAA
CGCCCTCCAATCGGGTAACTCCCAGGAGAGTGTCAC
AGAGCAGGACAGCAAGGACAGCACCTACAGCCTCAG
CAGCACCCTGACGCTGAGCAAAGCAGACTACGAGAA
ACACAAAGTCTACGCCTGCGAAGTCACCCATCAGGG
CCTGAGTTCGCCCGTCACAAAGAGCTTCAACAGGGG
AGAGTGTTAAGGGTTCGATCCCTACCGGTTAGTAATG
AGTTTAAACTCGACAATCAACCTCTGGATTACAAAATT
TGTGAAAGATTGACTGGTATTCTTAACTATGTTGCTC
CTTTTACGCTATGTGGATACGCTGCTTTAATGCCTTT
GTATCATGCTATTGCTTCCCGTATGGCTTTCATTTTC
TCCTCCTTGTATAAATCCTGGTTGCTGTCTCTTTATG
AGGAGTTGTGGCCCGTTGTCAGGCAACGTGGCGTG
GTGTGCACTGTGTTTGCTGACGCAACCCCCACTGGT
TGGGGCATTGCCACCACCTGTCAGCTCCTTTCCGGG
ACTTTCGCTTTCCCCCTCCCTATTGCCACGGCGGAA
CTCATCGCCGCCTGCCTTGCCCGCTGCTGGACAGG
GGCTCGGCTGTTGGGCACTGACAATTCCGTGGTGT
TGTCGGGGAAGCTGACGTCCTTTCCATGGCTGCTC
GCCTGTGTTGCCACCTGGATTCTGCGCGGGACGTC
CTTCTGCTACGTCCCTTCGGCCCTCAATCCAGCGGA
CCTTCCTTCCCGCGGCCTGCTGCCGGCTCTGCGGC
CTCTTCCGCGTCTTCGCCTTCGCCCTCAGACGAGT
CGGATCTCCCTTTGGGCCGCCTCCCCGCCTGGAAA
CGGGGGAGGCTAACTGAAACACGGAAGGAGACAAT
ACCGGAAGGAACCCGCGCTATGACGGCAATAAAAAG
ACAGAATAAAACGCACGGGTGTTGGGTCGTTTGTTC
ATAAACGCGGGGTTCGGTCCCAGGGCTGGCACTCT
GTCGATACCCCACCGAGACCCCATTGGGGCCAATAC
GCCCGCGTTTCTTCCTTTTCCCCACCCCACCCCCCA
AGTTCGGGTGAAGGCCCAGGGCTCGCAGCCAACGT
CGGGGCGGCAGGCCCTGCCATAGCAGATCTGCG

References

1. Hagemeyer CE, Ahrens I, Bassler N, Dschachutaschwili N, Chen YC, Eisenhardt SU, Bode C, Peter K (2010) Genetic transfer of fusion proteins effectively inhibits VCAM-1-mediated cell adhesion and transmigration via inhibition of cytoskeletal anchorage. J Cell Mol Med 14:290–302
2. Green LL (1999) Antibody engineering via genetic engineering of the mouse: Xenomouse strains are a vehicle for the facile generation of therapeutic human monoclonal antibodies. J Immunol Methods 231:11–23
3. Tomizuka K, Shinohara T, Yoshida H, Uejima H, Ohguma A, Tanaka S, Sato K, Oshimura M, Ishida I (2000) Double trans-chromosomic mice: maintenance of two individual human chromosome fragments containing Ig heavy and kappa loci and expression of fully human antibodies. Proc Natl Acad Sci U S A 97:722–727
4. Terness P, Welschof M, Moldenhauer G, Jung M, Moroder L, Kirchhoff F, Kipriyanov S, Little M, Opelz G (1997) Idiotypic vaccine for treatment of human B-cell lymphoma. Construction of IgG variable regions from single malignant b cells. Hum Immunol 56:17–27
5. Hakim R, Benhar I (2009) "Inclonals": IgGs and IgG-enzyme fusion proteins produced in an E. coli expression-refolding system. MAbs 1:281–287
6. Kipriyanov SM (2003) Generation of antibody molecules through antibody engineering. Methods Mol Biol 207:3–25
7. Bird RE, Hardman KD, Jacobson JW, Johnson S, Kaufman BM, Lee SM, Lee T, Pope SH, Riordan GS, Whitlow M (1988) Single-chain antigen-binding proteins. Science 242:423–426
8. Kim SJ, Park Y, Hong HJ (2005) Antibody engineering for the development of therapeutic antibodies. Mol Cells 20:17–29
9. Olafsen T, Sirk SJ, Betting DJ, Kenanova VE, Bauer KB, Ladno W, Raubitschek AA, Timmerman JM, Wu AM (2010) Immunopet imaging of B-cell lymphoma using 124i-anti-CD20 scFv dimers (diabodies). Protein Eng Des Sel 23:243–249
10. Yokota T, Milenic DE, Whitlow M, Schlom J (1992) Rapid tumor penetration of a single-chain Fv and comparison with other immunoglobulin forms. Cancer Res 52:3402–3408
11. Kipriyanov S (2002) High-level periplasmic expression and purification of scFvs. In: O'Brien PM, Aitken R (eds) Antibody phage display, vol 178. Humana Press, New Jersey, pp 333–341
12. Bach H, Mazor Y, Shaky S, Shoham-Lev A, Berdichevsky Y, Gutnick DL, Benhar I (2001) Escherichia coli maltose-binding protein as a molecular chaperone for recombinant intracellular cytoplasmic single-chain antibodies. J Mol Biol 312:79–93
13. Kapust RB, Waugh DS (2000) Controlled intracellular processing of fusion proteins by TEV protease. Protein Expr Purif 19:312–318
14. Foti M, Granucci F, Ricciardi-Castagnoli P, Spreafico A, Ackermann M, Suter M (1998) Rabbit monoclonal Fab derived from a phage display library. J Immunol Methods 213:201–212
15. Itoh K, Suzuki K, Ishiwata S, Tezuka T, Mizugaki M, Suzuki T (1999) Application of a recombinant Fab fragment from a phage display library for sensitive detection of a target antigen by an inhibition elisa system. J Immunol Methods 223:107–114
16. Hexham JM (1998) Production of human Fab antibody fragments from phage display libraries. Methods Mol Biol 80:461–474
17. Skerra A (1994) A general vector, pask84, for cloning, bacterial production, and single-step purification of antibody Fab fragments. Gene 141:79–84
18. Shaki-Loewenstein S, Zfania R, Hyland S, Wels WS, Benhar I (2005) A universal strategy for stable intracellular antibodies. J Immunol Methods 303:19–39
19. Kapust RB, Waugh DS (1999) Escherichia coli maltose-binding protein is uncommonly effective at promoting the solubility of polypeptides to which it is fused. Protein Sci 8:1668–1674
20. Huston JS, Levinson D, Mudgett-Hunter M, Tai MS, Novotny J, Margolies MN, Ridge RJ, Bruccoleri RE, Haber E, Crea R et al (1988) Protein engineering of antibody binding sites: recovery of specific activity in an anti-digoxin single-chain Fv analogue produced in Escherichia coli. Proc Natl Acad Sci U S A 85:5879–5883
21. Gibson DG, Young L, Chuang RY, Venter JC, Hutchison CA 3rd, Smith HO (2009) Enzymatic assembly of DNA molecules up to several hundred kilobases. Nat Methods 6:343–345
22. Lei X, Ahn K, Zhu L, Ubarretxena-Belandia I, Li YM (2008) Soluble oligomers of the intramembrane serine protease YqgP are catalytically active in the absence of detergents. Biochemistry 47:11920–11929

23. Nomine Y, Ristriani T, Laurent C, Lefevre JF, Weiss E, Trave G (2001) Formation of soluble inclusion bodies by HPV E6 oncoprotein fused to maltose-binding protein. Protein Expr Purif 23:22–32
24. Zanier K, Nomine Y, Charbonnier S, Ruhlmann C, Schultz P, Schweizer J, Trave G (2007) Formation of well-defined soluble aggregates upon fusion to MBP is a generic property of E6 proteins from various human papillomavirus species. Protein Expr Purif 51:59–70
25. Gal-Tanamy M, Zemel R, Berdichevsky Y, Bachmatov L, Tur-Kaspa R, Benhar I (2005) HCV NS3 serine protease-neutralizing single-chain antibodies isolated by a novel genetic screen. J Mol Biol 347:991–1003

INDEX

Michael Steinitz (ed.), *Human Monoclonal Antibodies: Methods and Protocols*, Methods in Molecular Biology, vol. 1904, https://doi.org/10.1007/978-1-4939-8958-4, © Springer Science+Business Media, LLC, part of Springer Nature 2019

E

F

G

H

I

K

L

M

N

O

P

R

S

T

V

Y